THE UNIVERSITY
of EDINBURGH

Evaluation of the antitumour activity of novel flavonoids on pre-clinical models of breast and ovarian cancer

Carlos Martínez-Pérez

Thesis submitted in fulfilment of the requirements of the degree of

Doctor of Philosophy

University of Edinburgh

August 2016

Declaration

This is to certify that this thesis has been composed by me. The work contained within is entirely my own unless otherwise stated, where work was carried out as part of a collaboration as credited to the contributors. No part of this thesis has been submitted for any other degree or professional qualification.

Carlos Martínez-Pérez

August 2016

Abstract

New drugs are needed for better cancer management. Clinical trials are currently underway to assess the use of flavonoids (natural polyphenols) as anticancer agents. Among them, myricetin has been shown to induce cell cycle arrest and apoptosis in pre-clinical cancer models. We hypothesised that myricetin-derived novel flavonoids designed to enhance this natural potential and improve on the drug-likeness limitations of myricetin might have increased potential for their application in the management of breast and ovarian cancer.

The effect of a library of novel flavonoids was screened on 3 panels of breast and ovarian cancer cell lines, representing different molecular subtypes and phenotypes, to assess their potency. The second-generation bi-methoxylated analogue AO-1530-OMe (Oncamex) was identified as the most effective candidate in the library, with sub-micromolar concentrations exerting a strong antiproliferative effect across almost all models studied. Results suggested that changes in the hydroxylation profile, the addition of methoxylations and a decyl alkyl chain were some of the structure-activity relationships contributing to this improved efficacy.

Plate assays showed 8 h treatment with Oncamex reduced cell viability and induced cytotoxicity and apoptosis, concomitant with caspase activation and PARP cleavage. Pre-incubation with an antioxidant partially blocked these effects, suggesting the possible involvement of ROS modulation in the mechanism of action of Oncamex. Fluorescence microscopy reported the quick and stable delivery of Oncamex to the mitochondria. Fluorescent probes showed that Oncamex can induce mitochondrial superoxide production at concentrations associated with its antiproliferative effects. Study of the electrochemical properties of Oncamex by cyclic voltammetry supported this.

Differential gene expression analysis following a microarray experiment showed Oncamex induces changes in the expression of genes controlling cell cycle and apoptosis. Together with previous results, the findings from this analysis led to the postulation of a model for the mechanism of action of Oncamex: due to its enhanced reactivity and mitochondrial targeting, Oncamex can generate mitochondrial superoxide, leading to mitochondrial dysfunction, membrane permeabilisation and the activation of the JNK pathway and the transcription factor FOXO3, which together contribute to the induction of intrinsic apoptosis and the inhibition of proliferation.

Further proliferation assays on cell culture models also reported enhanced effect of Oncamex when administered in combination with paclitaxel and TRAIL. These improved responses were observed in breast and ovarian cancer models, including cells lines characterised by their treatment-resistant phenotype. Cotreatment with Oncamex also improved the effect of tamoxifen on anti-oestrogen resistant LCC9 breast cancer cells.

Results from preliminary *in vivo* studies in mice implanted with the MDA-MB-231 breast cancer xenograft were consistent with an antiproliferative effect of Oncamex (25mg/kg/day) *in vivo*, as treatment inhibited tumour growth and reduced the expression of the marker of proliferation Ki-67 without signs of systemic toxicity. Tissues from this experiment also allowed for preliminary *in vivo* validation of the proposed mechanism of action of Oncamex by immunohistochemistry. The *in vivo* cytostatic effect of Oncamex was confirmed in a second *in vivo* experiment, which also investigated the effect of Oncamex at higher doses or in combination with paclitaxel.

In conclusion, the novel flavonoid Oncamex has shown a promising antiproliferative effect in pre-clinical models of breast and ovarian cancer, including models of treatment-resistant cancers. Preliminary *in vivo* studies have demonstrated a partial recapitulation of the effect of Oncamex. A mechanistic model has been proposed by which Oncamex induces intrinsic apoptosis through its redox reactivity and mitochondrial targeting. These results support the potential of this prototypic candidate, although possible work in the structure and formulation of this candidate and further study and validation of its mechanism of action is needed for its continued development as an anticancer agent.

Lay Abstract

Flavonoids are a type of plant natural products being studied for their potential as anticancer agents. Myricetin has been shown to reduce proliferation and cause cell death in pre-clinical cancer models. This project is based on the hypothesis that novel flavonoids, designed from the natural structure of myricetin to enhance its natural properties and address its limitations as a drug, could be used to treat breast and ovarian cancer.

Testing of a library of flavonoids on 3 groups of cell lines representing different types of breast and ovarian cancer identified the second-generation analogue Oncamex as the most potent compound. Results showed that, thanks to the changes in its structure, Oncamex can reduce proliferation and cause cell death (apoptosis) after 8 hours.

Microscopy studies showed that Oncamex targets the mitochondria, which are the main sites of energy production and are involved in many processes. There, Oncamex can generate reactive oxygen species (ROS), oxygen-derived molecules that can create oxidative stress but also play an important role as messengers in many processes. Other results showed that Oncamex also regulates proliferation and apoptosis by altering gene expression. Together, these results suggested that Oncamex may work by generating ROS in the mitochondria, which then cause stress, the release and activation of proteins and changes in gene expression that can lead to cell death.

Other work also showed that Oncamex could be used in combination with chemotherapy or hormonal therapy, improving the response of resistant cells. *In vivo* experiments showed that Oncamex also had a partial effect in mice implanted with breast cancer xenografts, blocking tumour growth without obvious signs of a toxic effect to animals. Other work also supported part of the model for the mechanism of Oncamex in early validation experiments.

In conclusion, this project has shown that Oncamex, based on a natural product, can induce an antiproliferative and apoptotic effect on breast and ovarian cancers *in vitro* and this effect was also partially translated into initial experiments in mice. Results showed that Oncamex may also have potential to be combined with other therapies. Although more work is needed to confirm these results and improve its solubility, the work shown here suggests that Oncamex holds potential to be developed further for its use as an anticancer drug.

Acknowledgements

Collaborations

Some parts of this project have been the result of collaborative work. In particular, I would like to thank and acknowledge the following for their contributions:

- Peter Mullen shared information from the previous set-up of cell culture experiments with novel flavonoids in in our lab.
- Donald McPhail and Graeme Cook (from Antoxis Ltd) contributed unpublished results from previous research on novel flavonoids.
- Dr Colin Campbell and Dr Patrick Thomson assisted in the electrochemical analysis of Oncamex and Dr Thomson contributed results from cyclic voltammetry.
- Parts of the RNA extraction and processing and IHC staining were done in collaboration with Edward Jarman, James Meehan and Chrysi Xintaropoulou, with the assistance of Sonya Uddin and Dr Arran Turnbull.
- Dr Arran Turnbull also provided assistance and guidance in differential gene expression analysis work and, specifically, carried out the cross-platform normalisation and contributed dissimilarity matrices and MDS.
- Dr Simon Langdon carried out the animal experiments on mice, implanting xenografts, administering treatments and collecting tissues at the end of the experiment.

Thanks

Firstly, I would like to thank my primary supervisors Dr Simon Langdon and Dr Carol Ward, for their continued support and guidance throughout this project and particularly during the final write-up process. I would also like to thank Prof David Harrison for, together with Dr Langdon, organising the project in collaboration with Antoxis and securing funding. From Antoxis, I am thankful to Donald McPhail and Graeme Cooke for providing the library of compounds studied in this project and for their willingness to share their advice and expertise on this field. Funding for this project was provided by the Scottish Universities Life Sciences Alliance (SULSA) through their BioSKAPE (Bio-industry Skills Knowledge and People Exchange) industrial PhD studentships, with contribution from Antoxis Ltd.

I am also thankful to Prof Val Brunton and Dr Colin Campbell for their helpful advice as members of the committee for my first and second year reviews. In the lab, I would like to thank Peter Mullen and Dr Carol Ward for getting me started in cell culture; Hannah Webb for her assistance in setting up ovarian experiments; as well as Paul Perry and Arran Turnbull for their helpful advice on microscopy and AQUA technology. I am also grateful to Helen Caldwell and Elaine McLay for their help in the day-to-day work in the lab and to Kate Britton for taking care of administration for the project.

I would specially like to thank all my friends in the Division of Pathology Laboratories (University, though, don't leave NHS orders with us) for making my 5 years (and counting) at the lab so enjoyable. To my teammates James, Ed, Chrysi, Kyle and Ghassan for their day-to-day support in the lab. To Laura, Jenny, Danny, Fiach and everyone else for all the coffee breaks (of which there were many), Metro quizzes and general tomfoolery, which helped make the lab a nice place to come to work every day.

I recently discovered that the University of Edinburgh's official motto is "*Nec temere, nec timide"*, a phrase coined by Aristotle which translates as "Neither rashly, nor timidly". I find that rather fitting, for doing a PhD is no easy task and I think requires both patience and resilience. It obviously takes brains, sure. But sometimes it also takes *cojones* – if you'll pardon my Spanish – to carry on working, particularly in the final stretch, when you feel like you really *cannae be bothered* anymore. Edison sure was on to something with his "99% perspiration" dictum.

For all of the above I am, finally, most indebted to the people closest to me, without whom I wouldn't have been able to finish my PhD. To my friends, in Edinburgh and elsewhere, for helping make these years enjoyable. To my parents, Ángel and Paz, for supporting me when I first decided to move to the UK and continuing to do so throughout, particularly in the last few months, when any mention of my thesis risked a snappy complaint. To my brother Pablo for his encouragement and his nonsensical texts, which are always welcome. And to my best friend Arran for, somewhat annoyingly, being "the glue that keeps this lab together" (not my words!) and for all his support during these years.

Thank you all.

Publications

Section 1.1.5. in Chapter 1 was the basis for a published literature review:

Novel flavonoids as anti-cancer agents: mechanisms of action and promise for their potential application in breast cancer

Martínez-Pérez C, Ward C, Cook G, Mullen P, McPhail D, Harrison, DJ and Langdon SP.

Biochemical Society Transactions **42**, 1017-1023 (2014)

Chapters 3 and 4 were the basis for a published research article:

Antitumour activity of the novel flavonoid Oncamex in preclinical breast cancer models

Martínez-Pérez C, Ward C, Turnbull AK, Mullen P, Cook G, Meehan J, Jarman EJ, Thomson PIT, Campbell CJ, McPhail D, Harrison, DJ and Langdon SP.

British Journal of Cancer 114, 905-906 (2016)

Both publications are enclosed in Appendix 3.

Table of contents

List of figures

List of tables

Supplementary materials

Appendix 1: Supplementary figures

Appendix 2: Gene lists

List of abbreviations

5-FU: 5-fluorouracil

Ab: antibody

ABC: ATP-binding cassette transporter

ABCG2: breast cancer resistance protein

ACIN1: apoptotic chromatin condensation inducer 1

ADME: the administration, distribution, metabolism and elimination

AhR: aryl hydrocarbon receptor

AI: aromatase inhibitor

AJCC: American Joint Committee on Cancer

AKT: protein kinase B

AMPS: Ammonium Persulphate

ANOVA: analysis of variance

AP-1: activator protein 1

APAF1: apoptotic protease activating factor 1

ATCC: American Type Culture Collection

ATP: adenosine triphosphate

AQUA: automated quantitative analysis

AURKA: Aurora kinase A

AURKB: Aurora kinase B

αTOS: α-tocopheryl succinate

BAD: BCL2-associated death promoter

BAK: BCL2 homologous antagonist/killer

BaP: benzo(a)pyrene

BAX: BCL2-associated X protein

BB: blocking buffer

BCA: Bicinchoninic Acid

BCL2: B-cell lymphoma 2 protein (family)

BCL-XL: B-cell lymphone-extralarge or BCL2-like 1 isoform 1

BCRP: breast cancer resistance protein

BCS: breast conserving surgery

BH3: BCL2 homology 3 domain

BIM: BCL2-like protein 11

BNIP3: BCL2/adenovirus E1B 19 KDa protein-interacting protein 3

BNIP3L: BNIP3-like, also referred to as NIX

BRCA: breast cancer gene family

BSA: bovine serum albumin

c-Jun: Jun proto-oncogene

CA-125: cancer antigen 125

CCNA2: Cyclin-A

CCNB1: Cyclin-B1

CCND1: Cyclin-D1

CCNG2: Cyclin-G2

CDCA2: cell division-associated protein 2, also referred to as Repo-man

CDC20: cell division cycle protein 20

CDDP: cis-platinum

CDK: cyclin-dependent kinases

CENPF: centromere protein F, also referred to as mitosin

COX1/2: cyclooxygenases 1 and 2

CSFCS: foetal calf serum charcoal-stripped of steroids

CV: cyclic voltammetry

CVα: ATP synthase subunit alpha

CYP1: cytochrome P450 enzyme

CYP1A1/A2/B1: cytochrome P450 enzyme isoforms

Cyp19: cytochrome P450 19 aromatase

Cyt c: cytochrome c

DAB: 3,3'-diaminobenzidine

DAPI: 4',6-diamidino-2-phenylindole

DAVID: Database for Annotation, Visualisation and Integrated Discovery

DCFDA: 2',7'-dichlorofluorescein diacetate

DCIS: ductal carcinoma *in situ*

DEDD2: death effector domain-containing 2

DMEM: Dulbecco's Modified Eagle Medium

DMSO: Dimethylsulfoxide

DNA: deoxyribonucleic acid

e^-: electron

E_2: 17β-oestradiol

EDI: estimated dietary intake

EDTA: ethylene-diamine-tetra-acetic acid

EGFR: epidermal growth factor receptor

EMT: epithelial to mesenchymal transition

ENO2: enolase 2

ER: estrogen receptor

ErbB: avian erythroblastosis oncogene B

ERBB2: human epidermal growth factor receptor 2

ERK: extracellular signal-regulated kinases

ERα: estrogen receptor α

ERβ: estrogen receptor β

ETC: electron transport chain

FADD: Fas-associated death domain

FCS: foetal calf serum

FFPE: formalin-fixed, paraffin-embedded

FIGO: International Federation of Gynaecology and Obstetrics

FIH: factor inhibiting HIF-1

FISH: fluorescence *in situ* hybridisation

FLICE: FADD-like interleukin-1beta-converting enzyme

FLIP: FLICE-like inhibitory protein (also known as CFLAR)

FOXO3: forkhead class O transcription factor 3a

FUNDC1: FUN14 domain-containing 1

GAPDH: glyceraldehyde-3-phosphodehydrogenase

GPI: phosphoglucose isomerase

GLUT1: glucose transporter 1

GLUT3: glucose transporter 3

GnRH: gonadotropin-releasing hormone

GO: gene ontology

GPX: glutathione peroxidase

HE4: human epididymis protein 4

HER2: human epidermal growth factor receptor 2

HH/GLI: Hedgehog/Glioma-associated oncogene cascade

HIF: hypoxia-inducible factor

HIF-1(α): hypoxia-inducible factor 1 (subunit α)

HK2: hexokinase 2

HOMO: highly occupied molecular orbital

HSD: 17β-hydroxysteroid dehydrogenase

HSP: heat shock protein

hTERT: human telomerase reverse transcriptase

H&E: haematoxylin and eosin

IC_{50}: half maximum inhibitory concentration

IDC: invasive/infiltrating ductal carcinoma

IHC: immunohistochemistry

IF: immunofluorescence

ILC: invasive/infiltrating lobular carcinoma

IM: inner mitochondrial membrane

IMS: industrial methylated spirit

IMS: intermembrane space

IU: International Units

JNK: c-Jun N-terminal kinases

LC3: microtubule-associated protein 1A/1B-light chain 3

LCIS: lobular carcinoma *in situ*

LCMS: liquid chromatography mass spectrometry

LDHA: lactate dehydrogenase A

LIR: LC3-interacting region

mAb: monoclonal antibody

MAC: mitochondrial apoptosis-induced channel

MAPK: mitogen-activated protein kinase

MAPKK: MAPK kinase kinase

MCM5: minichromosome maintenance complex component 5

MCT4: monocarboxylate transporter 4

MDR: multidrug resistance

MDS: multidimensional scaling

MeV: MultiExperiment Viewer

mH_2O_2: mitochondrial hydrogen peroxide

MMF: Morgan-Mercer-Flodin model

MOMP: mitochondrial outer membrane permeabilisation

MTP: mitochondrial permeability transition

mPTPC: mitochondrial permeability transition pore complex

MRP1/2: multidrug resistance proteins 1 and 2

mSO: mitochondrial superoxide

mTOR: mechanistic target of rapamycin

MUC1: mucin-1

NAC: N-acetyl-L-cysteine

NADPH: nicotinamide adenine dinucleotide phosphate

NBD: nucleotide binding domain

NF-κB: nuclear factor-kappa B

NHE: normal hydrogen electrode

NIX: BNIP3-like

NMR: nuclear magnetic resonance

NOS: no otherwise specified breast cancer

Nrf2: nuclear factor (erythroid-derived 2)-like 2

NST: no special type breast cancer

OD: optical density

OHT: 4-hydroxytamoxifen

OM: outer mitochondrial membrane

P-gp: P-glycoprotein

pAb: polyclonal antibody

PAGE: Polyacrylamide gel electrophoresis

PAH: polycyclic aromatic hydrocarbons

PARP: poly ADP-ribose polymerase

PBS: phosphate buffered saline

PDH-E1α: pyruvate dehydrogenase subunit E1-alpha

PFA: paraformaldehyde

PFK1: phosphofructose kinase

PGAM1: phosphoglycerate mutase

PGK1: phosphoglycerate kinase

PI3K: phosphatidylinositol 3 kinase

PKM2: pyruvate kinase isoenzyme type M2

PPP: pentose phosphate pathway

PR: progesterone receptor

PVDF: Polyvinylidene fluoride

RAD1: checkpoint DNA exonuclease

REVIGO: reduce + visualise gene ontology

RIP1: serine-threonine kinase receptor-interacting protein 1

RFU: relative fluorescence units

RLU: relative luminescence units

RMI: risk of malignancy index

RNA: ribonucleic acid

ROCA: risk of ovarian cancer algorithm

ROMA: risk of ovarian malignancy algorithm

ROS: reactive oxygen species

rpm: revolution per minute

RPMI: Rosswell Park Memorial Institute Medium

SAR: Structure-activity relationship

SD: standard deviation

SERD: selective oestrogen receptor down-regulators

SERM: selective oestrogen receptor modulators

SOD: superoxide dismutase

Smac: second mitochondria-derived activator of caspase

SRB: Sulforhodamine B

STAT3: signal transducer and activator of transcription 3

STR: short tandem repeat

SV40: simian virus 40

TBA·PF6: tetrabutylammonium hexafluorophosphate

TCA: tricarboxylic acid

TCA: trichloroacetic acid

TDLU: terminal ductal luminal units

TEMED: Tetramethylethylenediamine

TERT: telomerase reverse transciptase

TNBC: triple negative breast cancer

TPI: triosephosphate isomerase

TPP^+: triphenylphosphonium

TRAIL: TNF-related apoptosis-inducing ligand

UICC: Union for International Cancer Control

UKCTOCS: UK Collaborative Trial of Ovarian Cancer Screening

VDAC/ANT: voltage-dependent anion channel/adenine nucleotide translocase

VEGF: vascular endothelial growth factor

VEGFR: vascular endothelial growth factor receptor

WHO: World Health Organisation

wt: wild type

1. Introduction

1.1. Background

1.1.1. Cancer as a global disease

1.1.1.1. What is cancer?

Cancer (often referred to as a malignant tumour or neoplasm) is a generic term for a large group of diseases characterised by the uncontrolled growth and invasion of abnormal cells[1]. The development of cancer (or carcinogenesis) can be influenced by a wide range of environmental (lifestyle, pathogens or exposure to carcinogens, amongst others) or inherited factors. The general consensus is that the development of neoplastic disease is the result of a multistep process[2]. In brief, the accumulation of somatic mutations leads to the alteration of the genome and eventual transformation of normal cells into malignant ones[3,4].

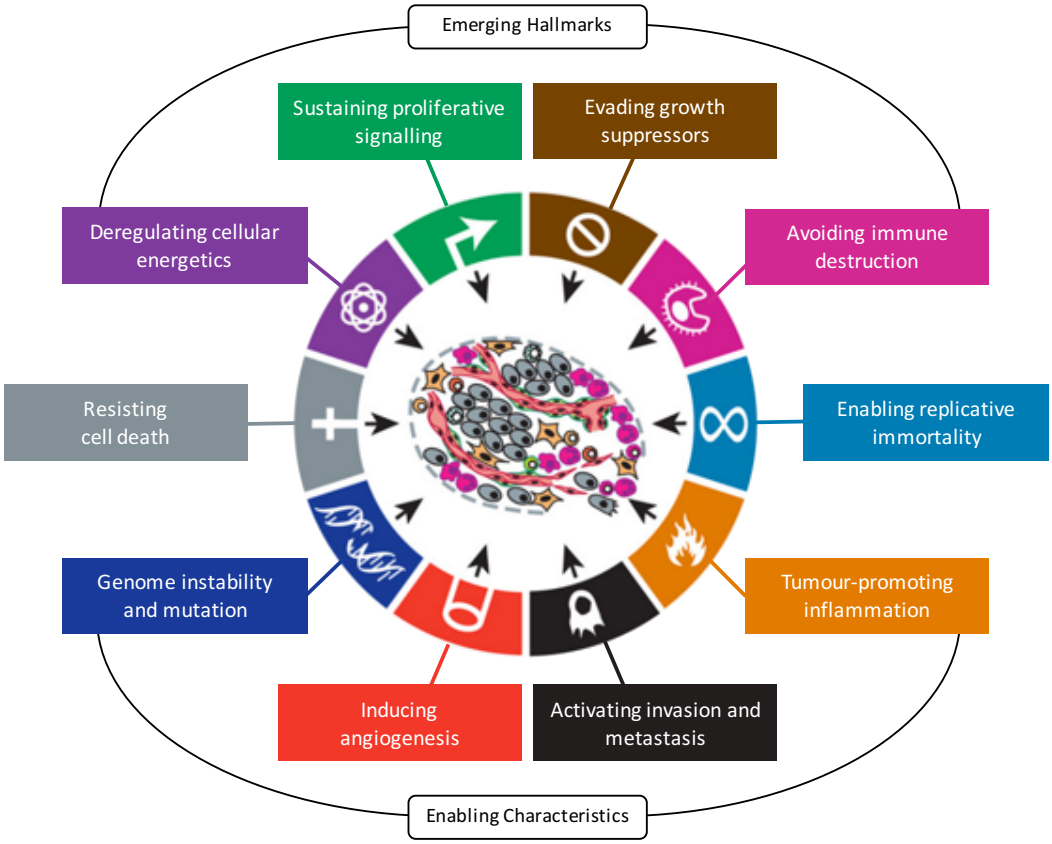

***Figure 1* Hallmarks of Cancer.** *In 2000 Hanahan and Weinberg published their "Hallmarks of Cancer", seeking to rationalise the complexities of neoplastic disease by describing six defining traits acquired during carcinogenesis and common to all cancers[2]. They revised and updated their article in 2011 to include a further four traits, highlighted here as emerging hallmarks and enabling characteristics[5]. Diagram adapted from Hanahan & Weinberg (2011).*

Cancer can affect any cell type with replicative potential in the body and more than 100 different types have been described, making its understanding as a single pathology extremely complex. In line with this, in 2000 Hanahan and Weinberg published a list of six common biological capabilities acquired during the multistep process of carcinogenesis[2]. This seminal article has been adopted as a reference for simplified description of the characteristics of all neoplasms and has since been revisited and updated[5] (see *Figure 1*).

1.1.1.2. Cancer epidemiology worldwide

Despite constant advances and breakthroughs in both the research and clinical settings, cancer is still among the leading causes of death worldwide, with lung, breast, colorectal and prostate being the most common cancer types (see *Figure 2* for worldwide figures on incidence of different cancer types). According to a recent report by the World Health Organisation (WHO), in 2012 approximately 14.1 million new cancer cases were detected, 8.2 million cancer-related deaths (most due to metastases) were recorded and 32.6 million people were living with cancer[6]. Most of these cancers occurred in less developed regions (57% of diagnoses and 65% of deaths)[6], in which the mortality rate is much higher. These figures are predicted to increase by about 70% to approximately 24 million new cases per year in 2 decades[7].

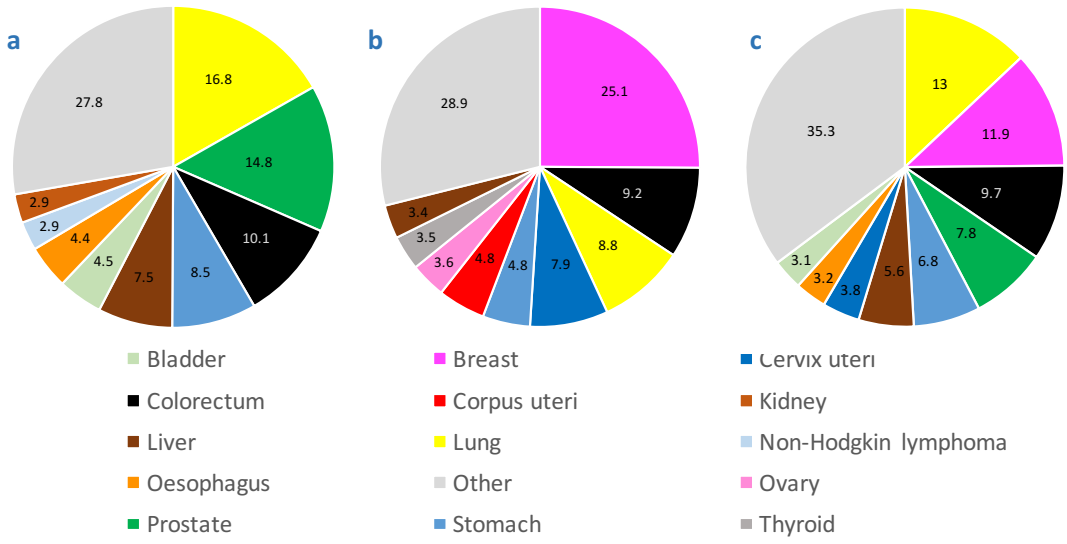

***Figure 2* Incidence of different cancer types worldwide:** *for men (a), women (b) and both sexes (c) according to the most recent WHO reports[6].*

1.1.1.3. Cancer epidemiology in the United Kingdom

Incidence and mortality rates vary considerably across continents and nations. In the United Kingdom 338,623 cases and 161,823 cancer-related deaths were recorded in 2012, according to Cancer Research UK[8]. In 2014, cancer was the leading cause of premature death in England, causing 42% of deaths in under-75s[9] and almost 30% of the total deaths across the UK[10]. In lay terms, someone in the UK is diagnosed with cancer every two minutes and more than one person dies from it every four minutes.

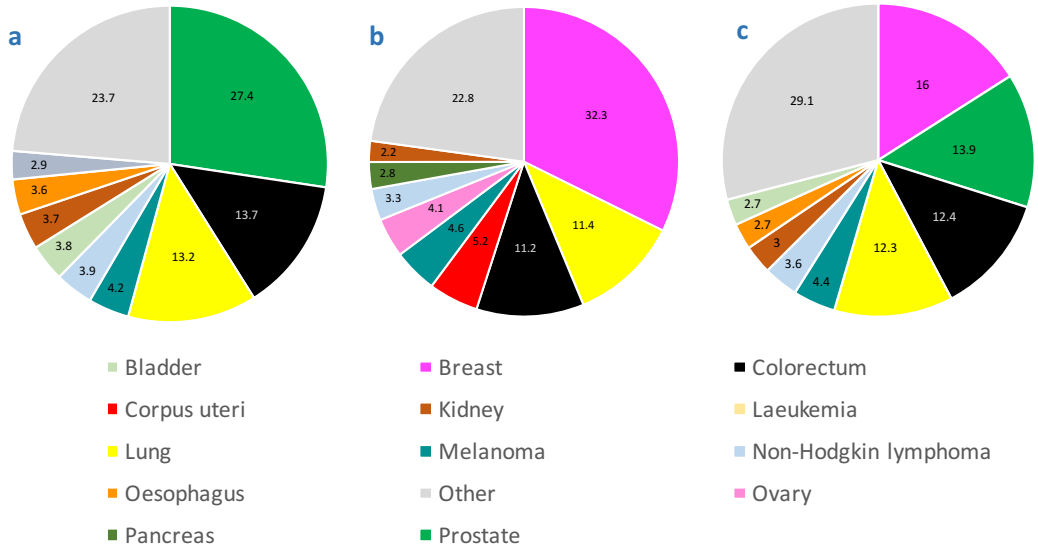

***Figure 3* Incidence of different cancer types in the UK:** *for men (a), women (b) and both sexes (c) according to the most recent WHO reports[10,11].*

In the UK, the incidence of different cancer types varies slightly from the worldwide trends (see *Figure 3* for UK figures on cancer incidence). However, the most frequent types considering both sexes are still breast, prostate, colorectal and lung tumours, which together account for over half (53%) of all new cases of cancer each year[8,11].

1.1.2. Current status of breast cancer

1.1.2.1. Breast cancer statistics

As previously mentioned, reports have shown that breast cancer is the second most common cancer in the world, the most common in the majority of high income regions (including the UK) and, by a wide margin, the most common amongst females[6] (see *Figures2* and *3*). Indeed, breast cancer incidence has increased by 51% since the 1970s to become the most frequent type (see *Figure 3*). Almost a third of all cancers detected in the UK are breast tumours, with 51,103 diagnoses and 11,716 deaths in 2012[12] (see *Figure 4a*). Greater awareness and the introduction of systematic screenings in 1988 have meant an increase in incidence but also have led, together with improved treatments, to a reduction in mortality (see *Figure 4b*). Death rates have decreased by 40% since peaking in the 1980s and the current 10-year survival rate is 78% (see *Figure 4c*).

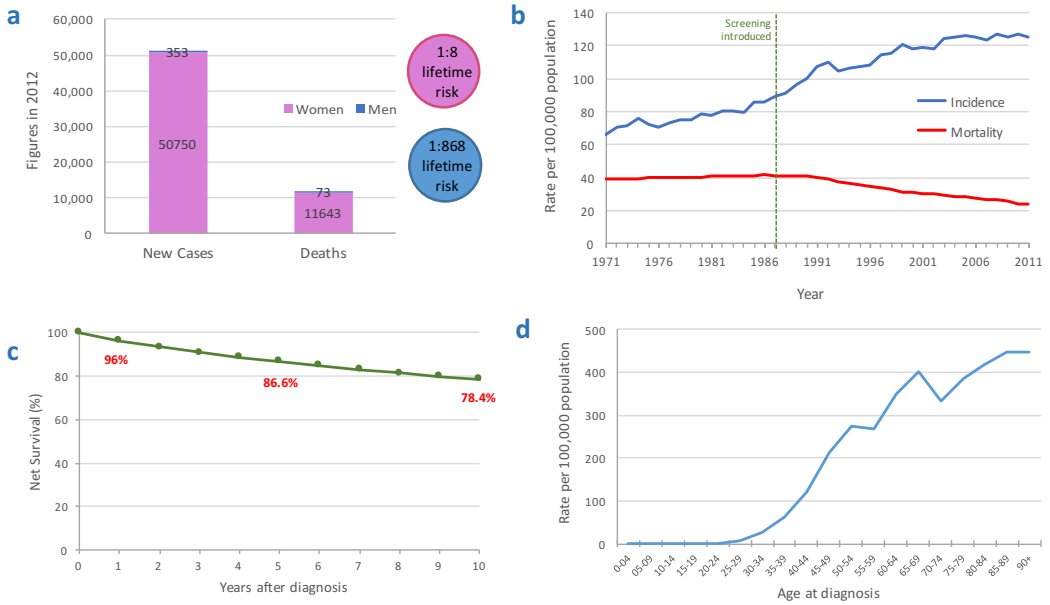

***Figure 4* Breast cancer statistics according to the latest reports[12,13].** *51,103 new breast cancer cases and 11,716 breast cancer-related deaths were recorded in 2012, the vast majority of which were female, as suggested by the higher lifetime risk in women (*a*). Incidence has risen and mortality has decreased since the introduction of systematic screening for breast cancer in 1987 (*b*), while survival has widely improved in the last three decades, with 78.4% of patients surviving for at least 10 years (*c*). Age is an important risk factor, with 13% of all new cancers being detected in patients in the 60-64 age group (*d*).*

A number of factors can contribute to the development of cancer. The biggest risk factor for breast cancer is gender, with the vast majority of cases found in females: although men

can also develop breast carcinomas, male cases account for less than 1% of all incidences (0.69% of the 51,103 new cases detected in 2012) (see *Figure 4a*). A British woman currently has a 1 in 8 lifetime risk of developing breast cancer, while a man has a risk of 1 in 868. In crude incidence rates this means that there are 157 new breast cancer cases for every 100,000 women, but only 1 for every 100,000 men[12].

After gender, the second biggest risk factor for breast cancer is age. Incidence is closely linked to the age group, with a peak in registrations among those aged 60 to 64 (see *Figure 4d*). Approximately 80% of all new cases each year are detected in patients aged over 50[13]. Additionally, it is estimated that about 27% of cases are linked to lifestyle and environmental factors, such as obesity, smoking, alcohol consumption and a sedentary lifestyle[14]. Family history is also associated with an increased risk of developing breast cancer[15].

1.1.2.2. Histological classification of breast cancer

As a first classification, breast cancer can be broadly categorised into *in situ* (or pre-cancer, corresponding to stage 0) and invasive or infiltrating carcinomas (stages I-IV) based on microscopic evaluation. Pre-cancers originate from the epithelial lining of the terminal ductal lobular units (TDLU) in the breast, which comprise each lobule (the milk-producing glands at the end of the breast ducts[16], considered the functional unit of the breast) and its respective intra- and extra-lobular terminal lactiferous duct. Depending on where in the TDLU growths originate they can be either ductal carcinomas *in situ* (DCIS) or lobular carcinomas *in situ* (LCIS) (see *Figure 5* for diagrams).

DCIS are more common, corresponding to about 90% of all pre-cancer detected[17,18] and can be further sub-classified depending on the architecture of the tumour into comedo, cribriform, micropapillary, papillary or solid DCIS[16]. Diagnosis of DCIS and LCIS has increased in recent years, particularly in pre-menopausal women, due to more thorough screening procedures. These are considered pre-malignant and indicate a higher risk of developing cancer in the future, as in some cases they can develop into invasive tumours[18–21].

An invasive cancer is defined by the breakage and trespass of the basal membrane of the duct or lobule. Invasive carcinomas can be divided into 7 different histological groups depending on their origin and structure: invasive ductal, invasive lobular, ductal/lobular, mucinous (or colloid), tubular, medullary and papillary carcinomas (see *Figure 5* for diagrams). Invasive ductal carcinoma (IDC), also referred to as no special type (NST) or not otherwise specified (NOS), is the most common subtype of invasive breast carcinomas,

accounting for about 80% of all breast cancers diagnosed in the UK[22,23]. Invasive lobular carcinoma (ILC) accounts for about 10% of all cancers diagnosed[24]. IDC can be further stratified depending on its histological scoring (see next section) as: well-differentiated (grade 1), moderately differentiated (grade 2) or poorly differentiated (grade 3)[25].

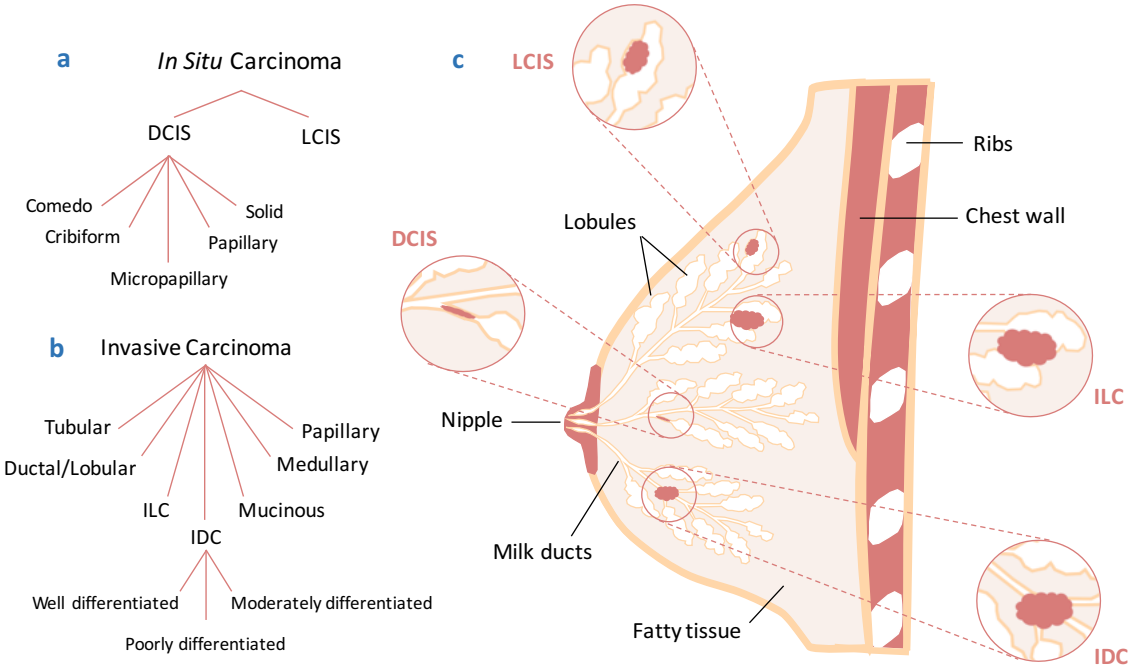

***Figure 5* Summary of the histological classification of breast cancers.** *Depending on their spread, breast tumours are classified as in situ* (a) *or invasive* (b)*. Each of these can be further sub-classified depending on the origin and location of the growth in the breast* (c)*, as well as factors such as tumour architecture and grade. DCIS: ductal carcinoma in situ; LCIS: lobular carcinoma in situ; ILC: invasive lobular carcinoma; IDC: invasive ductal carcinoma. Diagram adapted from Cancer Research UK.*

Besides the histological types described above, there are less common malignancies and related disorders. The growth of a locally advanced breast cancer to block the lymph nodes in the breast can lead to the development of inflammatory breast cancer. This is one of the most aggressive breast cancer types and receives its name by the development of inflammation-like symptoms in the affected breast, which can lead to misdiagnosis as mastitis[26]. Another example of a disorder related to breast cancer is the development of Paget's disease of the breast, a rare disorder of the nipple-areola caused by an underlying *in situ* or invasive carcinoma[27].

1.1.2.3. Histological grading of breast cancer

Breast cancer is a heterogeneous disease, both pathologically and genetically[28]. Consequently, different classification systems have been developed in an attempt to stratify neoplasms beyond their histological origin, according to their stage of development, molecular properties and clinical behaviour.

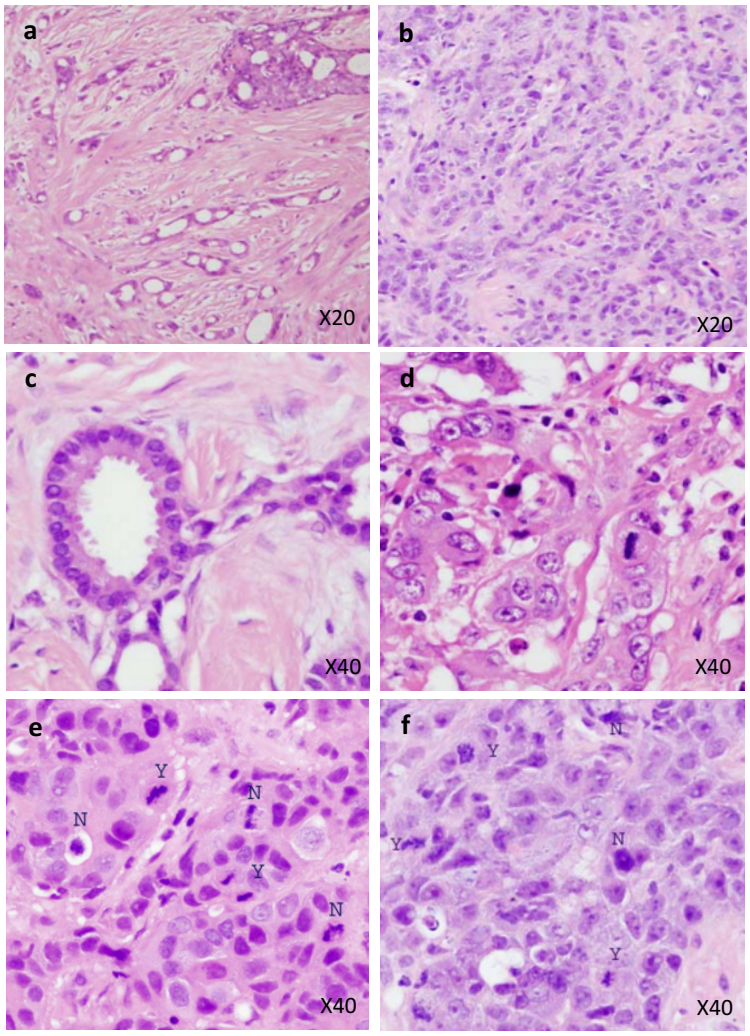

Figure 6 ***Microscopic examination of haematoxylin and eosin (H&E) stained formalin-fixed, paraffin-embedded (FFPE) section of human breast tissues.*** *In histological grading, tissue sections are scored for the overall tubule formation with the more frequent presence of tubular structures (*a*) receiving a lower score than tumours with less differentiated cells and, hence, lower tubular formation (*b*). Nuclear pleomorphism is scored in the worst areas depending on the presence of normal nuclei with even chromatin patterns (*c*) or more uneven, vesicular nuclei (*d*). For mitosis scoring (*e-f*) several fields are scored depending on the abundance of dividing cells, as judged by the specialist pathologist (Y marks cells considered mitotic; N, those considered non-dividing). Images courtesy of Dr Jeremy Thomas (Lead Consultant Pathologist, Edinburgh Breast Unit).*

Traditionally, breast cancers have been classified according to histological grading following the method developed by Bloom and Richardson in the 1950s[29], which has been subsequently updated and optimised[30,31]. The histological grading system considers (i) tubule formation (loss of normal cellular organisation in the tissue), (ii) nuclear pleomorphism (related to the distinctive morphology of the nuclei) and (iii) hyperchromatic and mitotic nuclei (regarding the mitotic count of cells)[29] (see *Figure 6*). Each factor is graded between 1 and 3 by microscopic observation of the tissue and scores are added to obtain an overall tumour score: non-tumour (scores under 3), grade 1 (score 3-5), grade 2 (score 6-7) or grade 3 (score 8-9). Higher grades indicate more poorly differentiated cancer and, hence, more advanced disease and worse prognosis.

1.1.2.4. TNM staging of breast cancer

The TNM classification is the agreed staging method for breast cancer worldwide. It consists of two steps: first scoring 3 different cancer-related categories (tumour size, node invasion and metastasis) that can then be grouped into overall stages (I-IV). The TNM system was first described by Denoix in the 1940s[32] and first applied to breast cancer in the 1960s[33]. Since then, it has been maintained and regularly updated for the specifications of each cancer type by the AJCC (American Joint Committee on Cancer) and the UICC (Union for International Cancer Control)[34–37].

Tumour size (T)	TX	Primary tumour cannot be evaluated
	T0	No evidence of primary tumour
	Tis	Carcinoma *in situ* (LCIS or DCIS)
	T1-T4	Size of the tumour
Invasion of lymph nodes (N)	NX	Regional lymph nodes cannot be evaluated
	N0	No regional lymph node involvement
	N1-N3	Involvement of regional lymph nodes
Metastasis (M)	M0	No distant metastasis
	M1	Distant metastasis

***Table 1* Simplified description of TNM staging system.** *Each of the 3 categories observed are scored according to the agreed standards[38–40]. LCIS: lobular carcinoma in situ; DCIS: ductal carcinoma in situ.*

In brief, this system scores a cancer based on 3 categories: tumour size (T), invasion of sentinel nodes (N) and distant metastasis (M) (see *Table 1* for details on scoring). Some authors have suggested the limitations of the TNM system to comprehensively categorise the biological heterogeneity of the disease[38], but this method remains the common standard for staging, allowing for the universal comparison of clinical data.

As with histological grading, these individual factors can then be combined to assign an overall stage of the disease. TNM scores are considered together according to established consensus[35] to designate the stage of the disease, between stages 0 and IV (see *Table 2* for descriptions of each stage in breast cancer). Thus, anatomic staging by TNM scoring is translated into 4 prognostic groups, which are useful to describe succinctly the overall characteristics of cancers across different types[40].

Stage 0		Abnormal cells in the lining of breast lobule or duct that have not spread to surrounding tissues	*In situ*	
Stage I		Tumour has spread from lobules or ducts to surrounding tissues, with a size ≤ 2cm, but has not spread to the lymph nodes	Invasive breast cancer	Early
Stage II		Tumour size of 2 to 5cm. May have spread to the lymph nodes		
Stage III	IIIA	Tumour size ≥ 5cm or has spread to axillary lymph nodes		
	IIIB	Locally advanced cancer. Tumour has spread into the skin, chest wall or further lymph nodes		Advanced
	IIIC			
Stage IV		Metastatic cancer which has spread to other parts of the body		

***Table 2* Simplified overall numerical staging for breast cancer.** *These stages are associated with different advance and, hence, prognosis of the disease at diagnosis. They are used across different cancer types to summarise the defining characteristics of the cancer as determined by TNM staging. This table describes what each stage implies to the specifics of breast cancer[40,41].*

1.1.2.5. Molecular subtyping of breast cancer

With the increasing understanding of the molecular heterogeneity of breast cancer[28], the definition of molecular subtypes has shaped the diagnosis and management of the disease in the last few decades. Stratification according to the expression of molecular markers has become standard practice thanks to its relevance in the clinical setting.

The presence of oestrogen receptor alpha (ER), human epidermal growth factor 2 (HER2 or ERBB2) and progesterone receptor (PR) are used to stratify patients at diagnosis. ER and PR are measured on IHC slides using the Allred score, which considers the abundance and intensity of positively-stained cells[42,43]. HER2 is measured by immunohistochemistry (IHC) using a scoring system (0 to 3+), complemented with detection of the HER2 gene by fluorescence *in situ* hybridisation (FISH) for cases with a medium IHC score (2+)[44–46].

Together with grading, staging and histological subtyping, the determination of a cancer's hormone receptor status has become an essential tool in guiding clinical decisions, allowing for a more informed selection of better, more targeted alternatives for the management of the disease [25,47–51].

ER receptor status, or classification of breast tumours as hormone-dependent (ER-positive, ER^+) or independent (ER-negative, ER^-), has been of particular clinical relevance. About 75% of cancers are ER^+ and dependent on hormonal regulation for their growth. Hence, the application of endocrine therapy plays an essential role in the management of these cancers (see section *1.1.2.7.*).

Despite the incorporation of hormone receptor status as a tool in the clinical decision-making process, the molecular heterogeneity of breast cancer has made a more thorough stratification of the disease necessary. In the early 2000s, Perou and Sørlie described and validated a series of molecular subtypes of breast cancer[52–54], confirming observations previously made from clinical evidence and epidemiological studies[55,56]. For this they applied microarray-based gene expression analysis and unbiased hierarchical clustering, an approach previously used to study genetic differences across different cancers[57,58]. They identified 5 different subtypes:

- Basal-like, triple negative breast cancer (TNBC), with negative status for all 3 hormonal receptors described (ER^-, PR^-, $HER2^-$), they express basal cytokeratins and epidermal growth factor receptor (EGFR).
- HER2, with enriched expression of HER2 (ER^-, PR^-, $HER2^+$).
- Normal breast-like, with a genetic signature similar to that of normal epithelial tissue of the breast ($ER^{+/-}$, PR^-, $HER2^-$).
- Luminal A, first of 2 ER^+ subtypes (ER^+, PR^+, $HER2^{-/low}$).
- Luminal B, second ER^+ subtype (ER^{low}, $PR^{+/-}$, $HER2^{+/-}$), with high proliferation.

An additional subtype referred to as claudin-low has since been described[59,60]. This is also TNBC with a genetic profile similar to that of the basal-like subtype but characterised by an epithelial to mesenchymal transition (EMT) phenotype.

Notably, these molecular subtypes displayed highly significant differences in prediction of survival[52–54] and appearance of metastasis[53] and have been shown to correlate well with clinical groups, predicting disease outcome[61,62]. They also allowed for the distinction of 2 different ER^+ subtypes, which had not been made before and was of interest given the clinical relevance of hormonal receptor status. Consequently, these intrinsic molecular subtypes have become a working model for the better stratification of breast cancer and have been the basis for a prominent branch of translational studies in the last fifteen years.

Subsequent work has focused on understanding the transformation of normal breast cells into aberrant cells, suggesting that arrest at different stages of development may lead to the development of different molecular subtypes[63–65]. Other authors have elaborated on this work, describing further sub-categorisations[66,67] and identifying specific biomarkers[68–72] to aid the targeted management of specific, molecularly distinct tumours with worse prognosis. Overall, the first clinical applications derived from this better understanding of the molecular heterogeneity of breast cancer have now arrived at the clinical setting and research continues to progress toward a more personalised management of breast cancer.

1.1.2.6. Breast cancer screening and diagnosis

The main tool for breast cancer screening is mammography. In the UK, a national screening programme has been in place since 1988 by which all women between the ages of 50 and 70 are invited to undertake a routine mammographic screening every 3 years[73]. Despite the acknowledgement of the incidence of overdiagnosis[74,75] and the need for refinement of the protocols in place (including the suggestion to expand the patient age group from 47 to 73[76]), recent reports highlighted the overall positive effect of the national screening programme[75–79]. Indeed, in the last 25 years it has led to a reduction in mortality by 20% and has saved about 1300 lives per year[75–77].

In recent years different clinical trials have investigated the potential of the incorporation of other technologies such as ultrasonography or magnetic resonance as supplementary or alternative diagnostic tools[80–82]. However, mammography remains the mainstay for screening in the general population and these other methods are normally only

used to follow up on unsatisfactory screening results or for monitoring of evolution during treatment.

When screening leads to the detection of a tumour by clinicians a core biopsy is customarily performed for histopathological assessment, since the best treatment strategy currently considers tumour grade, stage and molecular properties (receptor status), as previously described, together with over relevant factors such as age and menopausal status of the patient.

As previously mentioned, recent years have seen the arrival of the first clinical applications of molecular stratification of breast cancers through gene expression-based prognostic signatures. Tools such as MammaPrint (based on a 70-gene signature[62]) or Oncotype DX (21-gene[83]) can stratify patients into different risk groups and provide an estimation of probability of recurrence. Although these tests are not a replacement for the more traditional clinico-pathological features, they can be useful tools in those cases in which other measures of clinical risks might be doubtful (e.g., intermediate ER expression or histological grade), often aiding clinicians in decision-making for the administration of chemotherapy is necessary in cases where clinical features are non-conclusive[84,85]. The development of tests to predict the response to specific chemotherapy agents has been less successful and has led to no real clinical application to date[84,86], while new tools for the prediction of response to endocrine therapy are currently being developed[87].

1.1.2.7. Breast cancer treatment

A number of options are available for the treatment of breast cancers: surgery, radiotherapy, chemotherapy, endocrine therapy or targeted biological therapy. Historically, surgery has played the most important role and is still applied, alone or in combination, in most cases. Reports show the application of breast surgery as far back as 3000 BC[88], although it was an early attempt at what we now call radical mastectomy (removal of the breast, pectoral muscle and axillary lymph) by American surgeon William Halsted in 1882 that set the basis for most modern surgical techniques[88,89].

Surgery can be directed to remove only part of the breast tissue (lumpectomy or breast-conserving surgery, BCS) or the whole breast (mastectomy). In most women with stage I or II cancers BCS followed by radio- and/or chemo-therapy is as effective as mastectomy[90]. Mastectomies can be either simple (removal of one whole breast), bilateral or double (removing both breasts) or modified radical mastectomies (including the removal of sentinel

lymph nodes in the axilla)[90]. Biopsy of the sentinel nodes (first lymph nodes to which the cancer is most likely to spread as determined by injection of a tracer) is used for a better diagnosis and assessment of the progression of the cancer.

Besides removal of tumours, surgery can also be applied as a prophylactic measure in patients likely to develop cancer[91,92]. Reconstructive surgery is also a common procedure to reduce the impact of a mastectomy in the patient and is often performed in the same intervention[93].

Radiotherapy is often used after surgery to prevent regression. Depending on the type of surgery and advance of the cancer, radiation can be applied to irradiate the remaining breast tissue, the chest wall or sentinel lymph nodes[94]. The application of radiation post-surgery has been shown to have a positive effect on rates of local recurrence and 15-year survival and mortality[95].

Chemotherapy consists of the administration of cytotoxic drugs to halt the proliferation and induce the death of cancer cells. A range of different compounds are used for this purpose, including alkylating agents, taxanes and anthracyclines. Chemotherapy can be used after surgery (adjuvant setting), often in combination with radiotherapy, or prior to surgery to shrink the tumour when the size of the tumour makes it inoperable (neo-adjuvant setting)[96]. A number of factors is normally considered in deciding the administration of adjuvant chemotherapy. The finding of positive sentinel nodes after biopsy can be decisive in the use of chemotherapy, while other tools, such as genetic signature-based tests, can also be of aid in decision making in less conclusive cases, as previously described[84,85].

Chemotherapy can greatly influence recurrence and survival rates, but side effects are very common and can vary in severity and duration, ranging from temporary hair loss[97] to severe life threatening problems[98] that can ultimately lead to a lower quality of life for survivors[99,100]. The last decades have seen an increase in the awareness of the importance of selecting the right combination of cytotoxic agents for each case depending on type and stage of breast cancer[96]. Risk-benefit calculations have become more sophisticated and gene profiling is being applied to assess the best possible treatment strategy[101].

Endocrine therapy is administered to patients with hormone-dependent breast cancer, in which tumour growth is regulated by oestrogen (17β-oestradiol, E_2). The link between hormonal regulation and breast cancer goes back to the 19th century[102]. Since then, the discovery of oestrogen receptors in breast tumours[103,104] and the introduction of

tamoxifen[105,106], pharmacological ovarian ablation[107,108] and inhibitors of oestrogen biosynthesis[109,110] have contributed to the development of endocrine therapy.

In short, endocrine therapy targets the oestrogenic signalling pathway by disrupting either the synthesis or the activity of the hormone[111]. It is a major treatment modality in ER^+ cancers (up to 75% of all breast cancers[43]), where it can be more effective than chemotherapy and have fewer and less severe side effects[111,112]. As with chemotherapy, endocrine therapy might be applied in the adjuvant or neo-adjuvant setting depending on the case.

Endocrine treatment includes three main approaches: ovarian suppression, aromatase inhibitors and anti-oestrogens. In pre-menopausal women, where the main source of oestrogen is still the ovaries, endocrine treatment can entail ovarian suppression by resection of the ovaries (oophorectomy) or the pharmacological ablation of oestrogen production in the ovary using gonadotropin-releasing hormone (GnRH) agonists such as goserilin[113–115].

In post-menopausal women, oestrogen is mostly synthesised from androgen precursors by the enzyme aromatase in peripheral adipose tissue or in fibroblasts locally in the breast. In these cases oestrogen synthesis is blocked using Aromatase Inhibitors (AI), which can be either (i) steroidal, irreversible competitors such as exemestane, or (ii) non-steroidal, reversible competitors such as anastrozole and letrozole[116–118]. A third type of endocrine therapy is the use of anti-oestrogens to block the effect of the hormone in the breast. Selective oestrogen receptor modulators (SERMs), such as tamoxifen, exclude oestrogen by competitively binding ER and causing a conformational change that leads to a down-regulation of oestrogen-regulated genes, although SERMs can also have partial agonist effect[111]. Selective oestrogen receptor down-regulators (SERDs) or pure anti-oestrogens, such as fulvestrant, also exclude oestrogen from binding ER, as well as promoting degradation of the receptor, and have only an oestrogen-antagonist effect[119].

Lastly, another therapeutic strategy in breast cancer management is the application of targeted biological therapy or immunotherapy. This refers to the specific inhibition of molecular targets playing an important role in cancer progression[120–122]. A case of particular relevance is that of HER2 (or ERBB2, human epidermal growth factor 2), a receptor overexpressed in about 20% of breast cancers[123]. Targeting of HER2 by specific monoclonal antibody trastuzumab (commercialised as Herceptin) has proved an effective therapeutic target in $HER2^+$ (HER2-positive) tumours, which is particularly relevant given the fact that most of these cancers are also ER^- and, thus, not susceptible to endocrine therapy[124–127].

Other targeted therapies currently under investigation have tackled the mTOR (mechanistic target of rapamycin) pathway[121,128,129], receptors MUC1 (mucin-1)[130–132] or VEGFR (vascular endothelial growth factor receptor)[121,133,134] or enzymes PARP (poly-ADP ribose polymerase)[121,135] and transcriptase hTERT (human telomerase reverse transcriptase)[120,136].

1.1.3. Current status of ovarian cancer

1.1.3.1. Ovarian cancer statistics

Ovarian cancer is the sixth most common type of cancer in women in the UK (see *Figure 3)* with 7,029 new cases diagnosed in 2012[137] (see *Figure 7a*). It is often detected at a more advanced stage than breast cancer and its prognosis is usually worse. Indeed, despite a recent decrease in mortality and incidence rates in the UK by about 10% in the last decade (see *Figure 7b*), ovarian cancer remains the most lethal gynaecological malignancy, with 4,271 deaths recorded in 2012 and a 10-year survival rate of 34.5%[137] (see *Figure 7a-c*).

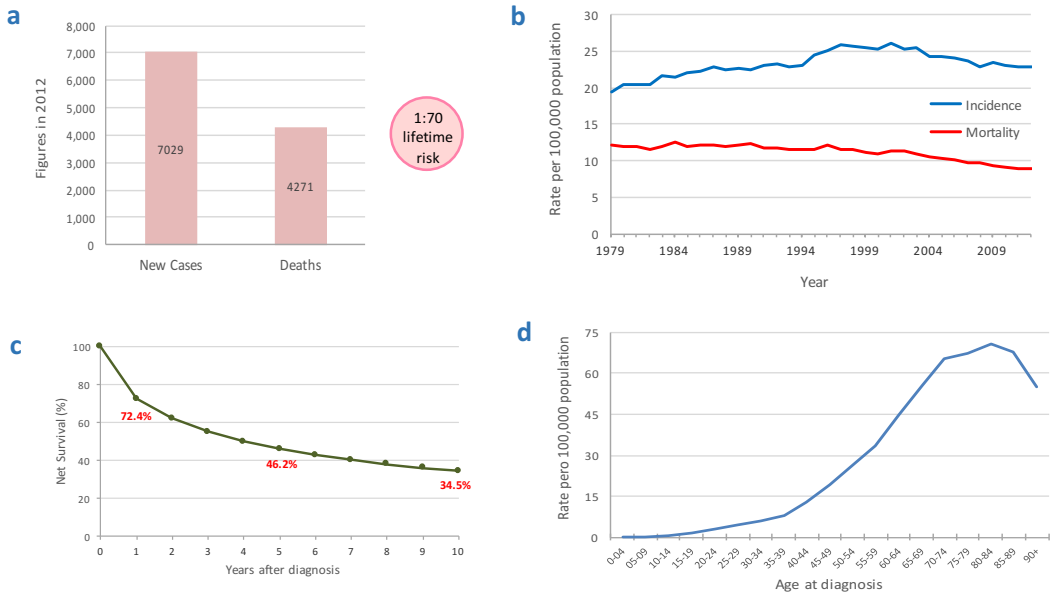

Figure 7 ***Ovarian cancer statistics according to the latest reports***[137]***.*** *7,029 new ovarian cancer cases and 4,271 ovarian cancer-related deaths were recorded in 2012, which corresponded to a lifetime risk of developing ovarian cancer of 1 in 70 for women in the UK (*a*). Both incidence and mortality rates have decreased over the last decade (*b*), but survival is still low, with only 34.5% of patients surviving for at least 10 years after diagnosis (*c*). Age is an important risk factor, with 74% of all new cancers being detected in patients aged over 55 (*d*).*

Like breast carcinomas, ovarian cancer is strongly related to age, with the highest incidence rates being found in older women: incidence rates rise sharply around the age of 35-39 and peak in the 80-84 age group (see *Figure 7d*). A number of factors can contribute to carcinogenesis, with an estimated 21% of all ovarian cancers being linked to lifestyle and environment[137].

The most important risk factor is family history of breast and ovarian cancer and genetic factors such as mutation in the BRCA genes[13,138,139]. Indeed, family history can lead to an increased risk of cancer, with large cohort studies showing that 1 in 5 women with ovarian cancer present inherited genetic mutations[140]. Ashkenazi Jewish populations are also at increased risk of development of cancer due to their higher rates of BRCA mutations. Interestingly, studies have found that the presence of BRCA mutations in these populations was independent of family history in at least a third of the women[141,142].

In contrast, other factors such as oral contraceptives, childbearing and breastfeeding can have protective effects[137,143]. In fact, the increasing widespread use of oral contraceptives has been suggested as a factor in the reduction of incidence in western Europe and the USA, whereas reduced fecundity could be linked to a corresponding rise in Southern and Eastern Europe[144].

1.1.3.2. Histological classification and staging of ovarian cancer

Like most cancers, ovarian cancer includes different histological subtypes of cancer, which have been linked to different molecular features and genetic changes. Traditionally, ovarian neoplasms have been classified as epithelial or non-epithelial depending on their tissue of origin. Epithelial tumours account for 90% of ovarian cancers and include high-grade serous (70-80% of all cases[145]), low-grade serous, mucinous and endometrioid carcinomas, as well as rarer types including Brenner tumours, clear cell, transitional, squamous, mixed and undifferentiated cancers. Non-epithelial histology subtypes include germ cell and sex cord-stromal tumours.

Besides histological classification, ovarian cancers are also subject to staging according to the degree of advance of the disease for better clinical stratification. In the case of ovarian neoplasms, they are classified into stages from I to IV using ovarian cancer-specific guidelines defined by FIGO (International Federation of Gynaecology and Obstetrics) (see *Table 3* for details).

1.1.3.3. Ovarian cancer diagnosis

The high mortality and poor survival rates in ovarian cancer have been attributed at least partly to the frequent delay of its diagnosis[146]. Indeed, in 75% of the cases patients present advanced disease in stages III or IV (see *Table 3* for description of FIGO staging) by the time it is detected[147].

Early stages of ovarian cancer are often asymptomatic[147], while symptoms of more advanced disease can be non-specific, including abdominal bloating or fullness, pelvic pain, gastrointestinal irregularities or weight loss[148–150]. This makes ovarian cancer a difficult disease to diagnose. Both the National Institute for Health and Care Excellence in the UK and the National Comprehensive Cancer Network in the US recommend symptom-triggered testing[151,152].

Stage I	Tumour limited to the ovaries	IA	Limited to one ovary		
		IB	Limited to both ovaries		
		IC	Tumour rupture, tumour on ovarian surface and/or malignant cells in ascites or peritoneal washings	IC1	Surgical spill
				IC2	Rupture before surgery or surface tumour
				IC3	Malignant cells in ascites or peritoneal washing
Stage II	Tumour involves one or both ovaries with pelvic extensions	IIA	Extensions in uterus or tube		
		IIB	Extensions to other pelvic tissues		
Stage III	One or both ovaries with peritoneal metastasis outside the pelvis or retroperitoneal or inguinal node metastasis	IIIA	Microscopic extrapelvic metastasis	IIIA1	Retroperitoneal lymph nodes only
				IIIA2	Retroperitoneal nodes and extrapelvic involvement
		IIIB	Macroscopic, extrapelvic growths ≤ 2cm		
		IIIC	Growths > 2cm		
Stage IV	Distant metastasis to visceral organs or a malignant pleural effusion	IVA	Pleural effusion with positive cytology		
		IVB	Hepatic or splenic metastasis or metastasis to extra-abdominal organs, including lymph nodes		

***Table 3* FIGO (International Federation of Gynaecology and Obstetrics) ovarian cancer staging system as per the recent update[153].** *The international consensus categorises ovarian carcinomas according to their size, spread and metastasis.*

In cases where ovarian cancer is suspected, guidance recommends testing for CA-125 (cancer antigen 125) levels in blood. CA-125 is a relatively specific ovarian cancer marker that

is raised in more than 80% of patients with advanced disease[147], but only raised in 50% of stage I ovarian cancers[154] and can be increased in other conditions, both benign and malignant[149]. Hence, CA-125 is currently used as a diagnostic tool together with ultrasound for better specificity[155]. Low levels of CA-125 (<35 IU/mL) are considered as suggestive of absence of advanced ovarian cancer, although careful monitoring of symptoms is recommended. When levels are higher further examination by abdominopelvic ultrasonography is advised[154].

Although there is currently no universally validated scoring system for ultrasonography, in the UK a risk of malignancy index (RMI)[156] is often applied to estimate the likelihood of a complex mass observed by ultrasound being malignant. The RMI considers the ultrasonic features of the cysts identified (between 1 and 3), the menopausal status of the patient (1 for pre-menopausal and 3 for post-menopausal) and the CA-125 level in blood. All three parameters are multiplied to obtain a final score that when >200 is considered as indicative of significant risk of malignancy. Another effort by the International Tumor Analysis Group has led to the development of a logistic regression model that also considers both clinical and ultrasonographical variables to categorise masses as benign or malignant[157].

Additionally, other tools have received FDA approval for their application in assisting in diagnosis of ovarian cancer: OVA1 is a multivariate index assay that considers 5 different biomarkers (including CA-125) to detect ovarian malignancies[158], while the biomarker HE4 (human epididymis protein 4) can be used together with CA-125 to stratify patients into high or low-risk for epithelial ovarian cancer through the risk of ovarian malignancy algorithm (ROMA)[159,160].

Unlike breast cancer, systematic screening for ovarian cancer is not currently in place. The largest randomised controlled trial to date, the UK Collaborative Trial of Ovarian Cancer Screening (UKCTOCS) has been carried out comprising 200,000 women to evaluate a screening method based on a risk of ovarian cancer algorithm (ROCA). Recently published results have reported a 2-fold increase in the number of cancers detected[161] and reduction in mortality in years 7-14[162], suggesting the promise of this screening method if efficacy and cost-effectiveness were to be found satisfactory for its systemic application in the future.

1.1.3.4. Ovarian cancer treatment

The mainstay for treatment of ovarian carcinoma is a combination of surgery and chemotherapy[163]. The purpose of surgery is both to provide a better diagnosis and staging of

any ovarian growth and to remove the cancerous tissue. In patients with organ-confined tumours, surgery alone can be curative in more than 90% of cases[164], but more than 80% of patients present more advanced cancers by the time of diagnosis[147,164].

Depending on the spread of the cancer, surgery may involve tumour debulking, unilateral or bilateral salpingo-oophorectomy (removal of ovary and Fallopian tube), total hysterectomy (removal of the uterus) or omentectomy (removal of tissue supporting stomach and colon)[150], as well as removal of lymph nodes for FIGO staging (see *Table 3*). Preventive salpingo-oophorectomy can also be performed as a protective measure in women with a high risk of developing cancer due to high-risk genetic factors[165].

Following surgery, the grade and stage of the cancer removed is often used to make an informed decision on the administration of adjuvant chemotherapy[166]. Staging can prevent the use of chemotherapy in patients with stage I disease or help identify occult advanced disease in up to 30% of patients[167]. For patients with advanced-stage cancers platinum-based chemotherapy (carboplatin or cisplatin) is administered, often in combination with a taxane[168,169]. Follow-up is recommended by monitoring of CA-125 levels, although studies have suggested no additional survival benefit from early treatment based on raised CA-125 alone[170].

Chemotherapy can also be applied neo-adjuvantly prior to tumour debulking surgery in patients with stage IIIC or IV cancer. In these cases, surgery is typically delayed until after three chemotherapy cycles. Studies have suggested that this approach has similar survival outcomes to those of surgery followed by adjuvant chemotherapy but leads to lower post-surgery morbidity[171,172].

A number of clinical trials have investigated the potential of different agents as maintenance chemotherapy[173]. These include both the combination with cytotoxic agents or novel treatments strategies based on specific molecular targets. For instance, PARP inhibitors are a new type of drug with potential therapeutic application in high-grade serous cancers characterised by BRCA mutations[150,174], whereas VEGF inhibitors are being studied as antiangiogenic treatments that may lead to prolonged disease control when used in combination with chemotherapy[150,175].

The patients with the best prognosis are typically those presenting early stage disease or advanced disease in which the tumour can be completely removed and the disease is sensitive to platinum-based chemotherapy[154]. However, for the latter group even in the cases

with the best prognosis 70% of patients will relapse within 18 months[176]. In the event of relapse most patients will receive second-line chemotherapy, dependent on the platinum-sensitive or resistant status of the patient. Secondary surgery can be beneficial to patients with platinum-sensitive disease[177], but is only performed occasionally in platinum-resistant cancer to palliate issues such as intestinal obstruction[150]. Endocrine therapy is also used in relapsed ovarian cancers presenting resistance to other treatments, although its application has not been systematically evaluated[178].

1.1.4. Need for novel therapeutic strategies

1.1.4.1. Issue of resistance and need for new therapies

Despite the constant advances in cancer therapy over the decades, no cancer treatment is infallible. Resistance to any treatment is possible and remains a major limitation in the management of the disease. Resistance can be intrinsic to the cancer, having developed prior to the diagnosis or treatment of the tumour, or acquired, when it emerges during treatment after an initial response[179].

Intrinsic resistance can be linked to inherent mutations in molecular targets or to environmental factors[180–184], meaning innate molecular characteristics of the host that may hinder the efficacy of a treatment. This often involves factors that affect pharmacokinetics of the agents administered, such as poor absorption or delivery or rapid metabolism or excretion.

Acquired resistance arises from cancer cells adapting through different mechanisms to escape cancer treatment after an initial response. A number of factors have been described in the study of causes for the development of acquired resistance. Interestingly, it has been suggested similar mechanisms may be involved in the loss of efficacy of different therapies, including chemotherapeutic, hormonal and targeted treatments[183,185]. In short, cancer cells evolve specific genetic or epigenetic alterations to give rise to adaptive mechanisms, allowing them to escape from treatment[179].

Alterations in drug transport may lead to reduced intake or excessive efflux of the drug into or from cancer cells[180,184,186], while changes in drug metabolism may lead to defective drug activation necessary for its anticancer effect[183,184,187,188] or to mechanisms that inactivate agents or detoxify their effect[182–184]. Another major mechanism for evasion of treatment is the development of alterations in drug targets, normally by mutation, amplification or overexpression of the oncogenes being targeted by treatment[183–185], which allow cancer cells to escape or surpass the inhibitory effect of the drug. Additionally, adaptive responses can promote cancer cell survival by preventing drug-induced cell damage from leading to the desired induction of cell death. This can involve over-activation of DNA repair mechanisms, de-regulation of apoptotic signals or compartmentalisation[180,183,184]. Changes in the tumour microenvironment can also lead to the development of resistance to chemotherapeutic or targeted treatments, following alterations in adhesion molecules and growth factor

levels[183,189–191]. In the specific case of ovarian cancer, the development of a hypoxic microenvironment has long been linked to radio- and chemo-resistance[192].

Several different mechanisms can contribute to a cancer adapting to gain resistance to treatment. It has been suggested that, depending on the therapy, the type of cancer and its stage, one or several alterations may be necessary for the cancer to become resistant[179,193,194].

Besides these adaptive changes emerging after treatment, tumour heterogeneity may also contribute to resistance by positive selection of innately resistant cells[183,184]. In short, treatment may successfully target sensitive cells, so that resistant cells are selected, remaining unaffected and able to spread further. Indeed, evidence has shown the presence of such subpopulations in cancers prior to treatment that may have subsequently given rise to resistant tumours[195–197].

As with other cancer types, and despite the notable advances in treatment in the last few decades, the development of resistance to treatment is also an important hurdle to successfully manage breast and ovarian cancers. In breast cancer, standard therapies are effective in 90% of primary breast cancer[198], but approximately 30% of patients with early-stage disease will experience recurrence, often as metastases[199–201], which have much lower response rates. These limited or temporary responses are observed across all types of standard treatments in breast cancer[198]. For example, in the specific case of endocrine therapy, success rates depend on the clinical setting[202] but it is estimated that between 30 and 50% of ER^+ patients with early stage breast cancer develop resistance to treatment and relapse at some point[203–205], while the majority of patients with advanced disease develop acquired resistance within 3 years of commencing treatment[202,206].

Similar issues are faced in the treatment of ovarian cancer, where resistance to treatment is one of the two major factors (the other one being late diagnosis) responsible for the poor survival rates in ovarian cancer (see section *1.1.3.1.*)[207]. Although the initial response to carboplatin-containing treatment is high, with 75-80% of patients with advanced disease showing an initial response[207,208], the majority develop resistance and relapse within 2 years[208]. A direct link between drug resistance, treatment failure and eventual death of more than 90% of patients with metastatic ovarian cancer has been suggested[164]. It has been suggested that the majority of ovarian cancers have some innate degree of resistance that eventually leads to the loss of responsiveness to treatment, contributing to the high relapse and poor survival rates[208,209].

In conclusion, there is an urgent need for new therapies in breast and ovarian cancer, including new combinatorial treatment strategies and drugs. One approach is the study of the mechanisms of resistance for its better understanding and the development of rational combination strategies. The application of different drugs may not only tackle the issue of acquired resistance, but also allow for a better targeting of the different mechanisms that may be involved in the development and progression of the cancer due, in no small part, to the inherent heterogeneity of the disease. A better monitoring of the development of resistance would also mean an improved management of its emergence in the clinical setting[185].

Additionally, the development of novel drugs has been and continues to be a necessary step for the advancement of cancer treatment. New, better drugs need to be developed for a more effective suppression of oncogenic signalling pathways, whether as single anticancer agents or as drugs that may aid treatment in combination with agents currently used in the clinic. For this, efforts are being made to identify biomarkers that may aid rational targeting of new therapies[178], as well as to assess and exploit libraries of drugs from different sources in an effort to identify and develop novel compounds with potential anticancer application[185].

1.1.4.2. Natural product drug discovery

Historically, natural products in general and plant-derived compounds in particular have been the basis for traditional medicine across civilisations[210]. In 1985, WHO estimated that 65% of the world's population was still reliant on these traditional treatments for their primary health care[211]. Besides the prevalence of traditional therapies in developing countries, natural products have been the source of a wide range of drugs of current clinical relevance in developed countries. Indeed, reviewers have pointed out that almost half (47%) of all new drugs developed and approved since the 1940s had a natural origin, either by the use of the actual natural molecules, the direct derivation of active compounds or their use as sources for novel structures of pharmacophores[210,212–214]. These include drugs such as steroids, analgesics, antitussives, antihypertensives, antimalarials, anaesthetics, muscle relaxants and anticancer agents[215,216]. From a pharmacoeconomic point of view, authors have suggested that plant-derived drugs represent about 25% of the prescription drug market[217–219] and have a multi-billion dollar annual retail value in the United States alone[220].

A remarkable example of the long-standing and current relevance of natural products as sources for therapeutic agents can be seen in the Swedish Karolinska Institutet awarding the Nobel Prize in Physiology or Medicine to William C Campbell and Satoshi Ömura (for their discovery of avermectins) and to Youyou Tu (for her discovery of artemisinin) in December 2015[221]. Both discoveries have had revolutionary impact in the fight against parasitic diseases, with avermectins reducing incidence of onchorcerciasis (or river blindness) and filariasis (elephantism) and artimisinin playing a substantial role in reducing mortality associated with malaria[222]. These agents are great examples of natural products with unique structures and chemical properties that were identified for their potential therapeutic applications and subsequently optimised to develop the semi-synthetic analogues that eventually had such important clinical applications.

In the wake of this award, some authors have talked of a "New Golden Age" of natural product drug discovery, emphasising the continuing relevance of natural products as a reservoir for novel therapies[223]. This has highlighted the role of this approach over more modern strategies favoured by the pharmaceutical industry in recent years, which rely on high-throughput screening of novel synthetic libraries and have correlated with a substantial decline in the identification and subsequent approval of successful new drugs[224].

1.1.4.3. Natural products as sources for anticancer agents

Plant-derived compounds have a long history of application in cancer therapy. These include a wide variety of natural derivatives that have proven anticancer properties both *in vitro* and *in vivo*[225]. More importantly, some drugs of a natural source are also currently in clinical use. A few examples are chemotherapeutic and cytotoxic agents such as (i) vinca alkaloids vinblastine and vincristine (isolated directly from plant extracts[226]), (ii) etoposide and teniposide (semisynthetic derivatives of natural product epipodophyllotoxin[227]), or (iii) topotecan and irinotecan (modified derivatives of natural camptothecin[228,229]), all of which have proven effective against different cancer types[225,230].

A particularly relevant example is that of the antimitotic chemotherapeutic agent paclitaxel. Since its discovery in the late 1970s[231,232], it was approved for clinical use against ovarian and breast cancers in the 1990s and it has gone on to become a major chemotherapeutic tool[210]. Paclitaxel belongs to the taxane family of drugs and is commercialised as Taxol, taking its name from its natural source, as it can be found in the bark and leaves of various plant species belonging to the *Taxus* genus[233]. Its success has

meant annual sales of over $1 billion in the United States alone[210] and has led to the development of the close derivatives docetaxel and cabazitaxel[234], as well as different formulation alternatives for paclitaxel[210,235].

In conclusion, evidence suggests that, despite changes and constant progress in the process of drug discovery and development, a great untapped potential remains to be exploited from natural products[236]. Their great structural and chemical diversity makes natural compounds good sources for new leads, which in turn, through direct modification of their structure and properties (or semisynthesis), have the potential to yield novel therapeutic tools with better pharmacological activity and fewer side effects[230].

A large number of compounds derived from natural products are currently being studied[237] and undergoing clinical trials[238–241]. This highlights the potential for the specific development of novel agents against breast and ovarian cancers that could provide new therapeutic strategies or tackle the issues currently found in the management of these diseases[225], such as the development of resistance to treatment.

In relation to these current studies of novel agents in drug development, the concept of clinical trials bears a short description for future reference in this text. These trials refer to the clinical research carried out to assess whether an agent that has shown promising activity in pre-clinical studies can be further developed toward its clinical application. Clinical trials are typically divided into phase I (study of safety in healthy humans), phase II (testing of effectiveness and safety in affected individuals), phase III (larger scale safety, effectiveness and efficacy study, particularly in comparison with standard of care for the disease being treated) and phase IV (an ongoing, post-marketing surveillance study to ensure long term safety).

1.1.5. Novel flavonoids as antitumour agents

1.1.5.1. What are flavonoids?

Flavonoids account for the largest group of secondary metabolites in the plant kingdom[242]. These compounds were not referred to as flavonoids, or bioflavonoids until the 1940s, receiving their name from the latin *flavum* (yellow), given the colour they customarily present[243]. They comprise a broad range of over 5000 polyphenolic compounds and hold a ubiquitous and essential role in plants[242,244]. Although flavonoids have long been known as the phytochemicals responsible for pigmentation of plant tissues, they have also been identified as essential in the development of many other biochemical processes, including hormonal, plant growth and stress protection roles[242,244,245].

Flavonoids are categorised as polyphenolic derivatives and their chemical backbone consists of two fused rings (aromatic A ring and heterocyclic C ring) connected to another aromatic B ring through a carbon-carbon bridge[246,247] (see *Table 4*). According to changes in this molecular backbone and the presence of hydroxyl groups and other moieties, they can then be categorised into a further 7 subclasses: flavones, flavonols, flavanonols, flavanones, anthocyanidins, isoflavones and flavonols (see *Table 4*). Research has identified relevant example compounds in numerous dietary sources for most of these subclasses, evidencing their ubiquitous presence in modern western diets[248,249]. They are most commonly found as glycosides in fruits, vegetables and herbs[250].

1.1.5.2. Flavonoids as therapeutic agents

Beyond the role of flavonoids in plants, in the last few decades their role as antioxidants and potential therapeutic agents has also been studied. Their use as dietary supplements, has been found to have health-promoting properties and protective effects against cancer, cardiovascular and neurodegenerative disease[251–253]. Such application of natural compounds in the treatment of cancer is most definitely not uncommon. As previously mentioned, natural products and their derivatives play a crucial role in drug discovery[237,240].

Among other health-promoting properties, numerous studies have reported interesting preclinical activity of flavonoids in models for a wide range of cancers, including the four leading types in the United Kingdom[254]: breast[255], prostate[242], lung[256,257] and colorectal cancer[258]. Other cancers targeted have been leukaemia[259], glioma[260,261], hepatic[262] or pancreatic cancer[252].

Subclass	Structure	Examples	Dietary sources	EDI (mg)
Flavonols	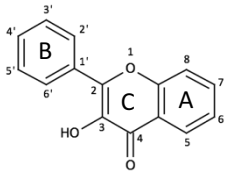	Quercetin, kaempferol, myricetin and their glycosides	Onions, red wine, tea, fruits, berries and herbs	12.9
Flavones	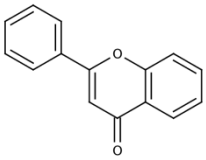	Luteolin, apigenin and tangeretin	Herbs, celery and chamomile tea	1.6
Flavanones	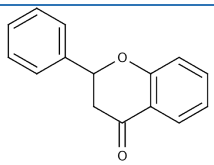	Naringenin, hesperetin (found in diet mainly as glycosides)	Citrus fruits	14.4
Flavanols	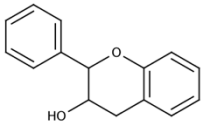	Catechin, epicatechin, epigallocatechin	Cocoa or dark chocolate, apples, grape, red wine and green tea	156.9
Anthocyanidins	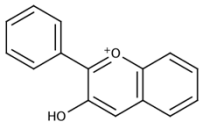	Cyanidin, delphinidin, pelargonidin, malvidin	Berries and other fruits	3.1
Isoflavones	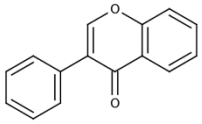	Genistein, daidzein, glycitein and their glycosides	Soy products	1.2
Flavanonol	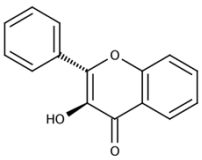	Taxifolin, aromadedrin	N/A	N/A

***Table 4* Flavonoid subtypes.** *Flavonoids are polyphenolic plant metabolites consisting of a 3-ring basic backbone. According to changes in the basic molecular backbone and the presence of hydroxyl groups and other moieties can be further categorised into 7 subclasses. This table details the estimated dietary intake (EDI) for each subtype*[248,249,263,264]*. Estimates for flavononols are not available (N/A), as they have not been reported at significant levels in dietary sources.*

1.1.5.3. Mechanisms of action of flavonoids as anticancer agents

Research has reported the involvement of numerous mechanisms in the effect of flavonoids against cancer. Evidence supports the potential of these compounds to target different pathways underlying the complexity of cancer as a disease. Here we will summarise the different mechanisms that could have relevant applications in the management of breast or ovarian cancer models.

1.1.5.3.1. Oestrogen signalling regulators

An interesting feature of flavonoids, especially regarding their potential application in the treatment of breast or ovarian cancer, is their ability to induce oestrogenic effects in humans. Indeed, flavonoids have been referred to as phytoestrogens, a term used to describe plant compounds with oestrogen-like biological activity[265], and extensive research on these oestrogen-mimicking properties has been carried out in the last few decades.

Despite their plant origin, flavonoids can mimic oestrogen-like responses due to their structural similarity to the main steroid in humans, 17β-oestradiol (E_2)[266,267]. This similarity is based on the existence of hydroxyl groups and phenolic rings in flavonoids, which are required for binding oestrogen receptors α and β (ERα and ERβ). This means that the pseudo-oestrogenic effects exerted by different subtypes of flavonoids can vary significantly due to their different backbones or substitutions[268].

Numerous authors have reported the ability of flavonoids to bind both isoforms of ER, mainly as agonists competing with E_2[242,269,270]. Indeed, they induce various biological responses traditionally associated with the binding of the natural hormone E_2 (including transactivation of ER, induction of immunodetection, up-regulation of oestrogen target genes and downregulation of ERα mRNA and protein levels) in a dose-dependent manner[251,271,272].

Some authors have reported the affinity of flavonoids for ER to be lower than that of the natural ligands of the receptor[273,274]. Other studies have reported that some of the ER-mediated responses are nonetheless induced by flavonoids to levels comparable, or even higher, to those induced by physiological levels of E_2, reason why some flavonoids are still described as full oestrogen agonists[275–277].

Unlike E_2, which binds both isoforms of ER with similar affinity, several studies have reported a stronger affinity of flavonoids for the ERβ isoform[278–280] and also that flavonoids binding ERβ induce the transcription of oestrogen target genes to much greater levels than

when binding ERα[275]. This preferential affinity for one isoform over the other is significant in that ERβ is known to frequently exert a response opposing the proliferative effects of ERα activation[281–283]. Indeed, interaction between both types of receptors and their substrates provides a regulation for the overall effect of oestrogens[284] and the ratio of ERα/ERβ can be used as a prognostic marker in breast tumours, such that ERβ predominance is a marker for more benign tumours, while ERα predominance indicates more aggressive ones[285,286].

In studying the role of flavonoids as phytoestrogens, the stronger affinity and effect on ERβ over ERα means that the antiproliferative effects of the former receptor will be favoured over the cell growth and proliferation mediated by the latter. Hence, physiological levels of phytoestrogens are likely to activate ERβ but not the ERα-mediated pro-cancer signalling (or activate this to a much lower extent), therefore exerting a practical antioestrogenic, antiproliferative effect[287,288].

Phytoestrogens can also alter oestrogenic signalling through other mechanisms, albeit unrelated to their binding to ER, such as at the level of oestrogen biosynthesis. Some phytoestrogens (mainly flavones and flavonones, due to structural features[289]) can act as aromatase inhibitors (AI), particularly on cytochrome P450 19 aromatase (CYP19A1), 17β-hydroxysteroid dehydrogenases (HSD) and oestrone sulfatase and sulfotransferase[290], all involved in the generation of oestradiol in breast tissue. These flavonoids have been shown to induce a significant decrease in circulating oestrogen concentration, although with IC_{50} values between 100 and 1000 higher than those for clinically used steroidal aromatase inhibitors[291]. Nevertheless, these compounds could still have a beneficial application in tissues non-respondent to common therapies, since these enzymes are the main executers of endogenous oestrogens synthesis and their overexpression or increased activity has been associated with breast cancer[292–294]. Extensive research has also been carried out on the ability of flavonoids to alter oestrogen-metabolising enzymes, thus reducing the production of genotoxic metabolites[288]. Some *in vivo* studies have been carried out on animal models[295–297], although the complexity of these modulations needs to be further elucidated.

It is worth noting that the oestrogen-mimic/E_2-agonist effects mentioned have been observed at concentrations as low as in the nano- or picomolar range[270,271], whereas the inhibition of steroidogenic enzymes required higher concentrations[290]. This brings us to the fact that different polyphenols, such as genistein, quercetin, resveratrol or myricetin, demonstrate a biphasic effect, so that for low concentrations they can act as oestrogen

agonists and may cause proliferation of tumour tissues in an ER-dependent manner, whereas for higher concentration in the micromolar range they exert AI and cytotoxic effects[271,277].

Moreover, a series of studies have been carried out that suggest the consumption of flavonoids has a positive influence in breast cancer risk[298,299], although other authors have dismissed this hypothesis[300]. Interestingly, some studies have noted that post-menopausal women may obtain more benefit from flavonoid consumption than pre-menopausal women[301,302]. Other authors have also suggested that flavonoid consumption at an early age might also affect the ER status of breast tumours developed later in life[303].

Finally, interesting observations have been made in terms of the ER status of a breast cancer and its potential responsiveness to flavonoid treatment. Although the effects summarised in this section are obviously ER-dependent and thus only of relevance to certain types of oestrogen-regulated cancers, other non-genomic changes occur independently of ER status[271,277,304]. This pleiotropic effect of flavonoids explains not only their broad effect against different cancer types, which will be reviewed in the following sections, but also the fact that flavonoids have also been shown to exert antitumour effects in TBNC, which do not rely on oestrogen signalling for their proliferation.

1.1.5.3.2. Redox regulators: anti- and pro-oxidants

The role of flavonoids as antioxidants and the potential of these properties for the preservation of foods and, more interestingly, the prevention of disease have been a subject of research for decades[305–307]. The numerous hydroxyl groups in their structure, in combination with a highly conjugated, π-electron system allow flavonoids to donate electrons or hydrogen atoms[306]. This way they act as scavengers, stabilising free radicals, or they can block the formation of reactive oxygen species (ROS) through chelation of redox-active, transition metal ions[307]. These interactions can confer flavonoids chemopreventive properties against cancer (by reducing events such as oxidative damage to DNA) or cardiovascular disease (by inhibiting the oxidation of low-density lipoproteins)[308].

Research on cell line models has shown polyphenols and specifically flavonoids can have a strong inhibitory effect on breast cancer by scavenging or inhibiting the production of ROS[270,309]. They have been found to scavenge active oxygen species such as H_2O_2, peroxidation-derived malonaldehyde, superoxide anion (O_2^-) and free hydroxyl radicals (·OH)[270,310].

Interestingly, and despite the fact that flavonoids have long been considered potent antioxidants, there is also evidence that they can act as pro-oxidants[311,312]. Compounds such as myricetin are known to be able to undergo auto-oxidation and reduce molecular oxygen to active species, also generating superoxide or ·OH radicals that can potentially produce cellular damage[310,312].

Indeed, as redox compounds, flavonoids can act as either anti- or pro-oxidants depending on factors such as pH, presence of oxygen and transition metals, temperature, concentration, number of hydroxyl groups in their structure and redox potential[313–315]. This biphasic effect suggests that a balance of both anti- and pro-oxidant properties might be essential to the therapeutic effect of individual flavonoids[276,316,317].

It has been suggested that the former may have beneficial chemopreventive effects. In contrast, pro-oxidant activities are linked to other beneficial effects in the form of cytotoxic, anticancer effects. Indeed, application of novel flavonoids could lead to targeted regulation of ROS production and other molecular pathways. Importantly, the pro-oxidant effect of some flavonoids could enable them to act as selected anticancer agents. Indeed, recent years have seen a growing interest in the potential of ROS modulation as an anticancer strategy[318–321], as discussed in the context of the role of flavonoids as mitocans (see section *1.1.5.3.7.*).

Finally, it bears mentioning that the biphasic effect of flavonoids has been linked to a concentration gradient, so that dietary levels of some flavonoids can have protective and chemopreventive effects, whereas slightly higher concentrations can have therapeutic applications while still being non-toxic due to their natural origin (see section *1.1.5.4.1.* for further discussion of biphasic effects). It can be noted that the potential of flavonoids to act as both antioxidant and pro-oxidant compounds is reminiscent of the effect oestrogenic compounds can have in different environments[322]. This once again evidences the relevant structural and functional similarities between both groups, as discussed in the previous section.

1.1.5.3.3. CYP1 regulators

Diet and environment are considered important factors in the development and progression of cancer. This is partially due to the exposure to xenobiotic carcinogenic compounds, which when processed by the body can give rise to cancer. This is the case of polycyclic aromatic hydrocarbons (PAHs) such as benzo(α)pyrene (BaP), found in tobacco smoke or charred foods.

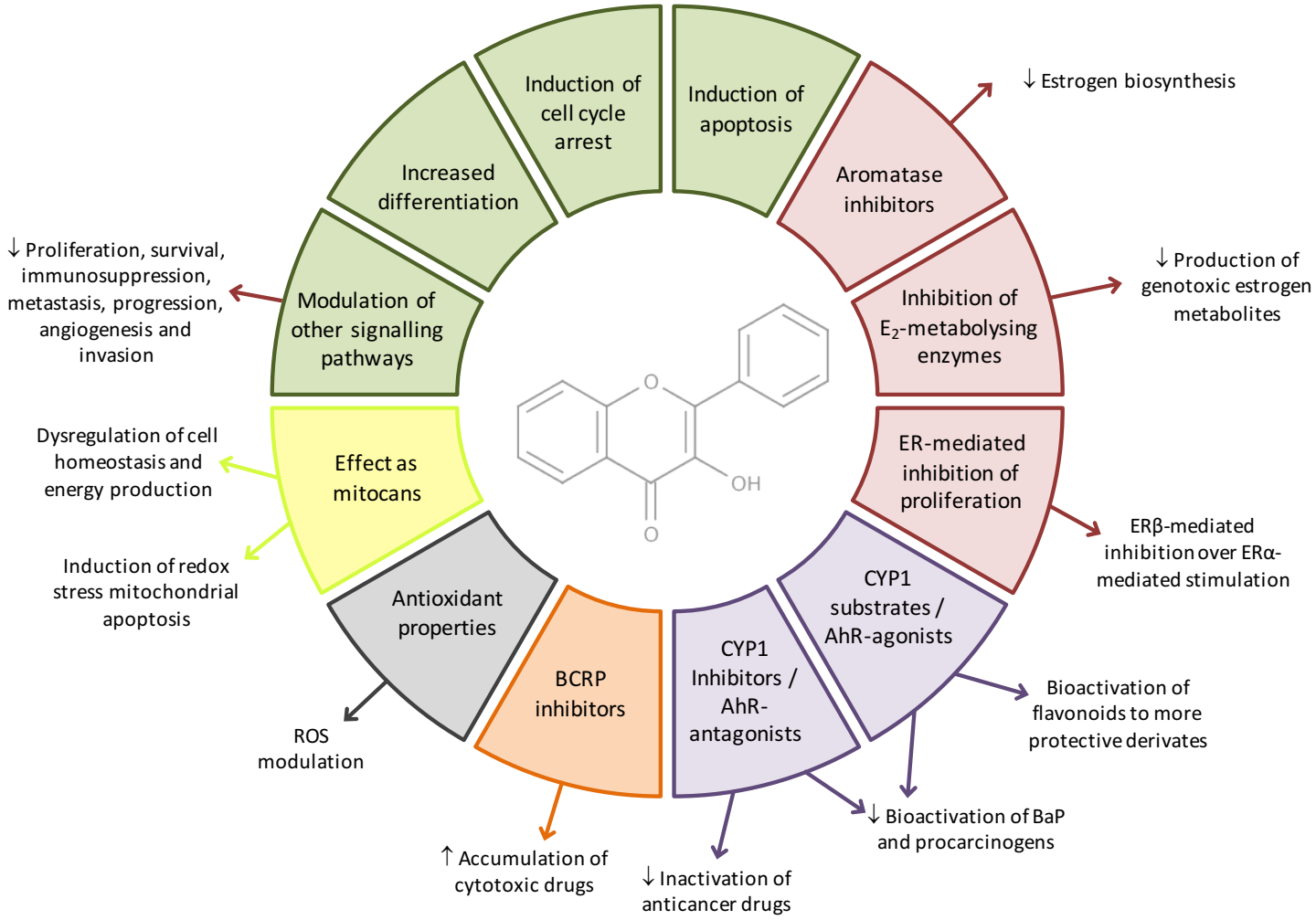

Figure 8 ***Anticancer effects of flavonoid.*** *Research has shown that flavonoids can exert a wide range of anticancer properties. Besides their known antioxidant properties, they have been shown to modulate oestrogenic signalling though different mechanisms, interact with CYP1 as inhibitors and substrates and inhibit MDR through inhibition of ABC transporters such as BCRP. Several flavonoids have been observed to act as mitocans. Numerous studies in models for different cancer types, both* in vitro *and* in vivo*, have also shown the ability of flavonoids to induce apoptosis and cell cycle arrest and to alter numerous signalling pathways linked to cancer development and progression.*

Compounds like these are typically subject to oxidation by cytochrome P450 (CYP1), a family of extrahepatic enzymes with monooxygenase activity. This family consists of several isoforms (including CYP1A1, CYP1A2 and CYP1B1) and has been implicated in carcinogenesis and cancer progression through three main mechanisms[323,324]:

- Firstly, the CYP1 family takes part in the modification and activation of PAHs and other pro-carcinogens[325,326]. The best established model defines that compounds such as BaP act as ligands to the aryl hydrocarbon receptor (AhR), a mediator in the transactivation of the CYP genes. The subsequent expression of these enzymes, leads to bioactivation of PAHs, allowing them to bind DNA and give rise to cellular and genetic damage, both essential phenomena in the cancer initiation stage[327].
- Secondly, the CYP1B1 isoform (one of the oestrogen-metabolising enzymes previously discussed) is involved in the modification of steroidal hormones such as E_2, also contributing to the initiation of mammary carcinogenesis[328].
- Finally, the same CYP1B1 isoform has also been shown to hinder cancer treatment by inactivation of a range of clinically used anticancer drugs[329].

Research has focused on tackling the effects of CYP1, given its role in carcinogenesis. Among other compounds, flavonoids have been identified as potent inhibitors of the induction of CYP1 both *ex vivo* and *in vivo* by acting as competitive antagonists for AhR[330–335]. This may be due to structural similarities between flavonoids and typical AhR ligands[336]. Studies have shown that different compounds have more potent inhibitory effects in different isoforms of the enzyme (for example, myricetin and quercetin are potent CYP1B1 inhibitors but appeared to be less effective on CYP1A1 and CYP1A2[337]).

Interestingly, in recent years flavonoids have also been described as possible AhR agonists and CYP1 substrates[336]. Through this mechanism, the expression of CYP1 isoforms is facilitated via AhR-mediated induction of the *Cyp1* gene, but the structural similarity of flavonoids with steroid hormones makes them likely substrates[337], consequently diminishing the harmful activity of the enzymes when flavonoids are target to their activity in lieu of PAHs and other pro-carcinogens. Additionally, enzymatic modification of flavonoids by CYP1 often gives rise to structures with beneficial anticancer properties[336].

Therefore, flavonoids and other polyphenols can exert different effects on the CYP1 family, acting either as antagonists for AhR/inhibitors for CYP1, as AhR agonists/substrates for CYP1 or having a combined inhibitor/substrate effect (such as in the case of resveratrol[338–340]). Interestingly, as mentioned above, the main argument for both types of response is

based on the chemical structure of these compounds. This evidences the complex role that structural conformation has in the anti-tumour properties of flavonoids, with the lipophilic or hydrophilic properties of the molecules being linked to their role as inhibitors or substrates, respectively[341]. Studies have also identified methoxylated flavonoids as the most potent chemopreventive agents, associating this moiety with accessibility to the tumour site and the active site of the enzyme[341]. Other research has highlighted the relevance of sugar chains in the flavonoids or aminoacidic residues in the different CYP1 isoforms[342].

Overall, flavonoids have been shown to exert beneficial effects on the process of bio-activation of pro-carcinogens by CYP1. This anticancer effect is also supported by the fact that CYP1 has been shown to be selectively expressed in a wide range of cancers (both in tumour cells and in pre-malignant tissue), not being significantly present in normal surrounding tissues[337]. This suggests the potential for the development of therapies targeted specifically to the abnormal tissue. This specificity could also be enhanced by the *in situ* bioactivation of some flavonoids when exposed to the effect of these enzymes.

Additionally, research has shown that flavonoids do not hinder other natural anticancer processes (such as the effect of phase II detoxifying enzymes[343]). The positive effects of flavonoids on CYP1 are observed at micromolar concentrations, which could be associated with normal dietary intake. This suggests these therapeutic strategies could be translated to the clinical setting more easily that in the case of other antimutagens and anticarcinogens, which require administration at unrealistically high doses which would not usually reflect the normal human exposure[344].

1.1.5.3.4. ABC transporters regulators

The ATP-binding cassette (ABC) superfamily is an evolutionarily-conserved family of transporters mainly expressed in the membrane of epithelial organs such as the gastrointestinal track, kidney and liver and several physiological barriers[345]. The ABC family comprises P-glycoprotein (P-gp), breast cancer resistance protein (BCRP, also known as ABCG2) and multidrug resistance proteins 1 and 2 (MRP1 and 2). These membrane proteins are involved in the absorption, disposition and secretion of xenobiotic compounds and have been described as the main family of drug efflux transporters[346], playing an important role in the disposition of drugs clinically used in the treatment of a range of pathologies, including cancer.

BCRP in particular has been detected in a number of human tumours[347–350] and has been shown to represent a prominent mechanism for the development of multidrug resistance (MDR). Its overexpression in tumour sites leads to active exclusion of cytotoxic agents, limiting their absorption and intracellular accumulation and therefore hindering the effect of some cancer treatments[351–354].

There is accumulating evidence of the existence of flavonoid-drug interaction with BCRP[353,355,356], highlighting the potential of these natural compounds as a way of tackling MDR. Indeed, in the last decade extensive screenings[346,357,358] have proved the effect of flavonoids as inhibitors of BCRP, both *in vitro* and *in vivo*, in different cancers, including lung, breast, kidney and ovarian tumours[346,353,359,360]. Most of these studies have shown that exposure to flavonoids during cancer treatment can cause an increase in the bioavailability an accumulation of antineoplastic agents[359,361], such as tripling the accumulation of cytotoxic compounds[359], reversing MDR. Flavonoids exert this effect in an additive manner, the reason why the combination of different polyphenols administered concomitantly with anticancer treatments has been suggested as one of the promising strategies for the application of flavonoids in cancer treatment[357,362,363].

Flavonoids induce these effects by acting as inhibitors of the transporters, limiting the ATP-hydrolysing action that leads to exclusion of anticancer drugs from tumour tissues [353,364]. This probably takes place by binding to a nucleotide binding domain (NBD), which is targeted by flavonoids both in BCRP and P-gp[365].

Despite the positive alteration of drug pharmacokinetics induced by flavonoids, their interaction with BCRP is yet to be completely understood. Interestingly, some authors have suggested that these compounds can also act as BCRP substrates, competing for the transporter with other substrates[346]. Other research has suggested the possibility of detrimental effects in some cases[366]. This highlights the importance of a thorough study of this mechanism before their potential clinical application, particularly considering the variable effects that different flavonoid subtypes may have on BCRP or the consequences of long term exposure to compounds as ubiquitous as these[353,359,365].

1.1.5.3.5. Apoptotic inducers

Numerous authors have reported the role of flavonoids as apoptosis inducers in models for different cancer types, including breast[367,368] and ovarian cancers[368,369]. Different compounds have been found to induce cell death through both main apoptotic pathways: (i)

intrinsic, caspase-9 and mitochondrial-driven apoptosis and (ii) extrinsic, caspase-8 and death receptor-driven apoptosis[370,371].

Flavonoids have been shown to activate different caspases[372,373] and have been linked to activation of PARP (poly ADP-ribose polymerase)[256,372] by cleavage. They can also act as modulators of other important regulators of apoptosis, such as anti-apoptotic protein families FLIP (FADD-like inhibitory protein) and Bcl-2 (B-cell lymphoma 2)[261,372,374–376]. Their apoptosis-inducing effect has also been linked to the functional status of regulatory genes such as *TP53* (protein 53)[242,369]. A flavonoid-derived drug currently under development targets a different step in apoptosis signalling by inhibition of sphingosine kinase, an enzyme involved in the induction of apoptosis[377], whose overexpression in tumours helps evade the pro-apoptotic effect of anticancer drugs[242,378]. Flavonols such as quercetin have been reported to deactivate protein kinase B (AKT), which is involved in the activation of anti-apoptotic proteins[379,380].

Ultimately, these examples reflect the well-established effect of flavonoids as pro-apoptotic drugs. Evidence suggests the complex modulation of cell death exerted by flavonoids through different mechanisms. In fact, some flavonoids have also been noted to act as competitive inhibitors for some caspases, possibly leading to alternative, non-caspase dependent induction of apoptosis[381].

1.1.5.3.6. Cell cycle inhibitors

The anti-proliferative and anti-cancer effect of flavonoids can also be linked to the inhibition of cell cycle progression. Both naturally-occurring and novel flavonoids have been shown to arrest proliferation at the G2/M checkpoint in several different cancer types[242,270,382], mainly through modulation of the expression level of different cyclins[256]. These antiproliferative effects have been reported in numerous cancer types[382–385], including breast[386] and ovarian[372].

1.1.5.3.7. Flavonoids as mitocans

The last decade has seen the emergence of mitochondria as targets in the development of new cancer therapies[387,388]. Mitochondria are at the centre of many essential cellular processes, as they are the main site of energy production, regulate cell homeostasis and are heavily involved in the initiation of cell death. Importantly, mitochondrial metabolism can be deregulated in cancer cells and markedly different from that of normal cells, making these organelles promising candidates for the selective treatment of cancer cells.

In short, mitochondrial metabolism relies on the creation of an electrochemical proton gradient across the mitochondrial inner membrane that originates through the electron transport chain (ETC). This electrochemical gradient generates a large mitochondrial membrane potential ($\Delta\psi_{mm}$), which is negative to the matrix, normally in the range of -150 to -170mV[389] (see *Figure 9*). This potential provides the stored force for the production of ATP as protons move into the mitochondrial matrix through the inner membrane-embedded ATP synthase. This normal mitochondrial metabolism is altered in cancer cells, where mitochondrial respiration is reduced in favour of aerobic glycolysis as the main mechanism for energy production, a phenomenon known as the Warburg effect[390,391]. Together with alterations in the respiratory enzyme complexes and associated regulators this leads to the accumulation of ROS and higher $\Delta\psi_{mm}$[389,392].

In a healthy cell the levels of ROS generated as by-products of the ETC are controlled within the constraints of the cellular redox system in order for the cell to sustain the necessary signalling processes[393]. The alterations in the mitochondrial metabolism of cancer cells lead to an accumulation of higher levels of ROS in the mitochondrial matrix. Consequently, cancer cells show lower antioxidant capacity than normal cells and are more sensitive to agents that may create further oxidative stress through redox modulation and creation of more ROS[393]. In a non-malignant cell the effect of such an agent may be absorbed by the protective enzymes present in its matrix (such as superoxide dismutase, SOD), whereas in cancer cells, in which mitochondrial metabolism is already deregulated, oxidative stress can trigger the initiation of apoptosis more easily. This increased sensitivity to the accumulation of higher ROS levels has contributed to the increasing interest in ROS modulation as a strategy for the selected targeting of cancer cells[318–321].

Changes in the mitochondrial metabolism also lead to cancer cells having a markedly greater $\Delta\psi_{mm}$ than non-malignant cells, with cancer cells presenting at least a 60mV higher net negative potential[389,394–396] (see *Figure 9*). The existence of a high $\Delta\psi_{mm}$ in the mitochondria plays an important role in the delivery of certain molecules to these organelles, particularly lipophilic, positively-charged compounds that may target the mitochondria. Indeed, the plasma membrane potential ($\Delta\psi_{pm}$) is lower than the mitochondrial membrane potential but negative to the extracellular matrix (normally -40 to -80mV), aiding such molecules to permeate into the cytoplasm from the extracellular space thanks to their lipophilicity and positive charge. In turn, the much stronger $\Delta\psi_{mm}$ drives these compounds to permeate though the mitochondrial membranes and into the mitochondrial matrix. The

greater $\Delta\psi_{mm}$ can lead to a 10-fold greater accumulation of such lipophilic charged compounds in cancer cells than in non-malignant cells[395]. In the field of drug design, this has led to the addition of positively-charged moieties such as triphenylphosphonium (TPP^+) as side groups to achieve mitochondrial targeting in anticancer drug candidates (see *Figure 9*).

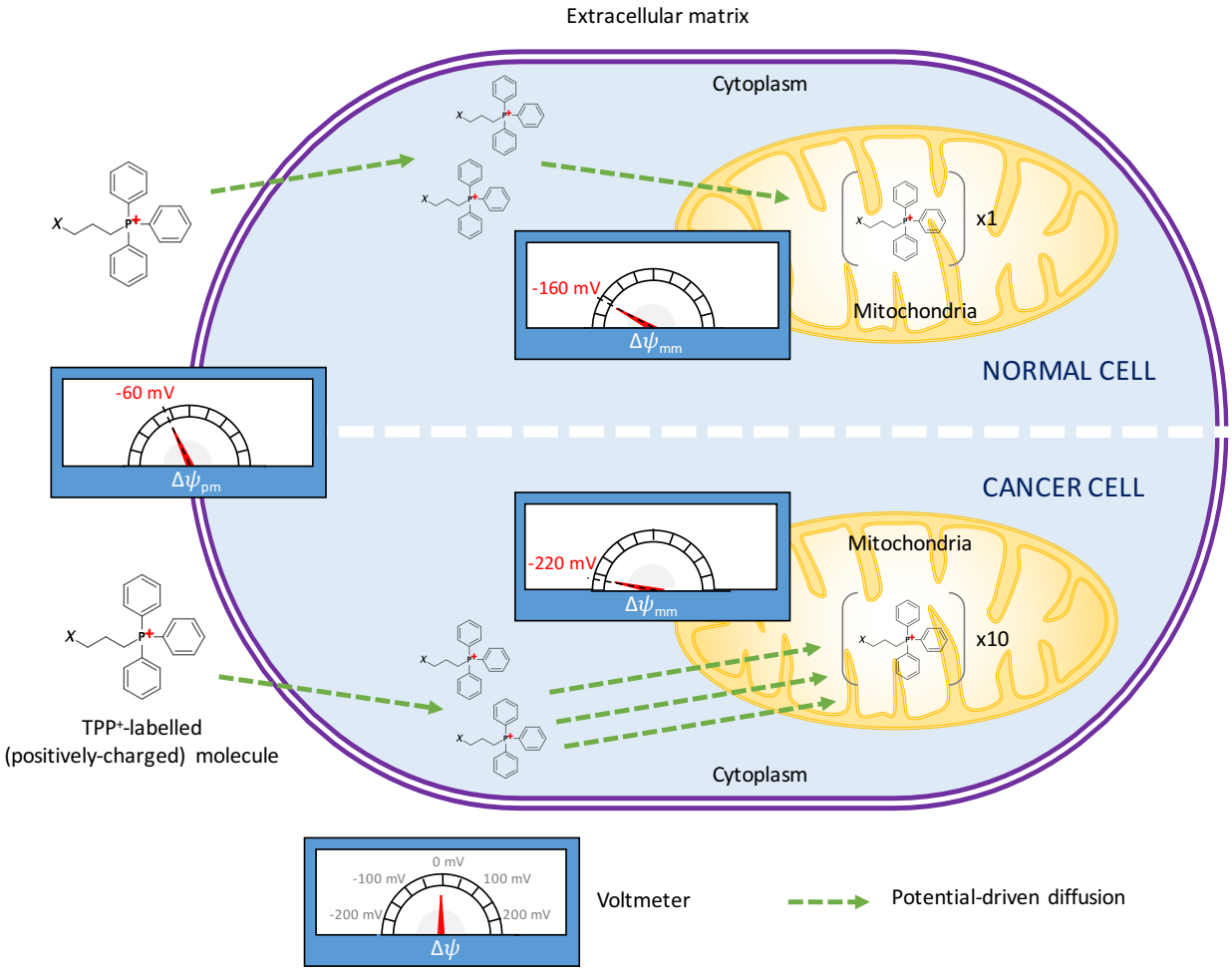

***Figure 9* Membrane potentials in normal and cancer cells.** *Transmembrane potential ($\Delta\psi$) gradients are essential to cell homeostasis, signalling and transport. This has been used to target molecules to the mitochondria by labelling them with positive-charged side chains such as triphenylphosphonium (TPP^+). The plasma membrane potential ($\Delta\psi_{pm}$) is normally between -40 and -80 mV. The mitochondrial membrane potential ($\Delta\psi_{mm}$) is between -150 and -170 mV in normal cells, while cancer cells have been noted to have a $\Delta\psi_{mm}$ at least a further 60 mV more negative[389,394–396], leading to a 10-fold greater accumulation of positively-charged molecules and a greater susceptibility to anticancer agents that may work as mitochondrial deregulators.*

In summary, alterations in mitochondrial metabolism make cancer cells more sensitive to redox stress-inducing agents and more likely to accumulate certain molecules. Thus,

mitochondria-targeted agents offer an alternative for therapeutic approaches that are not only effective, but also selective for cancer cells. Anticancer drugs that function through the specific targeting of the mitochondria are referred to as mitocans[389,393,397]. Given the central role of these organelles in cell homeostasis, mitocans can affect mitochondria through different mechanisms. The effect of flavonoids on general redox modulation or apoptosis, both heavily linked to mitochondrial function, has already been discussed. Nevertheless, several flavonoids have been noted to act as mitocans affecting mitochondrial function through other specific molecular targets[392,398].

Class I mitocans include inhibitors of the enzyme hexokinase[393], which supports the alternative energy-production glycolytic mechanism favoured in cancer cells and has been linked to tumour growth[399]. Oroxylin A (an O-methylated flavone) has been noted to inhibit glycolysis through targeting of hexokinase in breast cancer cell line models[400].

Flavonols such as myricetin and quercetin have been identified as class III mitocans inhibiting the thiol redox system[401], involved in the maintenance of cellular redox homeostasis and whose overexpression is associated with tumour growth and drug resistance in cancer[402,403].

Quercetin and some of its derivatives have also been shown to disrupt mitochondrial function through other mechanisms. Quercetin acts as a class IV mitocan by targeting the VDAC/ANT (voltage-dependent anion channel, adenine nucleotide translocase) mitochondrial membrane transporter complex to trigger apoptosis[404]. As class V and VI mitocans, novel quercetin derivatives affect mitochondrial function in cancer cells by targeting the ETC and the mitochondrial inner membrane[405,406], while quercetin can also act as a class VII mitocan by stimulating the activity of tricarboxylic acid cycle (TCA) enzymes[407], which is typically impaired in cancer cells[408].

1.1.5.3.8. Effect on other cancer-promoting signalling pathways

Flavonoids have also been reported to exert anticancer effects through modulation of proliferation, invasion or inflammatory signals[380], which has been described as an inhibition of several hallmarks or cancer[250]. In some cases, these effects have been linked to the previously discussed mechanisms linked to the properties of flavonoids as oestrogen-agonists, antioxidants or CYP1-inhibitors.

For instance, the polyphenol resveratrol inhibits cyclooxygenases 1 and 2 (COX1 and COX2)[409–411], involved in the production of prostaglandins that subsequently leads to cell

proliferation, angiogenesis and immunosuppression[412,413]. Other studies have shown inhibitory effects of flavonoids on different cancer-promoting pathways, such as the PI3K-AKT-mTOR[414,415], the EGFR[416] or the STAT3[417] signalling pathways. Research has also reported a broad-spectrum antitumour effect that can induce apoptosis through mitochondrial dysfunction and activation of the mitogen-activated protein kinase (MAPK) pathway[418–421].

A recent meta-analysis of controlled intervention trials has also shown the relation between consumption of flavonoids and the reduction of chronic systemic inflammation mediators[422]. Additionally, another review has noted the accumulation of evidence on flavonoids' ability to inhibit metastasis, invasion and progression, with a wide range of compounds being able to inhibit the different phenomena involved in these processes, from epithelial-mesenchymal transition to angiogenesis[422–425]. In the specific case of breast cancer, studies both *in vitro* and *in vivo* have shown that flavonoids can also have a protective effect by increasing breast tissue differentiation[426,427]. Myricetin has also been shown to down-regulate TERT (telomerase reverse transcriptase) activity in breast cancer models[428].

Different flavonoids have been reported to down-regulate both the transcription factor nuclear factor-kappa B (NF-κB)[429–432] and its subunit p65[428], therefore inhibiting proliferation and survival. Research has also shown flavonoids to inhibit crosstalk between NF-κB, ErbB receptors (avian erythroblastosis oncogene B family of receptors, which include EGFR), and the HH/GLI (Hedhehog/Glioma-associated) cascade pathways, which also play an important role in neoplastic transformation[433]. A recent review has summarised the extensive evidence accumulated on the anticancer effect of flavonoids in this and other cancer-promoting pathways[434].

It is also worth noting that most of the effects of flavonoids on apoptosis, cell cycle and other signalling pathways mentioned work in a dose and time-dependent manner. They also have been observed at concentrations as low as in the nano- and picomolar range and are specific to cancer cells[242,270], all of which are truly advantageous characteristics that add to the potential of these compounds in cancer treatment.

1.1.5.4. Pharmacological properties of flavonoids

The potential of flavonoids for their application as novel anticancer agents is based not only on their antitumour effects, but also on pharmacokinetic, pharmacodynamic and other properties that make them particularly desirable for their potential pharmacological application as chemotherapeutic agents.

1.1.5.4.1. Biphasic effect of drugs

Firstly, the anti-tumour effect of flavonoids has been shown to be not only concentration and time-dependent, but also biphasic[374]. As reviewed in the previous sections, flavonoids have been shown to exert a complex, pleiotropic but ultimately therapeutic effect against a broad variety of cancer types. Depending on the structural differences of each flavonoid type or specific compound and on its concentration, flavonoids can modulate a wide range of molecular pathways to exert either: (i) a chemopreventive effect, reducing the risk of oncogenesis, at lower concentrations; or (ii) a cytotoxic effect, blocking proliferation and inducing death of cancer cells, when administered at higher concentrations. Hence, lower concentrations that could easily derive from dietary intake may have cytoprotective and cancer risk-reducing effects, whereas higher concentrations can be pro-apoptotic through different mechanisms[435,436].

For instance, low concentrations of flavonoids such as quercetin or myricetin have been noted to have oestrogen-mimicking effects through their binding to ER[270,271](although possibly not a growth-inducing effect due to a higher affinity for ERβ[278–280]), whereas higher concentrations can play a role as AI[290] or exert cytotoxic effects. Thus, low concentrations may modulate oestrogen-regulated proliferation in an ER-dependent manner, whereas higher levels of flavonoids may induce both ER-dependent and independent anticancer effects through different mechanisms[271,277].

Although higher concentrations have been linked to cytotoxic effects of flavonoids, some authors have reported the increase of concentration linked to these biphasic effects to differ by only a factor of 5 or 10[436]. These levels are still feasible from a pharmacological point of view, in contrast with other models in which anti-mutagens and anti-carcinogens are administered at unrealistically high doses, which would probably hinder the translation of these therapeutic strategies to the clinical setting[344].

Research has shown that, despite the complex interaction of mechanisms and the dose-dependent balance of cytoprotective and cytotoxic effects, the application of flavonoids can result in beneficial antitumour effects. Indeed, meta-analyses of controlled intervention trials and studies *in vivo* have shown that, despite the complexity of their effect, the application of flavonoids in the right setting and conditions can ultimately lead to positive outcomes: decreasing indicators of inflammation, limiting proliferation, increasing latency and reducing both tumour size and metastasis[267,422].

1.1.5.4.2. Broad, cancer-specific effect

Another interesting feature of flavonoids is the fact that they exert their antiproliferative and cytotoxic effect in a selective and cancer-specific manner. They have been shown to exert broad-spectrum effects against numerous cancer types, which might arguably be due to their targeting of a wide range of molecular pathways linked to the main hallmarks of cancer (such as prolonged proliferation and survival or apoptosis), as reviewed above, rather than other more specific targets linked to the specific aetiology or mechanism of each cancer type.

Despite this broad-spectrum of different cancer types, the effect of flavonoids does appear to be cancer-specific, with normal cells being typically unaffected[374,437] by concentrations exerting cytotoxic effects on malignant cells. This might be due to the natural origin of these compounds, which grants them low general toxicity when they interact with molecular targets that are specifically dysregulated in cancer cells. For instance, flavonoids have been shown to target the CYP1 enzyme family, which is selectively expressed in tumour cells and pre-malignant tissue but has not been found to be significantly expressed in normal surrounding tissues[337].

1.1.5.4.3. Other properties of flavonoids as anticancer agents

Research has shown that while exerting their anti-tumour effects flavonoids do not hinder other anticancer natural processes, such as the effect of phase II detoxifying enzymes[343]. Hence, flavonoids can work concomitantly with natural cellular protective mechanisms.

Interestingly, authors have reported that flavonoids can be bioactivated when exposed to tumour cell-specific enzymes[337]. As discussed in previous sections, in addition to acting as inhibitors of the carcinogenesis-promoting CYP1, flavonoids can also act as substrates for this enzymes and be transformed into more effective metabolites *in situ* [336,438,439]. This could allow for the administration of flavonoids including moieties that improve their metabolic stability and bioavailability to then be converted to more reactive anticancer agents in cancer cells. Through this interaction the cancer specificity generally observed in flavonoids is enhanced by an also specific activation, occurring only in malignant cells. This could lead to great potential for the development of therapies targeted specifically to the abnormal tissue.

Reports have shown that flavonoids can exert some of their anti-tumour effects, such as BCRP inhibition, in an additive manner. A recent review has collected the accumulated

evidence of combinations of different polyphenols exerting more efficient anticancer effects than single treatment[434]. Studies have shown, both *in vivo* and *in vitro*, that combined flavonoids induce synergistic effects by several of the different mechanisms of action of previously discussed, including cell cycle arrest[440–442], induction of apoptosis[443,444] or modulation of signalling pathways linked to proliferation and progression[445,446]. Therefore, the use of different polyphenols administered concomitantly or in combination with anticancer treatments has been suggested as one of the promising strategies for their application[357,362,363].

1.1.5.5. Previous applications of flavonoids in cancer research

1.1.5.5.1. Evidence of the flavonol myricetin as an anticancer agent

Myricetin (3,5,7-trihydroxy-2-(3,4,5-trihydroxyphenyl)-4-chromenone) is a natural secondary plant metabolite belonging to the flavonol subclass of flavonoids (see *Figure 12a* or *Table 7* for molecular structure). It is a common dietary flavonoid due to its ubiquitous presence in plant products and is the most abundant flavonoid in many berries, herbs, wines and teas[447,448]. It was first isolated in the late 19th century from the bark of *Myrica nagi* (box myrtle or bayberry), a shrub or small tree found at high altitudes in India and Nepal[449–451].

Among flavonoids, myricetin has been reported to have particularly potent redox-regulating properties *in vitro* due to its structure and hydroxylation profile[307,312,452]. Research has shown a wide range of beneficial effects, including cytoprotective, antiviral, and antimicrobial activities[310,437,453], as well as possible therapeutic applications in a range of pathologies, including the prevention and treatment of cardiovascular disease[454,455] or diabetes[456–458].

The different molecular mechanisms described for flavonoids have been discussed above. This section will highlight some of the evidence on the wide range of anticancer properties associated with myricetin in particular. Evidence suggests that myricetin may exert this antitumour effect through mechanisms targeting several cancer hallmarks.

Firstly, myricetin has been shown to work as a regulator of proliferation in different cancer types, inducing arrest of the cell cycle G_0/G_1 and G_2/M phases[459–461] by inhibition of cyclins B1[459,460] and D1[461], as well as of different members of the cyclin-dependent kinases (CDK)[459].

Myricetin has also been reported to induce cell death through apoptosis across different cancer types, inducing the mitochondrial apoptotic pathway through cytochrome C release,

caspase activation and PARP cleavage[383,462], as well as regulation of pro- and anti-apoptotic proteins in the Bcl-2 family[259,460,462–464]. Interestingly, some authors have reported the ability of myricetin to work synergistically in combination with other therapies. This includes improved effects in combination with radiotherapy[465], chemotherapy[466] and TRAIL[261].

Several authors have also reported the inhibitory effect of myricetin on metastasis, by targeting matrix metalloproteinases (MMPs)[467] and the invasion-linked ERK (extracellular signal-regulated kinases) signalling pathway[257], and angiogenesis by inhibition of VEGF (vascular endothelial growth factor) and related neovascularisation-promoting factors[468,469].

In summary, myricetin is a good example of the promising anticancer effects of flavonoids previously discussed. It stands out from other similar compounds for its particularly active redox profile, while different mechanisms have been linked to its beneficial effects, including but not limited to the inhibition of proliferation and the induction of apoptosis, across different cancer types.

1.1.5.5.2. Previous clinical studies of novel flavonoids as anticancer agents

As previously summarised, flavonoids represent a natural reservoir of varied, polyphenolic plant secondary metabolites with a great potential in the prevention and treatment of cancer. This promise has led to numerous attempts to develop novel, semi-synthetic flavonoid derivatives. Decades of research on natural compounds have generated a wealth of knowledge on structure-activity relationships relevant to the different effects exerted by flavonoids or their bioavailability. Indeed, the number and location of different substitutions on the flavonoid rings can enhance or inhibit different effects[314,359,470,471]. Bioavailability profiles vary widely between different flavonoids[249,472] and evidence has suggested that substitution with larger groups such as sugars or lipophilic chains may improve distribution[341,453]. The application of this knowledge has allowed for the design and synthesis of new molecules with different substitutions and enhanced properties.

Recent years have seen the development of many of these semi-synthetic novel flavonoid derivatives (see *Figure 10* for structures of some examples). The novel flavone LZ-207 showed promising effects in colon cancer cell line models, inducing apoptosis and inhibiting inflammation[473], while the novel, wogonin-derived flavone V8 has also shown anti-inflammatory effects on cervical cancer cells[474].

Interestingly, a large part of this research has focused on application in breast cancer. Several groups have designed, synthesised and tested novel flavonoids with antiproliferative

effects on breast cancer cells[475–477]. For instance, the novel flavonoid derivative VI-14 has been shown to inhibit migration and invasion in different cancer models[477]. Another interesting approach consisted of the synthesis of flavonoid dimers such as FD18, which has shown promising results, reverting multidrug resistance to allow better distribution of chemotherapeutic agents such as paclitaxel in a human breast cancer xenograft model[478].

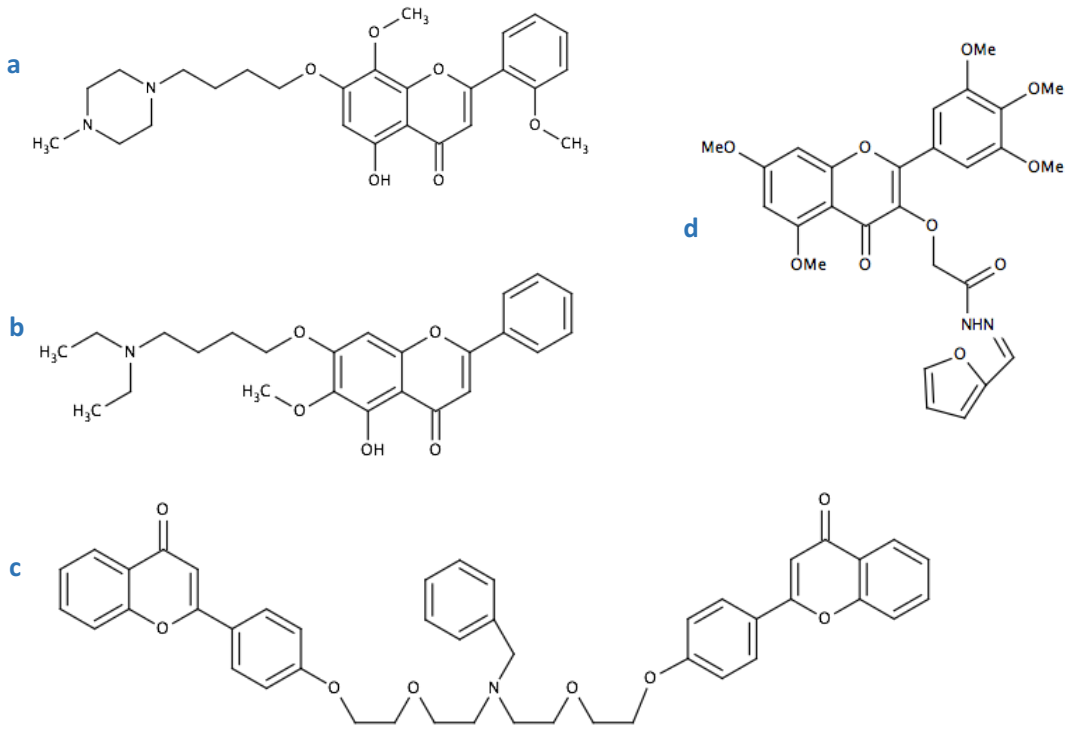

Figure 10 ***Examples of novel flavonoid structures.*** *The last few years have seen the development of different semi-synthetic compounds based on the natural flavonoid backbone. These include LZ-207 (*a*), VI-14 (*b*), dimers such as FD18 (*c*) or novel myricetin-based derivates (*d*).*

A recent study has reported the design and synthesis of novel myricetin derivatives with a range of substitutions, including multiple methoxylations and complex chains. Results have identified promising candidates with strong activity as telomerase modulators, inhibiting expression of hTERT (human telomerase reverse transcriptase) and the related factor p65 in an *in vitro* breast cancer cell line model[428].

The development of novel flavonoids has also taken some candidates beyond the pre-clinical stages of research. Most notably, Australian pharmaceutical company Novogen and its California-based subsidiary company MEI Pharma (previously known as Marshall-Edwards) have developed a series of compounds as part of their proprietary flavonoid technology platform (see *Figure 11*).

Their first candidate was Phenoxodiol, a novel derivative of the isoflavone genistein, promoted as an anticancer drug with promising beneficial effects and low toxicity[240,479]. Extensive pre-clinical work showed the ability of cell Phenoxodiol to induce cell cycle arrest and induce apoptosis in a range of cancer types, including prostate[480,481] and ovarian[482,483] cancers. Further work characterised Phenoxodiol as a particularly promising chemosensitiser to be used in combination with chemotherapy[484,485].

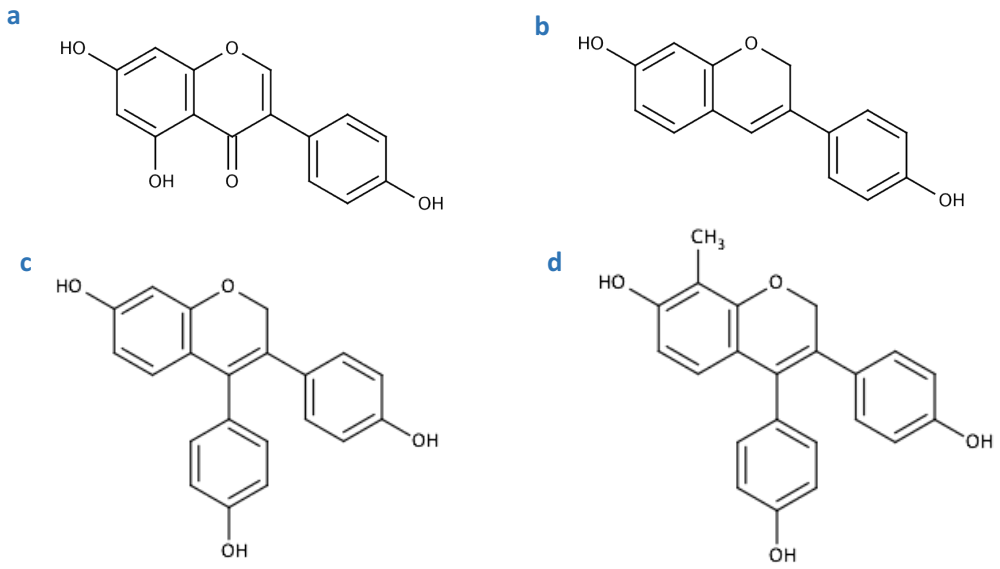

***Figure 11* MEI Pharma novel flavonoid platform technology.** *MEI Pharma have developed a series of new chemical entities based on the natural structure of the isoflavone genistein (*a*). From this backbone they designed Phenoxodiol (*b*) and its second-generation analogues ME-143 (*c*) and ME-344 (*d*).*

A phase I in-human dose escalation clinical trial (NCT00022295) reported moderate anticancer properties[479,486] and a promising pharmacokinetic profile[487]. This was followed by phase II studies to assess the effect of intravenous Phenoxodiol in combination with chemotherapy[488] (NCT00091377, NCT00303888). Progress was halted at the phase III trial stage of the OVARTURE (ovarian tumour response) clinical trial (NCT00382811) of orally administered Phenoxodiol in combination with carboplatin, due to lack of a statistically significant effect on either progression-free or overall survival[489,490], although the fact the trial was underpowered and no efficacy studies of oral Phenoxodiol had been conducted at phase II may have contributed to the lack of success of the study.

Nevertheless, work has continued on a second generation-derivative of Phenoxodiol, ME-143. A first-in-human dose escalation phase I study showed limited effect of ME-143 as

monotherapy on patients with solid tumours[490,491] (NCT01401868). However, a better understanding of the mechanism of action of ME-143 as an inhibitor of tumour-specific mitochondrial NADH oxidase[492] has led to plans for a phase II trial in combination with cytotoxic chemotherapy[490,491].

An additional lead compound currently under development by MEI Pharma is ME-344, another novel isoflavone with promising anticancer properties. Like ME-143, ME-344 also acts as an inhibitor of mitochondrial complex I in cancer cells[492]. Research has reported the ability of ME-344 to decrease the tumour burden *in vivo* when used as maintenance therapy post-chemotherapy in ovarian cancer[493]. A phase I clinical trial of ME-344 as a single agent in patients with solid tumours (NCT01544322) reported promising results, with 38% of patients showing improvement after treatment[494]. A phase II trial of ME-344 in combination with chemotherapy was underway but has been recently terminated due to lack of efficacy (NCT02100007). Additionally, recent findings have shown a synergistic effect of ME-344 in combination with VEGF inhibitors in an *in vivo* breast xenograft model[495]. These results are expected to lead to further studies in breast cancer models.

In summary, the last few years have seen the development of many novel semi-synthetic compounds with the aim to exploit the promising anticancer properties of natural flavonoids. This work has yielded numerous pre-clinical studies, as well as a few compounds that are already undergoing clinical trials. Together, this supports the promise of this approach for the development of new therapeutic and sets an example for similar studies based on different unique molecules that may target cancer cells through new mechanisms.

1.1.5.5.3. A library of novel, myricetin-derived flavonoids

This introduction has summarised the potential of flavonoids as therapeutic and, more specifically, anticancer agents, as well as highlighting the promise of myricetin as a natural scaffold and previous examples of novel flavonoids.

Following this, Aberdeen-based pre-clinical drug discovery company Antoxis Ltd have developed a proprietary platform of novel flavonoids for their study as potential therapeutic agents. This is based on the patented myricetin-derived molecular Kromex scaffold[496] (see *Figure 12*). Their strategy seeks to combine the redox ability and therapeutic potential of the myricetin scaffold with structural features that may enhance its drug-likeness and improve its potential *in vivo* activity.

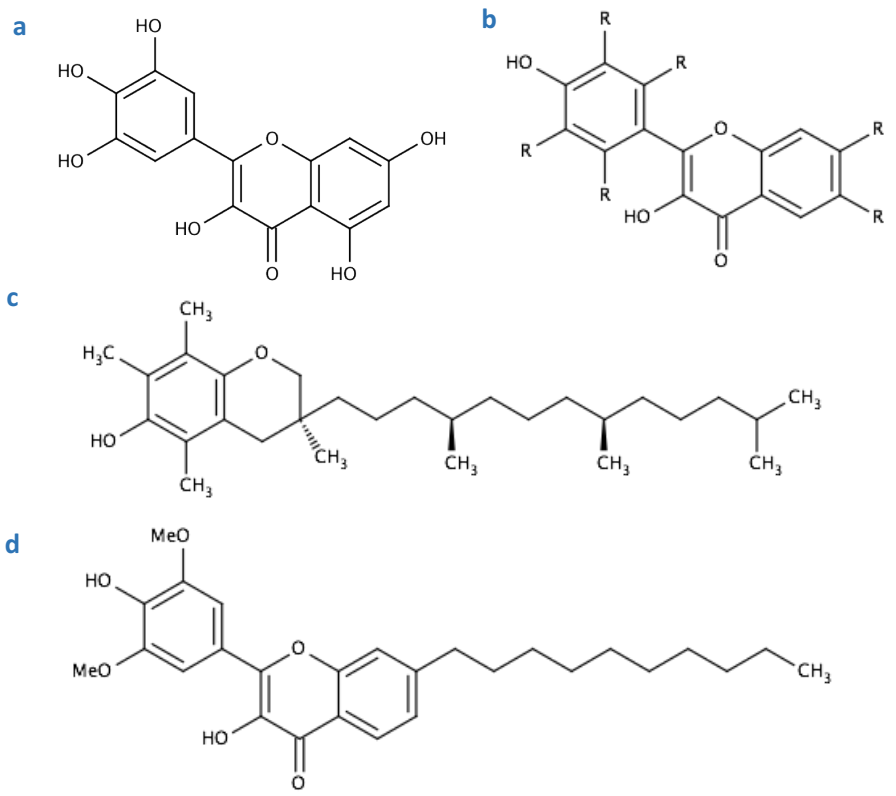

***Figure 12* Antoxis novel flavonoid platform technology.** *Antoxis Ltd have developed a library of novel semi-synthetic flavonoids derived from the natural structure of myricetin (*a*). From this backbone they have developed their patented proprietary Kromex scaffold (*b*). Addition of substitutions like hydrophobic chains similar to the one found in* d*-α-tocopherol (*c*) have led to the design of novel candidates such as AO-1530-OMe (*d*).*

The term 'drug-likeness' bears further description, as it is commonly used in the early stages of lead and drug discovery. It refers to the different physicochemical properties that impact the molecular behaviour of a compound *in vivo* (specifically its pharmacokinetics), including criteria such as bioavailability, solubility, permeability, metabolic stability and transport[497]. Thus, drug-likeness is often used as a qualitative property of compounds that make them likely to function as orally active compounds[498].

The concept of drug-likeness originated with the "rule of 5" described by Chris Lipinski in the late 1990s, which defined four physicochemical parameters (molecular weight ≤ 500, log *P* ≤ 5, H-bond donors ≤ 5, H-bond acceptors ≤ 10) associated with 90% of orally active drugs that achieve phase II clinical status[499]. This rule aimed to rationalise compound design and quickly became a standard in drug development. While Lipinski's rule has been subsequently criticised for its oversimplification of the properties necessary for a compound

to be a viable drug candidate[500,501], it led to subsequent refinement and research of what makes a compound 'drug-like'[501,502]. Importantly, this has led to greater awareness of the importance of considering aspects such as bioavailability or permeability in the early stages of drug development, as these are determining factors for the administration, distribution, metabolism and elimination (ADME) of chemicals *in vivo* and limitations in these properties contribute significantly to the high attrition rates in drug development[497,502,503].

In line with this, Antoxis's approach seeks to address the drug-likeness deficiencies hindering the application of myricetin and many other flavonoids in cancer therapy. Indeed, despite its promising properties, the successful application of myricetin has been hampered by its relatively poor bioavailability and low cell membrane solubility, physiological instability, oxidative degradation and metabolic transformations[452,504–507].

Antoxis have designed a large library of novel analogues which combine the ringed scaffold and substituents of myricetin with other beneficial structural traits to generate targeted, more potent candidates which also present physicochemical properties that improve their likelihood to be viable drug candidates *in vivo* [452,508,509]. These proposed compounds have been designed to present properties such as improved stability, rapid cell uptake, mitochondrial targeting and enhanced redox potential[510].

For instance, the Kromex scaffold has been combined with a side chain reminiscent of that found in *d*-α-tocopherol (the main constituent of vitamin E[511]), which allows for good uptake, transport and anchoring of the molecule to cell membranes (see *Figure 12*), all factors that can contribute to a chemical entity's drug-likeness. As previously mentioned, research has highlighted the potential of agents targeting the mitochondria as anticancer agents. Interestingly, some of these mitocans support the promise of Antoxis's new analogues, since semisynthetic analogues of both vitamin E[512–514] and natural flavonoids have shown promising results[392].

Previous work has showed the ability of one of Antoxis's first generation novel flavonoids, AO-1530, to confer protection against acute oxidative stress in both human neuronal and mouse embryonic stem cell models[510,515]. Results suggested the relevance of its novel chimeric structure and mitochondrial targeting. A larger library of these new chemical entities is now ready to undergo pre-clinical assessment in order to identify promising lead candidates and study their mechanism of action for their potential application in the treatment of breast and ovarian cancer.

1.2. Hypothesis and project rationale

We hypothesised that novel, myricetin-derived flavonoids developed by Antoxis Ltd with specific mitochondrial targeting, enhanced redox reactivity and optimised physicochemical properties and drug-like attributes may have potential for their application as anticancer agents in breast and ovarian cancer.

Mitochondria have been identified as promising targets for the effective and selective treatment of cancer, due to their central role in the cell and the changes in mitochondrial metabolism of cancer cells[387,388]. The specific role of oxidative stress in the development of cancer has long been established[516–518] and mitochondrial metabolism is known to be a major source of ROS and other active species[519,520], which are involved in and regulate many signalling pathways linked to the hallmarks of cancer development and progression.

As mentioned before, myricetin has been shown to induce mitochondria-dependent apoptosis[259]. This pro-apoptotic effect, together with its potential role as chemosensitiser, have set a strong basis for the development of novel, semi-synthetic flavonoids that may improve the drug-likeness and efficacy of the natural scaffold of myricetin and enable specific targeting of the mitochondria in cancer cells.

1.3. Aim and objectives

Based on this hypothesis and rationale, this project aimed to identify and study novel, myricetin-derived flavonoids with antitumour effects in preclinical models of breast and ovarian cancer for their potential development towards clinical study.

For this, we sought to accomplish a series of objectives:

- Evaluation of the effect of a small library of novel flavonoids on a panel of breast cancer cell lines representing diverse molecular types and a panel of ovarian serous adenocarcinoma cell lines representing different response to treatment, and identification of lead compounds in the library.
- Description of structure-activity relationships (SARs) of relevance for the anticancer properties and optimal pharmacokinetic and drug-like attributes observed.
- Assessment of the specificity of the expected mitochondrial targeting of the compounds studied and the relevance of this aspect to their possible anticancer effects.
- Investigation of the ROS-modulating effect of the compounds studied and the relevance of this mechanism to their possible anticancer effects.
- Study of the mechanism of action by which lead novel flavonoid candidates may exert anticancer properties, including any signalling pathways or hallmarks of cancer that may be altered by treatment.
- Investigation of the potential of novel flavonoids for their application in combination with other therapeutic strategies of current clinical relevance, including chemotherapy and endocrine therapy.
- Evaluation of the optimal setting for the application of novel flavonoids in the treatment of breast and ovarian cancer, as single or combination agents.
- Study of the effect of novel flavonoids in initial *in vivo* mouse models.

2. Materials and Methods

2.1. Materials

2.1.1. Cell lines

Two panels of cell lines representing different cancer types, subtypes or phenotypes were used as pre-clinical *in vitro* models throughout the project, including 7 breast cancer cell lines (see *Table 5*) and 6 ovarian cancer cell lines (see *Table 6*).

Cell line	Origin	Classification	Description
MCF-7	Pleural effusion of patient with adenocarcinoma	Luminal A	ER^+ (*wt* and variants) / PR^+ / $HER2^-$
MDA-MB-231	Pleural effusion of patient with adenocarcinoma	Basal B	ER^- / PR^- / $HER2^-$ (TNBC)
BT-549	Invasive ductal tumour	Basal B	ER^- / PR^- / $HER2^-$ (TNBC)
HBL-100	Milk from healthy nursing mother	Basal B	ER^- / PR^- / $HER2^-$ (TNBC) Harbours SV40 genome
LCC1	MCF-7 variant: Subpopulation derived from MCF-7 by selection for hormone independence	Luminal	ER^+ / PR^+ / $HER2^-$ Oestrogen-independent but endocrine therapy-responsive
LCC2	MCF-7 variant: Subpopulation derived from LCC-1 by selection for tamoxifen resistance	Luminal	ER^+ / PR^+ / $HER2^-$ Oestrogen-independent and tamoxifen-resistant
LCC9	MCF-7 variant: Subpopulation derived from LCC-1 by selection for fulvestrant (ICI 182,780) resistance	Luminal	ER^+ / PR^+ / $HER2^-$ Oestrogen-independent and fulvestrant- and tamoxifen-resistant

***Table 5* Breast cancer cell lines studied.** *The effect of a library of novel flavonoids was assessed on a panel consisting of 7 breast cancer cell lines with different molecular classification and traits*[59,521,522] *and response to endocrine therapy*[523–526]*. ER, oestrogen receptor; wt, wild type; PR, progesterone receptor; HER2, human epidermal growth factor receptor 2; TNBC, triple negative breast cancer; SV40, Simian Virus 40.*

Cell line	Origin	Treatment	Status
PEA1	Pleural effusion (PEA1) or peritoneal ascites (PEA2) in patient (MK) with poorly differentiated serous adenocarcinoma	Collected prior to treatment	Sensitive
PEA2		Collected on relapse after CDDP and prednimustine treatment	Resistant
PEO1	Peritoneal ascites in patient (DB) with poorly differentiated serous adenocarcinoma	Collected after CDDP, 5-FU and chlorambucil treatment	Sensitive
PEO4		Collected after clinical resistance developed to above agents	Resistant
PEO14	Peritoneal ascites in patient (EM) with well differentiated serous adenocarcinoma	Collected prior to treatment	Sensitive
PEO23		Collected on relapse after CDDP and chlorambucil	Resistant

***Table 6* Ovarian cancer cell lines panel.** *The effect of a library of novel flavonoids was assessed on a panel consisting of 3 pairs of ovarian cancer cell lines showing sensitivity or resistance to different chemotherapeutic agents* [527]*. CDDP: cis-platinum. 5-FU: 5-fluorouracil.*

The breast cancer cell lines MCF-7, MDA-MB-231, BT-549 and HBL-100 (all obtained from the American Type Culture Collection, ATCC) represent different molecular subtypes of breast cancer. Hormone-dependent MCF-7 cells express the oestrogen receptor (ER^+), while MDA-MB-231, BT-549 and HBL-100 are triple negative breast cancer (TNBC) cell lines, lacking in receptors for oestrogen (ER^-), progesterone (PR^-) and human epidermal growth factor ($HER2^-$) and are, consequently, hormone-independent.

LCC1, LCC2 and LCC9 cells (gifted by Prof Robert Clarke) are hormone-independent cells established by derivation of selected subpopulations of MCF-7 cells [523–525]. LCC1 cells were obtained through selection for oestrogen-independent growth. LCC2 and LCC9 cells were then derived from LCC1 cells by selection for antioestrogen-resistant phenotypes (see *Table 5* for description).

The panel of ovarian cancer cells used included 3 pairs of chemotherapy sensitive/resistant serous adenocarcinomas cell lines: PEA1/PEA2, PEO1/PEO4 and PEO14/PEO23 (see *Table 6*). For each pair cells were established from the same patient with collection before or after the development of resistance to treatment. They were all established by and obtained from Dr Simon Langdon[527].

All cell lines were authenticated by STR (short tandem repeat) profiling undertaken by Public Health England (Salisbury, UK) in December 2014.

2.1.2. Drug library

Novel flavonoids studied were supplied by Antoxis Limited (Aberdeen, UK) from their library of proprietary compounds[508] (see *Table 7*). They were custom synthesised and their purity was ascertained to be >95% by LCMS (liquid chromatography mass spectrometry) and NMR (nuclear magnetic resonance). It should be noted that AO-1530-OMe was also referred to as Anto-028 or Oncamex at different stages of the project. Myricetin was purchased from Sigma-Aldrich.

All flavonoids were obtained in powder form and stored at 4^{o}C. For use in cell culture treatments, they were made up to 10mM stock solutions in dimethylsulfoxide (DMSO) and stored at -20^{o}C degree before dilution to treatment concentrations.

2.1.3. Publically-available datasets

Differential gene expression analysis included the use of publically available datasets from published Affymetrix microarray experiments. These included MCF-7 cells exposed to (i) 0.025% DMSO for 2, 4 or 6 h[528], or (ii) 0.1% DMSO for 6 h[529]. These datasets were obtained from the National Center for Biotechnology Information Gene Expression Omnibus[530] under the accession numbers GSE28662[528] and GSE45853[529].

2.2. Methods

2.2.1. Cell culture

MCF-7, MDA-MB-231, BT-549 and HBL-100 cells were cultured in Dulbecco's Modified Eagle Medium (DMEM) supplemented with 10% heat-inactivated foetal calf serum (FCS) and 100IU/mL penicillin/streptomycin.

LCC1, LCC2 and LCC9 cells were cultured in Phenol Red-free (to prevent its weak oestrogenic effect[531]) DMEM supplemented with 5% heat-inactivated FCS charcoal-stripped of steroids (CSFCS) (see method below) and 100IU/mL penicillin/streptomycin.

All ovarian cancer cell lines were cultured in Roswell Park Memorial Institute 1640 Medium (RPMI) supplemented with 10% heat-inactivated FCS and 100IU/mL penicillin/streptomycin.

All cells were incubated at 37°C in a humidified atmosphere containing 5% CO_2 and following the recommended guidelines[532]. They were grown to confluence with periodic medium changes and harvested by brief incubation with trypsin/EDTA (ethylene-diamine-tetra-acetic acid) solution.

2.2.2. Heat-inactivation and charcoal treatment of FCS

All FCS used for cell culture is customarily heat-inactivated by incubation at 37°C for 15 min, then 56°C for 30 min in order to inactivate the complement present in the serum[533]. Hormone-independent cell lines need to be cultured in the absence of any oestrogenic effects. Phenol Red-free medium was used to avoid its weak oestrogen-mimicking activity[531]. In order to strip FCS of any steroids present, it was first incubated for 2 h at 37°C in the presence of 2000 IU of type IV sulphatase per litre and pH was adjusted to 4.2. A charcoal mix was prepared by adding 5g of charcoal and 25mg of Dextran T70 to 50mL of dH_2O and stirring at 4°C. The activated charcoal mix was then added to the FCS and stirred overnight at 4°C and in darkness. Charcoal was separated by centrifugation at 4000g for 1 h at 4°C, followed by re-adjustment of pH to 4.2. This charcoal treatment was repeated once more as described. Finally, pH was adjusted to 7.2 and any remaining traces of charcoal were removed by filtering using a Stericup filter (0.1µM pore, Millipore).

2.2.3. Sulforhodamine B proliferation assay

The sulforhodamine B (SRB) assay was developed in 1990 as a new method for anticancer drug screening[534]. This colorimetric method relies on the ability of the protein dye

SRB to bind electrostatically to the basic aminoacids of fixed proteins in a pH-dependent manner[534,535]. As this is a rapid and inexpensive method, SRB assays are commonly applied to assess drug-induced cytotoxicity based on the sensitive measurement of total cell protein content[535,536]. SRB assays can be used to rank chemically similar compounds in *in vitro* screenings as part of pre-clinical studies in drug development[537]. This method was applied to assess the effect of different treatments on cell culture models throughout the project.

In all instances, after relevant treatment and incubation, cells were fixed with 50µL/well of cold 25% trichloroacetic acid (TCA) for 1 h at 4°C and washed 10 times with H_2O. Fixed cells were stained for 30 min with 50µL/well of 0.4% (wt/vol) SRB (in 1% acetic acid) and washed 4 times with 1% acetic acid. Protein-bound SRB was solubilised in 150µL/well of 10mM Tris solution pH 10.5 for 1 h, followed by measurement of optical density (OD) at 540nm in a BP800 Microplate Reader (Biohit). Results were processed, subtracting average values of blanks and day zero controls and normalising to vehicle controls.

2.2.4. Drug-induced cytotoxicity assays

Breast and ovarian cancer cells (500-2000 cells/well, depending on doubling time) were plated in 96-well microplates. Medium was changed to 2.5% FCS (or CSFCS) after 24 h, following preliminary experiments that showed an improved effect of drugs in lower serum concentrations (see *Supplementary Figure 1*), and cells were incubated for a further 24 h before treatment.

Cells were treated with a library of 8 compounds, including myricetin and lead compounds AO-1530 and AO-1530-OMe (see *Table 7*). Treatments included a range of micromolar concentrations between 0.01 and 100µM for all compounds, maintaining the vehicle concentration at the minimum possible (≤1%). Treatments were typically maintained for 96 h, followed by fixing and quantifying of changes in cell protein content by SRB assays, as previously described, in order to assess drug-induced cytotoxicity. Additional experiments looked at the timing of the effect of flavonoids by repeating these assays with varying incubation times.

For analysis of cytotoxicity and other plate-based assays, all experiments were repeated at least once and 6 technical replicates were always used to calculate means and standard deviation. Results were processed, subtracting average values of blanks and day zero controls and normalising to untreated controls.

2.2.5. Data analysis and IC_{50} calculations

The half maximum inhibitory concentrations (IC_{50}) of compounds in the library studied were calculated from dose-response curves representing the cytotoxic effect of each flavonoid, as shown by pooled data from biological replicate SRB assays. These curves were fitted to a regression model using the Excel package Fit Designer 2D, excluding outliers outside of a 95% confidence interval. The mathematical sigmoidal growth model Morgan-Mercer-Flodin (MMF) was used, as it provided the best fit and regression coefficient in all cases. IC_{50} values for all compounds in the library studied were obtained for the 4 breast cancer cell line models. For oestrogen-independent breast cancer cell lines and ovarian cancer cell line models IC_{50} values were determined only for lead compounds AO-1530 and AO-1530-OMe and the natural compound myricetin.

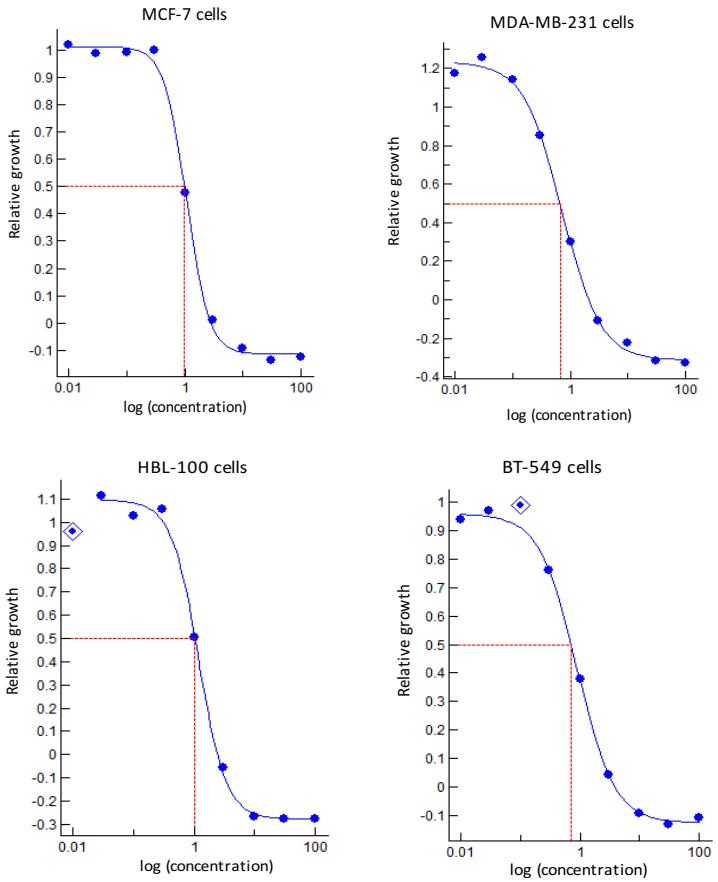

Figure 13 ***Fitting dose-response curves to sigmoidal growth models.*** *Example of graphs showing the modelling of the response of 4 breast cancer cell line models to AO-1530-OMe. In order to determine IC_{50} values Each curve was fitted to a sigmoidal model in order to determine IC_{50} values. The Morgan-Mercer-Flodin mathematical sigmoidal model, with high regression coefficient and exclusion of outliers outside of a 95% confidence interval (shown as boxed points). All graphs can be found in Supplementary Figures 2-9.*

2.2.6. Cytospin slides preparation

10^5 MCF-7 cells/well were plated in triplicate in 6-well plates. After treatment and incubation, medium was collected to prevent loss of any floating apoptotic cells that may have lost adherence. Remaining cells attached on the wells were trypsinised, combined with previously collected medium and centrifuged for 5 min at 2000rpm. Resulting pellets were resuspended in 100µL of FCS and transferred to Cytofunnels EZ Single (Fisher) mounted on Superfrost Plus slides (VWR International) to be spun for 3min at 500rpm in a Cytospin 4 Cytocentrifuge (Thermo Fisher). Slides were allowed to air-dry and stained using the Reastain Quick Diff kit (Reagena), to fix and dye both protein and DNA. After rinsing and air-drying, cells were observed on an Olympus BX51 microscope and images were captured using the software package Q-Capture Pro (Q Imaging).

2.2.7. Fluorescence microscopy

Cells were grown on coverslips and treated with Oncamex for 15 min, 1 h or 6 h at 37°C, adding 25nM Mitotracker Deep Red (Life) for the last 30 min (or 15 min for the shortest incubation). Cells were fixed in 4% paraformaldehyde (PFA) for 45 min, washed 3 times in phosphate buffered saline (PBS) and allowed to air-dry before mounting on Superfrost Plus microscope slides (Thermo Scientific) using ProLong Gold antifade mountant with DAPI (4',6-Diamidino-2-Phenylindole, Life).

Oncamex possesses fluorescent properties, with a stable signal measurable at $550nm_{EXC}/570nm_{EM}$. Other markers were detected at their excitation and emission spectra, as per the manufacturer's description: $644nm_{EXC}/665nm_{EM}$ for Mitotracker, $358nm_{EXC}/461nm_{EM}$ for DAPI. Cells were visualised, captures obtained and analysed using a HistoRX PM-2000 AQUA (Automated Quantitative Analysis) system and an Axioplan 2 fluorescent microscope (Zeiss).

2.2.8. Analytical electrochemistry

To prepare solutions of analytes, 0.5 mg of compound in powder form was suspended in 1 mL of 100mM tetrabutylammonium hexafluorophosphate ($TBA{\cdot}PF_6$) dissolved in acetonitrile (MeCN), and the suspension was treated with ultrasound in a water bath (40°C) for 30 min. Cyclic voltammograms were acquired using a Autolab PGStat (Eco-Chemie, Utrecht) at a scan rate of 100 mV/s, using only the tenth and final scan, to estimate the reduction potential of the analytes. A saturated calomel (Hg_2Cl_2) electrode was used as a reference and a fine platinum gauze (0.1mm wire, $1cm^2$) as a counter-electrode. A straight

platinum wire (1mm diameter) was used as a working electrode, and the experiments were carried out under a blanket of argon. All analytical chemistry reagents were purchased from Sigma-Aldrich and used without further purification.

2.2.9. Measurement of ROS production

Changes in ROS signalling were first assessed using 2 plate-based methods. Each experiment included at least 2 biological replicates. For detection of changes in overall ROS levels with DCFDA (2',7'-dichlorofluorescein diacetate, Abcam) cells were grown in Phenol Red-free DMEM to prevent interference of the colour of the medium with the detection of fluorescence. Black-walled 96-well microplates were used to prevent the overlap of signals between adjacent wells. Following the manufacturer's guidelines, cells were stained with 25µM DCFDA for 45 min prior to treatment and fluorescence ($485nm_{EXC}/535nm_{EM}$) was measured in a Labsystems Fluoroskan Ascent FL (Thermo) plate reader.

For detection of hydrogen peroxide (H_2O_2) the ROS-Glo H_2O_2 plate assay (Promega) was applied following the manufacturer's guidelines. Cells were grown in Phenol Red and FCS-free DMEM to prevent interference with luminescent signals. White-walled plates were used for optimal detection of luminescence and to prevent overlap of signals between adjacent wells. Luminescence was measured in a Labsystems Fluoroskan Ascent FL (Thermo) plate reader.

Finally, mitochondrial ROS production was measured using fluorescence microscopy. For this, the method described above for fluorescence microscopy was followed with additional staining of cells with mitochondrial probes following the manufacturers' guidelines, incubating with 10µM MitoPY1[538] (Tocris) or 2.5µM MitoSOX[539] (Life) to detect mitochondrial production of hydrogen peroxide and superoxide, respectively. Fluorescent signals were quantified using the HistoRX PM-2000 AQUA system. This methodology has been described elsewhere[540]. In short, this system calculated AQUA scores by measuring fluorescence signal intensity in each pixel of a field of view capture and normalising according to the mitochondrial mask determined by the signal of Mitotracker.

2.2.10. Plate-based assays

The CellTox Green Cytotoxicity and ApoTox-Glo Triplex assay kits (both purchased from Promega) were used to measure cytotoxicity at different timepoints and to assess the mechanism of action of the drugs studied, respectively. First, 10^4 cells/well were plated in 96-well microplates. Black-walled 96-well microplates were used for CellTox assays to

prevent auto-fluorescence, while white-walled plates were used for ApoTox-Glo assays for better detection of luminescence. For both assays culture medium was changed to Phenol Red-free DMEM after 24 h to prevent quenching of signals. The protocols were carried out following the manufacturer's instructions and fluorescence and luminescence were measured in a Labsystems Fluoroskan Ascent FL (Thermo) plate reader.

2.2.11. Collection of whole-cell lysates

To prepare whole-cell lysates $3x10^6$ cells/dish were grown in $140cm^2$ Petri dishes. After treatment, cells were washed in PBS and incubated for 10min on ice in 400µL of Lysis Buffer (50mM Tris, 5mM EGTA, 150mM NaCl) containing: Complete Protease Inhibitor Tablet (Roche, 1 tablet/10mL), 1:100 of phosphatase inhibitor cocktails 2 and 3 (Sigma), 1:200 aprotinin (Sigma) and 1:100 TritonX (Sigma). Lysates were centrifuged at 13000rpm and 4°C for 6 min. Supernatants were recovered, flash-frozen and stored at -70°C.

2.2.12. Bicinchoninic acid assay

Protein concentration in cell lysates was determined by bicinchoninic acid (BCA) assay. Bovine serum albumin (BSA, G Biosciences) was used as protein standard, preparing serial dilutions (0-1000µg/mL) in distilled water (dH_2O), while aliquots of cell lysates were also diluted 1:10 in dH_2O. 1mL of a 1:50 Copper Sulfate:BCA solution was added to 50µL of each protein solution in borosilicate glass tubes. Tubes were incubated at 60°C for 15 min, allowing for a protein concentration-dependent colour change, before dispensing replicates of each solution to a 96-well microplate. OD at 540nM was measured in a BP800 Microplate Reader (Biohit) and protein concentration in each lysate was extrapolated from BSA dilutions standard curves.

2.2.13. Polyacrylamide gel electrophoresis

Cell lysates (40µg of protein in 1:4 volume of 5X Loading buffer (5% SDS, 25% 2-mercaptoethanol, 50% glycerol, 0.02% bromophenol blue, 0.04M Tris)) were denatured at 60°C for 1 h. Samples were then electrophoretically separated by polyacrylamide gel electrophoresis (PAGE) on Mini-gel equipment (BioRad), using a 3.6% polyacrylamide stacking gel and a 7.5% resolving gel and running buffer (0.1% SDS, 25mM Tris Base, 0.192M glycine). Prestained Broad Range Protein Markers (7-175kDa, New England BioLabs), were included as a standard for protein size.

2.2.14. Western blotting

Proteins were transferred to a PVDF (polyvinylidene fluoride) membrane for 90 min at a constant voltage of 100V in cold, stirred transfer buffer (25mM Tris, 0.192mM glycine). After blocking for 1 h at 4°C in BB:PBS (1:1 dilution of Odyssey Blocking buffer (Li-Cor) in PBS), membranes were incubated with primary antibodies of interest (diluted in BB:PBS) overnight at 4°C. Detection with secondary antibodies (diluted in 0.01%SDS BB:PBS) for 1h at room temperature was followed by scanning on Li-Cor Odyssey Scanner (Li-Cor). Analysis and quantification was performed using the ImageStudio software package (Image Studio Lite, version 5.2.5, Li-Cor).

Antibodies used included: mouse anti-Cleaved PARP (Poly (ADP-ribose) polymerase) mAb (Cell Signaling, 1:8000 dilution) and rabbit anti-β-tubulin (Abcam, 1:6000 dilution) as loading control. Secondary antibodies included IRDye 800CW- or 680CW-labelled goat anti-mouse and anti-rabbit Ab and IRDye 680CW-labelled donkey anti-goat Ab (all Li-Cor, 1:10000).

2.2.15. RNA processing, microarray hybridisation and data analysis

Samples were collected comprising 5 breast cancer cell lines (MCF-7, MDA-MB-231, LCC1, LCC2 and LCC9) and 2 ovarian cancer cell lines (PEA1 and PEA2) in different conditions: low (2h in 0.3μM Oncamex), high treatment (6 h in 10μM Oncamex) and vehicle control (1% DMSO 6h). Where possible, an untreated control was also included (for MCF-7 and MDA-MB-231 cells). For each sample, ~$3x10^6$ cells per cell line were treated, collected by trypsinisation and stored at -70°C.

This was part of a larger microarray experiment which also included MCF-7 and MDA-MB-231 cells exposed to different conditions, including acute (24 h in 0.5% oxygen) or chronic hypoxia (10 weeks in 0.5% oxygen).

RNA was extracted using the Qiagen RNeasy Mini kit, amplified and labelled using the Ambion Illumina TotalPrep RNA Amplification kit (in both steps as per manufacturers' instructions). Samples were then shipped to Hologic Ltd (Manchester, UK), where they were hybridised to HumanHT-12 v4 Illumina BeadChips and the arrays were scanned using an Illumina iScan. Hologic Ltd then provided the raw microarray scan result files and all further processing and gene expression analysis were performed by the author as detailed in the following section and throughout this text.

2.2.16. Differential gene expression analysis

Raw gene expression files were log2-transformed and quantile-normalised using the *lumi* Bioconductor package[541]. Raw and normalised gene expression files were deposited at the National Center for Biotechnology Information Gene Expression Omnibus[530] under the accession number GSE70949. Probes were mapped to Ensembl gene identifiers and detection-filtered using re-annotation and pre-processing approaches previously described[542]. Where necessary Emsembl identifiers were converted to official gene IDs using DAVID (Database for Annotation, Visualization and Integrated Discovery) Bioinformatics Resources 6.7[543,544]. Differentially expressed genes between control and treated samples were selected applying a ±0.4 log 2-scale threshold.

Dissimilarity heatmaps based on Pearson correlations were drawn in R using the gplots package available from the Comprehensive R Archive Network. Data from MCF-7 samples (untreated, vehicle control, low Oncamex treatment and high Oncamex treatment) were combined with MCF-7 data (vehicle control samples exposed to different DMSO concentrations and incubation times) from 2 publically available Affymetrix datasets (see section *2.1.3.*). Data from the 3 studies was normalised, re-annotated to Ensembl gene identifiers and combined, retaining only genes common to all three datasets. Possible batch differences were reduced using empirical Bayes ComBat in R, which has been validated as an appropriate method for cross-platform normalisation and batch correction[542,545].

A dimension-reducing ordination technique known as multidimensional scaling (MDS) based on all of the genes selected in the combined dataset was performed to visualise the similarity between samples in two dimensions[546,547]. The same procedure was followed to compare control and treated MCF-7 and LCC1/2/9 cells from the Illumina microarray experiment alone.

Functional enrichment analysis of differentially expressed genes was performed using the Gene Ontology Consortium[548,549], followed by processing using the REVIGO (reduce + visualize gene ontology) online tool[550] to obtain gene ontology summary graphs.

Heatmaps of differentially expressed genes were generated using log2 fold change expression values calculated between treated and control conditions for each cell line. Heatmaps were generated using TM4 microarray software suite's MultiExperiment Viewer (MeV)[551,552] for hierarchical clustering following Pearson correlation with complete linkage. The biological functions linked to each gene cluster were identified using gene enrichment

analysis as described above. Where necessary, absolute gene expression levels (in exponential scale) were used for direct comparison of expression across samples and calculation of fold changes.

2.2.17. Combination treatment studies

The effect of Oncamex in combination with other therapeutic agents was investigated in ovarian and breast cancer cell lines. The PEA1/PEA2 cell line pair was selected as a model for the study of combinatorial effects in ovarian cell lines due to their selection for chemotherapy-sensitive/resistant phenotypes. MDA-MB-231 cells were also selected as a breast cancer model to assess possible combinatorial effect. Additionally, possible synergistic effects in combination with endocrine therapy were studied in the oestrogen-independent, antioestrogen-resistant cell line LCC9, in comparison to its parent cell line MCF-7.

First, the cytotoxic effect of other agents in these models to was assessed using SRB assays. PEA1, PEA2 and MDA-MB-231 were treated with a range of concentrations of the chemotherapeutic agent paclitaxel and TNF-related apoptosis inducing ligand (TRAIL), in order to establish the differential sensitivity to these agents. Similarly, the effect of the anti-oestrogen 4-hydroxytamoxifen (OHT) in MCF-7 cells and MCF-7-derived oestrogen-independent LCC9 cells was assessed to corroborate their expected phenotype of response and insensitivity to anti-oestrogenic therapy, respectively.

In order to study combinatorial effects, concentrations in the submicromolar range of Oncamex were combined with a range of concentrations of paclitaxel/TRAIL or OHT. A series of experiments assessed the effect of different treatment schedules, comparing treatment with each compound as a single agent to combinations, including concomitant treatment with both agents or sequential incubation with one agent before the other.

2.2.18. Xenograft experiments

The xenograft studies were undertaken under a UK Home Office Project Licence in accordance with the Animals (Scientific Procedures) Act 1986. The recommended guidelines for welfare and use of animals in research were followed[553] and the studies were approved by the University of Edinburgh Animal Ethics Committee.

In the first experiment, MDA-MB-231 xenografts were implanted subcutaneously into the flanks of adult (>8 weeks) female CD-1 immunodeficient mice (from Charles River Laboratories). Each of the 2 experimental groups included 10 xenografts in a total of 6 mice, implanted in one or both flanks.

Treatment was started when mean tumour volume reached 0.25 cm^3 (Day 0) and mice were treated daily intraperitoneally with Oncamex (25 mg/kg/day) or with solvent control (10% DMSO in saline) for 2 weeks (on days 0-4 and 7-11). Changes in tumour size over 14 days were measured using Vernier callipers and volumes calculated ($V = l \times w^2/2$). Changes in mean body weight were also recorded over 14 days.

In a second experiment, mice were again implanted with MDA-MB-231 xenografts as previously described. In this case the experiment included 5 experimental groups, each including between 7 and 10 xenografts, implanted in one or both flanks of between 5 and 8 mice, depending on the group. Mice were treated intraperitoneally with either (i) solvent control, (ii) 25 mg/kg/day Oncamex, (iii) 50 mg/kg/day Oncamex, (iv) paclitaxel (10 mg/kg/week) or (v) a combination of low dose Oncamex and paclitaxel.

Treatment was administered for 2 weeks, daily for Oncamex and control treatments (on days 0-4 and 7-11) and once a week (on days 0 and 7) for paclitaxel. For high dose treatment with Oncamex the mice were treated with double the volume of the low dose Oncamex concentration, due to solubility limitations. As in the previous experiment, changes in tumour size and mean body weight were recorded periodically over the 21 days of the experiment.

2.2.19. Immunohistochemistry

Xenograft tissue was collected, fixed in formalin and embedded in paraffin before sectioning for immunohistochemistry (IHC). Sections were dewaxed in xylene for 5 min and washed in alcohol and water before incubating in heated antigen retrieval solution (0.1M sodium citrate, 0.1M citric acid ph 6). Slides were washed in PBS, incubated in 3% dH_2O_2 for 10 min and washed again in PBST (0.1% Tween-20 PBS) before incubating for 10 min in Total Protein Block (Dako).

Sections were incubated for 1 h in the primary antibody of interest, followed by 30 min in Envision labelled polymer (Dako) and 10 min in DAB (1:50 dilution in buffer, Dako), with washes in PBST between each step. Finally, slides were counterstained in haematoxylin for 1 min and taken through graded alcohols to xylene before mounting in DPX mountant medium (Sigma-Aldrich).

IHC was applied for the detection of Ki-67 (mouse monoclonal antibody, 1:300 dilution, Dako; or rabbit monoclonal antibody, 1:250 dilution, Abcam) in tissue from all xenografts in the 2 *in vivo* experiments performed. Nuclear staining was considered to obtain Ki-67 scoring in 10 representative fields of view for each section. Results are presented as percentage of

positively-stained nuclei, using the average of calculations by 3 users to ensure unbiased estimations and. The percentage of viability was assessed using the image-processing package Image J (NIH) to measure the viable areas in each section.

IHC was also used to measure the expression levels of other proteins. For this, tests were performed on sections from 3 xenografts in each experimental group (control or treated) in the first *in vivo* experiment, staining with antibodies against proteins of interest that had been previously validated in-house. These included antibodies against Cyclin B1 (rabbit polyclonal, 1:100 dilution, Abcam), Cyclin D1 (rabbit monoclonal, 1:50 dilution, BioSource), pan-c-Jun (rabbit monoclonal, 1:400 dilution, Cell Signalling), phospho-c-Jun Ser63 (rabbit monoclonal, 1:100 dilution, Cell Signalling), phosphor-c-Jun-Ser73 (rabbit monoclonal, 1:200 dilution, Cell Signalling), pan-JNK (rabbit polyclonal, 1:100 dilution, Cell Signalling), HK2 (rabbit monoclonal, 1:100 dilution, Cell Signalling), LDHA (mouse monoclonal, 1:100 dilution, Abcam) and HIF1α (rabbit polyclonal, 1:25 dilution, Cell Signalling).

IHC scores were obtained from 10 representative fields of view for each section. For proteins with a clear nuclear staining (c-Jun antibodies) the proportion of positively-stained nuclei was counted as previously described for Ki-67. For other antibodies, scores were estimated by adding a proportion score (0: no positive cells; 1: ≤1% positive; 2: 1-10% positive; 3: 11-33% positive; 4: 34-66% positive; 5: 67-100% positive) to an intensity score (0: negative; 1: weak; 2: intermediate; 3: strong) to obtain a final semi-quantitative estimation (0-8) of the expression of the protein of interest.

2.2.20. Statistical analysis

For analysis of SRB and other plate-based assays, all experiments were repeated (n≥2) and included 6 technical replicates, unless otherwise stated. Average values of blanks and day zero controls were subtracted before results were typically normalised to vehicle controls included in every experiment. Pooled normalised data from biological replicate experiments were always used for calculations and analyses.

GraphPad Prism 6 was used for statistically analysis of results from AQUA, combination treatments, gene expression, xenografts and IHC experiments. First, column statistics analysis was performed to confirm the normal distribution of data. Further analyses were performed to assess where the means of different datasets were significantly different. Unpaired *t*-tests were performed when comparing 2 different experimental groups. When comparing 3 or more groups, one-way analysis of variance (ANOVA) was used, followed by a

post hoc analysis if the test found differences between the means of these datasets. For this, a Tukey-Kramer multiple comparison test was performed to find which datasets' means were significantly different from each other, as shown by the adjusted P-values for the comparisons of all possible pairs.

3. Screening a library of novel flavonoids in breast and ovarian cancer cell lines: differential efficacy and relevant SARs

3.1. Introduction

The first stage of this project sought to screen a library of novel semisynthetic flavonoids (see *Table 7*) in order to assess their possible inhibitory effect on cancer cell line models and identify the most promising analogues for further study.

This library of compounds has been developed by Antoxis from the natural scaffold of myricetin, a flavonol with particularly promising therapeutic effects on pre-clinical cancer models (see section *1.1.5.5.1.*). Rational design from this scaffold has led to the synthesis of novel derivatives with modified structural features that aim to exploit and enhance these natural properties.

Specifically, these compounds have been designed to combine the natural therapeutic potential of myricetin with improved drug-likeness. This seeks to address the drug-likeness deficiencies often encountered in the application of natural compounds such as myricetin, which presents poor bioavailability and low cell membrane solubility, physiological instability, oxidative degradation and metabolic transformations[452,504–507].

The library of proprietary novel flavonoids developed by Antoxis presents changes in the substituents of the natural 3-ring scaffold[452,508,509]. This includes the addition of lipophilic chains reminiscent of that found in *d*-α-tocopherol (the main constituent of vitamin E[511]), which allows for a good uptake, transport and anchoring of the molecule to cell membranes (see *Figures 12* and *24*), as well as methoxylation of residues in some analogues. These novel compounds are expected to exhibit improved stability and membrane permeability in order to improve on the drug-likeness of myricetin[510].

Additionally, some of these compounds are expected to specifically target the mitochondrial compartment and present an enhanced redox potential[510]. This seeks to potentially enable further anticancer properties to these compounds, since as previously mentioned (see sections *1.1.5.3.7.* and *1.1.5.5.3.*), compounds targeting mitochondrial metabolism and oxidative status have been described as promising anticancer agents, given the central role of these organelles in the cell and the changes in mitochondrial metabolism of cancer cells[387,388].

Compound	Structure	Characteristics/Properties
Myricetin	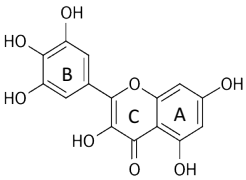	Naturally occurring flavonoid identified as particularly powerful antioxidant.
AO-1530	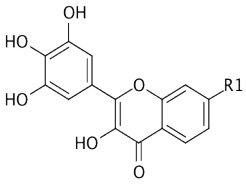	Myricetin-based novel flavonoid with active redox properties and expected mitochondrial targeting. Non-redox-active OH groups removed and a decyl chain similar to the one found in vitamin E added to improve permeability and targeting.
AO-1530-OMe (R1)		Bi-methoxylated second-generation analogue of AO-1530.
AO-1486 (R2)	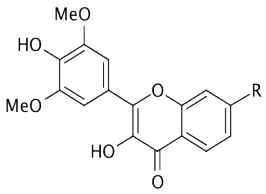	Same backbone as AO-1530-OMe, but different side chain and expected non-specific targeting.
AO-1487 (R3)		Same backbone as AO-1530-OMe, but different side chain and expected non-specific targeting.
AO-594 (R4)		Same backbone as AO-1530-OMe, but different side chain and expected weaker specificity for the mitochondrial compartment.
AO-155-179	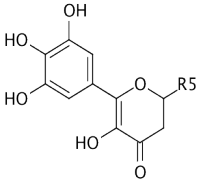	Similar backbone to that of AO-1530 but one of the fused rings has been removed, leaving a less flavonoid-like structure.
AO-714A	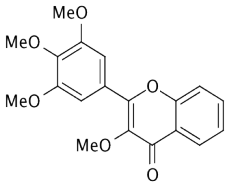	Fully blocked redox activity.

Radicals: R1, $(CH_2)_9$-CH_3; R2, $(CH_2)_3$-NH-$(CH_2)_4$-NH_2; R3, CH_2-(C_6H_8)-NH_2.HCl; R4, H; R5, $(CH_2)_{10}$-CH_3

Table 7 ***Library of novel flavonoids.*** *A library of 8 compounds was screened for their antitumour properties. The addition of different moieties and radicals granted distinctive redox potential and intracellular targeting to the 7 novel flavonoids included in the study.*

The library studied includes 7 novel compounds with slight variations in their structure. Among them is first generation AO-1530, which incorporates changes in its substitutions and a 7-alkyl chain. From this, a series of second-generation analogues presenting methoxylated residues and different chains have also been designed (see *Table 7*).

Previous work with this library of compounds has focused on the cytoprotective ability of first-generation novel flavonoid AO-1530, particularly for its application to confer protection against acute oxidative stress in both human neuronal and mouse embryonic stem cell models[510,515].

However, only preliminary unreported work has assessed the possible application of these compounds in the treatment of cancer. Limited tests have looked at the effect of AO-1530 in glioma and renal cancer cell line models, while the intracellular targeting of some other compounds in the library has been assessed in renal cancer cells (see *Supplementary Figures 10-13*).

Thus, this project aimed to investigate the possible antitumour abilities of a library of these new chemical entities, specifically in breast and ovarian cancers and aimed to gain a better understanding of the possible mechanism of action and the best potential application of these agents.

This first chapter aims to study the effects of this library of compounds in 3 panels of cell lines. This seeks to evaluate their efficacy as potential anticancer agents and identify the most promising analogues that may be subsequently studied in more detail in the following chapters. Comparison of the potency of the effects which different analogues may exert will also allow for the identification of some of the structural modifications contributing to these abilities.

3.2. Effect on a panel of breast cancer cell lines

3.2.1. Study on a first panel of cell lines

The first stage of the project studied the effect of the library of flavonoids described on breast cancer cell line models. For this, a series of SRB assays were carried out to determine the drug-induced cytotoxic effect of these compounds on a first panel of 4 breast cancer cell lines corresponding to different molecular subtypes: MCF-7, MDA-MB-231, BT-549 and HBL-100 (see *Table 5*). Testing of concentrations in the micromolar range (between 0.01µM and 100µM) produced concentration-response curves reflecting the concentration-dependent effect of these compounds (see *Figure 14* and *15*).

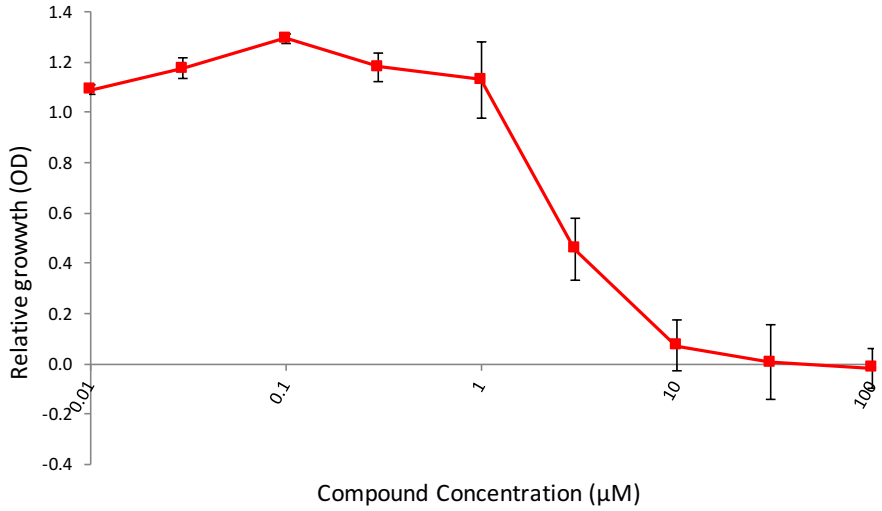

***Figure 14* Antiproliferative effect of AO-1530 on MCF-7 cells.** *Graph shows a typical example of the tests repeated for each compound and cell line in the panel. Each experiment was repeated (n=2, with 6 technical replicates for each concentration). This graph shows the effect of 96 h treatment with AO-1530 from a representative experiment, normalised to the vehicle control. Each data point represents the average of 6 technical replicates for each treatment condition in this biological repeat, with error bars representing standard deviation (SD).*

Treatment with concentrations in the micromolar range of all novel flavonoids reduced cell density below the initial levels before treatment. This is reflected by the negative values in relative growth, as a result of the subtraction of the 'Day 0' controls (see *Figure 15*). This "negative growth" suggests that the reduction in cell growth is not only due to the arrest of cell proliferation, but that the induction of cell death might also be involved. The mechanisms involved in this antiproliferative effect will be discussed in detail in the next chapter.

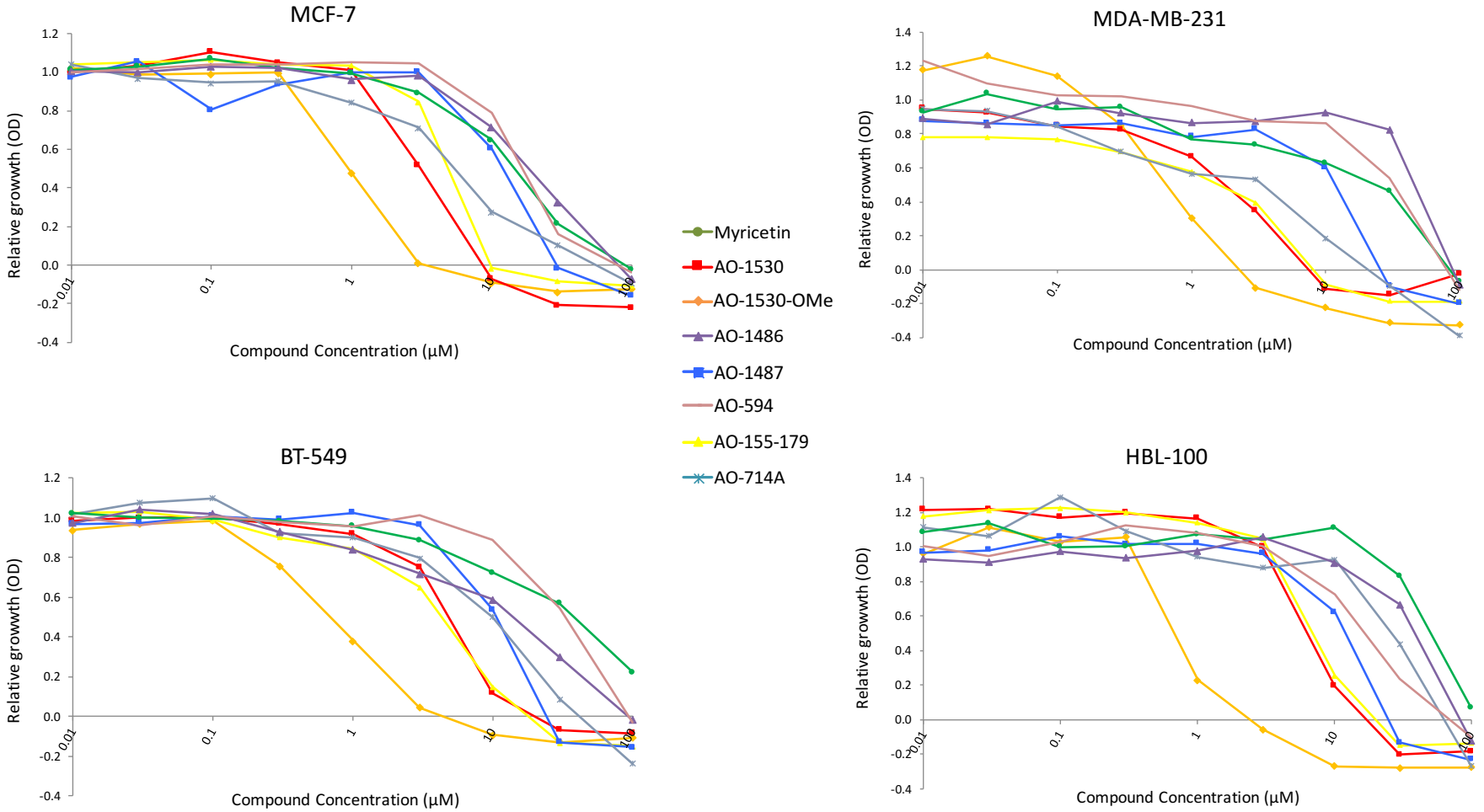

Figure 15 ***Summary of the effect of compounds in the library of novel flavonoids on a panel of 4 breast cancer cell lines.*** *Graphs represent the concentration-dependent growth-inhibiting effect of treatment with each compound for 96 h. Each experiment was repeated (n=2, with 6 technical replicates per concentration). These graphs show pooled results, with each data point representing the average from biological replicate experiments for each treatment condition, normalised to vehicle controls.*

In order to quantify the antiproliferative properties of these compounds, these results were used to calculate the half maximum inhibitory concentration (IC_{50}) of each compound for all 4 cell lines (see *Table 8*). The calculation of IC_{50} values allowed for the ordering of the analogues according to their potency on each cell line for a clearer assessment of the effect of the less potent agents (see *Table 9*).

	MCF-7	MDA-MB-231	HBL-100	BT-549
Myricetin	14.27	18.99	41.37	39.88
AO-1530	3.15	1.80	6.61	4.84
AO-1530-OMe	0.99	0.67	1.04	0.72
AO-1486	19.47	63.37	40.70	13.09
AO-1487	11.78	11.61	11.59	10.39
AO-549	16.37	30.87	17.09	32.81
AO-155-179	4.59	1.79	7.25	4.10
AO-714A	5.56	1.61	28.80	9.45

***Table 8* Half maximum inhibitory concentration (IC_{50}, in µM) of each compound in the library for the 4 breast cancer cell line models.** *Results show the growth-inhibiting effect of different compounds in the library, from pooled data combining results from biological replicate experiments (n=2, with 6 technical replicates for each treatment condition).*

	More potent > > > Less potent							
MCF-7	AO-1530-OMe	AO-1530	AO-155-179	AO-714A	AO-1487	Myricetin	AO-594	AO-1486
MDA-MB-231	AO-1530-OMe	AO-714A	AO-155-179	AO-1530	AO-1487	Myricetin	AO-594	AO-1486
HBL-100	AO-1530-OMe	AO-1530	AO-155-179	AO-1487	AO-594	AO-714A	AO-1486	Myricetin
BT-549	AO-1530-OMe	AO-155-179	AO-1530	AO-714A	AO-1487	AO-1486	AO-594	Myricetin

***Table 9* Comparison of relative potency between compounds across cell lines.** *Compounds are presented in hierarchical order according to the IC_{50} concentrations calculated for comparison of the potency of the growth-inhibiting effect of different novel flavonoids.*

All of the 8 compounds tested (see *Table 7*) exerted antiproliferative effects in the range of concentrations applied, with comparable results across the 4 cell lines initially studied (see *Figure 15*). However, comparison of the concentration-response curves and the IC_{50} concentrations obtained showed variation in the potency of these effects between compounds (see *Tables 8* and *9*).

Among the compounds assessed the second-generation bi-methoxylated analogue AO-1530-OMe exhibited the strongest antiproliferative effect on all 4 cell lines studied. This surpassed the potency of first-generation compound AO-1530, which bears the same structure except for the lack of methoxy residues on its B ring (see *Table 7* or *Figure 23*).

Compounds AO-714A (fully methoxylated and lacking a side chain) and AO-155-179 (non-methoxylated and presenting a different poly-ring backbone) exerted effects similar to those of AO-1530, with IC_{50} concentrations in the low micromolar range (see *Tables 8* and *9*). The remaining compounds, AO-1486, AO-1487 and AO-594, which present the same structure as AO-1530-OMe except for the inclusion of different side chains in the 7 position, exerted weaker effects, with IC_{50} values much closer to those of the natural myricetin.

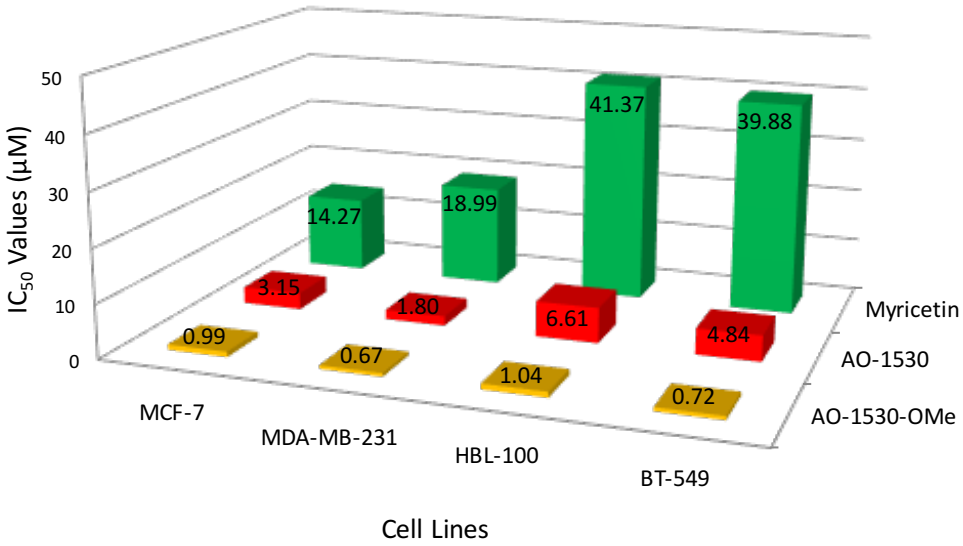

Figure 16* IC_{50} *values for myricetin, AO-1530 and AO-1530-OMe on breast cancer cell lines. *Visual representation for comparison of the different potency of the growth-inhibiting effects of the natural compound and both first and second-generation novel flavonoids, as quantified by the IC_{50} concentrations calculated from pooled data combining results from biological replicate experiments.*

Overall, these results suggest that at least some of the novel flavonols in the library studied successfully improved on the antiproliferative properties of the natural compound. AO-1530-OMe appeared as the most promising agent in the library, as it presented the

lowest IC_{50} concentrations for all 4 cell lines studied. Comparatively, myricetin had values between 15 and 55 times larger than those of AO-1530-OMe (see *Figure 16*). Given this stronger efficacy, AO-1530-OMe was selected as the lead candidate for the study of its effect and mechanism of action throughout the rest of the project, often alongside its first-generation analogue AO-1530 and the natural compound myricetin.

Although a number of factors might influence the actual therapeutic value of this compound *in vivo*, the structural features in AO-1530-OMe appear to confer the best antiproliferative abilities of the compounds in the library, whereas other analogues exerted weaker and less consistent effects. Observations on the possible structure-activity relationships involved in the differential effects of the compounds in this library will be discussed in further detail in the following paragraphs (see section *3.4.*).

Interestingly, results suggest that the apparent antiproliferative effect of these novel flavonoids, and AO-1530-OMe in particular, in breast cancer cell line models is independent of their hormone receptor status. This is evidenced by the ER^+ model (MCF-7) showing similar responsiveness to treatment as the TNBC models (such as MDA-MB-231). The following sections will study whether this broad effect across breast cancer subtypes is recapitulated in other cancer subtypes and types, particularly ovarian cancer.

3.2.2. Study on a panel of oestrogen-independent cell lines

Following the results on the panel of 4 breast cancer cell lines, the effect of the most potent compounds was tested on a group of MCF-7-derived, oestrogen-independent cells: LCC1, LCC2 and LCC9 (see *Table 5*). Work on these cell lines focused only on AO-1530-OMe, its first-generation analogue AO-1530 and the original natural compound myricetin as a reference for relative comparison of the novel agents' efficacy and the cell lines' responsiveness to treatment in general.

Although the first results reported in the paragraphs above suggested the effect of the novel flavonoids studied may not depend on oestrogen-signalling, this is not to say that the apparent broader effect of AO-1530-OMe on breast cancer models could not be suitable for its application in cancers that have developed resistance to endocrine treatment. As the development of resistance to endocrine treatment is a common obstacle in the clinical management of the disease (see section *1.1.4.1.*), novel therapeutic approaches that may offer alternative treatment strategies or improve responsiveness to standard-of-care treatments are an important necessity.

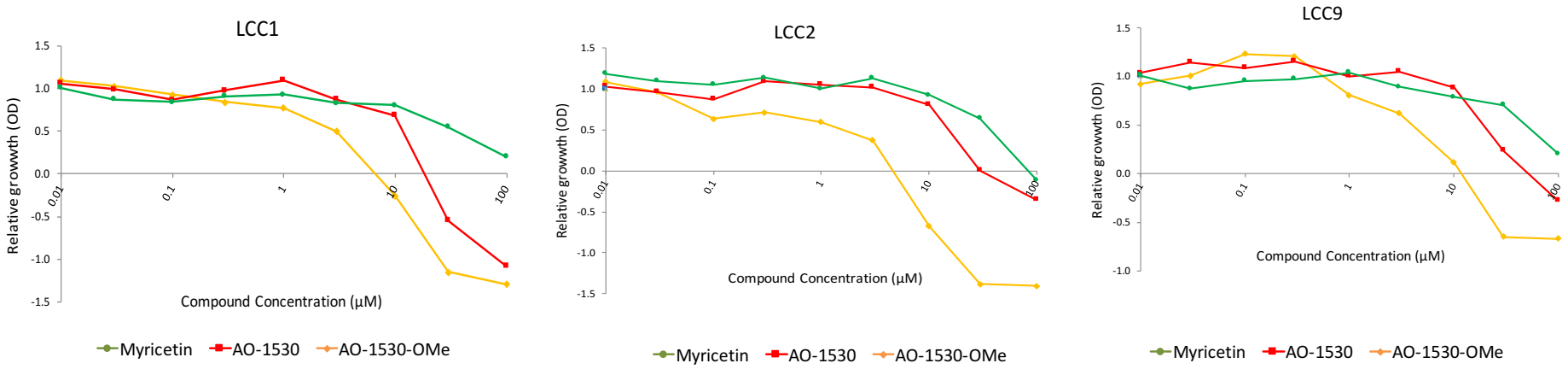

Figure 17 ***Effect of myricetin, AO-1530 and AO-1530-OMe on LCC1, LCC2 and LCC9 cells.*** *Graphs report the concentration-dependent growth-inhibiting effect of treatment with each compound for 96 h. Each experiment was repeated (n=2, with 6 technical replicates per concentration). These graphs show pooled results, with each data point representing the average from biological replicate experiments for each treatment condition, normalised to vehicle controls.*

Results from proliferation assays showed a recapitulation of the previous results. Second-generation analogue AO-1530-OMe exerted the strongest antiproliferative effect, followed by AO-1530, and both novel analogues improved on the efficacy of myricetin (see *Figure 17*).

These cells appeared to be less responsive to treatment with any of the compounds in comparison to MCF-7 cells, from which they were derived (see *Figure 18*). Indeed, the IC_{50} values for AO-1530-OMe were between ~2 and ~4 times larger than those for MCF-7, a larger ratio than that observed between other breast cancer cell lines.

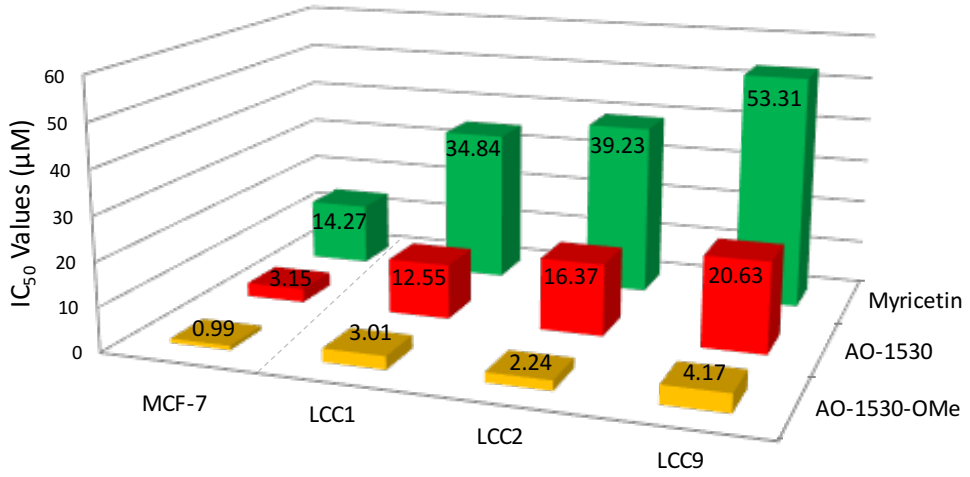

***Figure 18* Half maximum inhibitory concentrations (IC_{50}) for myricetin, AO-1530 and AO-1530-OMe on oestrogen-dependent and independent cell lines.** *Values show the different potency of the growth-inhibiting effect of the natural compound and both first and second-generation novel flavonoids on original MCF-7 cells and MCF-7-derived oestrogen-independent cells. Each value was obtained from pooled data combining results from biological replicate experiments.*

These cells have been selected for their oestrogen-independent (for all 3 cell lines) and antioestrogen-resistant (for LCC2 and LCC9) phenotypes (see *Table 5* for detailed description of cells' origin and characteristics[523–525]). Consequently, these cells are more recalcitrant than MCF-7 cells and could be expected to be more resistant not only to antioestrogen therapy but also other treatments. As previously discussed, evidence has suggested that the same mechanisms can be involved in the development of resistance to different therapeutic strategies (see section *1.1.4.1.*).

Interestingly, in comparing the effect of AO-1530-OMe among the 3 oestrogen-independent cell lines, LCC9 cells appear to be the least sensitive to all compounds tested (see *Figures 18* and *19*). These cells present the most recalcitrant phenotype, as they are both oestrogen-independent and resistant to 2 different antioestrogen therapies (tamoxifen and fulvestrant, despite having been obtained by selecting only for fulvestrant resistance). This further supports the notion that inherent mechanisms of resistance to an agent could also hinder the effect of AO-1530-OMe on cancer cells. Nevertheless, AO-1530-OMe still exhibited a potent antiproliferative effect, successfully improving on the ability of natural myricetin, which provides an encouraging basis for its potential application in this niche population of resistant cancers.

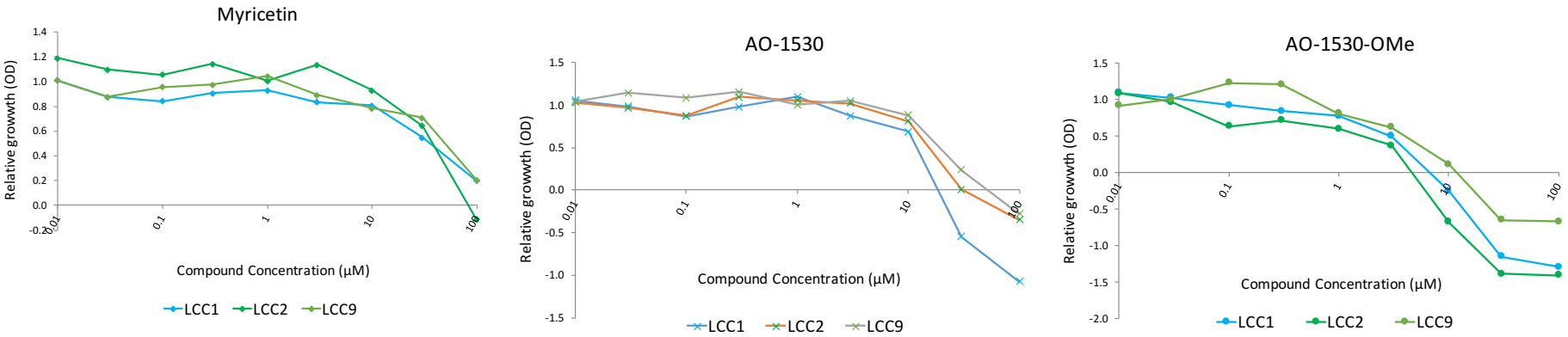

Figure 19 ***Comparison of the effect of myricetin, AO-1530 and AO-1530-OMe on oestrogen-independent cell lines.*** *Graphs report the concentration-dependent growth-inhibiting effect of treatment with each compound for 96 h, as previously shown. Here the effect of each compound in each of the 3 cell lines is presented together for direct comparison of the differential responsiveness of these oestrogen-independent cell lines.*

3.3. Effect on a panel of ovarian cancer cell lines

The efficacy of novel flavonoids was also studied on a panel of ovarian cancer cell lines in order to assess the possible application of these agents in a different cancer type. As in the case of oestrogen-independent breast cancer cell lines, this experimental section focused only on lead compounds AO-1530-OMe and AO-1530 and the natural product myricetin.

Ovarian cancer is a suitable model following its similarities with breast cancer, such as the role hormonal regulation can play in its development and progression. Like many other cancer types, it also presents common obstacles in its clinical management that need to be addressed, particularly the appearance of resistance to treatment. Furthermore, ovarian cancer has been a field of study of previous attempts to develop novel flavonoids as therapeutic alternatives, as previously discussed (see section *1.1.5.5.2.*).

Results showed the same trends observed in breast cancer models, with all 3 compounds exerting anti-proliferative effects at the 96 h timepoint (see *Figure 21*). Both novel flavonoids improved on the efficacy of myricetin and AO-1530-OMe exerted the strongest effect, with IC_{50} concentrations between ~4 and ~46 times smaller than those for myricetin (see *Figure 20*). These values were comparable to those determined for the initial panel of breast cancer cell lines, also in the low or sub-micromolar concentration range.

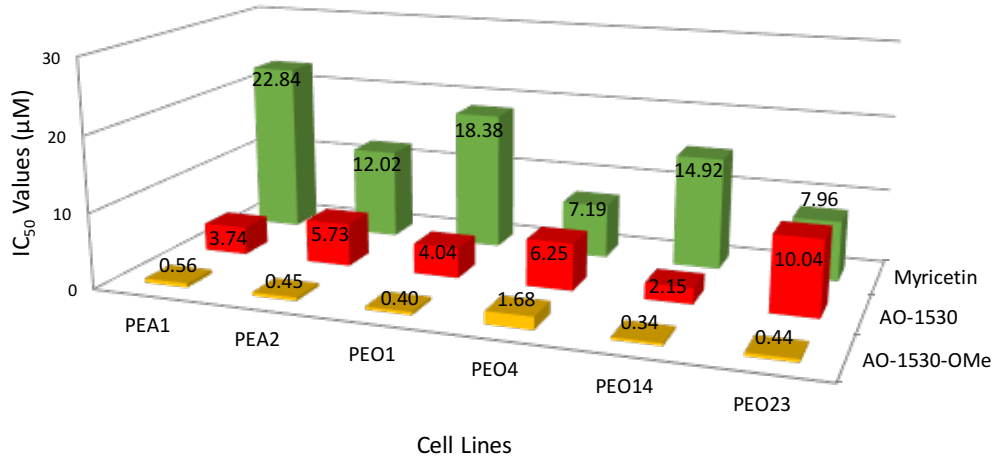

***Figure 20* Half maximum inhibitory concentrations (IC_{50}) for myricetin, AO-1530 and AO-1530-OMe on ovarian cancer cell lines.** *Values show the different potency of the growth-inhibiting effect of the natural compound and both first and second-generation novel flavonoids on chemotherapy-sensitive and resistant ovarian cancer cell lines. Each value was obtained from pooled data combining results from biological replicate experiments.*

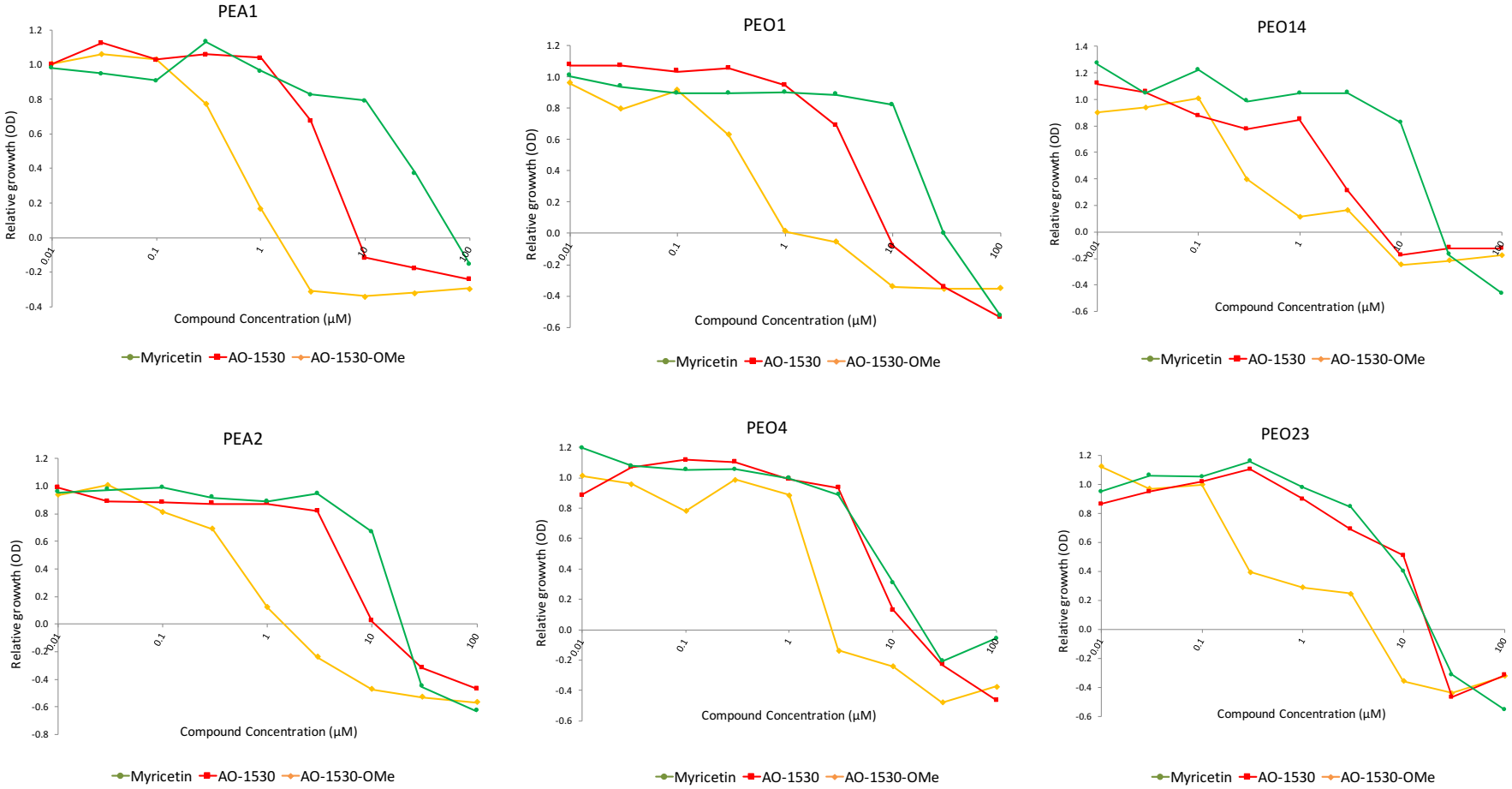

Figure 21 ***Effect of myricetin, AO-1530 and AO-1530-OMe on ovarian cancer cell lines.*** *Graphs report the concentration-dependent growth-inhibiting effect of treatment with each compound for 96 h. Each experiment was repeated (n=2, with 6 technical replicates per concentration). These graphs show pooled results, with each data point representing the average from biological replicate experiments for each treatment condition, normalised to vehicle controls.*

The panel studied included 3 pairs of cell lines, each of them consisting of a serous adenocarcinoma cell line of different origin and a variant cell line selected for a phenotype of resistance to chemotherapeutic agents (see *Table 6*). This allowed for interesting observations in terms of the relative potency of AO-1530-OMe on the cells of each pair.

Interestingly, the effect exerted by AO-1530-OMe was comparable for both chemo-sensitive and chemo-resistant cell lines in the PEA1/PEA2 and PEO14/PEO23 pairs, with very similar IC_{50} concentrations. For the other cell line pair, the resistant cell line (PEO4) exhibited lower responsiveness to treatment with both AO-1530-OMe and AO-1530 than its respective sensitive parent cell line (PEO1) (see *Figure 20*). Indeed, the IC_{50} for AO-1530-OMe was more than 5 times larger in chemotherapy-resistant cells. This recapitulates the previous observations on breast cancer cell lines, which demonstrated the lower susceptibility to treatment in cells already resistant to another form of treatment.

On the contrary, the opposite trend was observed in the case of myricetin, as treatment with the natural flavonol appeared to be more effective against chemotherapy-resistant cells. Despite this, the antiproliferative ability of AO-1530-OMe was still considerably stronger than that of myricetin in both chemo-resistant (between 4 and 27-fold lower IC_{50} concentrations) and chemo-sensitive (between 41 and 46-fold) cells, suggesting the possible application of the former in these cancers should this efficacy translate into a therapeutic effect *in vivo*.

3.4. Structure-activity relationship observations

The novel compounds tested in this project have been designed from the natural scaffold of myricetin to combine its redox ability and therapeutic potential with structural features that may enhance its drug-likeness and possible *in vivo* activity. This sought to address issues such as poor bioavailability and low membrane solubility[504,505], common to many natural flavonoids.

Modifications have included the optimisation of the redox properties of novel compounds and the incorporation of new moieties and chains (see *Table 7* and *Figure 23* for structures). These changes have yielded a library of novel compounds with potentially enhanced redox reactivity, bioavailability and mitochondrial targeting.

The previous sections have reported on the efficacy of these different novel chemical entities as antiproliferative agents: of the library studied AO-1530, previously identified as the most potent myricetin analogue to date, shows strong antiproliferative effects and, in particular, its second generation bi-methoxylated analogue AO-1530-OMe has proved to be an even stronger candidate compound. Indeed, this was the most potent of all compounds in the treatment of all cell lines studied, with IC_{50} values between ~4 and ~46 times smaller than those for the natural compound myricetin.

The differences in the effect exerted by these and other compounds with a similar backbone on a panel of breast cancer cell lines (see section *3.2.1.*) allowed for the identification of possible structure-activity relationships (SARs), i.e., specific moieties or structural features influencing the anticancer efficacy of novel flavonoids. This section will analyse these differences in the potency of compounds in the library to identify relevant SARs and discuss them in the context of the literature on flavonoids chemistry which supports the rational design of this novel library.

3.4.1. OH groups and redox reactivity

The redox potential of flavonoids is due to their highly-conjugated poly-ring scaffold, which creates extensive conjugated π-electron systems that allow for ready donation of electrons or hydrogen atoms from the hydroxyl moieties to free radicals[306]. The library of compounds studied was designed to enhance these properties, following existing knowledge on the contribution of different structural features to the redox ability of flavonols.

As previously discussed, myricetin has demonstrated particularly powerful redox properties *in vitro*. It has been shown to be more readily reduced and to have better reaction

kinetics and stoichiometry than many other flavonoids with redox abilities[307,452]. Previous research has linked the particularly strong reactivity of myricetin to the conjugation of OH groups on the flavonoid B and C rings. In particular, the presence of the 4'-OH group (believed to be the best hydrogen atom donor[452]) and of the 3-OH group attached to the 2,3-double bond and adjacent to the 4-cabonyl in the C ring have been linked to optimum redox reactivity[554]. This way, the substitution with electron-donating groups allows for an electronically extended conjugated system with a diffuse π orbital in which electrons are delocalised and can be more readily donated.

Modelling of the highly occupied molecular orbital (HOMO) of myricetin supports these observations (see *Figure 22*, from previously unreported data). This model shows the predicted distribution of the electrons with the highest energy level, which are the most readily available for donation and thus the most relevant to the redox ability of a compound.

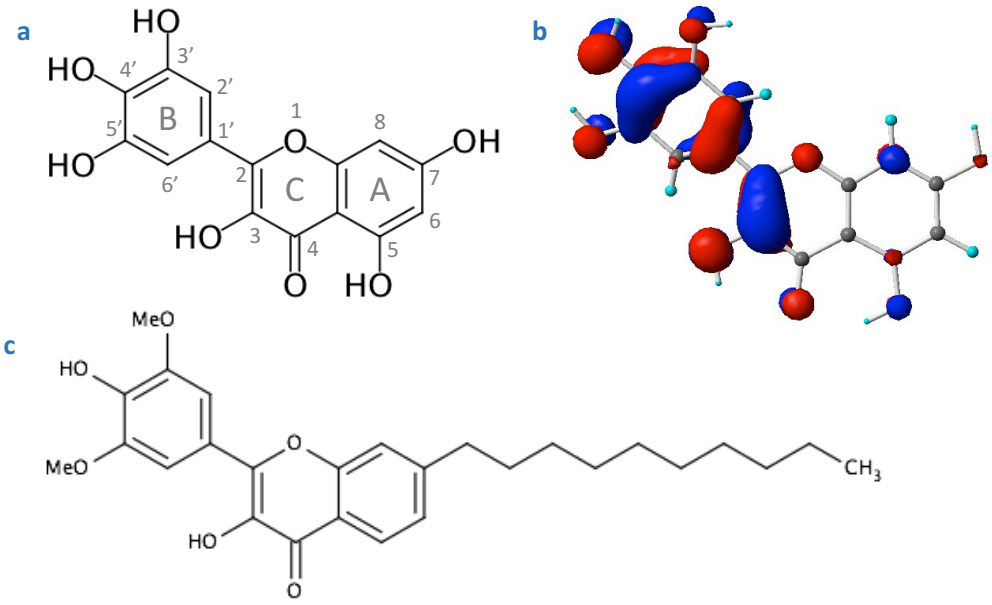

***Figure 22* Predicted highest occupied molecular orbital (HOMO) for myricetin.** *Natural scaffold of myricetin (*a*) and its predicted HOMO distribution (*b*). This model (obtained using the Gaussian chemistry modelling program) represents the distribution of the orbital containing the outermost electrons, which occupy the highest energy level and are easiest to donate. These more readily accessible electrons are the ones of relevance to the redox activity of the compound. This distribution is likely to be recapitulated in the myricetin-based novel flavonoid AO-1530-OMe (*c*). Image courtesy of Donald McPhail (Antoxis), from previously unreported studies.*

This model suggests the importance of the B and C rings and their substitutions, but not the A ring, to the potency of myricetin as a redox active compound and, consequently, as a

potential therapeutic agent. Indeed, the B and C rings appear to contribute significantly to this molecular orbital, particularly the OH substitutions and the presence of the 2-3 double bond. This model also supports the notion that the 4'-OH group would be the most important electron-donating group among the B ring substitution, most likely due to its position in the aromatic ring[555]. This distribution is likely to be similar to that of novel flavonoid in this library, based on the myricetin scaffold.

In the context of the library of novel flavonoids studied, the 4'-OH group is conserved in all but one compound (the fully methoxylated analogue AO-714A), while the OH groups in the 3' and 5' positions are present in AO-1530 but replaced by methoxy groups (OMe) in AO-1530-OMe and other analogues. The presence of more OH groups in the 3' and 5' positions of the B ring may aid the ability of 3 and 4' to donate electrons. However, other substitutions may provide more beneficial properties to the structure without blocking the reactivity provided by 4'-OH and 3-OH, as will be discussed in the next paragraphs.

The A ring and its substituents appear to be less relevant to the redox reactivity, given the distribution of conjugation in the molecule. Indeed, results reported here suggest that the removal of the 5-OH and 7-OH groups in the design of novel flavonoids did not lead to a reduction in their efficacy when compared to that of myricetin. The removal of these moieties would mean an improvement in the drug-likeness of the compounds by reducing the number of H-bond donors[499] and would enhance their lipophilicity by (i) avoiding the presence of hydrophilic OH groups in the A ring and (ii) also allowing for the beneficial addition of a lipophilic side chain in the 7 position, as will be further discussed in this chapter.

3.4.2. OMe substitutions

A second structural modification of relevance in this library of novel flavonoids is the incorporation of methoxy moieties (OMe) , a functional group not found in the original myricetin scaffold, in their structure. The most potent compound in the library, AO-1530-OMe, presents two of these substitutions in the 3' and 5' positions. This supports the notion that, although OH groups in those positions would probably contribute more to the strong redox ability of the molecule, substitution with other groups may provide ultimately more beneficial properties. In this case, methoxy groups in the 3' and 5' groups would also be expected to be electron-donating groups[555], although weaker than OH groups. More importantly, these substitutions would improve the drug-likeness of the molecule by further reducing the number of H-bond donors[498,499].

Additionally, methoxy residues may improve the efficacy of these novel flavonoids by enhancing their pharmacokinetic properties and increasing their stability. Indeed, methoxylated compounds are less prone to modifications such as glucuronidation and sulfation, and are consequently more chemically and metabolically stable[341]. It has been suggested that methoxylation improves the cell uptake and selectivity for cancer cells of flavonoids[556,557]. Researchers have also shown that methoxylation can improve solubility and prevent both metabolic conjugation and auto-oxidation in the mitochondria[405,558]. Added to improved uptake and membrane transport, such alterations may contribute to an increased bioavailability of these compounds[336,559].

Furthermore, as previously discussed (see section *1.1.5.4.3.*), it has been reported that, upon cell delivery, methoxylated compounds are targeted by tumour-specific O-demethylases that provide free hydroxyl groups and hence an increase in redox properties[336,560]. Thus, these novel methoxylated flavonoids, represented by lead analogue AO-1530-OMe, may benefit from the presence of methoxy residues which improve the delivery and biostability of the compound without necessarily hindering its subsequent anticancer properties.

Interestingly, previous research has suggested that the number and location of methoxy substitutions can influence differently the various properties observed in flavonoids. For instance, it has been reported that they may have unfavourable steric effects, compromising redox-modulating and Cytochrome P450 (CYP1)-inhibitory capabilities[336,561], while the extent of the BCRP-inhibitory properties of flavonoids also depends on the number and location of these modifications [346,358,470]. Nevertheless, results reported in this chapter have suggested that the presence of methoxylations did not hinder the antiproliferative ability of compounds, but rather may enhance them, as AO-1530-OMe has been highlighted as the most potent novel flavonoid in the library.

It is worth noting that other compounds in the library besides AO-1530-OMe also present methoxy residues: AO-1486, AO-1487 and AO-594 present the same substitutions as the lead compound with different chains in the 7 position, while AO-714A is a fully methoxylated compound bearing no side chain (see *Table 7* or *Figure 23* for structures).

AO-1486, AO-1487 and AO-594 were observed to exert the weakest effects of all 7 novel flavonoid tested in most breast cancer cell line models, with IC_{50} values much closer to those of myricetin (see *Tables 8* and *9*). This suggests that, while the bi-methoxylation in AO-1530-OMe enabled a stronger efficacy than the fully-hydroxylated but otherwise identical AO-

1530, the side chain added to these molecules is one of the most determining factors for their antitumoural activity. The relevance of these chains will be discussed in the next section.

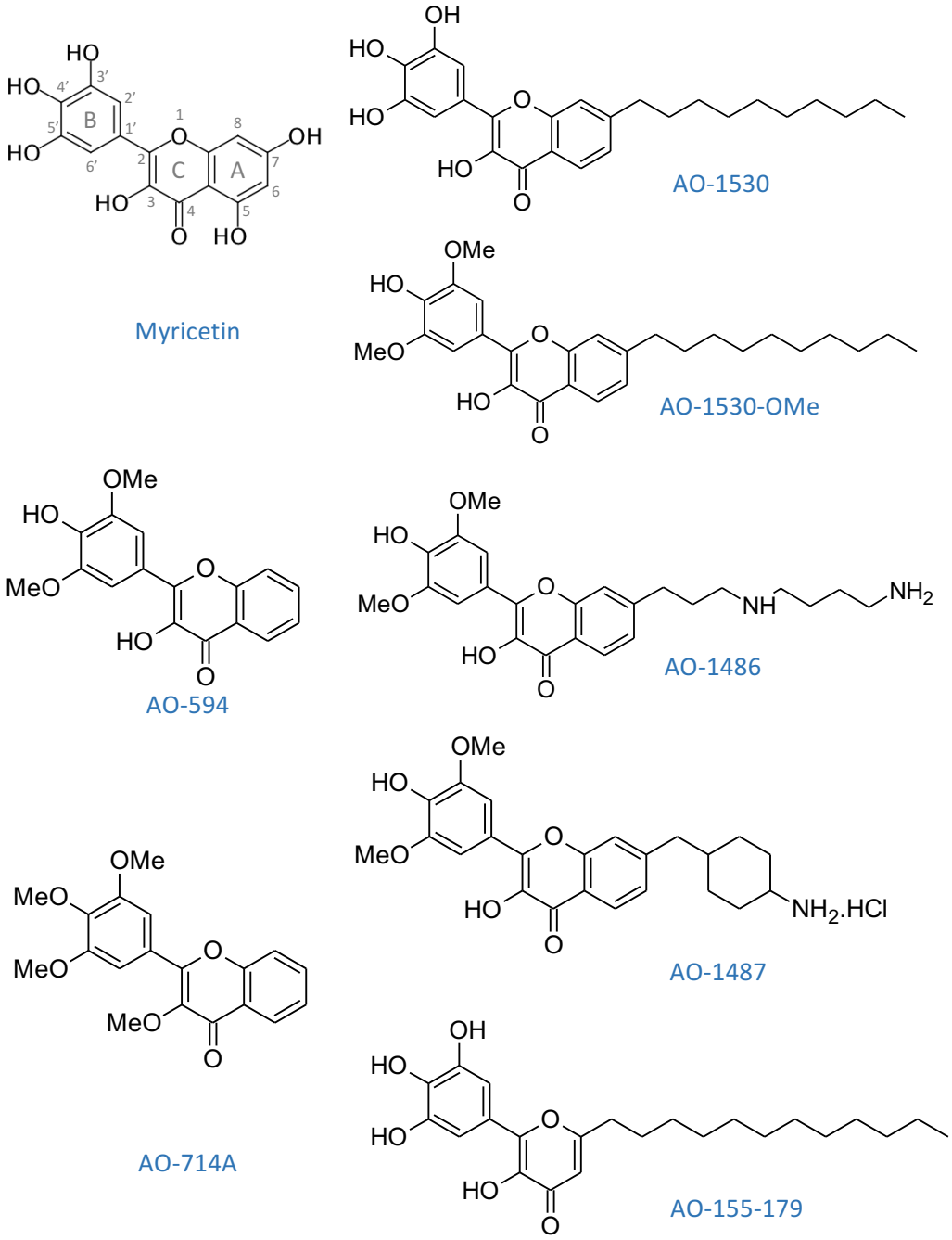

***Figure 23* Full structures of the novel flavonoids studied.** *The natural structure of myricetin was used as a backbone, removing OH groups on position 5 and 7 and adding methoxylation residues and side chains in different positions to generate a library of new chemical entities.*

Interestingly, the fully methoxylated molecule AO-714A showed a relatively potent antiproliferative effect on the models studied: while not as strong as the lead compound, AO-714A had generally low IC_{50} values in comparison to myricetin and other less potent analogues (see *Tables 8* and *9*). AO-714A may benefit from an improved biostability granted by the methoxylations in its structure, but its case is particularly interesting, given the absence of any redox-active OH groups or side chains that could improve the redox ability or delivery of the drug.

Regarding the limited expected redox reactivity of AO-714A, its antiproliferative effect can be interpreted in two ways. The relative efficacy of the compound could suggest that different, redox-independent mechanisms might be involved in the anticancer effects of some of these novel flavonoids. In fact, AO-714A presents methoxy groups in the 3, 3', 4' and 5' positions, reported as structural features that significantly increase some of the anticancer activity of flavonoids[346,358]. The pleiotropic effect of flavonoids has been previously reviewed (see section *1.1.5.*) and, for instance, myricetin has been previously noted to induce oxidative phosphorylation-independent cell death[259].

On the other hand, it can be argued that the fact that AO-714A is not rendered completely inactive by the lack of OH groups further supports the notion that flavonoids may not require free hydroxyl groups *per se* to be active anticancer agents due to their propensity to undergo demethylation by O-demethylases in the cells[336]. As mentioned above, previous research has suggested that upon cell delivery the methoxylations present in the structure of AO-714A could be converted into OH groups, providing the compound with an active redox profile.

The effect of AO-714A is also interesting in comparison to that of AO-594, which only differs in the presence of an OH group in the 4' position but also presents no side chain in the 7 position. Although the lack of a lipophilic chain most likely limits the efficacy of both these analogues, AO-714A exerts a stronger effect than AO-594. This once again suggests that, while these chains are relevant to the biological efficacy of the drug, in compounds with the same side chain the addition of methoxy substitutions appears to provide an advantage.

3.4.3. Side chains

A third major consideration in the design of these compounds was the addition of different side chains. As previously mentioned, AO-1530 and its second-generation analogue AO-1530-OMe present a decyl straight chain in the 7 position reminiscent of that in vitamin

E (see *Figures 12* and *24*). Vitamin E is a key antioxidant *in vivo* due to the combination of its scavenging properties with said hydrophobic chain, which allows for effective membrane anchorage[562].

Previous research has studied the effect of variations in the tail length and position in the structure, assessing the antioxidant abilities of novel flavonoids as an indication of their efficacy and bioactivity[509]. Changes in chains have been shown to influence the potency of novel flavonoids by altering their lipophilicity and orientation of the head group (the flavonoid scaffold) and, consequently, their membrane permeability and bioavailability.

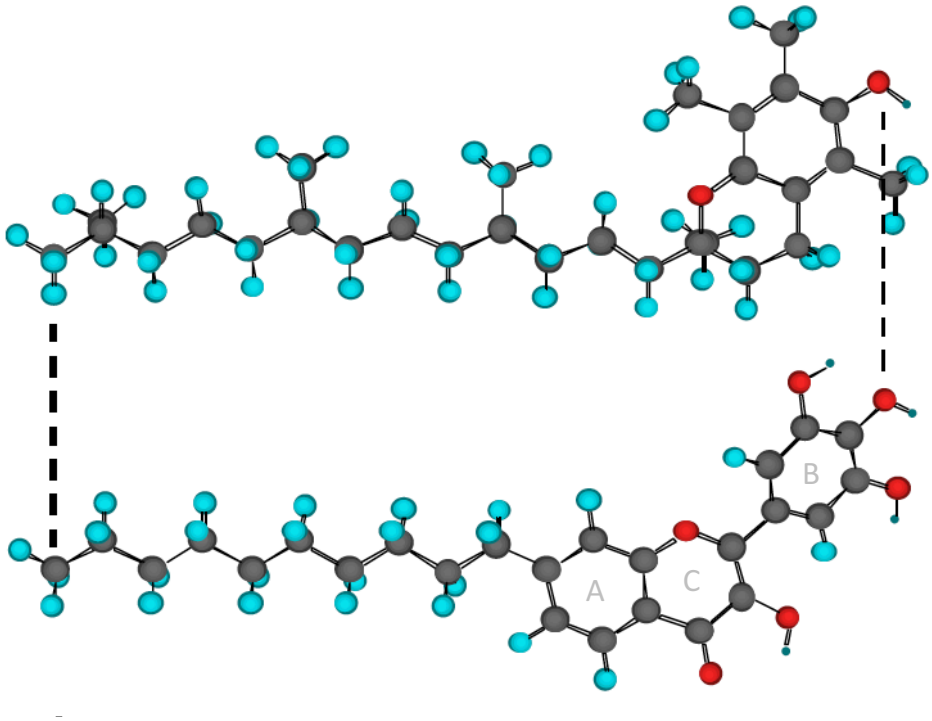

***Figure 24* Alignment of the structure of AO-1530 with that of vitamin E.** *Chem3D molecular mechanics (MM2) force field modelling of d-α-tocopherol (above) and AO-1530 (below). Figure adapted from Bennett* et al *(2004)*[452].

Previous results had reported optimum redox reactivity for compounds with chains ranging between 8 and 10 C atoms in length[452]. The structure of lead compound AO-1530-OMe follows this work, which showed the candidates with the most promising redox reactivity were 7-alkylflavonoids, in which the 7-OH group was substituted by an alkyl chain of similar length to that of vitamin E, particularly when a straight 10-C alkyl chain was added (see *Figure 24*)[452]. Vitamin E presents a 12-C, branched alkyl chain which could provide a slight advantage in terms of better lipophilicity but can produce different stereoisomers. Thus, a shorter, a straight decyl chain like the one in AO-1530 and AO-1530-OMe might

present a slightly lower lipophilicity but would reduce the chiral possibilities of a more complex, branched chain, making the compound bearing it more drug-like.

In terms of the position where the side chain is inserted, it has been reported that the addition of a decyl chain in the 7 position of a novel flavonoid would cause a good alignment of the structure of the flavonoid with that of vitamin E. This includes the redox active 4'-OH group (believed to be the best hydrogen atom donor in the flavonoid scaffold[452]) being orientated favourably like the OH group in natural vitamin E when anchoring the membrane, hence further improving the permeability and bioavailability of the novel flavonoid (see *Figure 24*)[452]. The addition of chains in other positions led to reduced efficacy despite similar redox reactivity and lipophilicity[452], highlighting the influence of orientation on the bioactivity of compounds.

In short, results from the study of the library of flavonoids in breast and ovarian cell line panels support the relevance the addition of a side chain in the 7 position can have to the efficacy of these novel compounds. The presence of a straight decyl chain in particular appears to provide the greatest advantage, with AO-1530-OMe exhibiting the strongest antitumour properties, which is supported by previous evidence. As a 7-alkylflavonol, it presents an optimum, achiral chain that may enable improved membrane permeability and orientation, thus enhancing the delivery, bioavailability and drug-likeness of the compound.

As briefly discussed in previous paragraphs, other interesting observations can be made by comparison of the different novel flavonoids in the library that present long chains in the 7 position. AO-1486 and AO-1487 are identical to AO-1530-OMe except for the architecture of their chains (see *Figure 23*) and they exert weaker antiproliferative effects on the cell lines studied. This supports the notion that not any chain in the 7 position of the flavonol scaffold enhances its abilities to the same extent. On the contrary, results suggest that the addition of a chain with a more complex, suboptimal structure like the ones in AO-1486 and AO-1487 can reduce their efficacy, despite the added potential provided by other changes in their redox profile or conjugation with stabilising methoxy groups. Indeed, the chains in AO-1486 and AO-1487 reduce their antiproliferative efficacy significantly, to similar levels to that of AO-594, which lacks a chain in the 7 position altogether.

3.4.4. Poly-ring structure

An interesting case is that of the compound AO-155-179, which preserves all the features believed to be relevant to the efficacy of flavonols. It presents an alkyl chain very

similar to the one present in AO-1530 and AO-1530-OMe. It also has a similar expected redox ability, as it presents a similar substitution profile, conserving the OH substitutions in the B and C rings and the presence of the 2-3 double bond in the C ring. However, this compound differs in that it has a less flavonoid-like structure, due to the removal of the A ring (see *Figure 23).*

Results on breast cancer cell line models have shown that this compound exerts a weaker effect than the methoxylated lead compound but its IC_{50} values are comparable to those of AO-1530. This suggests that, as expected, the A ring is not essential to the redox ability and, ultimately, the therapeutic efficacy of these novel flavonoids. This further supports the notion that, while the natural scaffold of flavonoids presents a 3-ring structure, their antitumour abilities seem to be mostly dependent on the combination of the B and C rings, their conjugation with OH and OMe groups and the addition of a suitable lipophilic chain.

3.5. Conclusion

This chapter has summarised the work carried out to assess the antiproliferative properties of a library of novel, myricetin-based flavonoids in 3 different cell line panels. A series of experiments on panels of breast and ovarian cancer cell line models determined the effect of the different compounds and their relative efficacy and identified the most potent candidate.

Results show all compounds were capable of inducing antiproliferative effects in cancer cell line models in the range of micromolar and sub-micromolar concentrations assessed. Although there was considerable variation in the potency of these effects, some of these compounds successfully improved on the antiproliferative abilities of myricetin. Indeed, these results have highlighted the second-generation bi-methoxylated analogue AO-1530-OMe as the lead candidate in this library, with the most potent antiproliferative effect on all 13 cell lines studied. Other species in the library exerted less potent and more variable effects across different models. This might be due to a weaker efficacy or the involvement of different, less effective mechanism of actions than in the case of AO-1530-OMe.

Importantly, the effect of this lead analogue is recapitulated across models representing cancers with different molecular and histological characteristics and even different cancer types. Indeed, sub-micromolar concentrations of AO-1530-OMe exerted a strong antiproliferative effect on both breast (ER^+ or ER^-) and ovarian cancer models.

This effect was also observed, albeit to a slightly lesser extent, on models with treatment-resistant phenotypes: both antioestrogen-resistant breast cancer cells and chemotherapy-resistant ovarian cancer cells responded to treatment with micromolar concentrations of AO-1530-OMe. The effect exerted in these more recalcitrant treatment-resistant models, despite their different molecular behaviour *in vitro*, which is in turn representative of the clinical complexity of the cancers they model, presents a particularly interesting niche for the potential application of AO-1530-OMe, as these represent more clinically-challenging diseases for which novel therapeutic tools are urgently needed.

This broad antiproliferative effect also suggests that, if this activity is translated into a therapeutic outcome *in vivo*, AO-1530-OMe could hold potential for its possible application as a novel anticancer agent across different and diverse cancer types. Other chapters will investigate the effect of this lead compound and its possible application as an antitumour agent in more detail.

Overall, the effect across different cancer types and subtypes and on treatment-resistant models suggests that the effects observed may be exerted through a mechanism of action common to different molecular subtypes and types of breast cancer. Redox modulation might be involved in these effects, given the expected redox ability of these compounds and the link between changes in the redox status of cancer cells and the development of resistance to treatment[563]. The mechanism of action of AO-1530-OMe will be better investigated in the next chapter.

Finally, the aforementioned differences in the effect of compounds across the library studied has led to the description of structural features which may linked to improved potency of these novel chemical entities. While more in-depth work such as mathematical modelling would be necessary to ascertain and quantify the contribution of different SARs, this preliminary analysis provides an overview of the features found in each the analogues studied which may be relevant to their differential potency. This was done in the context of previous knowledge on the chemistry of flavonoids and supported by the rational design of the library of flavonoids studied.

	Optimum redox profile	OMe substituents	Side chain in 7 position	3-ring backbone
Myricetin	✘	✘	✘	✔
AO-1530	✔	✘	✔	✔
AO-1530-OMe	✔	✔	✔	✔
AO-1486	✔	✔	✔	✔
AO-1487	✔	✔	✔	✔
AO-549	✔	✔	✘	✔
AO-155-179	✔	✘	✔	✘
AO-714A	✘	✔	✘	✔

***Table 10** **Summary of relevant SARs and compliance of each novel flavonoid studied.** A number of structural traits have been observed to contribute to the antiproliferative effect of novel flavonoid analogues. This table summarises the structural features present (✔) or not (✘) in the structure of each analogue in the library studied to highlight how different modifications may contribute to the overall antiproliferative efficacy of each compound.*

Results suggest several SARs might contribute to the antiproliferative activity observed. Although further studies in the design of novel flavonoids could potentially lead to more potent analogues, lead compound AO-1530-OMe is the most potent candidate in the library to date as a result of the combination of several traits that contribute to its antitumour effect, drug-likeness and biostability (see *Table 10* for summary). These SARs include the combination of the B-C poly-ring flavonoid backbone with (i) a modified substitution profile expected to enable optimum redox reactivity, (ii) methoxylations that enhance stability, bioavailability and drug-likeness and (iii) a lipophilic straight decyl chain in the 7 position that is expected to allow improved membrane intercalation and permeability and, consequently, cell delivery.

Overall, these structural alterations are likely to contribute to the efficacy of AO-1530-OMe by (i) enhancing the natural anticancer properties of myricetin and (ii) improving the drug-likeness of this novel candidate to surpass the obstacles previously discussed as hindrances in the efficacy of myricetin, such as stability, bioavailability and metabolic degradation (see section *1.1.5.5.3.*).

These observations suggest that the substitution with electron-donating moieties such as hydroxyl and methoxy groups may contribute to the reactivity of these compounds. The additional known influence of the latter groups on drug stability and delivery in combination with the permeability and improved delivery provided by different side chains may contribute to the stronger biological efficacy of this compound *in vitro*.

The following chapters will investigate the effect of these novel flavonoids at a molecular level to better understand the mechanisms of action involved and possible applications in the management of cancer. As AO-1530-OMe has been shown to have the strongest antiproliferative effect across all models, future work focused on its study as the best candidate to date. Given its identification as the lead candidate in the library, AO-1530-OMe was also renamed as Oncamex following Antoxis's initiative and will be referred to as such in the following chapters.

4. Investigation of the properties and mechanism of action of Oncamex

4.1. Introduction

The first stage of this project reported the promising anticancer effect of Oncamex on cell culture models for different cancer types and subtypes, particularly in comparison with myricetin and other novel flavonoids in the library studied (see Chapter 3). These novel flavonoids were designed to achieve a series of properties. This chapter describes the different properties of Oncamex contributing to its enhanced cytotoxic efficacy.

Firstly, the cell uptake and intracellular targeting of Oncamex were assessed. Previous unreported work by Antoxis had investigated the compartmental distribution of some of the compounds in this library in a renal cell carcinoma cell line (see *Supplementary Figure 10*). This preliminary study contributed to the initial rationale for the possible application of these compounds.

Detection of these compounds by virtue of their fluorescent spectra indicated the specific delivery of lead compounds AO-1530 and Oncamex to the mitochondrial compartment, and their exclusion from the nuclei. AO-155-179 also appeared to be localised in the mitochondria in renal cancer cells, although the weaker fluorescence of this analogue (most likely due to the absence of the complete 3-ring flavonoid scaffold observed in other analogues) prevented a better observation of this distribution. In contrast, the second-generation analogues AO-1486 and AO-1487 exhibited weaker compartmental specificity.

As Oncamex has been identified as the most promising candidate in this library, this chapter includes investigates the targeting of this compound in particular in breast cancer cells, to assess if this specific mitochondrial delivery is recapitulated. The rapidity and stability of this delivery is also studied and the possible contributing structure-activity relationships are discussed.

Another important factor in the design of the library of novel flavonoids studied was the development of a semisynthetic scaffold with an optimised substitution profile and, consequently, expected enhanced potential reactivity. As discussed in the previous chapter (see section *3.4.*), the improvement on the antiproliferative properties of myricetin suggested that these changes to the basic flavonoid poly-ring backbone succeeded in enhancing its natural abilities. This was supported by previous knowledge regarding the

chemistry of flavonoids. This chapter investigates this expected redox ability, as well as the possible effect of this compound on mitochondrial and cell homeostasis, in order to better understand the role redox modulation might play in the mechanism of action of Oncamex.

To further elucidate possible modes of action for Oncamex, the molecular responses induced by treatment that may be responsible for the observed antiproliferative effect were studied. A number of methods sought to measure the changes on cellular processes associated with the hallmarks of cancer and the possible induction of antitumour responses. Results from this work, together with differential gene expression analysis described in the next chapter, will be used to postulate an informed possible mechanistic model for Oncamex (see Chapter 5).

4.2. Assessment of the cell uptake, intracellular targeting and delivery of Oncamex

In order to assess the delivery and distribution of Oncamex in breast cancer cells, its localisation was monitored in MDA-MB-231 cells (selected for their better adherence and growth on coverslips) by fluorescence microscopy. Results illustrated the quick and specific delivery of Oncamex to the mitochondria (see *Figure 25*).

By 15 min after administration, Oncamex was primarily localised in the mitochondria and excluded from the nuclear compartment, as evidenced by the overlap of its fluorescent signal with that of the mitochondrial marker Mitotracker Deep Red but not with the nuclear stain DAPI (4',6-diamidino-2-phenylindole, dihydrochloride). This specificity appeared to be conserved over time, as Oncamex remained mostly in the mitochondria at the 1 h and 6 h timepoints. Visualisation of the cells at greater magnifications showed changes in cell morphology and apparent condensation of the nuclear material after 6 h, consistent with the induction of cell death.

These results support the specificity of Oncamex for the mitochondrial compartment in breast cancer cells. This was previously observed in a renal cell carcinoma cell lines (see *Supplementary Figure 10*, from unpublished results courtesy of Graeme Cook, Antoxis Ltd) and the effect of Oncamex appears to be similar across both models studied.

The effect of different structural features on the properties of novel flavonoids has been previously discussed (see section *3.4.*). However, the description of SARs linked to the mitochondrial targeting of Oncamex is a more complex matter. Indeed, the mechanism by which some compounds target the mitochondria is poorly understood.

In the case of Oncamex, some observations can be made *a priori* from knowledge of the structural features of the compound. The improved lipophilicity granted by the 7-decyl chain in Oncamex has been previously discussed (see section *3.4.3.*) and is supported by the quick cell uptake and subsequent delivery into the mitochondria reported in this section. This chain is likely to not only allow for the intake of the molecule into the cell, but also aid its entry into the mitochondrion through the mitochondrial membrane, which bears structural similarities to the plasma membrane.

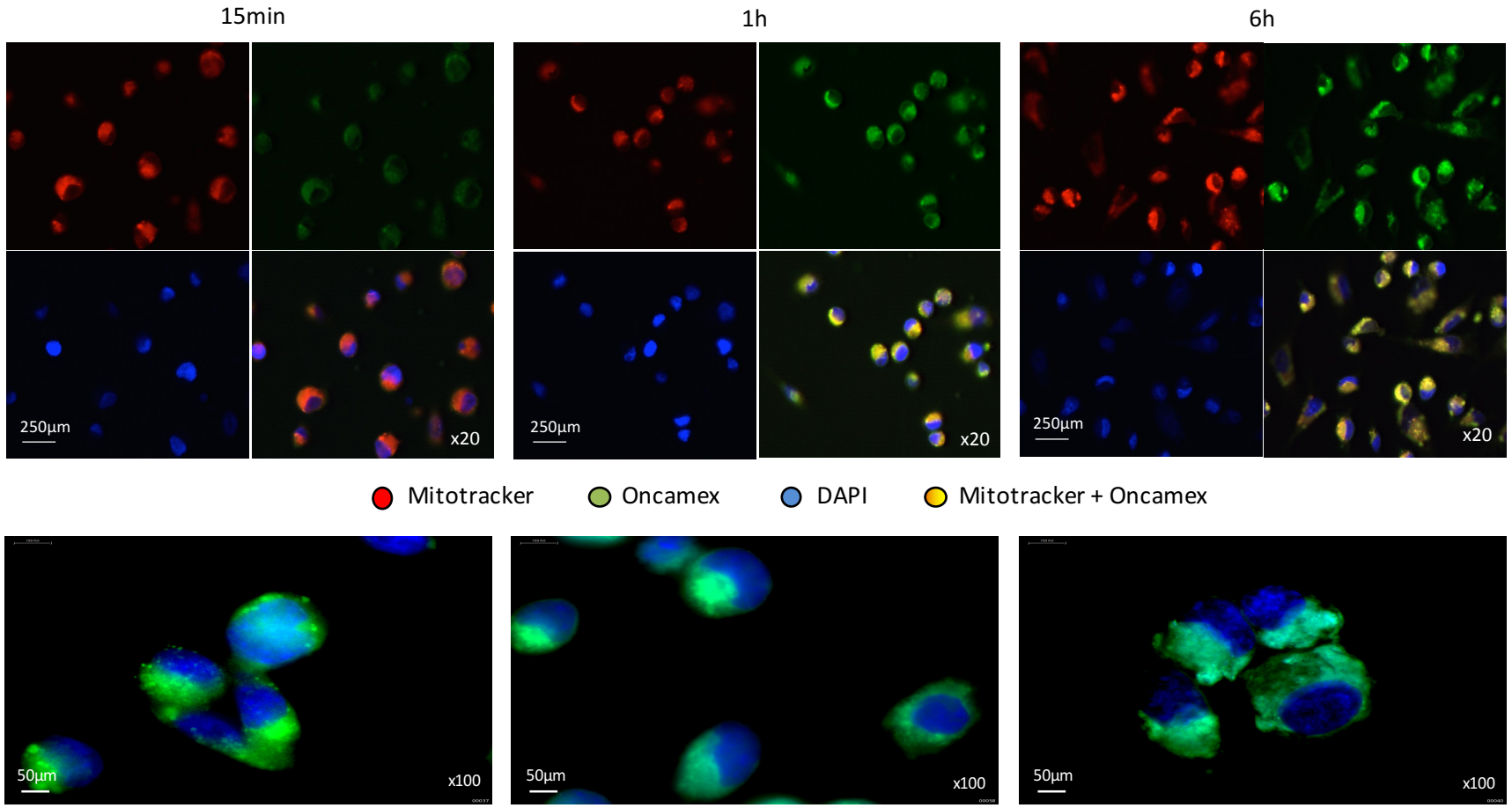

Figure 25 ***Intracellular localisation of Oncamex.*** *Fluorescence microscopy of MDA-MB-231 cells treated with Oncamex monitored the delivery of the drug and its localisation within the mitochondrial compartment. Oncamex was detected thanks to its fluorescence spectrum (550nm$_{EXC}$/570nm$_{EM}$). Overlap of the drug's fluorescent signal with that of the far-red fluorescent dye Mitrotracker Deep Red resulted in an orange-yellow signal. This experiment was repeated (n=2, in triplicate).*

As previously summarised (see section *1.1.5.3.7.*), the potential of mitochondria as targets in anticancer treatment led to the development of compounds engineered to target this compartment. The compound MitoVE makes for an interesting example. It is a semisynthetic derivative of vitamin E that incorporates the lipophilic cation triphenylphosphonium (TPP^+) to enhance the mitochondrial targeting and apoptotic effect of the simpler scaffold[564]. This strategy relies on the attraction of this positively-charged molecule toward the strong transmembrane potential in the mitochondria and its ability to permeate into the mitochondrial matrix, enabled by its lipophilicity.

Interestingly, even though conjugation with TPP^+ grants MitoVE improved efficacy, the simpler first-generation semysinthetic analogue on which it is based, α-tocopheryl succinate (αTOS), also targets the mitochondria specifically despite the absence of a cationic moiety in its structure[565–567]. Indeed, αTOS has been identified as an inhibitor of the complex II of the electron transport chain, although the mechanics of its targeting to the mitochondria are not as well established as in the case of its second-generation derivative MitoVE.

Like MitoVE, Oncamex also bears a lipophilic side chain that enables good permeability across the plasma and mitochondrial membranes. The presence of electron-donating moieties and its reported redox reactivity suggest that it may become ionised and, thus, be attracted to the mitochondria by a force similar to that employed in the TPP^+ targeting strategy. Mitochondrial potential could play a role in the expected targeting of this organelle by Oncamex, but the potential positive charge gained by the compound prior to its delivery to the mitochondria would most likely be weak in comparison to examples such as TPP^+-conjugated structures. Together with the fact that non-positively charged species such as αTOS can also present specific targeting, this suggests that the presence of a charge that may be pulled towards the mitochondrial potential may not be essential, so that Oncamex may successfully target this compartment independently of its ionisation in the extracellular matrix or the cytosol and because of its good membrane permeability.

Previous results had suggested a link between the lipophilicity of novel flavonoids and their cytotoxic efficacy (see section *3.2.1.*). Data reported here suggest a similar influence of lipophilicity on the ability of a compound to be specifically delivered to the mitochondria. Indeed, results from MDA-MB-231 cells have shown the strong specificity of the lead candidate Oncamex for the mitochondrial compartment, with a quick delivery and stable accumulation over time (see *Figure 25*).

Previous unreported work by Antoxis, albeit in a different model, provides interesting additional information to help understand this targeting, as it showed the poorer specificity for the mitochondria of compounds such as AO-1486 and AO-1487 (see *Supplementary Figure 10*), which bear complex, less lipophilic chains and exhibited weaker antiproliferative efficacy in breast cancer cells (see *Table 8*). The analogue AO-155-179, which presents a side chain more similar to that found in AO-1530 and Oncamex (see *Table 7* or *Figure 23* for structures), was observed to also target the mitochondrial compartment and exerted a comparatively stronger effect than AO-1486 or AO-1487 on breast cancer cells (see *Table 8*).

As previously discussed (see section *3.4.3.*), previous research has investigated the effect of different side chains in the lipophilicity of compounds[509] and highlighted 7-decyl as the best structural feature in the design of lipophilic novel flavonoids[452]. Together with the observations made here, this supports the notion that lipophilicity is directly proportional, and may also be a determining factor, to both the specificity of a novel flavonoid for the mitochondrial compartment and, in turn, its potency as a potential anticancer agent. Thus, the lipophilic decyl chain in Oncamex is most likely responsible for its mitochondrial targeting. These observations also suggest that the antiproliferative properties of Oncamex depend on this targeting and, consequently, its mechanism of action might be based on changes in the mitochondria.

As for the stability of the mitochondrial accumulation of Oncamex, this may be due to its modification once it interacts with the mitochondrial metabolism. The possible changes will be discussed in the next section according to results on the redox properties of the compound.

4.3. Study of the redox and ROS-modulating properties of Oncamex

4.3.1. Electrochemical properties of Oncamex

One of the defining features of the novel flavonoids studied in this project is the optimisation of the natural backbone of myricetin expected to enhance their redox reactivity. In order to investigate this, the electrochemical properties of Oncamex were studied using cyclic voltammetry (CV).

This method allowed for the study of the electrochemical properties of Oncamex in solution (see *Figure 26*). With the change in potential (between the working and reference electrodes) the cathodic current (flowing between the working and counter electrodes) increased as the available analyte was reduced, until the cathodic peak was reached and current decreased due to the depletion of reducible Oncamex. The reverse reaction led to a similar change with current of reverse polarity as the analyte was oxidised.

These CV results demonstrated the redox abilities of Oncamex. The cyclic voltammogram obtained shows that Oncamex is capable of undergoing a reversible reduction, so that the molecule can be reduced until exhausted to then be oxidised, with this redox reaction potentially occurring cyclically (see *Figure 26*).

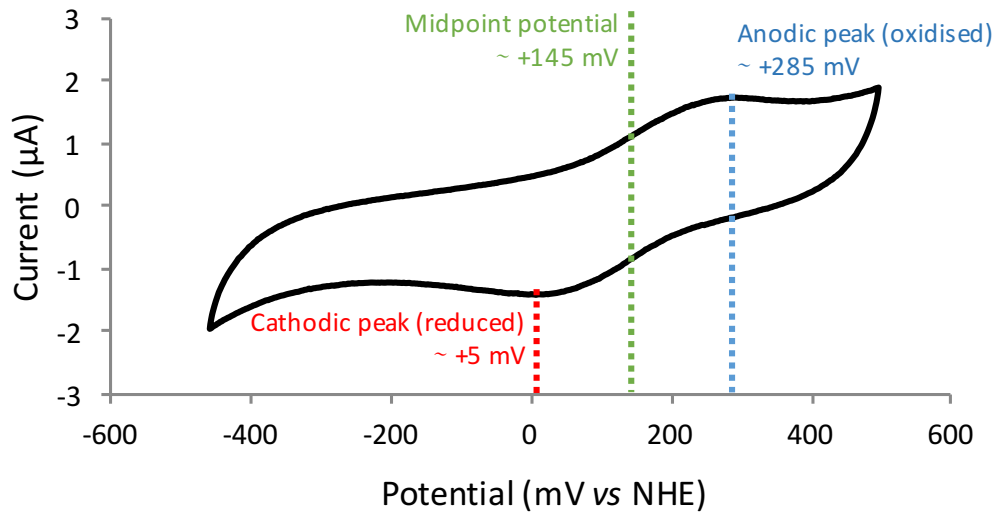

***Figure 26* Electrochemical profile of Oncamex.** *The plotting of the changes in current (between the working and counter electrodes) versus the applied voltage (potential between the working and reference electrodes) provided a cyclic voltammogram reflecting changes in the redox status of the analyte. NHE: normal hydrogen electrode (standard reference). Figure courtesy of Dr Patrick Thomson (Department of Chemistry, University of Edinburgh).*

CV results show the cathodic peak (the potential for which all Oncamex is reduced) is around +5 mV, the anodic peak (all Oncamex is oxidised) is around +285 mV and the midpoint potential (equal proportion of reduced and oxidised species) at +145 mV (see *Figure 26*). This electrochemical activity was detected with the analyte suspended in acetonitrile (MeCN), given the limited solubility of Oncamex in water.

These results suggest the redox ability of Oncamex. Importantly, the midpoint potential of +145 mV is much more positive than the physiological resting potential in either the cytosol or the mitochondria[568,569], which are significantly negative, particularly in the case of the mitochondria in cancer cells (see section *1.1.5.3.7.*). This suggests that, upon its specific delivery to the mitochondrial matrix, Oncamex would most likely be reduced, gaining electrons due to the strong negative electric potential in the compartment. In the mitochondria, this would enable Oncamex to in turn donate electrons to oxygen to form the superoxide radical anion ($O_2^{\cdot-}$), thus dysregulating mitochondrial ROS metabolism.

Additionally, deprotonation of Oncamex due to the mitochondrial pH could make it more strongly oxidising, enhancing its ability to release electrons. In short, the electrochemical properties observed here suggest a possible ROS-modulating effect which might be part of the mechanism of action by which Oncamex exerts the antiproliferative effect previously observed. This will be investigated in the next sections.

The possible deprotonation of Oncamex upon its delivery to the mitochondria could lead to changes in its polarity or charge, altering its membrane permeability and aiding its accumulation in this compartment due to the electrostatic repulsion of a possible negative charge by the mitochondrial membrane.

Additionally, the fact that Oncamex may undergo redox cycling means its activity may not be exhausted when all the compound available is reduced. Although drug metabolism could factor in its stability and reactivity, Oncamex could potentially further alter the mitochondrial redox status with every redox cycle it undergoes. This could lead to its effect being amplified, thus contributing to its efficacy, which results have suggested is already supported by (i) its stable and specific delivery to the mitochondria and (ii) its active, reversible redox ability.

4.3.2. Effect of Oncamex on overall ROS levels

The results showing the electrochemical properties of Oncamex support the notion that it may exert its antiproliferative effects through regulation of reactive oxygen species (ROS)

and changes in the redox homeostasis. Different methods were applied in an effort to monitor possible changes in ROS levels following treatment with this compound.

Firstly, changes in overall ROS levels were measured using the dye DCFDA (2',7'-dichlorofluorescein diacetate), which becomes oxidised and fluorogenic in the presence of ROS. Results from this assay reported a temporary increase in overall ROS levels quickly after treatment with Oncamex at concentrations in the high micromolar range (see *Figure 27*).

A second method was applied to detect specific changes in hydrogen peroxide (H_2O_2) levels using bioluminescence. This assay reported an increase over time in H_2O_2 after treatment with Oncamex concentrations in the low micromolar range only. This increase was observed over longer incubations and peaked at 6 h (see *Figure 27*).

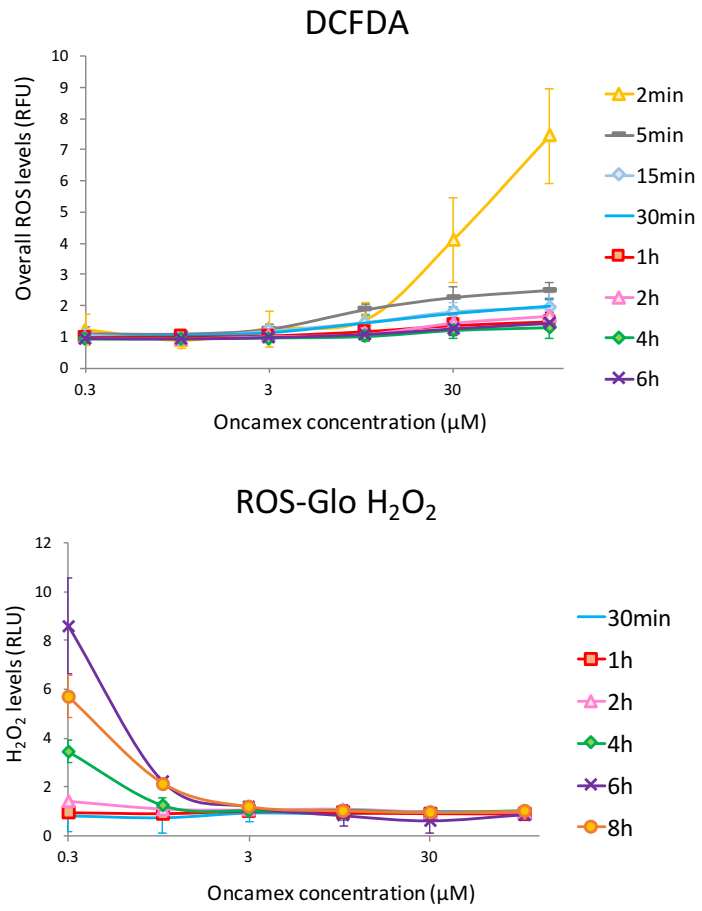

***Figure 27* Changes in ROS levels.** *Measurement of changes in overall ROS (above) and H_2O_2 levels (below) using the DCFDA fluorescence dye and ROS-Glo H_2O_2 luminescent plate assay, respectively. Each experiment was repeated (n=3, with 3 technical replicates per concentration). These graphs show pooled results, with each data point representing the average from biological replicate experiments for each treatment condition, normalised to vehicle controls, and error bars representing standard deviation (SD). RFU, relative fluorescence units; RLU, relative luminescence units.*

These methods appear to report opposed changes in ROS levels, showing the difficulty of both identifying and interpreting these changes by means of plate-based methods. In particular, these methods are based on the detection of changes in fluorescence and luminescence in cells in culture. Despite following the manufacturers' instructions, changes in the culture medium itself could interfere, feasibly creating artefactual results.

In the case of DCFDA-stained cells in particular, previous research has reported the oxidation of polyphenols in cell culture medium[570], which could lead to artefactual measurements. This is also supported by the fact that the increase in ROS levels is observed early after treatment but decreases over longer incubations. This method may also be affected by the colour of Oncamex in solution possibly interfering with the reading of the fluorescence signal. The application of other methods was necessary to provide a better insight into the effect of Oncamex on ROS signalling at a molecular level. This will be assessed in the next section.

4.3.3. Effect of Oncamex on mitochondrial ROS modulation

Following apparently conflicting results from 2 different methodologies seeking to assess ROS modulation induced by treatment with Oncamex, other technologies were applied in order to investigate these changes specifically in the mitochondrial compartment. This follows results that indicated the rapid and specific delivery of Oncamex into the mitochondria and its active electrochemical profile, which suggested this compound is likely to induce changes in this compartment.

For this, fluorescent probes that specifically detect changes in mitochondrial hydrogen peroxide (mH_2O_2) and mitochondria superoxide (mSO) were used. The study of changes in the mitochondria may provide more accurate results, as this is where Oncamex is known to be accumulated and is, hence, likely to be the place of initiation of the effects it may exert. The use of probes applied on fixed cells and detected using fluorescence microscopy may also prevent any issues arising from the interference of culture medium with fluorescent or luminescent signals.

The fluorescent probe MitoPY1 indicated changes in levels of mH_2O_2 in MDA-MB-231 cells treated with concentrations in the low micromolar range (0.3µM) of Oncamex after 1 h (see *Figure 28*). Changes in the fluorescence of MitoPY1 were not quantifiable but increases in levels of mH_2O_2 were qualitatively detected, with mH_2O_2 production observed as bright specks in the cells, also observed in a positive controls treated with 100µM H_2O_2 to induce

oxidative stress that would dysregulate the mitochondrial redox status. Treatment with higher Oncamex concentrations or for longer incubation periods did not show increased levels of mH_2O_2 production.

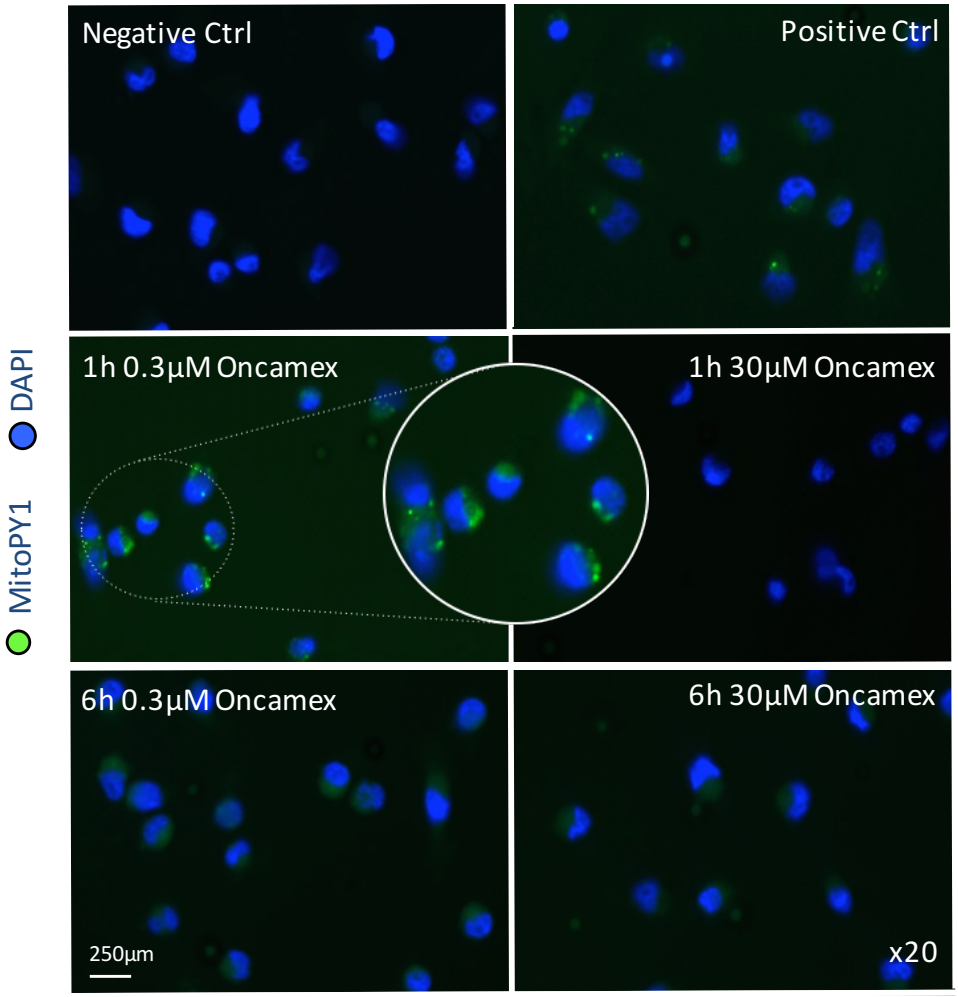

***Figure 28* Changes in mitochondrial hydrogen peroxide (mH_2O_2).** *The fluorescent probe MitoPY1 was used to specifically detect changes in mH_2O_2 levels in MDA-MB-231 cells treated with Oncamex. Negative (vehicle) and positive (100µM H_2O_2) controls were included. Each experiment was repeated (n=2, in triplicate). Positive results were not quantified but were qualitative, appearing as bright specks in cells.*

Staining with the fluorescent probe MitoSOX allowed for detection of changes in levels of mSO in MDA-MB-231 cells (see *Figure 29*). This species appeared to be generated and accumulated in a different fashion, with increased levels after longer incubations with higher concentrations of Oncamex. While other treatment conditions led to production of lower levels of mSO, treatment with 30µM Oncamex for 6 h generated high levels of mSO, which were quantitatively larger than those for the H_2O_2-treated positive control.

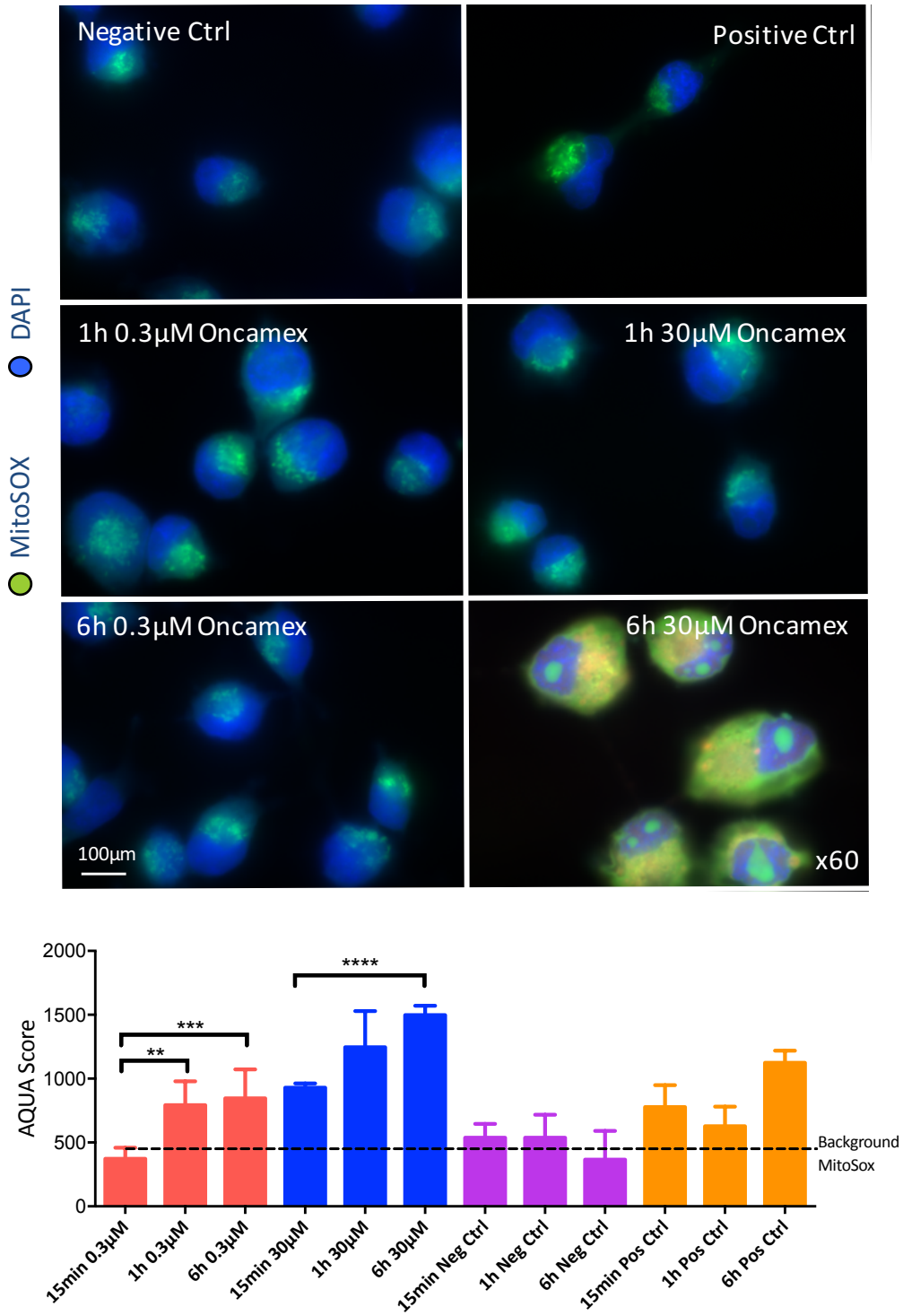

Figure 29 ***Changes in mitochondrial superoxide (mSO).*** *The fluorescent probe MitoSOX was used to specifically detect changes in mSO levels in MDA-MB-231 cells treated with Oncamex. Negative (vehicle) and positive (100µM H_2O_2) controls were included. Each experiment was repeated (n=2, in triplicates). Results were quantified using the AQUA system. Results show averages of 5 measured sections in a representative slide, with error bars representing standard deviation (SD). P-values from unpaired t-test: **P<0.01; ***P<0.001; ****P<0.0001. Where not shown P>0.05 (nonsignificant).*

These results show differential effects of Oncamex in the production of both mitochondrial ROS, mH_2O_2 and mSO, which could be interpreted as indicating that Oncamex can exert different effects on mitochondrial ROS metabolism in a concentration and time-dependent manner. Flavonoids have been previously described as having a biphasic effect in that different concentrations of some compounds may modulate different responses through several mechanisms (see sections *1.1.5.3.2.* and *1.1.5.4.1.*).

Nevertheless, although Oncamex may still exert a pleiotropic mechanism of action elsewhere, Oncamex has been shown to be delivered in a rapid and specific manner to the mitochondrial compartment and its electrochemical properties suggest its propensity to lead to the production of superoxide (see previous sections). Thus, the different changes in mH_2O_2 and mSO may reflect the reaction of the metabolic machinery to the redox stress induced by Oncamex.

The normal functioning of respiration in the mitochondria of abnormal cells also includes the generation of mitochondrial ROS as by-products of the electron transport chain (ETC). As part of mitochondrial respiration, mSO is produced and released into the mitochondrial matrix and the mitochondrial intermembrane space as a consequence of the leakage of electrons (e^-) from the complexes I and III in the ETC, respectively. This mSO is dismutated to mH_2O_2 by enzymes in the superoxide dismutase (SOD) family in both compartments. In turn, mH_2O_2 is fully reduced by glutathione peroxidase (GPX) to produce water (see *Figure 30*) or it may escape the mitochondrial compartment, as this species can diffuse out to the cytoplasm, unlike mSO[571].

Given its redox profile, Oncamex might lead to the production of mSO even at low concentrations. In the mitochondrial matrix SOD2 may dismutate this mSO, thus absorbing the stress created by Oncamex treatment and leading to the increase in mH_2O_2 production reported here. This would explain the detection of mH_2O_2 production, but low mSO levels, in cells treated with lower concentrations of Oncamex.

In comparison, the exposure to higher concentrations of Oncamex or for a longer length of time would generate higher levels of mSO that may surpass the enzymatic capacity of SOD, particularly considering the fact that the redox status of mitochondria in cancer cells is known to be altered and more susceptible to further stress (see section *1.1.5.3.7.*).

The application of specific mitochondrial fluorescent probes allowed for microscopic evaluation of the changes in ROS levels occurring *in situ* in this compartment, suggesting the

relevance of these results over previous ones obtained from less specific plate-based assays (see previous section and *Figure 27*).

As discussed in the previous section, a number of factors could have influenced the results observed in cells stained with DCFDA dye. Results obtained using the ROS-Glo H_2O_2 assay indicated an increase in H_2O_2 levels over time in cells treated with low concentrations of Oncamex. Although the significance of these results is hard to ascertain, in light of the results reported here by detection with MitoPY1, the changes observed by means of the ROS-Glo assay could be due to the release into the medium of mH_2O_2 generated in the mitochondria, as this species is known to be able to diffuse across membranes[571]. In any instance, given the delivery and reactivity of Oncamex in the mitochondria, results obtained by means of detection of MitoPY1 and MitoSOX are likely to provide a more relevant insight into the effect of Oncamex at a molecular level.

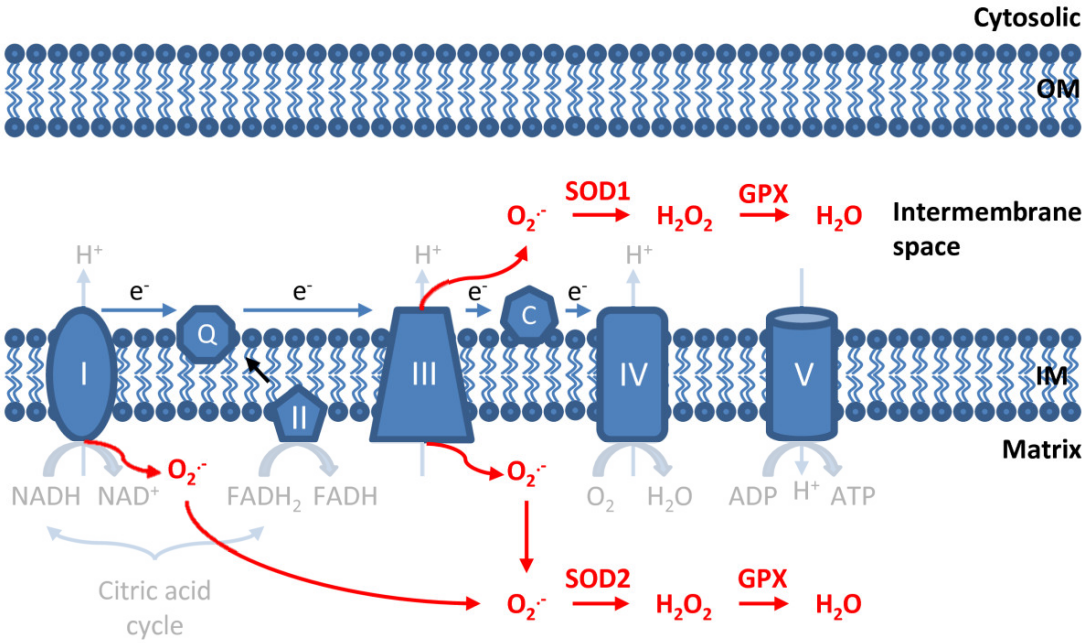

Figure 30 ***Production and disposal of mitochondrial ROS.*** *The process of mitochondrial respiration leads to the production of mSO ($O_2^{\cdot-}$) as a by-product from the leakage of electrons (e^-) from the electron transport chain. mSO is then dismutated into mH_2O_2 by the activity of superoxide dismutases (SOD1 and SOD2), which is then reduced to water (H_2O) by glutathione peroxidase (GPX). OM, outer mitochondrial membrane; IM, inner mitochondrial membrane. Figured adapted from Li et al (2013)*[572].

To conclude, results from methods assessing changes in mitochondrial ROS demonstrated the induction of mSO production by treatment with Oncamex, which is supported by the electrochemical properties of this novel flavonoid. In short, the mitochondrial enzymatic machinery might be able to absorb the weaker redox stress

generated by low concentrations of Oncamex in the form of low levels of mSO by converting it to mH_2O_2, but this response mechanism is surpassed when higher compound concentrations lead to production of higher levels of mSO and stronger redox stress. This production of high levels of mSO reported here could in turn cause major mitochondrial dysregulation and potentially disruption, which may lead to the previously observed cytotoxic effects of Oncamex in cancer cell line models. This possible mechanism of action will be further investigated in the next sections.

4.4. Investigation of the functional responses exerted by Oncamex

Previous sections have investigated the properties of Oncamex in terms of its cellular uptake, mitochondrial delivery and redox reactivity. These abilities, granted by the addition of structural modifications to the natural scaffold of myricetin, are likely to contribute to its enhanced antiproliferative effects on breast and ovarian cancer models. This section will investigate the cellular responses exerted by Oncamex that may lead to this effect in an attempt to understand the mechanism of action of this novel agent.

Firstly, the overall effect of Oncamex on cells was studied by microscopic observation of morphologic changes in treated cells, which were spotted, fixed and stained on cytospin slides for their study (see *Figure 31*). Untreated cells generally exhibited normal overall morphology, including presence of mitotic cells, as shown by the staining of chromosomes in division (*Figure 31a*). Treatment with Oncamex for 24 h induced a reduction of cell density and no evidence of cell division was observed (*Figure 31b*). Additionally, treated cells presented changes in morphology and abnormal or dead cells were observed after 24 or 48 h (*Figure 31c-d*). These changes were generalised 72 h after treatment (*Figure 31e*).

Most cells exposed to treatment with Oncamex presented morphological features suggestive of necrosis rather than apoptosis[573] (see *Figure 31b-e*). These include the lack of generalised chromatin condensation (pyknosis) or nuclear fragmentation (karyorrhexis) associated with the later stages of apoptosis, while the observed cytoplasmic swelling (oncosis) and the apparent loss of membrane integrity are typically found in necrotic cells.

However, these morphological features are common to two different "types" of necrotic processes[573,574]: necroptosis (or primary necrosis), a serine-threonine kinase receptor-interacting protein 1 (RIP1)-regulated form of active cell death; and secondary necrosis, a phenomenon by which, in the absence of scavengers with phagocytic capacity that could carry out the heterolytic degradation and clearance of cells (efferocytosis), the apoptotic process leads to the induction of necrosis for the autolytic degradation of dying cells.

Secondary necrosis often occurs as an *in vitro* artefact due to the absence of said scavenger cells with phagocytic abilities in cell culture. Interestingly, some authors have argued that this second necrotic phase might be the natural outcome of apoptosis[573], as observed in unicellular eukaryotes, and can serve as a self-sufficient process for auto-elimination of dying cells if clearance by other phagocytic cells present in multicellular organisms is not possible.

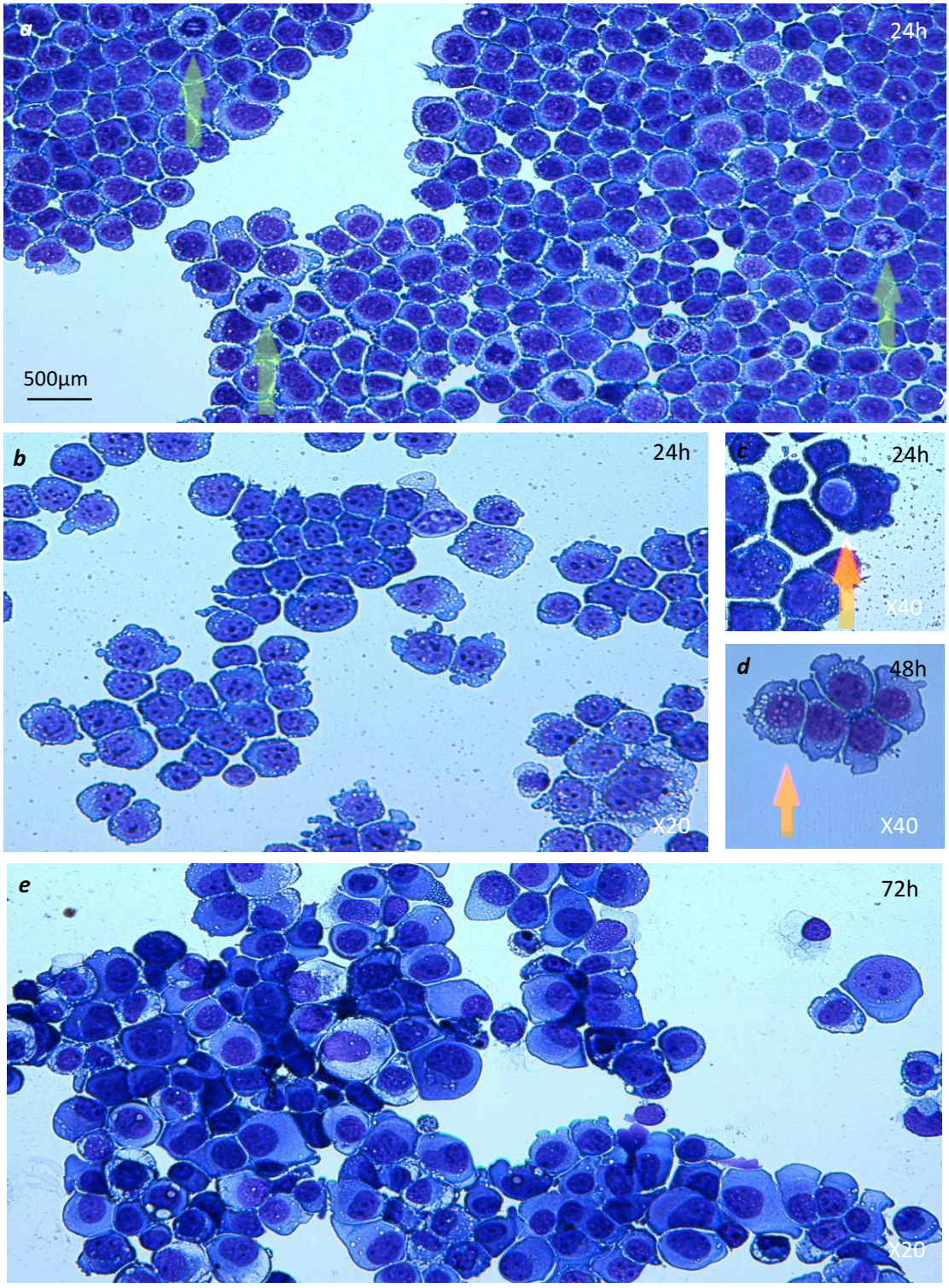

***Figure 31* Visualisation of changes in cell morphology.** *Untreated (vehicle control) MCF-7 cells (a) were observed in comparison to MCF-7 cells treated with 10µM Oncamex for different lengths of time (b-e). Each experiment was repeated (n=3, with 3 technical replicates in each experiment). Captures show representative examples. Green arrows indicate examples of untreated cells undergoing cell division. Orange arrows indicate treated cells presenting abnormal morphological features.*

In short, the results reported here support previous observations from SRB assays on the cytotoxic effect of Oncamex on cancer cells, suggesting that this agent may act by both inhibiting cell proliferation and inducing cell death. Previous results reported in this chapter have shown the quick cellular uptake and delivery of Oncamex to the mitochondria (see section *4.2.*), where it induces ROS production (see section *4.3.*). While this could suggest the induction of cell death by mitochondrial-dependent apoptosis, the observation of necrotic features reported here, which are common to both primary necrosis and apoptosis-triggered secondary necrosis, indicates that further work is needed to better assess the mechanism of action of Oncamex. Other tests were carried out in order to discern whether the cytotoxic effect previously observed at the 96 h timepoint is indeed linked to the induction of apoptosis or, contrarily, whether a different RIP1-related primary necrosis mechanism may be involved.

In a first attempt to better assess the mechanism of action of Oncamex, SRB assays were repeated to assess the timing for the induction of these responses. Results suggested the quick delivery of Oncamex may lead to the rapid induction of antiproliferative effects on cancer cells: although these may accumulate overtime, the changes in proliferation induced after 8 h are comparable to those observed at later timepoints (see *Figure 32*).

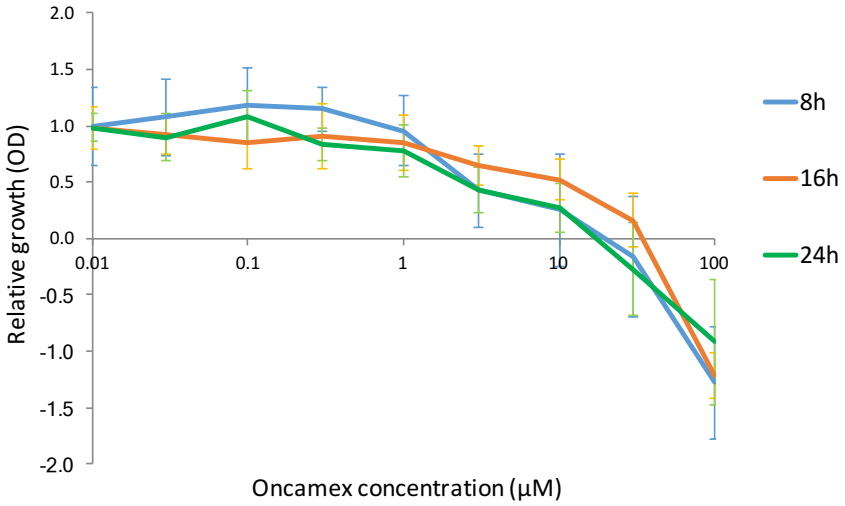

***Figure 32* Study of the timing of the antiproliferative effect of Oncamex.** *Previous assays on MCF-7 cells were repeated including treatment and incubation with Oncamex for different lengths of time (8, 16 or 24 h). From the same initial cell density, cells were treated and fixed after the desired incubation, followed by assessment of changes in proliferation by SRB assays. (n=3, with 6 technical replicates per concentration). This graph shows pooled results, with each data point representing the average from biological replicate experiments for each treatment condition, normalised to vehicle controls, and error bars representing standard deviation (SD).*

These results suggested the effects of Oncamex might be triggered after 8 h treatment or less with concentrations in the micromolar range. This is supported by its quick delivery of to the mitochondria and, more importantly, the strong effect on mitochondrial ROS levels (see *Figure 29*) induced by this incubation time. Consequently, 8 h treatment might be an appropriate timepoint for the investigation of the effects exerted by Oncamex.

The molecular changes exerted by Oncamex were further studied using plate-based methods designed to measure changes in different cell responses and functions. Firstly, the CellTox Green assay was applied to monitor the induction of cytotoxicity over time in treated cells (see *Figure 33*), as this assay includes a dye that becomes fluorogenic when staining DNA in dead cells.

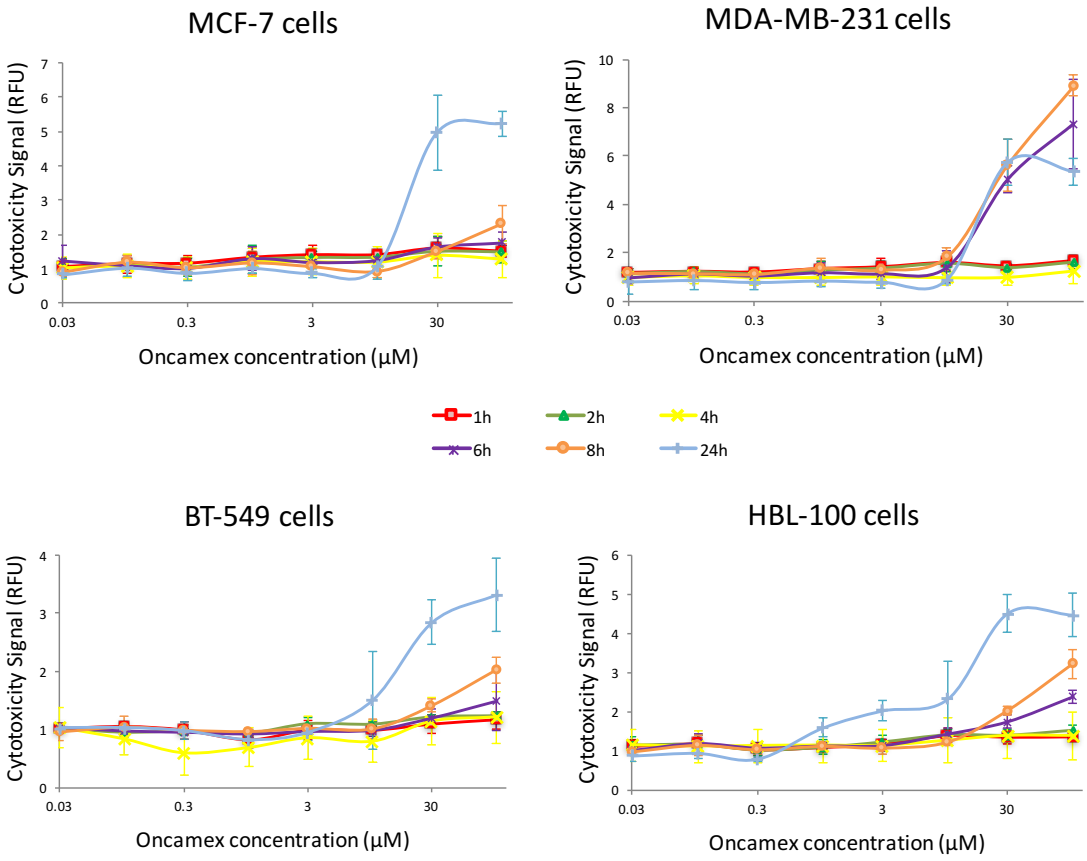

***Figure 33* Induction of cytotoxicity in breast cancer cells by Oncamex.** *The CellTox Green assay was used to measure the induction of cytotoxicity in breast cancer cells over time. Each experiment was repeated (n=2, with 6 technical replicates per concentration). These graphs show pooled results, with each data point representing the average from biological replicate experiments for each treatment condition, normalised to vehicle controls, and error bars representing standard deviation (SD). RFU, relative fluorescence units.*

Results supported previous observations on the timing of the effect of Oncamex: although there was some variation across cell lines, cytotoxicity was induced between 6 and 8 h after treatment in all models studied, normally reaching higher levels after 24 h (see *Figure 33*). Interestingly, cytotoxicity appeared to be induced more quickly and to higher relative levels in MDA-MB-231 and HBL-100 cells.

These results suggested the induction of cytotoxicity by micromolar concentrations of Oncamex. Lower concentrations may require longer incubation times to achieve levels of cytotoxicity leading to the effects observed after 96 h. Since this method relies on the entrance of the non-permeable dye into the cell in order to generate fluorescence, these results are consistent with the induction of disruption of membrane integrity previously suggested by the microscopic observation of necrosis-like changes in cell morphology.

The ApoTox-Glo triplex assay was applied to assess the possible induction of apoptosis 8 h after treatment with Oncamex (see *Figure 34*). Instead of monitoring membrane integrity, this method relies on fluorescent substrates to measure the activity of healthy and dead cell proteases in order to monitor cell viability and cytotoxicity, respectively, while a bio-luminescent substrate reports on the induction of apoptosis when cleaved by active caspases. Thus, the measurement of changes in caspase activation could help discern whether the mechanism by which Oncamex may induce cell death involves the induction of primary necrosis or apoptosis

Results recapitulated the induction of cytotoxicity previously observed and also showed the inversely-correlated decrease in cell viability and the increase in caspase activity (see *Figure 34*). A decrease in viability without induction of cytotoxicity or apoptosis would have suggested a cytostatic effect, whereas inversely-correlated changes in viability and cytotoxicity without caspase activity would have indicated primary necrosis. Since Oncamex treatment induced the loss in cell viability and the induction of both cytotoxicity and caspase activation (see *Figure 34*), these results support the notion that Oncamex induces apoptosis as part of its mechanism of action.

MDA-MB-231 and HBL-100 cells again appear to be more susceptible to the effects exerted by Oncamex, as both cytotoxicity and apoptosis are induced to greater relative levels in these models. For instance, MDA-MB-231 cells treated with 30 µM Oncamex exhibit a 5-fold increase in caspase activity, while MCF-7 cells levels are below 2-fold. Interestingly, apoptosis induction is measured through the cleavage of a luminescent substrate by caspases 3 and 7. MCF-7 cells are known to be deficient in caspase 3[575], while BT-549 cells have also

been shown to express lower levels of this protein than normal epithelial breast cells[576]. This further contributes to the notion that Oncamex relies on the induction of apoptosis as part of its mechanism of action, as models deficient in caspase 3 were less sensitive to changes in cytotoxicity or cell viability 8 h after treatment. The fact that Oncamex had similar IC_{50} concentrations in these 4 models suggests that caspase deficiencies do not necessarily lead to a weaker efficacy after longer incubations but possibly only a delay in the initiation of apoptosis, as other caspases may aid the triggering of the apoptotic cascade.

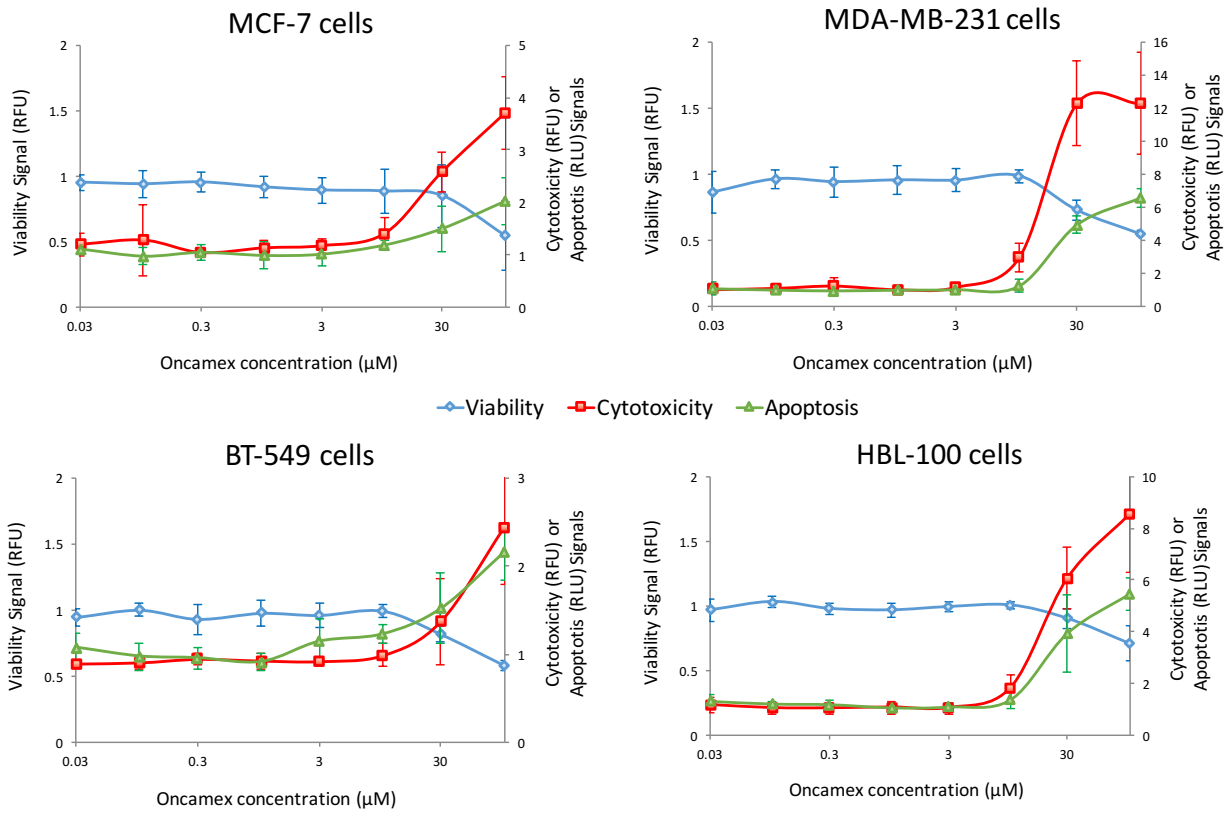

***Figure 34* Induction of apoptosis in breast cancer cells by Oncamex.** *The ApoTox-Glo Triplex assay was applied to assess the induction of apoptosis in cells treated with Oncamex for 8 h. Each experiment was repeated (n=2, with 6 technical replicates per concentration). These graphs show pooled results, with each data point representing the average from biological replicate experiments for each treatment condition, normalised to vehicle controls, and error bars representing standard deviation (SD). RFU, relative fluorescence units; RLU, relative luminescence units.*

Finally, the induction of apoptosis was corroborated by detection of poly ADP-ribose polymerase (PARP) cleavage. PARP, an enzyme involved in DNA repair, is a down-stream target in the apoptosis cascade and its cleavage by caspases is a well-established marker for the induction of apoptosis[577,578].

Detection by Western blotting showed the induction of PARP cleavage by treatment with Oncamex (see *Figure 35*). At the 8 h timepoint only the higher concentration of 100µM induced PARP cleavage, while 24 h were required for cleavage in cells treated with lower concentrations. Incubation for 24 h with the highest concentration led to no detection of PARP in either its whole or cleaved form, suggesting this treatment condition might have led to further cell death (possibly secondary necrosis) and protein degradation. As PARP is targeted by caspases 3 and 7, its cleavage may occur more quickly or more efficiently in cells depending on caspase activity.

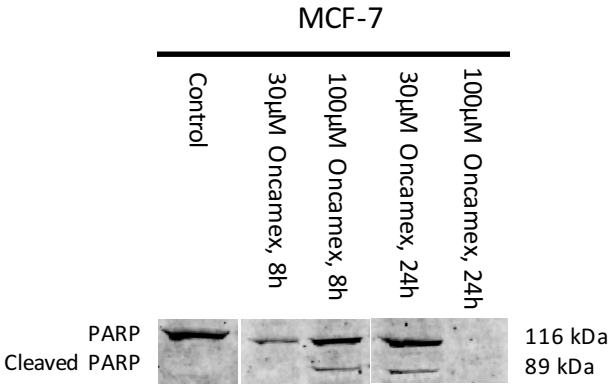

***Figure 35* Detection of PARP cleavage.** *The pro-apoptotic effect of Oncamex was assessed by Western blotting, comparing the timing of the induction of PARP cleavage after treatment with different concentrations of Oncamex. The experiment was repeated (n=2).*

Importantly, the detection of PARP cleavage supports the previous results from the ApoTox-Glo Triplex assay showing caspase activation. Indeed, in detecting the induction of caspase activation and PARP cleavage, these results support the role of in the mechanism of action of Oncamex. Together, these results suggest that 8 h treatment with concentrations in the micromolar range of Oncamex may induce cytotoxicity and the advancement of the apoptotic cascade, including PARP cleavage at later stages, leading to the more generalised induction of apoptosis after 24 h.

The noted necrotic features following treatment might be the outcome of the apoptotic program, which can lead to the induction of secondary necrosis in *in vitro* models, as previously discussed. Additionally, the ROS-modulating effect of Oncamex could also contribute to the induction of necrotic-like changes: besides possibly triggering mitochondria-dependent apoptosis, accumulating high levels of mSO (see *Figure 29*) could spill out of this compartment and into the cellular matrix, possibly coming into direct contact with and oxidising the plasma membrane, leading to its disruption and loss of membrane integrity.

In short, results suggest that the delivery and redox ability of Oncamex in the mitochondria can trigger the induction of apoptosis. Results have also suggested that treatment with this agent can also lead to the induction of necrosis: as secondary necrosis linked to said advancement of the apoptotic program and/or as a result of the oxidative offence (or other types of stress) exerted by the compound. While both of these different modes of cell death would contribute to the observed effect of Oncamex, further work will focus on the suggested pro-apoptotic mechanism, as this activity appears to be the result of targeted changes in the rational design of the novel compounds being studied.

As previously mentioned, the notion of apoptosis playing a role in the mechanism of action of Oncamex was supported by this compound's ability to target and induce ROS production in the mitochondria, which play a central role in cell homeostasis and the regulation of apoptosis (see next section for further discussion). In order to validate the hypothetical link between this ROS-modulating effect in the mitochondria and the induction of apoptosis, further experiments were designed incorporating a pretreatment stage with an antioxidant agent. N-acetyl-L-cysteine (NAC) acts as a free radical scavenger and inhibitor of ROS signalling[579,580] and is commonly used to confirm the involvement of ROS in different processes, including drug-induced apoptosis[581].

Incubation with 10mM NAC for 30 min prior to treatment with Oncamex led to partial blockade of its apoptotic effect (see *Figure 36*). Indeed, this pretreatment prevented a stronger induction of the effect of Oncamex as reported by microscopic observation of changes in cell density and morphology (*Figure 36a-b*) or by measurement of cell viability, cytotoxicity and apoptosis using ApoTox-Glo Triplex assays (*Figure 36c-g*). For instance, in comparing the responses induced by treatment of MDA-MB-231 cells with 30µM Oncamex, NAC-treated cells showed a 1.5-fold decrease in cytotoxicity and 2-fold decrease in caspase activation.

To conclude, this shows the involvement of ROS as mediators in the effect of Oncamex. The fact that the effect of Oncamex was only partially blocked could be due to the involvement of other mechanisms. However, it seems plausible that a 30 min incubation with NAC may not provide enough protection against the ROS-generating effect of Oncamex. Since it has been shown to lead to the production of high levels of mSO and results have shown its ability to become redox-cycled, it could potentially continue to exert its ROS-modulating effect once the effect of the pretreatment with NAC is exhausted.

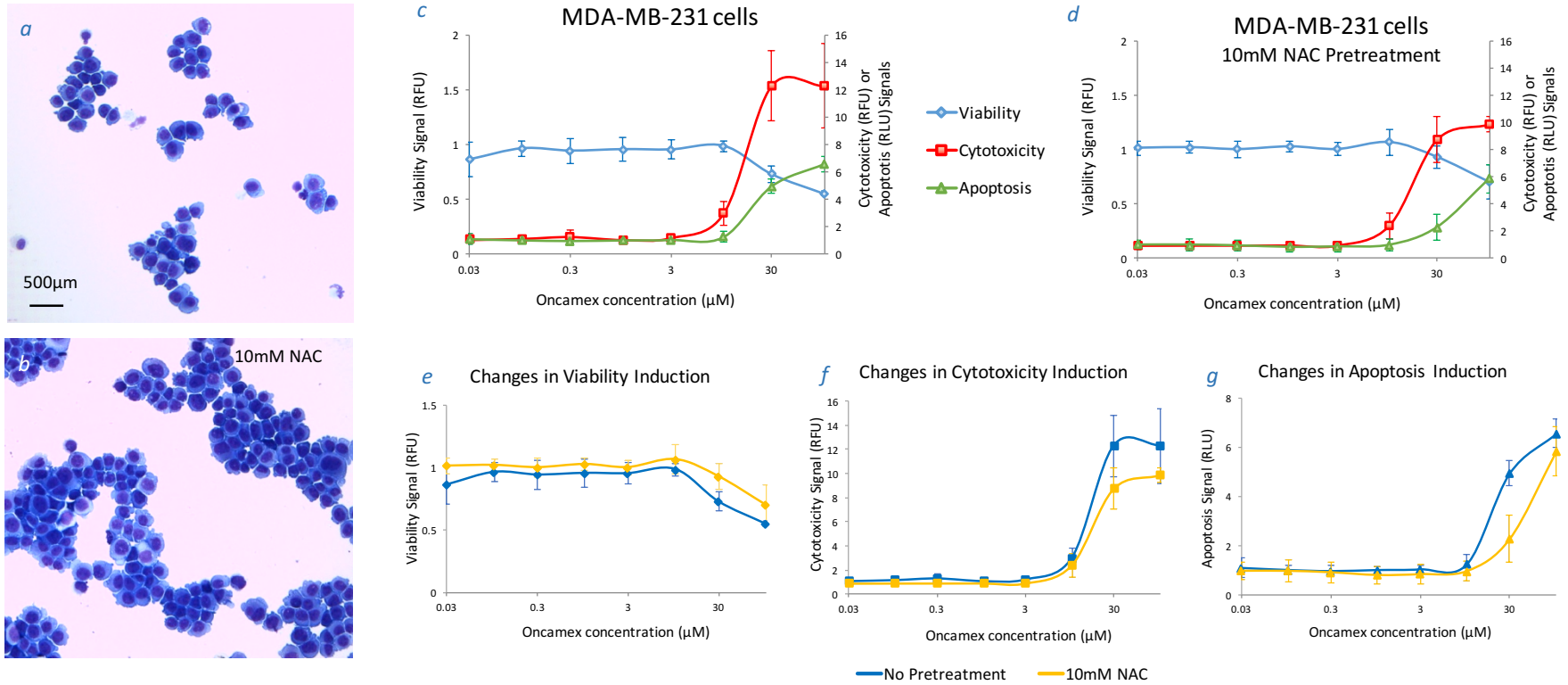

***Figure 36* Inhibition of induction of apoptosis by pretreatment with an antioxidant.** *Experiments were repeated including a 30 min pretreatment in 10mM NAC to assess the possible effect of the antioxidant. applied to assess the induction of apoptosis in cells treated with Oncamex for 8 h. Cytospin slides were prepared comparing the effect of treatment with 10µM Oncamex alone (a) or preceded by pretreatment with NAC. This experiment was repeated (n=2, with 3 technical replicates in each experiment). Captures show representative examples. ApoTox-Glo Triplex assays assessed changes in the effect exerted by Oncamex on MDA-MB-231 cells (c) when cells were pretreated with 10mM NAC (d). Graphs also compare the changes in viability (e), cytotoxicity (f) and apoptosis (g) in both conditions. Each experiment was repeated (n=2, with 6 technical replicates per concentration). These graphs show pooled results, with each data point representing the average from biological replicate experiments for each treatment condition, normalised to vehicle controls, and error bars representing standard deviation (SD). RFU, relative fluorescence units; RLU, relative luminescence units.*

4.5. Conclusions

Results reported in this chapter demonstrated the specific targeting of Oncamex for the mitochondrial compartment (see section *4.2.*) and its ROS-modulating effect there (see section *4.3.*). As previously discussed, the electrochemical properties of Oncamex suggested that it is likely to undergo reversible reduction in the mitochondria (see *Figure 26*), becoming negatively charged, and thus it may be able to react with oxygen to form mitochondrial superoxide ($O_2^{\cdot-}$ or mSO). This would regenerate the uncharged species of Oncamex, allowing for its continued redox cycling and the accumulation of increased levels of mSO.

While the potential modification of Oncamex by drug metabolism could alter its redox properties, its efficacy in generating mSO was supported by detection of mitochondrial ROS using specific fluorescent probes. Results suggested that the levels of mSO generated by lower concentration of Oncamex might be converted to mH_2O_2 (see *Figure 28*), most likely by the normal enzymatic activity of SOD1 and SOD2 (see *Figure 30* and section *4.3.*). However, results also suggested that higher concentrations of Oncamex may induce a greater production of mSO (see *Figure 29*) which can surpass the capacity of SOD enzymes, leading to accumulation of the anion. This may lead to the induction of oxidative stress and the disruption of mitochondrial function, which is already more susceptible to stress in cancer cells (see section *1.1.5.3.7.*). Thus, the study of ROS modulation in the mitochondria was suggestive of the possible role of apoptosis, tightly regulated by these organelles, in the mechanism of action of Oncamex. Further work sought to assess this (see section *4.4.*).

The initial observation of changes in cell morphology (see *Figure 31*) and detection of changes in membrane integrity using a fluorescent dye for the measurement of cytotoxicity (see *Figure 33*) suggested the induction of a necrosis-like effect. However, other results showed that the effect exerted by Oncamex (at least as early as 8 h after treatment) coincided with caspase activation, as also confirmed by the detection of PARP cleavage. This suggests the role of apoptosis as the main mechanism of Oncamex-induced cell death, with the necrotic-like features likely being the result of late apoptosis progressing into secondary necrosis. Results also showed the inhibition of the pro-apoptotic and cytotoxic effect of Oncamex by pre-incubation with the antioxidant NAC (see *Figure 36*), supporting the notion that ROS regulation is at least partially involved in the induction of the cellular responses observed.

The mechanism by which an increase in mSO can lead to the induction of apoptosis in the mitochondria bears further discussion. Despite the initial belief that apoptosis was a primarily nuclear event[582], mitochondria have long been known to play a key role in the initiation of apoptosis in mammalian cells[583–586]. The intrinsic (or mitochondria-dependent) apoptosis pathway can be triggered by multiple stimuli, including elevated ROS and oxidative stress, regulation by pro-apoptotic members of the BCL2 family or hypoxia, all of which can lead to the release of pro-apoptotic mitochondrial IMS proteins into the cytosol. Indeed, this apoptotic pathway relies on the release of pro-apoptotic proteins in the mitochondrial intermembrane space (IMS) such as cytochrome c (Cyt c) or Smac (second mitochondria-derived activator of caspase) that lead to the formation of the apoptosome, caspase activation, PARP cleavage and the subsequent development of apoptosis[584,587].

There are different, not necessarily mutually exclusive mechanisms for mitochondrial protein release[388,584,587–590]: (i) mitochondrial permeability transition (MPT) through the opening of a mitochondrial permeability transition pore complex (mPTPC) in the inner membrane[584,591], or (ii) mitochondrial outer membrane permeabilisation (MOMP) due to the creation of large channels in the outer membrane, such as the mitochondrial apoptosis-induced channel (MAC)[584,587], formed by pro-apoptotic members of the BCL2 family.

Both of these mechanisms cause substantial changes to the mitochondria, including membrane depolarisation and mitochondrial permeabilisation, which lead to the release of the pro-apoptotic signals into the cytosol (see *Figure 37* for summary of mechanism). Additionally, this process hampers the overall mitochondrial function, leading to the loss of ATP production, further ROS production and pH alterations[592].

Importantly, these pro-apoptotic mechanisms can be triggered by changes in levels of mitochondrial superoxide; in conjunction with other regulatory mechanisms such as calcium accumulation, increased ROS levels can lead to the formation of the mPTPC and the subsequent decrease of the mitochondrial transmembrane potential ($\Delta\psi$mm) and induction of apoptosis[593–597].

The induction of mitochondrial permeabilisation and apoptosis is subject to complex regulation by the BCL2 protein family[583,586,587,598–600], which includes both (i) anti-apoptotic members such as BCL2 and BCL-XL (B-cell lymphoma-extra large or BCL2-like 1 isoform 1) and (ii) pro-apoptotic members such as BAD (BCL2-associated death promoter), BAK (BCL2 homologous antagonist/killer) and Bax (BCL2-associated X protein).

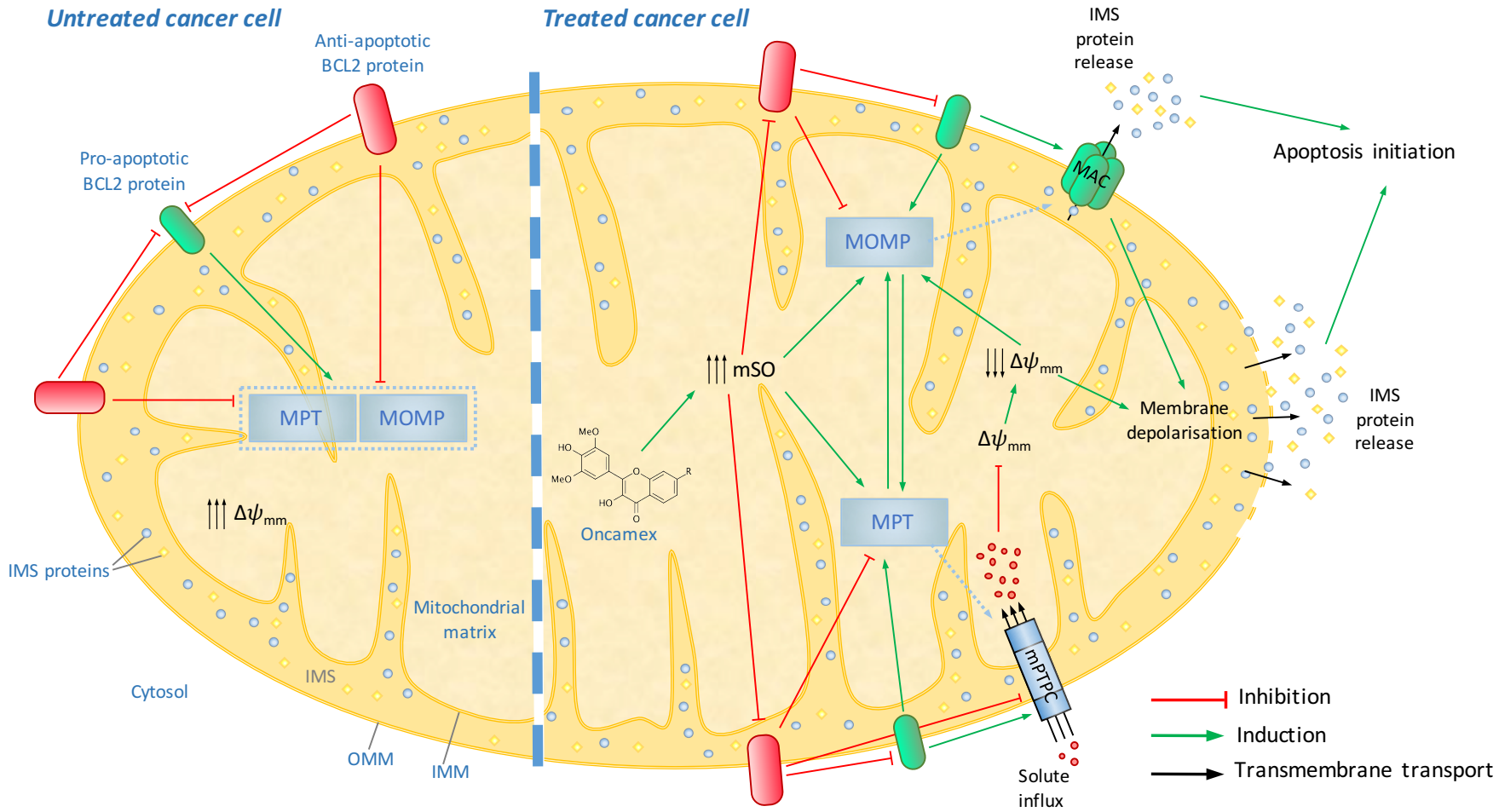

Figure 37 ***Mechanisms of initiation of mitochondria-dependent apoptosis.*** *The mitochondrion plays an essential role in the initiation of the intrinsic apoptosis pathway. The BCL2 protein family and ROS levels regulate mechanisms that can lead to the induction of apoptosis. Oncamex, like many anti-cancer agents, may lead to mitochondrial permeability transition (MPT) and mitochondrial outer membrane permeabilisation (MOMP), which cause the release of pro-apoptotic proteins in the mitochondrial intermembrane space (IMS) and can initiate caspase activation and the apoptosis signalling pathway in the cytosol. Δψmm, mitochondrial transmembrane potential; OMM, outer mitochondrial membrane; IMM, inner mitochondrial membrane; mSO, mitochondrial superoxide; mPTPC, mitochondrial permeability transition pore complex; MAC, mitochondrial apoptosis-induced channel.*

Interestingly, research has also shown a direct, antagonistic relation between levels of mitochondrial superoxide and anti-apoptotic regulator protein BCL2[588,601], since mSO can induce the degradation and down-regulation of BCL2[601–603]. Increases in mitochondrial ROS have also been shown to lead to acidification of the cytosol and conformational changes of BAX, which aide the induction and advancement of apoptosis[604].

Besides the direct effect of ROS accumulation in the triggering of MPT and MOMP, mSO can also induce mitochondrial dysfunction by damaging enzymes, either by direct oxidation or by reacting with nitric oxide (·NO) to form peroxynitrite ($ONOO^-$), an even more reactive oxidant[597,605]. Oxidation can lead to the release of ferrous iron from the iron sulphur centre of enzymes such as aconitase[606]. In the presence of ferrous or cuprous ions, mH_2O_2 obtained from the dismutation of mSO by SOD enzymatic activity can form hydroxyl radicals (·OH), another highly reactive species capable of inducing oxidative damage in the mitochondria[605,607].

In short, the production of mSO triggers the production of a series of reactive species that can lead to damaging effect to lipids, proteins and nucleic acids[597,608]. This effect is particularly impactful to the mitochondrial function of cancer cells and can lead to a decrease in mitochondrial ATP synthesis and cellular calcium dyshomeostasis, further contributing to mitochondrial permeabilisation and the induction of apoptosis. As previously mentioned, the accumulation of mSO may also lead to its spillage into the cytosol and direct oxidation of the plasma membrane, which could contribute to the observed loss of membrane integrity.

To conclude, there is extensive evidence on the essential role that mitochondria and changes in mitochondrial ROS levels can play in the induction of apoptosis. In particular, levels of mSO have been shown to inhibit anti-apoptotic signals and induce the release of pro-apoptotic factors. The pro-apoptotic role of mitochondrial ROS has led to the application of compounds capable of inducing oxidative stress in the mitochondria as anti-cancer agents[388,609,610]. Chemotherapeutic agents such as doxorubicin or cisplatin[611] and the anti-oestrogen tamoxifen[612] have been shown to induce ROS production as part of their mechanisms of action.

The results reported in this chapter suggest that Oncamex may rely in a similar mechanism. Through its specific mitochondrial targeting and redox properties, Oncamex can generate mSO, leading to mitochondrial dysregulation and, in turn, the induction of cytotoxicity and the initiation of ROS and mitochondria-dependent apoptosis. The relevance of these findings will be further discussed in the context of results from differential gene

expression analysis in order to postulate and informed model for the possible mechanisms of action of Oncamex (see section *5.4.*), considering information on the effect of Oncamex on both protein interaction and cellular responses (as described in this chapter) and gene expression (as reported in the next chapter).

5. Study of the effect of Oncamex on gene expression

5.1. Introduction

Following results from previous sections investigating the properties of Oncamex and the cellular responses it exerted *in vitro*, this section will further assess its effect by studying the changes induced at gene expression level. Differential gene expression analysis was undertaken to study the effect of Oncamex in breast and ovarian cancer cell line models. This methodology sought to study whether the observed antiproliferative and pro-apoptotic effects of this novel flavonoid were reflected in changes in the expression levels of genes regulating these processes, as well as to investigate other possible changes that may contribute to the effect of Oncamex in pre-clinical *in vitro* models and gain a better understanding of its mechanisms of action.

Following previous work, differential gene expression analysis assessed the effect of Oncamex in 5 breast cancer cell lines representing different molecular subtypes and phenotypes: triple negative MDA-MB-231, ER^+ MCF-7 and oestrogen-independent, MCF-7-derived LCC1, LCC2 and LCC9. This experiment also included the chemotherapy-sensitive/resistant ovarian cancer cell line pair PEA1 and PEA2.

Some constraints had to be factored into the design of this microarray experiment. Due to limited space in the chips, only 1 replicate per treatment condition and cell line could be included. Thus, for each of the 7 breast and ovarian cell lines studied the experiment included 1 sample each for the following treatment conditions:

(i) 10µM Oncamex for 6 h, as previous results suggested the ability of these treatment conditions to exert the initiation of changes in mitochondrial homeostasis, proliferation and apoptosis;

(ii) 0.3µM Oncamex for 2 h, as these conditions were tested for their possible beneficial effect in combination with other agents (see Chapter 6);

(iii) vehicle control (1% DMSO) for 6 h.

Where possible, untreated controls were also included (for MCF-7 and MDA-MB-231 cells). In order to assess the effect of Oncamex on these models, cells were processed and hybridised in a microarray experiment as previously described (see section *2.2.15.*) and resulting data was log2-transformed and normalised for its analysis (see section *2.2.16.*).

5.2. Preliminary analysis of the effect of treatment across breast and ovarian cancer cell line models

5.2.1. Analysis of dissimilarities between treated and control breast cancer samples

Preliminary analysis investigated the similarity of all treated and control breast cancer cells in an attempt to assess the overall differences across cell lines and the extent of the effects of Oncamex. For this, breast samples were clustered based on Pearson correlation of the 1000 most differentially expressed genes. Results showed the expected clustering of cells according to their biological similarities (see *Figure 38*).

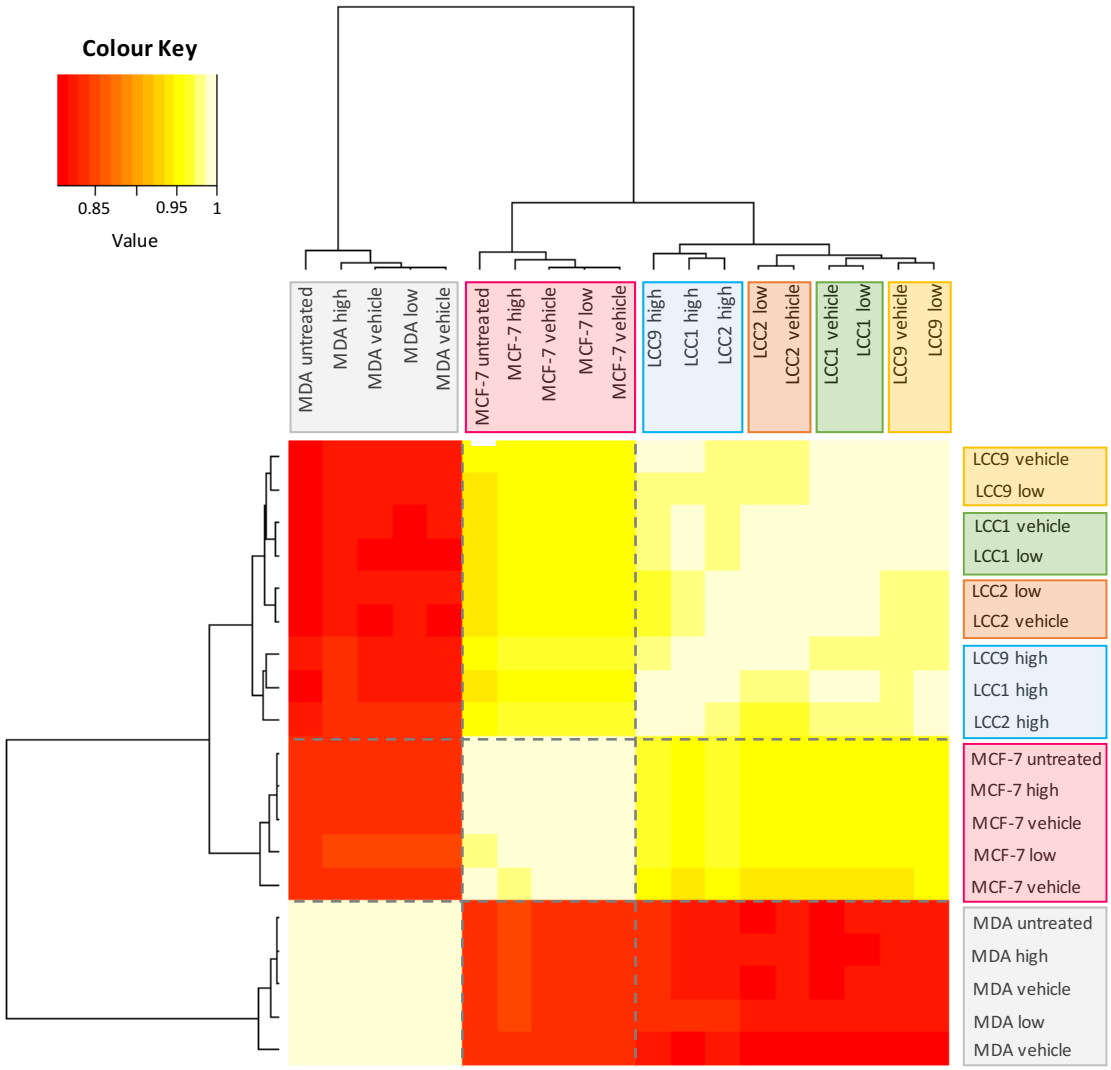

***Figure 38* Preliminary study of the differences between breast cancer cells.** *Samples were hierarchically clustered based on Pearson correlation using the 1000 most variable genes across all samples. This heatmap represents the level of similarity (light yellow for greater to red for lower) for each pair of samples. The dendrogram represents the samples' association, with coloured boxes indicating different branches.*

Indeed, the dendrogram from a dissimilarity matrix separated all the triple negative MDA-MB-231 samples from the ER^+ samples. Among the latter, MCF-7 samples were clustered together and separately from MCF-7-derived cells: LCC1, LCC2 and LCC9. Interestingly, all LCC cells treated with the higher concentration of Oncamex were clustered together, while controls and low treated-cells were clustered separately by pairs. This suggests that unlike with MDA-MB-231 and MCF-7 cells, the effect of treatment with Oncamex may induce changes greater than the inherent differences between LCC1, LCC2 and LCC9 cells.

Treatment with 10µM Oncamex appeared to induce an effect in every cell line studied, with treated samples being separated according to their dissimilarity from cells exposed to different conditions. In comparison, cells exposed to 0.3µM or a vehicle control were clustered the closest, indicating the similarity of the gene expression profile of each pair of samples. This suggests treatment with the lower dose of Oncamex may not induce a significant effect in addition to that of the vehicle at the 2 h timepoint studied. This was investigated further in subsequent analysis.

5.2.2. Preliminary study of a possible vehicle effect

Prior to further discussion of differential gene expression analysis results, the caveat of the possible effect of the vehicle (1% DMSO) bears mentioning. The concentration of the vehicle was kept to the minimum possible across experiments and never surpassed 1% in any treatment solution. However, the limited solubility of the novel flavonoids tested prevented the use of ideally lower concentrations of DMSO.

Previous experiments had incorporated untreated and vehicle controls and no apparent vehicle effects were observed. Additionally, previous research has found that DMSO may be applied as an organic solvent in cell culture without apparent toxic effect up to a concentration of 2%, with only limited effects in the regulation of drug-metabolising enzymes being consistently observed at gene level[613]. In this analysis, initial study of similarity across treated and control samples suggested the solvent may induce some effect, as cells exposed to a vehicle control (1% DMSO for 6 h) were clustered closer to samples exposed to low Oncamex treatment (0.3µM Oncamex for 2 h) than to untreated samples (see *Figure 38*).

Following these observations, preliminary analysis sought to assess the extent of the effect that DMSO may induce on the gene expression profiles of cells. The effect on MCF-7 cells of exposure to DMSO was studied by combining gene expression data from untreated,

vehicle control and Oncamex-treated samples in this microarray experiment with data from other publically-available datasets which included MCF-7 cells exposed to (i) 0.025% DMSO for 2, 4 or 6 h[528], or (ii) 0.1% DMSO for 6 h[529], as previously described (see sections *2.1.3.* and *2.2.17.*). Following integration and batch correction, multidimensional scaling (MDS) plotted samples according to the similarity of their gene expression profiles (see *Figure 39*).

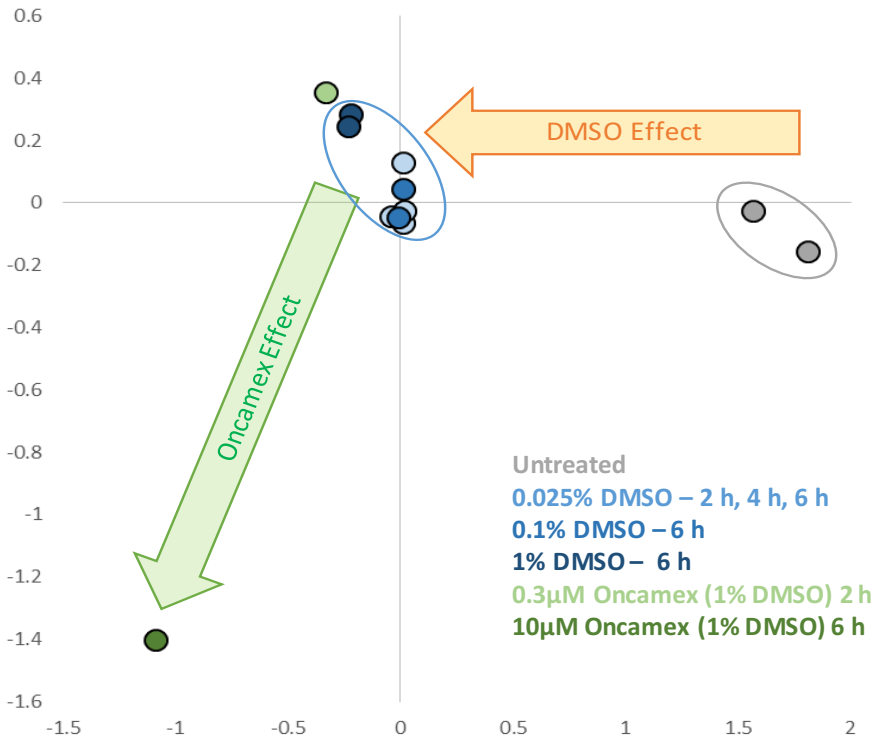

Figure 39 ***Multidimensional scaling of DMSO-treated MCF-7 cells.*** *Samples from the microarray described here and another 2 publically-available gene expression studies*[528,529] *were combined to assess the overall effect on the gene expression profile of MCF-7 cells of exposure to DMSO, at different concentrations and exposure times. MDS converted the gene expression information for these samples into a bi-dimensional scale, allowing for their plotting and clustering according to their similarity.*

Results showed that exposure to DMSO led to a shift in comparison to untreated cells. Treatment with 10µM Oncamex (in 1% DMSO, for 6 h) lead to a greater shift, which was consistent with Oncamex inducing a significantly greater effect than the vehicle. Cells treated with 0.3µM Oncamex (in 1% DMSO, for 2 h) were grouped together with vehicle controls, suggesting that the low concentration of the drug may not exert additional effects on the gene expression profile of MCF-7 cells beyond those of the vehicle. Importantly, MDS showed a similar effect of different vehicles, as DMSO-treated samples were clustered together irrespective of concentration (0.025, 0.1 or 1% DMSO) or length of exposure (2, 4 or 6 h).

In short, treatment with Oncamex required its administration in an organic solvent and, due to the limited solubility of the compound, 1% DMSO was required. MDS analysis demonstrated that, while DMSO induced an effect in the gene expression profile of MCF-7 cells, this effect was small in comparison to that of Oncamex. The poor solubility of the drug meant this effect was unavoidable and, importantly, results also suggested that the use of a lower concentration of DMSO would not have prevented this weaker vehicle effect, as samples treated with concentrations 40 times lower appeared to induce comparable effects. Indeed, MCF-7 cells exposed to 0.025% DMSO for 2 h clustered closely with cells treated with 1% DMSO for 6 h. Thus, the vehicle effect in this microarray experiment may be the minimal that could be expected in a study were the use of an organic solvent like DMSO was necessary. Evidence suggested that this vehicle effect may not be significant in comparison to the greater effect of high treatment with Oncamex, particularly if conservative thresholds are applied to select differentially expressed genes. However, the correct approach for further gene expression analysis was to consider this vehicle effect as a caveat, comparing vehicle to untreated controls were available and assessing the biological function of any genes altered by the solvent.

5.2.3. Overlapping changes in breast and ovarian cells

Differential gene expression analysis in this chapter focused on the effect of the higher treatment with Oncamex, as the 0.3µM concentration was included in relation to combination experiments (reported in Chapter 6). Initial analysis investigated gene changes induced by treatment with 10µM Oncamex in different breast and ovarian cancer models (see *Table 11*). A 0.4 log2-scale fold change threshold was applied to select genes whose expression level was up- or down-regulated (positive or negative changes between vehicle control and treated cells).

Results showed that treatment changed the expression levels of several hundred genes in all cell lines (see *Table 11* and *Appendix 2* for gene lists). Nevertheless, the extent of these changes varied between models, demonstrating the inherent differences between these different cell lines. For instance, Oncamex induced changes in a larger number of genes in MDA-MB-231 cells than in MCF-7 cells (766 vs 550). Interestingly, results showed that LCC9 cells underwent a greater change in their gene expression profile, with more genes being differentially expressed after treatment with Oncamex; more than double the number of genes than LCC1 and LCC2 and greater than 5 times more genes than MCF-7. Given the common origin of these 4 cell lines, this suggests the greater inherent dissimilarity of LCC9

cells, which are characterised by their oestrogen-independence and resistance to anti-oestrogens. The differential effect of Oncamex on these niche population of cell lines will be further discussed in the following chapter.

	MDA-MB-231	MCF-7	LCC1	LCC2	LCC9	PEA1	PEA2
Up-regulated genes	393	247	582	530	1496	522	389
Down-regulated genes	373	303	667	618	1546	245	412

Table 11 ***Differentially expressed genes in breast and ovarian cancer cells.*** *Comparison of gene expression levels between treated and control cells, using a threshold of 0.4 log2-scale fold change, led to the identification of genes whose expression was altered by treatment with 10μM Oncamex for 6 h.*

Previous results (see Chapters 3 and 4) have shown the ability of Oncamex to exert similar antiproliferative and pro-apoptotic effects in different cancer models. Consequently, further analysis assessed the number of genes whose expression levels were consistently altered by treatment with Oncamex across different models.

Venn diagrams obtained using online tools[614,615] represented the overlap in the differentially expressed genes in treated MDA-MB-231 and MCF-7 cells (see *Figure 40* and *Appendix 2* for gene lists). Results showed that, despite the apparent similar effects in cell culture tests, only a limited percentage of these genes were differentially expressed in both of these models: 59 genes were up-regulated and 27 down-regulated in both models.

Comparison of changes in MCF-7 and MCF-7-derived cell lines (LCC1, LCC2 and LCC9) showed greater similarity in the differential expression of genes induced (see *Figure 41* and *Appendix 2* for gene lists). This was to be expected due to the common origin of these 4 cell lines. Indeed, results showed 80 genes were up-regulated in these 4 models, while 59 were down-regulated.

Further analysis looked at the overlap between the gene expression changes induced by Oncamex in the PEA1/2 pair of ovarian cancer cell lines. Results reported a greater overlap of changes than in previous comparisons (see *Figure 42* and *Appendix 2* for gene lists): 129 up-regulated genes were conserved across both cell lines, while 67 genes were consistently down-regulated.

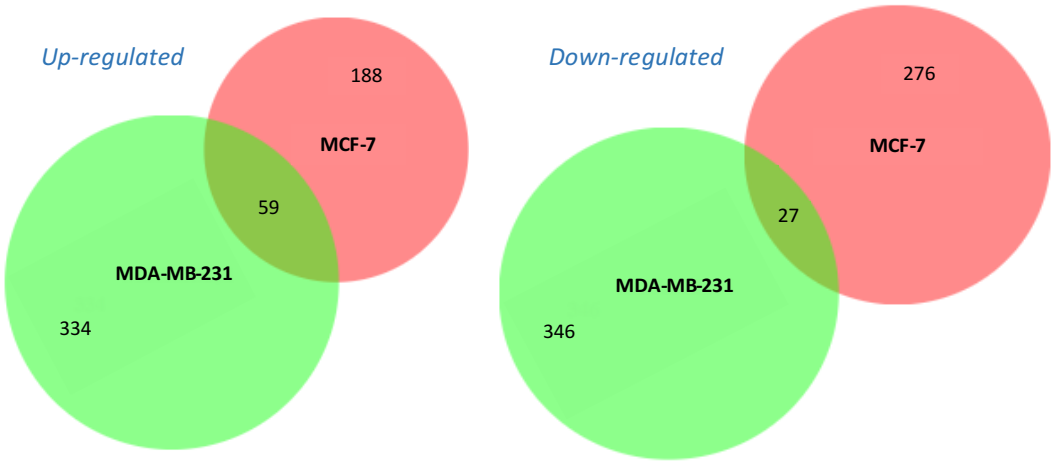

Figure 40 ***Overlapping differentially expressed genes across MDA-MB-231 and MCF-7 cells.*** *Genes whose expression level had changed by at least a 0.4 log2-scale fold change between control and treated (10μM Oncamex for 6 h) cells were considered differentially expressed. Venn diagrams represent the overlap in up- (left) and down-regulated (right) genes between both models. The relative size of each circle and overlapping areas is directly proportional to the number of genes in each group.*

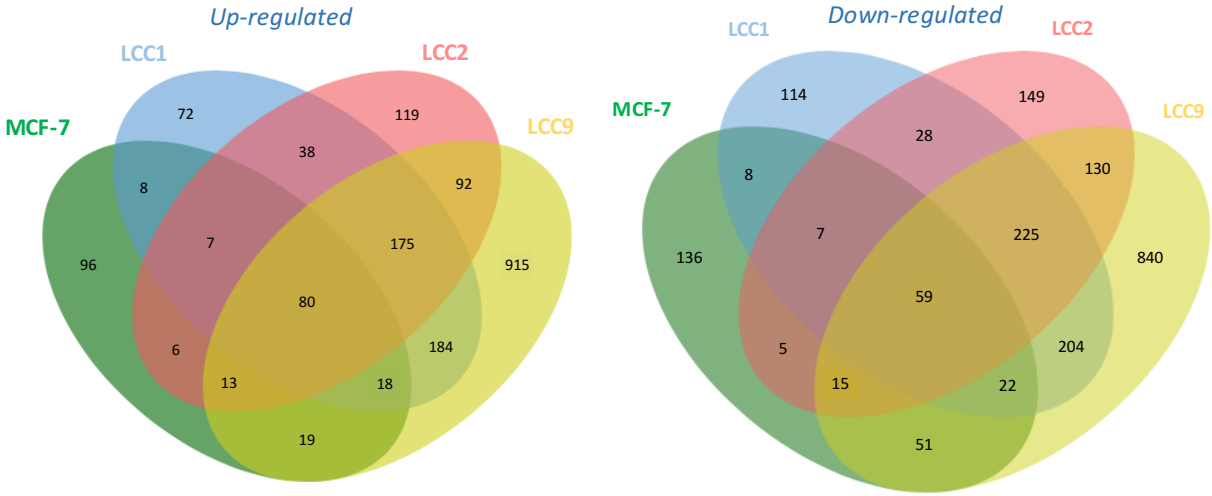

Figure 41 ***Overlapping differentially expressed genes across MCF-7 and LCC1/2/9 cells.*** *Genes whose expression level had changed by at least a 0.4 log2-scale fold change between control and treated (10μM Oncamex for 6 h) cells were considered differentially expressed. Venn diagrams represent the overlap in up- (left) and down-regulated (right) genes between both models.*

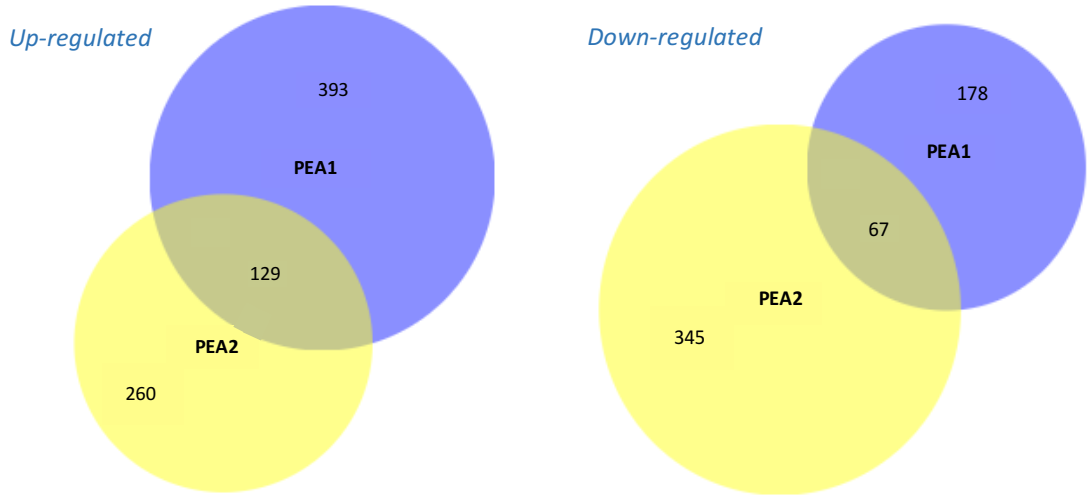

***Figure 42* Overlapping differentially expressed genes across PEA1 and PEA2 ovarian cancer cells.** *Genes whose expression level had changed by at least a 0.4 log2-scale fold change between control and treated (10μM Oncamex for 6 h) cells were considered differentially expressed. Venn diagrams represent the overlap in up- (left) and down-regulated (right) genes between both models. The relative size of each circle and overlapping areas is directly proportional to the number of genes in each group.*

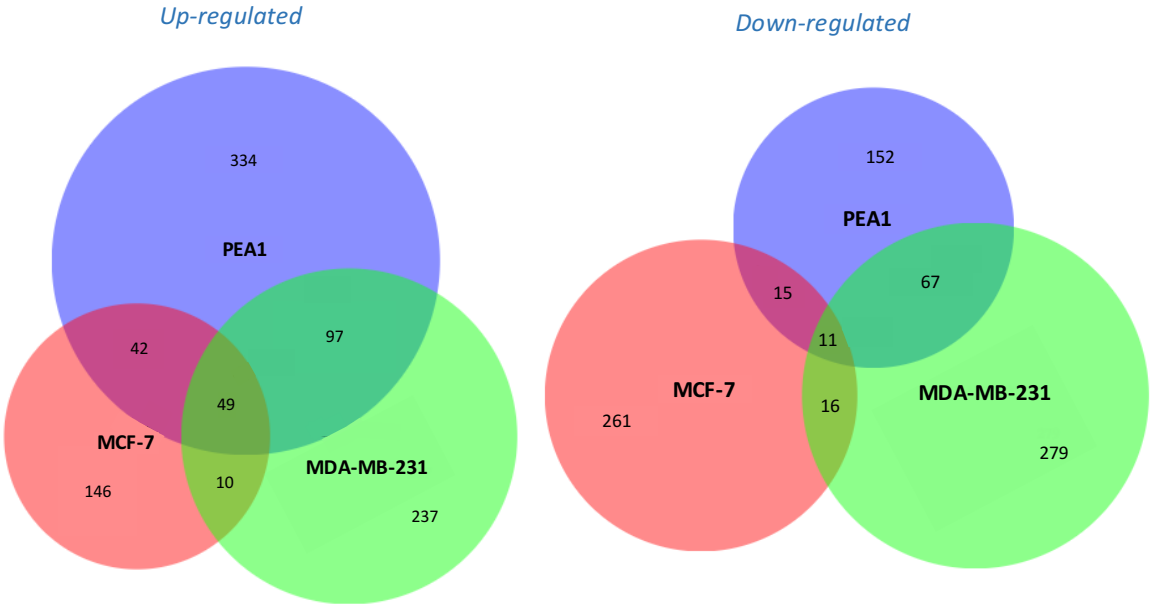

***Figure 43* Overlapping differentially expressed genes across breast and ovarian cancer cells.** *Genes whose expression level had changed by at least a 0.4 log2-scale fold change between control and treated (10μM Oncamex for 6 h) cells were considered differentially expressed. Venn diagrams obtained using the online tool jvenn[614] represent the overlap in up- (left) and down-regulated (right) genes between both models. The relative size of each circle and overlapping areas is directly proportional to the number of genes in each group.*

Finally, the overlap of differentially expressed genes was also assessed in comparison of 3 of the previous models known to be more biologically different: triple negative breast cancer cell line MDA-MB-231, ER^+ breast cancer cell line MCF-7 and ovarian cancer cell line PEA1 (see *Figure 43* and *Appendix 2* for gene lists). Results again reported only a partial overlap across all 3 cell lines of up-regulated (49) and down-regulated (11) genes.

In short, preliminary analysis of differentially expressed genes in treated cancer cells demonstrated the effect of Oncamex on the gene expression profiles of different breast and ovarian cancer cell line models. However, the extent of the effect of Oncamex on these gene expression profiles varied across cell lines and only part of the differentially expressed genes observed overlapped between different models. Results reported a greater overlap of up- or down-regulated genes between cell lines with a common biological origin, such as MCF-7-derived breast cancer cells or the chemo-sensitive/resistant ovarian cancer cell line pair PEA1/2. Interestingly, all comparisons demonstrated a greater overlap in those genes that were up-regulated by treatment with Oncamex, rather than down-regulated.

Further work sought to investigate whether these overlapping changes across different models exposed to 10μM Oncamex were related to a common effect that may contribute to the mechanism of action of Oncamex. For this, functional gene enrichment analysis was performed to obtain the gene ontology (GO) terms associated with these consistently differentially expressed genes. These terms provide an insight into the biological processes, molecular functions or cellular components linked to the activity of these genes[548,549].

Using the REVIGO (reduce + visualize gene ontology) online tool[550], these GO terms were summarised to identify and interpret the signalling pathways and processes regulated by these genes. Analysis of overlapping genes up-regulated in both MDA-MB-231 and MCF-7 cells showed the involvement of 2 main biological processes: glycolysis and response to oxygen levels/hypoxia (see *Figure 44*). GO functional enrichment analysis of overlapping down-regulated genes reported no statistically significantly enriched biological functions.

Interestingly, similar analysis reported the same enriched biological functions in overlapping genes differentially expressed in (i) MCF-7 and LCC1/2/9 cells (see *Figure 45*) and (ii) PEA1 and PEA2 cells (see *Figure 46*). Indeed, although a larger number of genes overlapped across both sets of cell lines due to their common biological origin, both glucose metabolism and response to oxygen levels/hypoxia were similarly enriched. In these instances, functional enrichment analysis also reported no significantly enriched biological functions for overlapping down-regulated genes.

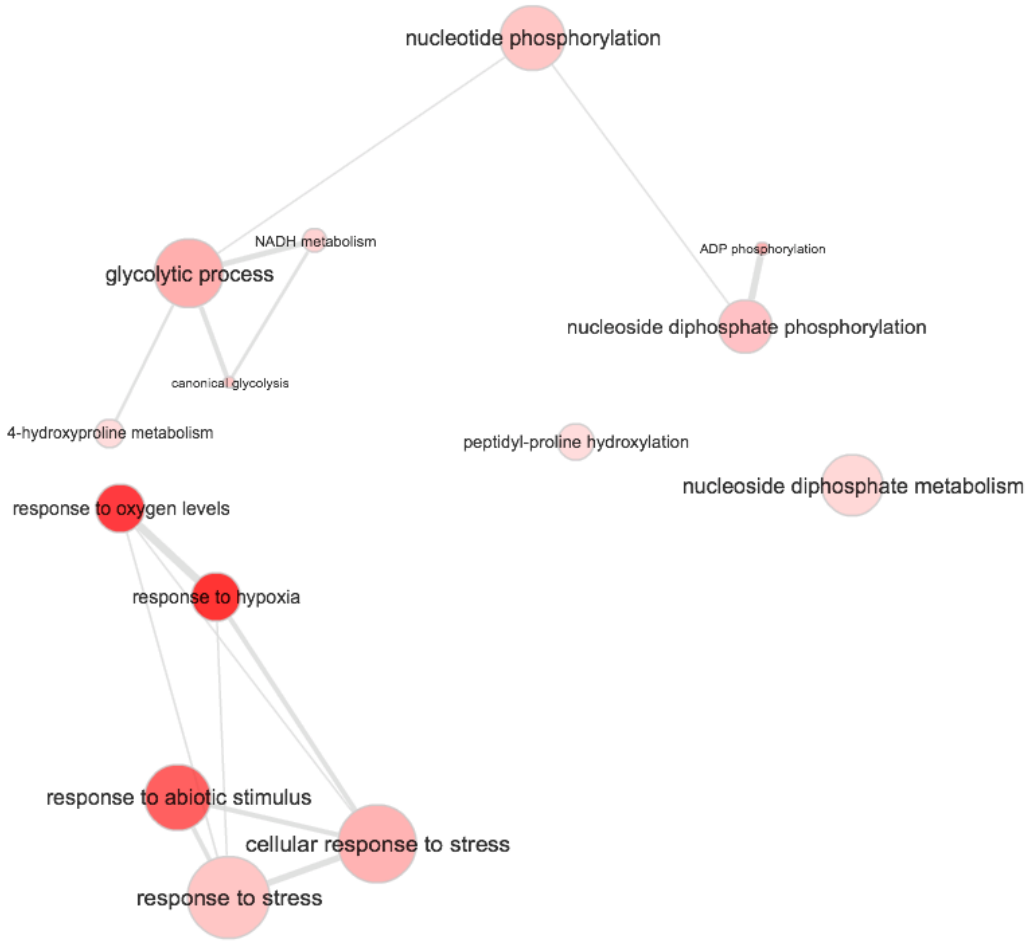

Figure 44 ***GO functional enrichment analysis with overlapping genes up-regulated by high Oncamex treatment in both MDA-MB-231 and MCF-7 breast cancer cells.*** *The REVIGO online tool was used to summarise the biological processes, molecular functions or cellular components linked to differentially expressed genes. Node colour indicates the statistical significance of the enrichment as per the adjusted P-values obtained from GO functional gene enrichment analysis, while node size indicates the frequency of each term in the underlying database. Highly similar nodes are linked, with line width indicating the degree of similarity. REVIGO applies a force-directed layout algorithm to position more similar nodes together.*

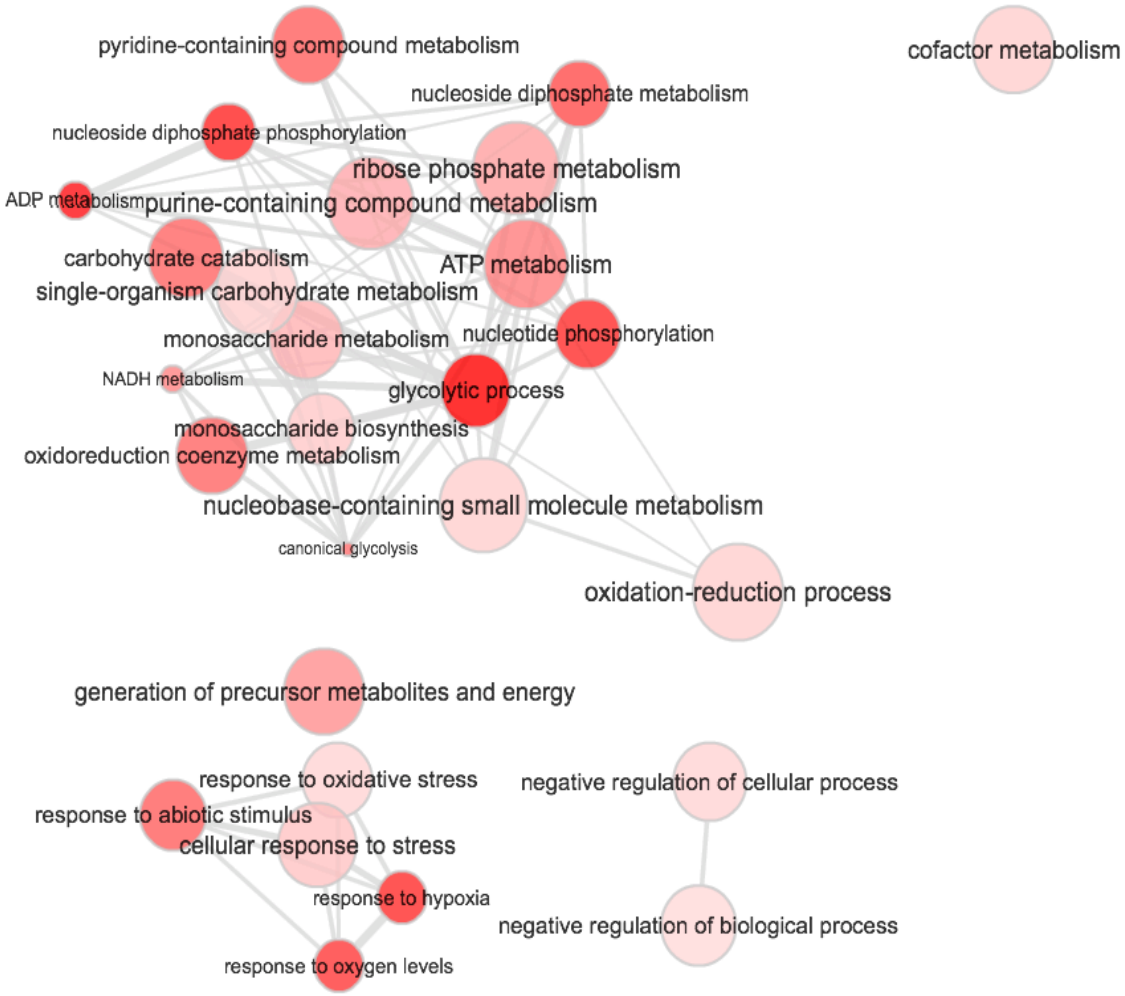

Figure 45 ***GO functional enrichment analysis with overlapping genes up-regulated by high Oncamex treatment in both MCF-7 and LCC1/2/9 breast cancer cells.*** *The REVIGO online tool was used to summarise the biological processes, molecular functions or cellular components linked to differentially expressed genes. Node colour indicates the statistical significance of the enrichment as per the adjusted P-values obtained from GO functional gene enrichment analysis, while node size indicates the frequency of each term in the underlying database. Highly similar nodes are linked, with line width indicating the degree of similarity. REVIGO applies a force-directed layout algorithm to position more similar nodes together.*

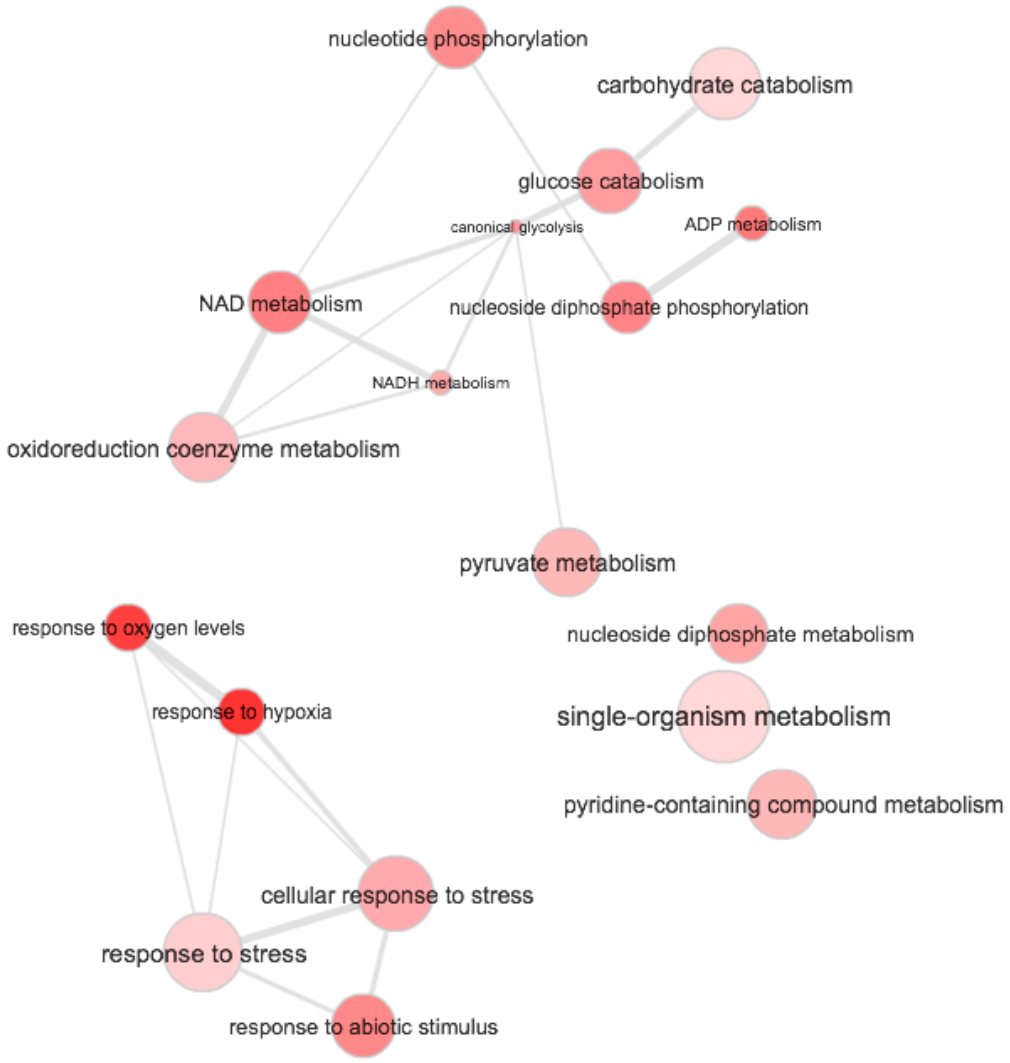

Figure 46 ***GO functional enrichment analysis with overlapping genes up-regulated by high Oncamex treatment in both PEA1 and PEA2 ovarian cancer cells.*** *The REVIGO online tool was used to summarise the biological processes, molecular functions or cellular components linked to differentially expressed genes. Node colour indicates the statistical significance of the enrichment as per the adjusted P-values obtained from GO analysis, while node size indicates the frequency of each term in the underlying database. Highly similar nodes are linked, with line width indicating the degree of similarity. REVIGO applies a force-directed layout algorithm to position more similar nodes together.*

In summary, results have shown that, despite differences across models in the number of genes that are consistently differentially expressed after treatment with Oncamex, the changes induced would translate into the modulation of the same biological functions. Indeed, REVIGO processing of GO functional enrichment analysis has shown the induction of changes in functions related to 2 general processes: (i) glucose metabolism and energy production and (ii) response to hypoxia, oxygen levels and other stresses.

These results suggest that the lack of a greater overlap in the changes in gene expression profiles induced is likely to be due to the inherent differences between models. Nevertheless, Oncamex appears to induce similar functional changes in different cell lines, which supports the notion of a similar effect and mechanism of action of these compounds across different cancer models and types.

These results suggest that Oncamex may exert its effect through modulation of these biological functions. Glycolysis has long been known to play an essential role in energy production in cancer cells, which are known to favour it over the most efficient process of oxidative phosphorylation in the mitochondria in what is called the Warburg effect[616,617]. The mechanisms behind cancer energy metabolism are complex, but it has been established that glycolysis is enhanced through hypoxia-induced factors. Indeed, these and other stress-related signals have been shown to influence the glycolysis/oxidative phosphorylation ratio in cancer cells and have also been linked to changes in mitochondrial function, oxidative stress and cell viability in cancer cells[616,618–620].

In this context, the preliminary results obtained from GO analysis of the changes induced by Oncamex suggest that this novel flavonoid might exert its observed *in vitro* antitumour effects through modulation of these biological functions. Thus, further gene expression analysis sought to investigate the changes induced by Oncamex in greater depth in an effort to better understand how the modulation of these biological functions might be linked to its observed mitochondrial targeting and pro-apoptotic abilities, demonstrated by previous results, and to describe a more detailed model for the mechanism of action of Oncamex.

5.3. In-depth analysis of Oncamex-induced differential gene expression

5.3.1. Study of the effect of Oncamex on a first breast cancer model

Firstly, work focused on studying the effect of Oncamex on MCF-7 breast cancer cells. Differentially expressed genes were selected by comparison of gene expression levels between cells treated with 10µM Oncamex or a vehicle control for 6 h, using a 0.4 log2-scale fold change threshold. The resulting genes were then clustered in TMeV using hierarchical clustering following Pearson correlation with complete linkage for 4 treatment conditions: untreated, vehicle control, low (0.3µM for 2 h) and high (10µM for 6 h) Oncamex treatment. This resulted in a heatmap presenting 3 distinct clusters (see *Figure 47*). Gene enrichment analysis of the genes in each cluster subsequently identified the most significantly represented GO terms (see *Figures 47*, *48* and *49*).

Cluster 1 included genes which were up-regulated by treatment with 10µM Oncamex (see *Figure 47*). Treatment with 0.3µM Oncamex induced a weaker effect, down-regulating the expression of the majority of these genes in comparison to untreated cells. This effect was similar to that observed in cells treated only with a vehicle control, suggesting the lower treatment with Oncamex did not exert a significant additional effect beyond that of the solvent, as previously discussed (see section *5.2.2.*).

Gene enrichment analysis showed several GO terms significantly represented in cluster 1. Indeed, results showed that treatment with 10µM Oncamex for 6 h up-regulated genes associated with glycolysis, the JNK (c-Jun N-terminal kinases) pathway, pro-apoptotic signals, mitophagy, cell cycle arrest and HSP (heat shock protein) stress response.

The most significant genes associated with each GO term in this cluster were also identified (see *Figure 48*). Oncamex induced an up-regulation of genes encoding key glycolytic enzymes[617,621,622]. These included *HK2* (encoding hexokinase 2, which couples glycolysis to oxidative phosphorylation by using ATP generated in the mitochondria to convert glucose to glucose-6-phosphate in the first enzymatic step of glycolysis[623–625]) and *PKM2* (pyruvate kinase isoenzyme type M2, responsible for ATP production in glycolysis[621,622]), as well as genes involved in the catalysis of other steps, such as *PGAM1* (phosphoglycerate mutase), *ENO2* (enolase 2) or *LDHA1* (lactate dehydrogenase A) (see *Figure 58* for a summary of glycolysis, glycolytic genes and their alteration by treatment with Oncamex).

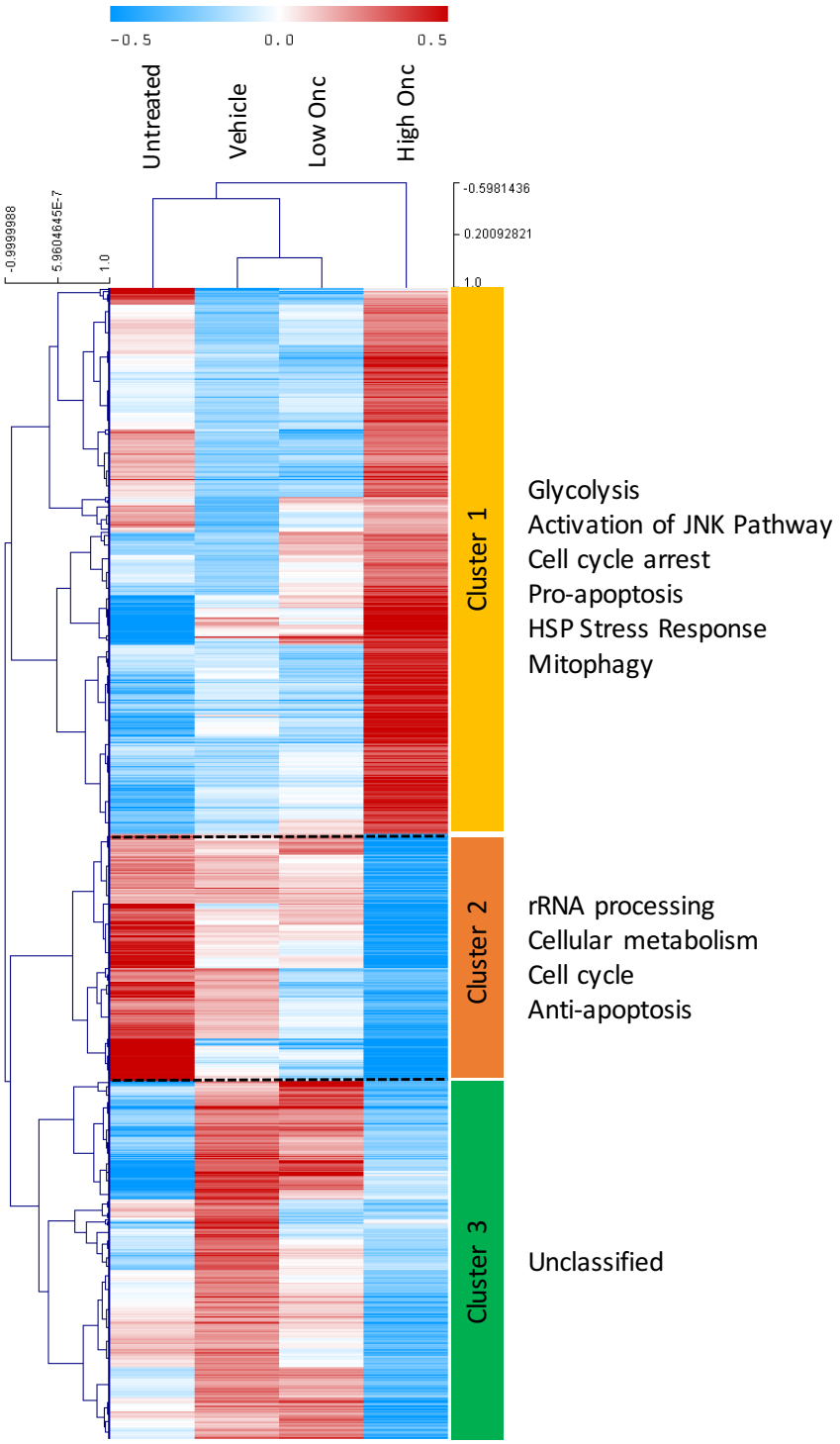

Figure 47 ***Differential gene expression profiles in MCF-7 cells treated with Oncamex.*** *Genes whose change in expression levels between high treated (10μM Oncamex for 6 h) and vehicle control (1% DMSO for 6 h) cells were greater than a 0.4 log2-scale cut-off were selected as differentially expressed. This heatmap is the result of hierarchical clustering of these genes following Pearson correlation with complete linkage for gene expression data of MCF-7 cells exposed to 4 treatment conditions. Red and blue represent relative high and low log2 expression values, respectively. Gene enrichment analysis provided a list of GO terms significantly represented in each cluster (right).*

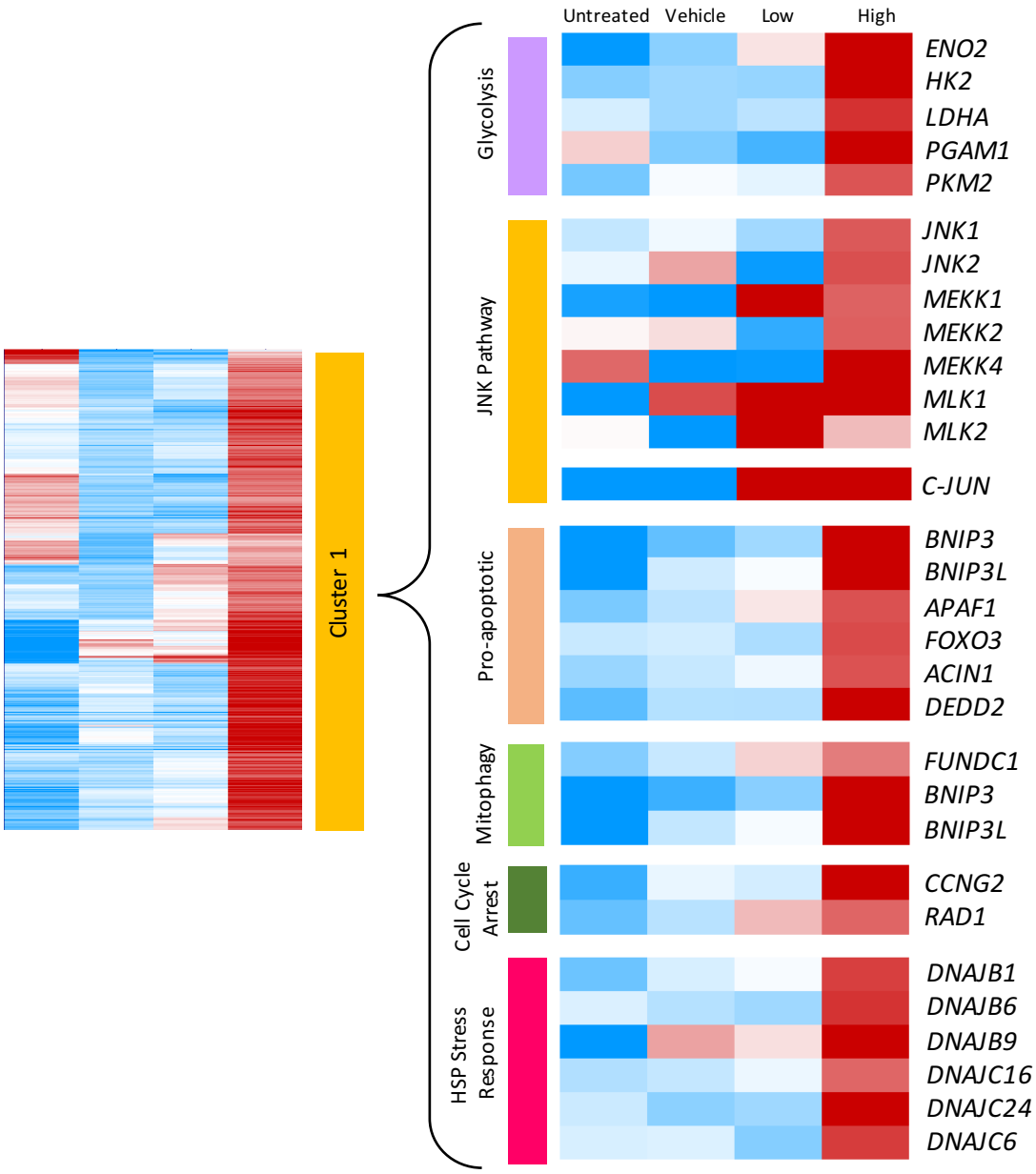

***Figure 48* Genes linked to functions significantly up-regulated by treatment with Oncamex.** *Gene enrichment analysis identified the biological processes, molecular functions or cellular components associated with cluster 1, which included genes differentially up-regulated in Oncamex-treated MCF-7 cells. Red and blue represent relative high and low log2 expression values, respectively. Significant examples of genes associated with each GO term are presented here.*

Treatment with Oncamex up-regulated genes in the JNK (c-Jun N-terminal kinases) pathway. This pathway can be induced by cellular stress through the MAPK (mitogen-activated protein kinase) pathway and is involved in the regulation of several biological processes, including cell survival proliferation, autophagy and apoptosis[626–628]. These changes included an increase in expression of *JNK1* and *JNK2*, as well as the genes encoding their

upstream activators belonging to the MAP3K (MAPK kinase kinase) family, such as *MEKK1*, *MEKK2* and *MEKK4* (also known as *MAP3K1*, *MAP3K2* and *MAP3K4*) or *MLK1* and *MLK2* (*MAP3K9* and *MAP3K10*)[626,629,630]. The effect of Oncamex on gene expression levels of these kinases varied, with *MEKK4* and *MLK1* being the most significantly up-regulated. Treatment also up-regulated expression of *C-JUN*, which encodes the protein c-Jun, a downstream target of phosphorylation by the JNK pathway which upon activation forms part of the early response transcription factor AP-1 (activator protein 1), involved in the regulation of processes including proliferation and apoptosis[626,631,632].

In relation to these changes, Oncamex also induced the up-regulation of genes involved in the induction of apoptosis. This included genes encoding pro-apoptotic members of the BCL2 apoptosis-regulating protein family[633–635]: *BNIP3* (BCL2/adenovirus E1B 19 KDa protein-interacting protein 3) and *BNIP3L* (BNIP3-like, also referred to as NIX). Other important pro-apoptotic genes whose expression was increased following treatment were *APAF1* (encoding the apoptotic protease activating factor 1, involved in the formation of the apoptosome and caspase activation[636–638]) and *FOXO3* (encoding the forkhead class O transcription factor 3a, involved in the response to ROS and oxidative stress and regulation of cell cycle arrest and cell death[639–642]), as well as *ACIN1* (apoptotic chromatin condensation inducer 1) and *DEDD2* (death effector domain containing 2), both involved in the initiation of apoptosis[643–645].

Another biological function identified by gene enrichment analysis in this cluster of genes up-regulated by Oncamex was mitophagy, a form of macro-autophagy involving the degradation of the mitochondria[646,647]. Pro-apoptotic genes *BNIP3* and *BNIP3L* have also been linked to the induction of this process[620,633,646,647]. Results also showed a modest increase in the expression of *FUNDC1* (FUN14 domain-containing 1), which encodes a mitochondrial outer-membrane protein associated with the induction of this process[620,646–648].

Gene enrichment analysis also showed the up-regulation of genes linked to the regulation of cell cycle progression: *CCNG2* (encoding Cyclin-G2, an unconventional cyclin involved in G2/M checkpoint cell cycle arrest[639,649]) and *RAD1* (encodes a checkpoint DNA exonuclease which forms part of a DNA damage checkpoint complex[650,651]). The increased expression levels of these 2 genes encoding key anti-proliferation markers is consistent with the induction of cell cycle arrest.

The final GO term represented in cluster 1 was response to HSP (heat shock protein) stress. This function was altered by Oncamex inducing the up-regulation of genes encoding HSP-40 co-chaperones type II (*DNAJB1*, *DNAJB6* and *DNAJB9*) and type III (*DNAJC16*, *DNAJC24*

and *DNAJC6*)[652]. As regulators of response to cellular stress, these genes are linked to changes in proliferation, glycolysis, cell survival and apoptosis[653–655].

Cluster 2 included genes that were down-regulated in cells treated with 10µM Oncamex, in comparison to baseline expression levels in untreated cells (see *Figure 47*). As in cluster 1, treatment with 0.3µM exerted a weaker effect in the expression level of these genes, which did not appear to induce a significant additional down-regulation beyond that caused by the solvent, as shown by the gene expression profile of the vehicle control cells.

Gene enrichment analysis showed that genes in this cluster were linked to rRNA processing, cellular metabolism, cell cycle and anti-apoptosis signals (see *Figure 49*). Among the most significant genes associated with cell cycle regulation were *CCND1* (encoding G1/S-specific Cyclin-D1) and *CCNB1* (G2/mitotic-specific Cyclin-B1), which are involved in the activation of successive stages of cell division through their interaction with cyclin-dependent kinases (CDKs) and are often over-expressed in cancer cells[656–659], as well as *CDC20* (cell-division cycle protein 20), linked to the promotion and control of mitosis[660]. Thus, the strong down-regulation of these genes induced by treatment with Oncamex is consistent with the induction of cell cycle arrest, as previously suggested by the up-regulation of cell cycle checkpoint regulator genes included in cluster 1 (see *Figure 48*).

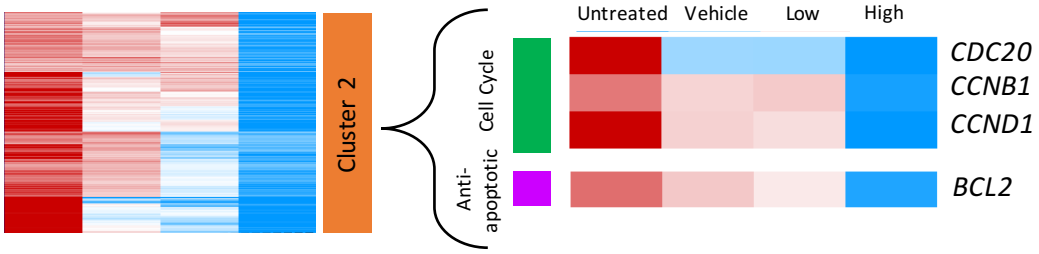

***Figure 49* Genes linked to functions significantly down-regulated by treatment with Oncamex.** *Gene enrichment analysis identified the biological processes, molecular functions or cellular components associated with cluster 2, which included genes differentially down-regulated in Oncamex-treated MCF-7 cells. Red and blue represent relative high and low log2 expression values, respectively. Significant examples of genes associated with each GO term are presented here.*

Cluster 2 also reflected the down-regulation of anti-apoptotic genes, most importantly *BCL2* (B-cell lymphoma 2), the founding member and main anti-apoptotic regulator of the BCL2 apoptosis-regulating protein family[661,662]. Together with the up-regulating effect on pro-apoptotic members of this family and associated factors, this down-regulation of *BCL2* is consistent with a strong pro-apoptotic effect of treatment with 10µM Oncamex.

Finally, cluster 3 included genes that were down-regulated in high treated cells, but also largely present at low expression levels in untreated cells (see *Figure 47*). These genes were clustered together due to the effect of the solvent, as demonstrated by the up-regulation in vehicle control cells. Similar expression patterns were observed in low treated cells.

Importantly, gene enrichment analysis showed no significant biological functions were attributed to the genes in this cluster. This suggests that the changes induced were not significantly linked to differential effects in any biological processes, molecular functions or cellular components. As previously discussed (see section *5.2.2.* and *Figure 39*), some effect of the vehicle on the gene expression of cells was expected, although these changes appeared to be weak in comparison to the effect of treatment with 10µM Oncamex. Indeed, these results suggest that the changes reflected in this cluster were the result of exposure to 1% DMSO, which induced a non-specific vehicle effect that was surpassed by high Oncamex treatment. In any instance, gene ontology analysis suggested that the solvent-induced changes reflected in cluster 3 were unlikely to be translated into a significant biological effect.

5.3.2. Recapitulation of changes in other breast cancer models

Following these results from the study of the gene expression changes induced by Oncamex in MCF-7, further analysis sought to assess whether other cells exhibited similar responses. For this, the expression levels of the significant genes identified in clusters 1 and 2 in MCF-7 cells were also studied in 4 other breast cancer cell lines: MDA-MB-231, LCC1, LCC2 and LCC9 (see *Figure 50*).

An important caveat to be observed in the comparison of these results across different models is how the baseline expression level of some genes in a particular cell line may affect the changes in expression levels observed here. Indeed, heatmaps reflect relative changes within each cell line in comparison to the baseline levels in vehicle controls. Thus, the potential modulating effect of Oncamex might be limited if the inherent baseline expression level for a gene is already as low or high as it may be.

For example, treatment with Oncamex induced a strong increase in expression of *C-JUN* in both MCF-7 and MDA-MB-231 cells, but comparatively this effect may not appear as strong in either of the 3 LCC cell lines (see *Figure 50*). Comparison of the changes in absolute expression values for *C-JUN* across these cell lines demonstrated that the lack of a greater relative increase is due to the expression of this gene already being high in untreated cells (see *Figure 51*).

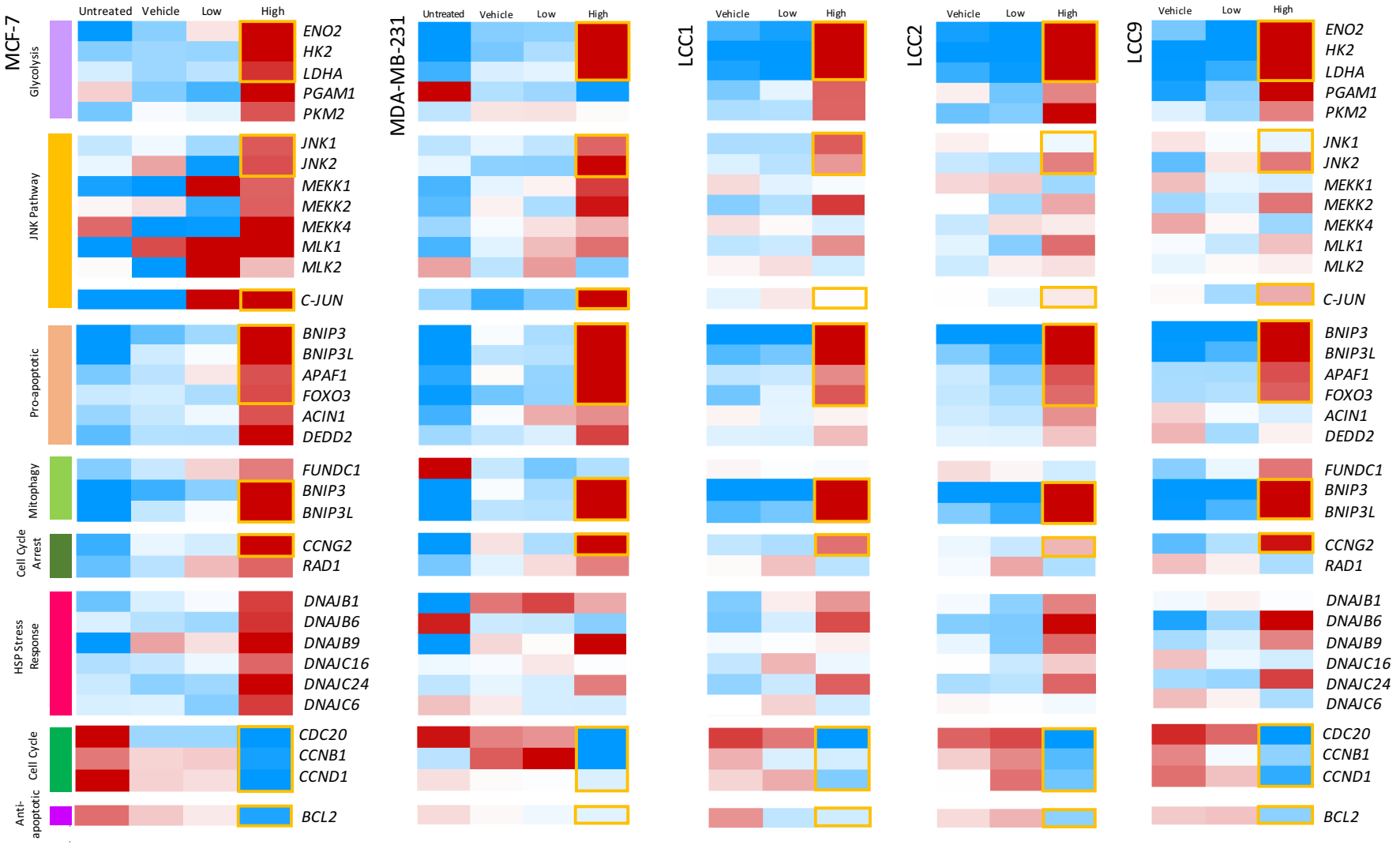

***Figure 50* Effect of Oncamex on biological functions across different breast cancer models.** *Data was adjusted and clustered as previously described. These heatmaps compare changes in relevant biological functions. Red and blue represent relative high and low log2 expression values, respectively. Some of the most significant, consistently altered genes are highlighted by orange boxes.*

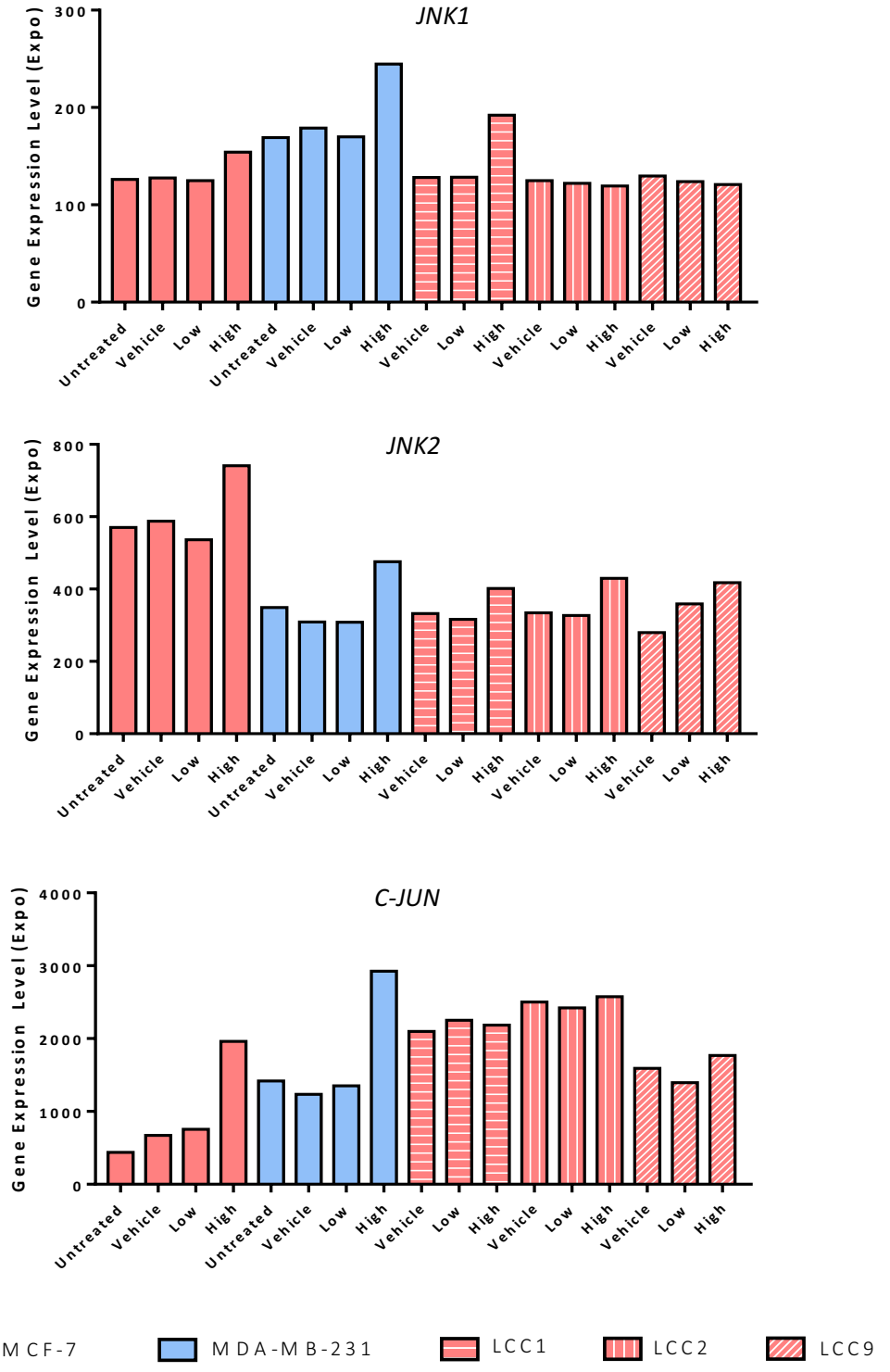

Figure 51 ***Absolute changes in expression levels of JNK pathway-related genes.*** *The expression levels for JNK1, JNK2 and C-JUN in breast cancer cells after exposure to different conditions are compared here. Expression values were reverted to an exponential scale for their comparison. Note the different y axis scales in each graph, for better representation of changes.*

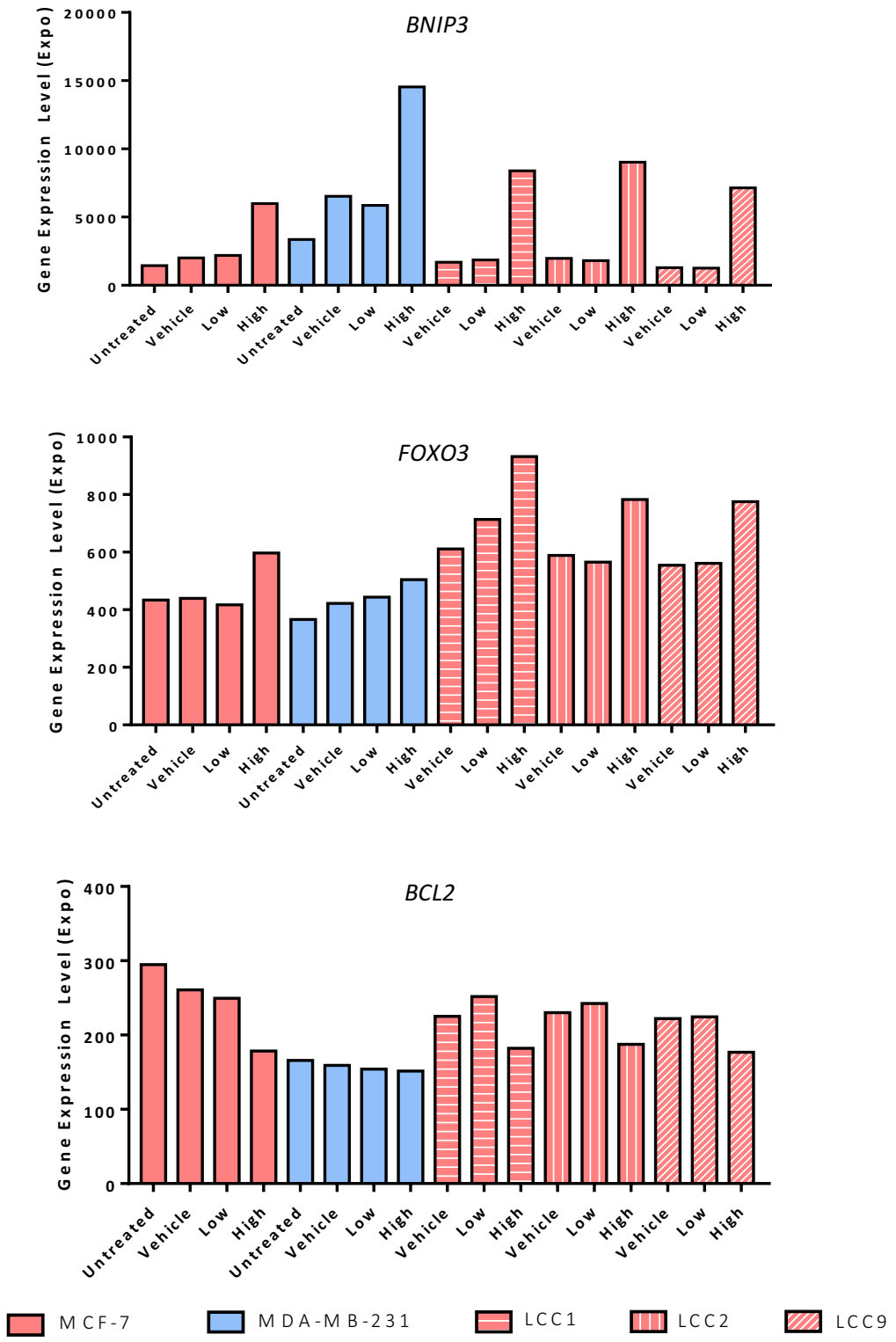

Figure 52 ***Absolute changes in expression levels of apoptosis-related genes.*** *The expression levels for BNIP3, FOXO3 and BCL2 in breast cancer cells after exposure to different conditions are compared here. Expression values were reverted to an exponential scale for their comparison. Note the different y axis scales in each graph, for better representation of changes.*

While the changes shown in the heatmaps could have been interpreted as indication that treatment with Oncamex led to a greater level of expression of this gene in MCF-7 than in LCC1, comparison of the absolute values showed that all cell lines exhibited similar levels of expression after treatment. Further analysis was carried out to highlight the changes in expression for genes related to the JNK pathway (see *Figure 51*) and apoptosis (see *Figure 52*), in comparison with the different baseline expression levels across cell lines.

Having considered this caveat, the effect of Oncamex on the biological functions previously identified as relevant using gene enrichment analysis was compared across different models (see *Figure 50*). Results showed an overall recapitulation of the Oncamex-induced changes previously observed in MCF-7 cells. Indeed, although some variation was observed in individual genes, the main genes for the same biological functions or pathways were up- or down-regulated.

Among glycolytic genes, *HK2*, *ENO2*, and *LDHA* (encoding essential enzymes) were strongly up-regulated in all cell lines. The up-regulating effect on genes related to the JNK pathway is also conserved, including changes in *JNK1/2* and *C-JUN*. Relative changes in the expression levels of these genes in LCC cells were less marked, but this was due to the higher baseline expression levels in these cells, as already discussed (see *Figure 51*).

Oncamex also exerted a similar effect in genes related to apoptosis and mitophagy across all models, with *BNIP3* and *BNIP3L* being strongly up-regulated. Expression levels of pro-apoptotic genes *APAF1* and *FOXO3* were also consistently increased by treatment in all cells studied, while the expression of anti-apoptotic gene *BCL2* was strongly reduced. The relative changes for genes such as *FOXO3* or *BCL2* appeared smaller in some cell lines due to their baseline expression levels (see *Figure 52*).

The overall effect on cell cycle progression was also consistent in all cells studied, with up-regulation of the gene encoding the growth-inhibiting Cyclin G2 and down-regulation of the expression levels of cell cycle-promoting *CDC20* and proliferation-inducing cyclins B1 and D1. The effect on HSP stress response was not as consistent, with only part of the genes observed in MCF-7 cells being consistently up-regulated across cell lines. However, it could be argued that the changes in this biological function may be indicative of a general stress response to the pro-apoptotic effect of the drug, rather than being intrinsic to the mechanism of action by which cell death is being induced. Indeed, these response mechanisms have been linked to general changes in proliferation, glycolysis, cell survival and apoptosis[653–655]. Thus, although some changes in HSP40-related genes are observed in all cell

lines, other stress-related alterations may have been triggered that were not found to be significant in MCF-7 cells.

Analysis of the fold changes in gene expression for some of the most relevant genes further supported the consistency of this differential expression across different cancer cell line models (see *Figures 56* and *57*). These effects were also found to be statistically significant. This will be further discussed in context with results from ovarian cancer models (see section *5.3.4.*).

5.3.3. Study of further changes in MDA-MB-231 cells

Previous preliminary studies showed differential overlap in the genes whose expression levels were altered by treatment with Oncamex between cell lines depending on their origin and biological similarities. As could have been expected, the changes induced in MCF-7 cells were more similar to those observed in its derived LCC cell lines (see *Figure 41*) than to the ones induced in more different, triple negative MDA-MB-231 cells (see *Figure 40*). Consequently, the global changes induced by treatment with Oncamex in the latter cells was also studied to prevent the exclusion of relevant results that could come from focusing only on genes identified from the initial study of MCF-7 cells.

For this, the previously described methodology was followed. Differentially expressed genes between cells treated with 10µM Oncamex or a vehicle control for 6 h were selected using a 0.4 log2-scale fold change threshold. Hierarchical clustering resulted in 3 main clusters (see *Figure 53*), which then underwent gene enrichment analysis for the identification of biological functions significantly represented in each of them, as shown by their gene ontology labels.

A first cluster appeared to represent a non-specific vehicle effect similar to that reflected in cluster 3 of the MCF-7 analysis (see *Figure 47*). These included genes that were up-regulated by treatment with 1% DMSO vehicle (and, partially, by lower treatment with Oncamex) in comparison with untreated cells. However, these changes were not recapitulated in cells exposed to high Oncamex treatment. Gene enrichment analysis failed to identify any biological functions significantly linked to the genes in these clusters. As in MCF-7 cells, this points to a non-specific vehicle effect that could not be avoided given the limited solubility of Oncamex but most likely did not translate into a significant effect in cells.

More importantly, another 2 main clusters demonstrated a strong effect of Oncamex in MDA-MB-231 cells. Cluster 3 included genes whose expression was significantly up-regulated

by treatment with Oncamex. The majority of these genes corresponded to the biological functions already discussed in MDA-MB-231 cells when assessing changes in genes first identified in MCF-7 (see *Figure 50*). Indeed, gene enrichment analysis linked the genes in cluster 3 to glycolysis, the JNK pathway, cell cycle arrest, pro-apoptosis signals and mitophagy (see *Figure 53*).

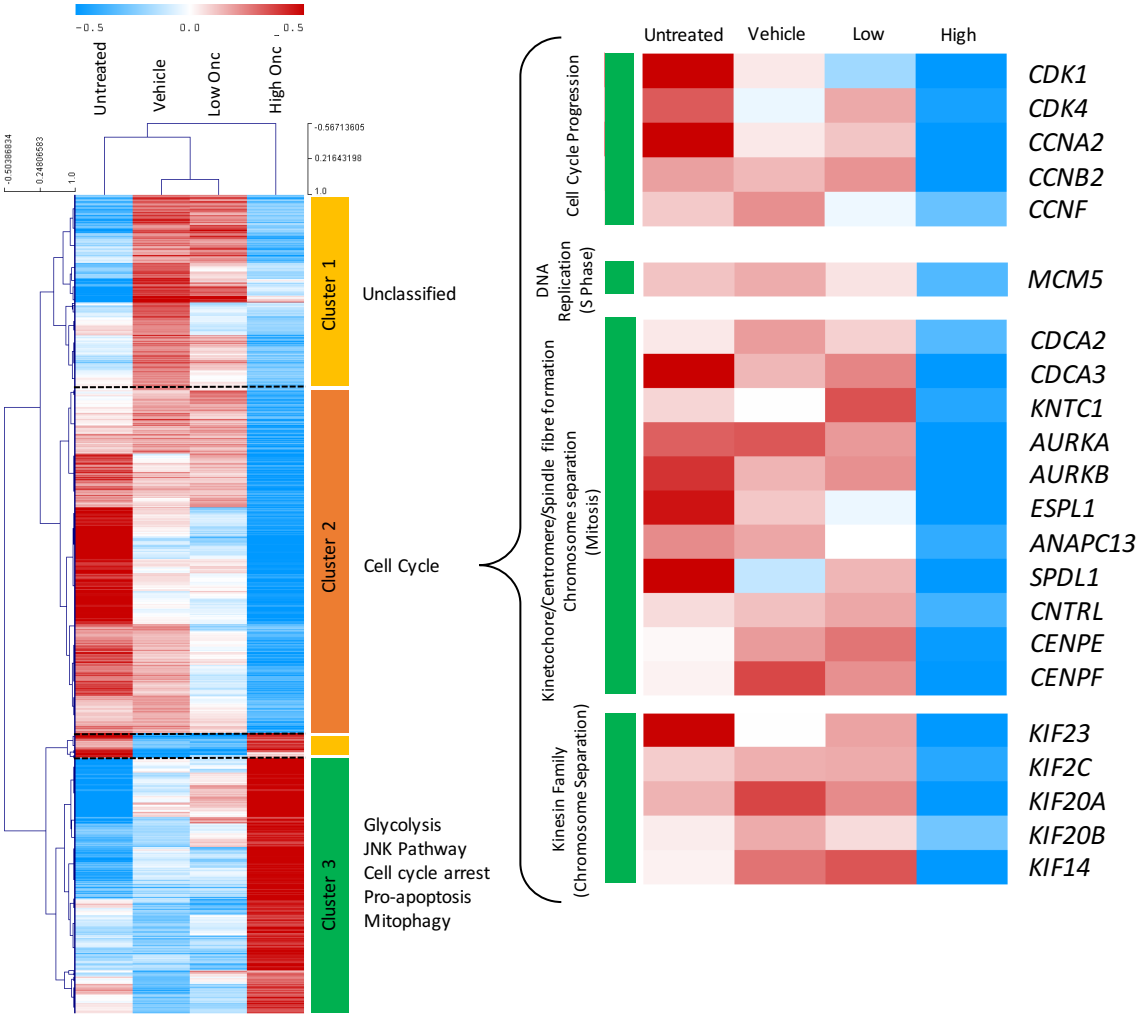

***Figure 53* Differential gene expression profiles in MDA-MB231 cells treated with Oncamex.** *Genes whose change in expression levels between high treated (10μM Oncamex for 6 h) and vehicle control (1% DMSO for 6 h) cells were greater than a 0.4 log2-scale cut-off were selected as differentially expressed. This heatmap is the result of hierarchical clustering of these genes following Pearson correlation with complete linkage for gene expression data of MDA-MB-231 cells exposed to 4 treatment conditions. Red and blue represent relative high and low log2 expression values, respectively. Gene enrichment analysis provided a list of GO terms significantly represented in each cluster and significant examples of genes associated with specific functions in cell division are presented here.*

Finally, cluster 2 included genes strongly down-regulated by high treatment with Oncamex (see *Figure 53*). Gene enrichment analysis linked this cluster of closely related genes (as suggested by the dendrogram) to the cell cycle. This could be misinterpreted as meaning that Oncamex exerted a stronger inhibition of proliferation in these cells, as a greater number of cell division-related genes were identified among the most differentially expressed.

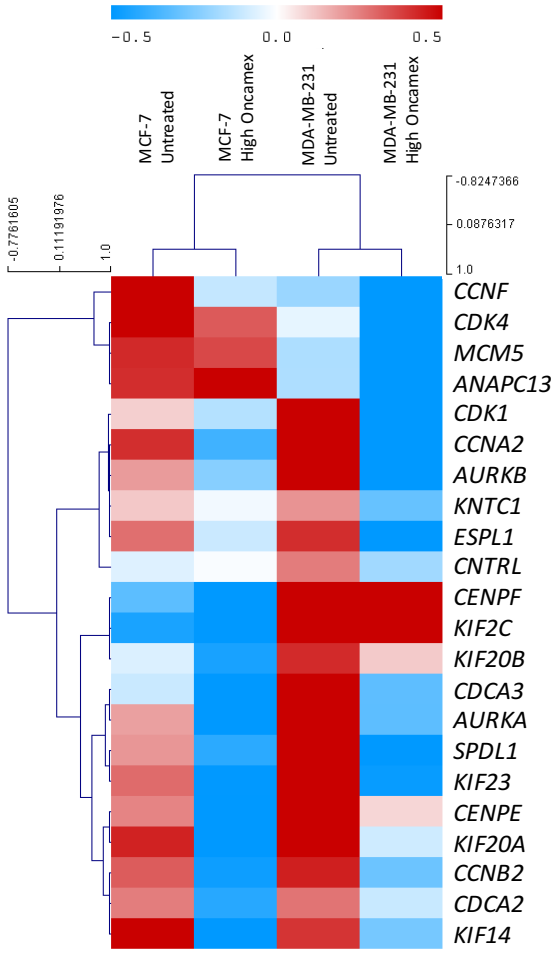

***Figure 54* Comparison of inherent levels of proliferation in MCF-7 and MDA-MB-231 cells.** *This heatmap represents the baseline expression levels for cell division-related genes in both cell lines and how these are affected by treatment with 10μM Oncamex for 6 h. Red and blue represent relative high and low log2 expression values, respectively.*

However, this is due to differences in the baseline levels of expression for certain genes and pathways across cell lines. Indeed, MDA-MB-231 cells exhibited a higher inherent level of proliferation, as shown by comparison of baseline expression levels for cell division-related genes between MDA-MB-231 and MCF-7 cells (see *Figure 54*). The same genes are down-regulated by treatment with Oncamex, but the relative changes in MCF-7 are smaller (and,

thus, may not be contained within the ± 0.4 log2-scale cut-offs applied) due to the lower inherent expression of these genes.

More detailed analysis of cluster 2 identified genes associated with different aspects of cell division and cell cycle promotion (see *Figure 53*). These included genes encoding closely-related cyclins and cyclin-dependent kinases involved in different cell cycle stages. For instance, cyclin A (encoded by *CCNA2*) is involved in the initiation of mitosis, inducing progression from phase S to G2 and then M through its interaction with CDK1[663–665].

Other down-regulated genes were associated with different steps of cell division. For instance, *MCM5* encodes a member of a family of helicases implicated in the initiation of DNA replication in phase S[666]. Aurora kinases A and B (encoded by *AURKA* and *AURKB*)[667], mitosin (encoded by *CENPF*)[668] and the kinesin family (represented by several downregulated genes)[669] are involved in chromosome segregation, while Repo-man (also referred to as cell division-associated protein 2 and encoded by *CDCA2*) is involved in post-mitotic chromatin reorganization[670].

5.3.4. Recapitulation of changes in ovarian cancer models

Finally, further analysis assessed the effect of treatment with Oncamex in 2 ovarian cancer models: the pair of chemotherapy-sensitive/resistant PEA1 and PEA2 cells. This focused on changes in the expression levels for genes previously identified as being differentially expressed and significantly linked to biological functions in breast cancer cells, including genes identified in both MCF-7 and MDA-MB-231 cells.

Results showed an overall recapitulation of the changes observed in breast cancer models following treatment with 10µM Oncamex (see *Figure 55*). As in previous models, the treatment with lower concentrations of Oncamex exerted a weaker effect that did not appear to induce any additional changes beyond those observed in control cells.

Analysis showed the Oncamex-induced up-regulation of genes related to glycolysis, the JNK pathway, pro-apoptotic signals, mitophagy and cell cycle arrest, while genes related to proliferation and anti-apoptotic signals were down-regulated. Interestingly, the inhibition of proliferation involved the down-regulation of a large number of genes, including those identified in both MCF-7 and MDA-MB-231 cells. This suggests that, like MDA-MB-231 cells, these ovarian cell lines may have inherently higher proliferation rates that are consequently susceptible to greater negative relative changes by treatment with Oncamex.

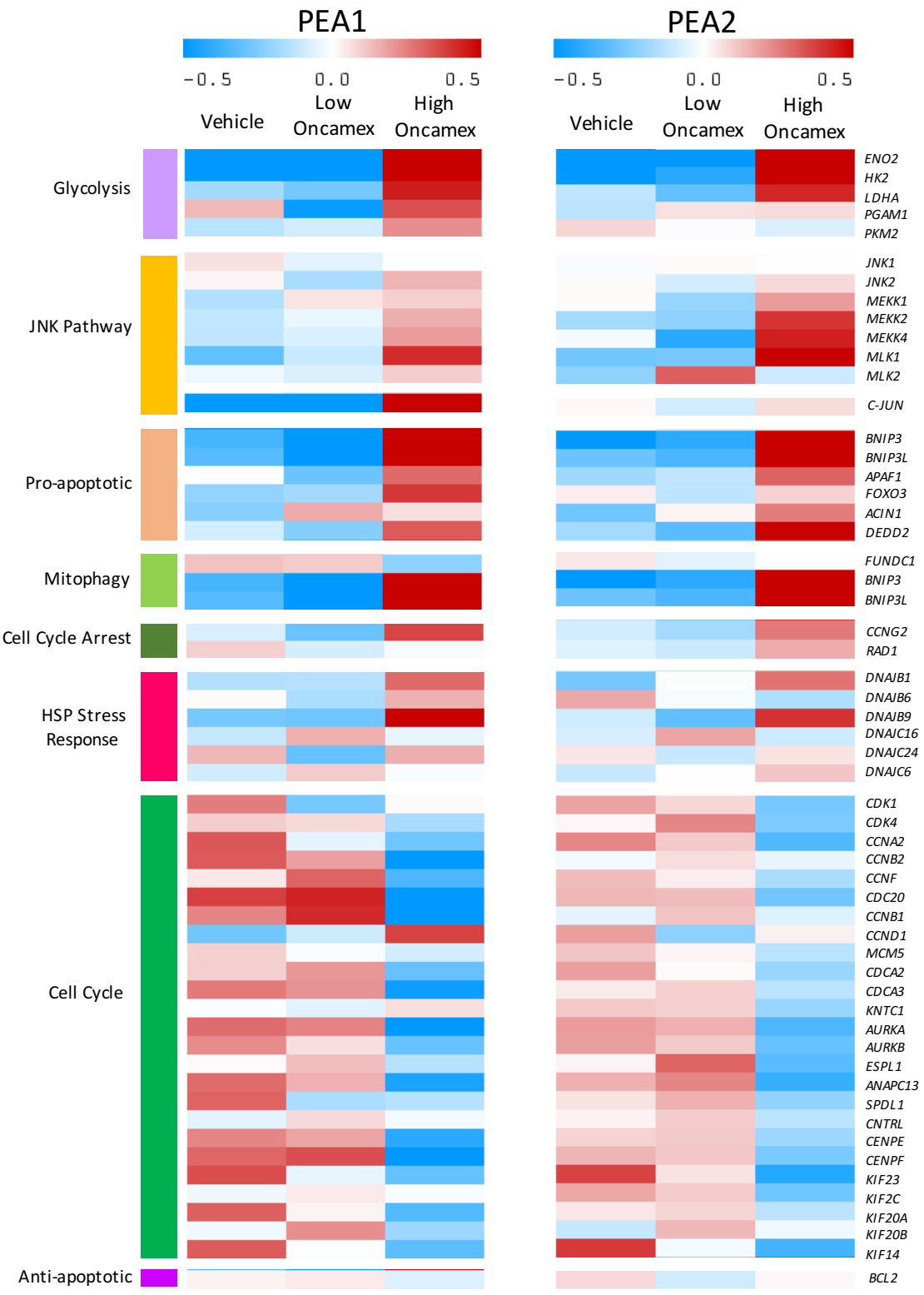

Figure 55 ***Differential gene expression profiles in ovarian cancer cells treated with Oncamex.*** *These heatmaps present the effect of treatment with a vehicle control (1% DMSO for 6 h), low (0.3µM for 2 h) or high (10µM for 6 h) Oncamex on PEA1 and PEA2 cells. The changes in relevant biological functions and the expression levels for genes previously identified as differentially expressed in MCF-7 and MDA-MB-231 breast cancer cells were assessed. Red and blue represent relative high and low log2 expression values, respectively.*

Following these results, further work analysed the Oncamex-induced fold changes in absolute expression for the main genes identified in relation to the biological functions. Results highlighted the consistency of the changes induced, which was also found to be statistically significant ($P<0.01$, or lower) (see *Figures 56* and *57*). This further supports the notion that Oncamex induces a similar effect in the functions studied, particularly considering that this analysis included 7 different cancer models representing different molecular subtypes and phenotypes of both breast and ovarian cancer.

Additionally, Oncamex also induced the up-regulation of the expression of other genes, such as *JNK1* or *C-JUN*, across cell lines, but these changes were not as obvious in terms of fold changes due to the inherent expression levels in some cell lines, as previously described (see *Figures 51* and *52*).

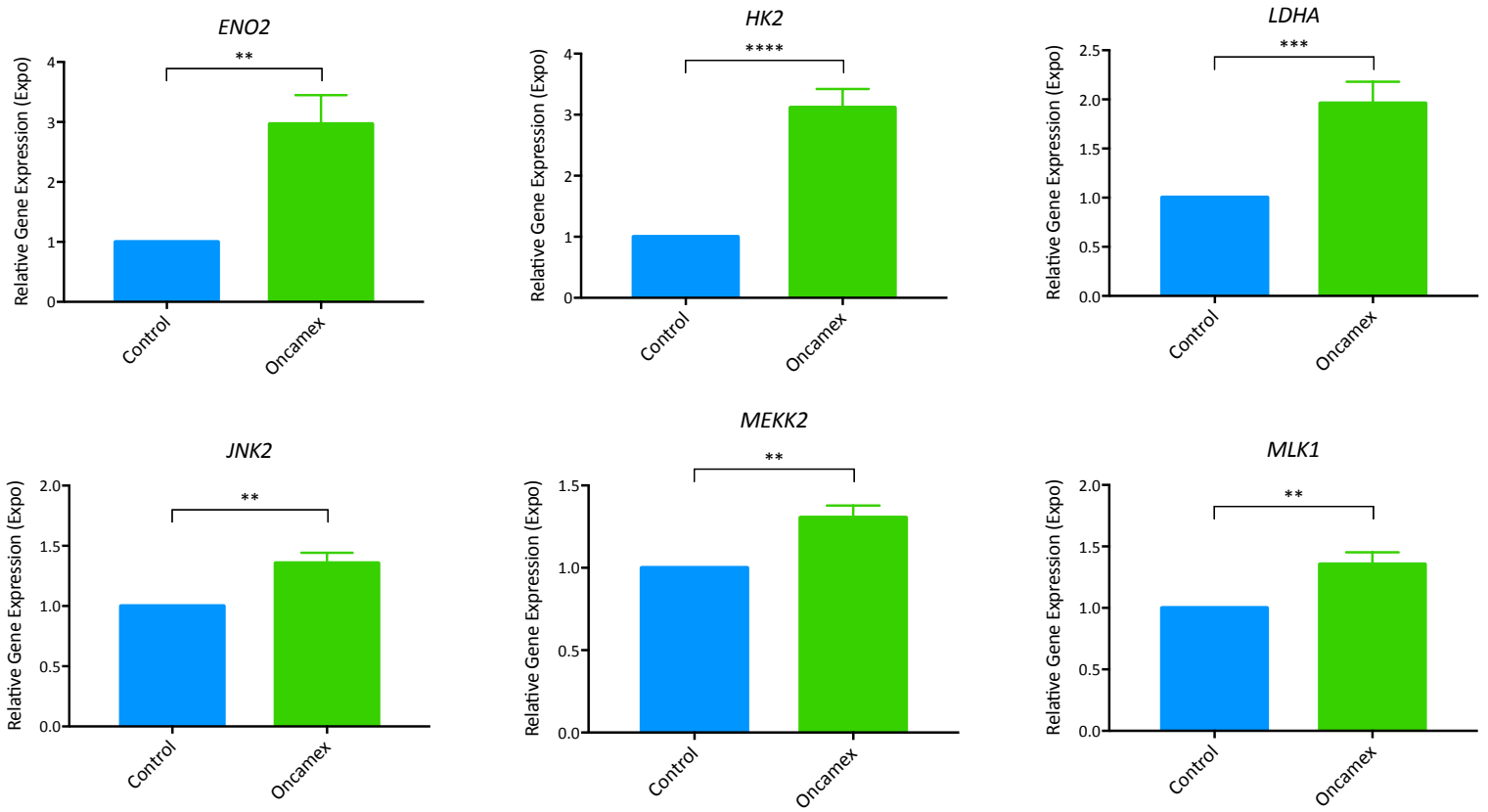

Figure 56 ***Summary of Oncamex-induced changes in the expression levels of the most significant genes linked to glycolysis and the JNK pathway in breast and ovarian models.*** *Graphs here represent the fold changes in absolute genes expression between vehicle controls and cells treated with 10μM Oncamex for 6 h. These graphs summarise results from 5 breast cancer cell lines (MCF-7, MDA-MB-231, LCC1, LCC2 and LCC9) and 2 ovarian cancer cell lines (PEA1 and PEA2). Columns represent averages from these population of cell lines (n=7), normalised to the vehicle control of each experiment, with error bars representing standard error (SEM). P-values from unpaired t-test comparing treated cells to vehicle controls: **P<0.01; ***P<0.01; ****P<0.0001. Where not shown P>0.05 (nonsignificant).*

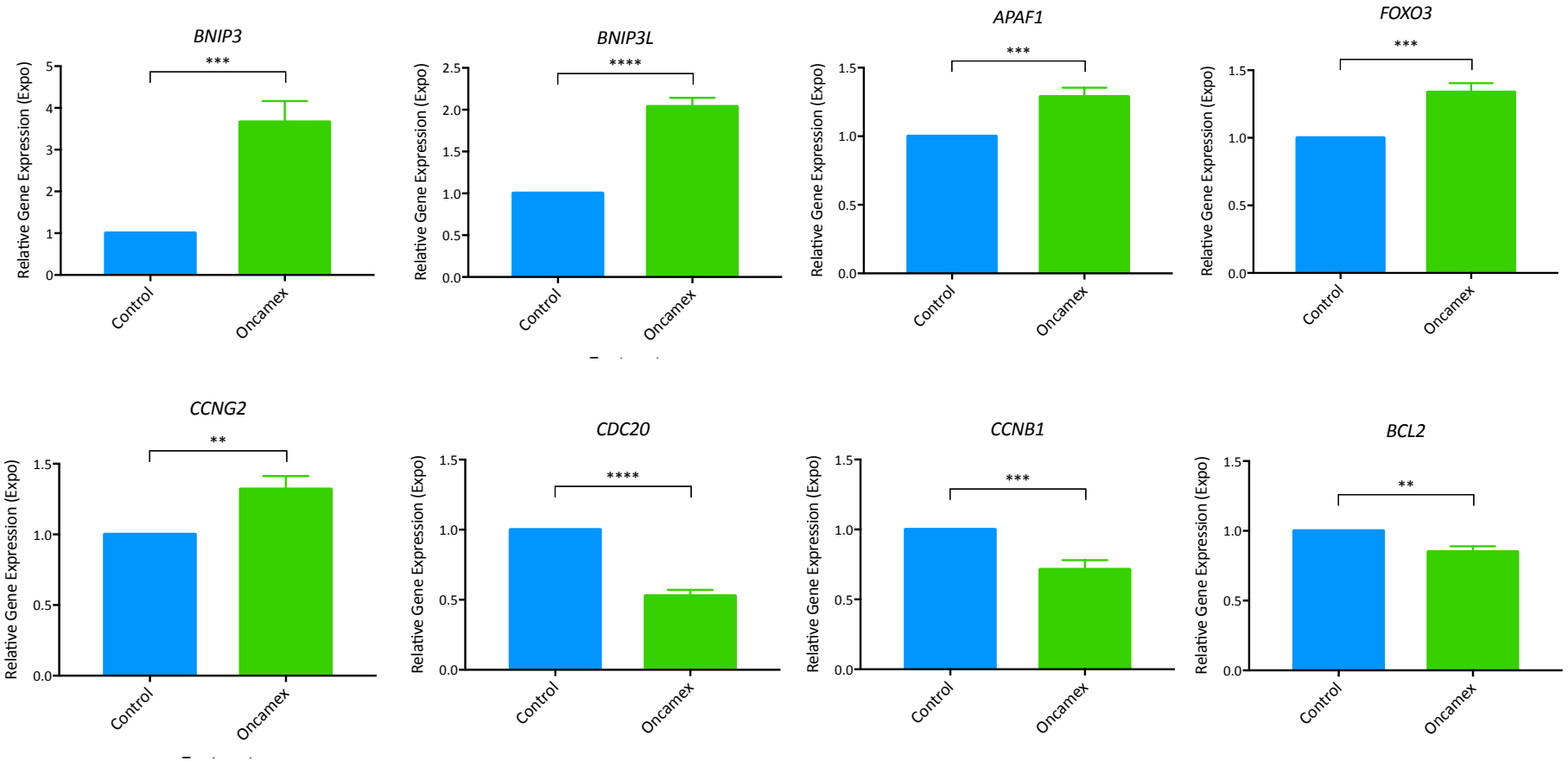

Figure 57 ***Summary of Oncamex-induced changes in the expression levels of the most significant genes linked to mitophagy, apoptosis and proliferation in breast and ovarian models****. Graphs here represent the fold changes in absolute genes expression between vehicle controls and cells treated with 10µM Oncamex for 6 h. These graphs summarise results from 5 breast cancer cell lines (MCF-7, MDA-MB-231, LCC1, LCC2 and LCC9) and 2 ovarian cancer cell lines (PEA1 and PEA2). Columns represent averages from these population of cell lines (n=7), normalised to the vehicle control of each experiment, with error bars representing standard error (SEM). P-values from unpaired t-test comparing treated cells to vehicle controls: **P<0.01; ***P<0.01; ****P<0.0001. Where not shown P>0.05 (nonsignificant).*

5.3.5. Summary of the effect of Oncamex on gene expression in breast and ovarian cancer cell line models

In summary, the results reported in this section have demonstrated the effect of treatment with 10µM Oncamex for 6 h on different biological processes, molecular functions and cellular components, as observed from differential gene expression analysis and gene enrichment analysis. These changes were observed across different cancer models and types, including both ER^+ and triple negative breast cancer and ovarian cancers.

Indeed, initial analysis of MCF-7 cells demonstrated the effect of Oncamex in the expression of genes linked to glycolysis, the JNK pathway, cell cycle regulation, apoptosis and mitophagy. These changes were largely recapitulated in other breast cancer cell lines (MDA-MB-231, LCC1, LCC2 and LCC9), as well as 2 models of ovarian cancer (PEA1 and PEA2). Interestingly, further study showed that the apparent smaller relative changes for some genes across cell lines may be due to inherent differences in baseline expression levels, such as in the case of proliferation-related genes in MDA-MB-231 cells.

Although practical limitations prevented the inclusion of replicates in this microarray, the statistically significant Oncamex-induced changes observed across these different models suggest a common and consistent effect and mechanism of action. Overall, differential gene expression analysis highlighted Oncamex-induced changes that suggest a complex mechanism involving the modulation of glycolytic metabolism and stress-response pathways to exert an antiproliferative and pro-apoptotic effect, which is consistent with previous evidence at protein level.

In relation to this, it is important to observe the caveat of the difference between changes at gene and protein level. The effect of Oncamex on the expression level of genes regulating these biological processes should be interpreted as informing and complementing results at protein level, but a number of variables may affect the correlation between changes at both levels: from regulation of transcription and translation to the differences in the half-life of mRNA and proteins, as well as post-transcriptional modification of proteins that define their interaction with other factors and, thus, their role in the cell[671]. This means that changes in gene expression levels may not necessarily correlate exactly with alterations in protein synthesis, in the same way that protein modification may induce a significant effect at molecular level that is nonetheless not reflected at gene expression level.

Consequently, results from gene expression analysis can inform previous results and provide greater insight into the seemingly complex mechanism underlying the effect of Oncamex on cancer cells. The next section will consider these results to propose a more detailed model for this mechanism of action in the context of previous findings (see results in previous chapters), knowledge of the compound being studied and its properties and the literature in the field. Subsequently, further work would be necessary for validation at protein level.

5.4. Description of a model for the mechanism of action of Oncamex

5.4.1. Oncamex, ROS and the mitochondria

Results reported in the previous chapter demonstrated the mitochondrial targeting and ROS-modulating properties of Oncamex. As previously discussed (see section *4.5.*), the electrochemical properties of the compound suggested its ability to induce the production of mitochondrial superoxide ($O_2^{\cdot-}$ or mSO), as observed using fluorescence microscopy. Results also reported the induction of cytotoxic and apoptotic responses across different cell line models.

In short, previous results suggested the possible effect of Oncamex through a mechanism by which changes in levels of mitochondrial ROS may lead to the induction of apoptosis. This was supported by the observed induction of mSO production and apoptotic responses following treatment with Oncamex, as well as the known involvement of this ROS species in both the inhibition of anti-apoptotic signals and the induction of the release of pro-apoptotic factors through mitochondrial membrane depolarisation.

These observations were also further supported by changes in gene expression reported in this chapter. Indeed, results from a microarray experiment have shown a significant down-regulation of BCL2 at gene level (see *Figure 50*), consistent with the proposed pro-apoptotic effect of Oncamex-induced mSO production.

The following sections will further discuss the results reported in this chapter in the context of these findings and the relevant literature in order to postulate an informed and comprehensive model for a possible mechanism of action of Oncamex, beyond its already established mitochondria-targeting and ROS-modulating properties.

5.4.2. Effect of Oncamex on the JNK pathway and FOXO3: role in apoptosis and proliferation

Beyond its direct effect on the induction of mitochondrial membrane permeabilisation, the mechanism by which ROS production may interact with BCL2 signalling or other pathways involved in the regulation of apoptosis (briefly discussed in section 4.5.) is complex. Recent years have seen an emphasis in the study of the JNK (c-Jun N-terminal kinases) signalling pathway and its role in the regulation of cell death, including oxidative stress-induced apoptosis[672].

Interestingly, differential gene expression analysis has shown a significant up-regulation of the JNK pathway by treatment with Oncamex, observed consistently in breast and ovarian

models (see *Figures 50* and *55)*. Indeed, the expression of both *JNK1* and *JNK2* was up-regulated, as well as that of genes encoding upstream activators belonging to the MAP3K pathway and downstream target c-JUN. The activation of JNK (formed by 10 isoforms encoded by *JNK1* and *JNK2*) by phosphorylation in turn leads to the activation of c-Jun, which interacts with c-Fos in the nucleus to form the early response transcription factor AP-1 (activator protein 1). The activity of c-Jun/AP-1 leads to the up-regulation of pro-apoptotic factors, most importantly the BAX subfamily of BCL2-related proteins[673–675]. Additionally, JNK also targets the anti-apoptotic members BCL2 and BCL-XL[676–679]. Their phosphorylation leads to the inhibition of their anti-apoptotic effect and ability to interact with and sequester pro-apoptotic members such as BAX[680]. JNK-dependent apoptosis has been linked to the mechanism of action of common chemotherapeutic agents, including microtubule inhibitors vinblastine[674,677] and paclitaxel[680].

Another important target of regulation by JNK signalling is FOXO3 (forkhead class O transcription factor 3a), consistently up-regulated after treatment with Oncamex (see *Figure 50* and *55*). This transcription factor has been found to inhibit proliferation and induce mitochondrial apoptosis through the activation of pro-apoptotic members of the BCL2 family in cancer cells[641,681,682], where it has been shown to antagonise the effect of the oncogenic transcription factor MYC[683].

FOXO3 can be activated in response to different stimuli, including changes in ROS levels which can trigger its translocation to the nuclei[672,684] and in turn leads to the alteration of the mitochondrial respiratory function and induces further ROS production[684]. However, FOXO3 is also down-regulated as a downstream target of the PI3K/AKT (phosphatydilinositol-3-kinases/protein kinase B) pathway, specifically being inactivated by the activity of AKT[682]. Although differential gene expression analysis showed no changes in the expression levels of AKT, its activation or deactivation occurs at protein level by post-translation modifications. Interestingly, different flavonoids have been noted to exert an inhibiting effect in the PI3K/AKT pathway[379,380,414,415]. Importantly, both AKT and FOXO3 are targets of JNK, which can both block the inhibitory effect of AKT[685,686] and phosphorylate FOXO3 itself directly[687–689] to prevent sequestration by other factors such as protein 14.3.3. Thus, JNK signalling can lead to an increase in the activity of FOXO3 and its translocation to the nucleus, where it inhibits proliferation-promoting genes[639,681] and up-regulates the expression of pro-apoptotic BCL2 members such as BIM (BCL2-like protein 11)[690].

FOXO3 has also been shown to regulate the activity of the BH3 (BCL2 homology 3) domain-containing proteins BNIP3 and BNIP3L (or NIX)[689,691], whose up-regulation has also been demonstrated by differential gene expression analysis (see *Figures 50* and *55*). These proteins have been linked to the induction of apoptosis, necrosis or autophagy[635,691]. However, the criteria determining the induction of BNIP3/NIX on either type of cell death are complex[692]. While BNIP3 and NIX can interact with anti-apoptotic proteins BCL-2 and BCL-XL[693], research has shown the ability of BNIP3 to induce an atypical form of mitochondria and caspase-independent apoptosis[635,694]. In any case, authors have suggested that the extent of the pro-apoptotic effect of BNIP3/NIX may be highly dependent on the balance of other pro- and anti-apoptotic factors and these receptors may only contribute to the advancement of apoptosis through the induction of other forms of cell death, such as autophagy[635,692]. Given the uncertain role of BNIP3/NIX in apoptosis, their role in the mechanism of action of Oncamex may be related to their better established role in the induction of mitophagy. This will be further discussed in an up-coming section (see section *5.4.4.*).

FOXO3 has also been found to regulate proliferation as part of its tumour suppressor activity. Indeed, this transcription has been shown to control the cell cycle machinery in response to different stimuli and under regulation by the PI3K/AKT pathway[639,695]. This includes its effect on the expression level of some of the proliferation-related genes observed to be differentially expressed following treatment with Oncamex. The unconventional cyclin G2, involved in the induction of G2/M cell cycle arrest, has been identified as a direct target for transcriptional up-regulation by FOXO3[639,696]. FOXO transcription factors have also been shown to down-regulate the expression of cell cycle-promoting cyclin D1[697,698] and B1[699]. FOXO3 can also stimulate the expression of its own genes, which are in contrast repressed by the activity of growth factors[700]. Interestingly, research has shown the involvement of FOXO3 in the anti-proliferative effect exerted by the flavonoid genistein[701].

Like FOXO3, its upstream regulator JNK has been found to be activated by several stimuli and forms of chemical or environmental stress[702], such as DNA damage[676] or radiation-induced stress[703]. Importantly, research has also found that superoxide production can lead to cell death through the activation of this pathway[704]. The efficacy of this mechanism has also been shown in the development of novel semisynthetic compounds. Indeed, both Bz-423 (a benzodiaxepine) and Phx-3 (an aminophenoxazine) have been found to cause apoptosis through induction of mitochondrial ROS production (specifically mSO in the case of Bz-423) that led to activation of the JNK pathway, BAK and BAX[705,706].

5.4.3. Oncamex and energy metabolism

As previously mentioned, a defining characteristic in cancer is the reliance on an altered mechanism for energy production (see section *1.1.5.3.7.*). The Warburg effect defines the phenomenon by which cancer cells present a higher rate of glycolysis, instead of oxidative phosphorylation in the mitochondria, even in aerobic conditions[390,391,617].

Otto Warburg's initial hypothesis supposed that the loss of mitochondrial respiratory function preceded the increase in aerobic glycolysis in cancer cells[707]. However, this notion was first challenged in the 1950s[708] and subsequent research has established that, while glycolysis is increased and the rate of oxidative phosphorylation may be reduced in malignant cells, the respiratory capacity of mitochondria is normally intact and these organelles continue to be essential for the functioning of the cell and tumourigenesis[609,616,709]. Indeed, it has been suggested that the majority of cancer cells undergo oncogene-directed metabolic reprogramming and utilise both of these pathways[710], with the increased glycolytic rate fuelling the demands of enhanced proliferation rates (see *Figure 58*) while oxidative phosphorylation continues to generate most of the ATP[710–712].

Interestingly, research has also shown that oxidative phosphorylation can function at oxygen levels as low as 0.5%[713]. Thus, in poorly perfused areas of solid tumours in which both nutrient and oxygen supplies are reduced, the glycolytic function may be impaired due to the limited glucose levels, while mitochondrial respiration continues to function. These observations further support how, as previously discussed, mitochondria are important targets for anti-cancer therapy and essential players in the induction of apoptosis.

The transcription factor HIF-1 mediates adaptive responses to changes in oxygen levels[714]. In hypoxia, HIF-1 acts as an activator of anaerobic glycolysis by up-regulating the expression of glucose transporters (GLUT1 and GLUT3) and 9 of the 10 enzymes catalysing the different steps in the glycolytic pathway[714,715] (see *Figure 58*). In normal cells, the presence of oxygen in normoxic conditions leads to the degradation of the HIF-1α subunit (hypoxia-inducible factor 1α) through the alteration of post-translational modifications by modulators such as FIH-1 (factor inhibiting HIF-1)[716,717].

Abbreviations:

GLUT1, glucose transporter 1;
GLUT3, glucose transporter 3;
MCT4, monocarboxylate transporter 4;
HK2, hexokinase 2;
GPI, phosphoglucose isomerase;
PFK1, phosphofructose kinase;
TPI, triosephosphate isomerase;
GAPDH, glyceraldehyde phosphate dehydrogenase;
PGK1, phosphoglycerate kinase;
PGAM1, phophoglycerate mutase 1;
ENO2, enolase 2;
PKM2, pyruvate kinase isoenzyme 2;
LDHA, lactate dehydrogenase;
PPP, pentose phosphate pathway;
TCA, tricarboxylic acid;
NADPH, nicotinamide adenine dinucleotide phosphate;
ATP, adenosine triphosphate;
HIF-1, hypoxia-inducible factor 1.

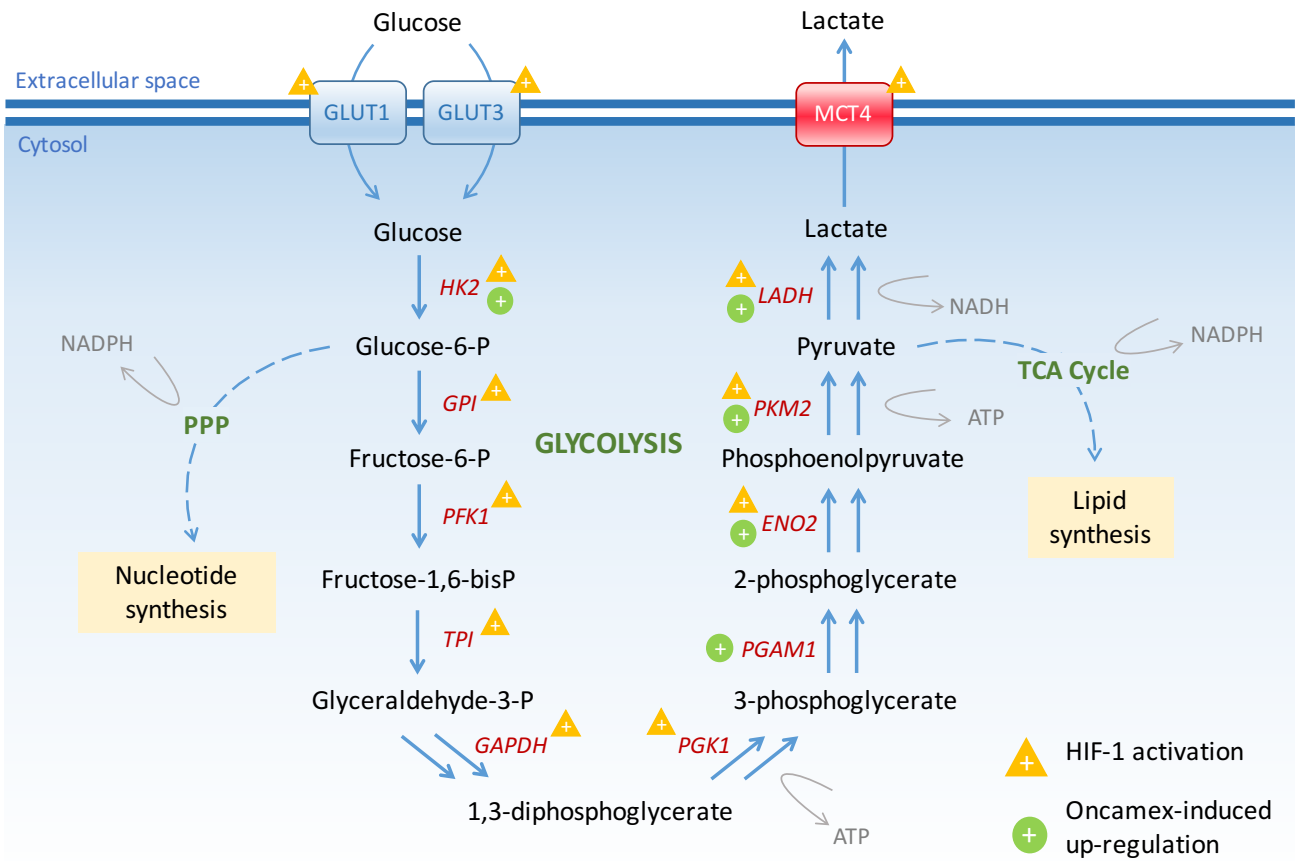

***Figure 58* Summary of glycolysis, activation of the pathway by HIF-1 and up-regulation of glycolytic genes by treatment with Oncamex.** *Cancer cells are characterised by an increase in their glycolytic rate even in aerobic conditions (Warburg effect). Contrary to the initial hypothesis, research has shown that most cells conserve their mitochondrial respiratory function, which continues to provide the majority of the ATP, while glycolysis fuels the enhanced proliferative rates by enabling the production of lipids and nucleotides*[710–712]*. In hypoxic conditions, and sometimes independently of oxygen levels in cancer cells, the transcription factor HIF-1 enhances glycolysis by induction of its target genes*[712,714,718,719]*. Results from a microarray experiment have shown an up-regulation of some glycolytic genes following treatment with 10µM Oncamex for 6 h. In this diagram, text in red represents the genes encoding each enzymatic step, which are the subject of up-regulation by HIF-1 or Oncamex treatment.*

However, in cancer cells glycolysis is often active independently of hypoxia, enabled by the dysregulation of oncogenic pathways such MYC and PI3K-AKT-mTOR. Research has shown that these oncogenes can induce glycolysis independently of HIF-1, as they share many target glycolytic genes[720–723], but can also induce HIF-1 overexpression as a mechanism for further enhancing glycolysis[724]. Indeed, HIF-1 overexpression has been observed in several different tumours, including breast, and particularly in metastases[725,726].

Differential gene expression analysis identified glycolysis as one of the biological functions significantly up-regulated by treatment with Oncamex (see *Figure 47*, *48* and *50*). Indeed, results from microarray experiments showed that treatment with 10μM Oncamex for 6 h induced a strong up-regulation in the expression of key glycolytic genes, to levels much higher than those of control cells in which this function would already be increased in comparison to normal cells.

More work sought to investigate the involvement of HIF-1 in this response. Initial analysis showed no significant changes were induced in the expression levels for the genes encoding HIF-1α and the HIF-1 modulator FIH-1 in any of these breast cancer cell lines after treatment with Oncamex (see *Figure 59*). However, as previously mentioned, the activity of this transcription factor is mostly regulated through post-translational modifications, so the lack of changes in these factors at gene level may not be a good indicator for the involvement of this transcription factor in the increased glycolytic rate observed after treatment with Oncamex. Indeed, these expression levels for HIF-1α were not higher in MCF-7 or MDA-MB-231 cells grown in hypoxic conditions, in which HIF-1 signalling would certainly be active.

Further analysis beyond the expression levels of this transcription factor was carried out to better assess its role in the up-regulation of glycolysis. The comparison of the changes induced by treatment with Oncamex and exposure to acute or chronic hypoxia suggested HIF-1 activation or the induction of a hypoxia-like mechanism may not play an important role. Indeed, for both MCF-7 and MDA-MB-231 only a relative small number of overlapping genes were identified as consistently differentially expressed after exposure to Oncamex and hypoxia (see *Figure 60* and *Appendix 2* for gene lists). Given the fact that this analysis compared changes induced by different conditions in the same model, it would be reasonable to expect a greater overlap if the effect induced by Oncamex involved the activation of a hypoxia-like mechanism.

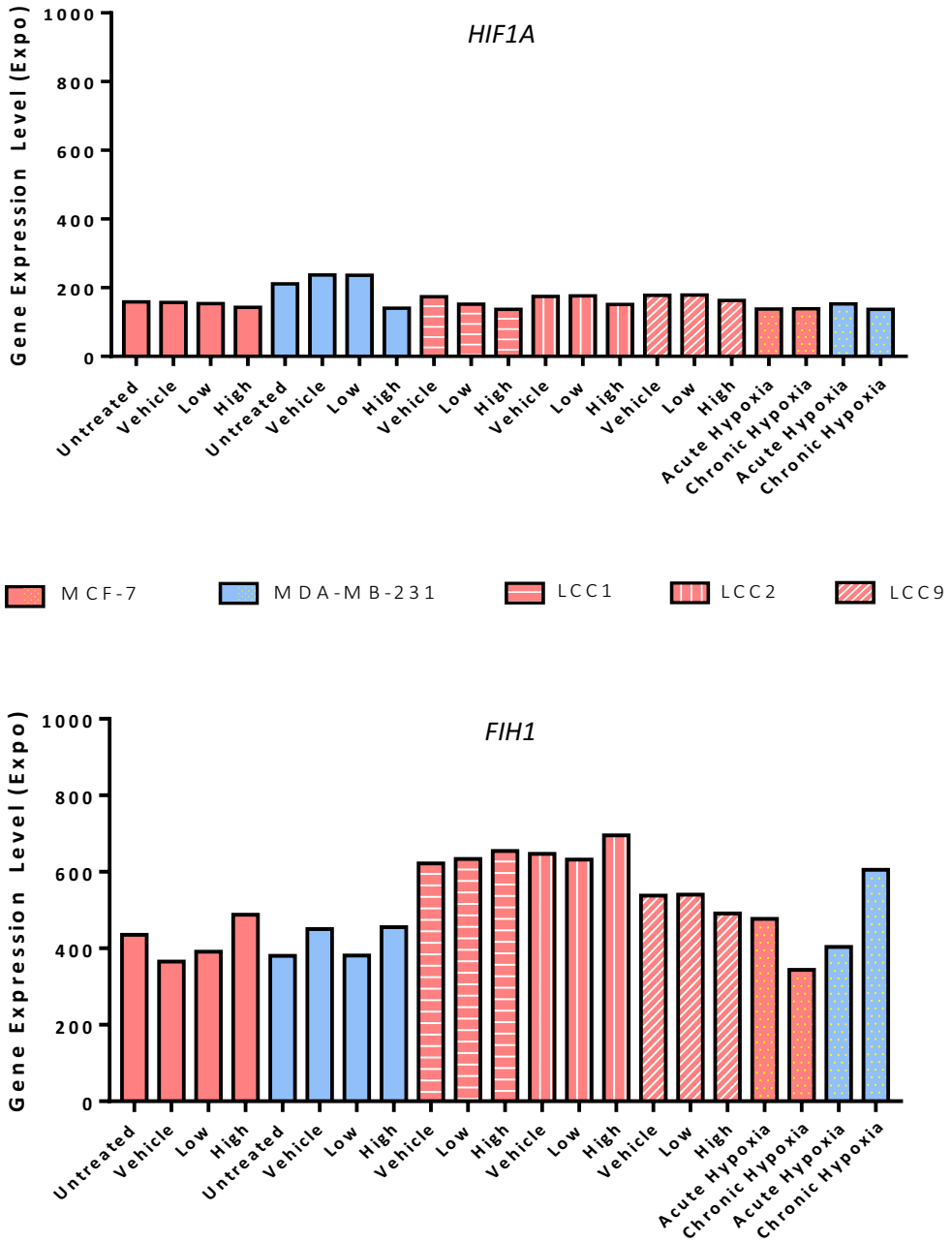

Figure 59 ***Absolute changes in expression levels of hypoxia-related genes.*** *The expression levels for HIF1A and FIH1 in breast cancer cells after exposure to treatment with Oncamex or hypoxic conditions are compared here. Expression values were reverted to an exponential scale for their comparison.*

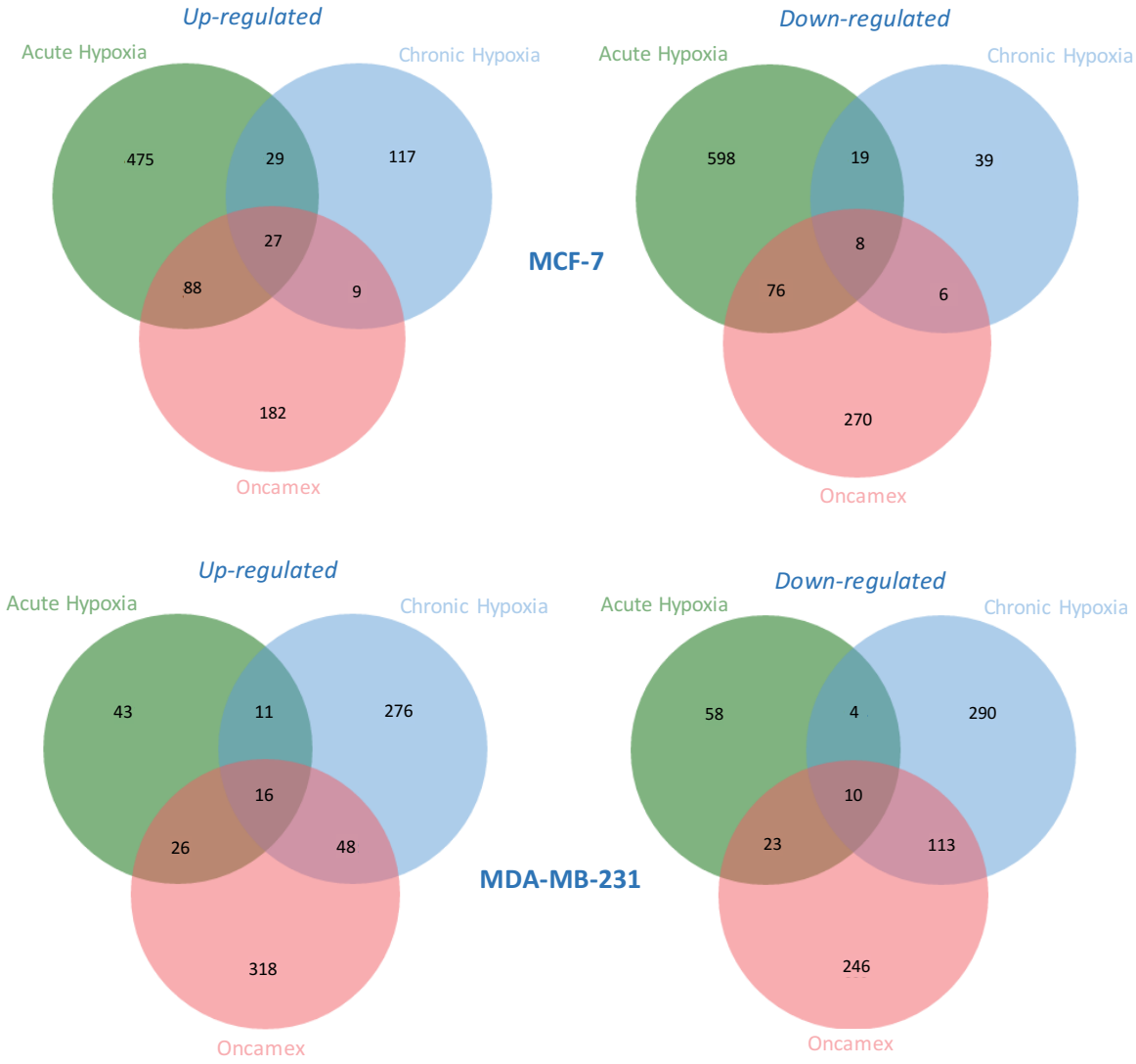

***Figure 60* Overlapping differentially expressed genes across MCF-7 and MDA-MB-231 cells exposed to different treatments or conditions.** *Following log2-transformation and normalisation of results from a microarray experiment, genes whose expression level had changed by at least a 0.4 log2-scale fold change between control and treated cells were considered differentially expressed. Venn diagrams shown here were obtained using the online tool jvenn*[614]*. These represent the overlap in up- (left) and down-regulated (right) genes in MCF-7 (above) and MDA-MB-231 (below) cells exposed to acute hypoxia (24 h in 0.5% oxygen), chronic hypoxia (10 weeks in 0.5% oxygen) or treatment with Oncamex (10μM for 6 h).*

Finally, further analysis compared the changes in expression levels of glycolytic genes and glucose transporters between Oncamex-treated cells and cells exposed to hypoxia (see *Figure 61*). Results highlighted the previously observed up-regulating effect of high treatment with Oncamex on the expression levels of 5 glycolytic genes. This expression pattern showed some variation in comparison to those of hypoxic cells, in which HIF signalling is expected to be involved in further up-regulating the glycolytic rate of cells. In particular, expression levels for genes corresponding to enzymes involved in the latter steps of glycolysis (*ENO2* and *PKM2*) appeared to be lower in Oncamex-treated cells.

Most importantly, Oncamex induced no significant changes in the expression of glucose transporters GLUT1 and GLUT3, which are important targets of HIF-1 regulation and were, indeed, up-regulated in cells exposed to hypoxia. These results suggest that, although results are consistent with an up-regulation in glycolytic genes by treatment with Oncamex across all cell lines studied (see *Figures 48* and *50*), the enhanced glycolytic rate observed may be independent of HIF-1 signalling.

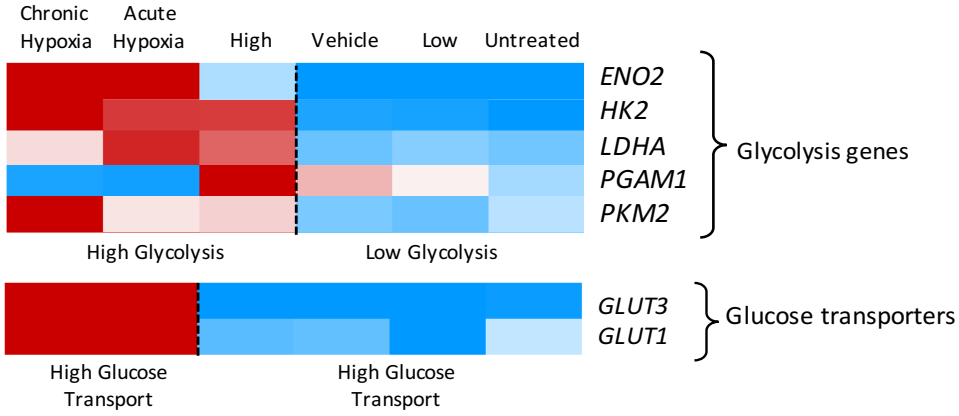

***Figure 61* Changes in expression levels of glycolysis-related genes in MCF-7 exposed to treatment with Oncamex or hypoxic conditions.** *This heatmap compares the changes in the expression levels of genes encoding 5 glycolytic enzymes and 2 glucose transporters cells in MCF-7 cells treated with low or high concentrations of Oncamex or control solutions, as well as cells grown in acute (24 h in 0.5% oxygen) or chronic (10 weeks in 0.5% oxygen) hypoxia. Red and blue represent relative high and low log2 expression values, respectively.*

Both glycolysis/metabolism and hypoxia/stress responses had been highlighted as significantly altered biological functions in preliminary gene ontology analysis (see *Figures 44*, *45* and *46*). However, the results reported here are consistent with the lack of HIF-1 signalling following treatment with Oncamex. This suggests that the initial results from gene ontology highlighting hypoxia as a significantly altered biological function may have reflected

changes in glycolysis-related genes, which would be labelled as hypoxia-related due to the normal induction of this metabolic pathway in hypoxic conditions.

Additionally, these preliminary analyses highlighted the GO term for response to hypoxia in close relation to other labels for stress response, such as abiotic stimulus, cellular response to stress or response to oxidative stress (see *Figures 44*, *45* and *46*). As previously mentioned in the discussion of the possible role of HSP40-related genes in the effect of Oncamex, this is consistent with changes reflecting an overall state of cellular stress, possibly as a consequence of the induction of apoptosis, rather than specific effects contributing to the mechanism of action of this novel flavonoid[653–655]. In any case, these initial gene ontology results were used as preliminary indicators of overall changes and the study of quantitative changes in gene expression reported in this section represents a more accurate method for the study of this mechanism.

The possible significance of this increase in glycolytic rate in the effect exerted by treatment with Oncamex may be of greater interest. This increase may be a response mechanism to the induction of mitochondrial dysfunction and apoptosis by Oncamex. Even if mitochondria continue to contribute most of the ATP in the majority of cancer cells, these rely on glycolysis to cover their energy demands once the mitochondrial function becomes compromised[709].

The Oncamex-induced accumulation of mSO would lead not only to the initiation of apoptosis, but also the hydrolysation of the ester phosphate bonds of ATP molecules and disruption of any undergoing oxidative phosphorylation[727], making it necessary for glycolysis to provide additional ATP supplies instead. Indeed, *PKM2*, which encodes the enzyme that generates the net gain of ATP from glycolysis, was significantly up-regulated by treatment with Oncamex. An increased glycolytic rate would also lead to a greater production of NADPH, a key anti-oxidant molecule commonly synthesised in cancer cells in an attempt to cope with oxidative stress[709]. Most likely, this metabolic effort could be directed to providing the energy necessary for the completion of apoptosis, as results have demonstrated the induction of cell death by Oncamex at both protein and gene levels and cells have been shown to use cytosolic ATP generated in glycolysis to undergo the energy-demanding process of cell death[728].

In summary, results from differential gene expression analysis are consistent with a mechanism by which the disruption of the mitochondrial function by treatment with

Oncamex leads to an increase in glycolysis as a response mechanism to cope with the stress and energetic demands associated with the initiation of apoptosis.

Following this, a possible combination with treatments capable of blocking glycolysis could lead to a stronger, beneficial effect, as the potential blockade of both pathways capable of energy production in the cell could induce an irreversible compromise of cell survival. The energy limitations could lead to the triggering of non-apoptotic death mechanisms: (i) autophagy, which can cooperate with apoptosis in response to stress[692,729], or (ii) necrosis, which can be derived from pro-apoptotic signals through TNF (tumour necrosis factor)[729,730] or death receptors such as FAS[731], particularly when apoptosis is blocked or ATP levels are too low.

This suggests a potential combination of Oncamex with glycolytic inhibitors against the glucose transporters or glycolytic enzymes, which are regulated by HIF-1 signalling and often over-expressed in cancer cells due to oncogenic activation[712,718,732,733]. Radiotherapy has also been shown to induce a switch from glycolysis to mitochondrial oxidative phosphorylation by inhibiting the activity of HK2 through an mTOR-dependent mechanism[734]. The combination of either of these therapeutic tools with a mitochondria-targeted agent such as Oncamex could be an interesting approach to be studied in further work.

5.4.4. Oncamex and the induction of mitophagy

Previous research has linked mitochondrial fragmentation and mitochondrial membrane depolarisation to the induction of mitophagy, a form of macro-autophagy involving the degradation of the mitochondria[646,647]. Indeed, mitochondrial dysregulation precedes the engulfment of mitochondria by the isolation membrane (or phagophore) through mechanisms involving (i) the activation of the ligase parkin by PINK1 (phosphatase and tensin homolog-induced putative kinase 1), or (ii) the BH3 (BCL2 homology 3) domain-containing receptors BNIP3 and BNIP3L (or NIX)[620,647,735].

Differential gene expression analysis results have shown a strong up-regulation of both BNIP3 and NIX across all models following treatment with Oncamex (see *Figures 50* and *55*). Although initial results in MCF-7 cells also showed a more modest increase in the expression of FUNDC1, this change was not consistent across different models, suggesting this protein may not be relevant to the otherwise common effect of Oncamex.

BNIP3 and NIX are redox-resistant homodimers whose integration in the outer mitochondrial membrane is dependent on dimerisation[633,735]. Besides their previously

discussed complex contribution to the induction of apoptosis (see section *4.6.1.*), they have been linked to the induction of stress-related mitophagy, interacting with LC3 (microtubule-associated protein 1A/1B-light chain 3), a protein embedded in the isolating membrane[736]. Through the LC3-interacting region (LIR) in their unstructured amino-termini[737], BNIP3 and NIX act as molecular adaptors for the targeting of the mitochondria by the isolating membrane and the formation of the autophagosome, where they can be captured and degraded.

As previously discussed, results have shown a consistent Oncamex-induced increase in the expression of the transcription factor FOXO3 across all models studied (see *Figures 50* and *55*). Besides its anti-proliferative and pro-apoptotic effect, FOXO3 has been shown to activate BNIP3/NIX-induced autophagy in response to stress[738]. While BNIP3 and NIX have been shown to be hypoxia-inducible, they may be activated by other sources of cellular stress and their modulation through FOXO3 could explain the activation of BNIP3/NIX in response to Oncamex-induced mitochondrial events such as increased ROS levels, alterations of the respiratory function or membrane depolarisation, which has been suggested by other authors[646]. Additionally, BNIP3 has also been linked to the modulation of oxidative phosphorylation and lipid metabolism in the mitochondria[739,740], suggesting its possible involvement in a mechanism of response to mitochondrial dysregulation.

In summary, BNIP3 and NIX act as inducers of cell death and mitophagy in response to hypoxia or mitochondrial stress. As discussed in the previous section, the expression profile for glycolysis-related genes suggested the absence of significant active HIF-1 signalling after treatment with Oncamex. Given their role in response to variation in oxygen levels, changes in BNIP3 and NIX levels may have also contributed to the identification of hypoxia response as a significant biological function in the effect of Oncamex in preliminary gene enrichment analysis.

In the context of these observations, the up-regulation of FOXO3 and previous results that have demonstrated the induction of mitochondrial dysregulation, the observed changes in BNIP3/NIX expression could reflect the induction of mitophagy as a mechanism of response, in an attempt to isolate and degrade dysfunctional mitochondria to prevent the induction of cell death triggered by the Oncamex-induced increase in ROS production and membrane permeabilisation. Mitophagy could be induced not only in addition to but also as a response mechanism to the pro-apoptotic effect of this novel flavonoid.

The possible role of mitophagy as a response mechanism to the effect of Oncamex suggests that, as in the case of increased glycolytic rates, the inhibition of this process concomitantly with treatment with this novel flavonoid could lead to improved efficacy. Although further work is needed in this field, some authors have suggested the inhibition of mitophagy as a possible therapeutic strategy, particularly for its application in cancer therapy, since the inhibition of this process would lead to an increase in ROS levels and cancer cells have been known to exhibit greater susceptibility to mitochondrial stress[620,646]. Through this mechanism of action, the potential combination of Oncamex with mitophagy inhibitors could not only impair one of the cell's apparent mechanisms of response that attempt to prevent the effect of the novel flavonoid, but also contribute to its mechanism of action. Indeed, reviewers have also highlighted the potential application of mitophagy inhibition in combination with other therapeutic tools capable of inducing mitochondrial stress[620].

5.5. Conclusion

Results reported in Chapters 4 and 5 have shown the mitochondrial targeting and ROS-modulating properties of Oncamex and demonstrated the induction of apoptosis at protein level, as well as changes in apoptosis-modulating pathways at gene level. These results are consistent with a mechanism by which Oncamex induces a rapid and strong production of mSO that leads to mitochondrial dysfunction and membrane permeabilisation, as well as to the activation of JNK signalling and its downstream target FOXO3, which together may contribute to a pro-apoptotic effect of this novel flavonoid.

Additionally, results have shown the induction of a HIF-1-independent increase in glycolysis and mitophagy. In the context of other altered biological functions and apoptotic responses, these changes are consistent with an increase in glycolysis and mitophagy as a response mechanism to the Oncamex-induced disruption of mitochondrial function, in an attempt to cope with the energy demands and stress associated with the induction of apoptosis.

As previously mentioned, this is a hypothetical model for the mechanism of Oncamex, based on results from the assessment of its effect at both protein and gene levels. As previously discussed (see section *5.1.*), practicalities limited the number of replicates that could be included in the microarray experiment. Differential gene expression analysis across different models for both breast and ovarian cancer have supported a common effect consistent with the mechanism described here. Nevertheless, further validation would be necessary to ascertain the specifics of this models, both to corroborate (possibly using qPCR) and to validate at protein level (with further protein work) changes observed in differential gene expression analysis.

In short, although further validation is required to corroborate it, the assessment of the effect of Oncamex through different methods has allowed for the postulation of a model for its mechanism of action, which results have suggested is consistent across different models of breast and ovarian cancers. The following chapters will study the application of Oncamex in combination with other agents (see Chapter 6) and assess its efficacy *in vivo* in initial xenograft experiments in mice (see Chapter 7).

6. Study of the effect of Oncamex in combination with other anticancer agents

6.1. Introduction

Previous chapters have focused on the assessment of the antiproliferative and pro-apoptotic effect of Oncamex as a single agent. This chapter seeks to study the possible applications of this compound in combination with different standard-of-care therapeutic agents, particularly the chemotherapy drug paclitaxel, TRAIL (TNF-related apoptosis-inducing ligand) and the anti-oestrogen tamoxifen.

As summarised in the introduction, previous research has reported numerous examples of flavonoids being able to exert beneficial effects in combination with other therapies (see section *1.1.5.5.1.*). Importantly, this includes the natural flavonol myricetin, from which Oncamex is derived, which has been observed to exert synergistic effects in combination with radiotherapy[465], chemotherapy[466] or TRAIL[261]. In the case of paclitaxel, research has previously described the ability of several flavonoids and polyphenols to induce an enhanced effect of the antimitotic agent through different mechanisms[741–744]. Different flavonoids and polyphenols have also been shown to enhance the efficacy of treatment with TRAIL[261,745–748]. Novel semi-synthetic flavonoids, similar to those in the library of compounds studied in this project, have also shown promising effects in combination with cytotoxic agents[484,485,488].

Oncamex has been observed to exhibit improved efficacy as a single agent and, importantly, to exert similar antiproliferative effects in models representing phenotypes of response and resistance to other treatments (see section *3.5.*). Additionally, previous unreported studies by Antoxis suggested Oncamex may have an additive or even synergistic effect when used in combination with cytotoxic agents in a glioblastoma cell line model (see *Supplementary Figures 11-13*, from unpublished results courtesy of Graeme Cook, Antoxis Ltd), although the effect on other cancer types has not been investigated and further work is needed. Following these results and the aforementioned evidence from previous studies with other flavonoids, the effect of Oncamex in combination with paclitaxel and TRAIL was investigated and is described in this chapter.

Flavonoids have also been observed to regulate oestrogen signalling through complex interaction with ER (see section *1.1.5.3.1.*). Results have shown the ability of Oncamex to exert antiproliferative effects in models representative of endocrine therapy-resistant breast

cancer models (see section *3.2.2.*) and previous research has shown the ability of some flavonoids to sensitise similar cancers to tamoxifen[749]. Following this evidence, this chapter also describes the effect of combination of Oncamex with endocrine therapy for its potential application in this niche group of cancers, as well as preliminary analysis investigating the possible changes in gene expression associated with this combination.

6.2. Oncamex in combination with paclitaxel and TRAIL

6.2.1. Study of combinatorial effects in ovarian cancer cells

A first panel of experiments investigated the effect of Oncamex in combination with the antimitotic agent paclitaxel (see section *1.1.4.3.*) and TRAIL. The PEA1/PEA2 pair of ovarian cell lines was selected as a model given their chemotherapy sensitive/resistant phenotype (see *Table 5*, section 2.1.1.). The sensitivity of these cell lines to paclitaxel and TRAIL was assessed prior to the start of the experiments (see *Figure 62*).

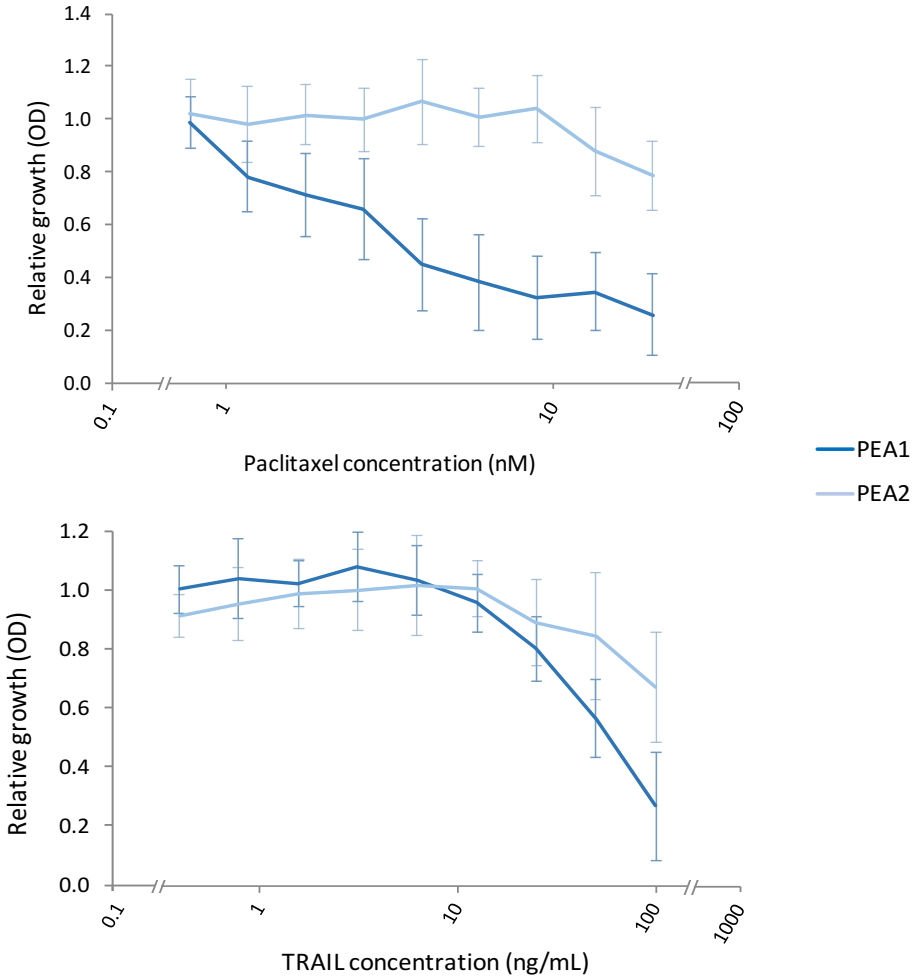

***Figure 62* Sensitivity of ovarian cancer cells to treatment with paclitaxel and TRAIL.** *The sensitivity of the PEA1/PEA2 ovarian cancer cell line pair to both agents was assessed by SRB assays after 48 h treatment. Each experiment was repeated (n=2, with 6 technical replicates per treatment condition). These graphs show pooled results, with each data point representing the average from biological replicate experiments for each treatment condition, normalised to vehicle controls, and error bars representing standard deviation (SD).*

Results showed a stronger response for the chemotherapy-sensitive cell line PEA1 to both agents. Indeed, both cell lines responded differently to treatment with concentrations in the nanomolar range of paclitaxel: proliferation appeared to be inhibited in PEA1 cells treated with concentrations higher than ~1.75nM, whereas treatment with 20nM was necessary to induce an effect in PEA2 cells. Similarly, treatment with 12.5ng/mL of TRAIL appeared to induce a considerable inhibition in PEA1 cells, while 50ng/mL were required to induce a similar effect in PEA2 cells.

Combination experiments sought to investigate a possible enhanced combinatorial effect between Oncamex and either paclitaxel or TRAIL, to assess whether concentrations of each agent that have limited efficacy as a single treatment may exert a significant effect in the models studied when combined. These experiments investigated the potential combinatorial effects achieved through different treatment regimens. Following results from preliminary experiments testing different combination alternatives (see *Supplementary Figure 14*), further work focused on assessing the effect of concomitant treatment with Oncamex and paclitaxel or TRAIL for 48h or a shorter pretreatment with the novel flavonoid followed by 48 h of concomitant treatment.

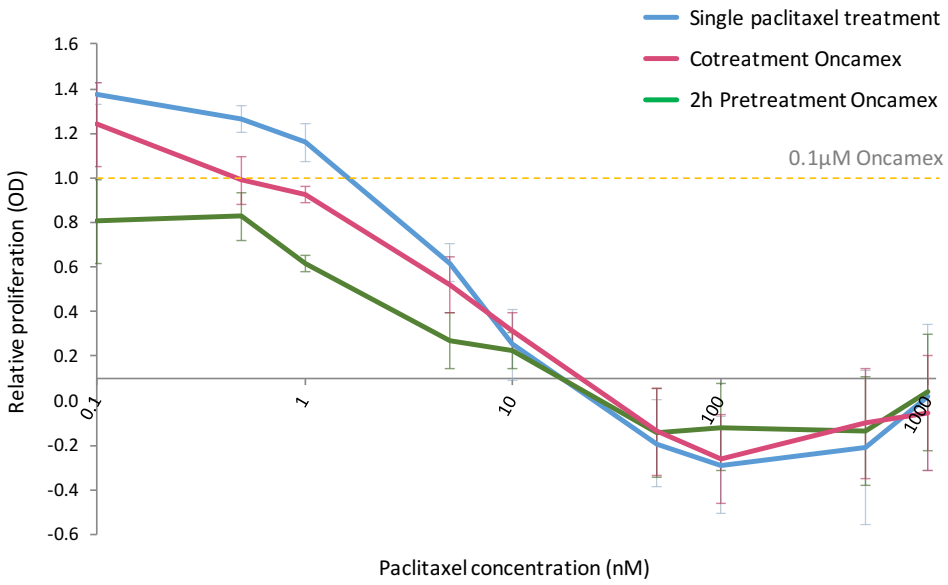

Figure 63 ***Preliminary results from screening of the combinatorial effect on PEA1 cells of 0.1µM Oncamex and a range of paclitaxel concentrations.*** *Initial experiments sought to identify concentrations of paclitaxel whose cytotoxic effect might be enhanced by combination with Oncamex. Each experiment was repeated (n=2, with 6 technical replicates per treatment condition). These graphs show pooled results, with each data point representing the average from biological replicate experiments for each treatment condition, normalised to vehicle controls, and error bars representing standard deviation (SD).*

Low concentrations of each agent were combined, as initial results suggested that co-administration with Oncamex could improve on the effect of paclitaxel only for concentrations of the latter in the nanomolar range that did not induce a strong cytotoxic effect (see *Figure 63*). Following this, combination experiments studied the effect of submicromolar concentrations of Oncamex (0.1μM or 0.3μM) when administered in combination with 1.75nM paclitaxel or 5ng/mL TRAIL. These treatment levels were selected as low concentrations which did not exert a strong antiproliferative effect on either cell line but were minimally effective on treatment-responsive PEA1 cells.

The effect of combination of Oncamex and paclitaxel in ovarian cancer cells was assessed first through SRB assays, measuring changes in protein biomass as an estimation of the effect of treatment on cell proliferation. Results demonstrated an enhanced effect on PEA1 and PEA2 cells when both agents were administered concomitantly or preceded by a short incubation with Oncamex, although some variation was observed depending on the concentration of Oncamex and the model (see *Figure 64*).

In PEA1 cells, concomitant treatment for 48 h had and enhanced inhibitory effect. For instance, combination of 0.3μM Oncamex with 1.75nM of paclitaxel led to proliferation levels below 70% control, significantly ($P<0.001$) lower than the effect of either single treatment, for which proliferation was >90% in comparison to vehicle controls. Interestingly, 2h pretreatment with either concentration of Oncamex prior to the administration of concomitant treatment induced a stronger beneficial effect in both models studied. Indeed, proliferation for both PEA1 and PEA2 cells was significantly reduced following this regimen: in comparison to vehicle controls, pretreatment with 0.3μM Oncamex led to <45% control proliferation in PEA1 cells and <75% in PEA2 cells.

Similar results were obtained in combination experiments with Oncamex and 5ng/mL TRAIL (see *Figure 65*). Combination of TRAIL with 0.1μM Oncamex induced a beneficial effect when administered as a pretreatment in PEA1 cells, leading to <80% control proliferation in comparison to the inefficacy (>100%) of either agent as a single agent.

Combination of 5ng/mL TRAIL with 0.3μM Oncamex appeared to induce significant combinatorial effects in both cell lines. In PEA1 cells, concentrations of TRAIL and Oncamex found to be ineffective as single agents (>100% proliferation) led to a significant effect when combined (<75%), particularly when preceded by pretreatment with Oncamex (<45%). In PEA2 cells, both regimens also induced modest but significant changes in proliferation.

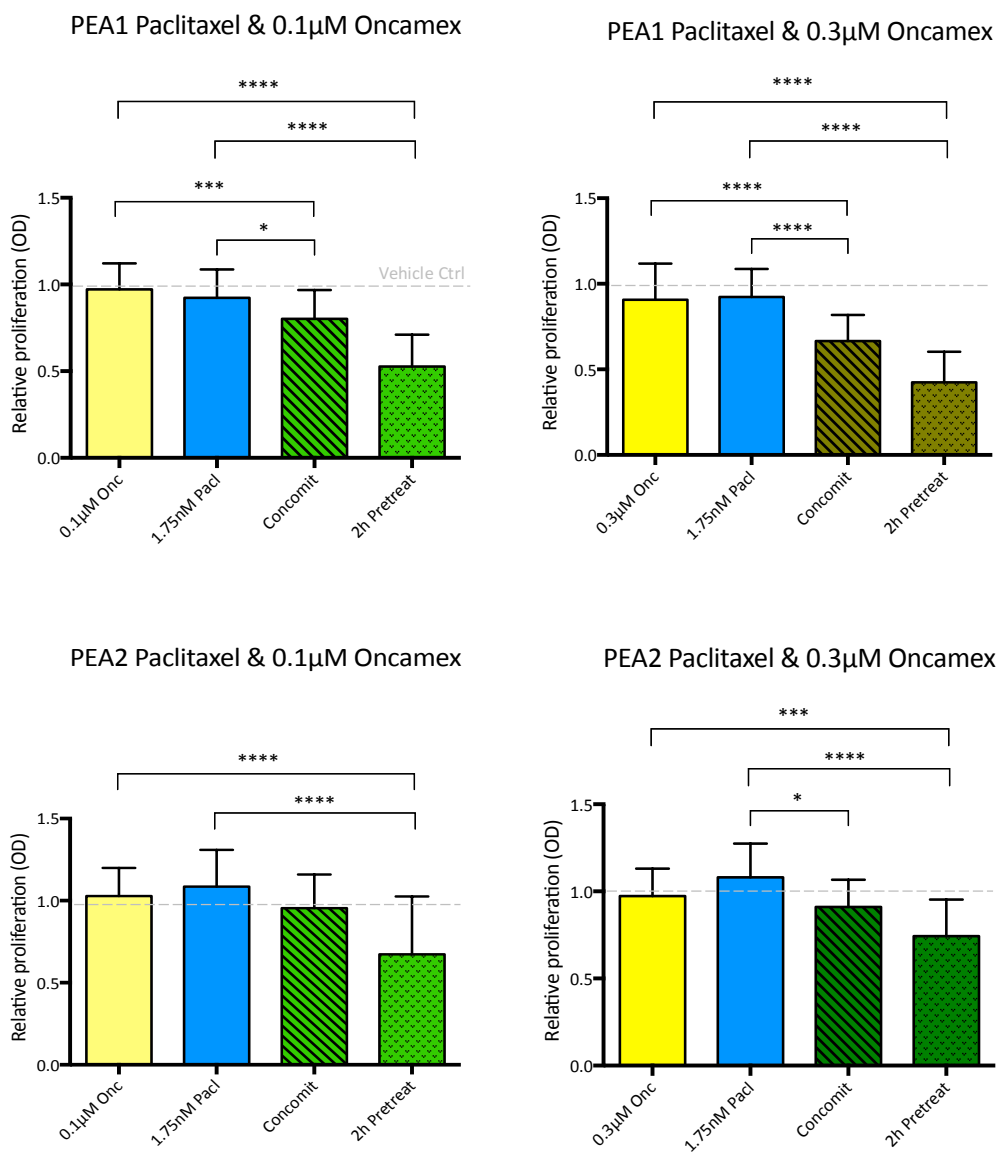

Figure 64 ***Combination treatment of ovarian cancer cell lines with Oncamex and paclitaxel.*** *Low concentrations of Oncamex and paclitaxel which had been observed to be ineffective as single treatment were combined concomitantly for 48 h, with or without a short pretreatment with Oncamex. Each experiment was repeated (n=3, with 6 technical replicates per treatment condition). These graphs show pooled results, with each data point representing the average from biological replicate experiments for each treatment condition, normalised to vehicle controls, and error bars representing standard deviation (SD). P-values from ANOVA followed by Tukey multiple comparison test: *P<0.05; ***P<0.001; ****P<0.0001. Where not shown P>0.05 (nonsignificant).*

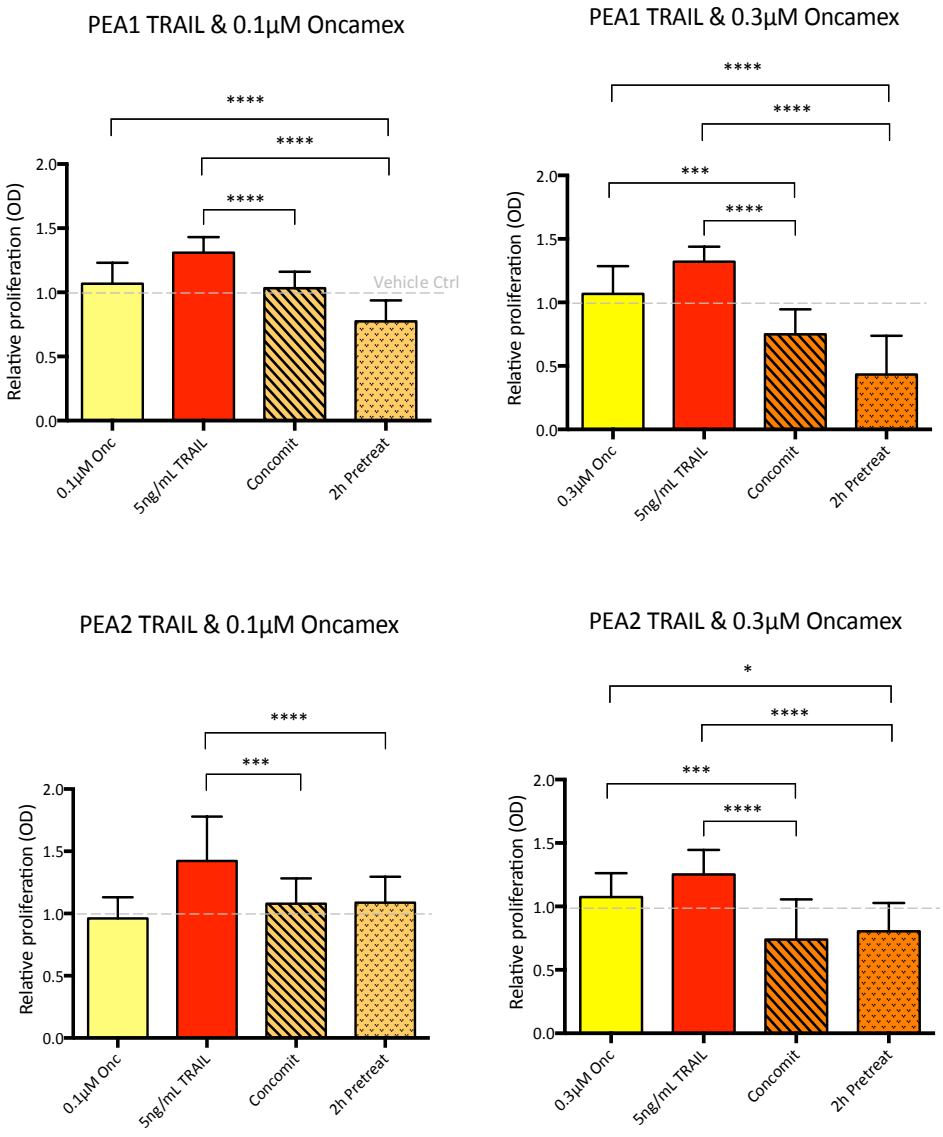

Figure 65 ***Combination treatment of ovarian cancer cell lines with Oncamex and TRAIL.*** *Low concentrations of Oncamex and TRAIL which had been observed to be ineffective as single treatment where combined concomitantly for 48 h, with or without a short pretreatment with Oncamex. Each experiment was repeated (n=3, with 6 technical replicates per treatment condition). These graphs show pooled results, with each data point representing the average from biological replicate experiments for each treatment condition, normalised to vehicle controls, and error bars representing standard deviation (SD). P-values from ANOVA followed by Tukey multiple comparison test: *P<0.05; ***P<0.001; ****P<0.0001. Where not shown P>0.05 (nonsignificant).*

In summary, the study of combination treatments with submicromolar concentrations of Oncamex and low levels of paclitaxel or TRAIL observed to be ineffective when administered as single agents has demonstrated some beneficial effects. Indeed, cotreatment with these agents led to a greater reduction in proliferation in both chemotherapy-sensitive and resistant ovarian cancer cell lines. Interestingly, the best observed response in all experiments corresponded to pretreatment for 2 h with 0.3µM Oncamex, followed by 48 h incubation with a concomitant treatment.

Finally, preliminary analysis of microarray data sought to assess whether changes in gene expression could be linked to the observed enhancing effect of 2 h pretreatment with 0.3µM Oncamex. Firstly, the effect of this treatment on genes whose expression levels were different (by a ±0.4 log 2-scale cut-off) at baseline between PEA1 and PEA2 cells was studied. Given the differences in response to chemotherapy, these inherent differences may be linked to the development of resistance in PEA2.

Hierarchical clustering of these genes as previously described resulted in 6 clusters (see *Figure 66*). Treatment with 0.3µM Oncamex for 2 h appeared to alter the gene expression of some of these genes (clusters 2 and 4) in PEA2, but not in PEA1 cells or after treatment with 10µM Oncamex. However, gene enrichment analysis found no significant GO terms associated with these changes. Thus, while results showed that 2 h pretreatment with 0.3µM Oncamex might exert a specific effect in PEA2 cells, gene ontology analysis suggested that these changes were unlikely to be translated into a significant biological effect.

Given the fact that the enhancing effect of 0.3µM Oncamex was observed not only in PEA2 cells, but also in their chemo-sensitive parent cell line PEA1, further analysis assessed the effect of this treatment on their overall gene expression profile, rather than just on those genes inherently different between both models. For this, genes whose expression levels were significantly changed (by a ±0.4 log 2-scale cut-off) between control and 0.3µM Oncamex-treated cells were selected.

Hierarchical clustering resulted in 6 distinct gene clusters (see *Figure 67*). Despite similar combinatorial effects in PEA1 and PEA2 cells, results showed that 2 h pretreatment with 0.3µM Oncamex induced a markedly different effect on both cell lines. Additionally, gene enrichment analysis again found no significant biological functions significantly represented in these clusters. In short, these results suggest that the observed changes induced by 0.3µM Oncamex on gene expression are unlikely to be translated into key biological effects.

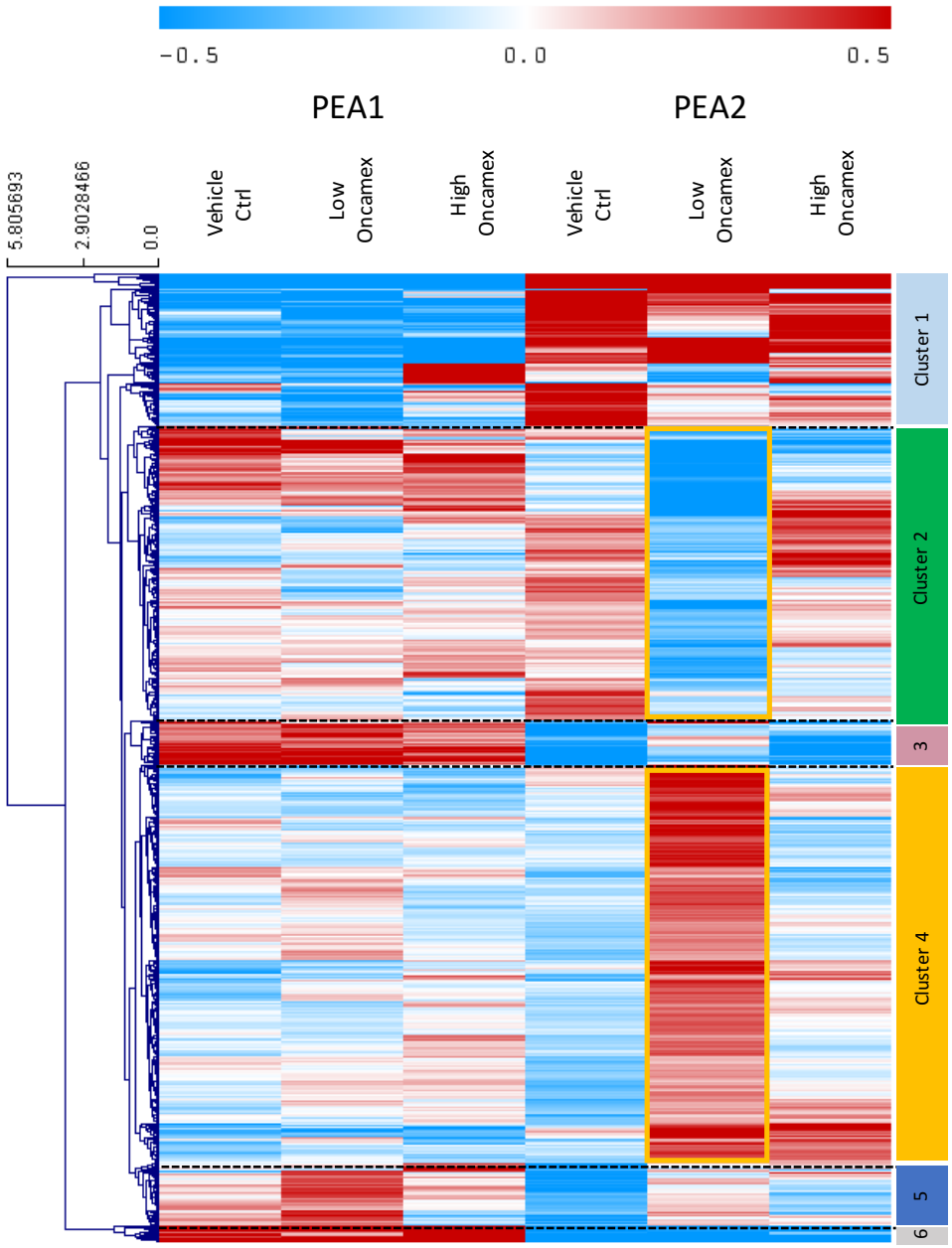

Figure 66 ***Effect of Oncamex on expression of genes differentially expressed at baseline in PEA1 and PEA2 cells.*** *Genes whose expression levels at baseline differed by more than a 0.4 log2-scale cut-off between control PEA1 and PEA2 cells were selected. This heatmap is the result of hierarchical clustering of these genes following Pearson correlation with complete linkage. Red and blue represent relative high and low log2 expression values, respectively. Gene enrichment analysis found no GO terms significantly represented in the clusters of interest.*

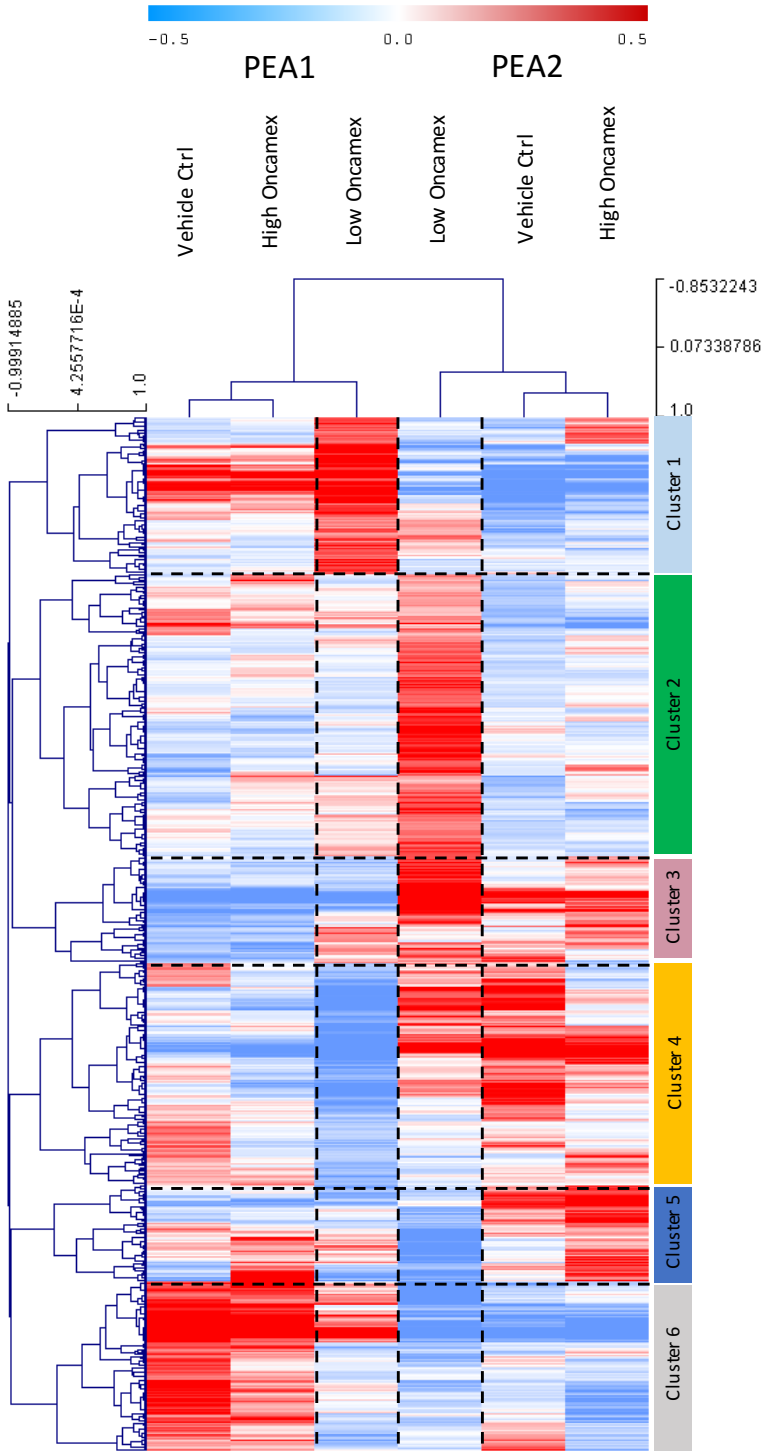

Figure 67 ***Differentially expressed genes in PEA1 and PEA2 cells following treatment with 0.3µM Oncamex for 2 h.*** *Genes whose expression levels at baseline differed by more than a 0.4 log2-scale cut-off between control and 0.3µM Oncamex-treated samples for either PEA1 or PEA2 cells were selected. This heatmap is the result of hierarchical clustering of these genes following Pearson correlation with complete linkage. Red and blue represent relative high and low log2 expression values, respectively. Gene enrichment analysis found no GO terms significantly represented in the clusters of interest.*

6.2.2. Study of combinatorial effect in breast cancer cells

Although initial work focused on ovarian cancer models due to their selected treatment-sensitive/resistant phenotypes, further experiments studied whether these combinatorial effects were recapitulated in breast cancer models. The inherent sensitivity of the breast cancer cell line MDA-MB-231 to paclitaxel and TRAIL was assessed in order to select appropriate concentrations to test in combination with Oncamex (see *Figure 68*).

Results showed the relative sensitivity of MDA-MB-231. Treatment with concentrations of paclitaxel higher than 15.625nM or with concentrations of TRAIL higher than 6.25ng/mL induced a strong inhibitory effect in MDA-MB-231, in comparison to cells exposed to a vehicle control.

Following these results, lower concentrations of these agents (5nM paclitaxel or 5ng/mL TRAIL) were applied in cotreatment experiments with submicromolar concentrations of Oncamex (0.1 or 0.3µM) in order to assess whether the beneficial combinatorial effects demonstrated in ovarian cancer cells were recapitulated in this breast cancer model. Similar treatment regimens were tested to compare the effect of each compound as a single agent or administered concomitantly, with or without 2h pretreatment with Oncamex.

Experiments assessed the effect of these combinations on MDA-MB-231 cells following the previous experimental design (see *Figure 69*). Results demonstrated a recapitulation of the beneficial combinatorial effects previously observed in ovarian cancer cells in this breast cancer model.

Combination with either 0.1 or 0.3µM Oncamex enhanced the effect of 5nM paclitaxel, with similar relative effects on either treatment regimen. Indeed, concomitant treatment with TRAIL and 0.1µM Oncamex led to a reduction in proliferation to levels below 50%, significantly improving on either compounds' effect as a single agent (>75%).

Results also demonstrated a beneficial combinatorial effect between Oncamex and TRAIL in MDA-MB-231 cells. Indeed, treatment with 5ng/mL TRAIL was ineffective (>100% in comparison to the vehicle control), while concomitant treatment with 0.1 or 0.3µM Oncamex lead to significant response (~56% and ~42%, respectively). Interestingly, in the case of combination with TRAIL in MDA-MB-231 cells pretreatment with Oncamex prior to the administration of concomitant treatment with both agents did not induce a beneficial effect in comparison to concomitant treatment alone.

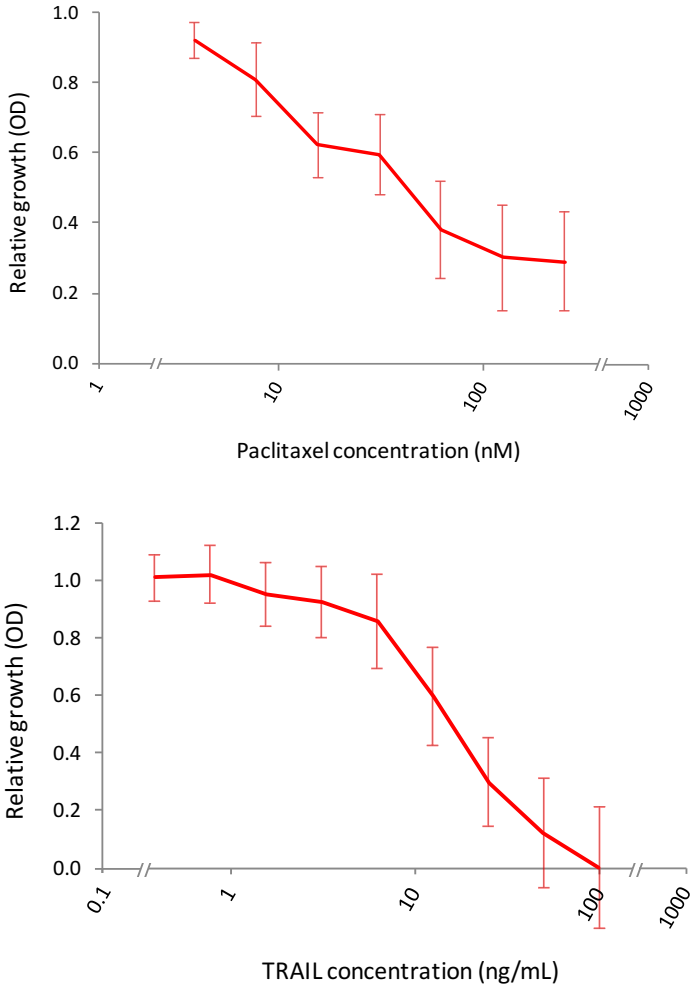

***Figure 68* Sensitivity of MDA-MB-231 breast cancer cells to treatment with paclitaxel and TRAIL.** *The sensitivity of MDA-MB-231 cells was assessed by SRB assays after 48 h treatment. Each experiment was repeated (n=2, with 6 technical replicates per treatment condition). These graphs show pooled results, with each data point representing the average from biological replicate experiments for each treatment condition, normalised to vehicle controls, and error bars representing standard deviation (SD).*

These results have shown that submicromolar concentrations of Oncamex may also lead to a beneficial effect in combination with paclitaxel and TRAIL in a breast cancer cell line model. Despite these significant changes, some variation can be observed in comparison to previous results in ovarian cells. For instance, the effect of paclitaxel appeared to be improved to a slightly further extent when combined with the lower concentration of Oncamex, while pretreatment with the novel flavonoid did not lead to a stronger response to concomitant treatment with TRAIL. This suggests the likely complexity of the mechanism underlying these effects and the need for further study and optimisation.

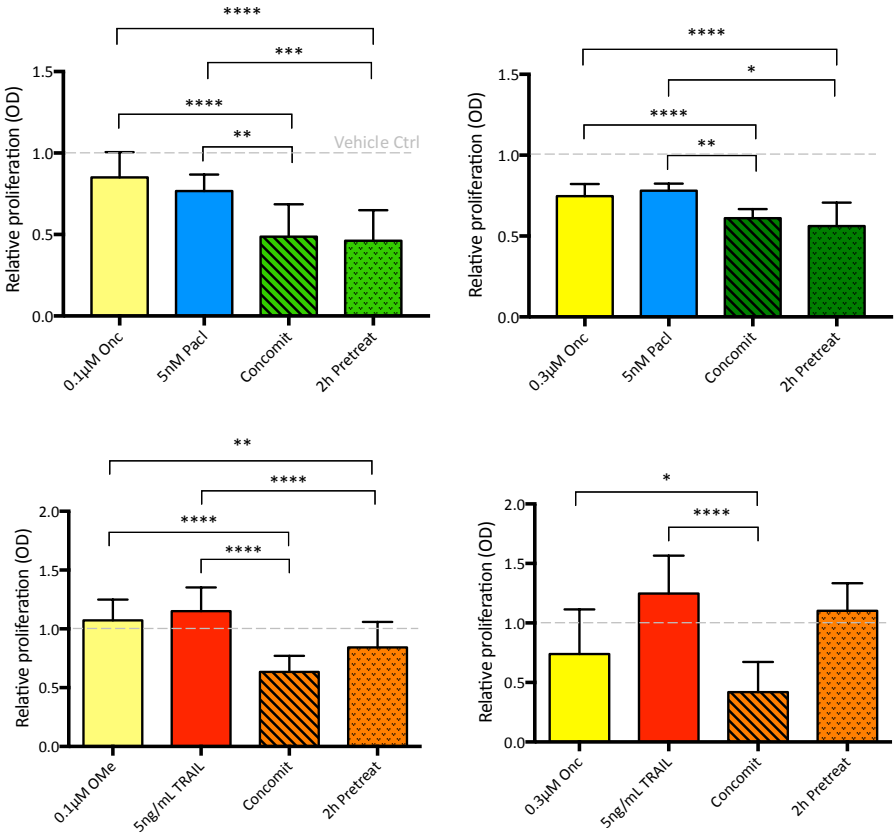

Figure 69 ***Combination treatment of MDA-MB-231 breast cancer cells with Oncamex and paclitaxel/TRAIL.*** *Low concentrations of Oncamex and paclitaxel/TRAIL paclitaxel which had been observed to be ineffective as single treatment where combined concomitantly for 48 h, with or without a short pretreatment with Oncamex. Each experiment was repeated (n=3, with 6 technical replicates per treatment condition). These graphs show pooled results, with each data point representing the average from biological replicate experiments for each treatment condition, normalised to vehicle controls, and error bars representing standard deviation (SD). P-values from ANOVA followed by Tukey multiple comparison test: *P<0.05; **P<0.001; ***P<0.001; ****P<0.0001. Where not shown P>0.05 (nonsignificant).*

6.2.3. Discussion of the possible mechanism underlying the effect of Oncamex as a combination agent

In summary, results reported here from experiments with both breast and ovarian cells suggest the potential of Oncamex to improve sensitivity to both paclitaxel and TRAIL. Importantly, although PEA1 cells demonstrated a greater relative response to combined treatment, a statistically significant effect was also observed in PEA2 cells, which were selected for their chemotherapy-resistant phenotype and have been shown to have a poorer inherent sensitivity to these agents. Additionally, in the same way that a similar effect of

Oncamex as a single agent was observed across different cancer types, these combinatorial effects were also recapitulated in breast cancer cells.

As previously discussed, research has suggested that similar mechanisms may be involved in the development of resistance to different treatments (see section *1.1.4.1.*). This is supported by the fact that PEA2 cells showed a phenotype of poorer sensitivity to paclitaxel and TRAIL despite having been selected for different chemotherapeutic agents (see *Table 6*, section 2.1.1.). The fact that Oncamex induced an enhanced effect in combination with different agents suggests it could exhibit similar combinatorial effects with other therapies.

The possible mechanism underlying the observed combinatorial effects, and in particular the improved effect of a short incubation with Oncamex observed in the majority of cases, bears further discussion.

Results from a preliminary gene expression analysis in PEA1 and PEA2 cells were consistent with a non-specific effect of 0.3µM Oncamex on gene expression level, which appeared unlikely to be translated into a biological effect. This suggests that the mechanism underlying the combinatorial effects reported here may not rely primarily on changes in gene expression. Given the low concentration of Oncamex applied, pretreatment may induce other changes that are unlikely to be translated into a modulation of gene expression after a short pretreatment of only 2 h. This synergy could be the result of subtoxic levels of Oncamex inducing weak pro-apoptotic changes in the mitochondria that may be bypassed by cancer cells when administered as a single treatment but could lead to effective changes when in combination.

This hypothesis is supported by previous results on the mechanism of action of Oncamex (see Chapter 4) and previous work investigating the effect of myricetin in combination with other treatments. Indeed, research has reported the ability of this flavonoid to sensitise cancer cells to TRAIL through induction of changes in the expression levels of apoptosis-regulating factors such as the BCL2 family when administered at subtoxic concentrations[261]. Down-regulation of BCL2 has also been linked to the ability of myricetin to induce an antiproliferative effect in ovarian cells with acquired resistance to the chemotherapeutic agent cisplatin[369].

The previously described ROS-modulating abilities of Oncamex could also play a role in the induction of these improved combinatorial effects. Research has shown that paclitaxel relies on the induction of ROS production to trigger cell death both *in vitro* and *in vivo*[750,751]

and its combination with pro-oxidative agents had been observed to improve its efficacy[752]. ROS generation has also been linked to the ability of the natural flavonoid wogonin to enhance the antitumour activity of TRAIL[753,754], while antioxidant enzymes have been linked to the development of resistance to this agent[755]. Treatment with low levels of Oncamex might induce the generation of ROS that, although insufficient to exert a strong pro-apoptotic effect alone, could enhance the effect of paclitaxel and TRAIL by contributing to their ROS-dependent mechanisms for the induction of cell death or facilitating the surpassing of mechanisms of resistance blocking these effects.

Additionally, the apparent ability of Oncamex to enhance the effect of different agents may point to the involvement of secondary mechanisms regulating drug metabolism or transport. The evidence on the interaction of flavonoids with these processes has been previously discussed (see sections *1.1.5.3.3.* and *1.1.5.3.4.*). In the case of combination with paclitaxel, previous work has suggested the ability of flavonoids to inhibit its metabolic degradation *in vivo*[756], while pretreatment with flavonoids has been noted to enable better bioavailability[757,758]. Nevertheless, further work is necessary in order to assess the involvement of these mechanisms in the combinatorial effects observed. Further, more in-depth studies, including *in vivo* testing, would be necessary to better evaluate the potential further development of Oncamex towards clinical application.

6.3. Oncamex in combination with endocrine therapy

In addition to cotreatments with paclitaxel or TRAIL, the potential application of Oncamex in combination with anti-oestrogens was also investigated. This follows previous research that has shown the ability of luteolin, a flavonol similar to myricetin, to improve sensitivity to tamoxifen *in vivo*[749]. As previously summarised, flavonoids have been noted to interact with oestrogen signalling through different mechanisms (see section *1.1.5.3.1.*).

Although the mechanisms of action of endocrine therapy are complex, several authors have linked tamoxifen treatment and the development of resistance to this agent to alterations in mitochondrial redox signalling[563,759]. In particular, the increased activity of antioxidant enzymes such as SOD has been observed in tamoxifen-resistant tumours[563]. Oncamex has shown antiproliferative efficacy as a single agent in anti-oestrogen resistant cells through regulation of the mitochondrial redox status. Additionally, Oncamex has shown an enhanced effect in combination with chemotherapy. Given the fact that the loss of efficacy of different therapies can involve similar mechanisms, further work sought to investigate whether this sensitising effect may be recapitulated in the instance of resistance to anti-oestrogens.

Initial experiments investigated the efficacy of treatment with 4-hydroxytamoxifen (OHT), an active metabolite of tamoxifen[760], in a panel of breast cancer cell lines. This included (i) the triple negative MDA-MB-231 cells, which lack ERα and are thus independent of oestrogen signalling for growth, as a control for resistant behaviour; (ii) MCF-7 cells, which are $ERα^+$ and expected to be responsive to treatment with the anti-oestrogen, as a control for responsiveness; and (iii) MCF-7-derived LCC1, LCC2 and LCC9 cells, which are expected to present different degrees of an oestrogen-independent and anti-oestrogen-resistant phenotype (see *Table 5*, section 2.1.1.).

Results showed the oestrogen-dependent effect of treatment with 1μM OHT on some of the cell lines studied (see *Figure 70*). This concentration of the anti-oestrogen induced a strong decrease in cell proliferation of MCF-7 cells, reducing proliferation to below 40% of that of vehicle controls.

The modulation of growth of LCC cells was more complex. Based on their origin, LCC1 cells would be expected to retain the sensitivity to anti-oestrogens of their parent cell line MCF-7, whereas LCC2 and LCC9 cells would both be expected not to be significantly affected by treatment, following their derivation from MCF-7 cells through selection for resistance to

anti-oestrogens. Interestingly, LCC9 cells exhibited the expected phenotype, with no statistically significant changes in proliferation after treatment with 1µM OHT. Indeed, changes in LCC9 cells were comparable to those observed in MDA-MB-231 cells. Conversely, LCC1 and LCC2 cells appeared to present an intermediate phenotype, with partial sensitivity to OHT. Indeed, treatment with OHT induced a decrease in proliferation of these cells, but this was statistically significantly smaller than that observed in MCF-7 cells. The effect on LCC1 was stronger than on LCC2, although this difference was not statistically significant.

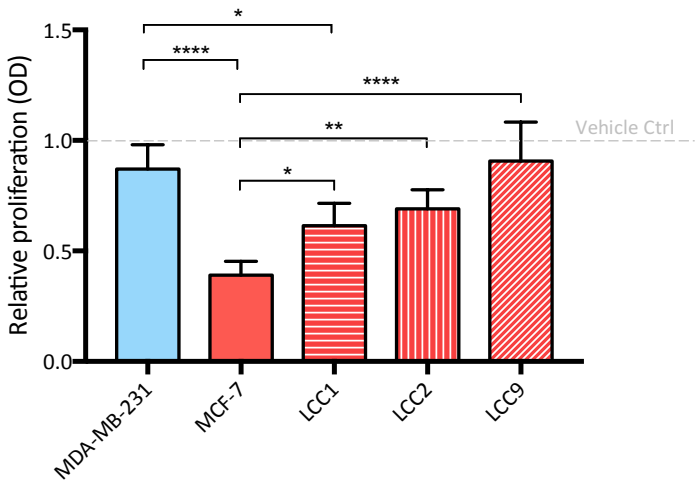

***Figure 70* Sensitivity of breast cancer cells to treatment with tamoxifen.** *SRB assays assessed the sensitivity of 5 breast cancer models to treatment with 1µM 4-hydroxytamoxifen (OHT) for 5 days. MDA-MB-231 and MCF-7 cells were treated in normal DMEM medium, containing FCS and Phenol Red. LCC1, LCC2 and LCC9 cells, grown in the absence of any oestrogenic effects with CSFCS and Phenol Red-free DMEM, were treated with OHT in the presence of 1nM E_2. Each experiment was repeated (n=3, with 6 technical replicates per treatment condition). These graphs show pooled results, with each data point representing the average from biological replicate experiments for each treatment condition, normalised to vehicle controls, and error bars representing standard deviation (SD). P-values from ANOVA followed by Tukey multiple comparison test: *P<0.05; **P<0.01; ****P<0.0001. Where not shown P>0.05 (nonsignificant).*

In short, 1µM OHT appeared to induce an ER-dependent effect in the breast cancer cell lines studied. Treatment with this anti-oestrogen active metabolite induced a strong effect in $ER\alpha^+$ MCF-7 cells but did not affect ER^- MDA-MB-231 or MCF-7-derived oestrogen-independent LCC-9 cells. As expected, LCC9 cells represented the best model for resistance to endocrine treatment. Consequently, they were selected for the assessment of possible combinatorial effects of Oncamex and OHT in further experiments.

Following the previous experimental design used to assess the effect of combination treatment with chemotherapy (see section *5.2.*), a range of concentrations of Oncamex (from subtoxic nanomolar to micromolar) were tested in combination with 1µM OHT. Initial results reported a potential combinatorial effect in cells treated with 1µM Oncamex (see *Figure 71*). Indeed, submicromolar concentrations observed to be subtoxic as single treatment (0.3µM) failed to improve the response to OHT, whereas higher micromolar concentrations (3-10µM) induced a strong cytotoxic effect that could not be enhanced by cotreatment with the anti-oestrogen. In contrast, treatment with 1µM Oncamex induced a partial decrease in LCC9 cell proliferation (~45% of control proliferation) that was enhanced when administered in combination with 1µM OHT (reduced to ~17%).

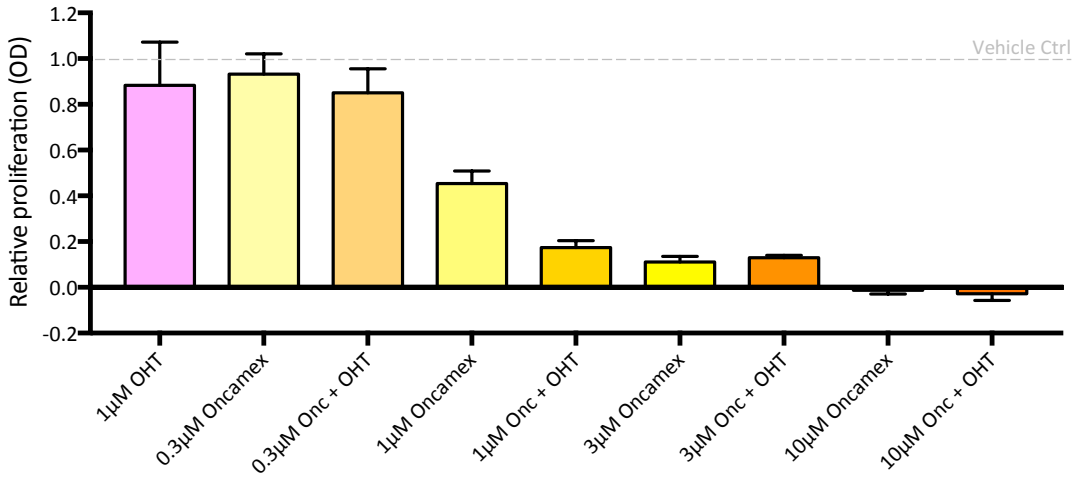

***Figure 71* Screening of Oncamex concentration for combination treatment with tamoxifen in LCC9 cells.** *A panel of experiments assessed the effect on LCC9 cells of treatment for 5 days with a range of Oncamex concentrations (0.3-10µM) in combination with 1µM OHT. This experiment was repeated (n=2, with 6 replicates per treatment condition). These graphs show pooled results, with each data point representing the average from biological replicate experiments for each treatment condition, normalised to vehicle controls, and error bars representing standard deviation (SD).*

These results suggested that concentrations of Oncamex in the low micromolar range might be more suitable for their assessment in combination with OHT. Following this, further work sought to confirm the results observed in combination with 1µM OHT. These experiments included the selected model LCC9, as well as MDA-MB-231 and MCF-7 cells to ascertain the dependence of any effects observed on the presence of ER and as reference for the comparison of anti-oestrogen effects, respectively.

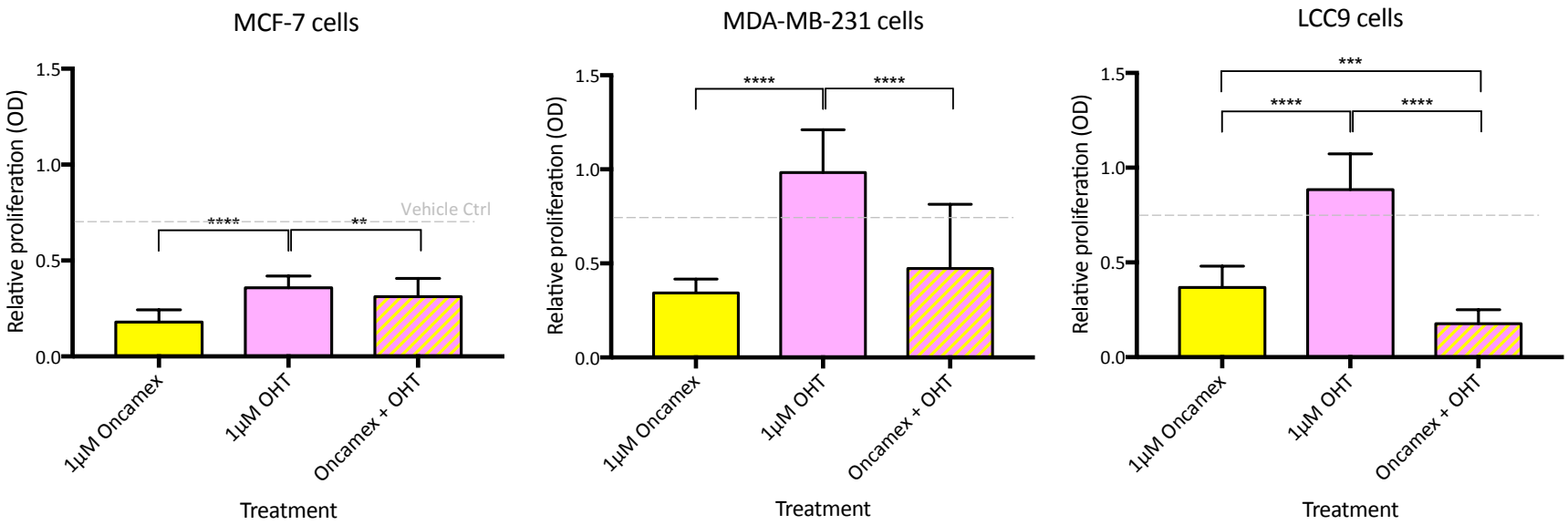

Figure 72 ***Combination treatment of breast cancer cell lines with Oncamex and tamoxifen.*** *Following optimisation experiments, the effect of treatment with a combination of 1µM Oncamex and 1µM OHT for 5 days was investigated in tamoxifen-resistant LCC9 cells, in comparison with MDA-MB-231 and MCF-7 cells. Each experiment was repeated (n=3, with 6 technical replicates per treatment condition). These graphs show pooled results, with each data point representing the average from biological replicate experiments for each treatment condition, normalised to vehicle controls, and error bars representing standard deviation (SD). P-values from ANOVA followed by Tukey multiple comparison test: **P<0.01; ***P<0.001; ****P<0.0001. Where not shown P>0.05 (nonsignificant).*

Results recapitulated the previous improved combinatorial effect in the administration of 1µM Oncamex concomitantly with 1µM OHT (see *Figure 72*). While treatment with this concentration of Oncamex exerted an antiproliferative effect in the 3 cell lines studied, its combination with OHT exerted a statistically significantly ($P<0.001$) stronger effect in LCC9 cells only. Indeed, the antiproliferative effect of Oncamex alone (37% in comparison to vehicle control) was almost halved (down to 18%) when the novel flavonoid was administered in combination with 1µM OHT. The response to this combination treatment was stronger than the effect of OHT observed in anti-oestrogen-sensitive MCF-7 cells.

This enhanced effect was not observed in MCF-7 cells, where the strong effect of the anti-oestrogen as a single agent (reducing proliferation to 36%) was not improved by combination with Oncamex. Cotreatment of MDA-MB-231 cells with Oncamex and OHT also failed to improve on the effect of either agent individually, although experimental variation across biological repeats led to high standard deviation, suggesting further work would be necessary for a better assessment of this response.

In summary, these results suggested the potential of Oncamex to exert an enhanced effect when administered in combination with OHT. The potential ability of Oncamex to improve the responsiveness of anti-oestrogen-resistant cells to treatment with tamoxifen would be of great interest given the high incidence of the development of acquired resistance to this widely applied standard-of-care primary therapy in ER^+ cancers (see sections *1.1.2.7.* and *1.1.4.1.*). However, further study would be necessary to elucidate whether this improved effect is the result of a partial reversal of resistance.

The possible interaction of the known properties of Oncamex with the mechanism of action of anti-oestrogen therapy bears further discussion. As previously discussed in the context of combinatorial effects with chemotherapy, the changes induced by Oncamex could improve the susceptibility of cancer cells to other agents.

Tamoxifen has been described to inhibit ER^+ cells not only through ER-dependent modulation of gene expression, but also through a mechanism of action involving the modulation of the mitochondria and, more specifically, mitochondrial ROS levels[563,759,761]. Indeed, tamoxifen has been shown to induce apoptosis by disrupting the mitochondrial function through a mechanism that requires the induction of high ROS levels, which also lead to changes in the BCL2 apoptosis-regulating protein family[759,761]. Interestingly, mechanisms inhibiting the accumulation of ROS lead to a reduction in the efficacy of tamoxifen[563,759,762], whereas the exposure of cells to other stimuli causing a decrease in the levels of anti-

apoptotic proteins such as BCL-XL or BCL2 can increase their susceptibility to this anti-oestrogen[761]. As previously discussed (see Chapter 5), treatment with Oncamex has been shown to modulate the expression of the anti-apoptotic protein BCL2.

Consequently, treatment with concentrations of Oncamex capable of dysregulating levels of mitochondrial ROS might improve the susceptibility to tamoxifen of cells that have developed acquired resistance through mechanisms that prevent the induction of this mitochondrial disruption by the anti-oestrogen. Together with results in combination with chemotherapy, these results suggest that Oncamex could have potential to be applied in combination with other therapeutic agents that also exert their effect through mitochondrial dysregulation and the induction of the intrinsic pathway of apoptosis.

In order to further understand the possible effect of Oncamex in the mechanisms of resistance to endocrine therapy, gene expression analysis assessed the possible differential effect of Oncamex specifically in LCC9 cells. Genes whose baseline expression levels were different (by a ±0.4 log 2-scale cut-off) between control MCF-7 and LCC9 cells were selected. Hierarchical clustering of these genes as previously described resulted in 4 clusters (see *Figure 73*). Results showed that among these differentially expressed genes, roughly half exhibited reduced expression in LCC9 cells (clusters 1 and 2), while the other half were increased in these cells (clusters 3 and 4).

Treatment with 0.3µM Oncamex for 2 h did not induce a significant change in expression of these genes in either cell line, as demonstrated by the similarity to the expression patterns of vehicle controls. Interestingly, treatment with 10µM Oncamex for 6 h induced changes in the genes included in clusters 2 and 4 only in LCC9 cells, altering their expression patterns to be more similar to those observed in MCF-7 cells.

Indeed, genes in cluster 2 that were lower in control LCC9 cells were up-regulated by treatment, achieving expression levels closer to those of control MCF-7 cells. A down-regulating effect was observed for cluster 4, which included genes up-regulated in vehicle control LCC9 cells in comparison to MCF-7 cells.

In short, this preliminary analysis has identified 2 groups of genes whose differential baseline expression between MCF-7 and LCC-9 cells could be linked to the mechanism underlying acquired resistance in the latter cells. Study of the effect of Oncamex has shown its ability to alter the expression pattern of some of these genes in LCC9 cells only, reverting them to expression levels closer to those of MCF-7 cells.

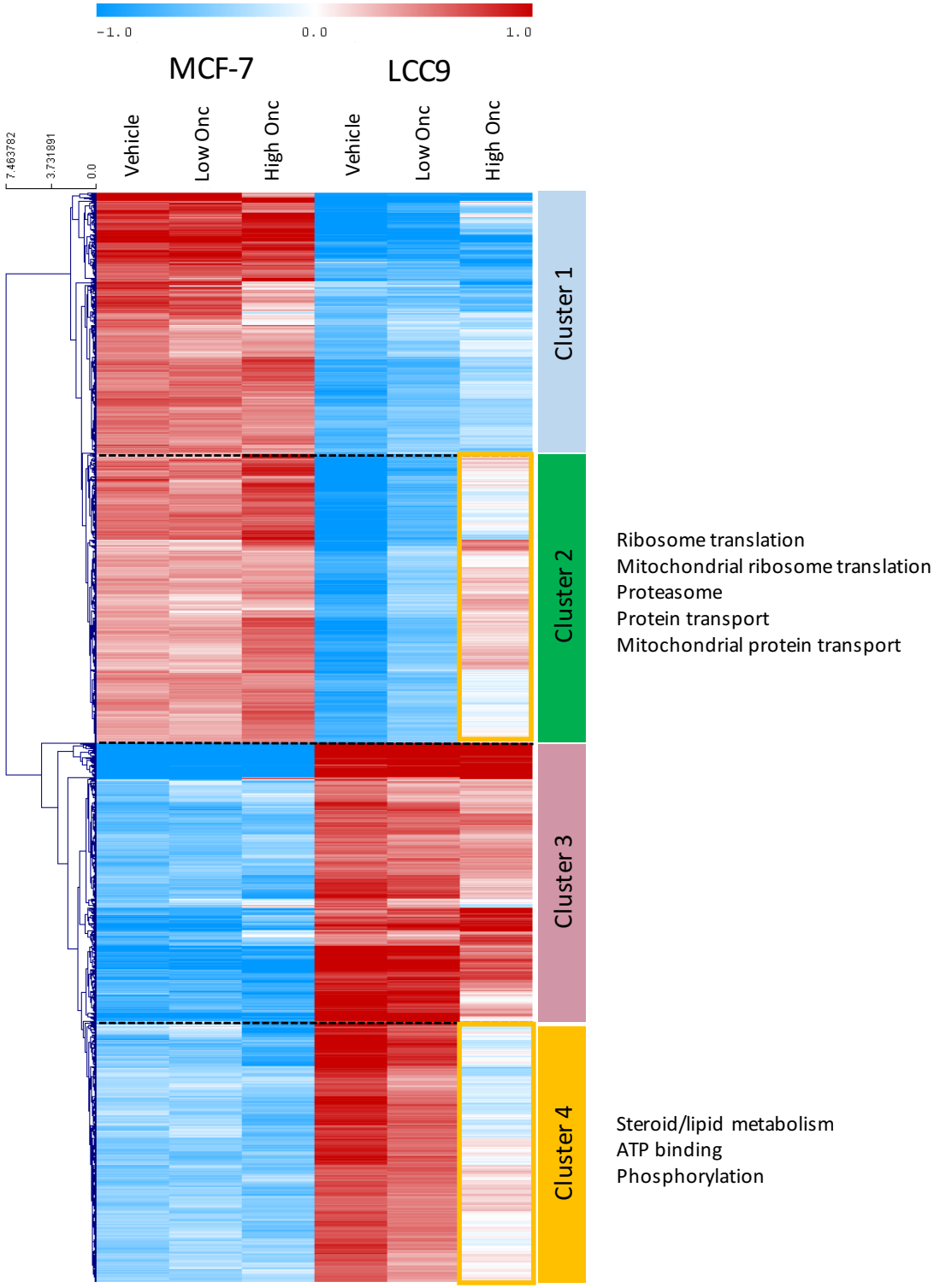

Figure 73 ***Effect of Oncamex on expression of genes differentially expressed at baseline in MCF-7 and LCC9 cells.*** *Genes whose expression levels at baseline differed by more than a 0.4 log2-scale cut-off between control MCF-7 and LCC9 cells were selected. This heatmap is the result of hierarchical clustering of these genes following Pearson correlation with complete linkage. Red and blue represent relative high and low log2 expression values, respectively. Gene enrichment analysis provided a list of GO terms significantly represented in the clusters of interest (right).*

The fact that these clusters were not altered by treatment with 10μM Oncamex in MCF-7 cells suggests that the genes included may not be related to the observed cytotoxic effect of this compound. Indeed, despite the suggested common mechanism of action of Oncamex across different cancer models (see Chapter 5), these preliminary results suggest it may also exert additional changes in this niche population of cells.

Gene enrichment analysis suggested that the genes up-regulated by Oncamex in LCC9 cells only (cluster 2) where linked to protein translation, transport and degradation, while genes specifically down-regulated by Oncamex (cluster 4) might be related to energy production, phosphorylation and lipid and steroid metabolism (see *Figure 73*). The latter is particularly interesting, given the fact that oestrogen is a steroid hormone and these are ER^+, anti-oestrogen-resistant cells.

Nevertheless, further analysis and experimenting would be necessary to elucidate whether these changes could be linked to the observed enhanced effect of tamoxifen in anti-oestrogen-resistant LCC9 cells when combined with Oncamex. Importantly, these changes at gene expression level have been observed following treatment with 10μM Oncamex, while the combinatorial effect with tamoxifen was observed following cotreatment with 1μM Oncamex. As previously discussed (see section *5.1.*), limitations in the microarray experiment prevented the inclusion of a greater range of treatment conditions, including 1μM Oncamex for 2 h. Hence, further work could also look at the effect on gene expression of this treatment for a better understanding of these changes and to assess their possible implication in a sensitising effect.

In any instance, the observed effect of 10μM Oncamex in LCC9 cells was interesting, given the apparent reversion of the expression pattern in these cells to be more similar to those of MCF-7. Multidimensional scaling assessed how these changes affected the overall similarity between both models by plotting control and treated samples for MCF-7, LCC1, LCC2 and LCC9 cells according to the similarities in their gene expression profiles.

Results showed the clustering of untreated LCC cells the furthest away from MCF-7 samples, consistent with their differences in phenotype and biology (see *Figure 74*). Treatment with low Oncamex did not induce a strong effect, with these samples being closely positioned, or even overlapping, with control samples. This recapitulates previous results suggesting the lack of strong effect of treatment with 0.3μM Oncamex for 2 h (see section *5.2.*).

Interestingly, treatment with 10µM Oncamex for 6 h, which was observed to induce changes in 2 clusters of genes differentially expressed between MCF-7 and LCC9, also led to a shift in the position of LCC samples in multidimensional scaling, particularly for treated LCC9 cells (see *Figure 74*). This suggests that Oncamex may increase the similarity between resistant cells and their parent cell line MCF-7. However, further work would be need to study the significance of these changes and to assess whether this may indicate a possible sensitising effect.

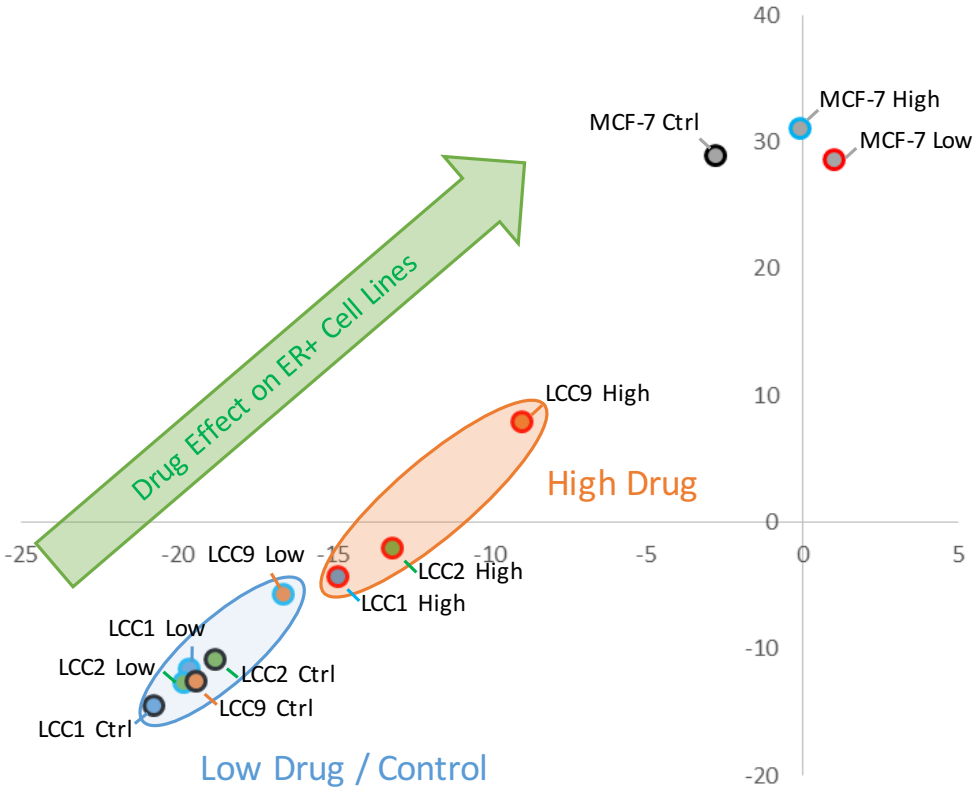

***Figure 74* Multidimensional scaling of MCF-7 and LCC9 cells.** *Control and Oncamex-treated samples from the microarray experiment described are represented here. MDS converted the gene expression information for these samples into a bi-dimensional scale, allowing for their plotting and clustering according to their similarity.*

6.4. Conclusion

This chapter has investigated the effect of Oncamex in combination with other agents in breast and ovarian cancer models *in vitro*. Firstly, results have demonstrated a modest but significant combinatorial effect of this novel flavonoid with paclitaxel and TRAIL. The administration of sub-micromolar concentrations of Oncamex was shown to lead to a beneficial effect in combination with levels of paclitaxel and TRAIL that were ineffective as single treatments.

This combinatorial effect was observed first in PEA1 ovarian cancer cells and, importantly, in related PEA2 cells, selected for their phenotype of resistance to chemotherapy. Similar enhanced responses to treatment were observed in MDA-MB-231 breast cancer cells cotreated with Oncamex and paclitaxel or TRAIL. The beneficial effects of cotreatment with Oncamex and a second agent concomitantly for 48 h appeared to be enhanced in most models when exposed to pretreatment with in Oncamex for 2 h.

These results suggest the potential application of Oncamex in combination with other cytotoxic agents. As its previously observed efficacy as a single agent, this effect of Oncamex appeared to be recapitulated across different cancer types and models. This is particularly relevant in the case of paclitaxel, which is commonly used in the clinic for the management of several cancer types, including breast and ovarian cancers. If the apparent ability of Oncamex to enhance the normal efficacy of cytotoxic agents were to be recapitulated *in vivo*, its application could allow for treatment with lower concentrations of paclitaxel. In turn, this could help reduce side effects associated with chemotherapy, which are a common issue and can play a role in the process of deciding the most suitable therapeutic strategies (see section *1.1.2.7.*). The recapitulation of this combinatorial effect in chemotherapy-resistant PEA2 cells is particularly relevant, as it suggests that cotreatment may not only improve the efficacy of treatment in responsive tumours, but also improve the sensitivity of resistant cancers.

This chapter also described the study of the effect of Oncamex in combination with anti-oestrogen therapy. Results reported here show an improved effect of tamoxifen on anti-oestrogen-resistant LCC9 cells when administered in combination with 1µM Oncamex. This enhanced effect may be linked to the at least partial reliance of both tamoxifen and Oncamex on a common mechanism of action, as both agents have been shown to enable mitochondrial apoptosis through the induction of ROS production. As with other therapies, this potential application could be relevant given the common issue of the development of acquired

resistance to endocrine therapy, which represents an important obstacle in the management of ER^+ tumours in 30-50% of early stage cases[203–205] and the majority of advanced cases[202,206] (see section *1.1.2.7.*).

Previous evidence of the effect that ROS production can have in improving response to chemotherapy or anti-oestrogens suggests that the observed combinatorial effects could be the result of subtoxic concentrations of Oncamex inducing changes in the mitochondria that, while not able to induce a significant inhibitory effect as a single treatment, may increase the susceptibility of these organelles to the activity of these other agents.

Preliminary gene expression analysis of data from PEA1 and PEA2 cells suggested that the combinatorial effect observed may not be dependent on changes in gene expression. On the other hand, the analysis of data from tamoxifen-sensitive and resistant models suggested that Oncamex may induce an additional effect on gene expression in LCC9 cells, beyond those changes observed across all cell lines and linked to the proposed common mechanism of action of action of this compound. Treatment altered the expression of some genes in LCC9 cells, making their expression pattern more similar to that of MCF-7 cells. These changes included a modest up-regulation in genes linked to protein synthesis, transport and degradation, as well as a modest down-regulation of genes related to energy production and steroid metabolism. While further work is needed to understand these changes, MDS analysis suggested that exposure to 10μM Oncamex leads to greater similarity of LCC1, LCC2 and LCC9 cells to their parent cell line MCF-7.

To conclude, while further work is needed to validate the enhanced effect of Oncamex when combined with chemotherapy or anti-oestrogens and to investigate the underlying mechanisms, the results reported here suggest the potential of this novel flavonoid for its application as a combination agent.

7. Study of the effect of Oncamex in an initial *in vivo* model

7.1. Introduction

The first part of this project studied the efficacy of Oncamex as an agent capable of inducing antiproliferative and pro-apoptotic effects in breast and ovarian cancer cell line models. Since *in vitro* work implies the maintenance of very restricted conditions, the subsequent study of the activity of a compound in *in vivo* models is an essential step for the further advancement of any promising agent. This chapter describes the study of the efficacy of Oncamex in preliminary *in vivo* experiments carried out in immunocompromised mice implanted with MDA-MB-231 breast cancer xenografts.

A first experiment sought to assess whether the antiproliferative effect of Oncamex observed *in vitro* was recapitulated in this *in vivo* setting. A second xenograft experiment sought to not only validate results from the first experiment, but also carry out a first *in vivo* test of the effect of Oncamex in combination with the chemotherapy drug paclitaxel, following results that described the improved effect of certain combinations of Oncamex with other agents (see Chapter 6).

Finally, this chapter also describes results from preliminary IHC experiments seeking to assess whether the previously described model for the mechanism of action of Oncamex (see Chapter 5) was recapitulated. For this, xenograft tissue from the first xenograft experiment was used to assess changes in the expression levels of selected proteins identified as potential players in this proposed mechanism of action, to obtain preliminary data that may both support this model and confirm its recapitulation *in vivo*.

7.2. Study of the effect of Oncamex in a first xenograft experiment

A first *in vivo* experiment assessed the effect of treatment with 25 mg/kg/day Oncamex in immunodeficient mice implanted with the MDA-MB-231 breast cancer xenograft. Results demonstrated a strong cytostatic effect of Oncamex, with the size of treated xenografts being significantly lower than that of time-matched, vehicle-treated controls (see *Figure 75*).

This difference in tumour size between both treatment conditions was observed as soon as day 2 after the start of treatment and was also maintained over the length of the experiment, including 3 days after treatment ended. Indeed, control xenografts showed a constant growth trend over time, with the final average volume having more than doubled over the duration of the experiment. In contrast, treatment with Oncamex inhibited tumour growth during treatment and the average tumour volume at the end of the experiment was still significantly lower than that of animals treated with a vehicle control ($P<0.001$).

Results showed no significant difference in mean body weight of mice between both experimental groups (see *Figure 75*). Additionally, treatment with Oncamex did not induce any meaningful changes in mean body weight of the animals, with less than 2% variation from the initial weight through the duration of the experiment. According to the current animal welfare standards[544], this could be considered as indicative of the absence of adverse effects induced by treatment.

The effect of Oncamex was further assessed using immunohistochemistry (IHC). A significant reduction ($P<0.001$) in the expression of the cellular marker of proliferation Ki-67, consistent with an antiproliferative effect, was observed (see *Figure 76*). Indeed, treatment with Oncamex produced a 24% reduction in mean expression of Ki-67 (from 60% in controls to 36% in treated cells).

The measurement of viable cellular zones in the xenograft tissue (delineated using Image J) also demonstrated a statistically significant effect, with viability being reduced by 19% in xenografts treated with Oncamex (from 56% to 37%). These changes were measured in tissue collected 3 days after the end of treatment. Thus, these results support the maintained effect of the treatment, although the reduction in levels of the proliferation marker may be higher during prolonged exposure to Oncamex. The loss of viability observed may be due to a recapitulation of the pro-apoptotic effect observed *in vitro* and/or the associated induction of necrosis, although further study of the changes taking place at a molecular level would be required to assess this.

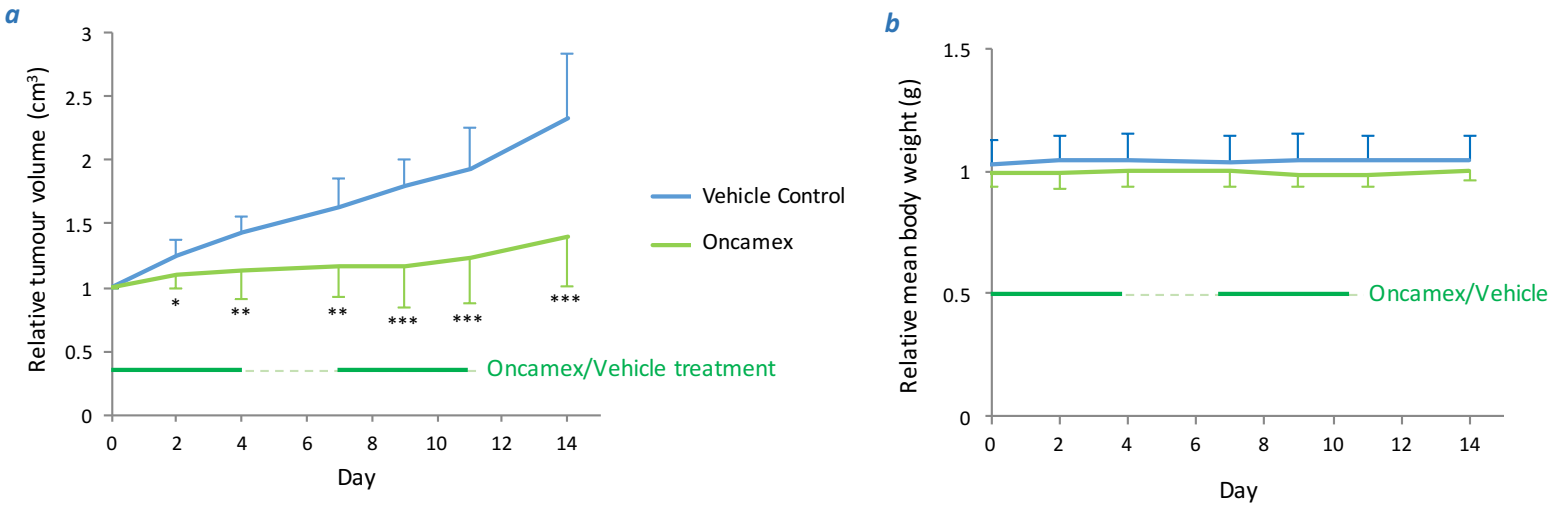

Figure 75 ***Investigation of the effect of Oncamex in a first* in vivo *xenograft experiment.*** *Two experimental groups included 6 CD-1 immunodeficient mice each, which were implanted in both flanks with a total of 10 MDA-MB-231 xenografts per group. Once xenografts reached a volume of 0.25cm^3 (day 0) mice were treated intraperitoneally with Oncamex (25 mg/kg/day) or with solvent control (10% DMSO in saline) on days 0-4 and 7-11. Changes in tumour size were recorded periodically and normalised to the volume at day 0 (*a*). All values depicted are the average of all 10 xenografts in each group, with error bars representing standard deviation (SD). Changes in mean body weight were similarly recorded over time (*b*). All values depicted are the average of all 6 mice in each group, with error bars representing standard deviation (SD). P-values from unpaired t-test: *P<0.05; **P<0.01; ***P<0.001. Where not shown P>0.05 (nonsignificant).*

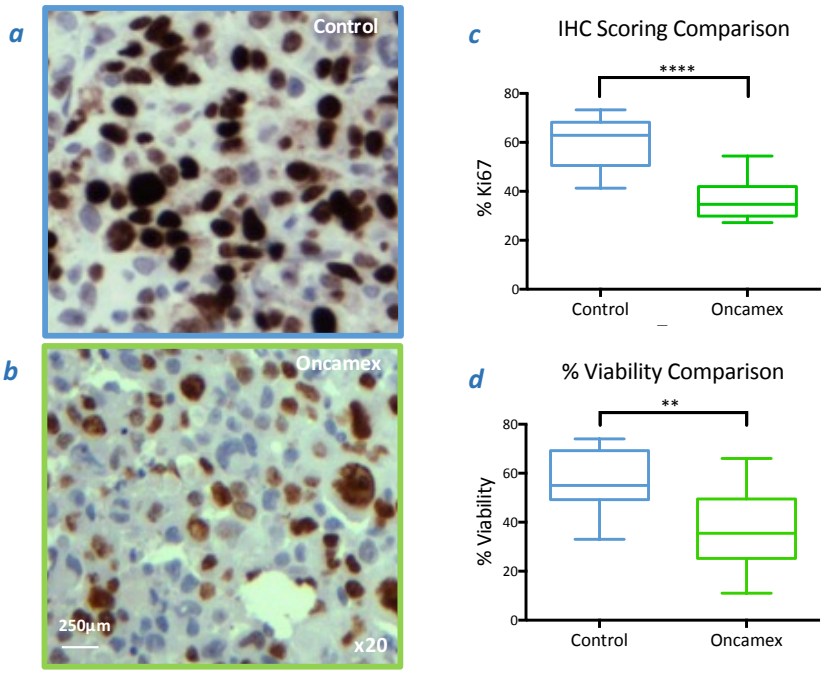

e

	Vehicle Control	Oncamex	P value
IHC Score Mean (%)	60.20 ± 0.11	36.34 ± 0.08	<0.0001
Viability Mean (%)	56 ± 12	37 ± 17	0.008

***Figure 76* Measurement of Oncamex-induced changes by immunohistochemistry.** *Xenograft tissue from an* in vivo *experiment was sectioned and stained for the cellular marker of proliferation Ki-67 (*a-b*). Proliferation was measured by scoring the positive nuclear staining in control and Oncamex-treated xenografts (*c, e*) and viability was assessed by measurement of viable areas using an image-processing package (d, e). These box plots represent the average measurements and distribution from representative sections of every xenograft in each experimental group. P-values from unpaired t-test: **P<0.01; ****P<0.0001.*

7.3. Further study in a second xenograft experiment

7.3.1. Validation of previous results on the effect of Oncamex *in vivo*

A second xenograft experiment was carried out in order to validate the previous results and test other treatment alternatives. These included the testing of a higher concentration of Oncamex and the assessment of the effect of Oncamex in combination with the chemotherapeutic agent paclitaxel, following previous results obtained *in vitro* which supported a potential synergistic effect (see section *6.2.*).

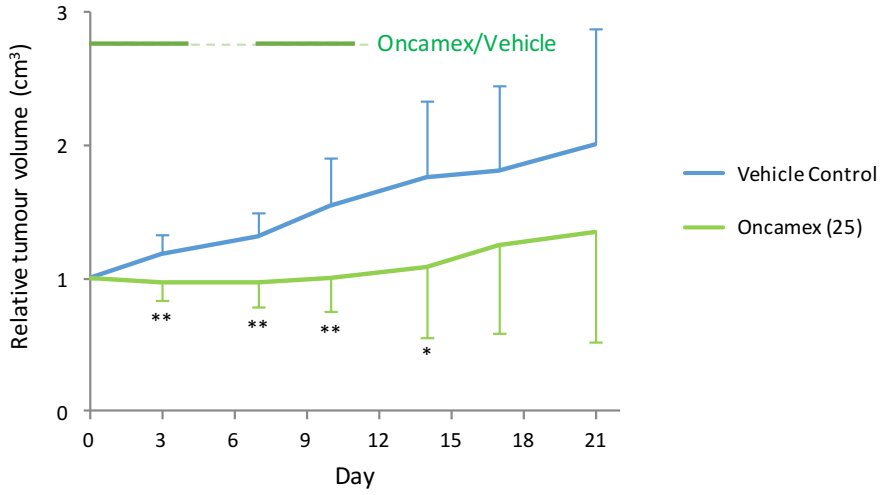

***Figure 77* Investigation of the effect of Oncamex in a second in vivo xenograft experiment.** *CD-1 immunodeficient mice (8 for control group and 5 for treated group) were implanted in both flanks with MDA-MB-231 xenografts (with a total of 10 xenografts for control or high dose groups and 7 for treated group). Mice were treated intraperitoneally with Oncamex (25 mg/kg/day) or with solvent control (10% DMSO in saline) on days 0-4 and 7-11. Changes in tumour size were recorded periodically and normalised to the volume at day 0 (left). All values depicted are the average of all xenografts in each group, with error bars representing standard deviation (SD). P-values from unpaired t-test: *P<0.05; **P<0.01. Where not shown P>0.05 (nonsignificant).*

Firstly, the effect of 25 mg/kg/day Oncamex was re-assessed in this second experiment. Previous results were recapitulated, with Oncamex inducing a statistically significant cytostatic effect in treated xenografts (see *Figure 77*). As found in the first experiment, this effect was maintained over the length of treatment and at least until day 14. In this instance, xenograft growth was monitored longer after treatment prior to tissue collection. Measurements of tumour volumes after day 14 still showed a difference between control and treated tumours. Indeed, average tumour volume showed the growth of untreated

xenografts to more than double their initial size, whereas the final growth of treated tumours over the length of the experiment was of less than 35%. In summary, these results corroborated the previous *in vivo* antiproliferative effect of Oncamex.

7.3.2. Effect of a higher Oncamex concentration

This experiment also included mice treated with a higher concentration of Oncamex (50 mg/kg/day). The effect of this treatment was compared to that of the lower dose (25 mg/kg/day). Results demonstrated that the higher concentration also induced a statistically significant cytostatic effect (with at least $P<0.05$ at all times tested) in comparison to the control xenografts for the length of treatment and until day 14 (see *Figure 78*).

However, treatment with 50 mg/kg/day did not improve on the activity of the lower dose 25 mg/kg/day. This was supported by comparison of the effect of both treatments using an unpaired t-test, which found no statistically significant difference in tumour volume at any time ($P>0.05$), as well as by ANOVA followed by Tukey-Kramer multiple comparison test when comparing these groups with the control (see *Figure 78*). Neither dose of Oncamex tested appeared to induce relevant signs of systemic toxicity. Indeed, no weight loss larger than 2% was observed and no statistically significant differences in mean body weight of mice were found between the 3 experimental groups ($P>0.05$).

In summary, the administration of a higher dose of Oncamex recapitulated but did not improve on the previously observed effect of this agent. However, a relevant caveat should be considered in the limitations in the administration procedure. The initial 25 mg/kg/day dose was selected based on the limiting solubility of Oncamex in the vehicle used (10% DMSO in saline). Doubling of the concentration of the compound led to reduced stability in solution. Consequently, twice the dose volume was used to administer treatment with 50 mg/kg/day. Although this should yield the same treatment dose, these solubility limitations suggest that factors such as solvent composition and administration method may hinder the *in vivo* distribution and activity of Oncamex. These aspects should be optimised in future experiments for the further pre-clinical development of Oncamex as a drug candidate.

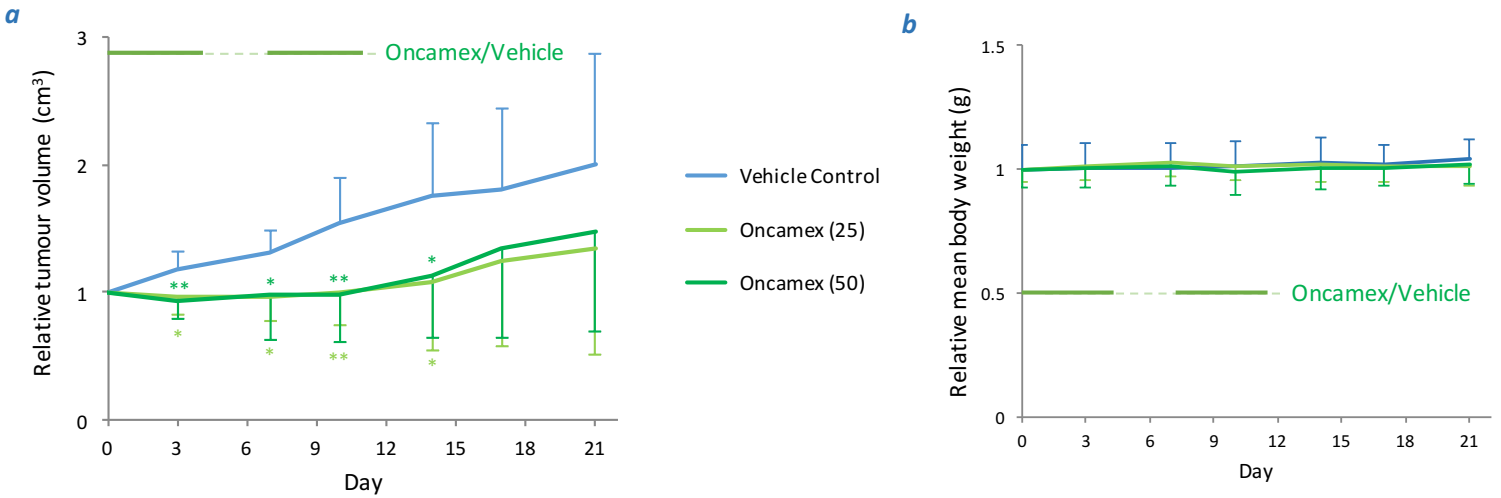

Figure 78 ***Investigation of the effect of Oncamex in a second* in vivo *xenograft experiment.*** *Further* in vivo *tests sought to confirm previous results and assess the effect of different doses of Oncamex. CD-1 immunodeficient mice (8 for control group, 5 for low dose group and 6 for high dose group) were implanted in one or both flanks with MDA-MB-231 xenografts (with a total of 10 xenografts for control or high dose groups and 7 for low dose group). Mice were treated intraperitoneally with Oncamex (25 or 50 mg/kg/day) or with solvent control (10% DMSO in saline) on days 0-4 and 7-11. Changes in tumour size were recorded periodically and normalised to the volume at day 0 (*a*). All values depicted are the average of all xenografts in each group, with error bars representing standard deviation (SD). Changes in mean body weight were similarly recorded over time (*b*). All values depicted are the average of all mice in each group, with error bars representing standard deviation (SD). P-values from ANOVA followed by Tukey-Kramer multiple comparison test, with * colour representing the P-value between that group and the vehicle control: *P<0.05. Where not shown P>0.05 (nonsignificant).*

7.3.3. Effect of Oncamex in combination with paclitaxel *in vivo*

A final analysis investigated the effect of treatment with Oncamex (25 mg/kg/day) in combination with paclitaxel (10 mg/kg/day). The experiment also included an experimental group treated with paclitaxel as a single agent for comparison. Results demonstrated the statistically significant cytostatic effect of both single treatments and their combination (see *Figure 79*). Although Tukey-Kramer multiple comparison tests found no significant difference between the 3 treated groups, the effect of combination treatment induced a slightly stronger reduction of xenograft volume during treatment and was found to have a higher statistical significance. Indeed, administration of the combination treatment did induce a reduction of the average volume of xenografts below their initial size at day 0 for the duration of treatment.

This combinatorial effect was not as significant as that observed when MDA-MB-231 cells were treated with a combination of Oncamex and paclitaxel *in vitro* (see *Figure 69*). However, those changes were the result of an optimised combination schedule in tightly controlled conditions in cell culture, which cannot be assumed in an animal model. Further experiments are needed in order to better optimise the combination alternatives *in vivo*.

As with previous tests, no significant differences were found between the mean body weights in the experimental groups (see *Figure 79*). Treatments did not appear to induce a relevant loss in body weight indicative of toxicity. Only mice treated with combination treatment exhibited a weak temporary decrease in mean body weight, but this was only 3.5% and coincided with the loss of volume of tumours. Overall, monitoring of mean body weight again suggested the absence of relevant systemic adverse effects induced by any of the compounds or the vehicle administered.

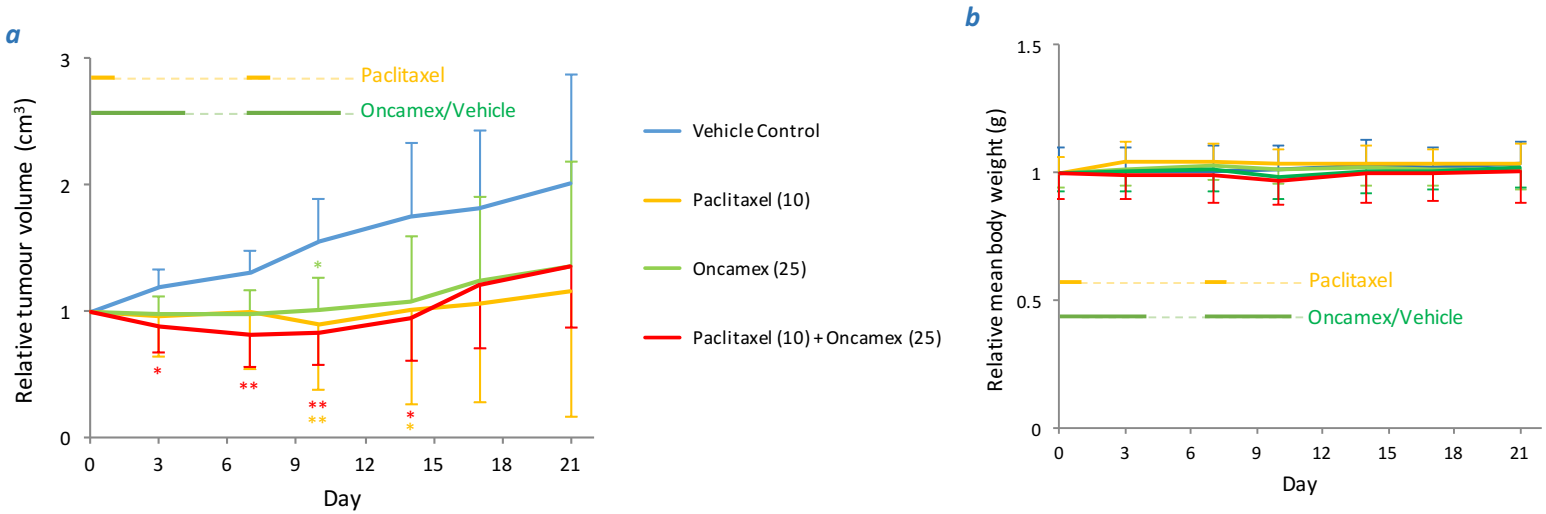

Figure 79 ***Investigation of the effect of Oncamex in combination with chemotherapy in a second* in vivo *xenograft experiment.*** *Further* in vivo *tests sought to assess the effect of treatment with Oncamex in combination with chemotherapeutic agent paclitaxel. CD-1 immunodeficient mice (8 for control group, 6 for paclitaxel group and 5 for Oncamex or combination groups) were implanted in both flanks with MDA-MB-231 xenografts (with a total of 10 xenografts for control group, 9 for paclitaxel or combination groups and 7 for Oncamex group). Mice were treated intraperitoneally with Oncamex (25 mg/kg/day) or with solvent control (10% DMSO in saline) on days 0-4 and 7-11, with paclitaxel (10 mg/kg/week) on days 0 and 7, or with both Oncamex and paclitaxel. Changes in tumour size were recorded periodically and normalised to the volume at day 0 (*a*). All values depicted are the average of all xenografts in each group, with error bars representing standard deviation (SD). Changes in mean body weight were similarly recorded over time (*b*). All values depicted are the average of all mice in each group, with error bars representing standard deviation (SD). P-values from ANOVA followed by Tukey-Kramer multiple comparison test, with * colour representing the P-value between that group and the vehicle control: *P<0.05; **P<0.01. Where not shown P>0.05 (nonsignificant).*

7.3.4. Assessment of changes in Ki-67

Changes in the expression level of the proliferation marker Ki-67 by IHC were used again as a measurement of the tumour growth-inhibiting effect of Oncamex *in vivo*. Results showed a strong statistically significant ($P<0.0001$) reduction in Ki-67 expression for all treated experimental groups (both concentrations of Oncamex, paclitaxel or combination) in comparison to the control group. (see *Figure 80*). This recapitulated the results from the first *in vivo* experiment, where 25 mg/kg/day Oncamex also induced a strong reduction of this marker (see *Figure 76*).

Importantly, in this second experiment xenograft tissue was collected later after treatment. Thus, these results suggest a lasting effect on proliferation of the treatments tested, given the significant difference in Ki-67 expression a week after the end of treatment.

Comparison of the levels of Ki-67 expression across different treatments showed no statistically significant ($P>0.05$) differences between both concentrations of Oncamex or between paclitaxel and the paclitaxel and Oncamex combination. This was consistent with the cytostatic effect of each treatment as suggested by changes in tumour volume. Finally, both treatments including paclitaxel induced stronger inhibition of Ki-67 expression, statistically significantly ($P<0.0001$) greater than the decreasing effect of Oncamex alone.

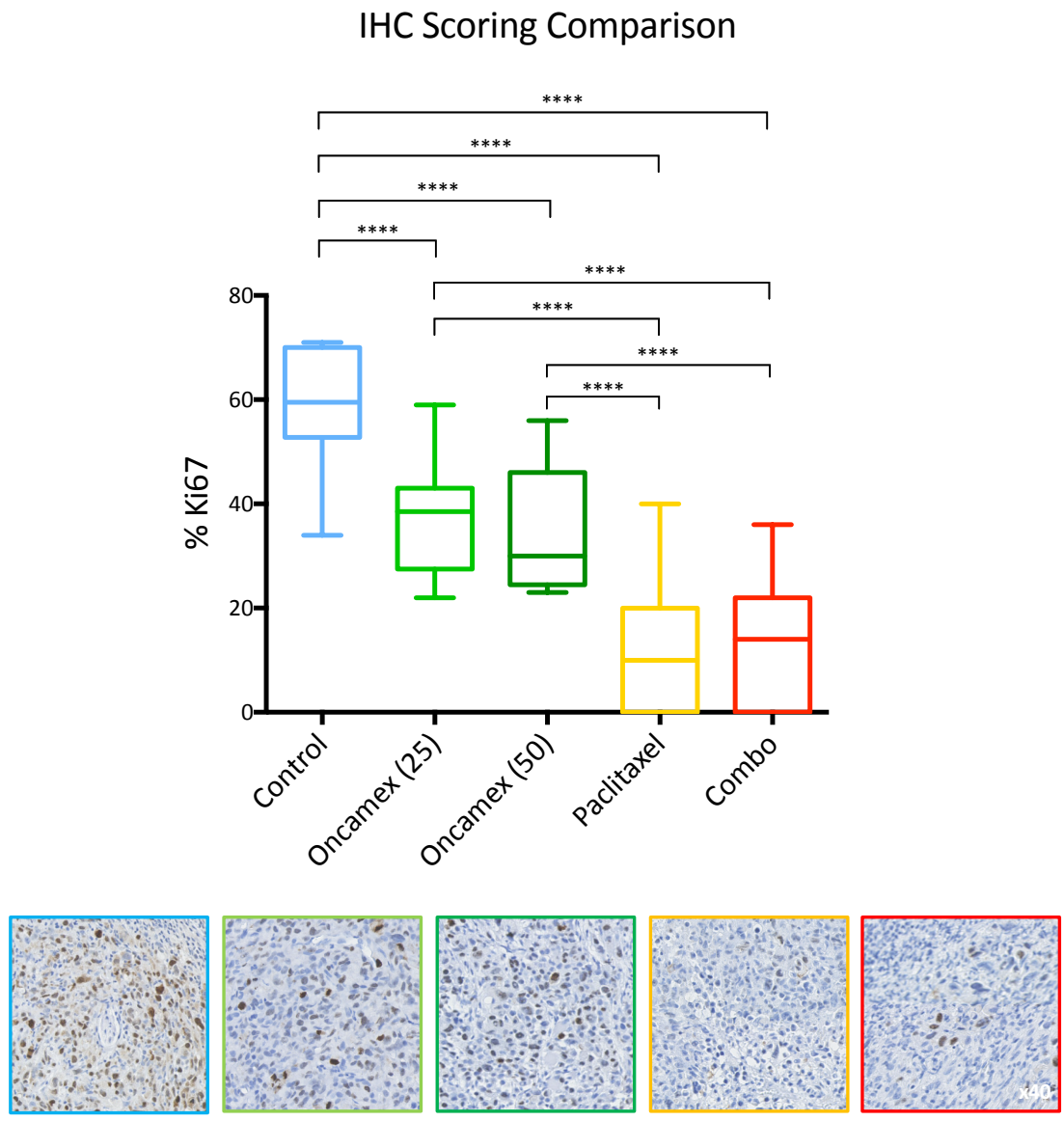

Figure 80 ***Measurement of treatment-induced changes by immunohistochemistry.*** *Xenograft tissue from a second* in vivo *experiment was sectioned and stained for the cellular marker of proliferation Ki-67. Proliferation was measured by scoring the positive nuclear staining in control and treated xenografts as previously described. These box plots represent the average measurements and distribution from representative sections of xenografts in each experimental group. P-values from ANOVA followed by Tukey-Kramer multiple comparison test: ****P<0.0001. Where not shown P>0.05 (nonsignificant).*

7.4. Initial *in vivo* validation of the mechanistic model for Oncamex

The study of the effect of Oncamex on ROS production, the activation of apoptosis-related proteins and changes at gene expression level led to the description of a model for its mechanism of action (see section *5.4.*). Following this, IHC was applied for preliminary validation, both at protein level and *in vivo*, of some of the proteins included in this model. For this, xenograft tissues from the first *in vivo* experiment described in this chapter were used to study Oncamex-induced changes (see section *2.2.19.* for description of scoring methods used and *Table 12* for summary of results).

Firstly, results from IHC showed an apparent reduction in the expression of Cyclin B1 (median score of 6 in control *vs* 2 in treated) and, to a lesser extent, Cyclin D1 (8 in control vs 5 in treated) (see *Figure 81*). The lower levels of these markers of proliferation, involved in the advance of cell division, is consistent with the effect observed in assays quantifying changes in total cell protein biomass and gene expression analysis *in vitro* (see Chapters 4 and 5). These observations are also consistent with the observed cytostatic effect of Oncamex *in vivo*, supported by measurement of changes in Ki-67 in both xenograft experiments (see *Figures 76* and *80*).

IHC was also used to assess the possible changes in the JNK-c-Jun signalling pathway. For this, previously validated antibodies were applied which detected either (i) endogenous levels of total c-Jun protein regardless of phosphorylation state (pan-c-Jun), or (ii) active forms of this protein presenting phosphorylation in specific residues (phospho-c-Jun Ser63 or Ser73).

Despite the increase in gene expression following treatment with Oncamex suggested by the analysis of microarray results, detection of the overall levels of c-Jun, irrespective of phosphorylation, showed similar expression levels in control and treated xenografts (81% and 85% of nuclei positively stained nuclei, respectively). Interestingly, results showed an apparent change in the levels of one of the phosphorylated active c-Jun only (see *Figure 82*): phospho-Ser63 c-Jun was not detected in either control or Oncamex-treated xenografts (0% of nuclei positively stained for either), while results showed a considerable increase in expression of phospho-Ser73 c-Jun, tripled in Oncamex-treated xenografts (60% of positively stained nuclei *vs* 20% in control).

This suggests that the observed initial up-regulation of gene expression may lead to an increase in the ratio of active/inactive c-Jun later after treatment. Although further work

would be needed for a better assessment of changes in expression and post-translational modifications, these preliminary validation results are consistent with the activation of c-Jun by treatment with Oncamex, which may lead to the formation of AP-1 (activator protein 1), involved in the regulation of apoptosis and proliferation.

a	Median scores (range: 0-8)	
	Control	Oncamex
Cyclin B1	6 (6-7)	2 (0-3)
Cyclin D1	8 (7-8)	5 (5-6)
pan-JNK	0 (0-2)	7 (7-8)
HK2	6 (4-6)	8 (7-8)
LDHA	6 (5-6)	8 (7-8)
HIF1A	5 (4-7)	5 (3-7)

b	Average scores (% positive nuclei)	
	Control	Oncamex
pan-c-Jun	81%	85%
p-c-Jun Ser63	0%	0%
p-c-Jun Ser73	20%	60%

Table 12 ***Scoring of immunohistochemistry for preliminary* in vivo *validation.*** *IHC tests were performed on sections from 3 xenografts in each experimental group (control or treated) in the first* in vivo *experiment. (a) For proteins with cytoplasmic staining, a proportion score (0-5) was added to an intensity score (0-3) to obtain a final semi-quantitative estimation (0-8) of the expression of the protein of interest. This table represents the median of a range of scores estimated for the cohort of 3 xenografts assessed in the control and treated experimental groups. (b) For proteins with a clear nuclear staining, the proportion of positively-stained nuclei was counted. Average percentages for the cohort of 3 xenografts assessed in the control and treated experimental groups are shown.*

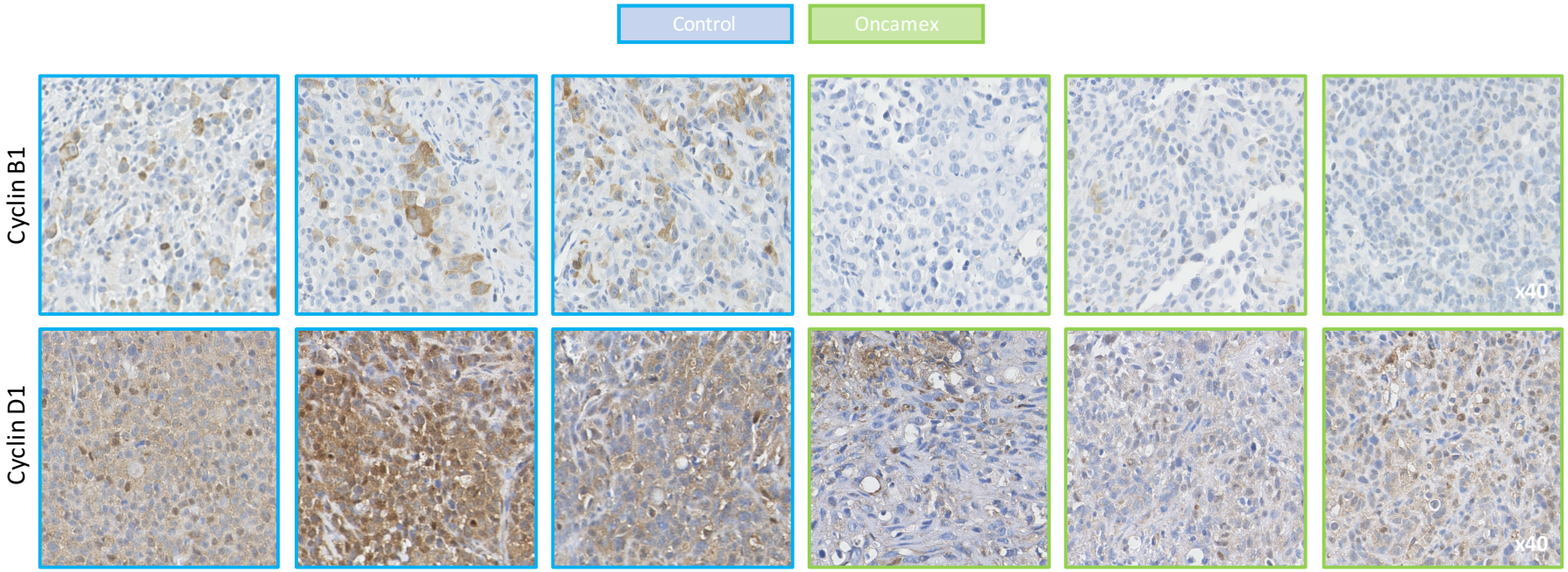

Figure 81 ***Preliminary assessment of changes in the expression of proliferation-related proteins in tissues from a first xenograft experiment.*** *Tissue from 3 xenografts in each experimental group (treated with a vehicle control or 25mg/kg/day Oncamex) in a first* in vivo *experiment was sectioned and stained for IHC detection of cyclins B1 and D1. Images shown here are representative captures from each of the xenografts studied (3 per group).*

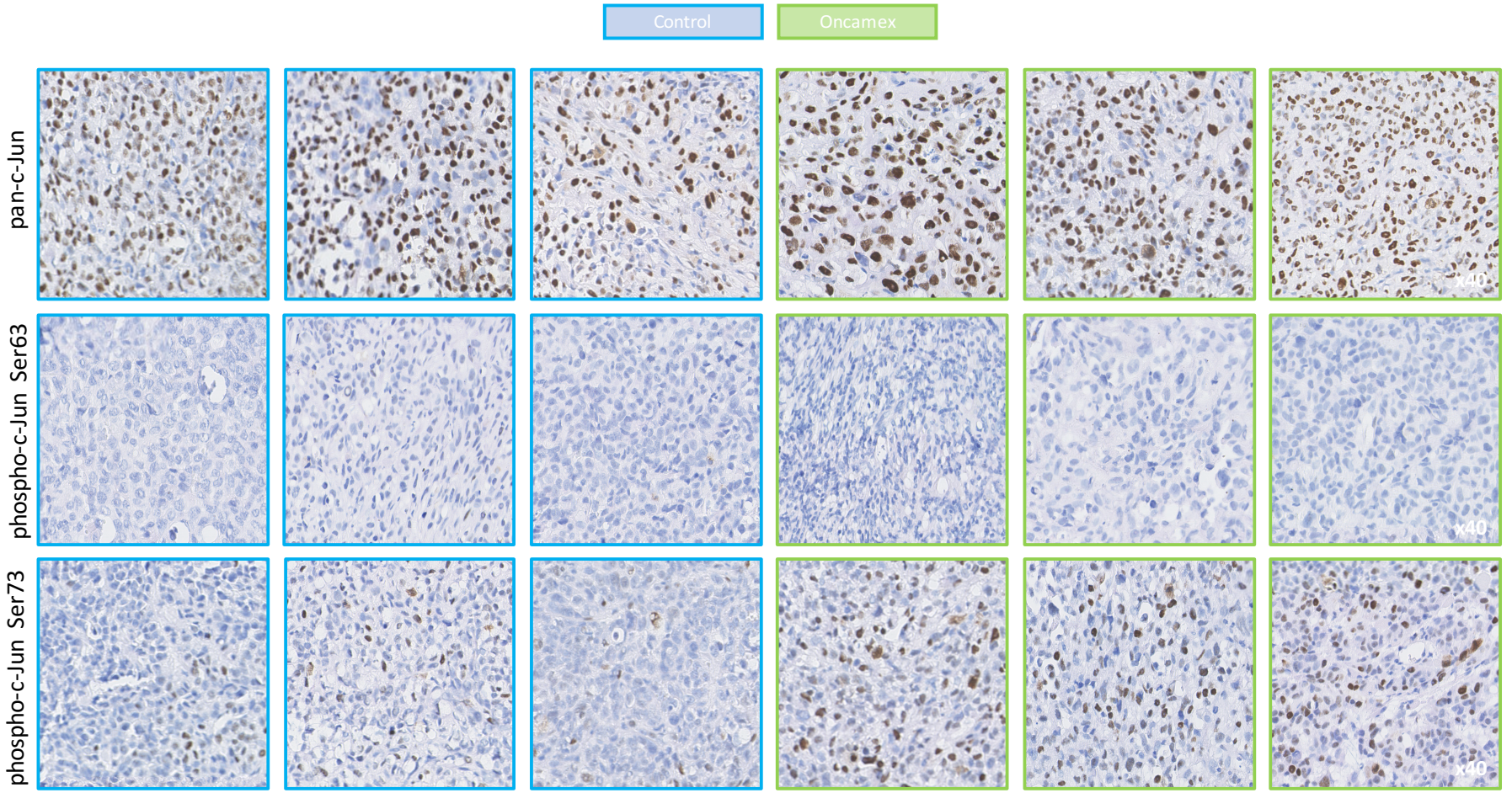

Figure 82 ***Preliminary assessment of changes in c-Jun expression in tissues from a first xenograft experiment.*** *Tissue from xenografts representative of the 2 treatment conditions in a first* in vivo *experiment (vehicle control or 25mg/kg/day Oncamex) was sectioned and stained for IHC detection of overall endogenous c-Jun or specific active forms phosphorylated in Ser63 or Ser73. Images shown here are representative captures from each of the xenografts studied (3 per group).*

Further IHC tests studied changes in the expression levels of overall JNK using a pan-JNK antibody capable of detecting both JNK1 and JNK2 irrespective of their phosphorylation state (see *Figure 83*). Results showed an increase in expression in Oncamex-treated tissue (median score of 7 in treated *vs* 0 in control), recapitulating the changes observed in gene expression analysis (see *Figures 50* and *51*). Additionally, this activation of JNK signalling is also consistent with the observed increase in phospho-c-Jun, since JNK acts as activator of c-Jun by phosphorylation.

Finally, preliminary IHC tests also assessed changes in the expression levels of key glycolytic genes HK2 and LDHA (see *Figure 84*). Results found that, while these glycolytic enzymes were expressed in untreated xenografts, Oncamex-treated tissue showed increased expression of both HK2 and LDHA (median score of 8 in treated *vs* 6 in control for both enzymes).

As previously discussed (see section *5.4.3.*), cancer cells would normally be expected to present high glycolytic rates. However, results from gene expression analysis showed that Oncamex may increase the expression level of enzymes related to this metabolic pathway in what has been hypothesised could be a mechanism of response to the pro-apoptotic effect of Oncamex. The results from preliminary IHC validation reported here are consistent with these previous findings.

Staining for HIF1α (see *Figure 84*) found similar expression levels in both experimental groups (median score of 5 for both treated and control). This recapitulated the absence of changes at gene expression level and previous results from gene expression analysis that suggested the observed up-regulation of glycolysis and mitophagy following treatment with Oncamex was HIF-1 signalling-independent and may instead occur in response to the loss of mitochondrial function and the induction of cell death.

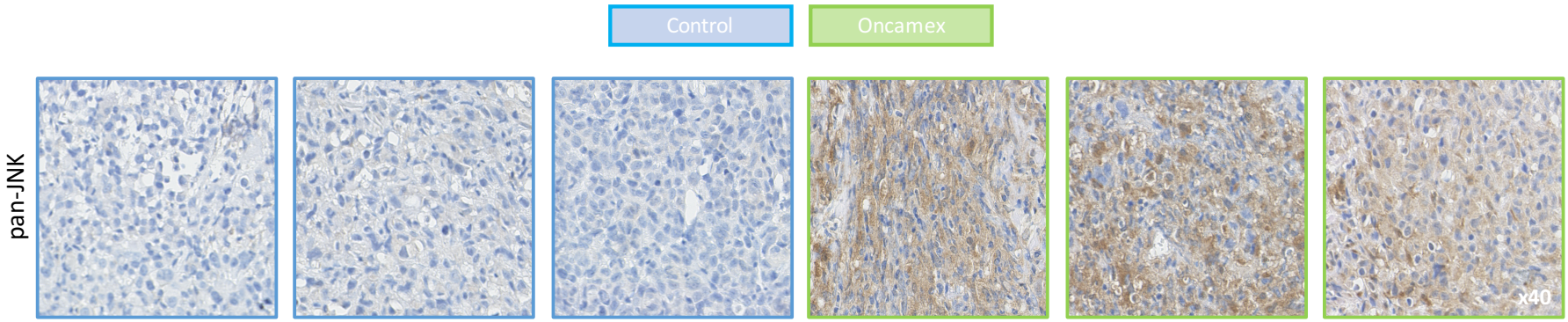

Figure 83 ***Preliminary assessment of changes in JNK expression in tissues from a first xenograft experiment.*** *Tissue from xenografts representative of the 2 treatment conditions in a first* in vivo *experiment (vehicle control or 25mg/kg/day Oncamex) was sectioned and stained for IHC detection endogenous forms of JNK1 or JNK2, irrespective of phosphorylation state Images shown here are representative captures from each of the xenografts studied (3 per group).*

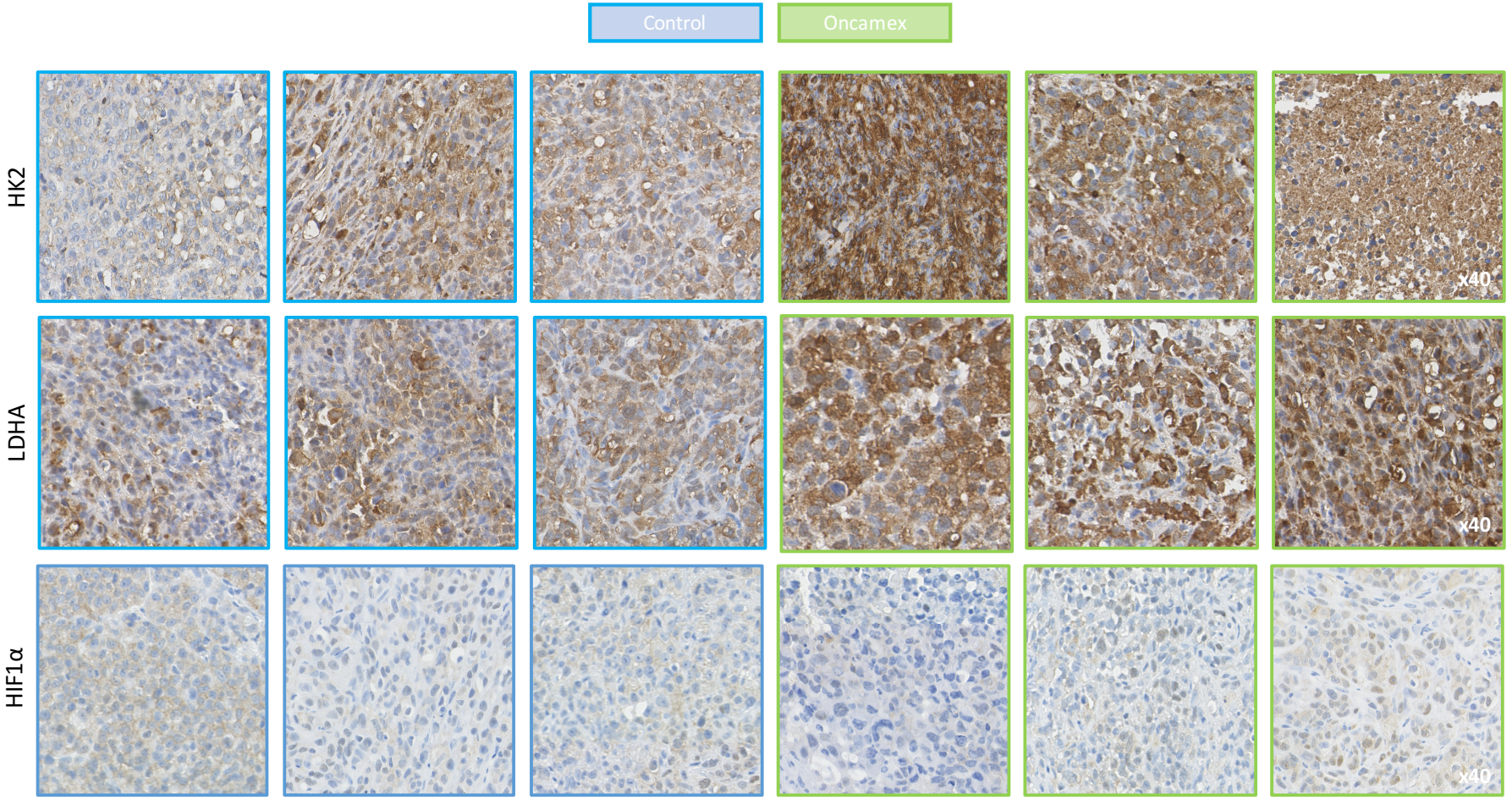

Figure 84 ***Preliminary assessment of changes in the expression of glycolysis and hypoxia-related proteins in tissues from a first xenograft experiment.*** *Tissue from xenografts representative of the 2 treatment conditions in a first* in vivo *experiment (vehicle control or 25mg/kg/day Oncamex) was sectioned and stained for IHC detection of HIF1α, HK2 and LDHA. Images shown here are representative captures from each of the xenografts studied (3 per group).*

7.5. Conclusion

Results reported in this chapter suggested the effect of Oncamex previously observed in cell culture models is at least partially translated into *in vivo* models. Treatment with 25 mg/kg/day of Oncamex was cytostatic and did not appear to reduce the size of MDA-MB-231 xenografts implanted in mice below their initial size throughout the duration of the experiment and at least 3 days after treatment ended. This inhibition coincided with a significant reduction in the expression of the cellular marker of proliferation Ki-67, also consistent with a cytostatic effect, as well as with a significant reduction in the viability of tumour tissue. Additionally, monitoring of the weight of animals demonstrated no significant changes (<2%) in the mean body weight of treated mice over time, suggesting no obvious adverse effects were induced by Oncamex or the solvent used.

Importantly, these results were validated in a second *in vivo* experiment. Further testing showed that the administration of higher concentrations (50 mg/kg/day) recapitulated but did not seem to improve on this cytostatic effect. Combination of 25mg/kg/day Oncamex with 10mg/kg/day paclitaxel led to a slight decrease in xenograft volumes, but this was not statistically significant in comparison to the effect of either agent alone. For all experimental groups, treatment did not induce any significant changes in mean body weight of the animals throughout the duration of the experiments, consistent with the previous absence of obvious adverse effects.

In summary, these results reported a partial recapitulation of the *in vitro* activity of Oncamex. Importantly, the *in vivo* effects observed did not present accompanying adverse effects or obvious indications of toxicity, as no changes in body mass were observed. However, these are only preliminary results from initial *in vivo* studies and further *in vivo* work is necessary for a better assessment of the potential efficacy of Oncamex *in vivo*, as well as to better monitor possible toxicity and optimise of aspects such as dosage or administration routes (see section *8.2.4.*).

Finally, IHC tests were carried out on xenograft tissues from the first *in vivo* experiment These were designed to provide a preliminary validation for the mechanistic model previously proposed in Chapter 5 at protein level, as well as to assess the possible recapitulation of this proposed mechanism, based on results from *in vitro* work, in a first *in vivo* setting. Results showed an apparent decrease in proliferation-related cyclins and an increase in activated phospho-c-Jun, together with higher expression of its up-stream

activator JNK. Results also showed an increase in the expression of glycolytic enzymes beyond the already high levels in untreated cells.

In summary, IHC results showed Oncamex induced changes consistent with the mechanistic model described so far. Although further work is required for a more detailed description and better corroboration, these tests provided a preliminary small-scale approach to its validation both at protein level and *in vivo*. This work is not a substitute for the validation of this model both at gene expression and protein levels in *in vitro* models, which should also be included in future work (see section *8.2.1.*).

8. Conclusion

8.1. Summary of findings

This project was based on the hypothesis that novel, myricetin-derived flavonoids with mitochondrial targeting, enhanced redox reactivity and improved physicochemical properties and drug-like attributes may hold potential for the treatment of breast and ovarian cancers, given the central role of mitochondria in cell homeostasis and regulation of cell death and the greater susceptibility to stress of these organelles in cancer cells. Accordingly, the work reported here aimed to study a library of 8 novel flavonoids, to assess their efficacy, possible modes of action and potential application as anticancer agents.

Firstly, a series of experiments assessed the antiproliferative properties of these compounds in 3 panels of breast and ovarian cancer cell lines (see sections *3.2.* and *3.3.*). Results showed that several of the compounds significantly improved on the efficacy of the novel flavonol myricetin. In particular, the second-generation methoxylated analogue AO-1530-OMe (Oncamex) was identified as the most potent compound in this library, leading to a reduction in cellular protein biomass on all models studied at concentrations in the low micromolar or submicromolar range. This effect was observed in breast (ER^+ or triple negative) and ovarian cancer cell lines, including models of resistance to anti-oestrogens and chemotherapy.

Comparison of the differential efficacy of the compounds studied in the context of the existing literature on structure-activity relationships suggested that several structural modifications may contribute to the improve potency of Oncamex (see section *3.4.*). These are likely to include the combination of the natural poly-ring flavonoid backbone with an improved substitution profile, the addition of methoxylations and the presence of the 7-decyl side chain. Following these observations, subsequent work focused on the properties and effect of the lead compound AO-1530-OMe (Oncamex).

Fluorescence microscopy experiments showed the specific targeting of Oncamex for the mitochondrial compartment and its quick and stable accumulation mainly in these organelles (see section *4.2.*). The application of specific probes in further microscopy studies demonstrated the ability of Oncamex to induce the generation of high levels of mitochondrial superoxide (mSO) at concentrations associated with its cytotoxic effects (see section *4.3.*). This was supported by the study of the electrochemical properties of the compound, which

suggested its ability to undergo reversible reduction and oxidation in the mitochondrial compartment.

Several different methods were applied to study the cellular responses exerted by treatment with Oncamex (see section *4.4.*). Microscopic observation and results from a membrane integrity-based assay suggested the induction of necrosis-like cell death. Further work reported the reduction in cell viability and induction of cytotoxicity and showed changes consistent with the induction of apoptosis following treatment for 6 to 8 h with micromolar concentrations of Oncamex, as supported by the measurement of caspase activation and the detection of PARP cleavage. This supported the role of this mode of cell death in the effect exerted by Oncamex, with the necrotic-like changes possibly being the result of secondary necrosis. Interestingly, these responses were attenuated by pre-incubation in antioxidant conditions, supporting the relevance of ROS modulation to the observed effects of Oncamex.

In order to gain greater insight into the possible mode of action of the compound, a microarray experiment assessed its effect on gene expression. Differential gene expression analysis showed treatment with 10μM Oncamex for 6 h exerted pro-apoptotic and anti-proliferative effects at gene expression level. Additionally, the JNK pathway, glycolysis and mitophagy appeared to be up-regulated by treatment. Importantly, these changes were consistent across all the breast and ovarian models studied (see section *5.3.*).

Together with previous results from the study of the compartmental distibution, ROS-modulating properties and pro-apoptotic effect of Oncamex, these results from gene expression analysis informed the description of a model for the mechanism of action of this novel flavonoid (see section *5.4.*). Results were consistent with a mechanism by which, due to its mitochondrial targeting and redox abilities, Oncamex can lead to the generation of mSO, which in turn may lead to mitochondrial dysfuntion, membrane permeabilisation and the activation of the JNK pathway and transcription factor FOXO3, which together lead to the induction of intrinsic apoptosis and the inhibition of proliferation. Additionally, results were consistent with an Oncamex-induced increase in glycolysis and mitophagy, independently of HIF-1 signalling, possibly in response to the energy demands and stresses induced by treatment. This hypothetical mechanistic model and the supporting evidence are summarised in *Figure 85*.

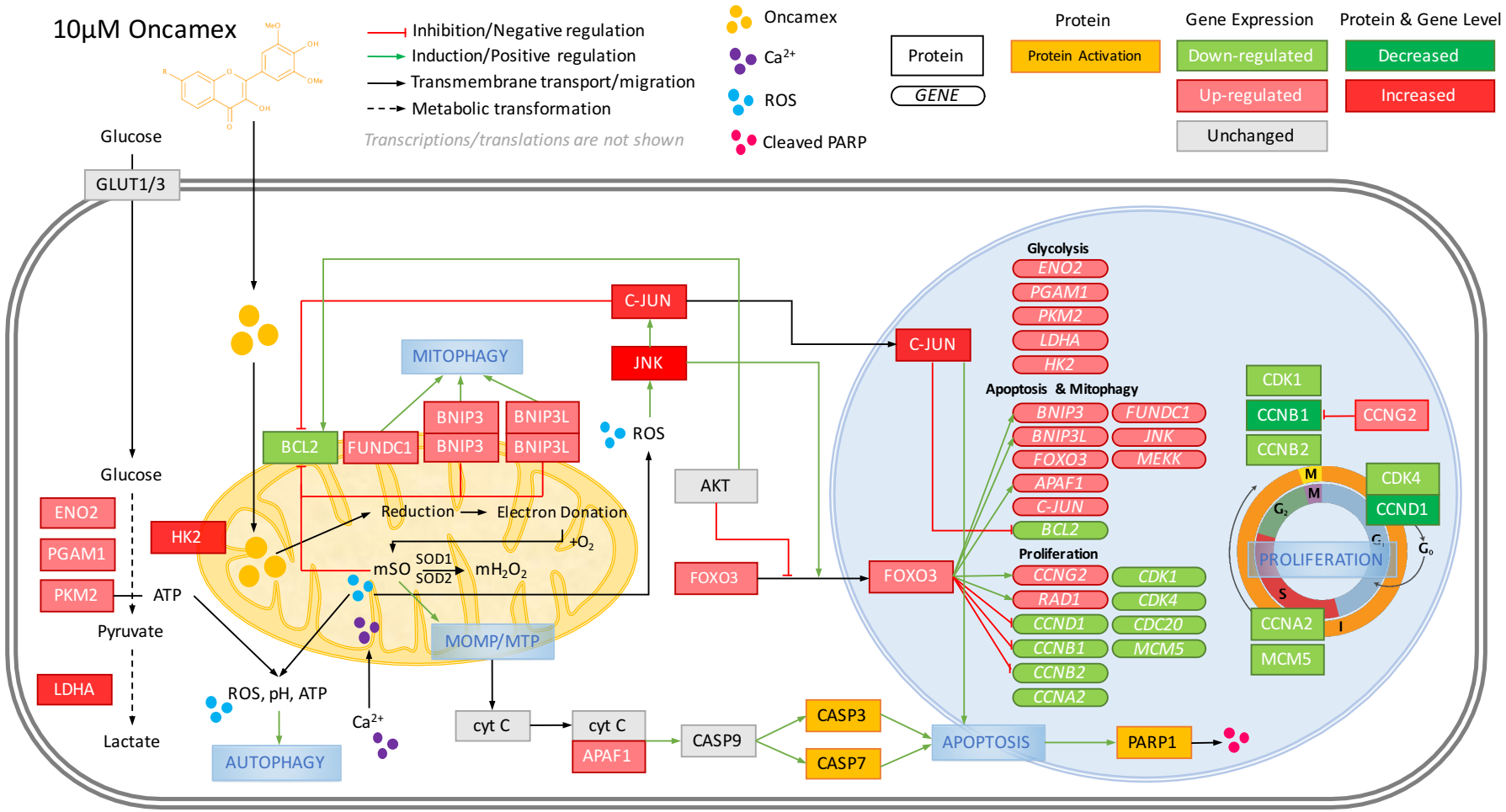

Figure 85 ***Proposed model for the mechanism of action of Oncamex.*** *Results from the study of the properties of Oncamex and its effect on ROS production, proliferation, apoptosis and gene expression allowed for the postulation of a mechanistic model. This diagram presents this model and summarises relevant results. Changes in protein activation are shown in orange, while up- or down-regulation of gene expression appear in light red and green, respectively. Gene changes that have been supported in preliminary validation experiments* in vivo *are shown in darker green or red, respectively, while interesting genes/proteins whose expression was unchanged by treatment with Oncamex but may play a role in its mechanism are shown in grey.*

Additional work assessed the possible combination of Oncamex with other anticancer agents. Results showed an enhanced effect when submicromolar concentrations of Oncamex, which were ineffective as mono-therapy, were combined with paclitaxel and TRAIL (see section *6.2.*). Importantly, this statistically significant effect was observed in both breast and ovarian cell lines, including chemo-resistant ovarian cell line PEA2.

Combination with Oncamex also improved the effect of tamoxifen in anti-oestrogen resistant ER^+ cells (section *6.3.*). Interestingly, differential gene expression analysis showed that Oncamex could induce changes in gene clusters which are inherently different between tamoxifen-sensitive and resistant models. Results showed that treatment with the novel flavonoid may increase the similarity between these models, suggesting a possible resensitising effect, although further work would be needed to better assess this.

Finally, preliminary animal experiments were carried out to explore the *in vivo* activity of Oncamex. A first experiment in immunodeficient mice implanted with MDA-MB-231 xenografts showed the ability of treatment with 25 mg/kg/day Oncamex to inhibit tumour growth (see section *7.1.*). Results also showed a significant reduction in the expression of the marker of proliferation Ki-67, consistent with a cytostatic effect. Importantly, monitoring of changes in mean body weight of mice showed no obvious adverse effects were induced by Oncamex or the solvent.

While a second xenograft experiment validated the previous results (see section *7.3.*), testing of treatment with a higher dose of Oncamex (50 mg/kg/day) recapitulated but did not improve on the previous anti-proliferative effect. Similarly, combination of Oncamex (25 mg/kg/day) with paclitaxel (10 mg/kg/day) did not yield a statistically significantly stronger antitumour effect than the individual treatments.

In short, this initial *in vivo* work showed a partial recapitulation of the *in vitro* effect of Oncamex, with a beneficial tumour growth-inhibiting effect in xenografts. Additionally, monitoring of changes in body weight showed no apparent signs of toxicity in any of the experimental groups, suggesting future tests could investigate the effect of higher treatment doses.

Finally, tissue from the first xenograft experiment was also used for preliminary assessment by IHC of the effect of Oncamex on protein expression *in vivo* (see section *7.4.*). Results showed a reduction in expression of cyclins, while JNK, its down-stream target c-Jun and glycolytic enzymes were increased. Although further work and analysis is needed, these

results provide a preliminary validation at protein level of part of the proposed model for the *in vitro* mechanism of action of Oncamex and are consistent with its at least partial recapitulation in a pre-clinical *in vivo* model.

8.2. Further work

Despite the advances made throughout this project in the understanding of the properties of Oncamex, its potential as an anticancer agent and its possible mechanism of action, further work is still needed. This section describes aspects that could be addressed in future experimental work in order to corroborate the findings reported here and build on the current knowledge of Oncamex and its efficacy, as well as for its potential continued development towards a possible clinical application.

8.2.1. Project limitations

The work reported here aimed to study the novel flavonoids of interest in a comprehensive, logical and sequential manner within the scope of this project. However, some practical limitations, either in terms of resources or time available for experiments, meant that some areas of the project presented limitations. This section will summarise some of these in the context of the overall work carried out and how these could be addressed in further work.

The first stage of the project focused on the study of the effect a library of flavonoids on panels of breast and ovarian cancer cell lines. While these tests allowed for the ranking of these compounds according to their relative potency and the identification of Oncamex as a lead candidate, time limitations prevented the inclusion of tests on normal epithelial breast or ovarian cells. The study of the effect of Oncamex in such models in further work could be of interest to assess its comparative cytotoxic effect in non-malignant cells.

Resources for the microarray experiment were limited and the inclusion of a wider range of breast and ovarian models meant that, as a compromise in the experimental design, only one replicate per sample (n=1) could be included. This design allowed for the study of changes in gene expression across different cancer cell line models, including preliminary assessment of possible differential effects of Oncamex in treatment-resistant models of disease. The fact that a large number of these changes were observed across different models supports their consistency and biological significance (see section *5.3.4.*). Nevertheless, the absence of more biological replicates (n≥2) was a limitation in this experiment that should ideally be addressed in further work (see section *8.2.2.*).

Limited resources also prevented a more thorough assessment of toxicity in the animal experiments performed. Thus, the tests reported here focused on the measurement of changes in the xenografts implanted in the mice, with monitoring of body weights changes

as the only assessment of toxicity and other tests (such as the analysis of histological changes in the liver) were outwith the limited scope of these first preliminary *in vivo* tests. Possible additional tests that could be performed in future studies are discussed later in this chapter (see section *8.2.5.*).

8.2.2. Validation of results

Further validation of some of the results reported here is needed to better describe the effect of Oncamex as a single agent and in combination with other therapies. For instance, further work should include validation of microarray results by quantitative PCR in order to corroborate the effect of Oncamex in the expression levels of relevant genes related to glycolysis, mitophagy, apoptosis, proliferation, the JNK signalling pathway or the transcription factor FOXO3 (see *Figures 56* and *57*).

Indeed, while several methods have shown the effect of Oncamex on ROS production, mitochondrial function and apoptosis, further validation is also needed to corroborate or refine the mechanistic model postulated, particularly given the need to bridge the gap between protein and gene expression results. Indeed, as previously discussed (see section *5.3.5.*), many aspects of transcriptional and post-transcriptional regulation can affect the correlation between changes in gene expression and protein function[662].

Further validation of changes in protein expression, activation and compartmental distribution by western blotting and immunohistochemistry could aid in the better understanding of the mechanism of action of Oncamex. For instance, further work could investigate the involvement of changes in the PI3K/AKT in the activation of FOXO3 or monitor the release of pro-apoptotic proteins from the mitochondrial intermembrane space.

Preliminary validation in tissues from a first *in vivo* experiment showed changes consistent with the described effect of Oncamex on proliferation, JNK signalling and glycolysis. Nevertheless, further analysis and experimentation are required to better validate whether not only the cytostatic effect of Oncamex, but also its suggested modes of action by induction of cell death, are recapitulated *in vivo*. This could include validation in tissues from the second xenograft experiment. Additionally, further xenograft experiments are needed for a better assessment of the effect of Oncamex *in vivo*, so validation of the mechanism in tests including different doses or treatment schedules would also be of interest.

8.2.3. Combination experiments

Chapter 6 has described results from preliminary combination experiments suggesting the enhanced beneficial effect of Oncamex in combination with other agents in cell culture models. A second xenograft experiment also assessed the effect of combination of Oncamex with paclitaxel *in vivo*.

In short, this work investigated some of the combination treatment alternatives, identifying concentrations and administration regimens that yielded improved effects in cell culture models. However, further studies are required to assess a greater range of combination alternatives and investigate whether a potential synergistic effect could be recapitulated *in vivo*.

Additionally, results from differential gene expression analysis have suggested the activation of glycolysis and mitophagy following treatment with Oncamex (see sections *5.4.3.* and *5.4.4.*). As previously discussed, confirmation of these aspects of its mechanism of action by further validation could open the door to possible combinations of Oncamex with glycolytic or mitophagy inhibitors or with other therapies capable of inhibiting this essential metabolic pathway in cancer cells.

8.2.4. Further study of the modes of action of Oncamex

While this project has focused on studying the effect on biological functions and possible mechanism of action of Oncamex as a single agent, further work could assess other effects that Oncamex may induce beyond this suggested mechanism. Despite the described specificity of this compound for the mitochondrial compartment, it could exert other effects given not only the central role of these organelles in cellular homeostasis[387,388], but also the well-established versatility of flavonoids, some of which have been described to interact with numerous cellular functions[448,754] (see section *1.1.5.3.*). This versatility could contribute, to some extent, to the observed effect of Oncamex, either as a single agent or in combination with other therapies.

Indeed, further work could also focus on the understanding of the apparent combinatorial effect of Oncamex with chemotherapy and anti-oestrogens. Results have shown the improved effect of these combinations in cell culture models, but further study is needed to understand the possible mechanisms underlying these responses, particularly to assess whether they are due to a resensitising effect of Oncamex on chemo- or endocrine therapy-resistant models.

Preliminary gene expression analysis also suggested that Oncamex may induce additional changes beyond those linked to the main mechanism of action proposed here, with lower concentrations altering some gene clusters in chemo-resistant PEA2 cells (see section *6.2.*), while higher concentrations might alter the expression levels of some genes in tamoxifen-resistant LCC9 cells only, reverting their expression profiles to levels more similar to those of anti-oestrogen-sensitive MCF-7 cells (see section *6.3.*). The study of these potential additional modes of action of Oncamex could open a new line of research.

Further work could include more in-depth analyses of changes in gene expression, followed by validation at protein level of possible findings. The latter could be of particular relevance to the possible mechanism underlying the combinatorial effect of Oncamex with paclitaxel, as this was partly observed following 2 h pretreatment with sub-micromolar concentrations of the novel flavonoid, suggesting protein interaction could play an important role independently of changes at gene expression level that may not have led to significant transcriptional changes by that timepoint.

8.2.5. Additional *in vivo* work

While most of the work reported here focused on cell culture models, given the importance of *in vitro* work for the earlier stages of drug discovery, chapter 7 has described initial *in vivo* work, also necessary for the further development of candidate compounds. As previously discussed (see section *8.1.*), promising results from two preliminary xenograft experiments, together with evidence from the previous development of similar agents, could be indicative of the potential of Oncamex but more work is needed to better understand its *in vivo* efficacy and possible further pre-clinical or clinical development. Extensive *in vivo* work would need to assess in greater detail aspects such as:

(i) the efficacy of the compound *in vivo* in further cancer models, to investigate whether the activity of Oncamex is potent enough to support further study;

(ii) definition of potential therapeutic levels and the maximum tolerated dose in animal models, since the absence of obvious treatment-induced toxicity in the form of significant changes in body weight in initial experiments suggested that higher doses could be applied;

(iii) administration options, both in terms of the best treatment regimens and the optimisation of treatment solvents or possible liposomal or micellar formulations, which could address the previously discussed issues with the

limited solubility of Oncamex (see sections *5.1.* and *7.3.*) and enable more desirable oral of intravenous administration routes;

(iv) pharmacodynamics studies, to assess not only the efficacy but also the specific effects and mechanisms of action of the compound *in vivo*, for which biomarkers identified in previous *in vitro* work should be considered; or

(v) pharmacokinetics studies, including monitoring of plasma or urine levels, to better understand the absorption, distribution, metabolism and elimination of the compound *in vivo*, to better understand how these may affect its efficacy.

Importantly, future experiments would also need to include a much more detailed monitoring for possible signs of toxicity, including the study of changes in behaviour and activity of the animals, physical discomfort or loss of appetite, as well as the monitoring of haematological parameters, signs for drug-induced neuropathy or damage to vital organs, such as the post-mortem examination of changes in histology, weight or morphology of the liver.

Given results from *in vitro* work, further xenograft studies could also assess other potential applications of Oncamex. This could include the assessment of the *in vivo* efficacy of Oncamex in other cancer models, including other breast and ovarian cancer xenografts. As previously mentioned (see section *8.2.3.*), further work could study its effect in combination with other agents, particularly in models for treatment-resistant cancers, given the fact that other novel flavonoids have shown particular promise for their applications as combination therapies (see section *1.1.5.5.2.*).

8.2.6. Further development of Antoxis's novel flavonoid platform

As previously discussed (see sections *1.1.5.5.3.* and *3.4.*), the compounds studied in this project were the result of Antoxis Ltd's efforts to optimise and improve the natural backbone of the flavonol myricetin through alteration of its substituents and side chains. Although results to date have already identified novel flavonoids improving on the anticancer efficacy of myricetin, this is not to indicate that further work could not aim to develop newer and more potent semi-synthetic analogues, in the same way that Oncamex was developed as a second-generation analogue of AO-1530.

Further work could build on the knowledge gained from the results reported here or subsequent work to improve the efficacy of this compounds or its effect in specific cellular functions. For instance, the potency of a fully methoxylated analogue of Oncamex could be

assessed. The potential of similar novel flavonoids based on other natural products could also be investigated.

Moreover, as mentioned in the previous section, further work could investigate possible improvements to the composition, solubility and stability in solution of these compounds. As discussed, the inclusion of a lipophilic side chain in the structure of Oncamex has been suggested as one of the factors contributing to its improved potency by enhancing its permeability. However, improved lipophilicity can also be linked to a reduction in solubility. Indeed, several authors have discussed the shift towards the development of chemical entities with increased lipophilicity, the often negative effect of this on drug solubility and the need to balance both properties[755–757]. Thus, the development of an Oncamex-based analogue with better solubility or an optimised solvent formulation could exhibit greater pharmacokinetic properties and hold greater potential for its continued pre-clinical or clinical development if it demonstrated an advantageous efficacy in further *in vivo* experiments.

8.3. Final remarks

In conclusion, the initial hypothesis on which this project was based has been validated. The results reported here have shown the improved efficacy of myricetin-derived novel flavonoids, and in particular lead analogue Oncamex, for the treatment of breast and ovarian cancers. Additionally, the results obtained have led to the postulation of a mechanism that suggests the antiproliferative and pro-apoptotic effect of Oncamex is dependent on its mitochondrial targeting, redox reactivity and improved physicochemical properties, which were the basis for this project's rationale. Importantly, this project has also included preliminary work to investigate the application of Oncamex as a combination agent with chemotherapy and anti-oestrogens, as well as initial validation of its activity *in vivo*.

In short, Oncamex represents a new candidate in a recent field of novel flavonoids with anti-cancer properties. While further work is needed, the results reported here represent an encouraging start to the development of Oncamex as a potential anticancer agent. The partial recapitulation of its efficacy *in vivo* also suggests the promise for its possible further pre-clinical development. This is also encouraged by the absence of obvious signs of drug-induced toxicity in the first *in vivo* experiments.

Oncamex is a derivative of the natural compound myricetin, which like many flavonoids has been noted to be non-toxic to normal cells[374,437] (see section *1.1.5.4.2.*). Recent years have seen the pre-clinical development of several other novel flavonoids, with promising results and limited *in vivo* toxicity[473,478,763] (see section *1.1.5.5.2.*). On the other hand, work to date has suggested that the limited solubility of Oncamex could represent a hindrance for its continued pre-clinical, or potentially clinical, development. In comparison, compounds such as ME-143 and ME-344 or the first generation compound in their class, Phenoxodiol, present better solubility that has allowed for their administration orally or intravenously in their clinical testing[487,491,494].

Together with further validation of results to date and the testing of other possible combinations or treatment alternatives, further work should aim to improve the solubility of Oncamex or develop an improved solvent composition that may allow its easier administration by oral, intravenous or intramuscular routes. If successful, this would allow for the further development of Oncamex to exploit its improved efficacy. Its improved structure, including methoxylations and lipophilic chains have been linked to the greater antiproliferative potency *in vitro*. In the same way that Oncamex exhibited greater efficacy

than its first-generation hydroxylated analogue AO-1530, these alterations may also lead to greater potency than ME-143 and ME-344, currently under development.

These agents have advanced to phase I and II clinical trials to assess their application as mono-therapies or in combination with other agents and their continued development towards potential clinical application[491,492,494]. Current work appears to focus on their combination with cytotoxic chemotherapy[491]. The first-generation analogue Phenoxodiol was previously tested in combination with cisplatin, paclitaxel and carboplatin[488,489]. A trial assessing the effect of ME-344 in combination with topotecan (NCT02100007) was started but recently terminated due to lack of efficacy, while a trial to study the effect of ME-143 in combination with cytotoxic chemotherapy has been announced, based on its efficacy in combination with a range of agents (including carboplatin, cisplatin and paclitaxel) in *in vitro* studies, although no further information has been made available.

In relation to this, Oncamex has been shown to improve the response to paclitaxel and TRAIL in both breast and ovarian cancer *in vitro* studies. Further work may assess if this effect translates to *in vivo* models and could be recapitulated in combination with other agents. As Oncamex bears unique structural features that appear to grant efficacy both as a single and combination agent *in vitro*, it may hold potential to enhance the effect of cytotoxic compounds more effectively than previously developed novel flavonoids. Additionally, Oncamex is the first novel flavonoid to date that has been observed to induce an enhanced response to anti-oestrogens in ER^+ resistant cells, representing a potential novel line of research.

In short, although Oncamex has limited solubility, the evidence to date suggests that, thanks to its improved structural features, this novel compound may hold potential for its application as an anticancer agent as a mono-therapy or in combination with chemotherapy or anti-oestrogens. Although further work is needed, the results reported represent an encouraging start for the continued development of Oncamex.

9. Bibliography

1. Cancer Research UK. Cancer Research UK: What is Cancer? Available at: http://www.cancerresearchuk.org/about-cancer/what-is-cancer. (Accessed: 25th November 2015)
2. Hanahan, D. & Weinberg, R. A. The Hallmarks of Cancer. *Cell* **100,** 57–70 (2000).
3. Watson, I. R., Takahashi, K., Futreal, P. A. & Chin, L. Emerging patterns of somatic mutations in cancer. *Nat. Rev. Genet.* **14,** 703–18 (2013).
4. Martincorena, I. & Campbell, P. J. Somatic mutation in cancer and normal cells. *Science (80-.).* **349,** 1483–1489 (2015).
5. Hanahan, D. & Weinberg, R. A. Hallmarks of cancer: the next generation. *Cell* **144,** 646–74 (2011).
6. World Health Organisation. GLOBOCAN 2012 - Cancer factsheets. (2012).
7. Stewart, B. & Wild, C. *World Cancer Report 2014*. (2014).
8. Cancer Research UK. Cancer Research UK - Cancer Statistics in the UK. Available at: http://www.cancerresearchuk.org/health-professional/cancer-statistics. (Accessed: 25th November 2015)
9. Department of Health. *Living Well for Longer: National Support for Local Action to Reduce Premature Avoidable Mortality*. (2014).
10. World Health Organisation. UK Cancer Profile 2014. (2014). Available at: http://www.who.int/cancer/country-profiles/gbr_en.pdf. (Accessed: 25th November 2015)
11. World Health Organisation. GLOBOCAN 2012 - UK population factsheet. (2012). Available at: http://globocan.iarc.fr/Pages/fact_sheets_population.aspx. (Accessed: 25th November 2015)
12. Cancer Research UK. Cancer Research UK - Breast cancer statistics. (2012). Available at: http://www.cancerresearchuk.org/health-professional/cancer-statistics/statistics-by-cancer-type/breast-cancer. (Accessed: 27th November 2015)
13. Office for National Statistics. *Cancer Statistics Registrations, No. 42*. (2013).
14. Parkin, D. M., Boyd, L. & Walker, L. C. The fraction of cancer attributable to lifestyle and environmental factors in the UK in 2010. *Br. J. Cancer* **105 Suppl,** S77-81 (2011).
15. Metcalfe, K. A. *et al.* Breast cancer risks in women with a family history of breast or ovarian cancer who have tested negative for a BRCA1 or BRCA2 mutation. *Br. J. Cancer* **100,** 421–5 (2009).
16. Malhotra, G. K., Zhao, X., Band, H. & Band, V. Histological, molecular and functional subtypes of breast cancers. *Cancer Biol Ther* **10,** 955–960 (2010).
17. Cancer Research UK. DCIS.
18. Cancer Research UK. LCIS. Available at: http://www.cancerresearchuk.org/about-cancer/type/breast-cancer/about/types/lcis-lobular-carcinoma-in-situ. (Accessed: 7th December 2015)
19. Afonso, N. & Bouwman, D. Lobular carcinoma in situ. *Eur. J. Cancer Prev.* **17,** 312–6 (2008).
20. Duggal, S., Robin, J. & Julian, T. B. Ductal carcinoma in situ: an overview. *Expert Rev. Anticancer Ther.* **13,** 955–62 (2013).
21. Venkitaraman, R. Lobular neoplasia of the breast. *Breast J.* **16,** 519–28 (2010).
22. Cancer Research UK. Invasive Ductal Carninoma.
23. Li, C. I., Uribe, D. J. & Daling, J. R. Clinical characteristics of different histologic types of breast cancer. *Br J Cancer* **93,** 1046–1052 (2005).
24. Cancer Research UK. Invasive Lobular Carcinoma.
25. Lester, S. C. *et al.* Protocol for the examination of specimens from patients with invasive carcinoma of the breast. *Arch Pathol Lab Med* **133,** 1515–1538 (2009).
26. Yamauchi, H. *et al.* Inflammatory breast cancer: what we know and what we need to learn. *Oncologist* **17,** 891–9 (2012).
27. Sakorafas, G. H., Blanchard, K., Sarr, M. G. & Farley, D. R. Paget's disease of the breast. *Cancer Treat. Rev.* **27,** 9–18 (2001).
28. Stingl, J. & Caldas, C. Molecular heterogeneity of breast carcinomas and the cancer stem cell hypothesis. *Nat Rev Cancer* **7,** 791–799 (2007).
29. Bloom, H. J. & Richardson, W. W. Histological grading and prognosis in breast cancer; a study of 1409 cases of which 359 have been followed for 15 years. *Br. J. Cancer* **11,** 359–377 (1957).

30. Elston, C. W. & Ellis, I. O. Pathological prognostic factors in breast cancer. I. The value of histological grade in breast cancer: experience from a large study with long-term follow-up. *Histopathology* **41,** 154–161 (2002).
31. Genestie, C. *et al.* Comparison of the prognostic value of Scarff-Bloom-Richardson and Nottingham histological grades in a series of 825 cases of breast cancer: Major importance of the mitotic count as a component of both grading systems. *Anticancer Res.* **18,** 571–576 (1998).
32. Denoix, P. Enquete permanent dans les centres anticancereaux. *Bull Inst Nat Hyg* 70–75 (1946).
33. Union for International Cancer Control (UICC). TMN Classification of malignant tumours. *TMN Classification of Malignant Tumours* (1968).
34. Sobin, L., Gospodarowicz, M. & Wittekind, C. *TNM Classification of Malignant Tumours*. (2009).
35. Edge, S. *et al.* in *AJCC Cancer Staging Manual 7th ed.* 347–376 (2010).
36. Singletary, S. E. Systemic treatment after sentinel lymph node biopsy in breast cancer: who, what, and why?11No competing interests declared. *J. Am. Coll. Surg.* **192,** 220–230 (2001).
37. Woodward, W. A. *et al.* Changes in the 2003 American Joint Committee on Cancer staging for breast cancer dramatically affect stage-specific survival. *J. Clin. Oncol.* **21,** 3244–8 (2003).
38. Benson, J. R. The TNM staging system and breast cancer. *Lancet Oncol.* **4,** 56–60 (2003).
39. Cancer Research UK. TNM Breast Cancer Staging. Available at: http://www.cancerresearchuk.org/about-cancer/type/breast-cancer/treatment/tnm-breast-cancer-staging. (Accessed: 6th December 2015)
40. American Joint Committee on Cancer (AJCC). What is cancer staging? Available at: What is the TNM Staging System? (Accessed: 6th December 2015)
41. Cancer Research UK. Number stages of breast cancer. Available at: http://www.cancerresearchuk.org/about-cancer/type/breast-cancer/treatment/number-stages-of-breast-cancer. (Accessed: 6th December 2015)
42. Allred, D. C., Harvey, J. M., Berardo, M. & Clark, G. M. Prognostic and predictive factors in breast cancer by immunohistochemical analysis. *Mod Pathol* **11,** 155–168 (1998).
43. Harvey, J. M., Clark, G. M., Osborne, C. K. & Allred, D. C. Estrogen receptor status by immunohistochemistry is superior to the ligand-binding assay for predicting response to adjuvant endocrine therapy in breast cancer. *J. Clin. Oncol.* **17,** 1474–1481 (1999).
44. Gown, A. M. *et al.* High concordance between immunohistochemistry and fluorescence in situ hybridization testing for HER2 status in breast cancer requires a normalized IHC scoring system. *Mod Pathol* **21,** 1271–1277 (2008).
45. Tvrdik, D. *et al.* Comparison of the IHC, FISH, SISH and qPCR methods for the molecular diagnosis of breast cancer. *Mol Med Rep* **6,** 439–443 (2012).
46. Slamon, D. J. *et al.* Human breast cancer: correlation of relapse and survival with amplification of the HER-2/neu oncogene. *Science (80-.).* **235,** 177–182 (1987).
47. Harris, L. *et al.* American Society of Clinical Oncology 2007 update of recommendations for the use of tumor markers in breast cancer. *J Clin Oncol* **25,** 5287–5312 (2007).
48. Rakha, E. A., Reis-Filho, J. S. & Ellis, I. O. Combinatorial biomarker expression in breast cancer. *Breast Cancer Res Treat* **120,** 293–308 (2010).
49. Payne, S. J. L., Bowen, R. L., Jones, J. L. & Wells, C. A. Predictive markers in breast cancer--the present. *Histopathology* **52,** 82–90 (2008).
50. Hortobagyi, G. N. Toward individualized breast cancer therapy: translating biological concepts to the bedside. *Oncologist* **17,** 577–584 (2012).
51. Maughan, K. L., Lutterbie, M. A. & Ham, P. S. Treatment of breast cancer. *American Family Physician* **81,** 1339–1346 (2010).
52. Sørlie, T. *et al.* Gene expression patterns of breast carcinomas distinguish tumor subclasses with clinical implications. *Proc Natl Acad Sci U S A* **98,** 10869–10874 (2001).
53. Sorlie, T. *et al.* Repeated observation of breast tumor subtypes in independent gene expression data sets. *Proc. Natl. Acad. Sci. U. S. A.* **100,** 8418–23 (2003).
54. Perou, C. M. *et al.* Molecular portraits of human breast tumours. *Nature* **406,** 747–752 (2000).
55. Fox, M. S. On the diagnosis and treatment of breast cancer. *J. Am. Med. Assoc.* **241,** 489–494 (1979).
56. Gruvberger, S. *et al.* Estrogen receptor status in breast cancer is associated with remarkably distinct gene expression patterns. *Cancer Res.* **61,** 5979–5984 (2001).

57. Golub, T. R. *et al.* Molecular classification of cancer: Class discovery and class prediction by gene expression monitoring. *Science (80).* **286,** 527–531 (1999).

58. Alizadeh, A. A. *et al.* Distinct types of diffuse large B-cell lymphoma identified by gene expression profiling. *Nature* **403,** 503–511 (2000).

59. Prat, A. *et al.* Phenotypic and molecular characterization of the claudin-low intrinsic subtype of breast cancer. *Breast Cancer Res.* **12,** R68 (2010).

60. Perou, C. M. Molecular stratification of triple-negative breast cancers. *Oncologist* **16 Suppl 1,** 61–70 (2011).

61. West, M. *et al.* Predicting the clinical status of human breast cancer by using gene expression profiles. *Proc. Natl. Acad. Sci. U. S. A.* **98,** 11462–11467 (2001).

62. Van't Veer, L. J. *et al.* Gene expression profiling predicts clinical outcome of breast cancer. *Nature* **415,** 530–536 (2002).

63. Prat, A. & Perou, C. M. Mammary development meets cancer genomics. *Nat Med* **15,** 842–844 (2009).

64. Lim, E. *et al.* Aberrant luminal progenitors as the candidate target population for basal tumor development in BRCA1 mutation carriers. *Nat Med* **15,** 907–913 (2009).

65. Kakarala, M. & Wicha, M. S. Implications of the cancer stem-cell hypothesis for breast cancer prevention and therapy. *J. Clin. Oncol.* **26,** 2813–20 (2008).

66. Lehmann, B. D. *et al.* Identification of human triple-negative breast cancer subtypes and preclinical models for selection of targeted therapies. *J Clin Invest* **121,** 2750–2767 (2011).

67. Teschendorff, A. E., Miremadi, A., Pinder, S. E., Ellis, I. O. & Caldas, C. An immune response gene expression module identifies a good prognosis subtype in estrogen receptor negative breast cancer. *Genome Biol* **8,** R157 (2007).

68. Das, P., Siegers, G. M. & Postovit, L. M. Illuminating luminal B: QSOX1 as a subtype-specific biomarker. *Breast Cancer Res* **15,** 104 (2013).

69. Katchman, B. A. *et al.* Expression of quiescin sulfhydryl oxidase 1 is associated with a highly invasive phenotype and correlates with a poor prognosis in Luminal B breast cancer. *Breast Cancer Res* **15,** R28 (2013).

70. Holland, D. G. *et al.* ZNF703 is a common Luminal B breast cancer oncogene that differentially regulates luminal and basal progenitors in human mammary epithelium. *EMBO Mol Med* **3,** 167–180 (2011).

71. Yanagawa, M. *et al.* Luminal A and luminal B (HER2 negative) subtypes of breast cancer consist of a mixture of tumors with different genotype. *BMC Res Notes* **5,** 376 (2012).

72. Curtis, C. *et al.* The genomic and transcriptomic architecture of 2,000 breast tumours reveals novel subgroups. *Nature* **486,** 346–352 (2012).

73. Hogben, R. K. F. Screening for breast cancer in England: a review. *Curr. Opin. Obstet. Gynecol.* **20,** 545–9 (2008).

74. Heywang-Koebrunner, S. *et al.* Mammography Screening - as of 2013. *Geburtshilfe Frauenheilkd.* **73,** 1007–1016 (2013).

75. Marmot, M. G. *et al.* The benefits and harms of breast cancer screening: an independent review. *Br. J. Cancer* **108,** 2205–40 (2013).

76. Patnick, J. Breast cancer screening: The UK independent review and update on breast screening in England. *Cancer Forum* **38,** 199–202 (2014).

77. Marmot, M. *et al.* The benefits and harms of breast cancer screening: an independent review. *Lancet* **380,** 1778–86 (2012).

78. Njor, S. *et al.* Breast cancer mortality in mammographic screening in Europe: a review of incidence-based mortality studies. *J. Med. Screen.* **19 Suppl 1,** 33–41 (2012).

79. Broeders, M. *et al.* The impact of mammographic screening on breast cancer mortality in Europe: a review of observational studies. *J. Med. Screen.* **19 Suppl 1,** 14–25 (2012).

80. Hooley, R. J., Andrejeva, L. & Scoutt, L. M. Breast cancer screening and problem solving using mammography, ultrasound, and magnetic resonance imaging. *Ultrasound Q.* **27,** 23–47 (2011).

81. Elmore, J. G., Armstrong, K., Lehman, C. D. & Fletcher, S. W. Screening for breast cancer. *JAMA* **293,** 1245–56 (2005).

82. Houssami, N., Lord, S. J. & Ciatto, S. Breast cancer screening: Emerging role of new imaging techniques as adjuncts to mammography. *Medical Journal of Australia* **190,** 493–498 (2009).

83. Paik, S. *et al.* A Multigene Assay to Predict Recurrence of Tamoxifen-Treated, Node-Negative Breast Cancer. *N. Engl. J. Med.* **351,** 2817–2826 (2004).

84. Reis-Filho, J. S. & Pusztai, L. Gene expression profiling in breast cancer: classification, prognostication, and prediction. *Lancet* **378,** 1812–23 (2011).

85. Sotiriou, C. & Pusztai, L. Gene-expression signatures in breast cancer. *N. Engl. J. Med.* **360,** 790–800+752 (2009).

86. Borst, P. & Wessels, L. Do predictive signatures really predict response to cancer chemotherapy? . *Cell Cycle* **9,** 4836–4840 (2010).

87. Turnbull, A. K. *et al.* Accurate Prediction and Validation of Response to Endocrine Therapy in Breast Cancer. *J Clin Oncol* (2015). doi:10.1200/JCO.2014.57.8963

88. Loukas, M. *et al.* The history of mastectomy. *Am. Surg.* **77,** 566–571 (2011).

89. Bland, C. S. The Halsted mastectomy: present illness and past history. *West. J. Med.* **134,** 549–555 (1981).

90. American Cancer Society. Surgery for Breast Cancer. (2014). Available at: http://www.cancer.org/cancer/breastcancer/detailedguide/breast-cancer-treating-surgery. (Accessed: 9th February 2016)

91. Eisen, A., Rebbeck, T. R., Wood, W. C. & Weber, B. L. Prophylactic surgery in women with a hereditary to breast and ovarian cancer. *J. Clin. Oncol.* **18,** 1980–1995 (2000).

92. Hartmann, L. C. *et al.* Efficacy of bilateral prophylactic mastectomy in women with a family history of breast cancer. *N. Engl. J. Med.* **340,** 77–84 (1999).

93. Walton, L., Ommen, K. & Audisio, R. A. Breast reconstruction in elderly women breast cancer: A review. *Cancer Treat. Rev.* **37,** 353–357 (2011).

94. Poortmans, P. Evidence based radiation oncology: Breast cancer. *Radiother. Oncol.* **84,** 84–101 (2007).

95. Abe, O. *et al.* Effects of radiotherapy and of differences in the extent of surgery for early breast cancer on local recurrence and 15-year survival: An overview of the randomised trials. *Lancet* **366,** 2087–2106 (2005).

96. Kelly, C. M. & Hortobagyi, G. N. Adjuvant chemotherapy in early-stage breast cancer: What, When, and for Whom? *Surg. Oncol. Clin. N. Am.* **19,** 649–668 (2010).

97. Paus, R., Haslam, I. S., Sharov, A. A. & Botchkarev, V. A. Pathobiology of chemotherapy-induced hair loss. *Lancet. Oncol.* **14,** e50-9 (2013).

98. Meinardi, M. T. *et al.* Long-term chemotherapy-related cardiovascular morbidity. *Cancer Treat. Rev.* **26,** 429–447 (2000).

99. Kayl, A. E. & Meyers, C. A. Side-effects of chemotherapy and quality of life in ovarian and breast cancer patients. *Curr. Opin. Obstet. Gynecol.* **18,** 24–28 (2006).

100. Schloßberger, A., Ditsch, N., Kahlert, S. & Untch, M. Chemotherapy. Long-term side effects in women with gynaecologic malignancies. *Onkologe* **11,** 785–792 (2005).

101. Akashi-Tanaka, S. Predicting responses to chemotherapy in breast cancer: From bench to bedside. *Breast Cancer* **17,** 92–96 (2010).

102. Beatson, G. T. ON THE TREATMENT OF INOPERABLE CASES OF CARCINOMA OF THE MAMMA: SUGGESTIONS FOR A NEW METHOD OF TREATMENT, WITH ILLUSTRATIVE CASES. *Lancet* **148,** 101–107 (1896).

103. Jensen, E. V, DeSombre, E. R. & Jungblut, P. W. in *Endogenous Factors Influencing Host-Tumor Balance* (ed. R.W. Wissler, T. L. S. and J. S. W. (eds. .) 15–30 (University of Chicago Press, 1967).

104. McGuire, W. L. Estrogen receptors in human breast cancer. *J. Clin. Invest.* **52,** 73–77 (1973).

105. Cole, M. P., Jones, C. T. & Todd, I. D. A new anti-oestrogenic agent in late breast cancer. An early clinical appraisal of ICI46474. *Br. J. Cancer* **25,** 270–275 (1971).

106. Jordan, V. C. Tamoxifen: A most unlikely pioneering medicine. *Nat. Rev. Drug Discov.* **2,** 205–213 (2003).

107. Robertson, J. F. R. & Blamey, R. W. The use of gonadotrophin-releasing hormone (GnRH) agonists in early and advanced breast cancer in pre- and perimenopausal women. *Eur. J. Cancer* **39,** 861–869 (2003).

108. Goel, S., Sharma, R., Hamilton, A. & Beith, J. LHRH agonists for adjuvant therapy of early breast cancer in premenopausal women. *Cochrane Database Syst. Rev.* (2009).

109. Carpenter, R. & Miller, W. R. Role of aromatase inhibitors in breast cancer. *Br. J. Cancer* **93,** S1–S5 (2005).

110. Miller, W. R. Aromatase inhibitors and breast cancer. *Minerva Endocrinol.* **31,** 27–46 (2006).

111. Johnston, S. R. D. & Dowsett, M. Aromatase inhibitors for breast cancer: Lessons from the laboratory. *Nat. Rev. Cancer* **3,** 821–831 (2003).

112. Larionov, A. A. & Miller, W. R. Challenges in defining predictive markers for response to endocrine therapy in breast cancer. *Futur. Oncol.* **5,** 1415–1428 (2009).

113. Prowell, T. M. & Davidson, N. E. What is the role of ovarian ablation in the management of primary and metastatic breast cancer today? *Oncologist* **9,** 507–517 (2004).

114. Schindler, A. E. GnRH-agonists in benign and malignant breast disease. *Curr. Obstet. Gynaecol.* **7,** 236–240 (1997).

115. Chengalvala, M. V, Pelletier, J. C. & Kopf, G. S. GnRH agonists and antagonists in cancer therapy. *Curr. Med. Chem. - Anti-Cancer Agents* **3,** 399–410 (2003).

116. Simpson, E. R. & Dowsett, M. Aromatase and its inhibitors: Significance for breast cancer therapy. *Recent Prog. Horm. Res.* **57,** 317–338 (2002).

117. Dowsett, M. *et al.* In vivo measurement of aromatase inhibition by letrozole (CGS 20267) in postmenopausal patients with breast cancer. *Clin. Cancer Res.* **1,** 1511–1515 (1995).

118. Howell, A. & Dowsett, M. Aromatase inhibitors versus antioestrogens. *Breast Cancer Res.* **6,** 269–274 (2004).

119. Johnston, S. J. & Cheung, K. L. Fulvestrant - A novel endocrine therapy for breast cancer. *Curr. Med. Chem.* **17,** 902–914 (2010).

120. Rosenberg, S. A., Yang, J. C. & Restifo, N. P. Cancer immunotherapy: Moving beyond current vaccines. *Nat. Med.* **10,** 909–915 (2004).

121. Wicki, A. & Rochlitz, C. Targeted therapies in breast cancer. *Swiss Med. Wkly.* **142,** w13550 (2012).

122. Torres, S. *et al.* Patterns in target-directed breast cancer research. *Springerplus* **5,** 109 (2016).

123. McArthur, H. L. & Hudis, C. A. Trastuzumab: a picky partner? *Clin Cancer Res* **15,** 6311–6313 (2009).

124. Herbst, R. S. *et al.* Clinical Cancer Advances 2005: major research advances in cancer treatment, prevention, and screening--a report from the American Society of Clinical Oncology. *J Clin Oncol* **24,** 190–205 (2006).

125. Esteva, F. J. Monoclonal antibodies, small molecules, and vaccines in the treatment of breast cancer. *Oncologist* **9,** 4–9 (2004).

126. Pegram, M. *et al.* Inhibitory effects of combinations of HER-2/neu antibody and chemotherapeutic agents used for treatment of human breast cancers. *Oncogene* **18,** 2241–2251 (1999).

127. Cobleigh, M. A. *et al.* Multinational study of the efficacy and safety of humanized anti-HER2 monoclonal antibody in women who have HER2-overexpressing metastatic breast cancer that has progressed after chemotherapy for metastatic disease. *J. Clin. Oncol.* **17,** 2639–2648 (1999).

128. Yardley, D. A. Combining mTOR Inhibitors with Chemotherapy and Other Targeted Therapies in Advanced Breast Cancer: Rationale, Clinical Experience, and Future Directions. *Breast Cancer (Auckl).* **7,** 7–22 (2013).

129. Li, R., Ma, W. & Zhang, S. Research progress of mTOR inhibitors in the treatment of breast cancer. *Cancer Research and Clinic* **27,** 646–648 (2015).

130. Kufe, D. W. MUC1-C oncoprotein as a target in breast cancer: activation of signaling pathways and therapeutic approaches. *Oncogene* **32,** 1073–81 (2013).

131. Singh, R. & Bandyopadhyay, D. A target molecule for cancer therapy. *Cancer Biology and Therapy* **6,** 481–486 (2007).

132. Kufe, D. W. Mucins in cancer: Function, prognosis and therapy. *Nat. Rev. Cancer* **9,** 874–885 (2009).

133. Ellis, L. M. & Hicklin, D. J. VEGF-targeted therapy: mechanisms of anti-tumour activity. *Nat. Rev. Cancer* **8,** 579–91 (2008).

134. Sharma, P. S., Sharma, R. & Tyagi, T. VEGF/VEGFR pathway inhibitors as anti-angiogenic agents: Present and future. *Current Cancer Drug Targets* **11,** 624–653 (2011).

135. Glendenning, J. & Tutt, A. PARP inhibitors--current status and the walk towards early breast cancer. *Breast* **20 Suppl 3,** S12-9 (2011).

136. Park, Y. P. *et al.* Human telomerase reverse transcriptase (hTERT): a target molecule for the treatment of cisplatin-resistant tumors. *Korean J. Lab. Med.* **28,** 430–7 (2008).

137. Cancer Research UK. Cancer Research UK - Ovarian cancer statistics. (2010). Available at: http://www.cancerresearchuk.org/cancer-info/cancerstats/types/ovary/. (Accessed: 30th November 2015)

138. Hemminki, K., Sundquist, J. & Brandt, A. Incidence and mortality in epithelial ovarian cancer by family history of any cancer. *Cancer* **117,** 3972–80 (2011).

139. Friebel, T. M., Domchek, S. M. & Rebbeck, T. R. Modifiers of cancer risk in BRCA1 and BRCA2 mutation carriers: systematic review and meta-analysis. *J. Natl. Cancer Inst.* **106,** dju091 (2014).

140. Alsop, K. *et al.* BRCA mutation frequency and patterns of treatment response in BRCA mutation-positive

women with ovarian cancer: a report from the Australian Ovarian Cancer Study Group. *J. Clin. Oncol.* **30,** 2654–63 (2012).

141. Manchanda, R. *et al.* Population testing for cancer predisposing BRCA1/BRCA2 mutations in the Ashkenazi-Jewish community: a randomized controlled trial. *J. Natl. Cancer Inst.* **107,** 379 (2015).
142. Manchanda, R. *et al.* Cost-effectiveness of population screening for BRCA mutations in Ashkenazi jewish women compared with family history-based testing. *J. Natl. Cancer Inst.* **107,** 380 (2015).
143. Lukanova, A. & Kaaks, R. Endogenous hormones and ovarian cancer: epidemiology and current hypotheses. *Cancer Epidemiol. Biomarkers Prev.* **14,** 98–107 (2005).
144. Brewster, W. R. Temporal trends in ovarian cancer: incidence and mortality across Europe. *Nat. Clin. Pract. Oncol.* **2,** 286–7 (2005).
145. Sundar, S. in *Obstetrics and gynaecology: an evidence based text for MRCOG* (Hodder, 2010).
146. Maringe, C. *et al.* Stage at diagnosis and ovarian cancer survival: evidence from the International Cancer Benchmarking Partnership. *Gynecol. Oncol.* **127,** 75–82 (2012).
147. Hennessy, B. T., Coleman, R. L. & Markman, M. Ovarian cancer. *Lancet (London, England)* **374,** 1371–82 (2009).
148. Friedman, G. D., Skilling, J. S., Udaltsova, N. V & Smith, L. H. Early symptoms of ovarian cancer: a case-control study without recall bias. *Fam. Pract.* **22,** 548–53 (2005).
149. Cannistra, S. A. Cancer of the ovary. *N. Engl. J. Med.* **351,** 2519–29 (2004).
150. Jayson, G. C., Kohn, E. C., Kitchener, H. C. & Ledermann, J. A. Ovarian cancer. *Lancet (London, England)* **384,** 1376–88 (2014).
151. National Comprehensive Cancer Network. NCCN guidelines for treatment of ovarian cancer. (2015). Available at: http://www.nccn.org/professionals/physician_gls/f_guidelines.asp#site. (Accessed: 17th April 2016)
152. National Institute for Health and Care Excellence. Ovarian cancer: recognition and initial management. (2011). Available at: https://www.nice.org.uk/guidance/CG122. (Accessed: 17th April 2016)
153. Prat, J. Staging classification for cancer of the ovary, fallopian tube, and peritoneum. *Int. J. Gynaecol. Obstet.* **124,** 1–5 (2014).
154. Sundar, S., Neal, R. D. & Kehoe, S. Diagnosis of ovarian cancer. *BMJ* **351,** h4443 (2015).
155. Menon, U. *et al.* Sensitivity and specificity of multimodal and ultrasound screening for ovarian cancer, and stage distribution of detected cancers: results of the prevalence screen of the UK Collaborative Trial of Ovarian Cancer Screening (UKCTOCS). *Lancet. Oncol.* **10,** 327–40 (2009).
156. Jacobs, I. *et al.* A risk of malignancy index incorporating CA 125, ultrasound and menopausal status for the accurate preoperative diagnosis of ovarian cancer. *Br. J. Obstet. Gynaecol.* **97,** 922–929 (1990).
157. Timmerman, D. *et al.* Logistic regression model to distinguish between the benign and malignant adnexal mass before surgery: a multicenter study by the International Ovarian Tumor Analysis Group. *J. Clin. Oncol.* **23,** 8794–801 (2005).
158. Ueland, F. R. *et al.* Effectiveness of a multivariate index assay in the preoperative assessment of ovarian tumors. *Obstet. Gynecol.* **117,** 1289–97 (2011).
159. Heliström, I. *et al.* The HE4 (WFDC2) protein is a biomarker for ovarian carcinoma. *Cancer Res.* **63,** 3695–3700 (2003).
160. Van Gorp, T. *et al.* HE4 and CA125 as a diagnostic test in ovarian cancer: prospective validation of the Risk of Ovarian Malignancy Algorithm. *Br. J. Cancer* **104,** 863–70 (2011).
161. Menon, U. *et al.* Risk Algorithm Using Serial Biomarker Measurements Doubles the Number of Screen-Detected Cancers Compared With a Single-Threshold Rule in the United Kingdom Collaborative Trial of Ovarian Cancer Screening. *J. Clin. Oncol.* **33,** 2062–71 (2015).
162. Jacobs, I. J. *et al.* Ovarian cancer screening and mortality in the UK Collaborative Trial of Ovarian Cancer Screening (UKCTOCS): a randomised controlled trial. *Lancet* **387,** 945–956 (2015).
163. McGuire, W. P. & Markman, M. Primary ovarian cancer chemotherapy: current standards of care. *Br. J. Cancer* **89 Suppl 3,** S3-8 (2003).
164. Agarwal, R. & Kaye, S. B. Ovarian cancer: strategies for overcoming resistance to chemotherapy. *Nat. Rev. Cancer* **3,** 502–16 (2003).
165. Kauff, N. D. *et al.* Risk-reducing salpingo-oophorectomy in women with a BRCA1 or BRCA2 mutation. *N. Engl. J. Med.* **346,** 1609–15 (2002).
166. Vergote, I. *et al.* Prognostic importance of degree of differentiation and cyst rupture in stage I invasive

epithelial ovarian carcinoma. *Lancet (London, England)* **357,** 176–82 (2001).

167. Powless, C. A., Aletti, G. D., Bakkum-Gamez, J. N. & Cliby, W. A. Risk factors for lymph node metastasis in apparent early-stage epithelial ovarian cancer: implications for surgical staging. *Gynecol. Oncol.* **122,** 536–40 (2011).
168. Ozols, R. F. *et al.* Phase III trial of carboplatin and paclitaxel compared with cisplatin and paclitaxel in patients with optimally resected stage III ovarian cancer: a Gynecologic Oncology Group study. *J. Clin. Oncol.* **21,** 3194–200 (2003).
169. Vasey, P. A. *et al.* Phase III randomized trial of docetaxel-carboplatin versus paclitaxel-carboplatin as first-line chemotherapy for ovarian carcinoma. *J. Natl. Cancer Inst.* **96,** 1682–91 (2004).
170. Rustin, G. J. & Van Der Burg, M. E. A randomized trial in ovarian cancer (OC) of early treatment of relapse based on CA125 level alone versus delayed treatment based on conventional clinical indicators (MRC OV05/EORTC 55955 trials). *J Clin Oncol* **27,** (2009).
171. Trimbos, J. B. *et al.* International collaborative ovarian neoplasm trial 1 and adjuvant chemotherapy in ovarian neoplasm trial: Two parallel randomized phase III trials of adjuvant chemotherapy in patients with early-stage ovarian carcinoma. *J. Natl. Cancer Inst.* **95,** 105–112 (2003).
172. Kehoe, S. *et al.* Primary chemotherapy versus primary surgery for newly diagnosed advanced ovarian cancer (CHORUS): an open-label, randomised, controlled, non-inferiority trial. *Lancet (London, England)* **386,** 249–57 (2015).
173. Markman, M. Maintenance chemotherapy in the management of epithelial ovarian cancer. *Cancer Metastasis Rev.* **34,** 11–7 (2015).
174. Fong, P. C. *et al.* Inhibition of poly(ADP-ribose) polymerase in tumors from BRCA mutation carriers. *N. Engl. J. Med.* **361,** 123–34 (2009).
175. Gotlieb, W. H. *et al.* Intravenous aflibercept for treatment of recurrent symptomatic malignant ascites in patients with advanced ovarian cancer: a phase 2, randomised, double-blind, placebo-controlled study. *Lancet. Oncol.* **13,** 154–62 (2012).
176. Vaughan, S. *et al.* Rethinking ovarian cancer: recommendations for improving outcomes. *Nat. Rev. Cancer* **11,** 719–25 (2011).
177. Harter, P. *et al.* Prospective validation study of a predictive score for operability of recurrent ovarian cancer: the Multicenter Intergroup Study DESKTOP II. A project of the AGO Kommission OVAR, AGO Study Group, NOGGO, AGO-Austria, and MITO. *Int. J. Gynecol. Cancer* **21,** 289–95 (2011).
178. Ledermann, J. A. & Kristeleit, R. S. Optimal treatment for relapsing ovarian cancer. *Ann. Oncol.* **21 Suppl 7,** vii218-22 (2010).
179. Foo, J. & Michor, F. Evolution of acquired resistance to anti-cancer therapy. *J. Theor. Biol.* **355,** 10–20 (2014).
180. Gottesman, M. M. Mechanisms of cancer drug resistance. *Annu. Rev. Med.* **53,** 615–27 (2002).
181. Gatti, L. & Zunino, F. Overview of tumor cell chemoresistance mechanisms. *Methods in molecular medicine* **111,** 127–148 (2005).
182. Wilson, T. R., Longley, D. B. & Johnston, P. G. Chemoresistance in solid tumours. *Ann. Oncol.* **17 Suppl 1,** x315-24 (2006).
183. Holohan, C., Van Schaeybroeck, S., Longley, D. B. & Johnston, P. G. Cancer drug resistance: an evolving paradigm. *Nat Rev Cancer* **13,** 714–726 (2013).
184. Zahreddine, H. & Borden, K. L. B. Mechanisms and insights into drug resistance in cancer. *Front. Pharmacol.* **4,** 28 (2013).
185. Groenendijk, F. H. & Bernards, R. Drug resistance to targeted therapies: déjà vu all over again. *Mol. Oncol.* **8,** 1067–83 (2014).
186. Gottesman, M. M., Fojo, T. & Bates, S. E. Multidrug resistance in cancer: Role of ATP-dependent transporters. *Nature Reviews Cancer* **2,** 48–58 (2002).
187. Kuffel, M. J. *et al.* Activation of the antitumor agent aminoflavone (NSC 686288) is mediated by induction of tumor cell cytochrome P450 1A1/1A2. *Molecular Pharmacology* **62,** 143–153 (2002).
188. Bardenheuer, W. *et al.* Resistance to cytarabine and gemcitabine and in vitro selection of transduced cells after retroviral expression of cytidine deaminase in human hematopoietic progenitor cells. *Leukemia* **19,** 2281–8 (2005).
189. McMillin, D. W., Negri, J. M. & Mitsiades, C. S. The role of tumour-stromal interactions in modifying drug response: challenges and opportunities. *Nat. Rev. Drug Discov.* **12,** 217–28 (2013).
190. Lesniak, D. *et al.* Beta1-integrin circumvents the antiproliferative effects of trastuzumab in human

epidermal growth factor receptor-2-positive breast cancer. *Cancer Res.* **69,** 8620–8 (2009).

191. Wilson, T. R. *et al.* Widespread potential for growth-factor-driven resistance to anticancer kinase inhibitors. *Nature* **487,** 505–9 (2012).
192. Tomida, A. & Tsuruo, T. Drug resistance mediated by cellular stress response to the microenvironment of solid tumors. *Anticancer. Drug Des.* **14,** 169–77 (1999).
193. Michor, F., Nowak, M. A. & Iwasa, Y. Evolution of resistance to cancer therapy. *Curr. Pharm. Des.* **12,** 261–71 (2006).
194. Michor, F. & Polyak, K. The origins and implications of intratumor heterogeneity. *Cancer Prev. Res. (Phila).* **3,** 1361–4 (2010).
195. Hofmann, W.-K. *et al.* Presence of the BCR-ABL mutation Glu255Lys prior to STI571 (imatinib) treatment in patients with Ph+ acute lymphoblastic leukemia. *Blood* **102,** 659–61 (2003).
196. Toyooka, S., Kiura, K. & Mitsudomi, T. EGFR mutation and response of lung cancer to gefitinib. *N. Engl. J. Med.* **352,** 2136; author reply 2136 (2005).
197. Inukai, M. *et al.* Presence of epidermal growth factor receptor gene T790M mutation as a minor clone in non-small cell lung cancer. *Cancer Res.* **66,** 7854–8 (2006).
198. Gonzalez-Angulo, A. M., Morales-Vasquez, F. & Hortobagyi, G. N. Overview of resistance to systemic therapy in patients with breast cancer. *Advances in Experimental Medicine and Biology* **608,** 1–22 (2007).
199. Parkin, D. M., Bray, F., Ferlay, J. & Pisani, P. Estimating the world cancer burden: Globocan 2000. *Int. J. cancer* **94,** 153–6 (2001).
200. Pisani, P., Bray, F. & Parkin, D. M. Estimates of the world-wide prevalence of cancer for 25 sites in the adult population. *Int. J. cancer* **97,** 72–81 (2002).
201. Jemal, A. *et al.* Cancer statistics, 2003. *Ca-A Cancer J. Clin.* **53,** 5–26 (2003).
202. Dixon, J. M. Endocrine Resistance in Breast Cancer. *New J. Sci.* **2014,** 27 (2014).
203. Murray, J., Miller, W. R. & Dixon, J. M. Neoadjuvant endocrine therapy models. *Methods Mol. Med.* **120,** 489–502 (2006).
204. Turnbull, A. K. Personalized medicine in cancer: where are we today? *Future Oncol.* **11,** 2795–8 (2015).
205. Ma, C. X., Sanchez, C. G. & Ellis, M. J. Predicting endocrine therapy responsiveness in breast cancer. *Oncology* **23,** 133–142 (2009).
206. Ring, A. & Dowsett, M. Mechanisms of tamoxifen resistance. *Endocr. Relat. Cancer* **11,** 643–658 (2004).
207. Holmes, D. Ovarian cancer: beyond resistance. *Nature* **527,** S217 (2015).
208. Blagden, S. & Gabra, H. Future directions in the management of epithelial ovarian cancer. *Future Oncol.* **4,** 403–11 (2008).
209. Greene, M. H., Clark, J. W. & Blayney, D. W. The epidemiology of ovarian cancer. *Semin. Oncol.* **11,** 209–26 (1984).
210. Cragg, G. M. & Newman, D. J. Natural products: a continuing source of novel drug leads. *Biochim. Biophys. Acta* **1830,** 3670–95 (2013).
211. Farnsworth, N. R., Akerele, O., Bingel, A. S., Soejarto, D. D. & Guo, Z. Medicinal plants in therapy. *Bull. World Health Organ.* **63,** 965–981 (1985).
212. Newman, D. J. & Cragg, G. M. Natural products as sources of new drugs over the last 25 years. *J. Nat. Prod.* **70,** 461–77 (2007).
213. Newman, D. J. & Cragg, G. M. Natural products as sources of new drugs over the 30 years from 1981 to 2010. *J. Nat. Prod.* **75,** 311–35 (2012).
214. Cragg, G. M. & Newman, D. J. Antineoplastic agents from natural sources: Achievements and future directions. *Expert Opinion on Investigational Drugs* **9,** 2783–2797 (2000).
215. Fabricant, D. S. & Farnsworth, N. R. The value of plants used in traditional medicine for drug discovery. *Environ. Health Perspect.* **109,** 69–75 (2001).
216. Pezzuto, J. M. Plant-derived anticancer agents. *Biochem. Pharmacol.* **53,** 121–133 (1997).
217. Farnsworth, N. R. & Morris, R. W. Higher plants - the sleeping giant of drug development. *Am. J. Pharm. Sci. Support. Public Health* **148,** 46–52 (1976).
218. Farnsworth, N. R. & Soejarto, D. D. Potential consequence of plant extinction in the United States on the current and future availability of prescription drugs. *Econ. Bot.* **39,** 231–240 (1985).
219. O'Neill, M. J. & Lewis, J. A. The renaissance of plant research in the pharmaceutical industry. *Human Medicinal Agents from Plants* 48–55 (1993).

220. Principe, P. P. Monetizing the pharmacological benefits of plants. *Medicinal Resources of the Tropical Rainforest* 191–218 (1996).

221. The Nobel Assembly at Karolinska Insitutet. The Nobel Prize in Phisiology or Medicine 2015 press release. (2015). Available at: http://www.nobelprize.org/nobel_prizes/medicine/laureates/2015/press.html. (Accessed: 26th May 2016)

222. Molyneux, D. H. & Ward, S. A. Reflections on the Nobel Prize for Medicine 2015 - The Public Health Legacy and Impact of Avermectin and Artemisinin. *Trends Parasitol.* **31,** 605–607 (2015).

223. Shen, B. A New Golden Age of Natural Products Drug Discovery. *Cell* **163,** 1297–1300 (2015).

224. Li, J. W.-H. & Vederas, J. C. Drug discovery and natural products: end of an era or an endless frontier? *Science* **325,** 161–5 (2009).

225. Prakash, O., Kumar, A., Kumar, P. & Ajeet, A. Anticancer Potential of Plants and Natural Products: A Review. *Am. J. Pharmacol. Sci.* **1,** 104–115 (2013).

226. Gueritte, F., Fahy, J., Roussi, F., Gueritte, F. & Fahy, J. in *Anticancer Agents from Natural Products* (eds. Cragg, G., Kingston, D. & Newman, D.) 177–198 (Taylor and Francis, 2005).

227. Lee, K.-H. & Xiao, Z. Podophyllotoxin and analogs. *Anticancer Agents from Natural Products* 95–122 (2012).

228. Potmesil, M. Camptothecins: from bench research to hospital wards. *Cancer Res.* **54,** 1431–9 (1994).

229. Garcia-Carbonero, R. & Supko, J. G. Current perspectives on the clinical experience, pharmacology, and continued development of the camptothecins. *Clin. Cancer Res.* **8,** 641–61 (2002).

230. Gordaliza, M. Natural products as leads to anticancer drugs. *Clin. Transl. Oncol.* **9,** 767–76 (2007).

231. Schiff, P. B. & Horwitz, S. B. Taxol stabilizes microtubules in mouse fibroblast cells. *Proc. Natl. Acad. Sci. U. S. A.* **77,** 1561–1565 (1980).

232. Wani, M. C., Taylor, H. L., Wall, M. E., Coggon, P. & McPhail, A. T. Plant antitumor agents. VI. The isolation and structure of taxol, a novel antileukemic and antitumor agent from Taxus brevifolia [12]. *Journal of the American Chemical Society* **93,** 2325–2327 (1971).

233. Kingston, D. G. I. Taxol and its analogs. *Anticancer Agents from Natural Products* 89–122 (2005).

234. Kingston, D. G. I. & Newman, D. J. Taxoids: Cancer-fighting compounds from nature. *Current Opinion in Drug Discovery and Development* **10,** 130–144 (2007).

235. Green, M. R. *et al.* Abraxane, a novel Cremophor-free, albumin-bound particle form of paclitaxel for the treatment of advanced non-small-cell lung cancer. *Ann. Oncol.* **17,** 1263–8 (2006).

236. Pan, L., Chai, H. & Kinghorn, A. D. The continuing search for antitumor agents from higher plants. *Phytochem. Lett.* **3,** 1–8 (2010).

237. Mishra, B. B. & Tiwari, V. K. Natural products: an evolving role in future drug discovery. *Eur. J. Med. Chem.* **46,** 4769–807 (2011).

238. Butler, M. S. The role of natural product chemistry in drug discovery. *J. Nat. Prod.* **67,** 2141–53 (2004).

239. Butler, M. S. Natural products to drugs: natural product derived compounds in clinical trials. *Nat. Prod. Rep.* **22,** 162–95 (2005).

240. Butler, M. S. Natural products to drugs: natural product-derived compounds in clinical trials. *Nat. Prod. Rep.* **25,** 475–516 (2008).

241. Butler, M. S., Robertson, A. A. B. & Cooper, M. A. Natural product and natural product derived drugs in clinical trials. *Nat. Prod. Rep.* **31,** 1612–61 (2014).

242. Brown DM. Kelly GE. Husband, A. Flavonoid compounds in maintenance of prostate health and prevention and treatment of cancer. *Molecular Biotechnology* **30,** 253–270 (2005).

243. Baier, W. E. Chemistry of bioflavonoids. *Ann. N. Y. Acad. Sci.* **61,** 639–645 (1955).

244. Winkel-Shirley, B. Biosynthesis of flavonoids and effects of stress. *Curr. Opin. Plant Biol.* **5,** 218–23 (2002).

245. Winkel-Shirley, B. Flavonoid biosynthesis. A colorful model for genetics, biochemistry, cell biology, and biotechnology. *Plant Physiol.* **126,** 485–93 (2001).

246. Weng, C.-J. & Yen, G.-C. Flavonoids, a ubiquitous dietary phenolic subclass, exert extensive in vitro anti-invasive and in vivo anti-metastatic activities. *Cancer Metastasis Rev.* **31,** 323–51 (2012).

247. Ververidis, F. *et al.* Biotechnology of flavonoids and other phenylpropanoid-derived natural products. Part I: Chemical diversity, impacts on plant biology and human health. *Biotechnol. J.* **2,** 1214–34 (2007).

248. Hooper, L. *et al.* Flavonoids, flavonoid-rich foods, and cardiovascular risk: A meta-analysis of randomized controlled trials. *American Journal of Clinical Nutrition* **88,** 38–50 (2008).

249. Manach, C., Scalbert, A., Morand, C., Rémésy, C. & Jiménez, L. Polyphenols: food sources and bioavailability.

Am. J. Clin. Nutr. **79,** 727–47 (2004).

250. Lea, M. A. Flavonol regulation in tumor cells. *J. Cell. Biochem.* **116,** 1190–4 (2015).
251. Maggiolini, M. *et al.* The red wine phenolics piceatannol and myricetin act as agonists for estrogen receptor alpha in human breast cancer cells. *J. Mol. Endocrinol.* **35,** 269–81 (2005).
252. Nöthlings, U., Murphy, S. P., Wilkens, L. R., Henderson, B. E. & Kolonel, L. N. Flavonols and pancreatic cancer risk: The multiethnic cohort study. *American Journal of Epidemiology* **166,** 924–931 (2007).
253. Cook, N. C. & Samman, S. Flavonoids - Chemistry, metabolism, cardioprotective effects, and dietary sources. *Journal of Nutritional Biochemistry* **7,** 66–76 (1996).
254. Ferlay, J. *et al.* GLOBOCAN 2008. Cancer Incidence and Mortality Worldwide. *IARC CancerBase No. 10* (2010).
255. Pan, H. *et al.* Genistein inhibits MDA-MB-231 triple-negative breast cancer cell growth by inhibiting NF-κB activity via the Notch-1 pathway. *Int. J. Mol. Med.* **30,** 337–43 (2012).
256. Park, K. Il *et al.* Induction of the cell cycle arrest and apoptosis by flavonoids isolated from Korean Citrus aurantium L. in non-small-cell lung cancer cells. *Food Chem.* **135,** 2728–35 (2012).
257. Shih, Y.-W. Y.-W., Wu, P.-F. P.-F., Lee, Y.-C., Shi, M.-D. M.-D. & Chiang, T.-A. T.-A. Myricetin suppresses invasion and migration of human lung adenocarcinoma a549 cells: Possible mediation by blocking the erk signaling pathway. *J. Agric. Food Chem.* **57,** 3490–3499 (2009).
258. Ko, C.-H., Shen, S.-C., Lee, T. J. F. & Chen, Y.-C. Myricetin inhibits matrix metalloproteinase 2 protein expression and enzyme activity in colorectal carcinoma cells. *Molecular Cancer Therapeutics* **4,** 281–290 (2005).
259. Ko, C. H., Shen, S.-C., Hsu, C.-S. & Chen, Y.-C. Mitochondrial-dependent, reactive oxygen species-independent apoptosis by myricetin: roles of protein kinase C, cytochrome c, and caspase cascade. *Biochem. Pharmacol.* **69,** 913–27 (2005).
260. Siegelin, M. D., Reuss, D. E., Habel, A., Herold-Mende, C. & von Deimling, A. The flavonoid kaempferol sensitizes human glioma cells to TRAIL-mediated apoptosis by proteasomal degradation of survivin. *Mol. Cancer Ther.* **7,** 3566–74 (2008).
261. Siegelin, M. D., Gaiser, T., Habel, A. & Siegelin, Y. Myricetin sensitizes malignant glioma cells to TRAIL-mediated apoptosis by down-regulation of the short isoform of FLIP and bcl-2. *Cancer Lett.* **283,** 230–8 (2009).
262. Huang, W.-W. *et al.* Kaempferol induces autophagy through AMPK and AKT signaling molecules and causes G2/M arrest via downregulation of CDK1/cyclin B in SK-HEP-1 human hepatic cancer cells. *Int. J. Oncol.* (2013). doi:10.3892/ijo.2013.1909
263. Chun, O. K., Chung, S. J. & Song, W. O. Estimated dietary flavonoid intake and major food sources of U.S. adults. *J. Nutr.* **137,** 1244–52 (2007).
264. Chun, O. K., Lee, S. G., Wang, Y., Vance, T. & Song, W. O. Estimated Flavonoid Intake of the Elderly in the United States and Around the World. *Journal of Nutrition in Gerontology and Geriatrics* **31,** 190–205 (2012).
265. Murkies, A. L., Wilcox, G. & Davis, S. R. Clinical review 92: Phytoestrogens. *J. Clin. Endocrinol. Metab.* **83,** 297–303 (1998).
266. Sirtori, C. R., Arnoldi, A. & Johnson, S. K. Phytoestrogens: End of a tale? *Annals of Medicine* **37,** 423–438 (2005).
267. Limer, J. L. & Speirs, V. Phyto-oestrogens and breast cancer chemoprevention. *Breast Cancer Res.* **6,** 119–27 (2004).
268. Le Bail, J.-C., Champavier, Y., Chulia, A.-J. & Habrioux, G. Effects of phytoestrogens on aromatase, 3β and 17β-hydroxysteroid dehydrogenase activities and human breast cancer cells. *Life Sciences* **66,** 1281–1291 (2000).
269. Brownson, D. M., Azios, N. G., Fuqua, B. K., Dharmawardhane, S. F. & Mabry, T. J. Flavonoid Effects Relevant to Cancer. in *International Research Conference on Food, Nutrition & Cancer* 3482–3489 (2002).
270. Damianaki, A. *et al.* Potent inhibitory action of red wine polyphenols on human breast cancer cells. *J. Cell. Biochem.* **78,** 429–41 (2000).
271. Maggiolini, M. *et al.* Estrogen receptor α mediates the proliferative but not the cytotoxic dose-dependent effects of two major phytoestrogens on human breast cancer cells. *Mol. Pharmacol.* **60,** 595–602 (2001).
272. Bowers, J. L., Tyulmenkov, V. V, Jernigan, S. C. & Klinge, C. M. Resveratrol acts as a mixed agonist/antagonist for estrogen receptors α and β. *Endocrinology* **141,** 3657–3667 (2000).
273. Miksicek, R. J. Interaction of naturally occurring nonsteroidal estrogens with expressed recombinant human

estrogen receptor. *Journal of Steroid Biochemistry and Molecular Biology* **49,** 153–160 (1994).

274. Collins, B. M., McLachlan, J. A. & Arnold, S. F. The estrogenic and antiestrogenic activities of phytochemicals with the human estrogen receptor expressed in yeast. *Steroids* **62,** 365–372 (1997).
275. Harris, D. M., Besselink, E., Henning, S. M., Go, V. L. W. & Heber, D. Phytoestrogens induce differential estrogen receptor alpha- or beta-mediated responses in transfected breast cancer cells. *Experimental Biology and Medicine* **230,** 558–568 (2005).
276. Van Der Woude, H. *et al.* The stimulation of cell proliferation by quercetin is mediated by the estrogen receptor. *Molecular Nutrition and Food Research* **49,** 763–771 (2005).
277. Matsumura, A., Ghosh, A., Pope, G. S. & Darbre, P. D. Comparative study of oestrogenic properties of eight phytoestrogens in MCF7 human breast cancer cells. *J. Steroid Biochem. Mol. Biol.* **94,** 431–43 (2005).
278. Kuiper, G. G. J. M. *et al.* Comparison of the ligand binding specificity and transcript tissue distribution of estrogen receptors and α and β. *Endocrinology* **138,** 863–870 (1997).
279. Kuiper, G. G. J. M. *et al.* Interaction of estrogenic chemicals and phytoestrogens with estrogen receptor β. *Endocrinology* **139,** 4252–4263 (1998).
280. Lehmann, L., Esch, H. L., Wagner, J., Rohnstock, L. & Metzler, M. Estrogenic and genotoxic potential of equol and two hydroxylated metabolites of Daidzein in cultured human Ishikawa cells. *Toxicology Letters* **158,** 72–86 (2005).
281. Omoto, Y., Eguchi, H., Yamamoto-Yamaguchi, Y. & Hayashi, S.-I. Estrogen receptor (ER) β1 and ERβcx/β2 inhibit ERα function differently in breast cancer cell line MCF7. *Oncogene* **22,** 5011–5020 (2003).
282. Ström, A. *et al.* Estrogen receptor β inhibits 17β-estradiol-stimulated proliferation of the breast cancer cell line T47D. *Proc. Natl. Acad. Sci. U. S. A.* **101,** 1566–1571 (2004).
283. Koehler, K. F., Helguero, L. A., Haldosén, L.-A., Warner, M. & Gustafsson, J.-Å. Reflections on the discovery and significance of estrogen receptor β. *Endocrine Reviews* **26,** 465–478 (2005).
284. McDonnell, D. P. The molecular determinants of estrogen receptor pharmacology. *Maturitas* **48,** S7–S12 (2004).
285. Balfe, P. *et al.* Estrogen receptor α and β profiling in human breast cancer. *European Journal of Surgical Oncology* **30,** 469–474 (2004).
286. Shaaban, A. M. *et al.* Declining Estrogen Receptor-β Expression Defines Malignant Progression of Human Breast Neoplasia. *American Journal of Surgical Pathology* **27,** 1502–1512 (2003).
287. McCarty, M. F. Isoflavones made simple - Genistein's agonist activity for the beta-type estrogen receptor mediates their health benefits. *Medical Hypotheses* **66,** 1093–1114 (2006).
288. Mense, S. M., Hei, T. K., Ganju, R. K. & Bhat, H. K. Phytoestrogens and breast cancer prevention: Possible mechanisms of action. *Environ. Health Perspect.* **116,** 426–433 (2008).
289. Kao, Y.-C., Zhou, C., Sherman, M., Laughton, C. A. & Chen, S. Molecular basis of the inhibition of human aromatase (estrogen synthetase) by flavone and isoflavone phytoestrogens: A site-directed mutagenesis study. *Environmental Health Perspectives* **106,** 85–92 (1998).
290. Rice, S. & Whitehead, S. a. Phytoestrogens and breast cancer--promoters or protectors? *Endocr. Relat. Cancer* **13,** 995–1015 (2006).
291. Sanderson, J. T. *et al.* Induction and inhibition of aromatase (CYP19) activity by natural and synthetic flavonoid compounds in H295R human adrenocortical carcinoma cells. *Toxicological Sciences* **82,** 70–79 (2004).
292. Li, K. X. Z., Smith, R. E. & Krozowski, Z. S. Cloning and expression of a novel tissue specific 17β-hydroxysteroid dehydrogenase. *Endocrine Research* **24,** 663–667 (1998).
293. Pasqualini, J. R. *et al.* Concentrations of estrone, estradiol, and estrone sulfate and evaluation of sulfatase and aromatase activities in pre- and postmenopausal breast cancer patients. *Journal of Clinical Endocrinology and Metabolism* **81,** 1460–1464 (1996).
294. Yue, W. *et al.* The potential role of estrogen in aromatase regulation in the breast. *Journal of Steroid Biochemistry and Molecular Biology* **79,** 157–164 (2001).
295. Lu, L.-J. W. *et al.* Increased urinary excretion of 2-hydroxyestrone but not 16α- hydroxyestrone in premenopausal women during a soya diet containing isoflavones. *Cancer Research* **60,** 1299–1305 (2000).
296. Wood, C. E., Kaplan, J. R., Stute, P. & Cline, J. M. Effects of soy on the mammary glands of premenopausal female monkeys. *Fertility and Sterility* **85,** 1179–1186 (2006).
297. Badawi, A. F., Cavalieri, E. L. & Rogan, E. G. Role of human cytochrome P450 1A1, 1A2, 1B1, and 3A4 in the 2-, 4-, and 16α-hydroxylation of 17β-estradiol. *Metabolism: Clinical and Experimental* **50,** 1001–1003

(2001).

298. Cutler, G. J. *et al.* Dietary flavonoid intake and risk of cancer in postmenopausal women: the Iowa Women's Health Study. *Int. J. Cancer* **123,** 664–71 (2008).

299. Hui, C. *et al.* Flavonoids, flavonoid subclasses and breast cancer risk: a meta-analysis of epidemiologic studies. *PLoS One* **8,** e54318 (2013).

300. Zamora-Ros, R. *et al.* Dietary flavonoid and lignan intake and breast cancer risk according to menopause and hormone receptor status in the European Prospective Investigation into Cancer and Nutrition (EPIC) Study. *Breast Cancer Res. Treat.* (2013). doi:10.1007/s10549-013-2483-4

301. Cho, Y. A. *et al.* Effect of dietary soy intake on breast cancer risk according to menopause and hormone receptor status. *European Journal of Clinical Nutrition* **64,** 924–932 (2010).

302. Wang, Q. *et al.* Soy isoflavones, CYP1A1, CYP1B1, and COMT polymorphisms, and breast cancer: a case-control study in southwestern China. *DNA Cell Biol.* **30,** 585–95 (2011).

303. Touillaud, M. S. *et al.* Effect of dietary intake of phytoestrogens on estrogen receptor status in premenopausal women with breast cancer. *Nutr. Cancer* **51,** 162–169 (2005).

304. Brownson, D. M., Azios, N. G., Fuqua, B. K., Dharmawardhane, S. F. & Mabry, T. J. Flavonoid effects relevant to cancer. *Journal of Nutrition* **132,** 3482S–3489S (2002).

305. Ames, B. N. Dietary carcinogens and anticarcinogens. Oxygen radicals and degenerative diseases. *Science* **221,** 1256–1263 (1983).

306. Bors, W. & Saran, M. Radical scavenging by flavonoid antioxidants. *Free Radic. Res. Commun.* **2,** 289–94 (1987).

307. McPhail, D. B., Hartley, R. C., Gardner, P. T. & Duthie, G. G. Kinetic and stoichiometric assessment of the antioxidant activity of flavonoids by electron spin resonance spectroscopy. *J. Agric. Food Chem.* **51,** 1684–90 (2003).

308. Duthie, G. G., Duthie, S. J. & Kyle, J. A. Plant polyphenols in cancer and heart disease: implications as nutritional antioxidants. *Nutr. Res. Rev.* **13,** 79–106 (2000).

309. Oyama, Y., Fuchs, P. A., Katayama, N. & Noda, K. Myricetin and quercetin, the flavonoid constituents of Ginkgo biloba extract, greatly reduce oxidative metabolism in both resting and Ca2+-loaded brain neurons. *Brain Res.* **635,** 125–129 (1994).

310. Ong, K. C. & Khoo, H.-E. E. Biological effects of myricetin. *Gen. Pharmacol.* **29,** 121–6 (1997).

311. Smith, C., Halliwell, B. & Aruoma, O. I. Protection by albumin against the pro-oxidant actions of phenolic dietary components. *Food Chem. Toxicol.* **30,** 483–489 (1992).

312. Chobot, V. & Hadacek, F. Exploration of pro-oxidant and antioxidant activities of the flavonoid myricetin. *Redox Rep.* **16,** 242–246 (2011).

313. Mendes, V., Costa, V. & Mateus, N. Involvement of the modulation of cancer cell redox status in the anti-tumoral effect of phenolic compounds. *RSC Adv.* **5,** 1–9 (2015).

314. Cao, G., Sofic, E. & Prior, R. L. ANTIOXIDANT AND PROOXIDANT BEHAVIOR OF FLAVONOIDS: STRUCTURE-ACTIVITY RELATIONSHIPS. *Free Radic. Biol. Med.* **22,** 749–760 (1997).

315. Bors, W., Michel, C. & Schikora, S. Interaction of flavonoids with ascorbate and determination of their univalent redox potentials: a pulse radiolysis study. *Free Radic. Biol. Med.* **19,** 45–52 (1995).

316. Araújo, J. R., Gonçalves, P. & Martel, F. Chemopreventive effect of dietary polyphenols in colorectal cancer cell lines. *Nutr. Res.* **31,** 77–87 (2011).

317. Magee, P. J. & Rowland, I. R. Phyto-oestrogens, their mechanism of action: current evidence for a role in breast and prostate cancer. *Br. J. Nutr.* **91,** 513–31 (2004).

318. Sosa, V. *et al.* Oxidative stress and cancer: An overview. *Ageing Res. Rev.* **12,** 376–390 (2013).

319. Gorrini, C., Harris, I. S. & Mak, T. W. Modulation of oxidative stress as an anticancer strategy. *Nat. Rev. Drug Discov.* **12,** 931–47 (2013).

320. Liu, J. & Wang, Z. Increased Oxidative Stress as a Selective Anticancer Therapy. *Oxid. Med. Cell. Longev.* **2015,** 1–12 (2015).

321. Trachootham, D., Alexandre, J. & Huang, P. Targeting cancer cells by ROS-mediated mechanisms: a radical therapeutic approach? *Nat. Rev. Drug Discov.* **8,** 579–591 (2009).

322. Kumar, S., Lata, K., Mukhopadhyay, S. & Mukherjee, T. K. Role of estrogen receptors in pro-oxidative and anti-oxidative actions of estrogens: a perspective. *Biochim. Biophys. Acta* **1800,** 1127–35 (2010).

323. Walle, T. Methoxylated flavones, a superior cancer chemopreventive flavonoid subclass? *Seminars in Cancer Biology* **17,** 354–362 (2007).

324. Androutsopoulos, V. P., Papakyriakou, A., Vourloumis, D. & Spandidos, D. a. Comparative CYP1A1 and CYP1B1 substrate and inhibitor profile of dietary flavonoids. *Bioorg. Med. Chem.* **19,** 2842–9 (2011).

325. Shimada, T. *et al.* Oxidation of xenobiotics by recombinant human cytochrome P450 1B1. *Drug Metabolism and Disposition* **25,** 617–622 (1997).

326. Kim, J. H. *et al.* Metabolism of benzo[α]pyrene and benzo[α]pyrene-7,8-diol by human cytochrome P450 1B1. *Carcinogenesis* **19,** 1847–1853 (1998).

327. Wen, X. & Walle, T. Methylated flavonoids have greatly improved intestinal absorption and metabolic stability. *Drug Metabolism and Disposition* **34,** 1786–1792 (2006).

328. Bugano, D. D. G., Conforti-Froes, N., Yamaguchi, N. H. & Baracat, E. C. Genetic polymorphisms, the metabolism of estrogens and breast cancer: A review. *European Journal of Gynaecological Oncology* **29,** 313–320 (2008).

329. Rochat, B., Morsman, J. M., Murray, G. I., Figg, W. D. & Mcleod, H. L. Human CYP1B1 and anticancer agent metabolism: Mechanism for tumor-specific drug inactivation? *Journal of Pharmacology and Experimental Therapeutics* **296,** 537–541 (2001).

330. Casper, R. F. *et al.* Resveratrol has antagonist activity on the aryl hydrocarbon receptor: Implications for prevention of dioxin toxicity. *Molecular Pharmacology* **56,** 784–790 (1999).

331. Ciolino, H. P., Daschner, P. J. & Yeh, G. C. Resveratrol inhibits transcription of CYP1A1 in vitro by preventing activation of the aryl hydrocarbon receptor. *Cancer Research* **58,** 5707–5712 (1998).

332. Ciolino, H. P. & Yeh, G. C. Inhibition of aryl hydrocarbon-induced cytochrome P-450 1A1 enzyme activity and CYP1A1 expression by resveratrol. *Molecular Pharmacology* **56,** 760–767 (1999).

333. Wen, X., Walle, U. K. & Walle, T. 5,7-Dimethoxyflavone downregulates CYP1A1 expression and benzo[a]pyrene-induced DNA binding in Hep G2 cells. *Carcinogenesis* **26,** 803–809 (2005).

334. Moon, Y. J., Wang, X. & Morris, M. E. Dietary flavonoids: Effects on xenobiotic and carcinogen metabolism. *Toxicology in Vitro* **20,** 187–210 (2006).

335. Puppala, D., Gairola, C. G. & Swanson, H. I. Identification of kaempferol as an inhibitor of cigarette smoke-induced activation of the aryl hydrocarbon receptor and cell transformation. *Carcinogenesis* **28,** 639–647 (2007).

336. Arroo, R. R. J. *et al.* Phytoestrogens as natural prodrugs in cancer prevention: Dietary flavonoids. *Phytochem. Rev.* **8,** 375–386 (2009).

337. Arroo, R. R. J. *et al.* Phytoestrogens as natural prodrugs in cancer prevention: A novel concept. *Phytochem. Rev.* **7,** 431–443 (2008).

338. Chun, Y. J., Kim, M. Y. & Guengerich, F. P. Resveratrol is a selective human cytochrome P450 1A1 inhibitor. *Biochemical and Biophysical Research Communications* **262,** 20–24 (1999).

339. Potter, G. A. *et al.* The cancer preventative agent resveratrol is converted to the anticancer agent piceatannol by the cytochrome P450 enzyme CYP1b1. *British Journal of Cancer* **86,** 774–778 (2002).

340. Piver, B. *et al.* Involvement of cytochrome P450 1A2 in the biotransformation of trans-resveratrol in human liver microsomes. *Biochemical Pharmacology* **68,** 773–782 (2004).

341. Androutsopoulos, V. P., Papakyriakou, A., Vourloumis, D., Tsatsakis, A. M. & Spandidos, D. a. Dietary flavonoids in cancer therapy and prevention: substrates and inhibitors of cytochrome P450 CYP1 enzymes. *Pharmacol. Ther.* **126,** 9–20 (2010).

342. Sousa, M. C., Braga, R. C., Cintra, B. a. S., de Oliveira, V. & Andrade, C. H. In silico metabolism studies of dietary flavonoids by CYP1A2 and CYP2C9. *Food Res. Int.* **50,** 102–110 (2013).

343. Kensler, T. W. Chemoprevention by inducers of carcinogen detoxication enzymes. *Environmental Health Perspectives* **105,** 965–970 (1997).

344. Knasmüller, S. *et al.* Search for dietary antimutagens and anticarcinogens: Methodological aspects and extrapolation problems. *Food and Chemical Toxicology* **40,** 1051–1062 (2002).

345. Fetsch, P. A. *et al.* Localization of the ABCG2 mitoxantrone resistance-associated protein in normal tissues. *Cancer Letters* **235,** 84–92 (2006).

346. Tan, K. W., Li, Y., Paxton, J. W., Birch, N. P. & Scheepens, A. Identification of novel dietary phytochemicals inhibiting the efflux transporter breast cancer resistance protein (BCRP/ABCG2). *Food Chem.* **138,** 2267–74 (2013).

347. Ross, D. D., Karp, J. E., Chen, T. T. & Doyle, L. A. Expression of breast cancer resistance protein in blast cells from patients with acute leukemia. *Blood* **96,** 365–368 (2000).

348. Kanzaki, A. *et al.* Expression of multidrug resistance-related transporters in human breast carcinoma.

Japanese Journal of Cancer Research **92,** 452–458 (2001).

349. Sargent, J. M. *et al.* Breast cancer resistance protein expression and resistance to daunorubicin in blast cells from patients with acute myeloid leukaemia. *British Journal of Haematology* **115,** 257–262 (2001).
350. Van Der Kolk, D. M. *et al.* Expression and activity of breast cancer resistance protein (BCRP) in de novo and relapsed acute myeloid leukemia. *Blood* **99,** 3763–3770 (2002).
351. Steinbach, D. *et al.* BCRP gene expression is associated with a poor response to remission induction therapy in childhood acute myeloid leukemia. *Leukemia* **16,** 1443–1447 (2002).
352. Friedrich, R. E., Punke, C. & Reymann, A. Expression of multi-drug resistance genes (mdr1, mrp1, bcrp) in primary oral squamous cell carcinoma. *In Vivo* **18,** 133–148 (2004).
353. Zhang, S., Yang, X. & Morris, M. E. Flavonoids are inhibitors of breast cancer resistance protein (ABCG2)-mediated transport. *Mol. Pharmacol.* **65,** 1208–1216 (2004).
354. Natarajan, K., Xie, Y., Baer, M. R. & Ross, D. D. Role of breast cancer resistance protein (BCRP/ABCG2) in cancer drug resistance. *Biochemical Pharmacology* **83,** 1084–1103 (2012).
355. Cooray, H. C., Janvilisri, T., Van Veen, H. W., Hladky, S. B. & Barrand, M. A. Interaction of the breast cancer resistance protein with plant polyphenols. *Biochemical and Biophysical Research Communications* **317,** 269–275 (2004).
356. Fleisher, B., Unum, J., Shao, J. & An, G. Ingredients in fruit juices interact with dasatinib through inhibition of BCRP: a new mechanism of beverage-drug interaction. *J. Pharm. Sci.* **104,** 266–75 (2015).
357. Imai, Y., Tsukahara, S., Asada, S. & Sugimoto, Y. Phytoestrogens/flavonoids reverse breast cancer resistance protein/ABCG2-mediated multidrug resistance. *Cancer Research* **64,** 4346–4352 (2004).
358. Katayama, K. *et al.* Flavonoids inhibit breast cancer resistance protein-mediated drug resistance: transporter specificity and structure-activity relationship. *Cancer Chemother. Pharmacol.* **60,** 789–97 (2007).
359. Zhang, S., Yang, X., Coburn, R. A. & Morris, M. E. Structure activity relationships and quantitative structure activity relationships for the flavonoid-mediated inhibition of breast cancer resistance protein. *Biochem. Pharmacol.* **70,** 627–639 (2005).
360. Karthikeyan, S. & Hoti, S. L. Development of fourth generation ABC inhibitors from natural products: A novel approach to overcome cancer multidrug resistance. *Anticancer. Agents Med. Chem.* **15,** 605–615 (2015).
361. Li, Y., Revalde, J. L., Reid, G. & Paxton, J. W. Interactions of dietary phytochemicals with ABC transporters: Possible implications for drug disposition and multidrug resistance in cancer. *Drug Metabolism Reviews* **42,** 590–611 (2010).
362. Zhang, S., Yang, X. & Morris, M. E. Combined effects of multiple flavonoids on breast cancer resistance protein (ABCG2)-mediated transport. *Pharm. Res.* **21,** 1263–73 (2004).
363. Alvarez, A. I. *et al.* Modulation of the activity of ABC transporters (P-glycoprotein, MRP2, BCRP) by flavonoids and drug response. *Journal of Pharmaceutical Sciences* **99,** 598–617 (2010).
364. Li, Y. & Paxton, J. W. The effects of flavonoids on the ABC transporters: consequences for the pharmacokinetics of substrate drugs. *Expert Opin. Drug Metab. Toxicol.* **9,** 267–85 (2013).
365. Morris, M. E. & Zhang, S. Flavonoid-drug interactions: effects of flavonoids on ABC transporters. *Life Sci.* **78,** 2116–30 (2006).
366. Tirona, R. G. & Bailey, D. G. Herbal product-drug interactions mediated by induction. *British Journal of Clinical Pharmacology* **61,** 677–681 (2006).
367. Huang, K. F., Zhang, G. D., Huang, Y. Q. & Diao, Y. Wogonin induces apoptosis and down-regulates survivin in human breast cancer MCF-7 cells by modulating PI3K-AKT pathway. *Int. Immunopharmacol.* **12,** 334–41 (2012).
368. Phan, V., Walters, J., Brownlow, B. & Elbayoumi, T. Enhanced cytotoxicity of optimized liposomal genistein via specific induction of apoptosis in breast, ovarian and prostate carcinomas. *J. Drug Target.* (2013). doi:10.3109/1061186X.2013.847099
369. Huang, H. *et al.* Myricetin inhibits proliferation of cisplatin-resistant cancer cells through a p53-dependent apoptotic pathway. *Int. J. Oncol.* **47,** 1494–502 (2015).
370. Kamsteeg, M. *et al.* Phenoxodiol - An isoflavone analog - Induces apoptosis in chemoresistant ovarian cancer cells. *Oncogene* **22,** 2611–2620 (2003).
371. Hengartner, M. O. The biochemistry of apoptosis. *Nature* **407,** 770–6 (2000).
372. Chang, H.-L. *et al.* Protoapigenone, a novel flavonoid, inhibits ovarian cancer cell growth in vitro and in vivo. *Cancer Lett.* **267,** 85–95 (2008).

373. Yang, P.-M., Tseng, H.-H., Peng, C.-W., Chen, W.-S. & Chiu, S.-J. Dietary flavonoid fisetin targets caspase-3-deficient human breast cancer MCF-7 cells by induction of caspase-7-associated apoptosis and inhibition of autophagy. *International Journal of Oncology* **40,** 469–478 (2012).

374. Ramos, S. Effects of dietary flavonoids on apoptotic pathways related to cancer chemoprevention. *J. Nutr. Biochem.* **18,** 427–42 (2007).

375. Huang, C. *et al.* Induction of Apoptosis by Icariside II through Extrinsic and Intrinsic Signaling Pathways in Human Breast Cancer MCF7 Cells. *Biosci. Biotechnol. Biochem.* **76,** 1322–1328 (2012).

376. Chung, H. *et al.* Anticancer effects of wogonin in both estrogen receptor-positive and -negative human breast cancer cell lines in vitro and in nude mice xenografts. *Int. J. Cancer* **122,** 816–22 (2008).

377. Pettus, B. J., Chalfant, C. E. & Hannun, Y. A. Ceramide in apoptosis: an overview and current perspectives. *Biochim. Biophys. Acta* **1585,** 114–25 (2002).

378. Senchenkov, A., Litvak, D. A. & Cabot, M. C. Targeting ceramide metabolism--a strategy for overcoming drug resistance. *J. Natl. Cancer Inst.* **93,** 347–57 (2001).

379. Kim, Y.-H. & Lee, Y. J. TRAIL apoptosis is enhanced by quercetin through Akt dephosphorylation. *J. Cell. Biochem.* **100,** 998–1009 (2007).

380. Senthilkumar, K. *et al.* Quercetin inhibits invasion, migration and signalling molecules involved in cell survival and proliferation of prostate cancer cell line (PC-3). *Cell Biochem. Funct.* **29,** 87–95 (2011).

381. White, J. B. *et al.* Some natural flavonoids are competitive inhibitors of Caspase-1, -3 and -7 despite their cellular toxicity. *Food Chem.* **131,** 1453–1459 (2012).

382. Gómez-Alonso, S. *et al.* Inhibition of colon adenocarcinoma cell proliferation by flavonols is linked to a G2/M cell cycle block and reduction in cyclin D1 expression. *Food Chem.* **130,** 493–500 (2012).

383. Feng, J. *et al.* Myricetin inhibits proliferation and induces apoptosis and cell cycle arrest in gastric cancer cells. *Mol. Cell. Biochem.* (2015). doi:10.1007/s11010-015-2492-1

384. Bishayee, K. *et al.* Quercetin induces cytochrome-c release and ROS accumulation to promote apoptosis and arrest the cell cycle in G2/M, in cervical carcinoma: signal cascade and drug-DNA interaction. *Cell Prolif.* **46,** 153–163 (2013).

385. Kim, S.-H. & Choi, K.-C. Anti-cancer Effect and Underlying Mechanism(s) of Kaempferol, a Phytoestrogen, on the Regulation of Apoptosis in Diverse Cancer Cell Models. *Toxicol. Res.* **29,** 229–34 (2013).

386. Androutsopoulos, V. P., Mahale, S., Arroo, R. R. J. & Potter, G. Anticancer effects of the flavonoid diosmetin on cell cycle progression and proliferation of MDA-MB 468 breast cancer cells due to CYP1 activation. *Oncol. Rep.* **21,** 1525–1528 (2009).

387. Fulda, S. & Kroemer, G. Mitochondria as therapeutic targets for the treatment of malignant disease. *Antioxid. Redox Signal.* **15,** 2937–49 (2011).

388. Fulda, S., Galluzzi, L. & Kroemer, G. Targeting mitochondria for cancer therapy. *Nat. Rev. Drug Discov.* **9,** 447–64 (2010).

389. Ralph, S. J., Low, P., Dong, L., Lawen, A. & Neuzil, J. Mitocans: mitochondrial targeted anti-cancer drugs as improved therapies and related patent documents. *Recent Pat. Anticancer. Drug Discov.* **1,** 327–46 (2006).

390. Vander Heiden, M. G., Cantley, L. C. & Thompson, C. B. Understanding the Warburg effect: the metabolic requirements of cell proliferation. *Science* **324,** 1029–33 (2009).

391. Hsu, P. P. & Sabatini, D. M. Cancer cell metabolism: Warburg and beyond. *Cell* **134,** 703–7 (2008).

392. Gorlach, S., Fichna, J. & Lewandowska, U. Polyphenols as mitochondria-targeted anticancer drugs. *Cancer Lett.* **366,** 141–9 (2015).

393. Neuzil, J., Dong, L.-F., Rohlena, J., Truksa, J. & Ralph, S. J. Classification of mitocans, anti-cancer drugs acting on mitochondria. *Mitochondrion* **13,** 199–208 (2013).

394. Modica-Napolitano, J. S. & Aprille, J. R. Basis for the selective cytotoxicity of rhodamine 123. *Cancer Res.* **47,** 4361–4365 (1987).

395. Modica-Napolitano, J. S. & Aprille, J. R. Delocalized lipophilic cations selectively target the mitochondria of carcinoma cells. *Adv. Drug Deliv. Rev.* **49,** 63–70 (2001).

396. Chen, L. B. Mitochondrial membrane potential in living cells. *Annu. Rev. Cell Biol.* **4,** 155–81 (1988).

397. Ralph, S. J. & Neuzil, J. Mitochondria as targets for cancer therapy. *Mol. Nutr. Food Res.* **53,** 9–28 (2009).

398. Biasutto, L., Dong, L.-F., Zoratti, M. & Neuzil, J. Mitochondrially targeted anti-cancer agents. *Mitochondrion* **10,** 670–81 (2010).

399. Bustamante, E., Morris, H. P. & Pedersen, P. L. Energy metabolism of tumor cells. Requirement for a form of hexokinase with a propensity for mitochondrial binding. *J. Biol. Chem.* **256,** 8699–8704 (1981).

400. Wei, L. *et al.* Oroxylin A induces dissociation of hexokinase II from the mitochondria and inhibits glycolysis by SIRT3-mediated deacetylation of cyclophilin D in breast carcinoma. *Cell Death Dis.* **4,** e601 (2013).

401. Lu, J. *et al.* Inhibition of Mammalian thioredoxin reductase by some flavonoids: implications for myricetin and quercetin anticancer activity. *Cancer Res.* **66,** 4410–8 (2006).

402. Wang, Y. *et al.* Inhibition of glutathione synthesis eliminates the adaptive response of ascitic hepatoma 22 cells to nedaplatin that targets thioredoxin reductase. *Toxicol. Appl. Pharmacol.* **265,** 342–50 (2012).

403. Lu, J. & Holmgren, A. Thioredoxin system in cell death progression. *Antioxid. Redox Signal.* **17,** 1738–47 (2012).

404. Ortega, R. & García, N. The flavonoid quercetin induces changes in mitochondrial permeability by inhibiting adenine nucleotide translocase. *J. Bioenerg. Biomembr.* **41,** 41–7 (2009).

405. Mattarei, A. *et al.* A mitochondriotropic derivative of quercetin: a strategy to increase the effectiveness of polyphenols. *Chembiochem* **9,** 2633–2642 (2008).

406. Biasutto, L. *et al.* Impact of mitochondriotropic quercetin derivatives on mitochondria. *Biochim. Biophys. Acta* **1797,** 189–96 (2010).

407. Buss, G. D. *et al.* The action of quercetin on the mitochondrial NADH to NAD(+) ratio in the isolated perfused rat liver. *Planta Med.* **71,** 1118–22 (2005).

408. Rocha, C. M. *et al.* Metabolic signatures of lung cancer in biofluids: NMR-based metabonomics of blood plasma. *J. Proteome Res.* **10,** 4314–24 (2011).

409. Jang, M. *et al.* Cancer chemopreventive activity of resveratrol, a natural product derived from grapes. *Science* **275,** 218–220 (1997).

410. Subbaramaiah, K. *et al.* Resveratrol inhibits cyclooxygenase-2 transcription and activity in phorbol ester-treated human mammary epithelial cells. *Journal of Biological Chemistry* **273,** 21875–21882 (1998).

411. Maccarrone, M., Lorenzon, T., Guerrieri, P. & Finazzi Agrò, A. Resveratrol prevents apoptosis in K562 cells by inhibiting lipoxygenase and cyclooxygenase activity. *European Journal of Biochemistry* **265,** 27–34 (1999).

412. O'Byrne, K. J. & Dalgleish, A. G. Chronic immune activation and inflammation as the cause of malignancy. *British Journal of Cancer* **85,** 473–483 (2001).

413. Romagnolo, D. F. & Selmin, O. I. Flavonoids and cancer prevention: a review of the evidence. *J. Nutr. Gerontol. Geriatr.* **31,** 206–38 (2012).

414. Jin, H. *et al.* Morin, a flavonoid from Moraceae, suppresses growth and invasion of the highly metastatic breast cancer cell line MDA-MB‐231 partly through suppression of the Akt pathway. *Int. J. Oncol.* **45,** 1629–37 (2014).

415. Li, C., Yang, X., Chen, C., Cai, S. & Hu, J. Isorhamnetin suppresses colon cancer cell growth through the PI3K‐Akt‐mTOR pathway. *Mol. Med. Rep.* **9,** 935–40 (2014).

416. Firdous, A. B. *et al.* Quercetin, a natural dietary flavonoid, acts as a chemopreventive agent against prostate cancer in an in vivo model by inhibiting the EGFR signaling pathway. *Food Funct.* **5,** 2632–45 (2014).

417. Li, X. *et al.* Quercetin potentiates the antitumor activity of rituximab in diffuse large B-cell lymphoma by inhibiting STAT3 pathway. *Cell Biochem. Biophys.* **70,** 1357–62 (2014).

418. Liu, H., Xiao, Y., Xiong, C., Wei, A. & Ruan, J. Apoptosis induced by a new flavonoid in human hepatoma HepG2 cells involves reactive oxygen species-mediated mitochondrial dysfunction and MAPK activation. *Eur. J. Pharmacol.* **654,** 209–16 (2011).

419. Wei, A., Zhou, D., Xiong, C., Cai, Y. & Ruan, J. A novel non-aromatic B-ring flavonoid: isolation, structure elucidation and its induction of apoptosis in human colon HT-29 tumor cell via the reactive oxygen species-mitochondrial dysfunction and MAPK activation. *Food Chem. Toxicol.* **49,** 2445–52 (2011).

420. Yuan, Q. *et al.* A novel, broad-spectrum antitumor compound containing the 1-hydroxycyclohexa-2,5-dien-4-one group: the disclosure of a new antitumor pharmacophore in protoapigenone 1. *Bioorg. Med. Chem. Lett.* **21,** 3427–30 (2011).

421. Chen, W.-Y. *et al.* Protoapigenone, a natural derivative of apigenin, induces mitogen-activated protein kinase-dependent apoptosis in human breast cancer cells associated with induction of oxidative stress and inhibition of glutathione S-transferase π. *Invest. New Drugs* **29,** 1347–59 (2011).

422. Peluso, I., Raguzzini, A. & Serafini, M. Effect of flavonoids on circulating levels of TNF-α and IL-6 in humans: A systematic review and meta-analysis. *Mol. Nutr. Food Res.* **57,** 784–801 (2013).

423. Christofori, G. New signals from the invasive front. *Nature* **441,** 444–50 (2006).

424. Thiery, J. P. Epithelial-mesenchymal transitions in tumour progression. *Nat. Rev. Cancer* **2,** 442–54 (2002).

425. Yang, J. & Weinberg, R. A. Epithelial-mesenchymal transition: at the crossroads of development and tumor metastasis. *Dev. Cell* **14,** 818–29 (2008).

426. Hilakivi-Clarke, L. *et al.* Prepubertal exposure to zearalenone or genistein reduces mammary tumorigenesis. *British Journal of Cancer* **80,** 1682–1688 (1999).

427. Whitsett, T., Carpenter, M. & Lamartiniere, C. A. Resveratrol, but not EGCG, in the diet suppresses DMBA-induced mammary cancer in rats. *Journal of Carcinogenesis* **5,** (2006).

428. Xue, W. *et al.* Novel myricetin derivatives: Design, synthesis and anticancer activity. *Eur. J. Med. Chem.* **97,** 155–163 (2015).

429. Huang, S.-M., Wu, C.-H. & Yen, G.-C. Effects of flavonoids on the expression of the pro-inflammatory response in human monocytes induced by ligation of the receptor for AGEs. *Mol. Nutr. Food Res.* **50,** 1129–39 (2006).

430. Banerjee, S., Bueso-Ramos, C. & Aggarwal, B. B. Suppression of 7,12-dimethylbenz(a)anthracene-induced mammary carcinogenesis in rats by resveratrol: Role of nuclear factor-κB, cyclooxygenase 2, and matrix metalloprotease 9. *Cancer Research* **62,** 4945–4954 (2002).

431. Kundu, J. K. & Surh, Y. J. Molecular basis of chemoprevention by hesveratrol: NF-KB and AP-1 as potential targets. *Mutat Res* **555,** 65–80 (2005).

432. Pozo-Guisado, E. *et al.* Resveratrol-induced apoptosis in MCF-7 human breast cancer cells involves a caspase-independent mechanism with downregulation of Bcl-2 and NF-κB. *Int. J. Cancer* **115,** 74–84 (2005).

433. Benvenuto, M. *et al.* Inhibition of ErbB receptors, Hedgehog and NF-kappaB signaling by polyphenols in cancer. *Front. Biosci. (Landmark Ed.* **18,** 1290–310 (2013).

434. Fantini, M. *et al.* In vitro and in vivo antitumoral effects of combinations of polyphenols, or polyphenols and anticancer drugs: perspectives on cancer treatment. *Int. J. Mol. Sci.* **16,** 9236–82 (2015).

435. Tan, X. *et al.* Differences of four catechins in cell cycle arrest and induction of apoptosis in LoVo cells. *Cancer Letters* **158,** 1–6 (2000).

436. Wätjen, W. *et al.* Low concentrations of flavonoids are protective in rat H4IIE cells whereas high concentrations cause DNA damage and apoptosis. *Journal of Nutrition* **135,** 525–531 (2005).

437. Semwal, D. K., Semwal, R. B., Combrinck, S. & Viljoen, A. Myricetin: A Dietary Molecule with Diverse Biological Activities. *Nutrients* **8,** 90 (2016).

438. Surichan, S. *et al.* Bioactivation of the citrus flavonoid nobiletin by CYP1 enzymes in MCF7 breast adenocarcinoma cells. *Food Chem. Toxicol.* **50,** 3320–8 (2012).

439. Melo-Filho, C., Braga, R. & Andrade, C. Advances in Methods for Predicting Phase I Metabolism of Polyphenols. *Curr. Drug Metab.* **15,** 120–126 (2014).

440. Ferrer, P. *et al.* Association between Pterostilbene and Quercetin Inhibits Metastatic Activity of B16 Melanoma. *Neoplasia* **7,** 37–47 (2005).

441. Sakamoto, K. Synergistic effects of thearubigin and genistein on human prostate tumor cell (PC-3) growth via cell cycle arrest. *Cancer Lett.* **151,** 103–109 (2000).

442. Somers-Edgar, T. J. *et al.* The combination of epigallocatechin gallate and curcumin suppresses ER alpha-breast cancer cell growth in vitro and in vivo. *Int. J. Cancer* **122,** 1966–71 (2008).

443. Wang, P., Heber, D. & Henning, S. M. Quercetin increased bioavailability and decreased methylation of green tea polyphenols in vitro and in vivo. *Food Funct.* **3,** 635–42 (2012).

444. Amin, A. R. M. R. *et al.* Enhanced anti-tumor activity by the combination of the natural compounds (-)-epigallocatechin-3-gallate and luteolin: potential role of p53. *J. Biol. Chem.* **285,** 34557–65 (2010).

445. Wang, P. *et al.* Increased chemopreventive effect by combining arctigenin, green tea polyphenol and curcumin in prostate and breast cancer cells. *RSC Adv.* **4,** 35242–35250 (2014).

446. Wang, P. *et al.* Enhanced inhibition of prostate cancer xenograft tumor growth by combining quercetin and green tea. *J. Nutr. Biochem.* **25,** 73–80 (2014).

447. Harnly, J. M. *et al.* Flavonoid content of U.S. fruits, vegetables, and nuts. *J. Agric. Food Chem.* **54,** 9966–77 (2006).

448. Devi, K. P., Rajavel, T., Habtemariam, S., Nabavi, S. F. & Nabavi, S. M. Molecular mechanisms underlying anticancer effects of myricetin. *Life Sci.* (2015). doi:10.1016/j.lfs.2015.10.004

449. Perkin, A. G. & Phipps, S. VIII. Notes on some natural colouring matters. *J. Chem. Soc. Trans.* **85,** 56 (1904).

450. Perkin, A. G. XXI. Myricetin. Part II. *J. Chem. Soc. Trans.* **81,** 203 (1902).

451. Perkin, A. G. & Hummel, J. J. LXXVI. The colouring principle contained in the bark of Myrica nagi. Part I. *J. Chem. Soc. Trans.* **69,** 1287 (1896).

452. Bennett, C. J. *et al.* Potential therapeutic antioxidants that combine the radical scavenging ability of myricetin and the lipophilic chain of vitamin E to effectively inhibit microsomal lipid peroxidation. *Bioorg. Med. Chem.* **12,** 2079–98 (2004).

453. Ross, J. A. & Kasum, C. M. Dietary flavonoids: Bioavailability, metabolic effects, and safety. *Annu. Rev. Nutr.* **22,** 19–34 (2002).

454. Hertog, M. G. L., Feskens, E. J. M., Hollman, P. C. H., Katan, M. B. & Kromhout, D. Dietary antioxidant flavonoids and risk of coronary heart disease: The Zutphen Elderly Study. *Lancet* **342,** 1007–1011 (1993).

455. Angelone, T. *et al.* Distinct signalling mechanisms are involved in the dissimilar myocardial and coronary effects elicited by quercetin and myricetin, two red wine flavonols. *Nutr. Metab. Cardiovasc. Dis.* **21,** 362–71 (2011).

456. Kang, S.-J., Park, J.-H. Y., Choi, H.-N. & Kim, J.-I. α-glucosidase inhibitory activities of myricetin in animal models of diabetes mellitus. *Food Sci. Biotechnol.* **24,** 1897–1900 (2015).

457. Ozcan, F., Ozmen, A., Akkaya, B., Aliciguzel, Y. & Aslan, M. Beneficial effect of myricetin on renal functions in streptozotocin-induced diabetes. *Clin. Exp. Med.* **12,** 265–72 (2012).

458. Li, Y. & Ding, Y. Minireview: Therapeutic potential of myricetin in diabetes mellitus. *Food Sci. Hum. Wellness* **1,** 19–25 (2012).

459. Zhang, X.-H., Zou, Z.-Q., Xu, C.-W., Shen, Y.-Z. & Li, D. Myricetin induces G2/M phase arrest in HepG2 cells by inhibiting the activity of the cyclin B/Cdc2 complex. *Mol. Med. Rep.* **4,** 273–7 (2011).

460. Sun, F. *et al.* Potential anticancer activity of myricetin in human T24 bladder cancer cells both in vitro and in vivo. *Nutr. Cancer* **64,** 599–606 (2012).

461. Maggioni, D. *et al.* Myricetin and naringenin inhibit human squamous cell carcinoma proliferation and migration in vitro. *Nutr. Cancer* **66,** 1257–67 (2014).

462. Zhang, X.-H. *et al.* Myricetin induces apoptosis in HepG2 cells through Akt/p70S6K/bad signaling and mitochondrial apoptotic pathway. *Anticancer. Agents Med. Chem.* **13,** 1575–81 (2013).

463. Kim, M. E., Ha, T. K., Yoon, J. H. & Lee, J. S. Myricetin induces cell death of human colon cancer cells via BAX/BCL2-dependent pathway. *Anticancer Res.* **34,** 701–706 (2014).

464. Kim, W. *et al.* Myricetin Inhibits Akt Survival Signaling and Induces Bad-mediated Apoptosis in a Low Dose Ultraviolet (UV)-B-irradiated HaCaT Human Immortalized Keratinocytes. *J. Radiat. Res.* **51,** 285–296 (2010).

465. Zhang, S., Wang, L., Liu, H., Zhao, G. & Ming, L. Enhancement of recombinant myricetin on the radiosensitivity of lung cancer A549 and H1299 cells. *Diagn. Pathol.* **9,** 68 (2014).

466. Yi, J. L. *et al.* Myricetin and methyl eugenol combination enhances the anticancer activity, cell cycle arrest and apoptosis induction of cis-platin against HeLa cervical cancer cell lines. *Int. J. Clin. Exp. Pathol.* **8,** 1116–1127 (2015).

467. Moulik, S., Pal, S., Biswas, J. & Chatterjee, A. Role of ERK in modulating MMP 2 and MMP 9 with respect to tumour invasiveness in human cancer cell line MCF-7 and MDA-MB-231. *J. Tumor* **2,** 87–98

468. Jung, S. K. *et al.* Myricetin inhibits UVB-induced angiogenesis by regulating PI-3 kinase in vivo. *Carcinogenesis* **31,** 911–7 (2010).

469. Huang, H. *et al.* Dietary compounds galangin and myricetin suppress ovarian cancer cell angiogenesis. *J. Funct. Foods* **15,** 464–475 (2015).

470. Pick, A. *et al.* Structure-activity relationships of flavonoids as inhibitors of breast cancer resistance protein (BCRP). *Bioorganic Med. Chem.* **19,** 2090–2102 (2011).

471. Ragab, F. A., Yahya, T. A. A., El-Naa, M. M. & Arafa, R. K. Design, synthesis and structure-activity relationship of novel semi-synthetic flavonoids as antiproliferative agents. *Eur. J. Med. Chem.* **82C,** 506–520 (2014).

472. Manach, C., Williamson, G., Morand, C., Scalbert, A. & Rémésy, C. Bioavailability and bioefficacy of polyphenols in humans. I. Review of 97 bioavailability studies. *The American journal of clinical nutrition* **81,** (2005).

473. Sun, J. *et al.* LZ-207, a Newly Synthesized Flavonoid, Induces Apoptosis and Suppresses Inflammation-Related Colon Cancer by Inhibiting the NF-κB Signaling Pathway. *PLoS One* **10,** e0127282 (2015).

474. He, A. *et al.* TLR4-MyD88-TRAF6-TAK1 Complex-Mediated NF-κB Activation Contribute to the Anti-Inflammatory Effect of V8 in LPS-Induced Human Cervical Cancer SiHa Cells. *Inflammation* **39,** 172–81 (2016).

475. Yao, N. *et al.* Novel flavonoids with antiproliferative activities against breast cancer cells. *J. Med. Chem.* **54,** 4339–49 (2011).

476. Ou, L. *et al.* Design, synthesis and 3D-QSAR study of cytotoxic flavonoid derivatives. *Mol. Divers.* **15,** 665–

75 (2011).

477. Li, F. *et al.* VI-14, a novel flavonoid derivative, inhibits migration and invasion of human breast cancer cells. *Toxicol. Appl. Pharmacol.* **261,** 217–26 (2012).

478. Yan, C. S. W. *et al.* A New Class of Safe, Potent, and Specific P-gp Modulator: Flavonoid Dimer FD18 Reverses P-gp-Mediated Multidrug Resistance in Human Breast Xenograft in Vivo. *Mol. Pharm.* **12,** 3507–17 (2015).

479. Choueiri, T. K., Wesolowski, R. & Mekhail, T. M. Phenoxodiol: Isoflavone analog with antineoplastic activity. *Curr. Oncol. Rep.* **8,** 104–107 (2006).

480. Mahoney, S. *et al.* Cytotoxic effects of the novel isoflavone, phenoxodiol, on prostate cancer cell lines. *J. Biosci.* **37,** 73–84 (2012).

481. Aguero, M. F., Venero, M., Brown, D. M., Smulson, M. E. & Espinoza, L. A. Phenoxodiol inhibits growth of metastatic prostate cancer cells. *Prostate* **70,** 1211–21 (2010).

482. Mor, G., Fu, H. H., Alvero, A. B. & Mor G. Fu HH. Alvero, A. Phenoxodiol, a novel approach for the treatment of ovarian cancer. *Current Opinion in Investigational Drugs* **7,** 542–548 (2006).

483. Alvero, A. B. *et al.* Molecular mechanism of phenoxodiol-induced apoptosis in ovarian carcinoma cells. *Cancer* **106,** 599–608 (2006).

484. Alvero, A. B., Brown, D., Montagna, M., Matthews, M. & Mor, G. Phenoxodiol-Topotecan co-administration exhibit significant anti-tumor activity without major adverse side effects. *Cancer Biol. Ther.* **6,** 612–7 (2007).

485. McPherson, R. A. C., Galettis, P. T. & de Souza, P. L. Enhancement of the activity of phenoxodiol by cisplatin in prostate cancer cells. *Br. J. Cancer* **100,** 649–55 (2009).

486. De Souza, P. L. *et al.* Phase I and pharmacokinetic study of weekly NV06 (Phenoxodiol), a novel isoflav-3-ene, in patients with advanced cancer. *Cancer Chemother. Pharmacol.* **58,** 427–33 (2006).

487. Howes JB. de Souza PL. West L. Huang LJ. Howes, L. Pharmacokinetics of phenoxodiol, a novel isoflavone, following intravenous administration to patients with advanced cancer. *BMC Clinical Pharmacology* (2011).

488. Kelly, M. G. *et al.* Phase II evaluation of phenoxodiol in combination with cisplatin or paclitaxel in women with platinum/taxane-refractory/resistant epithelial ovarian, fallopian tube, or primary peritoneal cancers. *International Journal of Gynecological Cancer* **21,** 633–639 (2011).

489. Fotopoulou, C. *et al.* Weekly AUC2 carboplatin in acquired platinum-resistant ovarian cancer with or without oral phenoxodiol, a sensitizer of platinum cytotoxicity: the phase III OVATURE multicenter randomized study. *Ann. Oncol.* **25,** 160–5 (2014).

490. Kurkjian, C. *et al.* ME-143 , a novel inhibitor of tumor-specific NADH oxidase (tNOX): Results from a first-in-human phase I study. in *2012 American Society of Clinical Oncology Annual Meeting* (2012).

491. Pant, S. *et al.* A first-in-human dose-escalation study of ME-143, a second generation NADH oxidase inhibitor, in patients with advanced solid tumors. *Invest. New Drugs* **32,** 87–93 (2014).

492. Lim, S. C., Carey, K. T. & McKenzie, M. Anti-cancer analogues ME-143 and ME-344 exert toxicity by directly inhibiting mitochondrial NADH: ubiquinone oxidoreductase (Complex I). *Am. J. Cancer Res.* **5,** 689–701 (2015).

493. Alvero, A. B. *et al.* Abstract LB-286: ME-344 delays tumor kinetics in an ovarian cancer in vivo recurrence model. *Cancer Res.* **73,** LB-286-LB-286 (2014).

494. Bendell, J. C. *et al.* Phase 1, open-label, dose escalation, safety, and pharmacokinetics study of ME-344 as a single agent in patients with refractory solid tumors. *Cancer* **121,** 1056–63 (2015).

495. Manevich, Y. *et al.* Abstract 5409: MEI-344, a novel isoflavone with activity as a mitochondrial oxygenase inhibitor. *Cancer Res.* **75,** 5409–5409 (2015).

496. Antoxis Ltd. Antoxis Platform Technology. Available at: http://www.antoxis.com/technology/technology. (Accessed: 11th April 2016)

497. Bickerton, G. R., Paolini, G. V, Besnard, J., Muresan, S. & Hopkins, A. L. Quantifying the chemical beauty of drugs. *Nat. Chem.* **4,** 90–8 (2012).

498. Lipinski, C. A. Lead- and drug-like compounds: the rule-of-five revolution. *Drug Discov. Today. Technol.* **1,** 337–41 (2004).

499. Lipinski, C. A., Lombardo, F., Dominy, B. W. & Feeney, P. J. Experimental and computational approaches to estimate solubility and permeability in drug discovery and development settings. *Adv. Drug Deliv. Rev.* **46,** 3–25 (2001).

500. Zhang, M.-Q. & Wilkinson, B. Drug discovery beyond the 'rule-of-five'. *Curr. Opin. Biotechnol.* **18,** 478–88 (2007).

501. Kubinyi, H. Opinion: Drug research: myths, hype and reality. *Nat. Rev. Drug Discov.* **2,** 665–668 (2003).

502. Ursu, O., Rayan, A., Goldblum, A. & Oprea, T. I. Understanding drug-likeness. *Wiley Interdis. Rev.: Comp. Mol. Sci.* **1,** 760–781 (2011).

503. Waring, M. J. *et al.* An analysis of the attrition of drug candidates from four major pharmaceutical companies. *Nat. Rev. Drug Discov.* **14,** 475–486 (2015).

504. Mullen, W. *et al.* Determination of Flavonol Metabolites in Plasma and Tissues of Rats by HPLC−Radiocounting and Tandem Mass Spectrometry Following Oral Ingestion of [2- 14 C]Quercetin-4'-glucoside. *J. Agric. Food Chem.* **50,** 6902–6909 (2002).

505. Mitchell, J. H. *et al.* Antioxidant efficacy of phytoestrogens in chemical and biological model systems. *Arch. Biochem. Biophys.* **360,** 142–8 (1998).

506. Kuntz, S. *et al.* Uptake and bioavailability of anthocyanins and phenolic acids from grape/blueberry juice and smoothie in vitro and in vivo. *Br. J. Nutr.* **113,** 1044–55 (2015).

507. Pandareesh, M. D., Mythri, R. B. & Srinivas Bharath, M. M. Bioavailability of dietary polyphenols: Factors contributing to their clinical application in CNS diseases. *Neurochem. Int.* **89,** 198–208 (2015).

508. Caldwell, S. T., Bennett, C. J., Hartley, R. C., McPhail, D. B. & Duthie, G. G. Flavonoid compounds as therapeutic antioxidants. **1,** 1–89 (2007).

509. Caldwell, S. T., McPhail, D. B., Duthie, G. G. & Hartley, R. C. Synthesis of polyhydroxylated flavonoids bearing a lipophilic decyl tail as potential therapeutic antioxidants. *Can. J. Chem.* **90,** 23–33 (2012).

510. McPhail, D. B., Cook, G. J., Johnstone, A. S. & Docherty, K. Protection of mESCs from oxidative stress-induced cell death by a novel class of mitochondrial-targeted, high-potency antioxidant. in *British Pharmacological Society Summer Meeting* **7,** (2009).

511. Brigelius-Flohé, R. & Traber, M. G. Vitamin E: function and metabolism. *FASEB J.* **13,** 1145–55 (1999).

512. Neuzil, J. *et al.* Vitamin E analogues as a novel group of mitocans: anti-cancer agents that act by targeting mitochondria. *Mol. Aspects Med.* **28,** 607–45 (2007).

513. Cheng, G. *et al.* Mitochondria-targeted vitamin E analogs inhibit breast cancer cell energy metabolism and promote cell death. *BMC Cancer* **13,** 285 (2013).

514. Cheng, G. *et al.* Antiproliferative effects of mitochondria-targeted cationic antioxidants and analogs: Role of mitochondrial bioenergetics and energy-sensing mechanism. *Cancer Lett.* **365,** 96–106 (2015).

515. Drummond, N. J. Targeting a custom-engineered flavonoid to the mitochondria protects against acute oxidative stress. (University of Edinburgh, 2014).

516. Toyokuni, S., Okamoto, K., Yodoi, J. & Hiai, H. Persistent oxidative stress in cancer. *FEBS Lett.* **358,** 1–3 (1995).

517. Hileman, E. A., Achanta, G. & Huang, P. Superoxide dismutase: an emerging target for cancer therapeutics. *Expert Opin. Ther. Targets* **5,** 697–710 (2001).

518. Hileman, E. O., Liu, J., Albitar, M., Keating, M. J. & Huang, P. Intrinsic oxidative stress in cancer cells: a biochemical basis for therapeutic selectivity. *Cancer Chemother. Pharmacol.* **53,** 209–19 (2004).

519. Kang, D. & Hamasaki, N. Mitochondrial oxidative stress and mitochondrial DNA. *Clin. Chem. Lab. Med.* **41,** 1281–8 (2003).

520. Pelicano, H., Carney, D. & Huang, P. ROS stress in cancer cells and therapeutic implications. *Drug Resist. Updat.* **7,** 97–110 (2004).

521. Holliday, D. L. & Speirs, V. Choosing the right cell line for breast cancer research. *Breast Cancer Res.* **13,** 215 (2011).

522. Gaffney, E. V. A cell line (HBL-100) established from human breast milk. *Cell Tissue Res* 563–568 (1982).

523. Thompson, E. W. *et al.* The invasive and metastatic properties of hormone-independent but hormone-responsive variants of MCF-7 human breast cancer cells. *Clin. Exp. Metastasis* **11,** 15–26 (1993).

524. Brünner, N. *et al.* MCF7 / LCC2 : A 4-Hydroxytamoxifen Resistant Human Breast Cancer Variant That Retains Sensitivity to the Steroidal Antiestrogen ICI 182,780. *Cancer Res.* **53,** 3229–3232 (1993).

525. Brünner, N. *et al.* MCF7 / LCC9 : An Antiestrogen-resistant MCF-7 Variant in Which Acquired Resistance to the Steroidal Antiestrogen ICI 182 , 780 Confers an Early Cross-Resistance to the Nonsteroidal Antiestrogen Tamoxifen MCF7ILCC9 : An Antiestrogen-resistant to the Nonste. *Cancer Res.* **57,** 3486–3493 (1997).

526. Jørgensen, L. *et al.* Steroid metabolism in the hormone dependent MCF-7 human breast carcinoma cell line and its two hormone resistant subpopulations MCF-7/LCC1 and MCF-7/LCC2. *J. Steroid Biochem. Mol. Biol.* **63,** 275–81 (1997).

527. Langdon, S. P. *et al.* Characterization and Properties of Nine Human Ovarian Adenocarcinoma Cell Lines. *Cancer Res.* **48,** 6166–6172 (1988).

528. Wei, G. *et al.* Chemical genomics identifies small-molecule MCL1 repressors and BCL-xL as a predictor of MCL1 dependency. *Cancer Cell* **21,** 547–62 (2012).

529. Santagata, S. *et al.* Tight coordination of protein translation and HSF1 activation supports the anabolic malignant state. *Science (80-.).* **341,** 1238303 (2013).

530. Barrett, T. *et al.* NCBI GEO: mining millions of expression profiles--database and tools. *Nucleic Acids Res.* **33,** D562-6 (2005).

531. Berthois, Y., Katzenellenbogen, J. a & Katzenellenbogen, B. S. Phenol red in tissue culture media is a weak estrogen: implications concerning the study of estrogen-responsive cells in culture. *Proc. Natl. Acad. Sci. U. S. A.* **83,** 2496–500 (1986).

532. Geraghty, R. J. *et al.* Guidelines for the use of cell lines in biomedical research. *Br. J. Cancer* **111,** 1021–46 (2014).

533. Soltis, R. D., Hasz, D., Morris, M. J. & Wilson, I. D. The effect of heat inactivation of serum on aggregation of immunoglobulins. *Immunology* **36,** 37–45 (1979).

534. Skehan, P. *et al.* New Colorimetric Cytotoxicity Assay for anticancer-drug screening. *J Natl Cancer Inst* **82,** 1107–1112 (1990).

535. Voigt, W. Sulforhodamine B assay and chemosensitivity. *Methods Mol. Med.* 39–48 (2005).

536. Vichai, V. & Kirtikara, K. Sulforhodamine B colorimetric assay for cytotoxicity screening. *Nat. Protoc.* **1,** 1112–1116 (2006).

537. Fricker, S. P. The application of sulforhodamine B as a colorimetric endpoint in a cytotoxicity assay. *Toxicol. Vitr.* **8,** 821–822 (1994).

538. Dickinson, B. C. & Chang, C. J. A targetable fluorescent probe for imaging hydrogen peroxide in the mitochondria of living cells. *J. Am. Chem. Soc.* **130,** 9638–9 (2008).

539. Robinson, K. M. *et al.* Selective fluorescent imaging of superoxide in vivo using ethidium-based probes. *Proc. Natl. Acad. Sci. U. S. A.* **103,** 15038–43 (2006).

540. Camp, R. L., Chung, G. G. & Rimm, D. L. Automated subcellular localization and quantification of protein expression in tissue microarrays. *Nat. Med.* **8,** 1323–1328 (2002).

541. Du, P., Kibbe, W. A. & Lin, S. M. lumi: a pipeline for processing Illumina microarray. *Bioinformatics* **24,** 1547–8 (2008).

542. Turnbull, A. K. *et al.* Direct integration of intensity-level data from Affymetrix and Illumina microarrays improves statistical power for robust reanalysis. *BMC Med. Genomics* **5,** 35 (2012).

543. Huang, D. W., Sherman, B. T. & Lempicki, R. A. Systematic and integrative analysis of large gene lists using DAVID bioinformatics resources. *Nat. Protoc.* **4,** 44–57 (2009).

544. Huang, D. W., Sherman, B. T. & Lempicki, R. A. Bioinformatics enrichment tools: paths toward the comprehensive functional analysis of large gene lists. *Nucleic Acids Res.* **37,** 1–13 (2009).

545. Johnson, W. E., Li, C. & Rabinovic, A. Adjusting batch effects in microarray expression data using empirical Bayes methods. *Biostatistics* **8,** 118–127 (2007).

546. Chen, Y., Meltzer, P. S., Chen, Y. & Meltzer, P. S. in *Current Protocols in Bioinformatics* 7.11.1-7.11.9 (John Wiley & Sons, Inc., 2005). doi:10.1002/0471250953.bi0711s10

547. Tzeng, J. *et al.* Multidimensional scaling for large genomic data sets. *BMC Bioinformatics* **9,** 179 (2008).

548. The Gene Ontology Consortium. Gene Ontology Consortium: going forward. *Nucleic Acids Res.* **43,** D1049–D1056 (2015).

549. Ashburner, M. *et al.* Gene Ontology: tool for the unification of biology. *Nat. Genet.* **25,** 25–29 (2000).

550. Supek, F., Bošnjak, M., Škunca, N. & Šmuc, T. REVIGO Summarizes and Visualizes Long Lists of Gene Ontology Terms. *PLoS One* **6,** e21800 (2011).

551. Saeed, A. I. *et al.* TM4: a free, open-source system for microarray data management and analysis. *Biotechniques* **34,** 374–8 (2003).

552. Saeed, A. I. *et al.* TM4 microarray software suite. *Methods Enzymol.* **411,** 134–93 (2006).

553. Workman, P. *et al.* Guidelines for the welfare and use of animals in cancer research. *Br. J. Cancer* **102,** 1555–77 (2010).

554. Rice-Evans, C. A., Miller, N. J. & Paganga, G. Structure-antioxidant activity relationships of flavonoids and phenolic acids. *Free Radic. Biol. Med.* **20,** 933–956 (1996).

555. Rice, J. E. *Organic Chemistry Concepts and Applications for Medicinal Chemistry (Chapter 3: Functional Groups)*. *Organic Chemistry Concepts and Applications for Medicinal Chemistry* (Elsevier, 2014).

doi:10.1016/B978-0-12-800739-6.00003-6

556. Walle, T. *et al.* Cancer chemopreventive properties of orally bioavailable flavonoids--methylated versus unmethylated flavones. *Biochem. Pharmacol.* **73,** 1288–96 (2007).

557. Lewandowska, U., Fichna, J. & Gorlach, S. Enhancement of anticancer potential of polyphenols by covalent modifications. *Biochem. Pharmacol.* **109,** 1–13 (2016).

558. Sassi, N. *et al.* Mitochondria-targeted Resveratrol Derivatives Act as Cytotoxic Pro-oxidants. *Curr. Pharm. Des.* **20,** 172–179 (2014).

559. Walle, T. Methylation of Dietary Flavones Greatly Improves Their Hepatic Metabolic Stability and Intestinal Absorption. *Mol. Pharm.* **4,** 166–170 (2007).

560. Androutsopoulos, V., Arroo, R. R. J., Hall, J. F., Surichan, S. & Potter, G. a. Antiproliferative and cytostatic effects of the natural product eupatorin on MDA-MB-468 human breast cancer cells due to CYP1-mediated metabolism. *Breast Cancer Res.* **10,** R39 (2008).

561. Heim, K. E., Tagliaferro, A. R. & Bobilya, D. J. Flavonoid antioxidants: chemistry, metabolism and structure-activity relationships. *J. Nutr. Biochem.* **13,** 572–584 (2002).

562. Bisby, R. H. & Parker, A. W. Reaction of ascorbate with the alpha-tocopheroxyl radical in micellar and bilayer membrane systems. *Arch. Biochem. Biophys.* **317,** 170–8 (1995).

563. Schiff, R. *et al.* Oxidative Stress and AP-1 Activity in Tamoxifen- Resistant Breast Tumors In Vivo. *J. Natl. Cancer Inst.* **92,** 1926–1934 (2000).

564. Dong, L.-F. *et al.* Mitochondrial targeting of α-tocopheryl succinate enhances its pro-apoptotic efficacy: a new paradigm for effective cancer therapy. *Free Radic. Biol. Med.* **50,** 1546–55 (2011).

565. Wang, X.-F. *et al.* Vitamin E analogues as anticancer agents: lessons from studies with alpha-tocopheryl succinate. *Mol. Nutr. Food Res.* **50,** 675–85 (2006).

566. Neuzil, J. *et al.* Induction of cancer cell apoptosis by alpha-tocopheryl succinate: molecular pathways and structural requirements. *FASEB J.* **15,** 403–15 (2001).

567. Prasad, K. N., Kumar, B., Yan, X.-D., Hanson, A. J. & Cole, W. C. Alpha-tocopheryl succinate, the most effective form of vitamin E for adjuvant cancer treatment: a review. *J. Am. Coll. Nutr.* **22,** 108–17 (2003).

568. Auchinvole, C. A. R. *et al.* Monitoring intracellular redox potential changes using SERS nanosensors. *ACS Nano* **6,** 888–96 (2012).

569. Mallikarjun, V., Clarke, D. J. & Campbell, C. J. Cellular redox potential and the biomolecular electrochemical series: a systems hypothesis. *Free Radic. Biol. Med.* **53,** 280–8 (2012).

570. Long, L. H., Clement, M. V. & Halliwell, B. Artifacts in Cell Culture: Rapid Generation of Hydrogen Peroxide on Addition of (−)-Epigallocatechin, (−)-Epigallocatechin Gallate, (+)-Catechin, and Quercetin to Commonly Used Cell Culture Media. *Biochem. Biophys. Res. Commun.* **273,** 50–53 (2000).

571. Szeto, H. H. Cell-permeable, mitochondrial-targeted, peptide antioxidants. *AAPS J.* **8,** E277-83 (2006).

572. Li, X. *et al.* Targeting mitochondrial reactive oxygen species as novel therapy for inflammatory diseases and cancers. *J. Hematol. Oncol.* **6,** 19 (2013).

573. Silva, M. T. Secondary necrosis: The natural outcome of the complete apoptotic program. *FEBS Lett.* **584,** 4491–4499 (2010).

574. Vanden Berghe, T. *et al.* Necroptosis, necrosis and secondary necrosis converge on similar cellular disintegration features. *Cell Death Differ.* **17,** 922–930 (2010).

575. Janicke, R. U. MCF-7 breast carcinoma cells do not express caspase-3. *Breast Cancer Res Treat* **117,** 219–221 (2009).

576. Devarajan, E. *et al.* Down-regulation of caspase 3 in breast cancer: a possible mechanism for chemoresistance. *Oncogene* **21,** 8843–8851 (2002).

577. Soldani, C. & Scovassi, A. I. Poly(ADP-ribose) polymerase-1 cleavage during apoptosis: An update. *APOPTOSIS* **7,** 321–328 (2002).

578. Lazebnik, Y. A., Kaufmann, S. H., Desnoyers, S., Poirier, G. G. & Earnshaw, W. C. Cleavage of poly(ADP-ribose) polymerase by a proteinase with properties like ICE. *Nature* **371,** 346–7 (1994).

579. Curtin, J. F., Donovan, M. & Cotter, T. G. Regulation and measurement of oxidative stress in apoptosis. *J. Immunol. Methods* **265,** 49–72 (2002).

580. Sun, S.-Y. N-acetylcysteine, reactive oxygen species and beyond. *Cancer Biol. Ther.* **9,** 109–10 (2010).

581. Halasi, M. *et al.* ROS inhibitor N-acetyl-L-cysteine antagonizes the activity of proteasome inhibitors. *Biochem. J.* **454,** 201–8 (2013).

582. Kerr, J. F. R., Wyllie, A. H. & Currie, A. R. Apoptosis: A Basic Biological Phenomenon with Wideranging Implications in Tissue Kinetics. *Br. J. Cancer* **26,** 239–257 (1972).

583. Estaquier, J., Vallette, F., Vayssiere, J. L. & Mignotte, B. in *Advances in Experimental Medicine and Biology* **942,** 157–183 (Springer Netherlands, 2012).

584. Wang, C. & Youle, R. J. The role of mitochondria in apoptosis. *Annu. Rev. Genet.* **43,** 95–118 (2009).

585. Parsons, M. J. *et al.* Mitochondria in cell death. *Essays Biochem.* **47,** 99–114 (2010).

586. Pradelli, L. A., Bénéteau, M. & Ricci, J.-E. Mitochondrial control of caspase-dependent and -independent cell death. *Cell. Mol. Life Sci.* **67,** 1589–1597 (2010).

587. Chalah, A. & Khosravi-Far, R. in *Advances in Experimental Medicine and Biology* **615,** 25–45 (Springer Netherlands, 2008).

588. Cai, J., Yang, J. & Jones, D. P. Mitochondrial control of apoptosis: the role of cytochrome c. *Biochim. Biophys. Acta* **1366,** 139–149 (1998).

589. Gogvadze, V., Orrenius, S. & Zhivotovsky, B. Multiple pathways of cytochrome c release from mitochondria in apoptosis. *Biochim. Biophys. Acta - Bioenerg.* **1757,** 639–647 (2006).

590. Chipuk, J. E., Bouchier-Hayes, L. & Green, D. R. Mitochondrial outer membrane permeabilization during apoptosis: the innocent bystander scenario. *Cell Death Differ.* **13,** 1396–1402 (2006).

591. Crompton, M. The mitochondrial permeability transition pore and its role in cell death. *Biochem. J.* **341 (Pt 2,** 233–249 (1999).

592. Indran, I. R., Tufo, G., Pervaiz, S. & Brenner, C. Recent advances in apoptosis, mitochondria and drug resistance in cancer cells. *Biochim. Biophys. Acta* **1807,** 735–45 (2011).

593. Tajeddine, N. How do reactive oxygen species and calcium trigger mitochondrial membrane permeabilisation? *Biochim. Biophys. Acta* **1860,** 1079–1088 (2016).

594. Zoratti, M. & Szabò, I. The mitochondrial permeability transition. *Biochim. Biophys. Acta - Rev. Biomembr.* **1241,** 139–176 (1995).

595. Madesh, M. & Hajnóczky, G. VDAC-dependent permeabilization of the outer mitochondrial membrane by superoxide induces rapid and massive cytochrome c release. *J. Cell Biol.* **155,** 1003–15 (2001).

596. Kuznetsov, A. V., Margreiter, R., Amberger, A., Saks, V. & Grimm, M. Changes in mitochondrial redox state, membrane potential and calcium precede mitochondrial dysfunction in doxorubicin-induced cell death. *Biochim. Biophys. Acta - Mol. Cell Res.* **1813,** 1144–1152 (2011).

597. Görlach, A., Bertram, K., Hudecova, S. & Krizanova, O. Calcium and ROS: A mutual interplay. *Redox Biology* **6,** 260–271 (2015).

598. Ola, M. S., Nawaz, M. & Ahsan, H. Role of Bcl-2 family proteins and caspases in the regulation of apoptosis. *Mol. Cell. Biochem.* **351,** 41–58 (2011).

599. Chipuk, J. E. & Green, D. R. How do BCL-2 proteins induce mitochondrial outer membrane permeabilization? *Trends Cell Biol.* **18,** 157–64 (2008).

600. Green, D. R. & Kroemer, G. The pathophysiology of mitochondrial cell death. *Science* **305,** 626–9 (2004).

601. Azad, N. *et al.* Role of oxidative/nitrosative stress-mediated Bcl-2 regulation in apoptosis and malignant transformation. *Ann. N. Y. Acad. Sci.* **1203,** 1–6 (2010).

602. Azad, N., Iyer, A. K. V, Manosroi, A., Wang, L. & Rojanasakul, Y. Superoxide-mediated proteasomal degradation of Bcl-2 determines cell susceptibility to Cr(VI)-induced apoptosis. *Carcinogenesis* **29,** 1538–45 (2008).

603. Luanpitpong, S. *et al.* Mitochondrial superoxide mediates doxorubicin-induced keratinocyte apoptosis through oxidative modification of ERK and Bcl-2 ubiquitination. *Biochem. Pharmacol.* **83,** 1643–1654 (2012).

604. Ahmad, K. A., Iskandar, K. B., Hirpara, J. L., Clement, M.-V. & Pervaiz, S. Hydrogen peroxide-mediated cytosolic acidification is a signal for mitochondrial translocation of Bax during drug-induced apoptosis of tumor cells. *Cancer Res.* **64,** 7867–78 (2004).

605. Beckman, J. S., Beckman, T. W., Chen, J., Marshall, P. A. & Freeman, B. A. Apparent hydroxyl radical production by peroxynitrite: implications for endothelial injury from nitric oxide and superoxide. *Proc. Natl. Acad. Sci. U. S. A.* **87,** 1620–1624 (1990).

606. Yan, L. J., Levine, R. L. & Sohal, R. S. Oxidative damage during aging targets mitochondrial aconitase. *Proc. Natl. Acad. Sci. U. S. A.* **94,** 11168–72 (1997).

607. Vásquez-Vivar, J., Kalyanaraman, B. & Kennedy, M. C. Mitochondrial aconitase is a source of hydroxyl radical. An electron spin resonance investigation. *J. Biol. Chem.* **275,** 14064–14069 (2000).

608. James, A. M. & Murphy, M. P. How mitochondrial damage affects cell function. *J. Biomed. Sci.* **9,** 475–87

(2002).

609. Scatena, R. in *Advances in Experimental Medicine and Biology* **942,** 287–308 (Springer Netherlands, 2012).

610. Huang, P., Feng, L., Oldham, E. A., Keating, M. J. & Plunkett, W. Superoxide dismutase as a target for the selective killing of cancer cells. *Nature* **407,** 390–395 (2000).

611. Yokomizo, A. *et al.* Cellular levels of thioredoxin associated with drug sensitivity to cisplatin, mitomycin C, doxorubicin, and etoposide. *Cancer Res.* **55,** 4293–4296 (1995).

612. Ferlini, C. *et al.* Tamoxifen induces oxidative stress and apoptosis in oestrogen receptor-negative human cancer cell lines. *Br. J. Cancer* **79,** 257–63 (1999).

613. Sumida, K. *et al.* Effects of DMSO on gene expression in human and rat hepatocytes. *Hum. Exp. Toxicol.* **30,** 1701–9 (2011).

614. Bardou, P. *et al.* jvenn: an interactive Venn diagram viewer. *BMC Bioinformatics* **15,** 293 (2014).

615. Hulsen, T. *et al.* BioVenn – a web application for the comparison and visualization of biological lists using area-proportional Venn diagrams. *BMC Genomics* **9,** 488 (2008).

616. Zheng, J. Energy metabolism of cancer: Glycolysis versus oxidative phosphorylation. *Oncology Letters* **4,** 1151–1157 (2012).

617. Koppenol, W. H., Bounds, P. L. & Dang, C. V. Otto Warburg's contributions to current concepts of cancer metabolism. *Nat. Rev. Cancer* **11,** 325–37 (2011).

618. Kroemer, G. Mitochondria in cancer. *Oncogene* **25,** 4630–4632 (2006).

619. Brown, N. N. S. *et al.* Hypoxia and oxidative stress in breast cancer. Oxidative stress: its effects on the growth, metastatic potential and response to therapy of breast cancer. *Breast Cancer Res.* **3,** 323–7 (2001).

620. Boland, M. L., Chourasia, A. H. & Macleod, K. F. Mitochondrial dysfunction in cancer. *Front. Oncol.* **3,** 292 (2013).

621. Granchi, C. & Minutolo, F. Anticancer agents that counteract tumor glycolysis. *ChemMedChem* **7,** 1318–50 (2012).

622. Granchi, C., Fancelli, D. & Minutolo, F. An update on therapeutic opportunities offered by cancer glycolytic metabolism. *Bioorg. Med. Chem. Lett.* **24,** 4915–4925 (2014).

623. Shan, D. *et al.* Abnormal partitioning of hexokinase 1 suggests disruption of a glutamate transport protein complex in schizophrenia. *Schizophr. Res.* **154,** 1–13 (2014).

624. Cárdenas, M. L., Cornish-Bowden, A. & Ureta, T. Evolution and regulatory role of the hexokinases. *Biochimica et Biophysica Acta - Molecular Cell Research* **1401,** 242–264 (1998).

625. Galluzzi, L., Kepp, O., Tajeddine, N. & Kroemer, G. Disruption of the hexokinase-VDAC complex for tumor therapy. *Oncogene* **27,** 4633–5 (2008).

626. Dhanasekaran, D. N. & Reddy, E. P. JNK signaling in apoptosis. *Oncogene* **27,** 6245–51 (2008).

627. Nishina, H., Wada, T. & Katada, T. Physiological Roles of SAPK/JNK Signaling Pathway. *J. Biochem.* **136,** 123–126 (2004).

628. Zhou, Y.-Y. *et al.* MAPK/JNK signaling: A potential autophagy regulation pathway. *Biosci. Rep.* **35,** 931–937 (2015).

629. Lin, A. Activation of the JNK signaling pathway: Breaking the brake on apoptosis. *BioEssays* **25,** 17–24 (2003).

630. Fanger, G. R., Gerwins, P., Widmann, C., Jarpe, M. B. & Johnson, G. L. MEKKs, GCKs, MLKs, PAKs, TAKs, and Tpls: upstream regulators of the c-Jun amino-terminal kinases? *Curr. Opin. Genet. Dev.* **7,** 67–74 (1997).

631. Karin, M. The regulation of AP-1 activity by mitogen-activated protein kinases. *Journal of Biological Chemistry* **270,** 16483–16486 (1995).

632. Shaulian, E. & Karin, M. AP-1 as a regulator of cell life and death. *Nat Cell Biol* **4,** E131-6 (2002).

633. Zhang, J. & Ney, P. A. Role of BNIP3 and NIX in cell death, autophagy, and mitophagy. *Cell Death Differ.* **16,** 939–46 (2009).

634. Imazu, T. *et al.* Bcl-2/E1B 19 kDa-interacting protein 3-like protein (Bnip3L) interacts with bcl-2/Bcl-xL and induces apoptosis by altering mitochondrial membrane permeability. *Oncogene* **18,** 4523–4529 (1999).

635. Burton, T. R. & Gibson, S. B. The role of Bcl-2 family member BNIP3 in cell death and disease: NIPping at the heels of cell death. *Cell Death Differ.* **16,** 515–23 (2009).

636. Zou, H., Henzel, W. J., Liu, X., Lutschg, A. & Wang, X. Apaf-1, a Human Protein Homologous to C. elegans CED-4, Participates in Cytochrome c–Dependent Activation of Caspase-3. *Cell* **90,** 405–413 (1997).

637. Li, P. *et al.* Cytochrome c and dATP-Dependent Formation of Apaf-1/Caspase-9 Complex Initiates an

Apoptotic Protease Cascade. *Cell* **91,** 479–489 (1997).

638. Zou, H., Li, Y., Liu, X. & Wang, X. An APAF-1·Cytochrome c Multimeric Complex Is a Functional Apoptosome That Activates Procaspase-9. *J. Biol. Chem.* **274,** 11549–11556 (1999).
639. Ho, K. K., Myatt, S. S. & Lam, E. W.-F. Many forks in the path: cycling with FoxO. *Oncogene* **27,** 2300–2311 (2008).
640. Fu, Z. & Tindall, D. J. FOXOs, cancer and regulation of apoptosis. *Oncogene* **27,** 2312–9 (2008).
641. Ferber, E. C. *et al.* FOXO3a regulates reactive oxygen metabolism by inhibiting mitochondrial gene expression. *Cell Death Differ.* **19,** 968–79 (2012).
642. Kops, G. J. P. L. *et al.* Forkhead transcription factor FOXO3a protects quiescent cells from oxidative stress. *Nature* **419,** 316–321 (2002).
643. Lee, J. C. *et al.* DEDD regulates degradation of intermediate filaments during apoptosis. *J. Cell Biol.* **158,** 1051–66 (2002).
644. Roth, W., Stenner-Liewen, F., Pawlowski, K., Godzik, A. & Reed, J. C. Identification and characterization of DEDD2, a death effector domain-containing protein. *J. Biol. Chem.* **277,** 7501–7508 (2002).
645. Sahara, S. *et al.* Acinus is a caspase-3-activated protein required for apoptotic chromatin condensation. *Nature* **401,** 168–73 (1999).
646. Chourasia, A. H., Boland, M. L. & Macleod, K. F. Mitophagy and cancer. *Cancer Metab.* **3,** 4 (2015).
647. Ding, W.-X. & Yin, X.-M. Mitophagy: mechanisms, pathophysiological roles, and analysis. *Biol. Chem.* **393,** 547–64 (2012).
648. Liu, L. *et al.* Mitochondrial outer-membrane protein FUNDC1 mediates hypoxia-induced mitophagy in mammalian cells. *Nat Cell Biol* **14,** 177–185 (2012).
649. Zimmermann, M. *et al.* Elevated cyclin G2 expression intersects with DNA damage checkpoint signaling and is required for a potent G2/M checkpoint arrest response to doxorubicin. *J. Biol. Chem.* **287,** 22838–22853 (2012).
650. Roos-Mattjus, P. *et al.* Genotoxin-induced Rad9-Hus1-Rad1 (9-1-1) chromatin association is an early checkpoint signaling event. *J. Biol. Chem.* **277,** 43809–43812 (2002).
651. Parrilla-Castellar, E. R., Arlander, S. J. H. & Karnitz, L. Dial 9-1-1 for DNA damage: The Rad9-Hus1-Rad1 (9-1-1) clamp complex. *DNA Repair* **3,** 1009–1014 (2004).
652. Sterrenberg, J. N., Blatch, G. L. & Edkins, A. L. Human DNAJ in cancer and stem cells. *Cancer Lett.* **312,** 129–142 (2011).
653. Huang, L., Yu, Z., Zhang, T., Zhao, X. & Huang, G. HSP40 interacts with pyruvate kinase M2 and regulates glycolysis and cell proliferation in tumor cells. *PLoS One* **9,** e92949 (2014).
654. Fulda, S., Gorman, A. M., Hori, O. & Samali, A. Cellular stress responses: Cell survival and cell death. *International Journal of Cell Biology* **2010,** 214074 (2010).
655. Beere, H. M. Death versus survival: functional interaction between the apoptotic and stress-inducible heat shock protein pathways. *J. Clin. Invest.* **115,** 2633–9 (2005).
656. Baldin, V., Lukas, J., Marcote, M. J., Pagano, M. & Draetta, G. Cyclin D1 is a nuclear protein required for cell cycle progression in G1. *Genes Dev.* **7,** 812–821 (1993).
657. Diehl, J. A. Cycling to cancer with cyclin D1. *Cancer Biology and Therapy* **1,** 226–231 (2002).
658. Gavet, O. & Pines, J. Progressive Activation of CyclinB1-Cdk1 Coordinates Entry to Mitosis. *Dev. Cell* **18,** 533–543 (2010).
659. De Souza, C. P. C., Ellem, K. A. O. & Gabrielli, B. G. Centrosomal and cytoplasmic Cdc2/cyclin B1 activation precedes nuclear mitotic events. *Exp. Cell Res.* **257,** 11–21 (2000).
660. Fang, G., Yu, H. & Kirschner, M. W. Direct binding of CDC20 protein family members activates the anaphase-promoting complex in mitosis and G1. *Mol Cell* **2,** 163–171 (1998).
661. Vaux, D. L., Cory, S. & Adams, J. M. Bcl-2 gene promotes haemopoietic cell survival and cooperates with c-myc to immortalize pre-B cells. *Nature* **335,** 440–442 (1988).
662. Youle, R. J. & Strasser, A. The BCL-2 protein family: opposing activities that mediate cell death. *Nat. Rev. Mol. Cell Biol.* **9,** 47–59 (2008).
663. Morgan, D. O. Cyclin-dependent kinases: engines, clocks, and microprocessors. *Annu Rev Cell Dev Biol* **13,** 261–291 (1997).
664. Yam, C. H., Fung, T. K. & Poon, R. Y. C. Cyclin A in cell cycle control and cancer. *Cell. Mol. Life Sci.* **59,** 1317–1326 (2002).

665. Gong, D. & Ferrell, J. E. The Roles of Cyclin A2, B1, and B2 in Early and Late Mitotic Events. *Mol. Biol. Cell* **21,** 3149–3161 (2010).

666. Maiorano, D., Lutzmann, M. & Méchali, M. MCM proteins and DNA replication. *Curr. Opin. Cell Biol.* **18,** 130–136 (2006).

667. Crane, R., Gadea, B., Littlepage, L., Wu, H. & Ruderman, J. V. Aurora A, Meiosis and Mitosis. *Biol. Cell* **96,** 215–229 (2004).

668. Bomont, P., Maddox, P., Shah, J. V, Desai, A. B. & Cleveland, D. W. Unstable microtubule capture at kinetochores depleted of the centromere-associated protein CENP-F. *EMBO J.* **24,** 3927–39 (2005).

669. Wordeman, L. How kinesin motor proteins drive mitotic spindle function: Lessons from molecular assays. **21,** 260–268 (2010).

670. Vagnarelli, P. in *Cancer Biology and the Nuclear Envelope* 401–414 (Springer New York, 2014). doi:10.1007/978-1-4899-8032-8_18

671. Vogel, C. & Marcotte, E. M. Insights into the regulation of protein abundance from proteomic and transcriptomic analyses. *Nat. Rev. Genet.* **13,** 227–232 (2012).

672. Sinha, K., Das, J., Pal, P. B. & Sil, P. C. Oxidative stress: the mitochondria-dependent and mitochondria-independent pathways of apoptosis. *Arch. Toxicol.* **87,** 1157–1180 (2013).

673. Lei, K. *et al.* The Bax Subfamily of Bcl2-Related Proteins Is Essential for Apoptotic Signal Transduction by c-Jun NH2-Terminal Kinase. *Mol. Cell. Biol.* **22,** 4929–4942 (2002).

674. Fan, M., Goodwin, M. E., Birrer, M. J. & Chambers, T. C. The c-Jun NH(2)-terminal protein kinase/AP-1 pathway is required for efficient apoptosis induced by vinblastine. *Cancer Res.* **61,** 4450–8 (2001).

675. Jin, H.-O. *et al.* Up-regulation of Bak and Bim via JNK downstream pathway in the response to nitric oxide in human glioblastoma cells. *J. Cell. Physiol.* **206,** 477–86 (2006).

676. Kharbanda, S. *et al.* Translocation of SAPK/JNK to Mitochondria and Interaction with Bcl-xL in Response to DNA Damage. *J. Biol. Chem.* **275,** 322–327 (2000).

677. Fan, M. *et al.* Vinblastine-induced Phosphorylation of Bcl-2 and Bcl-XL Is Mediated by JNK and Occurs in Parallel with Inactivation of the Raf-1/MEK/ERK Cascade. *J. Biol. Chem.* **275,** 29980–29985 (2000).

678. Matsuyoshi, S., Shimada, K., Nakamura, M., Ishida, E. & Konishi, N. Bcl-2 Phosphorylation Has Pathological Significance in Human Breast Cancer. *Pathobiology* **73,** 205–212 (2006).

679. Wei, Y., Sinha, S. C. & Levine, B. Dual Role of JNK1-mediated phosphorylation of Bcl-2 in autophagy and apoptosis regulation. *Autophagy* **4,** 949–951 (2008).

680. Haldar, S., Chintapalli, J. & Croce, C. M. Taxol Induces bcl-2 Phosphorylation and Death of Prostate Cancer Cells Taxol Induces bcl-2 Phosphorylation and Death of Prostate Cancer Cells1. *Cancer Res.* **56,** 1253–1255 (1996).

681. Schmidt, M. *et al.* Cell cycle inhibition by FoxO forkhead transcription factors involves downregulation of cyclin D. *Mol. Cell. Biol.* **22,** 7842–52 (2002).

682. Zhang, X., Tang, N., Hadden, T. J. & Rishi, A. K. Akt, FoxO and regulation of apoptosis. *Biochim. Biophys. Acta - Mol. Cell Res.* **1813,** 1978–1986 (2011).

683. Peck, B., Ferber, E. C. & Schulze, A. Antagonism between FOXO and MYC Regulates Cellular Powerhouse. *Front. Oncol.* **3,** 96 (2013).

684. Hagenbuchner, J. *et al.* FOXO3-induced reactive oxygen species are regulated by BCL2L11 (Bim) and SESN3. *J. Cell Sci.* **125,** 1191–203 (2012).

685. Sunters, A. *et al.* Paclitaxel-induced nuclear translocation of FOXO3a in breast cancer cells is mediated by c-Jun NH2-terminal kinase and Akt. *Cancer Res.* **66,** 212–20 (2006).

686. Sunayama, J., Tsuruta, F., Masuyama, N. & Gotoh, Y. JNK antagonizes Akt-mediated survival signals by phosphorylating 14-3-3. *J. Cell Biol.* **170,** 295–304 (2005).

687. Oh, S. W. *et al.* JNK regulates lifespan in Caenorhabditis elegans by modulating nuclear translocation of forkhead transcription factor/DAF-16. *Proc. Natl. Acad. Sci. U. S. A.* **102,** 4494–9 (2005).

688. Essers, M. A. G. *et al.* FOXO transcription factor activation by oxidative stress mediated by the small GTPase Ral and JNK. *EMBO J.* **23,** 4802–12 (2004).

689. Zhou, Y.-Y., Li, Y., Jiang, W.-Q. & Zhou, L.-F. MAPK/JNK signalling: a potential autophagy regulation pathway. *Biosci. Rep.* **35,** e00199 (2015).

690. Gilley, J., Coffer, P. J. & Ham, J. FOXO transcription factors directly activate bim gene expression and promote apoptosis in sympathetic neurons. *J. Cell Biol.* **162,** 613–22 (2003).

691. Chinnadurai, G., Vijayalingam, S. & Gibson, S. B. BNIP3 subfamily BH3-only proteins: mitochondrial stress

sensors in normal and pathological functions. *Oncogene* **27 Suppl 1,** S114-27 (2008).

692. Maiuri, M. C., Zalckvar, E., Kimchi, A. & Kroemer, G. Self-eating and self-killing: crosstalk between autophagy and apoptosis. *Nat. Rev. Mol. Cell Biol.* **8,** 741–752 (2007).
693. Ray, R. *et al.* BNIP3 heterodimerizes with Bcl-2/Bcl-X(L) and induces cell death independent of a Bcl-2 homology 3 (BH3) domain at both mitochondrial and nonmitochondrial sites. *J. Biol. Chem.* **275,** 1439–1448 (2000).
694. Guo, K. *et al.* Hypoxia induces the expression of the pro-apoptotic gene BNIP3. *Cell Death Differ.* **8,** 367–376 (2001).
695. Kops, G. J. P. L. *et al.* Control of cell cycle exit and entry by protein kinase B-regulated forkhead transcription factors. *Mol. Cell. Biol.* **22,** 2025–36 (2002).
696. Martinez-Gac, L., Marques, M., Garcia, Z., Campanero, M. R. & Carrera, A. C. Control of Cyclin G2 mRNA Expression by Forkhead Transcription Factors: Novel Mechanism for Cell Cycle Control by Phosphoinositide 3-Kinase and Forkhead. *Mol. Cell. Biol.* **24,** 2181–2189 (2004).
697. Signoretti, S. *et al.* Oncogenic role of the ubiquitin ligase subunit Skp2 in human breast cancer. *J. Clin. Invest.* **110,** 633–641 (2002).
698. Zou, G., Reddy, Y. K. & Falck, J. R. Ag(I)-promoted Suzuki–Miyaura cross-couplings of n-alkylboronic acids. *Tetrahedron Lett.* **42,** 7213–7215 (2001).
699. Takano, M. *et al.* Transcriptional cross talk between the forkhead transcription factor forkhead box O1A and the progesterone receptor coordinates cell cycle regulation and differentiation in human endometrial stromal cells. *Mol. Endocrinol.* **21,** 2334–49 (2007).
700. Essaghir, A., Dif, N., Marbehant, C. Y., Coffer, P. J. & Demoulin, J.-B. The Transcription of FOXO Genes Is Stimulated by FOXO3 and Repressed by Growth Factors. *J. Biol. Chem.* **284,** 10334–10342 (2009).
701. Qi, W. *et al.* Genistein inhibits proliferation of colon cancer cells by attenuating a negative effect of epidermal growth factor on tumor suppressor FOXO3 activity. *BMC Cancer* **11,** 219 (2011).
702. Davis, R. J. Signal Transduction by the JNK Group of MAP Kinases. *Cell* **103,** 239–252 (2000).
703. Wang, X., Chen, W. R. & Xing, D. A pathway from JNK through decreased ERK and Akt activities for FOXO3a nuclear translocation in response to UV irradiation. *J. Cell. Physiol.* **227,** 1168–1178 (2012).
704. Conde de la Rosa, L. *et al.* Superoxide anions and hydrogen peroxide induce hepatocyte death by different mechanisms: Involvement of JNK and ERK MAP kinases. *J. Hepatol.* **44,** 918–929 (2006).
705. Blatt, N. B., Boitano, A. E., Lyssiotis, C. A., Opipari, A. W. & Glick, G. D. Bz-423 superoxide signals apoptosis via selective activation of JNK, Bak, and Bax. *Free Radic. Biol. Med.* **45,** 1232–1242 (2008).
706. Che, X. F. *et al.* 2-Aminophenoxazine-3-one-induced apoptosis via generation of reactive oxygen species followed by c-jun N-terminal kinase activation in the human glioblastoma cell line LN229. *Int. J. Oncol.* **43,** 1456–1466 (2013).
707. Warburg, O. Über den Stoffwechsel der Carcinomzelle. *Naturwissenschaften* **12,** 1131–1137 (1924).
708. WEINHOUSE, S. On respiratory impairment in cancer cells. *Science (80-.).* **124,** 267–9 (1956).
709. Weinberg, S. E. & Chandel, N. S. Targeting mitochondria metabolism for cancer therapy. *Nat. Chem. Biol.* **11,** 9–15 (2015).
710. Ward, P. S. & Thompson, C. B. Metabolic reprogramming: a cancer hallmark even Warburg did not anticipate. *Cancer Cell* **21,** 297–308 (2012).
711. Zu, X. L. & Guppy, M. Cancer metabolism: facts, fantasy, and fiction. *Biochem. Biophys. Res. Commun.* **313,** 459–465 (2004).
712. Ros, S. & Schulze, A. Glycolysis back in the limelight: Systemic targeting of HK2 blocks tumor growth. *Cancer Discov.* **3,** 1105–1107 (2013).
713. Rumsey, W. L., Schlosser, C., Nuutinen, E. M., Robiolio, M. & Wilson, D. F. Cellular energetics and the oxygen dependence of respiration in cardiac myocytes isolated from adult rat. *J. Biol. Chem.* **265,** 15392–402 (1990).
714. Semenza, G. L. Targeting HIF-1 for cancer therapy. *Nat. Rev. Cancer* **3,** 721–732 (2003).
715. Macheda, M. L., Rogers, S. & Best, J. D. Molecular and cellular regulation of glucose transporter (GLUT) proteins in cancer. *J. Cell. Physiol.* **202,** 654–662 (2005).
716. Wang, E. *et al.* The role of factor inhibiting HIF (FIH-1) in inhibiting HIF-1 transcriptional activity in glioblastoma multiforme. *PLoS One* **9,** e86102 (2014).
717. Janke, K. *et al.* Factor inhibiting HIF-1 (FIH-1) modulates protein interactions of apoptosis-stimulating p53 binding protein 2 (ASPP2). *J. Cell Sci.* **126,** 2629–40 (2013).

718. Porporato, P. E., Dhup, S., Dadhich, R. K., Copetti, T. & Sonveaux, P. Anticancer targets in the glycolytic metabolism of tumors: a comprehensive review. *Front. Pharmacol.* **2,** 49 (2011).

719. Levine, A. J. & Puzio-Kuter, A. M. The control of the metabolic switch in cancers by oncogenes and tumor suppressor genes. *Science (80-.).* **330,** 1340–1344 (2010).

720. Shim, H. *et al.* c-Myc transactivation of LDH-A: implications for tumor metabolism and growth. *Proc. Natl. Acad. Sci. U. S. A.* **94,** 6658–63 (1997).

721. Dang, C. c-Myc target genes involved in cell growth, apoptosis, and metabolism. *Mol. Cell. Biol.* **40,** 66–9 (1999).

722. Arsham, A. M., Plas, D. R., Thompson, C. B. & Simon, M. C. Akt and hypoxia-inducible factor-1 independently enhance tumor growth and angiogenesis. *Cancer Res.* **64,** 3500–7 (2004).

723. Arsham, A. M., Plas, D. R., Thompson, C. B. & Simon, M. C. Phosphatidylinositol 3-Kinase/Akt Signaling Is Neither Required for Hypoxic Stabilization of HIF-1alpha nor Sufficient for HIF-1-dependent Target Gene Transcription. *J Biol Chem* **277,** 15162–70. (2002).

724. Laughner, E., Taghavi, P., Chiles, K., Mahon, P. C. & Semenza, G. L. HER2 (neu) signaling increases the rate of hypoxia-inducible factor 1alpha (HIF-1alpha) synthesis: novel mechanism for HIF-1-mediated vascular endothelial growth factor expression. *Mol. Cell. Biol.* **21,** 3995–4004 (2001).

725. Zhong, H. *et al.* Overexpression of hypoxia-inducible factor 1alpha in common human cancers and their metastases. *Cancer Res.* **59,** 5830–5 (1999).

726. Talks, K. L. *et al.* The Expression and Distribution of the Hypoxia-Inducible Factors HIF-1α and HIF-2α in Normal Human Tissues, Cancers, and Tumor-Associated Macrophages. *Am. J. Pathol.* **157,** 411–421 (2000).

727. Afanasev, I. Formation and damaging effects of superoxide in mitochondria: relevance to mitochondrial aging. in *International Association of Biomedical Gerontology 10th Conference* (2003).

728. Zamaraeva, M. V *et al.* Cells die with increased cytosolic ATP during apoptosis: a bioluminescence study with intracellular luciferase. *Cell Death Differ.* **12,** 1390–7 (2005).

729. Nikoletopoulou, V., Markaki, M., Palikaras, K. & Tavernarakis, N. Crosstalk between apoptosis, necrosis and autophagy. *Biochimica et Biophysica Acta - Molecular Cell Research* **1833,** 3448–3459 (2013).

730. Laster, S. M., Wood, J. G. & Gooding, L. R. Tumor necrosis factor can induce both apoptic and necrotic forms of cell lysis. *J. Immunol.* **141,** 2629–34 (1988).

731. Vercammen, D. *et al.* Dual signaling of the Fas receptor: initiation of both apoptotic and necrotic cell death pathways. *J. Exp. Med.* **188,** 919–30 (1998).

732. Dong, G. *et al.* PKM2 and cancer: The function of PKM2 beyond glycolysis. *Oncol. Lett.* **11,** 1980–1986 (2016).

733. Mohammad, G. H., Olde Damink, S. W. M., Malago, M., Dhar, D. K. & Pereira, S. P. Pyruvate Kinase M2 and Lactate Dehydrogenase A Are Overexpressed in Pancreatic Cancer and Correlate with Poor Outcome. *PLoS One* **11,** e0151635 (2016).

734. Lu, C. L. *et al.* Tumor cells switch to mitochondrial oxidative phosphorylation under radiation via mTOR-mediated hexokinase II inhibition - A Warburg-reversing effect. *PLoS One* **10,** (2015).

735. Novak, I. Mitophagy: A Complex Mechanism of Mitochondrial Removal. *Antioxid. Redox Signal.* **17,** 794–802 (2012).

736. Tanida, I., Ueno, T. & Kominami, E. LC3 and autophagy. *Methods Mol. Biol.* **445,** 77–88 (2008).

737. Hanna, R. A. *et al.* Microtubule-associated Protein 1 Light Chain 3 (LC3) Interacts with Bnip3 Protein to Selectively Remove Endoplasmic Reticulum and Mitochondria via Autophagy. *J. Biol. Chem.* **287,** 19094–19104 (2012).

738. Mammucari, C. *et al.* FoxO3 Controls Autophagy in Skeletal Muscle In Vivo. *Cell Metab.* **6,** 458–471 (2007).

739. Chourasia, A. H. *et al.* Mitophagy defects arising from BNip3 loss promote mammary tumor progression to metastasis. *EMBO Rep.* **16,** 1145–63 (2015).

740. Glick, D. *et al.* BNip3 regulates mitochondrial function and lipid metabolism in the liver. *Mol. Cell. Biol.* **32,** 2570–84 (2012).

741. Klimaszewska-Wisniewska, A. *et al.* Paclitaxel and the dietary flavonoid fisetin: a synergistic combination that induces mitotic catastrophe and autophagic cell death in A549 non-small cell lung cancer cells. *Cancer Cell Int.* **16,** 10 (2016).

742. Luo, T. *et al.* (-)-Epigallocatechin gallate sensitizes breast cancer cells to paclitaxel in a murine model of breast carcinoma. *Breast Cancer Res.* **12,** R8 (2010).

743. George, S. *et al.* Phase I study of flavopiridol in combination with Paclitaxel and Carboplatin in patients with

non-small-cell lung cancer. *Clin. Lung Cancer* **9,** 160–5 (2008).

744. Schwartz, G. K. Phase I Study of the Cyclin-Dependent Kinase Inhibitor Flavopiridol in Combination With Paclitaxel in Patients With Advanced Solid Tumors. *J. Clin. Oncol.* **20,** 2157–2170 (2002).
745. Yoshida, T. *et al.* Kaempferol sensitizes colon cancer cells to TRAIL-induced apoptosis. *Biochem. Biophys. Res. Commun.* **375,** 129–133 (2008).
746. Horinaka, M. *et al.* The combination of TRAIL and luteolin enhances apoptosis in human cervical cancer HeLa cells. *Biochem. Biophys. Res. Commun.* **333,** 833–838 (2005).
747. Ganapathy, S., Chen, Q., Singh, K. P., Shankar, S. & Srivastava, R. K. Resveratrol enhances antitumor activity of TRAIL in prostate cancer xenografts through activation of FOXO transcription factor. *PLoS One* **5,** (2010).
748. Szliszka, E., Czuba, Z. P., Jernas, K. & Król, W. Dietary flavonoids sensitize HeLa cells to tumor necrosis factor-related apoptosis-inducing ligand (TRAIL). *Int. J. Mol. Sci.* **9,** 56–64 (2008).
749. Tu, S.-H. *et al.* Luteolin sensitises drug-resistant human breast cancer cells to tamoxifen via the inhibition of cyclin E2 expression. *Food Chem.* **141,** 1553–61 (2013).
750. Alexandre, J., Hu, Y., Lu, W., Pelicano, H. & Huang, P. Novel action of paclitaxel against cancer cells: bystander effect mediated by reactive oxygen species. *Cancer Res.* **67,** 3512–7 (2007).
751. Alexandre, J. *et al.* Accumulation of hydrogen peroxide is an early and crucial step for paclitaxel-induced cancer cell death bothin vitro and in vivo. *Int. J. Cancer* **119,** 41–48 (2006).
752. Hadzic, T. *et al.* Paclitaxel combined with inhibitors of glucose and hydroperoxide metabolism enhances breast cancer cell killing via H2O2-mediated oxidative stress. *Free Radic. Biol. Med.* **48,** 1024–33 (2010).
753. Yang, L. *et al.* Wogonin enhances antitumor activity of tumor necrosis factor-related apoptosis-inducing ligand in vivo through ROS-mediated downregulation of cFLIPL and IAP proteins. *Apoptosis* **18,** 618–26 (2013).
754. Ding, J. *et al.* Wogonin and related natural flavones overcome tumor necrosis factor-related apoptosis-inducing ligand (TRAIL) protein resistance of tumors by down-regulation of c-FLIP protein and up-regulation of TRAIL receptor 2 expression. *J. Biol. Chem.* **287,** 641–9 (2012).
755. Song, I.-S. *et al.* Peroxiredoxin I contributes to TRAIL resistance through suppression of redox-sensitive caspase activation in human hepatoma cells. *Carcinogenesis* **30,** 1106–14 (2009).
756. Václavíková, R., Horský, S., Šimek, P. & Gut, I. Paclitaxel metabolism in rat and human liver microsomes is inhibited by phenolic antioxidants. *Naunyn. Schmiedebergs. Arch. Pharmacol.* **368,** 200–209 (2003).
757. Choi, J.-S., Choi, H.-K. & Shin, S.-C. Enhanced bioavailability of paclitaxel after oral coadministration with flavone in rats. *Int. J. Pharm.* **275,** 165–170 (2004).
758. Choi, J.-S., Jo, B.-W. & Kim, Y.-C. Enhanced paclitaxel bioavailability after oral administration of paclitaxel or prodrug to rats pretreated with quercetin. *Eur. J. Pharm. Biopharm.* **57,** 313–318 (2004).
759. Razandi, M., Pedram, A., Jordan, V. C., Fuqua, S. & Levin, E. R. Tamoxifen regulates cell fate through mitochondrial estrogen receptor beta in breast cancer. *Oncogene* **32,** 3274–85 (2013).
760. Yu, D. D. & Forman, B. M. Simple and Efficient Production of (Z)-4-Hydroxytamoxifen, a Potent Estrogen Receptor Modulator. *J. Org. Chem.* **68,** 9489–9491 (2003).
761. Kallio, A., Zheng, A., Dahllund, J., Heiskanen, K. M. & Härkönen, P. Role of mitochondria in tamoxifen-induced rapid death of MCF-7 breast cancer cells. *Apoptosis* **10,** 1395–1410 (2005).
762. Cho, S. K., Pedram, A., Levin, E. R. & Kwon, Y. J. Acid-degradable core-shell nanoparticles for reversed tamoxifen-resistance in breast cancer by silencing manganese superoxide dismutase (MnSOD). *Biomaterials* **34,** 10228–10237 (2013).
763. Pan, D. *et al.* LW-214, a newly synthesized flavonoid, induces intrinsic apoptosis pathway by down-regulating Trx-1 in MCF-7 human breast cells. *Biochem. Pharmacol.* **87,** 598–610 (2014).

Appendix 1: Supplementary figures

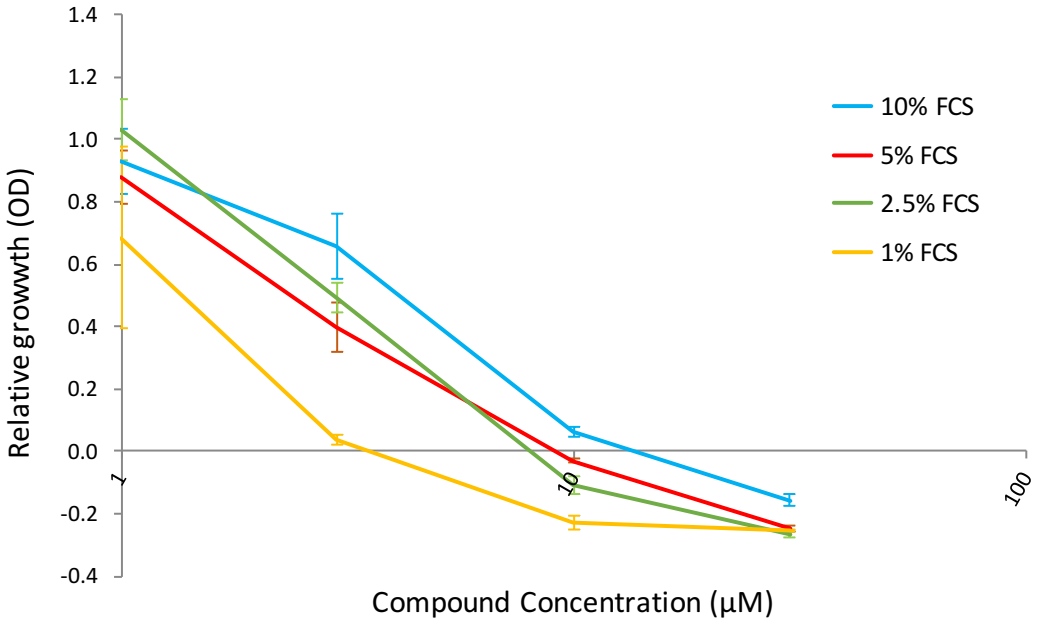

Supplementary Figure 1 ***Preliminary assessment of the effect of foetal calf serum concentration on the efficacy of AO-1530.*** *This graphs shows the differences in the concentration-dependent growth-inhibiting effect on MCF-7 cells (1000 cells/well) of treatment with AO-1530 for 96 h depending on the concentration of foetal calf serum (FCS) in the medium. Each data point represents the average of 3 technical replicates, with the errors bars representing the standard deviation (SD). All values were normalised to vehicle controls. Figure courtesy of Peter Mullen, from unpublished preliminary work.*

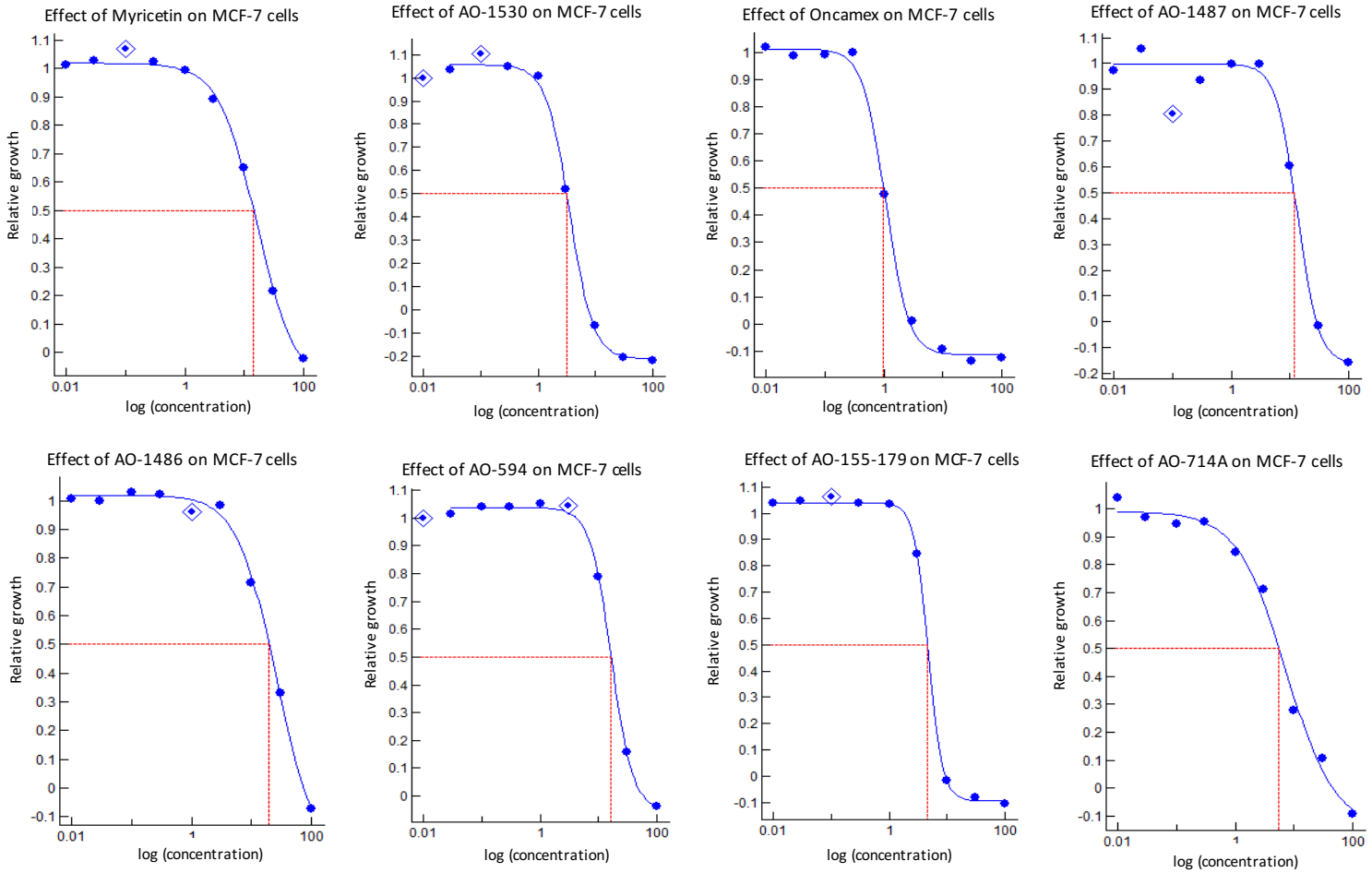

Supplementary Figure 2 ***Calculation of half maximum inhibitory concentrations (IC_{50}) for MCF-7 cells.*** *In order to determine IC_{50} values, dose-response curves from pooled results from biological replicate experiments (n=2) for each compound in the library studied were fitted to sigmoidal growth models. The Morgan-Mercer-Flodin mathematical sigmoidal model, with high regression coefficient and exclusion of outliers outside of a 95% confidence interval (shown as boxed points).*

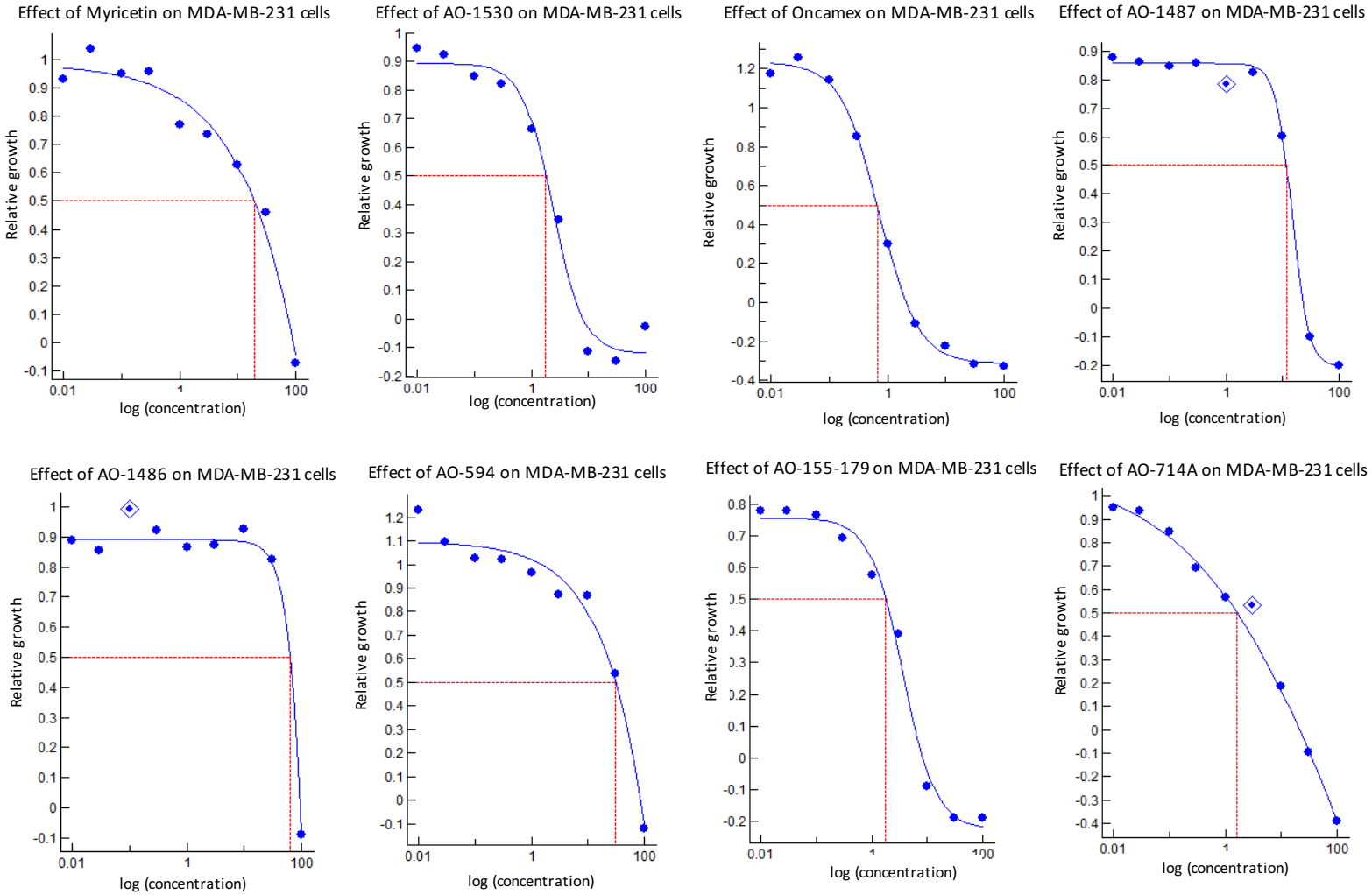

Supplementary Figure 3 ***Calculation of half maximum inhibitory concentrations (IC_{50}) for MDA-MB-231 cells.*** *In order to determine IC_{50} values, dose-response curves from pooled results from biological replicate experiments (n=2) for each compound in the library studied were fitted to sigmoidal growth models. The Morgan-Mercer-Flodin mathematical sigmoidal model, with high regression coefficient and exclusion of outliers outside of a 95% confidence interval (shown as boxed points).*

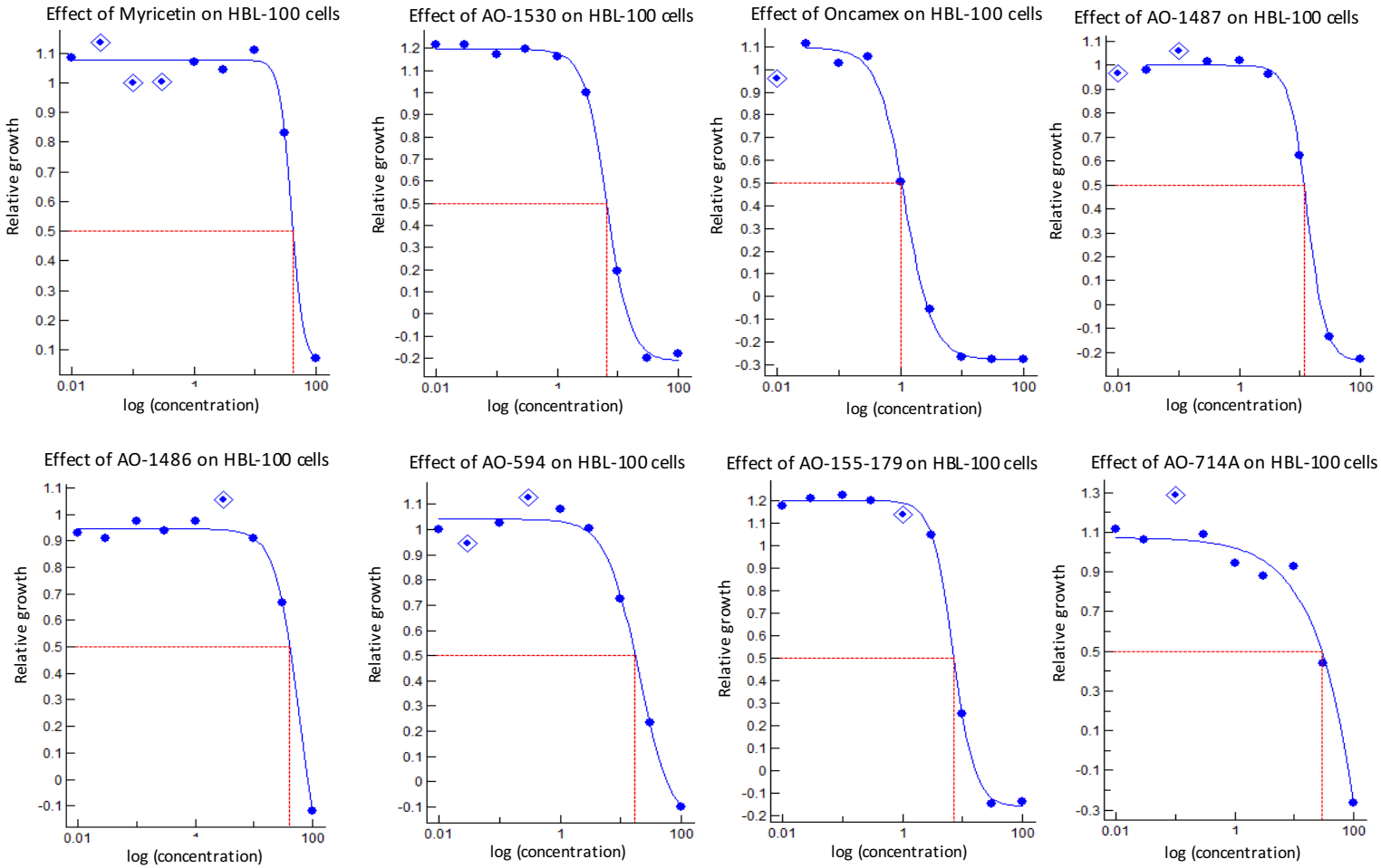

Supplementary Figure 4 ***Calculation of half maximum inhibitory concentrations (IC_{50}) for HBL-100 cells.*** *In order to determine IC_{50} values, dose-response curves from pooled results from biological replicate experiments (n=2) for each compound in the library studied were fitted to sigmoidal growth models. The Morgan-Mercer-Flodin mathematical sigmoidal model, with high regression coefficient and exclusion of outliers outside of a 95% confidence interval (shown as boxed points)*

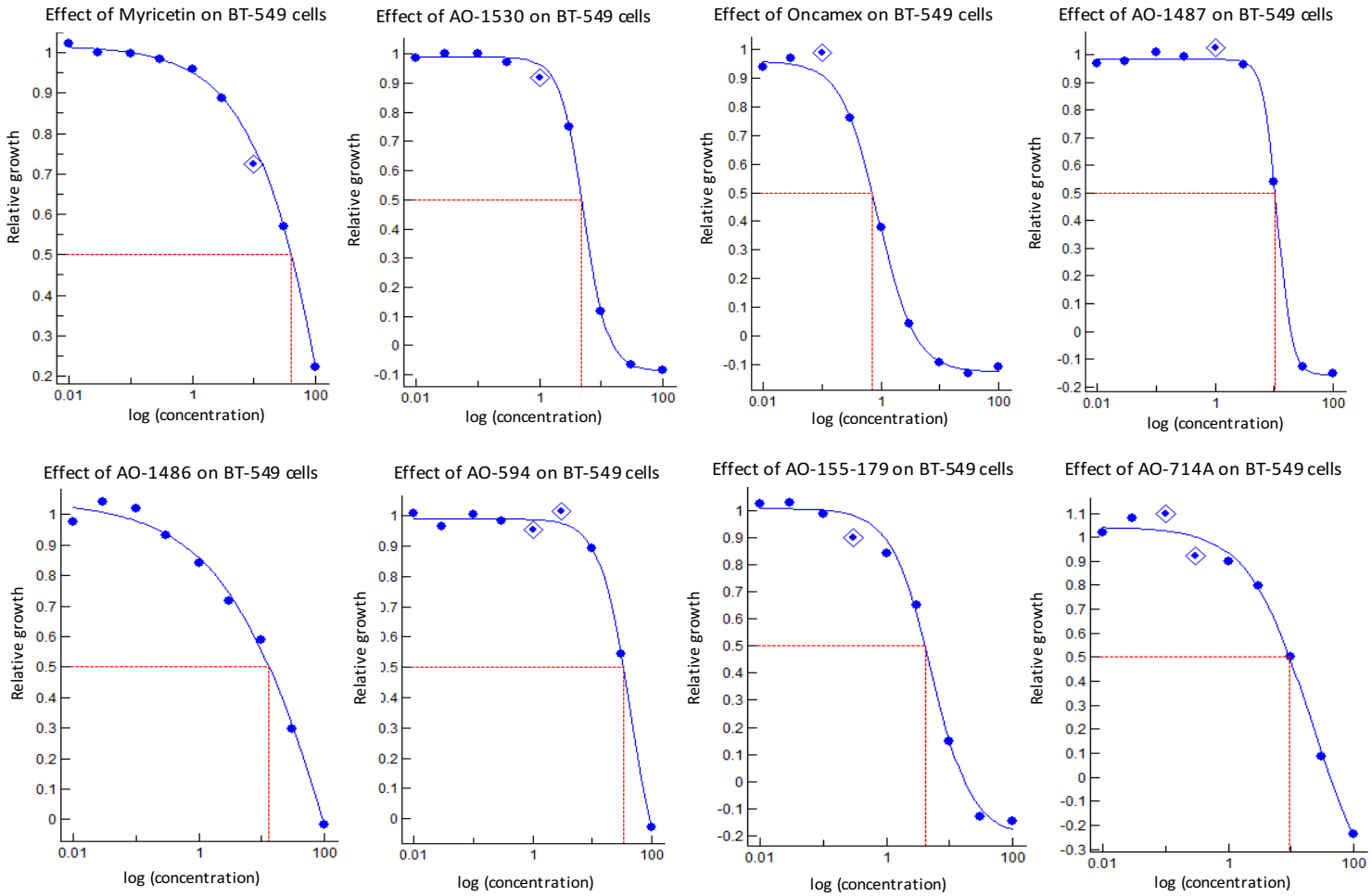

Supplementary Figure 5 ***Calculation of half maximum inhibitory concentrations (IC_{50}) for BT-549 cells.*** *In order to determine IC_{50} values, dose-response curves from pooled results from biological replicate experiments (n=2) for each compound in the library studied were fitted to sigmoidal growth models. The Morgan-Mercer-Flodin mathematical sigmoidal model, with high regression coefficient and exclusion of outliers outside of a 95% confidence interval (shown as boxed points).*

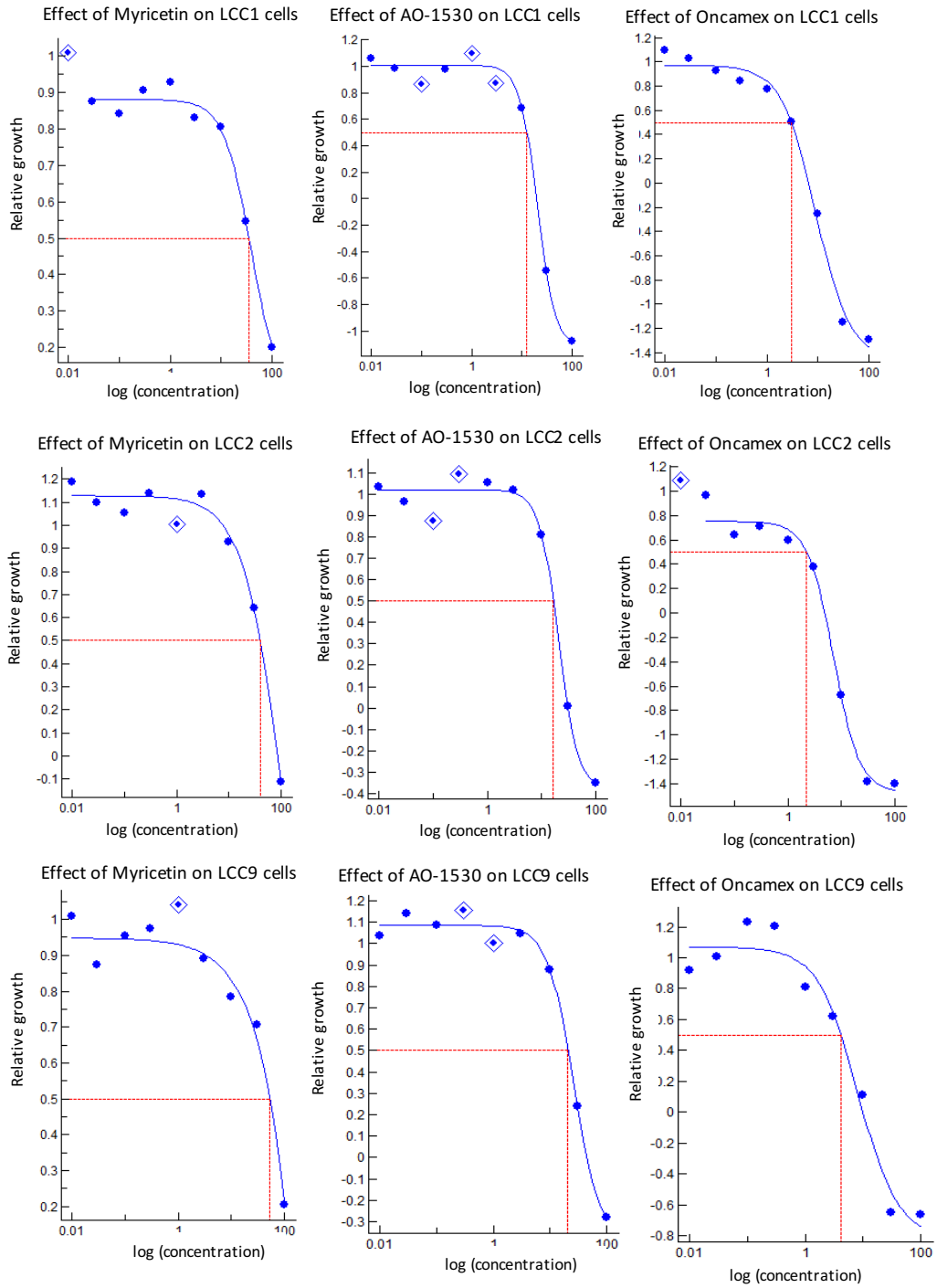

Supplementary Figure 6 ***Calculation of half maximum inhibitory concentrations (IC_{50}) for LCC1, LCC2 and LCC9 cells.*** *In order to determine IC_{50} values, dose-response curves from pooled results from biological replicate experiments (n=2) for each compound in the library studied were fitted to sigmoidal growth models. The Morgan-Mercer-Flodin mathematical sigmoidal model, with high regression coefficient and exclusion of outliers outside of a 95% confidence interval (shown as boxed points).*

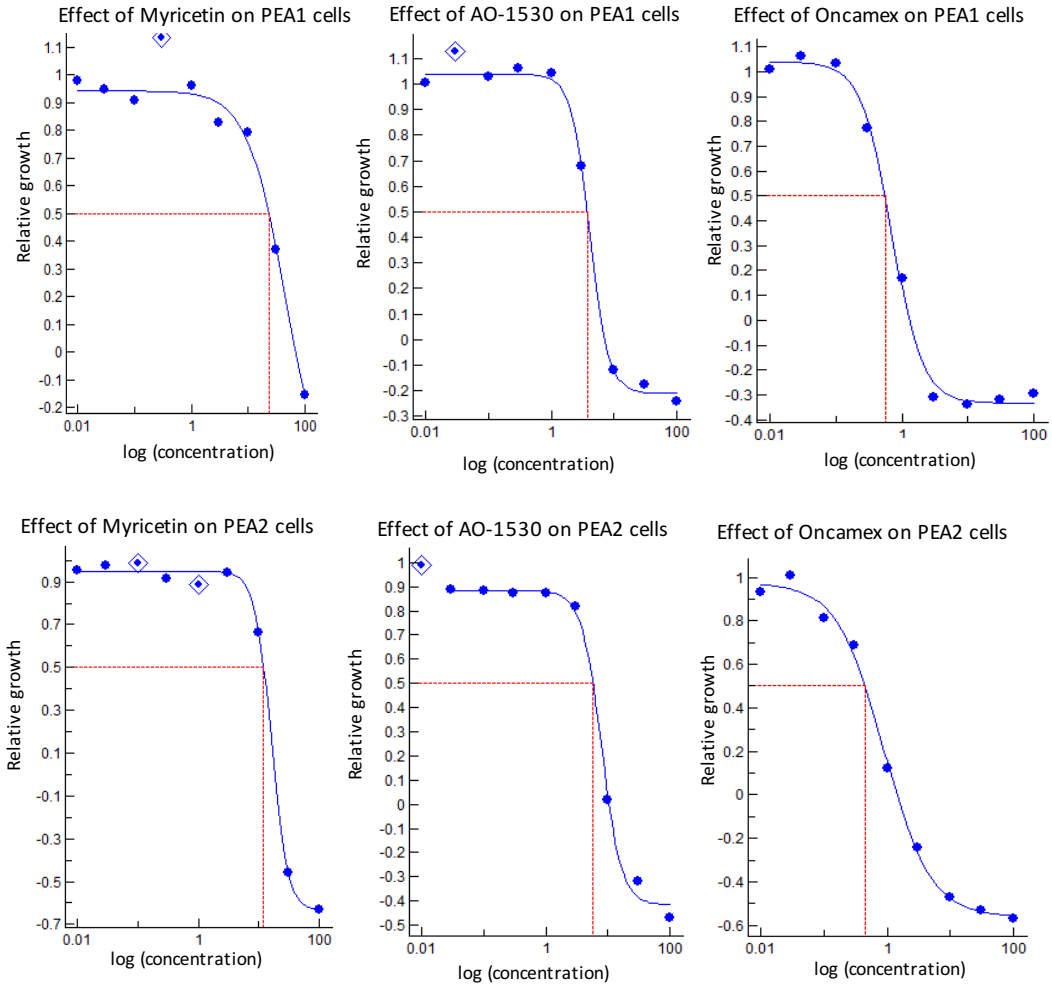

Supplementary Figure 7 ***Calculation of half maximum inhibitory concentrations (IC_{50}) for PEA1 and PEA2 cells.*** *In order to determine IC_{50} values, dose-response curves from pooled results from biological replicate experiments (n=2) for each compound in the library studied were fitted to sigmoidal growth models. The Morgan-Mercer-Flodin mathematical sigmoidal model, with high regression coefficient and exclusion of outliers outside of a 95% confidence interval (shown as boxed points).*

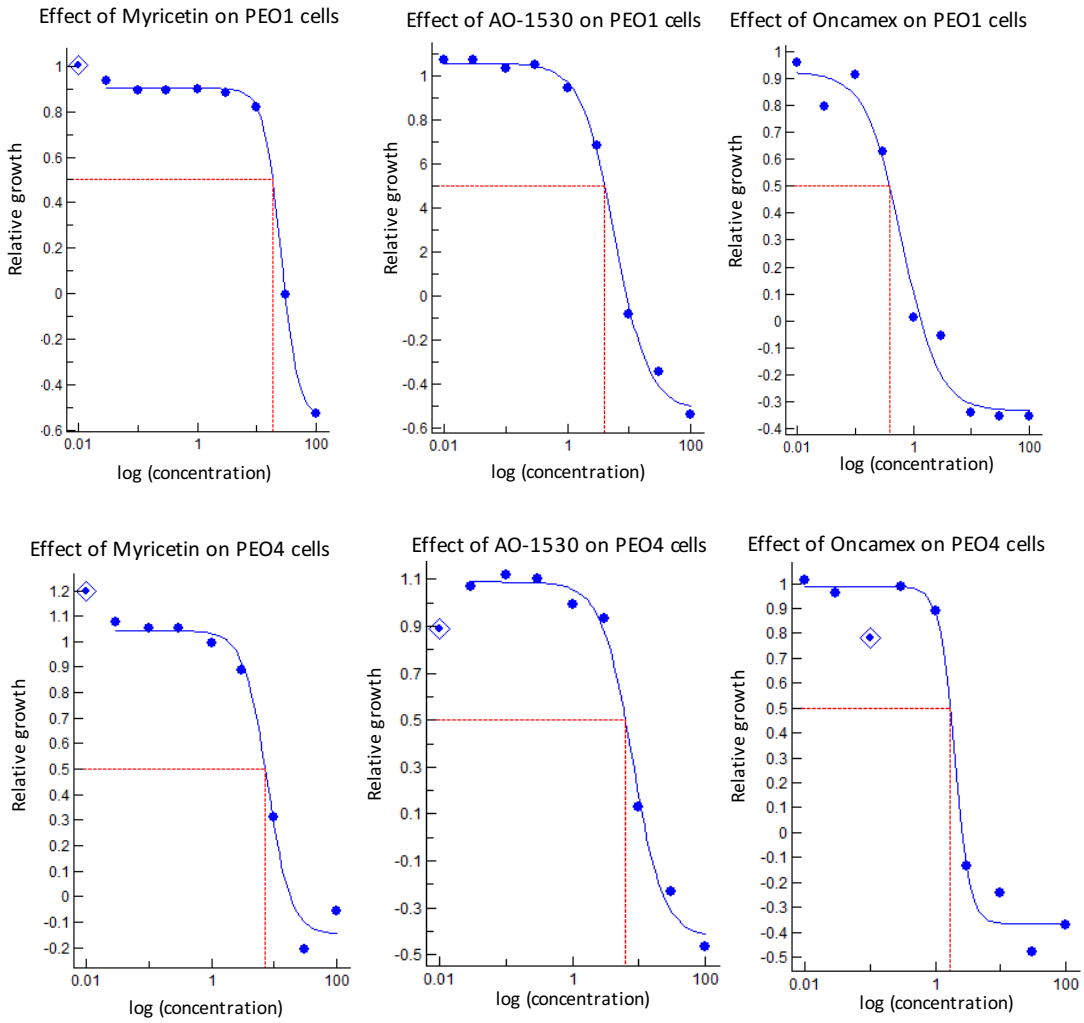

Supplementary Figure 8 ***Calculation of half maximum inhibitory concentrations (IC_{50}) for PEO1 and PEO4 cells.*** *In order to determine IC_{50} values, dose-response curves from pooled results from biological replicate experiments (n=2) for each compound in the library studied were fitted to sigmoidal growth models. The Morgan-Mercer-Flodin mathematical sigmoidal model, with high regression coefficient and exclusion of outliers outside of a 95% confidence interval (shown as boxed points).*

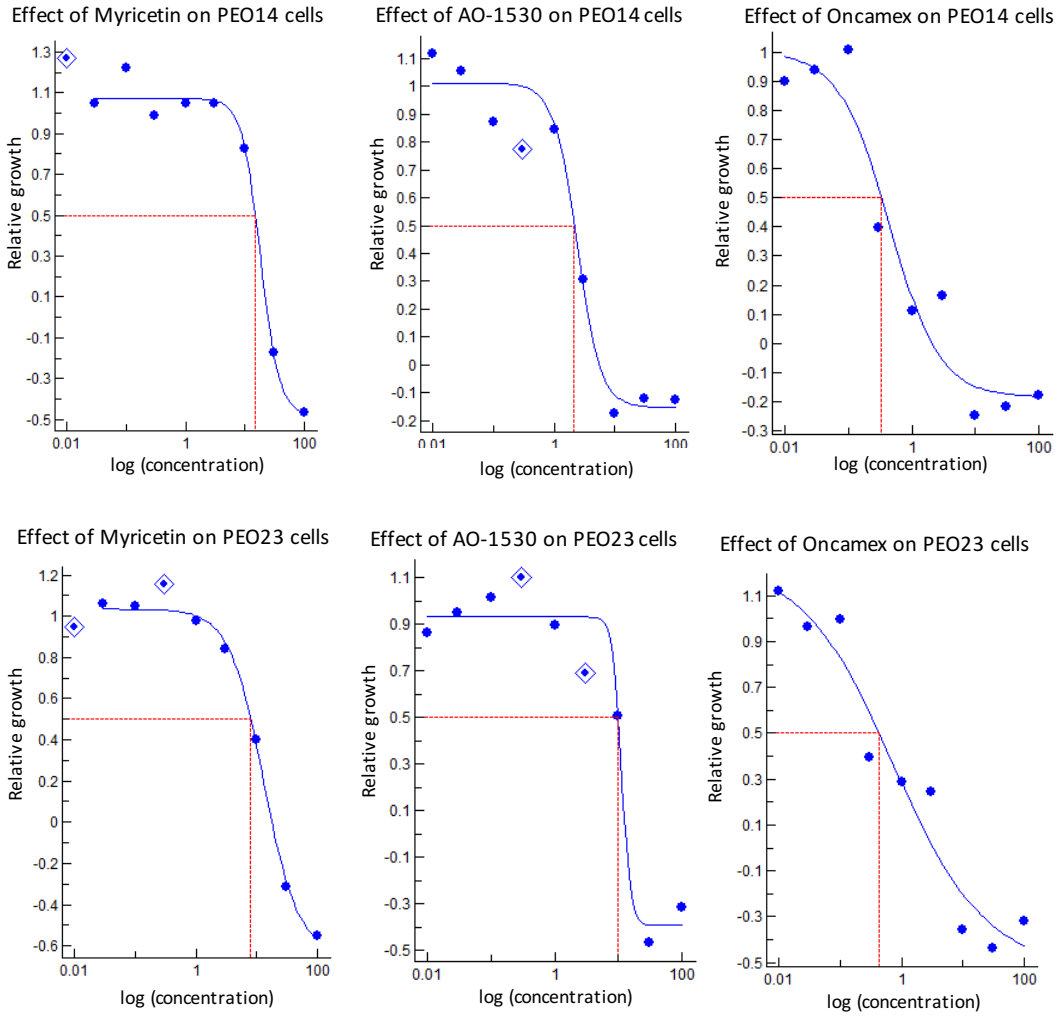

Supplementary Figure 9 ***Calculation of half maximum inhibitory concentrations (IC_{50}) for PEO14 and PEO23 cells.*** *In order to determine IC_{50} values, dose-response curves from pooled results from biological replicate experiments (n=2) for each compound in the library studied were fitted to sigmoidal growth models. The Morgan-Mercer-Flodin mathematical sigmoidal model, with high regression coefficient and exclusion of outliers outside of a 95% confidence interval (shown as boxed points).*

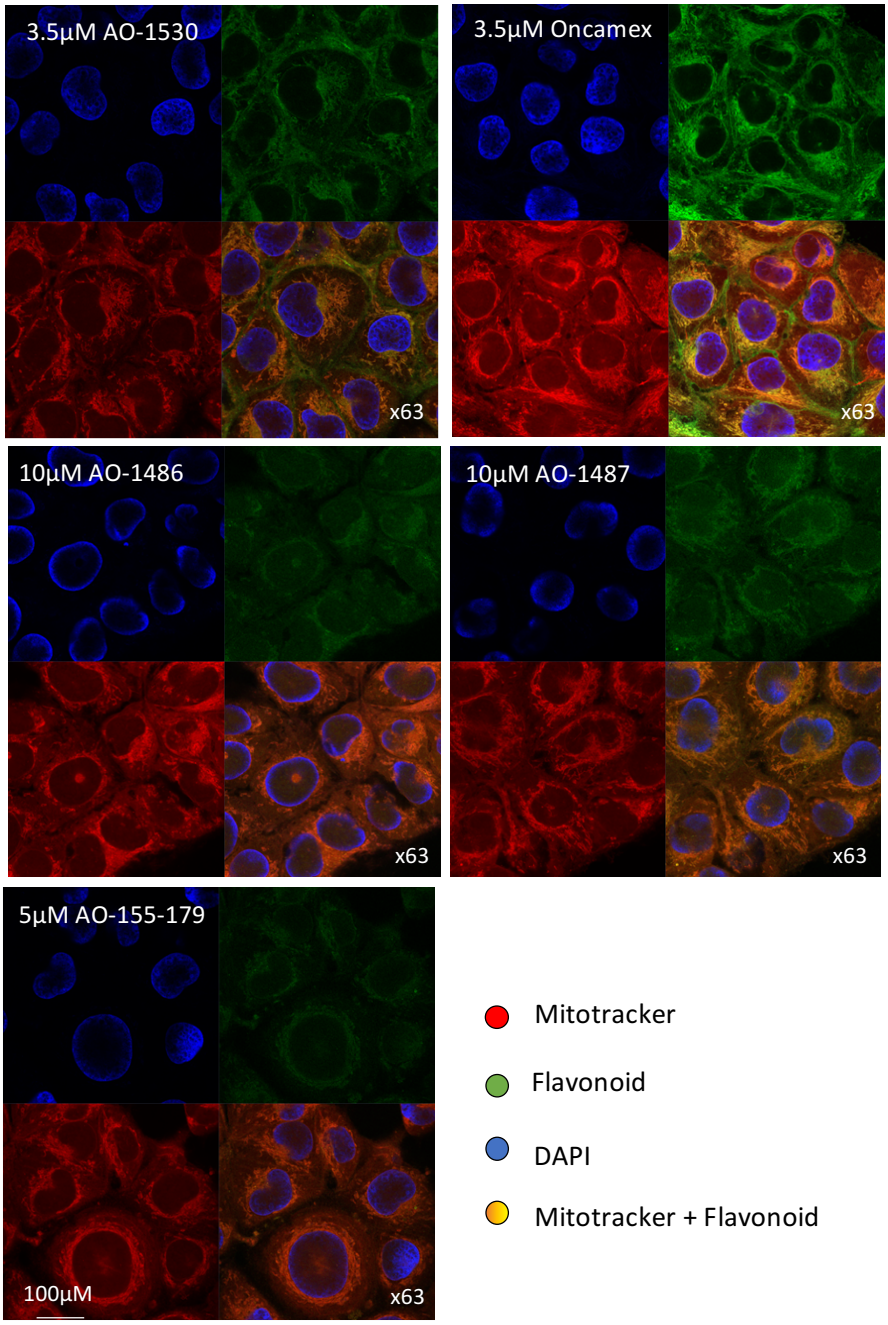

Supplementary Figure 10 ***Preliminary study of intracellular localisation of novel flavonoids.*** *Previous unreported work on renal cell carcinoma cells (RCC-30) investigated the compartmental distribution of novel flavonoids. Cells were visualised using a confocal fluorescence microscope after 1 h treatment with AO-1530, Oncamex, AO-1486, AO-1487 and AO-155-179. The natural fluorescence of these compounds allowed for detection of their distribution within the cell. Images courtesy of Graeme Cooke (Antoxis), from previously unpublished studies.*

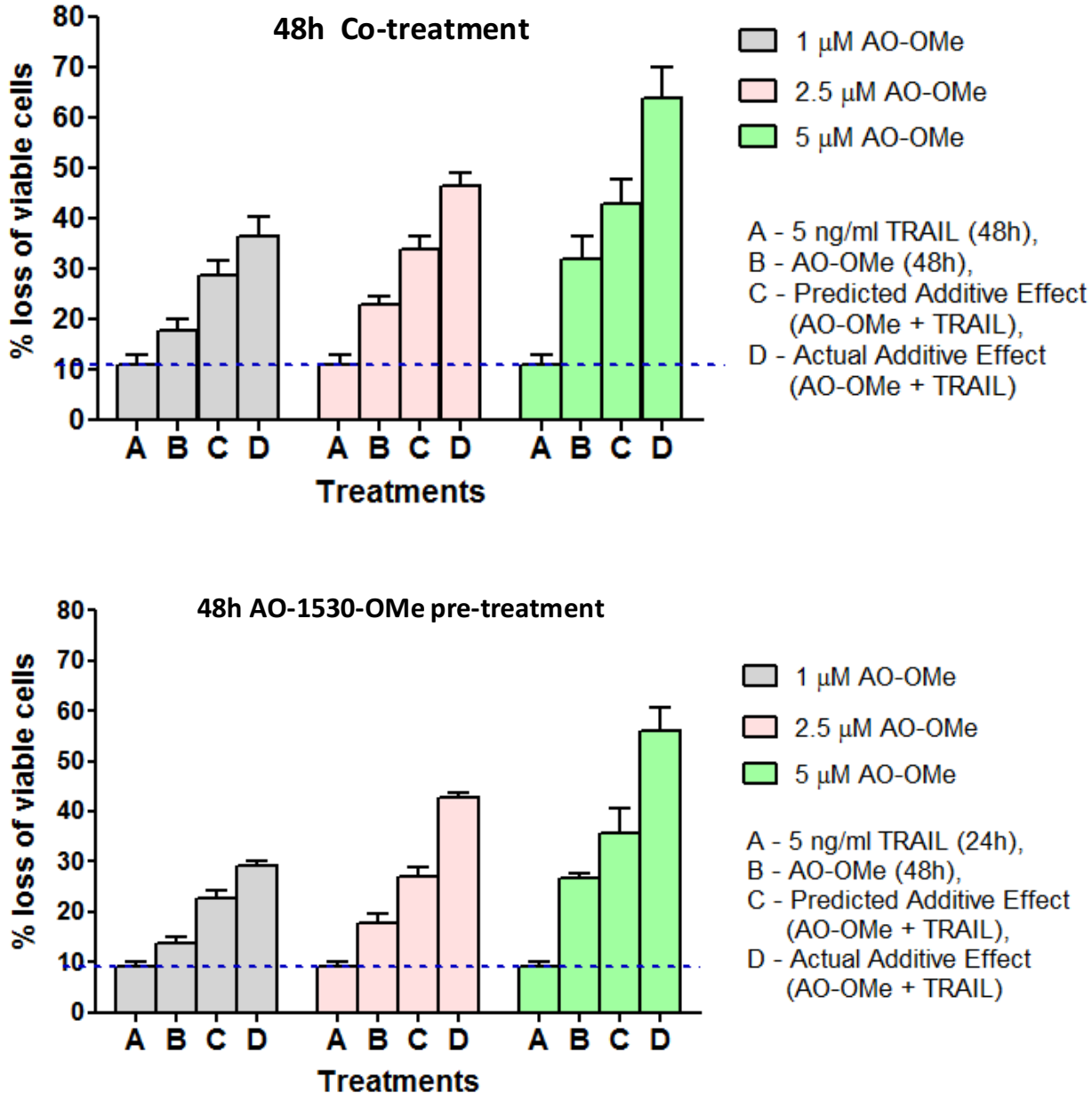

Supplementary Figure 11 ***Preliminary study of the effect on U87-MG glioblastoma cells of AO-1530-OMe in combination with TRAIL.*** *Previously unreported studies by Antoxis Ltd investigated the effect of a range of concentrations in the micromolar range of the novel flavonoid AO-1530-OMe (Oncamex) in combination with 5ng/mL TRAIL, either in co-treatment for 48 h (above) or with a 48 h pre-treatment with AO-1530-OMe followed by 24 h treatment with TRAIL. Graphs reflect the treatment-induced negative growth, with results presented as percentage of loss of viable cells. Graphs curtesy of Graeme Cook (Antoxis Ltd) from preliminary, previously unreported experiments.*

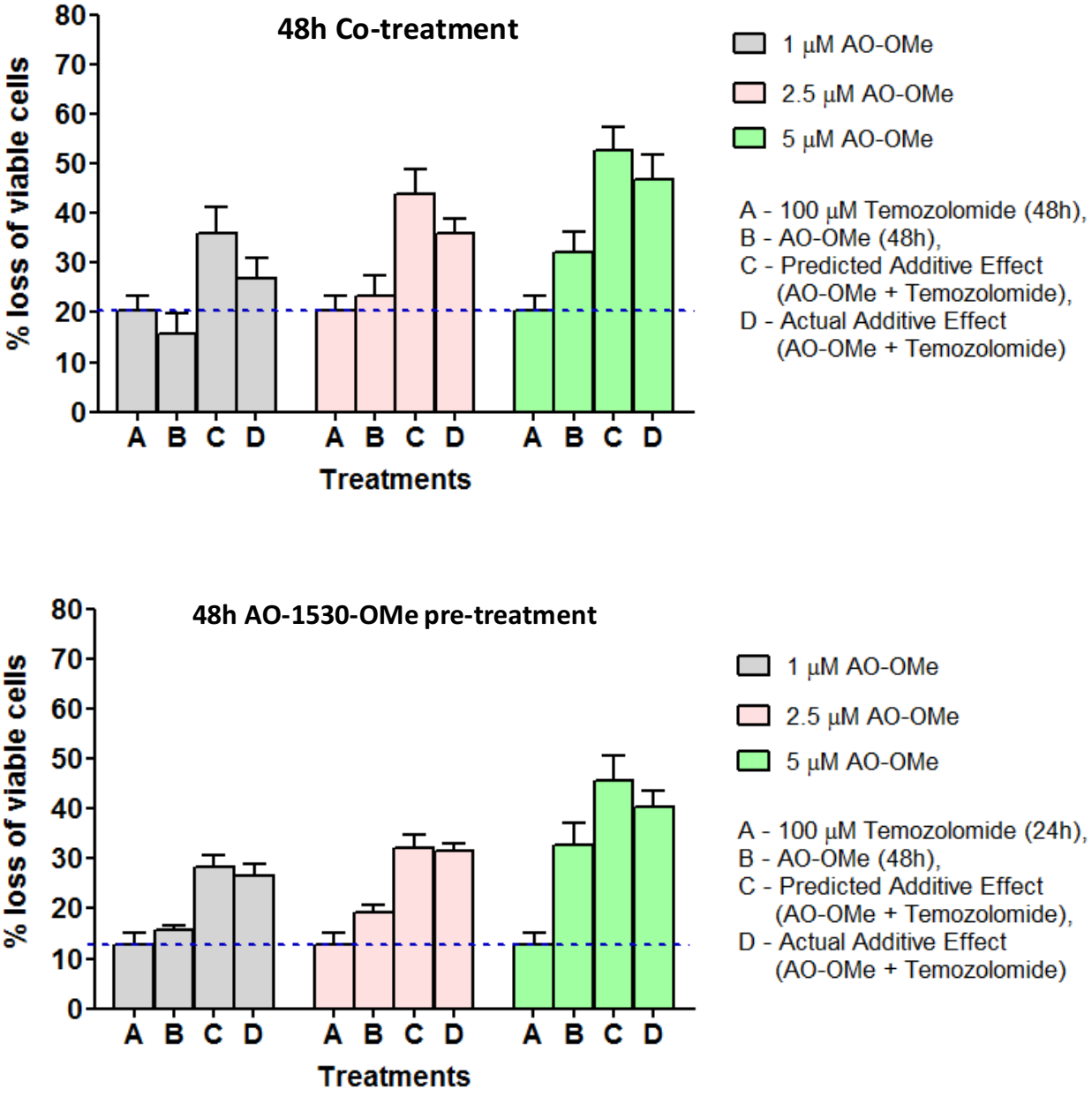

Supplementary Figure 12 ***Preliminary study of the effect on U87-MG glioblastoma cells of AO-1530-OMe in combination with temozolomide.*** *Previously unreported studies by Antoxis Ltd investigated the effect of a range of concentrations in the micromolar range of the novel flavonoid AO-1530-OMe (Oncamex) in combination with 100µM temozolomide, either in co-treatment for 48 h (above) or with a 48 h pre-treatment with AO-1530-OMe followed by 24 h treatment with TRAIL. Graphs reflect the treatment-induced negative growth, with results presented as percentage of loss of viable cells. Graphs curtesy of Graeme Cook (Antoxis Ltd) from preliminary, previously unreported experiments.*

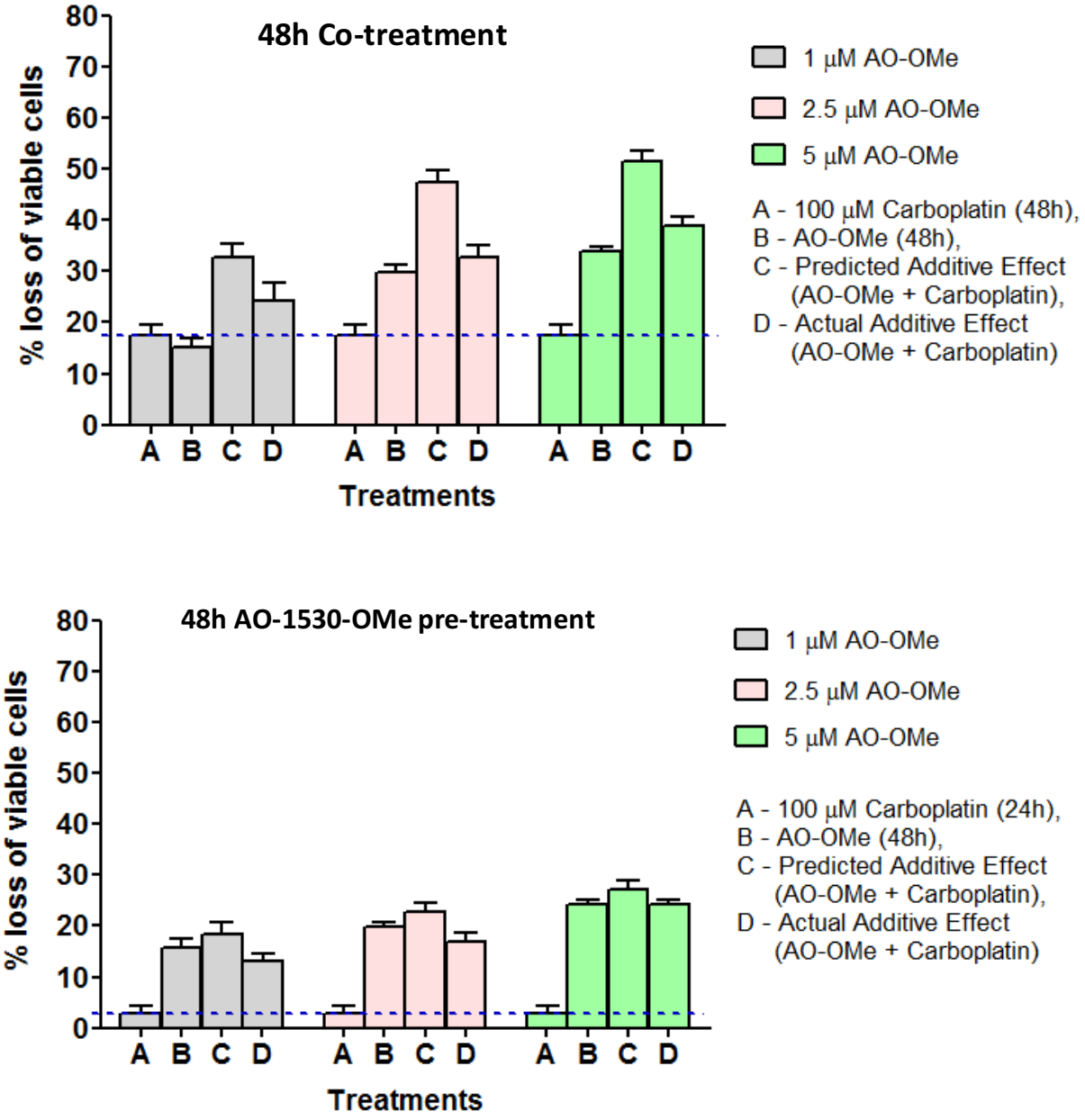

Supplementary Figure 13 ***Preliminary study of the effect on U87-MG glioblastoma cells of AO-1530-OMe in combination with carboplatin.*** *Previously unreported studies by Antoxis Ltd investigated the effect of a range of concentrations in the micromolar range of the novel flavonoid AO-1530-OMe (Oncamex) in combination with 100µM carboplatin, either in co-treatment for 48 h (above) or with a 48 h pre-treatment with AO-1530-OMe followed by 24 h treatment with TRAIL. Graphs reflect the treatment-induced negative growth, with results presented as percentage of loss of viable cells. Graphs curtesy of Graeme Cook (Antoxis Ltd) from preliminary, previously unreported experiments.*

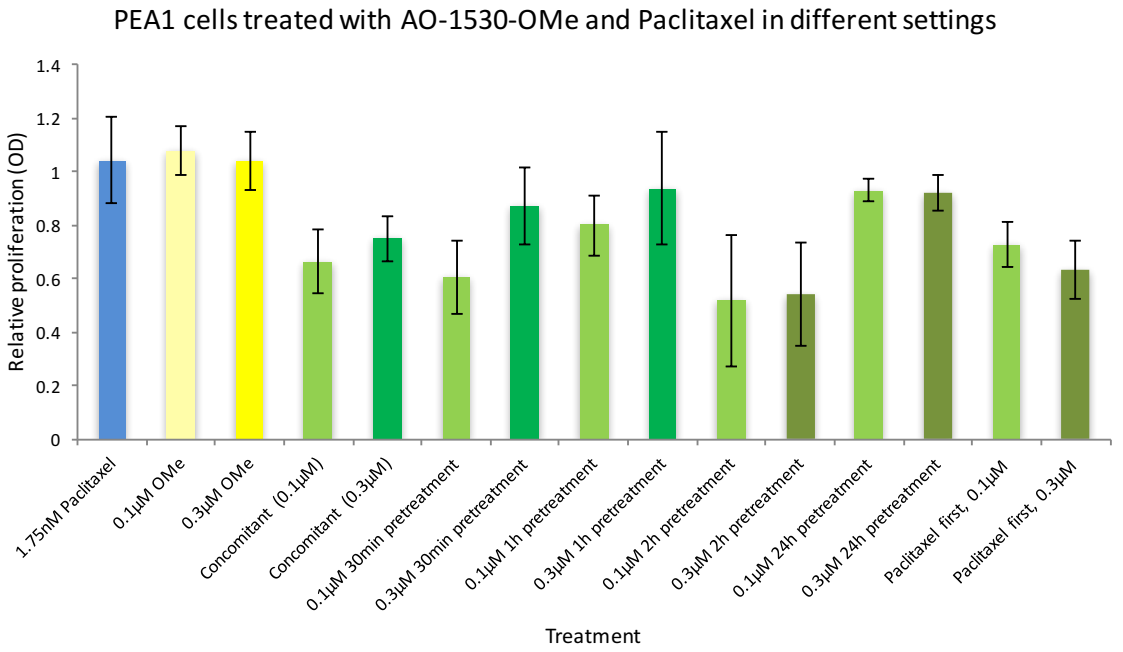

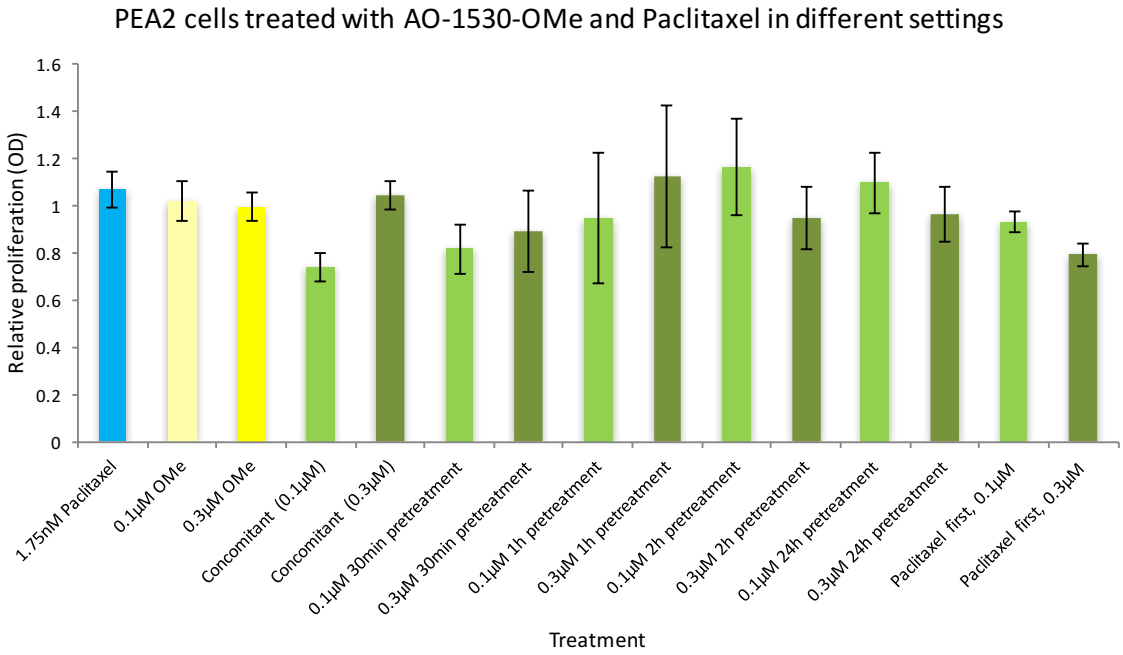

Supplementary Figure 14 ***Preliminary study of the effect on ovarian cancer cells of AO-1530-OMe in combination with paclitaxel following different administration schedules.*** *Concentrations in the sub-micromolar range of AO-1530-OMe (Oncamex) were combined with 1.75nM paclitaxel by cotreatment for 48 h alone, preceded by pretreatment with AO-1530-OMe (for 30 min or 1/2/24 h) or preceded by pretreatment with paclitaxel (for 24 h). Each experiment was repeated (n=2, with 6 replicates per treatment condition). These graphs show results from representative experiments, normalised to vehicle controls. Each data point represents the average of 6 technical replicates, with error bars representing standard deviation (SD).*

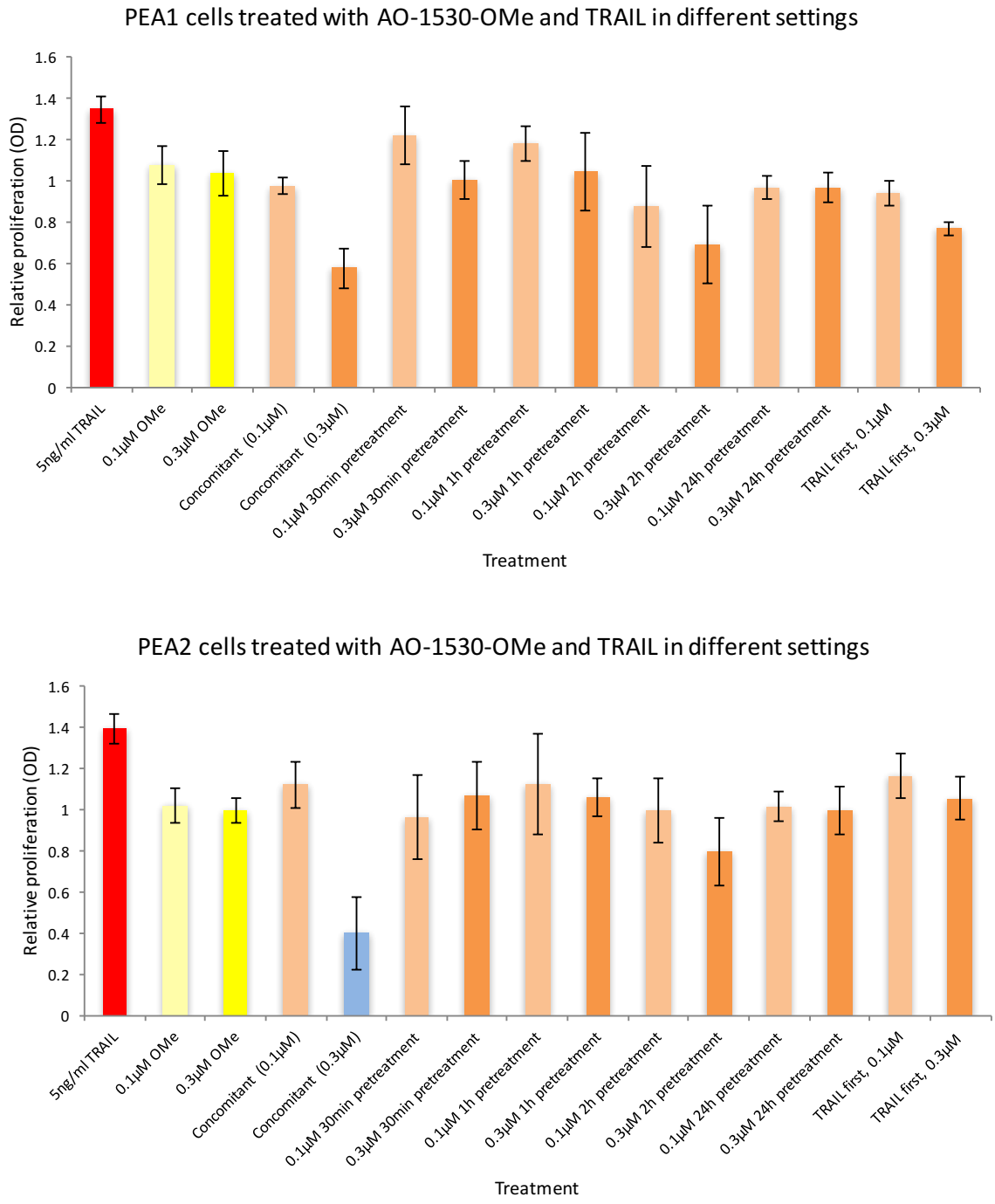

Supplementary Figure 15 ***Preliminary study of the effect on ovarian cancer cells of AO-1530-OMe in combination with TRAIL following different administration schedules.*** *Concentrations in the sub-micromolar range of AO-1530-OMe (Oncamex) were combined with 5ng/mL TRAIL by cotreatment for 48 h alone, preceded by pretreatment with AO-1530-OMe (for 30 min or 1/2/24 h) or preceded by pretreatment with TRAIL (for 24 h). Each experiment was repeated (n=2, with 6 replicates per treatment condition). These graphs show results from representative experiments, normalised to vehicle controls. Each data point represents the average of 6 technical replicates, with error bars representing standard deviation (SD).*

Appendix 2: Gene lists

Tables in this appendix include gene lists from gene expression analysis reported in chapter 5, including differentially expressed genes after treatment with Oncamex and groups of genes in each of the sections of Venn diagrams comparing the overlap in genes between different models or treatment conditions (groups for which there was no overlapping genes are not shown).

***Supplementary Table 1* Differentially expressed genes in MCF-7 cells after treatment with Oncamex.**

		MCF-7 (differentially expressed genes after high or low treatment with Oncamex)
High	Up	ADM, ADPGK, AKNAD1, ALDOC, ANGPTL4, ANKRD37, AP4B1, AQP3, ARID3A, ARL6IP6, ASF1B, ASNS, BAMBI, BCL6, BHLHE40, BNIP3, BNIP3L, BTBD11, BTG2, C10orf28, C11orf68, C11orf75, C17orf58, C17orf96, C1orf51, C2orf49, CCDC28A, CCNA2, CCNE2, CCNG2, CDK7, CDKN1B, CEBPD, CELF1, CENPW, CEP152, CGA, CHIC2, CHMP1B, CHRM3, CITED2, CLDN12, CLDND1, CLK3, CMC1, CMTM6, CNIH, CPOX, CRIPT, CRKL, CSRNP1, CSRP2, CXADR, DCUN1D3, DDIT4, DEDD2, DENND5A, DHX32, DLX2, DNAJB6, DNAJC24, DUSP1, E2F7, EFNA1, EGLN1, ELP4, ENO2, ERO1L, EXO1, FAM111A, FAM57A, FARP2, FBXO8, FHL3, FKBP15, FOS, FOXP1-IT1, FUT11, GADD45B, GBE1, GLCE, GON4L, GPR37, HES1, HILPDA, HK2, HMG20A, HOXA5, HSD17B1, HSPA1A, HSPA1B, HSPH1, ID1, IGHV5-78, INSIG2, IRF2BPL, JUN, JUNB, KBTBD2, KCTD6, KDM2A, KDM3A, KIAA0355, KIAA0907, KIDINS220, KIFAP3, KIRREL3-AS2, KLHL12, KLHL9, LDHA, LEMD3, LPIN1, MAP3K13, MAPK8, MAPK9, MED30, MFAP1, MFAP3, MIR21, MLL5, MMD, MTHFSD, MTRNR2L1, MXD4, NDRG1, NEK7, NFE2L1, NFIL3, NFYA, NMI, NPC1, NR4A2, NSMCE2, NUDT18, NXF1, NXN, OXSR1, P4HA1, P4HA2, PDRG1, PFKFB3, PFKFB4, PGAM1, PGAM4, PGK1, PGM1, PGPEP1L, PHF13, PIAS1, PIAS4, PIR, PLEKHA8P1, PNRC1, POLR2H, POLR3GL, POU2F1, PPFIA4, PPIP5K1, PPME1, PPP2R5B, PRDX3, PRKRIP1, PRPF3, PTPN21, RAB23, RAB2B, RAB30, RAB9A, RAD54B, RBM14, RBM4B, RFFL, RHBDL1, RIC8B, RIMKLA, RIOK3, RLF, RN7SL1, RNASEL, RNF122, RNF144A, RNF24, RNFT1, RNGTT, RNMT, RUNDC3B, SEC22A, SLC25A4, SLC38A2, SPRED1, SPRY1, SSH2, STARD3NL, STC1, STC2, STK3, SYT5, TBKBP1, TDO2, TERF2IP, TFAP2C, TICAM2, TOB1, TRIB1, TSPYL1, TTC1, TTI1, VLDLR, VPS4B, WDR26, WDR27, WDR54, WSB1, YEATS2, YPEL2, ZBTB41, ZC2HC1A, ZFP36, ZFYVE20, ZIC2, ZNF217, ZNF248, ZNF295, ZNF337, ZNF395, ZNF654, ZNF770, ZSWIM5, 19 other genes with no HGNC symbol
	Down	40787, ACOT4, ACSS1, AEN, AFF3, AK2P2, ALKBH2, ARHGEF16, ARHGEF19, ARPC3, ASAP3, AVEN, B4GALT1, BCL2, BLMH, BOP1, C10orf81, C14orf126, C14orf39, C15orf59, C16orf74, C17orf70, C19orf10, C19orf46, C4orf19, C6orf211, CA12, CABLES1, CAMK2N1, CAPN1, CCDC155, CCDC86, CCDC88C, CCDC94, CCNB1, CCND1, CDC20, CDH18, CENPB, CHD4, CHGA, CLN3, CMBL, COMTD1, COPG2, CREB3L4, CRIP2, CUTC, CXCL12, DBN1, DCAF13, DEGS2, DEPTOR, DHX33, DNAJC9, DNPEP, DRAM1, DUS1L, DUS3L, EFCAB4A, EFHD1, EIF3B, ELFN2, ELOVL2, EMG1, EML3, ERMP1, ESR1, EXOSC6, EXOSC8, F12, FADS1, FADS2, FAH, FAM173A, FAM195A, FAM213B, FAM35A, FAM5B, FAM63A, FAM65A, FAM70A, FBXO27, FDPS, FFAR2, FGD3, FHL2, FKBP4, FLNA, FLNB, FOXE3, GALNT6, GGT6, GJA1, GLA, GNB1L, GPR68, GRPR, GSDMD, GSTM3, HCG18, HIST1H1B, HIVEP3, HNRNPD, HPDL, HPGD, HSD3B7, HSPA5, HSPB8, ICAM3, IGFBP4, IGFBP5, IL17D, IL19, IL27RA, INPP4B, IPCEF1, ISOC2, ITPK1, KAZALD1, KIAA0182, KIAA0664, KIF12, KRT18P13, KRT18P17, KRT18P19, KRT18P28, KRT8P33, KRT8P9, KTN1-AS1, KYNU, LCP1, LDLR, LEPREL4, LMOD3, LPO, LRP5L, LRRFIP1, LTBR, LYRM1, MAML3, MAP3K14, MAPKAPK3, METTL1, MIR373, MIR635, MLLT6, MOCOS, MPPED2, MRP63, MRPS2, MRTO4, MTA2, MYADM, MYBBP1A, MYO3B, NAA10, NAGLU, NCOR2, NINJ1, NME2P1, NOP14, NOP16, NOP58, NPY1R, NR2E3, NR5A2, NTHL1, NUCB2, PACSIN3, PALLD, PBX1, PDCD4, PDIA3P, PER3, PHF15, PINK1-AS, PLIN5, PLXNB1, POLA2, POLR3K, PPP1R35, PPRC1, PREX1, PRKCD, PRLR, PRSS23, PTGR2, PUS1, RAB3IL1, RAC3, RAD50, RAI14, RAP1GAP, RASL11A, RASL11B, RBPMS2, RDBP, RELL2, REPIN1, RERG, RHBDL2, RPP40, RPS26P35, RPS26P47, RPUSD1, RRP1, RRS1, SAPCD2, SCARNA9, SCIN, SCNN1A, SDC1, SDC4, SELENBP1, SEMA3C, SEMA3F, SERPINH1, SFPQ, SGK3, SHANK2, SHISA5, SIPA1L3, SLC19A1, SLC25A11, SLC25A13, SLC25A22, SLC29A2, SLC39A10, SLC4A2, SLC7A2, SLC7A8, SLC9A3, SLC9A3R1, SLITRK4, SMARCD2, SNORD13, SOAT2, SPDEF, SPOCD1, SRF, SRM, SRPK1, SRSF6, SSH3, STARD10, STEAP3, SUSD3, SYS1-DBNDD2, SYT12, SYTL1, TBC1D16, TBL1X, TCEA3, TEAD2, TEKT4, TGFB3, TIGD5, TMEM229B, TOMM40, TRIB3, TRIM65, TRIP6, TRMT1, TRMT6, TRPS1, TSPAN4, TUFT1, TYRO3, UBL3, UFSP1, VASP, VPS11, VTRNA1-3, WDR46, WDR90, WSB2, XCR1, YBX2, ZHX2, ZNF239, ZNF346, ZNF358, ZNF467, ZNF593, ZNF75A, ZNF768, ZNF787, ZNHIT2, 14 other genes with no HGNC symbol
Low	Up	C16orf11, C1orf105, C5orf55, FAM110B, FAM210B, FAM83F, FGFBP3, GAS2L2, HERC2P2, KCND3, MFAP4, MIR26B, NFIX, OR2T11, PCDH9, PRSS30P, PTPRU, RNU6-15, SNORA2B, SNORD113-3, SUDS3, ZC3H6, 2 other genes with no HGNC symbol
	Down	ALX3, ATP2C2, C16orf74, C19orf10, CLDN4, CNGA3, COPG2, F12, FGF6, HIST3H2A, KRT18P19, MRPS34, MTMR8, NBPF20, PDIA3P, PINK1-AS, PLIN5, PPARGC1A, SERPINH1, SLC25A22, SNHG10, TEKT4, TMEM174, YIPF3, ZDHHC18, 13 other genes with no HGNC symbol

Supplementary Table 2 ***Differentially expressed genes in MDA-MB-231 cells after treatment with Oncamex.***

		MDA-MB-231 (differentially expressed genes after high or low treatment with Oncamex)
High	Up	38777, ABCB6, ABCD1, ABHD5, ADAM8, ADM, ADRB2, AHSA1, AK4, ANG, ANGPTL4, ANKRD37, ANKRD54, ANKZF1, ARC, ARHGEF16, ARHGEF40, ARID3A, ARID5B, ARMC7, ASNS, ASUN, ATAD2B, ATG12, ATG9A, AVL9, B3GALNT2, B3GNT5, BBC3, BCYRN1, BHLHE40, BLCAP, BLID, BLZF1, BMS1P5, BNIP3, BNIP3L, BTAF1, C10orf10, C10orf118, C10orf28, C11orf96, C12orf23, C17orf96, C2orf69, C3orf52, C3orf58, C5orf30, C7orf71, C8orf58, C8orf80, C9orf84, CAPN5, CAPRIN2, CARS, CBLB, CCND2, CCNE1, CCRN4L, CDC42EP2, CDK12, CDKN1C, CHIC2, CHMP7, CHPF, CHST11, CHSY1, CHSY3, CIR1, CITED2, CKB, CLCF1, CNOT8, CPO, CSF2, CSRNP1, CSRP2, CTSZ, CXCL1, DACT3, DCP2, DDA1, DDAH1, DDIT4, DENND2C, DGKQ, DLC1, DNAJB2, DNAJB9, DOK1, DUSP1, DUSP18, DUSP5, DUSP5P, EGLN1, EIF2C2, ELP2, ENO2, ENTPD7, ERO1L, ERRFI1, EYA3, F3, FAM107B, FAM117B, FAM13A, FAM162A, FAM179B, FAM195B, FAM46A, FAM57A, FAM63A, FAT4, FER1L4, FGFR3, FICD, FLNC, FUT11, FUT6, G0S2, GALNT3, GALNTL4, GBE1, GFPT2, GJA3, GLRX, GLS, GM2A, GNPNAT1, GOLGB1, GPR137B, GPT2, GSK3B, HAND1, HBEGF, HES4, HIATL2, HILPDA, HK2, HMHA1, HOXD1, HSD17B7, HSPA4L, IFFO1, IFT20, IGFBP3, IL11, IL1RAPL1, IL27RA, IL8, IMPA1, INSIG2, ISCA1P1, ITFG2, ITGA5, ITPK1-AS1, ITPKA, JUN, KCTD11, KDM3A, KDM5A, KIAA1715, KIAA1958, KIF1B, KIRREL, KLF6, KLHDC1, KRTAP2-3, LDHA, LGALS8, LIF, LIN37, LINC00342, LOX, LRRC14, LUZP1, MAFF, MAGT1, MAK16, MAN2A1, MAP1LC3B, MAP2K1, MAP6D1, MAPK8, MAPK9, MBD4, MCTS1, METRNL, MFHAS1, MGAT1, MGEA5, MIR1275, MIR17HG, MIR507, MIR759, MKNK2, MOB3A, MOSPD1, MT1X, MTF2, MYO3B, NANS, NARF, NCBP1, NDRG1, NFIL3, NFKBID, NIPA1, NIPAL1, NOC3L, NOG, NR2F2, NXF1, OBFC2A, ODZ1, OFD1, OR1S2, OR5C1, OSBPL8, P4HA1, P4HA2, P4HB, PABPC1L, PAG1, PAM, PANX1, PAPD7, PCNX, PCSK5, PDK1, PFKFB3, PFKFB4, PHF13, PHF23, PIK3C3, PIM1, PKIA, PLA2G15, PLAT, PLAUR, PLCXD1, PLEKHG3, PLOD2, PNP, PNPLA2, PNPLA8, POM121B, PPAN-P2RY11, PPFIA4, PPME1, PPP1R16A, PPP2R2A, PPP2R5B, PPP3R1, PPTC7, PRSS8, PUS3, RAB11FIP3, RAB20, RAB30, RAB38, RAD54L2, RALGAPA1, RASSF7, RBM15, RECQL4, RGS4, RIOK3, RLF, RNF113A, RNF24, RNMT, RORA, RPS4XP16, RRAD, RRAGD, RUNDC1, RUNDC3B, SAMD4A, SDC4, SEC11C, SEC63P1, SERPINB8, SERPINE1, SERPINE2, SGMS2, SH3BP5L, SIPA1L2, SLC22A25, SLC25A36, SLC2A1, SLC2A14, SLC2A3, SLC38A2, SLC41A1, SLC5A8, SLC6A10P, SLC6A8, SLC7A2, SLIT2, SMAP2, SNORA5C, SNX33, SOGA3, SPAG4, SPHK1, SPIRE1, SRGAP1, SSTR2, ST8SIA2, STC1, STK35, TAF15, TCF19, TCF24, TEAD3, TICAM2, TIGD5, TLR4, TMEM115, TMEM156, TMEM51, TMEM57, TNIP1, TNIP2, TPBG, TPI1P1, TRIM27, TRIM58, TRIP12, TTC14, TUBB2A, UAP1, UBE4A, UGCG, UGDH, UPRT, USP38, USP49, VEGFC, VGF, VLDLR, VMP1, VPS18, VPS37A, WFIKKN1, YEATS2, ZBTB40, ZCCHC12, ZCCHC6, ZDHHC18, ZFAND2A, ZFP36L1, ZNF140, ZNF148, ZNF17, ZNF175, ZNF193, ZNF207, ZNF215, ZNF224, ZNF322P1, ZNF335, ZNF35, ZNF470, ZNF653, ZNF668, ZNF672, ZNF695, ZNF770, ZNF772, ZNF786, ZNF800, ZNF841, ZNFX1, 18 other genes with no HGNC symbol
	Down	ABR, ADAM19, ADORA2B, AIMP2, AMD1, AMDHD2, ANAPC13, ANGPTL2, ANP32AP1, APCDD1L, APEX1, APOBEC3B, ARMCX1, ARMCX2, ASAP3, ASPM, ASXL1, AURKA, AURKB, BAIAP2L1, BAMBI, BMP4, BRI3, BTF3L4, BUB1, C12orf32, C15orf23, C16orf53, C17orf98, C1orf109, C1orf123, C20orf72, C7orf53, C9orf3, C9orf40, CA12, CABLES1, CALM3, CAP2, CARD10, CAV1, CAV2, CBR1, CBX1, CCDC102A, CCDC106, CCDC99, CCNA2, CCNB1, CCNB2, CCNF, CD207, CD58, CDC20, CDCA2, CDCA3, CDCA8, CDH11, CDK1, CDKN2D, CDKN3, CENPA, CENPB, CENPE, CENPF, CEP41, CEP55, CKAP2, CKAP2L, CKS2, CLIC6, CMBL, COL4A2, COQ2, CRADD, CREB3L4, CST1, CST4, CTDSPL, CTIF, CTNNBIP1, CUEDC2, CUL9, CYB5A, CYP1B1, CYR61, DBN1, DENND5B, DLGAP5, DNAAF2, DNAH2, DNAJC9, DSN1, EHBP1, ESPL1, ETS2, F2RL1, FAM171A1, FAM46B, FAM75A1, FAM83D, FHOD3, FKBP1C, FUT8, FZD2, GBAP1, GBP1, GCA, GEMIN2, GJB2, GLT25D2, GNG10, GNG12, GPR56, GTF2H4, H1F0, H2AFX, HAUS8, HCAR1, HDDC3, HES1, HIF1A, HIST1H2AC, HIST1H4C, HIVEP1, HLA-DPA1, HMBS, HMGB3, HMGCR, HMGCS1, HMGN1P38, HMMR, HNRNPA0, HNRNPA3, HNRNPD, HSPE1, HTRA2, HYLS1, ID3, IGF2BP3, IGFBP4, IMPA2, INSIG1, KCNN4, KIAA1671, KIF11, KIF14, KIF18A, KIF20A, KIF22, KIF23, KIF2C, KIF4A, KIFC1, KLF15, KRT80, LAMA5, LAMTOR1, LAYN, LDLR, LIMA1, LMNB2, LMTK3, LPAL2, LPP, LPXN, LRP5, LTV1, LYRM2, MAD2L1, MAMDC2, MAMLD1, MCM5, MED26, MELK, METTL5, MGAT2, MIR586, MKI67, MLPH, MMACHC, MRPL34, MRPS18C, MTA3, MXD3, MYLIP, MYO5C, MYOF, NASP, NCAPD2, NDC80, NDP, NDUFA12, NEDD8-MDP1, NEXN, NFE2L3, NGF, NIF3L1, NNMT, NOXA1, NPAS2, NR1H3, NR3C2, NREP, NRP1, NRXN1, NSMCE4A, NUP35, NUP37, NUSAP1, OBFC1, OGFR, OIP5, OLFML2A, OPRK1, OSBPL10, PAAF1, PACSIN3, PAFAH1B1, PAPPA, PARP4, PCCA, PDCD11, PDE7B, PER3, PFN2, PHF15, PHF19, PIF1, PIGT, PIGV, PIGY, PITX1, PKP2, PLAU, PLEK2, PLEKHA6, PLK1, PLK4, PLLP, PLXNA1, PMEPA1, POC1A, POC5, POLA2, POLE2, PPAP2B, PPAPDC1A, PPARG, PPIL1, PPP1R10, PPP5C, PRC1, PRDM8, PRDX3, PRICKLE2, PRIM1, PRNP, PSPC1P1, PSRC1, PXDN, RAB3IL1, RAB7L1, RACGAP1, RAD23B, RAD51AP1, RAN, RARRES3, REPIN1, RGS20, RHOJ, RPL39L, SAMD9L, SCNN1A, SCRN1, SDPR, SEMA3A, SH3PXD2A, SH3RF3, SHISA2, SLC29A2, SLC35B3, SLC37A1, SLC37A2, SLC46A3, SLCO4A1, SNORA73B, SNORD117, SNORD13, SNRPD1, SORBS2, SOX4, SPATS2L, SPCS1, SPDEF, SRBD1, SRF, SRRM1, SRSF6, SUN2, SUSD5, SUV39H1, SVIL, SYNCRIP, TACC2, TACC3, TANC1, TANC2, TCEA3, THBS1, THOC6, TIMELESS, TIMM10, TIMP3, TIPARP, TMCO3, TMEM116, TMEM14A, TMEM163, TMEM237, TMEM60, TMEM71, TMEM75, TNFRSF11B, TNFRSF14, TNFRSF21, TNS3, TOP2A, TOX2, TPX2, TRERF1, TRIM6, TRIM8, TRIP13, TRIP6, TROAP, TTF2, TTK, TUBB, TYMS, UBE2C, UBE2L6, UBE2T, UPF3AP1, UTP18, VIPR1, WDR67, WDR92, WEE1, ZFAND5, ZMIZ1, ZNF627, 21 other genes with no HGNC symbol
Low	Up	ADCY10, ARPC3, ATF5, CTSZ, DDI1, HMOX2, KIRREL, PLXDC1, PRR21, SCARNA14, TAF15, TRIB3, TXN2, VASP, ZNF365, 3 other genes with no HGNC symbol
	Down	ARL4D, BLOC1S1, C17orf65, C19orf10, CPXM2, CRISP1, CSF2, CST1, EDN1, FAM65B, HOGA1, KLF7, MIR23B, MVP, OPRK1, PAX9, PCP2, RAB13, SERPINA5, TFF1, TMEM65, TMEM75, ZNF785, 2 other genes with no HGNC symbol

Supplementary Table 3 ***Differentially expressed genes in LCC1 cells after treatment with Oncamex.***

		LCC1 (differentially expressed genes after high or low treatment with Oncamex)
High	Up	39142, ABCB6, ACP1, ACTG1, ACTL6A, ADM, ADORA2B, ADPGK, AGK, AGPAT5, AHCY, AK4, ALDOA, ALDOC, ALKBH5, ANAPC10, ANGPTL4, ANKRD12, ANKRD37, ANKS1A, ANKZF1, ANXA3, ANXA5, AP3M1, AP4E1, APLF, ARF4, ARGLU1, ARHGEF7, ARID3A, ARL8B, ARNTL, ATG9B, ATP5C1P1, ATP6V0E1, ATP6V1E2, B2M, B3GNT4, BCL11B, BCL2L13, BCL2L2, BHLHE40, BNIP2, BNIP3, BNIP3L, BRD1, BRI3, C12orf5, C14orf109, C14orf129, C14orf135, C15orf42, C17orf58, C17orf96, C18orf25, C1orf51, C3orf58, C3orf70, C4orf29, C4orf3, C7orf23, C7orf42, CA5B, CAB39, CACNB4, CAP2, CASC3, CCDC58, CCDC59, CCNE2, CDH10, CDKN3, CEBPD, CEBPG, CECR5, CELF1, CEP350, CFDP1, CFI, CGRRF1, CHD7, CHFR, CHIC2, CHMP1B, CHMP2B, CHRM3, CHST14, CHST7, CHSY1, CHURC1, CHURC1-FNTB, CISD2, CITED2, CLDN1, CLDN12, CLDND1, CLIC4, CLINT1, CLPX, CNIH, CNNM1, CNOT8, COMMD2, COMMD3, COPS8, COX20, COX7A2L, CPE, CREG1, CRKL, CRLS1, CSRNP2, CSRP2, CSTB, CTDSPL2, CUL2, CXADR, CXorf23, CYP1B1, CYP20A1, DDIT4, DDX18, DDX21, DDX3X, DDX41, DDX5, DDX50, DENND5A, DERA, DERL1, DHX29, DHX32, DMTF1, DNAJA1, DNAJB6, DNAJC24, DOCK7, DPYSL4, DSCR3, DTNA, DUSP1, DUSP14, DVL3, DYNC1I2, DYNLL1, EDA, EDEM1, EEF1A1P12, EEF1A1P19, EEF1A1P6, EEF1G, EGLN1, EIF1, EIF1B, EIF3J, EIF4A1P2, EIF4EBP2, EIF4G2, EIF4H, ELL2P1, ENDOG, ENO2, ENOSF1, ENY2, ERLEC1, ERO1L, ETFA, EXD2, EXOC2, FAF2, FAM110C, FAM129A, FAM162A, FAM210A, FAM220CP, FAM57A, FAM60A, FAM82A2, FAM84B, FBXO21, FBXO34, FBXO8, FCHO2, FEZ2, FJX1, FNBP1L, FOS, FOXO3, FSCN1, FUT11, FZD3, FZD6, FZD9, GALNTL4, GAPDH, GBE1, GCA, GDF15, GHITM, GLB1, GLO1, GOLGA5, GOLPH3, GOLT1B, GPI, GPT2, GRPEL1, GTF2A2, GYS1, H2AFZ, H3F3B, HAGH, HBXIP, HDAC3, HECTD1, HILPDA, HIRA, HIST1H2AC, HIST1H2BD, HIST1H2BG, HIST1H4E, HIST1H4H, HIST2H4A, HIST3H2A, HK2, HLA-A, HMGN2P7, HMGN4, HMOX1, HNRNPA2B1, HOXA5, HPRT1, HSD17B1, HSDL1, HSPA1B, HSPH1, IARS, IDH1, IFIT2, IFIT3, IMP3, ING2, INSIG2, ISCA1, ISCA1P6, JAG2, JKAMP, KBTBD2, KCTD11, KCTD9, KDELR2, KDM3A, KHDRBS1, KHDRBS3, KIAA0907, KIAA1191, KIDINS220, KLF9, KLHL12, KLHL9, KPNA3, KPNA4, LAMC1, LAPTM4B, LDHA, LGALS8, LIPA, LONRF2, LPIN2, LRP11, LRRC37BP1, MAL2, MALSU1, MANBA, MAP2K1, MAP3K13, MAP3K2, MAP6D1, MAPK6, MAPK8, MAPK9, MBD3L3, MBIP, MDH1, MED20, METAP1, METTL18, MFAP1, MFAP3, MGST3, MINPP1, MIR21, MKI67IP, MKRN2, MMADHC, MON2, MORF4L2, MSANTD3, MTERFD1, MTHFD2, MTX2, MTX3, MYO9A, NCKIPSD, NDRG1, NEDD8-MDP1, NETO2, NFE2L1, NFE2L2, NFIL3, NFYA, NIPA1, NMD3, NMI, NOL3, NOP58, NPHP3, NPIPP1, NRIP1, NUDT18, NUP37, ORC4, OSBPL10, OSTC, OTUD6B, OXSR1, P4HA1, P4HA2, PAICS, PALLD, PAM, PAPD7, PARP16, PCBP1, PDK1, PDK3, PELO, PEX11A, PEX13, PEX2, PFDN2, PFKFB3, PFKFB4, PFKP, PFN2, PGAM1, PGAM4, PGK1, PGM1, PGM3, PGRMC1, PHLPP2, PIGA, PIGY, PIM2, PIPSL, PKD1, PLCG2, PLEKHH1, PLOD2, PLS3, PNMA1, POLG, POLG2, POLR2D, PPA1, PPFIA4, PPME1, PPP1R3C, PPP1R3E, PPP2R2A, PPP2R5B, PPPDE1, PPWD1, PQLC3, PRDX2, PRDX4, PRKRIR, PROSER1, PRPSAP2, PRRC2C, PRSS53, PSAT1, PTGES3, PTRF, PTTG1IP, PUM1, PVRL4, RAB11FIP5, RAB20, RAB21, RAB2B, RAB32, RAB3GAP2, RAI1, RAI2, RALGAPA1P, RAP2A, RBM4B, RCOR2, RDX, REXO2, RIC8B, RIMKLA, RIOK3, RIPK4, RIT1, RNF113A, RNF144A, RNF145, RNF24, RNMT, RPL10A, RPL17, RPL18AP16, RPL18P13, RPL21, RPL26, RRAGA, RSBN1, RSL24D1, RUNDC1, SAP30, SART3, SAV1, SC5DL, SCAF8, SCO1, SCOC, SCYL2, SDF2, SEC23B, SEC61G, SEL1L3, SERTAD2, SESN1, SFXN1, SH2B2, SH3GL3, SH3GLB1, SLC22A25, SLC25A4, SLC2A1, SLC33A1, SLC35E3, SLC35F5, SLC41A2, SLC7A11, SLCO2A1, SMAD4, SMEK2, SMG1, SMG8, SMNDC1, SMS, SNRNP27, SPATA5L1, SPRED1, SPRY1, SRSF4, SRSF8, SRSF9, SRXN1, SSH1, STAM, STC1, STC2, STK39, STX3, SULT1C4, SYDE1, TBC1D14, TBK1, TERF2IP, TFRC, THAP6, THOC7, TIMM21, TJP1, TMED2, TMED5, TMEM123, TMEM126A, TMEM14B, TMEM18, TMEM185B, TMEM209, TMEM237, TMEM41A, TMEM43, TMEM74B, TMEM87A, TNKS2, TOR1AIP1, TPD52L1, TPI1, TRAM1, TRIM37, TRIT1, TRMT112, TSPYL1, TSPYL5, TUBA1A, TUBA1B, TUBB6, TXNIP, TXNRD1, TYMS, UAP1L1, USO1, USP10, VAMP7, VGF, VKORC1, VLDLR, VWA7, WASL, WDR26, WDR45L, WDR54, WDR61, WIPI1, WSB1, XPO1, XPOT, YAP1, YARS2, YEATS2, YWHAG, ZBED4, ZC3H12C, ZCCHC14, ZCCHC9, ZFAND5, ZFR, ZIC2, ZNF160, ZNF295, ZNF337, ZNF395, ZNF429, ZNF511, ZNF654, ZNF673, ZNF770, ZNF813, ZNF83, ZNHIT3, ZSWIM5, ZUFSP, 32 other genes with no HGNC symbol
	Down	38777, ABCA12, ABCB4, ABCD1, ACOX3, ACP2, ACSS1, ACSS2, ACTN4, ADAT3, ADCY10, AEBP1, AGAP11, AIP, AIRE, AK2P2, AKR1B1, ALDH16A1, ALG1L, ALKBH6, ALPP, ANKRD33, ANKRD34A, ANKRD44, APOF, ARAF, ARHGAP10, ARHGAP4, ARHGDIA, ARHGEF16, ARHGEF19, ARID5B, ARL2, ARMC5, ARMC7, ARMCX1, ASAP3, ASGR1, ASNA1, ATF5, ATG2A, ATHL1, ATIC, ATN1, ATP13A1, ATP2A3, B4GALNT1, B4GALT1, BASP1, BATF, BCYRN1, BEGAIN, BLOC1S1, BLVRA, BLVRB, BMP7, BMP8B, BNIPL, BOP1, BST2, C10orf27, C10orf81, C11orf2, C12orf66, C14orf28, C14orf80, C14orf93, C15orf52, C16orf42, C17orf28, C17orf53, C17orf67, C17orf70, C17orf82, C19orf46, C19orf53, C19orf54, C19orf66, C1orf138, C1orf86, C20orf27, C20orf94, C2CD4B, C6orf100, C6orf141, C9orf106, C9orf169, C9orf64, CAB39L, CACYBP, CALML5, CAMK1G, CAMK2N1, CAPN1, CBFA2T3, CBX5, CCDC137, CDC20, CDC42EP5, CDT1, CEACAM6, CECR7, CENPB, CERCAM, CGNL1, CHD4, CHD8, CHST1, CHST12, CISH, CITED4, CLIC3, CLN3, COASY, COL16A1, COX19, CPEB3, CPSF1, CRIP1, CROT, CRX, CRY2, CSRNP1, CTGF, CUEDC1, CUL7, CXXC1, CYR61, DAPK3, DBN1, DCAKD, DCLRE1C, DDAH2, DDX6, DEGS1, DENND1B, DIAPH2, DICER1-AS1, DLG4, DNAAF3, DNAJC3-AS1, DNAJC9, DOCK6, DOK4, DTX3, DUS2L, DUSP2, DUSP5, EDN1, EDN2, EEF1A2, EFCAB4A, EFEMP2, EGR2, EHBP1L1, EIF2AK4, EIF2B5, EIF2S1, EIF4G3, ELFN2, ELOVL6, EMD, EML3, ENC1, EOMES, ERBB2, ERCC2, ESR1, ESRRAP2, EVI5, EXD3, EXOC3L4, FAM100A, FAM107B, FAM113B, FAM211B, FAM43A, FAM46B, FAM46C, FAM50A, FAM65A, FAM71F1, FAM83A, FAM83H, FAT2, FBXO27, FDPS, FGD1, FHOD1, FIBCD1, FICD, FIZ1, FNIP2, FOLR2, FOSB, FZD2, GABARAP, GADD45G, GALNT14, GALNT3, GALNT6, GATS, GBP2, GCAT, GCGR, GNB2, GNL1, GPER, GPKOW, GRAMD1A, GSC, GSDMD, GTF2A1, GTF2F1, GUCY1B2, HAND2, HARS, HAUS2, HCFC1R1, HCG9, HDAC11, HDAC6, HDHD2, HES1, HIATL2, HIST1H1D, HIST1H4C, HIVEP3, HKR1, HLA-DMB, HMGCS1, HNRNPKP4, HOOK1, HOXC10, HOXC13, HOXC6, HOXC8, HOXC9, HSD17B7, HSD3B7, IFI35, IGSF9, IKBKE, IL16, IL27RA, IL4R, ILKAP, INPP4B, INPP5J, INPPL1, IPP, IQCC, IRF3, IRX3, ISOC2, ISYNA1, ITPK1, ITPRIP, KCNK12, KIAA0664, KIAA1683, KIF12, KIF18B, KIF22, KLF2, KLF6, KLHDC8B, KRT18P13, KRT18P17, KRT18P19, KRT18P28, KYNU, LAMB2, LCN2, LDLR, LETM1, LGALS12, LHPP, LILRB1, LINC00476, LINGO1, LMAN2, LMNA, LONP2, LRG1, LRP3, LRRC45, LTB, LTB4R, MAP2K2, MAP3K11, MAP3K12, MAP3K5, MAP9, MAPK3, MBD3, MBD4, MBTD1, MCF2L, MEPCE, MFSD11, MGAT3, MICAL1, MIR2278, MIR635, MIR7-3HG, MLLT6, MMAB, MMP25, MOB3C, MOV10, MRPL2, MSRB2, MT1G, MTA2, MTX1P1, MUC20, MVD, MVK, MVP, MX1, MX2, MYB, MYH14, NAGLU, NAPRT1, NAT14, NBEAL2, NBPF20, NCF1C, NCKAP5L, NCLN, NDE1, NDUFB10, NDUFC2, NDUFS7, NEK8, NELF, NEU4, NFYB, NINJ1, NKX2-2, NLRP8, NME3, NMNAT1, NPAS4, NPW, NR1H3, NR2F6, NRCAM, NRSN2, NSDHL, NTHL1, NUBPL, NXNL1, NYNRIN, OBSCN, ODZ3, OR11H12, OR5M4P, OR8B12, OSBPL5, OTUB1, OVGP1, PACS1, PACSIN3, PAF1, PAGE2B,

		PATE2, PBX1, PCDHA3, PCDHB9, PCNXL3, PCYT2, PDE9A, PDIA3P, PELP1, PGR, PHF15, PHKA2, PHLDA2, PIGQ, PIGU, PIGX, PITPNM1, PITX1, PKP1, PKP4P1, PLA2G3, PLA2G4F, PLBD2, PLEKHA4, PLEKHG2, PLIN5, PLK1, PLK2, PLXNB1, PMPCA, PNKP, PNPLA2, PNPLA6, POC1A, POF1B, POLA2, POLR1B, POMT2, POTEI, PPDPF, PPFIBP2, PPM1F, PPOX, PPP1R10, PPP1R13B, PRAF2, PRAMEF6, PRDM6, PREB, PRLR, PRODH, PRRC2A, PRRG2, PRRT3, PRSS8, PSCA, PSD4, PSMB10, PSMC3, PSORS1C2, PTDSS2, PTGER4, PTPLAD2, PXMP4, RAB13, RAB26, RAD54L2, RAD9A, RAP1GAP, RAP2C, RAPGEF3, RARA, RASD1, RASSF5, RAX2, RBM47, RBPMS2, RCHY1, RDBP, RDH16, RENBP, RGS17, RIMS2, RN5S9, RNASEH2B, RND1, RNU1-3, RNU1-5, RPL7L1, RTN4RL1, RUNX3, S1PR3, SALL4, SAMD11, SBK1, SCAMP5, SCARNA9, SCNN1A, SDC1, SDF2L1, SDSL, SEMA3F, SERPINA3, SFMBT2, SFN, SGSM2, SH3BGRL2, SIL1, SIX5, SLC10A4, SLC11A2, SLC12A9, SLC15A3, SLC16A3, SLC16A5, SLC25A10, SLC25A11, SLC25A23, SLC25A29, SLC29A2, SLC2A6, SLC30A3, SLC38A7, SLC43A2, SLC4A8, SLC52A3, SLC5A8, SLC7A8, SLC9A3R1, SLC9A3R2, SMCR5, SNAPC4, SNORD13, SNRPA, SNX29P2, SOGA3, SPC24, SPDEF, SPINK4, SPTBN2, SREBF1, SRF, SRGAP1, SRM, SSH3, SSPO, SSTR2, ST3GAL4, ST3GAL5, ST6GALNAC2, STAP2, STEAP3, STK19P, STK36, STXBP2, SUSD3, SWSAP1, SYMPK, SYNJ2BP, SYT12, SYT17, SYT2, TAF13, TAF6L, TBL3, TCEA3, TCHH, TEAD2, TEF, TGFB1, TGFB3, THOC2, THOP1, TIMP1, TIPARP, TJP3, TLCD1, TM4SF1, TMC6, TMEM120A, TMEM121, TMEM205, TMEM229B, TMEM241, TMEM44, TMEM79, TMEM97, TMSB4XP8, TNFAIP2, TNFRSF14, TOR2A, TP53INP2, TRAPPC9, TRIM3, TRMT1, TSEN54, TSPAN15, TSPAN31, TSPAN33, TSPAN4, TUFT1, TYRO3, UBA7, UROS, USP49, UXS1, VAPB, VASN, VCX, VIPR1, VPS11, WDR18, WDR24, WDR46, WDR73, WDR74, WDR83, WIBG, WNK4, WNT10B, WSB2, XAF1, YIPF3, YPEL3, YWHAE, ZC3H12A, ZCWPW1, ZDHHC1, ZDHHC24, ZER1, ZFYVE19, ZHX2, ZNF148, ZNF219, ZNF223, ZNF329, ZNF358, ZNF385A, ZNF428, ZNF444, ZNF462, ZNF467, ZNF468, ZNF486, ZNF593, ZNF600, ZNF618, ZNF641, ZNF738, ZNF750, ZNF75A, ZNF763, ZNF768, ZNF773, ZNF786, ZNF787, ZNF827, ZSCAN5A, ZSWIM7, 40 other genes with no HGNC symbol
Low	Up	ANO3, C19orf26, CADPS, CCDC19, CHODL, CTGF, EHD3, FADS6, FAM197Y8, FZD10, HNRNPA3, HNRNPA3P3, IER3, KCNJ8, MAML3, MIR708, MTX3, NFAM1, NRAP, NRIP1, OIT3, PRSS45, RAI2, RRH, SCGB3A2, SIAH2, SLC35F1, SLC41A2, SMCP, SULT1C4, TAS2R4, TIPARP, TM4SF20, 6 other genes with no HGNC symbol
	Down	ADCY10, ALPP, BLVRB, C1orf138, C8orf85, CIT, CRX, DDX6, EFEMP2, ETAA1, FAT2, FNIP2, GALNT3, GPR112, HAND2, HIST1H1D, KCTD8, LRFN2, MBTD1, MGAT3, MIR1267, MIR2278, MIR635, NDUFC2, NXT2, OTOF, PGLYRP4, PHC1, PLAA, PLIN5, POLR1A, PSAPL1, PSCA, PSORS1C2, RAD54L2, RPS26P35, RPS28, SCARNA9, SEC31B, SLC10A4, SLC38A11, SMCR5, SNX32, SPRR1B, SSTR2, SSU72P1, TOP1P1, TOR2A, WSB2, ZNF223, 8 other genes with no HGNC symbol

Supplementary Table 4 ***Differentially expressed genes in LCC2 cells after treatment with Oncamex.***

		LCC2 (differentially expressed genes after high or low treatment with Oncamex)
High	Up	ABCB6, ACP1, ADIPOR1, ADM, ADORA2B, ADPGK, ADPRHL2, AGPAT5, AGPAT9, AHCY, AHSA1, AK4, ALDOA, ALDOC, ALKBH5, ANGPTL4, ANKRD37, ANKZF1, ANXA3, ANXA5, AP2M1, AP4E1, APRT, ARHGAP28, ARID3A, ASCL2, ATG9A, ATG9B, ATP6V1E2, B3GNT4, B4GALT5, BET1, BEX2, BEX5, BHLHE40, BNIP2, BNIP3, BNIP3L, BOLA3, BRI3, BSPRY, BTG2, C14orf133, C15orf42, C15orf61, C17orf58, C17orf96, C19orf10, C1orf122, C1orf51, C2orf49, C3orf58, C4orf47, C7orf42, CA5B, CAB39, CAGE1, CALU, CANT1, CASC3, CBX8, CCDC58, CCNA1, CCRN4L, CDK7, CDKN2D, CEBPB, CEBPD, CECR5, CELF1, CFDP1, CHCHD2P9, CHD7, CHIC2, CHST14, CHST7, CHSY1, CHURC1-FNTB, CITED2, CLDN7, CLDND1, CLINT1, CNNM1, CNO, CNTNAP4, COMMD2, COPS8, COX17, COX20, COX7A2L, CPOX, CREG1, CRKL, CRLS1, CSRNP2, CSRP2, CSTB, CTSL3, CXADR, CXorf64, CYB5D1, DAD1, DALRD3, DCTN5, DCUN1D5, DDIT4, DDT, DDX18, DDX21, DDX41, DDX50, DEFB107B, DENND5A, DERL1, DHX32, DNAJB6, DNAJC5, DNMT3A, DOK3, DPH3, DPP4, DPYSL4, DSCR3, DTNA, DUSP1, DUSP14, DUSP18, DYNLL1, DYNLT1, E2F7, EDEM1, EEF1A1P12, EEF1G, EGLN1, EIF1B, EIF3J, EIF4E2, EIF4EBP2, ELF1, ELK1, ENDOG, ENO1P1, ENO2, ENOSF1, EPDR1, EPT1, ERO1L, ETFDH, FAM110C, FAM127B, FAM131A, FAM162A, FAM168B, FAM195A, FAM219A, FAM57A, FAM60A, FBXO34, FJX1, FNBP1L, FOS, FSCN1, FTL, FUT11, FZD3, FZD9, GADD45B, GALNTL4, GAPDH, GBE1, GDAP1, GDF15, GIGYF2, GLO1, GLS, GPI, GPT2, GRPEL1, GTF2A2, GYS1, H3F3B, HAGH, HBEGF, HBXIP, HBXIPP1, HERC1, HES3, HIBADH, HILPDA, HINT1, HIRA, HIST1H2BG, HIST1H4H, HK2, HLA-A, HLA-A, HLA-B, HLA-DRB1, HLA-DRB6, HLA-H, HOMER1, HOXA5, HPRT1, HSPA1A, HSPA1B, HSPA8, HSPH1, IARS, IARS2, ID1, IDH1, IFI27, IFIT2, IL17C, IMP3, INSIG2, ISCA1, ISCA1P6, JAG2, KBTBD2, KCTD11, KCTD5, KDELR2, KDM2A, KDM3A, KIAA0355, KIDINS220, KLHL12, KLHL35, KLHL9, LAMC1, LAMTOR1, LARP6, LDHA, LGALS8, LHX6, LPIN3, LRP11, LRRC58, LYPLAL1, MAD2L1BP, MAL2, MAP1LC3B, MAP2, MAP2K1, MAP6D1, MAPK6, MAPK7, MAPRE1, MDH1, MED20, MESDC1, MGST3, MIR21, MKI67IP, MKRN2, MLEC, MLL5, MORF4L1P1, MORF4L2, MORN2, MRPS23, MTHFD1L, MTHFD2, MTO1, NAF1, NARF, NAT10, NCKIPSD, NDRG1, NDUFA12, NDUFB2, NDUFB6, NEDD8-MDP1, NEUROG3, NFE2L1, NFIL3, NOL3, NOP10, NPHP3, NPIPP1, NSMCE2, NUP37, NXN, ODC1, ORAI2, ORC1, OSBPL10, OSGIN1, OTUD6B, OVOL1, OXSM, OXSR1, P4HA1, P4HA2, PAICS, PALLD, PAM, PAPD7, PCBP1, PDCD2L, PDK1, PDK3, PELI1, PEX11A, PEX11B, PEX13, PFKFB3, PFKFB4, PFKP, PGAM4, PGK1, PGM1, PIGA, PIM1, PIPSL, PITHD1, PKD1, PKM2, PLEKHH1, PLOD2, PNMA1, PNPO, POLG, POLR2B, POLR2D, POLR2H, PPFIA4, PPIL1, PPME1, PPP1R16A, PPP1R3C, PPP1R3E, PPP2R5B, PPPDE2, PRAMEF4, PRDX2, PRDX4, PRPSAP2, PRSS45, PRSS53, PSAT1, PTPN21, PTRF, PTTG1IP, PUS7, PYGL, QSOX1, RAB11FIP5, RAB2B, RAB32, RAB9A, RAN, RAP2A, RBBP5, RBM4B, RCOR2, REV1, RGS6, RIMKLA, RIOK3, RIPK4, RIT1, RNF122, RNF145, RNF24, RNF41, RNFT1, RNMT, RPL10A, RPL13AP7, RPL15P3, RPL17, RPL18AP16, RPL18P13, RPL26, RPL30, RPLP0, RPRD1B, RPS4X, RQCD1, RRP15, RUNDC1, SAMD4A, SAP30, SAV1, SC5DL, SEC23B, SEC23IP, SEC61G, SEL1L3, SERPINB8, SERTAD2, SH2B2, SH3BP1, SH3BP4, SIAH2, SKIV2L2, SLC25A4, SLC25A5, SLC2A1, SLC35B2, SLC35E3, SLC39A14, SLC7A1, SLC7A11, SLCO2A1, SMAD4, SMG1, SMS, SNORA67, SPAG4, SPATS2L, SPRED1, SPRED2, SPRY1, SRSF9, SRXN1, STC1, STC2, STIP1, STRAP, STX3, SYDE1, TAX1BP3, TBK1, TBP, TCF24, TFRC, THUMPD3, TINF2, TJP1, TMCO3, TMED2, TMED5, TMEM123, TMEM14B, TMEM174, TMEM18, TMEM185B, TMEM43, TMEM45A, TMEM74B, TNFAIP1, TNFRSF12A, TNFRSF21, TNKS1BP1, TOR1B, TP53, TPI1, TPI1P1, TRIT1, TSPYL5, TTC26, TUBA1A, TUBA1B, TUBB, TUBB2A, TUBB2B, TUBB4B, TUBB6, TXN, TXNIP, TXNRD1, TYMS, UBFD1, UFM1, UHRF2, ULBP1, UPK1A, USP37, VDAC1, VKORC1, VLDLR, WBP11P1, WBP4, WDR45L, WDR54, WDR61, WRAP73, XPNPEP1, XPOT, YARS2, YEATS2, ZCCHC9, ZIC2, ZNF295, ZNF395, ZNF511, ZNF770, ZNFX1, ZNHIT3, ZSWIM5, ZW10, 36 other genes with no HGNC symbol
	Down	ABCA12, ABCB4, ABCB7, ACAA2, ACACA, ACACB, ACP2, ACSF2, ACSS1, ACTG2, ADCY4, AFAP1L2, AK2P2, AKAP8L, ALCAM, ALG1L, ALKBH8, ALPP, ANKRD1, ANKRD34A, ANKRD44, APOA1, APOC1, APOF, AQP11, AR, ARHGAP4, ARID4B, ARID5B, ARL6IP5, ARMC1, ASAP3, ASGR1, ASNA1, ATHL1, ATIC, ATN1, ATP6V1C1, AURKA, B4GALNT1, BARD1, BASP1, BCAS1, BCL3, BCYRN1, BLVRA, BLZF1, BMF, BMP8B, BMS1P5, BRD3, C10orf27, C10orf68, C10orf81, C14orf28, C14orf93, C15orf52, C17orf53, C17orf67, C19orf46, C19orf71, C1orf162, C1orf54, C20orf94, C21orf56, C6orf225, C8orf37, C9orf169, CABLES1, CACYBP, CAMK2N1, CAPN9, CBX5, CC2D1A, CCDC149, CCDC25, CCNF, CD63, CDC20, CDC25B, CDC42EP4, CDKN2AIPNL, CECR7, CENPB, CENPF, CERS4, CFI, CGN, CGNL1, CHD4, CHD8, CHST12, CISH, CLIC3, CLLU1, CLN3, CMTM8, CNST, COASY, COL16A1, COL9A2, COX19, CPEB3, CREB3L4, CRISP2, CRYGB, CSN1S1, CSRNP1, CTDSPL, CTGF, CUEDC1, CYR61, DBN1, DCLRE1C, DDX6, DEM1, DHCR24, DIAPH2, DICER1-AS1, DLC1, DLG4, DLGAP5, DLX3, DNAAF3, DNAH2, DNAJC22, DOK4, DUSP19, DUSP2, DUSP5, E2F1, E4F1, ECT2, EDC4, EDN1, EDN2, EFCAB4A, EFNB3, EGR1, EGR2, EHBP1L1, EHD1, EID3, EIF2AK4, EIF2C2, ELF5, ELFN2, ELOVL6, EML3, ENDOV, EPN3, ERBB2, ERCC2, ERGIC1, ESR1, ETV6, EVI5, EXOC3L4, FAM100A, FAM107B, FAM113B, FAM175A, FAM183A, FAM200A, FAM211B, FAM27L, FAM46B, FAM46C, FAM63A, FAM83H, FAR1, FBXO18, FBXO27, FEZF2, FGD3, FGFR4, FHOD1, FIBCD1, FICD, FIZ1, FLT3LG, FOSB, FOXC1, FOXP1-IT1, FUT6, FZD4, GABARAP, GADD45G, GALM, GALNT3, GALNT6, GAS2L3, GATS, GCAT, GCN1L1, GNL1, GPER, GPR1, GPR37L1, GRM4, GSTM3, GUCY1B2, GYG2, HAUS2, HES1, HGD, HIATL2, HIST1H1D, HIST1H4C, HIVEP3, HMGB1P1, HMGCS1, HN1L, HOOK1, HOXC8, HOXC9, HSD17B7, IER2, IFT74, IGFBP5, IL20, INPP4B, INPP5J, IPP, IRF2BPL, IRS2, IRX3, IRX5, ISG20L2, ISOC2, ITPK1, ITPK1-AS1, ITPRIP, ITPRIPL2, JPX, KAZALD1, KCNJ13, KCNK5, KCNQ1OT1, KIAA0195, KIAA0664, KIAA1683, KIAA1731, KIF12, KIF22, KLF6, KLHL28, KRT18P13, KRT18P17, KRT18P28, KRT7, KYNU, LAMA5, LDLR, LEPREL4, LEPROT, LHPP, LIN52, LINC00174, LINC00476, LMOD3, LMTK3, LRCH4, LRP1, LRRC45, LRRCC1, LRRFIP1, LTB, LTB4R, MAGEB5, MAGT1, MAN2B2, MAP3K11, MAP3K12, MAP3K5, MAP9, MARVELD1, MARVELD3, MAST3, MBD4, MBTD1, MCF2L, MDK, MEPCE, MFSD11, MIDN, MIR1914, MIS18BP1, MLLT6, MMP25, MRPL28, MSRB2, MTA2, MTF2, MVD, MVK, MX1, MYB, MYO3B, N4BP2, NAGLU, NAT14, NAT9, NBEAL2, NBPF14, NBPF20, NBR2, NCAPG, NCKAP5L, NDE1, NEAT1, NEK8, NEMF, NFIB, NFIX, NFKBIA, NFKBIE, NFYB, NINJ1, NIPAL1, NIPAL3, NKX2-2, NLRP8, NME3, NR1H3, NR2F6, NR4A3, NRCAM, NTHL1, NUAK1, NUBPL, NUCB2, NUCKS1, NYNRIN, OAF, OBSCN, ODZ3, OSBPL5, OVGP1, PACS1, PACSIN3, PAPD5, PBX1, PCDHA3, PCDHB9, PCGF2, PCYOX1, PCYT2, PDE4C, PDZRN3, PELP1, PEX6, PGAP2, PHF15, PHKA2, PHLDB1, PI3, PIGX, PKIB, PKN2, PKP1, PKP4P1, PLA2G3, PLA2G4F, PLEKHA6, PLEKHF1, PLEKHN1, PLIN5, PLK2, PLXNA4, PLXNB1, PNKP, PNPLA6, PNPLA7, PODXL2, POLR1B, POLR3F, PPFIBP2, PPIG, PPM1F, PPP1R10, PPP1R13B, PPP1R9A, PRODH, PROM2, PRR11, PRRG2, PRRT3, PSD4, PSPC1P1, PTGER4, PTPLAD2, PXMP4, QRFPR, RAB13, RAB26, RAD9A, RAP1GAP, RARA, RASD1, RAX2, RBM12B, RBM42, RBPMS2, RDBP, RDH16, REC8, REEP5, RENBP, RFX1, RHBDL2, RHOBTB3, RHPN1, RIMS2, RIMS3, RN5S9, RND1, RNF31, RNU1-5, RPS6KA5, RYBP, S1PR3, SALL4, SAPCD2, SBK1, SCNN1A, SDC4, SDSL, SELENBP1, SEMA3F, SENP3, SERPINA3, SERTAD4, SF3B3, SFMBT2, SFN, SGSM2, SIPA1L3, SIX5, SKIV2L, SLC12A9, SLC16A3,

		SLC16A5, SLC25A25, SLC26A2, SLC29A2, SLC2A6, SLC30A7, SLC43A2, SLC4A11, SLC5A8, SLCO4C1, SMARCA4, SMCR5, SNAPC4, SNORD13, SNORD46, SNRPA, SOCS2, SOGA3, SPDEF, SREBF1, SRF, SRGAP1, SRSF6, SSH3, SSPO, SSTR2, ST3GAL4, ST3GAL5, ST6GALNAC2, STAC, STAR, STEAP3, STK36, STX16-NPEPL1, STXBP2, SUSD2, SUV39H1, SYMPK, SYNJ2BP, SYT17, TACC2, TACC3, TAGLN, TAOK1, TAS2R39, TBC1D10B, TBX2, TCEA1P2, TCEA3, TCF25, TDRD1, TEAD2, TERF1P4, TFEB, TGFB3, THOC2, TIPARP, TM4SF1, TMEM135, TMEM183A, TMEM229B, TMEM241, TMEM44, TMEM45B, TMEM91, TMSB4XP8, TNFRSF14, TNPO3, TNRC6B, TOB1, TP53INP1, TRAPPC9, TRIM38, TRIM66, TROAP, TTC12, TTC32, TTK, TUBD1, TUFT1, TYRO3, TYW3, UGDH, UPF3A, USP36, USP49, VAPB, VASN, VN1R2, VPS11, VTCN1, WDR34, WDR46, WDR73, WIBG, WSB2, XAF1, YPEL3, ZADH2, ZBTB2, ZBTB43, ZCCHC6, ZCWPW1, ZFHX3, ZFP2, ZG16, ZHX2, ZKSCAN1, ZMYND10, ZNF140, ZNF148, ZNF219, ZNF223, ZNF281, ZNF346, ZNF354A, ZNF358, ZNF385A, ZNF418, ZNF462, ZNF467, ZNF486, ZNF562, ZNF579, ZNF600, ZNF641, ZNF644, ZNF738, ZNF750, ZNF75A, ZNF763, ZNF773, ZNF785, ZNF786, ZNF816, ZNF827, ZNF860, ZNF91, ZSCAN5A, 37 other genes with no HGNC symbol
Low	Up	ASNA1, BAI2, C16orf74, C1orf109, CBX5, CLLU1, CRYGB, DYDC2, EID3, FAM132B, FAM27L, HOXD10, KLRG1, MIR1914, NEMF, NIPAL1, OBP2B, PKN2, PLIN5, RIBC1, SENP3, SNORD46, SNRPD3, SPTY2D1, STARD8, TELO2, TK2, TMEM81, ZMYND10, 7 other genes with no HGNC symbol
	Down	BATF2, C1orf216, C9orf57, CD1C, CDY2B, CUL3, EXOSC8, FGFBP3, FOSB, HIST1H2BO, HMCN2, HSPB8, IFI44L, IGFBP4, IL5RA, KRTAP5-10, MEGF10, MIR639, OR2AG2, OSMR, OTC, PLG, TBC1D3B, TKTL1, TNIP3, TSKU, TSSK6, UBQLN4P1, 1 other genes with no HGNC symbol

Supplementary Table 5 ***Differentially expressed genes in LCC9 cells after treatment with Oncamex.***

		LCC9 (differentially expressed genes after high or low treatment with Oncamex)
High	Up	39142, 39326, AASDHPPT, ABCB10, ABCB6, ABCE1, ABHD3, ABHD5, ABRACL, ACAP2, ACOX1, ACP1, ACTG1, ACTL6A, ACTR10, ACTR2, ACTR3, ACVR1, ADAT1, ADIPOR1, ADM, ADNP, ADORA2B, AFF4, AGGF1, AGPAT5, AHCY, AHSA1, AK4, ALDH18A1, ALDH9A1, ALDOA, ALDOC, ALG10B, ALG13, ALKBH5, ALS2, ALYREF, AMZ2, ANAPC10, ANAPC13, ANAPC7, ANGPTL4, ANKIB1, ANKRA2, ANKRD12, ANKRD37, ANKRD46, ANKRD49, ANKS1A, ANKZF1, ANLN, ANO6, ANXA3, ANXA5, ANXA7, AP1G1, AP1S1, AP1S2, AP2M1, AP3M1, AP3S1, AP4E1, AP5M1, APAF1, API5, APIP, ARCN1, ARF4, ARGLU1, ARID3A, ARIH1, ARL6, ARL6IP1, ARMC10, ARMCX5, ARPC1A, ARPC3, ARRDC4, ARV1, ASB8, ASCL1, ASF1A, ASH2L, ASNSD1, ASXL2, ATAD1, ATAD2, ATG16L1, ATG3, ATG4C, ATG9B, ATP2A2, ATP2C1, ATP5C1P1, ATP5F1, ATP5J, ATP6AP2, ATP6V1A, AUH, AZIN1, B2M, B3GNT4, BBS10, BCAR3, BCAS2, BCL11B, BCL2L13, BCL2L2, BECN1, BET1, BFAR, BHLHE40, BMI1, BMPR1A, BMPR2, BNIP2, BNIP3, BNIP3L, BOLA3, BRI3, BRK1, BRMS1L, BRP44, BRP44L, BSDC1, BTAF1, BTBD1, BTBD10, BTBD6, BTF3, BTF3L4, BTG2, BTG3, BTN2A1, C10orf32, C11orf1, C11orf67, C11orf73, C11orf82, C12orf23, C12orf26, C12orf5, C12orf75, C14orf109, C14orf129, C14orf135, C14orf149, C14orf166, C14orf167, C14orf2, C14orf43, C15orf24, C15orf61, C16orf80, C17orf58, C17orf96, C18orf25, C1orf131, C1orf43, C1orf51, C1orf52, C1orf53, C1orf55, C1orf63, C1QBP, C2orf28, C2orf47, C2orf49, C3orf14, C3orf38, C3orf58, C3orf70, C4orf27, C4orf47, C6orf72, C7orf23, C7orf42, C8orf59, C9orf46, C9orf78, C9orf89, CA5B, CAB39, CALM2, CALU, CAND1, CANT1, CAP2, CAPN7, CASC4, CASP7, CAT, CBFB, CBL, CBLL1, CBWD5, CBX1, CCDC112, CCDC117, CCDC47, CCDC53, CCDC59, CCDC72, CCDC99, CCNC, CCNDBP1, CCNE2, CCNG1, CCNG2, CCNYL1, CCT2, CCZ1B, CD2, CD2AP, CD46, CD58, CD9, CDC42SE1, CDC5L, CDH1, CDK1, CDK2, CDK7, CDK8, CDKN3, CECR5, CELF1, CENPK, CENPQ, CEP120, CEP350, CEP44, CERS2, CGRRF1, CHCHD2P6, CHCHD2P8, CHCHD2P9, CHCHD3, CHIC2, CHMP1B, CHMP2B, CHMP5, CHPT1, CHRM3, CHST14, CHST7, CHSY1, CHURC1, CHURC1-FNTB, CISD2, CITED2, CLASP2, CLDN12, CLDN23, CLDND1, CLIC4, CLINT1, CLNS1A, CLPX, CMAS, CMPK1, CMTM6, CNEP1R1, CNIH, CNO, CNOT7, CNOT8, COG6, COMMD10, COMMD2, COMMD3, COMMD6, COPB1, COPB2, COPS4, COPS5, COPS8, COX17, COX20, COX5B, COX6B1, COX6C, COX7A2L, COX7C, CPNE3, CRADD, CREBZF, CREG1, CRIPT, CRK, CRKL, CRLS1, CRY1, CSNK1G3, CSNK2A1, CSRNP2, CSRP2, CST9, CSTB, CTCF, CTDSPL2, CTNNAL1, CTSL2, CUL2, CUL5, CXADR, CYB5A, CYB5D1, CYB5R4, CYBASC3, CYC1, CYCSP55, CYFIP1, CYP1B1, CYP20A1, DAD1, DCUN1D5, DDIT4, DDT, DDX18, DDX21, DDX3X, DDX5, DDX60, DENND5A, DERA, DERL1, DET1, DHRS7, DHX15, DHX29, DHX32, DHX36, DIP2B, DLD, DLEU1, DMTF1, DNAAF2, DNAJA1, DNAJA4, DNAJB6, DNAJC24, DNAL4, DOCK7, DPF2, DPH3, DPM1, DPY19L1, DPY19L4, DPY30, DPYSL4, DR1, DSCR3, DTWD1, DUSP1, DUSP11, DUSP14, DUSP16, DVL3, DYNC1I2, DYNLL1, DYNLT1, DYNLT3, DYRK1A, E2F5, E2F7, EAF1, EDEM1, EDEM3, EEF1A1P12, EEF1A1P19, EEF1A1P27, EEF1A1P6, EEF1B2, EEF1E1, EEF1G, EFR3A, EGLN1, EHHADH, EI24, EID2, EIF1, EIF1B, EIF2AK3, EIF3J, EIF4A1P2, EIF4A3, EIF4B, EIF4E3, EIF4EBP2, EIF4G2, EIF4H, ELF1, ELL2P1, ELOVL5, EML4, ENDOG, ENO2, ENOPH1, ENOSF1, ENPP4, ENSA, ENY2, EPCAM, EPHB1, EPRS, EPT1, ERLEC1, ERLIN1, ERO1L, ESD, ETFA, EXD2, EXOC1, EXOC2, EXOC5, EXOSC3, F2RL1, F9, FAM122B, FAM126B, FAM149B1, FAM162A, FAM168B, FAM174A, FAM18B1, FAM18B2-CDRT4, FAM190B, FAM195A, FAM199X, FAM206A, FAM210A, FAM214A, FAM216A, FAM217B, FAM220CP, FAM3C2, FAM45A, FAM57A, FAM60A, FAM82A2, FAM82B, FAM83D, FAM84B, FAM96A, FAT1, FBXL3, FBXO21, FBXO28, FBXO33, FBXO34, FBXO45, FBXO8, FBXW11, FEZ2, FNBP1L, FNDC3B, FNTA, FOS, FOXA1, FOXN2, FRMD6, FSCN1, FTH1, FTH1P7, FTL, FTLP3, FTSJD1, FUNDC1, FUT11, FZD1, FZD3, FZD6, G3BP2, GABARAPL2, GALNT12, GALNTL4, GAPDH, GBE1, GCA, GCH1, GCSH, GDF15, GEMIN2, GFPT1, GGH, GHITM, GIGYF2, GJB2, GLB1, GLCE, GLO1, GLRX2, GLRX3, GNA13, GNAQ, GNG10, GNPTAB, GOLGA5, GOLPH3, GOLT1B, GPAM, GRAMD3, GRB2, GRPEL1, GTF2A2, GTF2B, GTF2E1, GTF2H5, GTF3C3, GYS1, H2AFZ, HAGH, HAT1, HBP1, HBXIP, HBXIPP1, HCAR1, HEATR5B, HECTD1, HELZ, HERC1, HIBADH, HIGD1A, HILPDA, HINT1, HIST1H2AC, HIST1H2AE, HIST1H2AG, HIST1H2BD, HIST1H2BG, HIST1H2BJ, HIST1H2BK, HIST1H3H, HIST1H4A, HIST1H4E, HIST1H4H, HIST2H2BB, HIST2H2BE, HIST2H3C, HIST2H4A, HIST3H2A, HK2, HLA-A, HLA-B, HLTF, HMGB2, HMGN1, HMGN2P17, HMGN2P7, HMGN4, HNRNPA0, HNRNPA1P12, HNRNPH1, HNRNPH2, HNRNPK, HNRNPKP4, HOMER1, HPRT1, HPS3, HRSP12, HSD17B4, HSP90B1, HSPA14, HSPA1A, HSPA1B, HSPA4L, HSPA8, HSPH1, HTATIP2, IARS, IARS2, ID1, ID2, ID3, IDH1, IFI44L, IFIH1, IFIT2, IFNK, IL6ST, IL8, ILF2, IMP3, IMPA1, IMPAD1, ING2, INSIG2, INTS2, IPO7P2, ISCA1, ISCA1P6, ISOC1, ITFG1, ITGA2, ITGAE, ITGAV, ITGB1, ITGB1BP1, ITGB3BP, ITM2B, ITPR1, JAK1, JKAMP, KAL1, KAT2B, KBTBD2, KBTBD4, KCNK1, KCTD11, KCTD18, KCTD3, KCTD5, KDELR2, KDM2A, KDM3A, KHDRBS1, KHDRBS3, KIAA0101, KIAA0196, KIAA0247, KIAA0355, KIAA0391, KIAA0907, KIAA1033, KIAA1191, KIAA1279, KIAA1324L, KIAA1468, KIAA1715, KIDINS220, KIF21A, KIF3B, KLF9, KLHDC2, KLHDC5, KLHL12, KLHL20, KLHL9, KPNA3, KPNA4, KRT10, LACTB, LAMC1, LAMP2, LAMTOR1, LANCL1, LAP3, LAPTM4B, LCLAT1, LCMT2, LDHA, LGMN, LHX2, LHX6, LIMA1, LINC00116, LINC00493, LIPA, LMBR1, LMBRD1, LNX2, LPIN2, LRP11, LRP8, LRRC57, LRRC58, LSM3, LTV1, LXN, LYPLAL1, LYRM2, LYRM5, LYSMD2, MAD2L1, MAD2L1BP, MAL2, MANBA, MAP2K1, MAP3K13, MAP3K8, MAP6D1, MAPK1IP1L, MAPK6, MAPK9, MAPRE1, MARCKS, MARS2, MBIP, MBLAC2, MBTPS1, MCEE, MCFD2, MCU, MDH1, ME1, ME2, MED27, MED30, MED7, MELK, METAP1, METTL21D, METTL23, METTL5, MEX3C, MEX3D, MFAP1, MFAP3, MFF, MFSD8, MGAT2, MGST3, MICA, MINPP1, MIR21, MKI67IP, MKRN2, MLH1, MMADHC, MMD, MMGT1, MNAT1, MOAP1, MOB1A, MOB4, MON2, MORF4L1P1, MORF4L2, MORN2, MPHOSPH6, MPP5, MRFAP1, MRPL13, MRPL18, MRPL22, MRPL32, MRPL33, MRPL39, MRPL45, MRPL50, MRPS18C, MRPS21, MRPS23, MRPS30, MRPS31, MRPS35, MRS2, MTDH, MTERFD1, MTHFD2, MTM1, MTMR6, MTPN, MTRNR2L1, MTX2, MTX3, MYC, MYO5C, MYOF, NAA20, NBN, NCAPG2, NCK1, NCOR1, NCSTN, NDFIP2, NDRG1, NDUFA12, NDUFA4, NDUFA7, NDUFB3, NDUFB5, NDUFB6, NDUFS4, NECAP1, NEDD8-MDP1, NEK7, NFE2L2, NFIL3, NFXL1, NGDN, NGRN, NIPA1, NMD3, NOA1, NOL3, NOL7, NOP10, NPC1, NPHP3, NPIPP1, NPM1P5, NPTN, NRBF2, NREP, NSA2, NSMCE2, NTAN1, NUDCD2, NUDT21, NUP153, NUP160, NUP37, NUP54, NUPL2, OAT, OBFC2A, OCRL, OR2D3, OSBPL10, OSGIN2, OST4, OSTC, OSTCP2, OTUD4, OTUD6B, OXR1, OXSM, OXSR1, P4HA1, P4HA2, PABPC3, PAICS, PAIP2, PAM, PAN3, PAPD4, PAPD7, PAPSS1, PAQR3, PARP4, PATE3, PCBP1, PCGF5, PCMTD1, PCMTD2, PCNA, PCNP, PDCD10, PDCD2, PDCD2L, PDE6D, PDIA6, PDIK1L, PDK3, PELO, PEPD, PERP, PEX1, PEX11A, PEX13, PEX2, PFKFB3, PFKFB4, PFKP, PFN2, PGAM1, PGAM4, PGK1, PGM1, PGM3, PGRMC1, PHACTR2, PHACTR4, PHF5A, PHLPP2, PI4K2B, PIAS2, PIAS3, PICALM, PIGA, PIGB, PIGC, PIGF, PIGH, PIGK, PIGP, PIGT, PIGY, PIK3C2A, PIK3CB, PIK3IP1, PIK3R4, PIPSL, PIR, PKD2, PLEKHA2, PLEKHH1, PLOD2, PLRG1, PLS1, PLS3, PLSCR1, PMS2P5, PNMA1, PNPLA8, PNPO, POC1B-GALNT4, POLG2, POLR2B, POLR2H, PON2, PPA1, PPAT, PPCS, PPFIA4, PPIAP29, PPIC, PPM1D, PPME1, PPP1CC, PPP1R12A, PPP1R2P3, PPP1R3C, PPP1R3D, PPP1R3E, PPP2CB, PPP2R5B, PPP3CC, PPP3R1, PPPDE1, PPPDE2, PPTC7, PPWD1, PQLC3, PRAMEF6, PRDM6, PRDX2, PRDX3, PRDX4, PREP, PREPL, PRKAG1, PRKAR1A, PRKRIR, PRMT10, PRMT3, PRMT6, PRNP, PROSER1, PRPF18, PRPS1, PRPSAP2, PRRC1, PRRC2C, PSAT1, PSMA3, PSMB5, PSMC1P9, PSMC4, PSMC6, PSMD10, PSMD6, PSMD7, PSMG1, PSMG2, PSPH, PTGES3, PTPLA, PTPLB, PTPN12, PTRF, PTS, PTTG1IP, PUM2, PUS7L, PWWP2A, RAB11FIP2, RAB20,

		RAB21, RAB22A, RAB2B, RAB5A, RAB9A, RABGGTB, RAD51C, RALGAPA1, RALGAPA1P, RAN, RAP2A, RAPGEF2, RARS2, RASA1, RB1CC1, RBBP5, RBM23, RBM43, RBM4B, RBX1, RC3H2, RCN2, RDH10, RDX, REXO2, RGL3, RIC8B, RIMKLA, RINT1, RIOK2, RIOK3, RIPK2, RIT1, RLF, RMI1, RNASEL, RND3, RNF103, RNF122, RNF13, RNF145, RNF4, RNF5P1, RNFT1, RNMT, RPAP3, RPL10A, RPL10P3, RPL12, RPL13AP7, RPL15, RPL15P3, RPL17, RPL18AP16, RPL18P13, RPL19P12, RPL21, RPL22, RPL23AP4, RPL23AP64, RPL24, RPL26, RPL26L1, RPL26P30, RPL29, RPL30, RPL31, RPL34, RPL35A, RPL39, RPL39L, RPL6, RPL9, RPL9P25, RPLP0, RPS15A, RPS17, RPS25, RPS27L, RPS3AP5, RPS4X, RPS5, RPS6, RQCD1, RRAGA, RRAS2, RRM2, RRP1B, RSBN1, RSBN1L, RSRC1, RTCD1, RUNDC1, RWDD3, SAP30, SAR1A, SAR1B, SAV1, SC5DL, SCAF8, SCFD1, SCML1, SCO1, SCOC, SCPEP1, SCYL2, SDCBP, SDF2, SDHB, SDHD, SEC11C, SEC23B, SEC23IP, SEC24A, SEC24D, SEC61G, SEH1L, SENP2, SENP5, SERINC1, SERP1, SERPINI1, SERTAD2, SETD9, SFT2D1, SFXN1, SH3BP1, SH3D19, SH3GL3, SH3GLB1, SHOC2, SHQ1, SIAH2, SIDT1, SIRT1, SKAP2, SKIV2L2, SLBP, SLC25A3, SLC25A36, SLC25A4, SLC25A46, SLC25A5, SLC2A1, SLC31A1, SLC31A2, SLC33A1, SLC35A3, SLC35E3, SLC35F5, SLC37A1, SLC39A14, SLC39A6, SLC39A8, SLFN5, SLIRP, SLK, SLMO2, SMAD4, SMARCAD1, SMEK2, SMG1, SMG8, SMNDC1, SMS, SNRNP27, SNRPB2, SNX19, SNX2, SNX27, SNX3, SNX30, SNX4, SNX5, SOX4, SPAG9, SPATA5L1, SPATS2, SPATS2L, SPCS1, SPG11, SPPL2A, SPRY1, SPTSSB, SQLE, SRP14, SRP54, SRP9, SRP9P1, SRRM1, SRSF7, SRSF8, SRSF9, SRXN1, SSFA2, SSR1, STAM, STARD3NL, STARD7, STC1, STC2, STK3, STRADBP1, STRAP, STRBP, STRN3, STX3, STXBP3, SUCLA2, SUMO2, SUMO2P3, SYBU, SYDE1, SYNCRIP, SYPL1, SYS1, SYVN1, TADA1, TAF12, TAF2, TAF4, TAF7, TANC1, TAX1BP3, TBC1D14, TBCAP1, TBCK, TBK1, TBL2, TBP, TEFM, TFB2M, TFDP1, TFF1, TFRC, THAP11, THAP6, THOC3, THOC7, THUMPD1, THUMPD3, TIA1, TIAL1, TIMM21, TJP1, TM2D1, TM2D3, TM9SF4, TMBIM4, TMCO3, TMED10, TMED2, TMED5, TMED7, TMEM123, TMEM126A, TMEM126B, TMEM14A, TMEM14B, TMEM14D, TMEM165, TMEM167A, TMEM185B, TMEM192, TMEM2, TMEM209, TMEM230, TMEM237, TMEM245, TMEM33, TMEM39A, TMEM41A, TMEM43, TMEM59, TMEM64, TMEM85, TMEM87A, TMTC2, TMTC3, TMX1, TNFAIP1, TNFRSF12A, TOMM20, TOP2A, TOP2B, TOR1AIP1, TOR1B, TPD52L1, TPGS2, TPI1, TPK1, TRAM1, TRAPPC11, TRAPPC4, TRAPPC8, TRIM32, TRIM33, TRIM37, TRIP4, TRIT1, TRMT112, TSC22D2, TSEN15, TSG101, TSHZ1, TSNAX, TSPAN13, TSPAN3, TSPYL1, TSPYL5, TTC19, TTC5, TTF2, TUBA1A, TUBA1B, TUBB, TUBB6, TUSC3, TWSG1, TXN, TXNDC16, TXNDC17, TXNIP, TXNRD1, TYMS, UBA5, UBB, UBE2A, UBE3C, UBE4A, UBFD1, UBL3, UBQLN1, UBXN2B, UCHL5, UFM1, UHRF2, UNC50, UPF3AP1, UQCRFS1, UQCRQ, USMG5, USO1, USP10, USP3, USP34, USP37, USP8P1, VAMP4, VAMP7, VBP1, VDAC1, VIM, VKORC1, VKORC1L1, VLDLR, VPS29, VPS4B, WASF3, WASL, WBP4, WDR12, WDR26, WDR36, WDR37, WDR45L, WDR47, WDR61, WDSUB1, WRB, WRNIP1, WSB1, XBP1, XPC, XPNPEP1, XPO1, XPOT, XRCC5, XRN2, YAP1, YARS2, YEATS2, YEATS4, YIPF6, YME1L1, YPEL2, YTHDF3, YWHAG, ZBED4, ZBTB34, ZC3H12C, ZC3H15, ZCCHC14, ZCCHC8, ZCCHC9, ZDHHC13, ZFAND1, ZFAND5, ZFAND6, ZFP106, ZFR, ZFX, ZIC2, ZNF189, ZNF217, ZNF277, ZNF295, ZNF330, ZNF395, ZNF397, ZNF511, ZNF614, ZNF654, ZNF680, ZNF770, ZNF791, ZNF83, ZNFX1, ZNHIT3, ZNHIT3, ZSWIM5, ZZZ3, 103 other genes with no HGNC symbol
	Down	36951, 38777, 40057, AAGAB, AARSD1, AATF, ABCA3, ABCA7, ABCB7, ABCC12, ABCD1, ABHD14B, ACACA, ACACB, ACAD9, ACP2, ACP6, ACSF2, ACSS1, ACSS2, ACTN1, ACTN4, ACTR1A, ACTR5, ADAP1, ADAT3, ADCK1, ADCK4, ADCY3, ADM2, ADRBK1, AEBP1, AES, AFAP1L2, AFF3, AGAP11, AGRN, AHR, AIP, AIRE, AK2P2, AKAP8L, AKR1D1, ALDH16A1, ALDH8A1, ALG1L, ALKBH2, ALKBH6, ALPP, AMDHD2, AMH, AMT, ANKMY1, ANKRD13B, ANKRD30A, ANKRD30B, ANKRD33, ANKRD34A, ANKRD44, ANKRD52, ANKRD54, ANKS3, ANO9, ANXA11, ANXA2R, AP5Z1, APOA5, APOE, APOF, APOL2, ARAF, ARAP1, ARFGAP1, ARFGAP2, ARHGAP10, ARHGAP4, ARHGDIA, ARHGDIB, ARHGEF16, ARHGEF19, ARHGEF2, ARID4B, ARL2, ARL6IP4, ARL6IP5, ARMC1, ARMC5, ARMC7, ARPC4-TTLL3, ARRB1, ASAP3, ASIC3, ASL, ASMTL, ATAD3A, ATF7IP2, ATG12, ATG16L2, ATG2A, ATG7, ATHL1, ATIC, ATN1, ATOX1, ATP13A1, ATP5D, ATP6AP1, ATP6V1B1, ATXN2, ATXN7L2, AURKAIP1, AZI1, B3GALT6, B3GAT3, B4GALNT1, B4GALT1, BAG6, BATF, BCAS4, BCKDK, BCYRN1, BGN, BIN3, BLMH, BLVRA, BLVRB, BLZF1, BMP7, BMP8B, BMS1P5, BNIPL, BOP1, BRAT1, BRD3, BRD9, BRF1, BRSK1, BSG, BST2, BTBD2, C10orf114, C10orf27, C10orf81, C11orf2, C11orf83, C12orf10, C12orf44, C14orf102, C14orf159, C14orf28, C14orf79, C14orf80, C14orf93, C15orf52, C16orf48, C16orf57, C16orf59, C16orf7, C16orf79, C16orf93, C17orf28, C17orf53, C17orf61, C17orf67, C17orf70, C19orf21, C19orf24, C19orf33, C19orf46, C19orf66, C1orf135, C1orf54, C1orf86, C20orf27, C20orf94, C20orf96, C21orf56, C21orf58, C22orf25, C2CD4B, C2orf55, C4orf48, C5, C6orf141, C6orf170, C6orf225, C6orf47, C6orf52, C7orf41, C7orf50, C8orf37, C8orf73, C8orf82, C9orf106, C9orf114, C9orf142, C9orf169, C9orf37, C9orf64, C9orf86, CABLES1, CACFD1, CACNA1H, CACYBP, CAD, CALML5, CAMK1, CAMK2B, CAMK2N1, CAMK2N2, CAPN9, CAPZB, CARD9, CARM1, CATSPER2, CBFA2T3, CBX5, CC2D1A, CCDC101, CCDC102A, CCDC12, CCDC124, CCDC125, CCDC154, CCDC92, CCDC94, CCND1, CCNF, CD320, CD63, CD96, CD99L2, CDC20, CDC34, CDC42EP2, CDC42EP5, CDK10, CDKN2AIPNL, CDT1, CEACAM6, CECR7, CEL, CENPB, CENPF, CENPT, CEP164, CERCAM, CERS4, CES2, CFB, CFLAR, CGN, CGNL1, CHAC1, CHD4, CHD5, CHD8, CHMP1A, CHPF, CHST1, CHST12, CHTF18, CIC, CIRH1A, CISH, CITED4, CIZ1, CLASRP, CLIC3, CLIP2, CLN3, CLN6, CLPTM1, CNNM3, CNST, CNTROB, COASY, COG2, COL16A1, COL1A1, COL5A1, COL6A1, COL7A1, COMTD1, CORO7, COX19, CPSF1, CPT1B, CREB3L4, CRIP1, CRIP2, CRIPAK, CROCC, CRY2, CRYBA2, CSF2RA, CSK, CSNK1G2, CSRNP1, CST1, CTC1, CTGF, CUEDC1, CUEDC2, CUL9, CUX2, CXXC1, CYB5R1, CYBA, CYP4F12, D2HGDH, DAGLB, DAPK3, DAXX, DBN1, DBNDD1, DBNL, DCAKD, DCLRE1C, DCXR, DDAH2, DDX27, DDX28, DDX39A, DDX51, DDX56, DDX6, DEF6, DEGS2, DEM1, DENND4B, DGAT1, DGAT2, DGCR5, DGCR6L, DGKD, DHCR24, DHCR7, DHRS2, DHX37, DIAPH2, DICER1-AS1, DIP2C, DIS3L, DLG4, DLX3, DMAP1, DMWD, DNAAF3, DNAJC22, DNAJC3-AS1, DNAJC9, DNM1, DOCK6, DOK7, DOLK, DPEP2, DPP9, DTNB, DTX3, DUS2L, DUS3L, DUSP19, DUSP2, DUSP5, E2F2, E4F1, EBF4, ECHDC2, ECSIT, EDC4, EDN1, EDN2, EFCAB4A, EFHD2, EFNB3, EGR1, EGR2, EHBP1L1, EHD1, EHMT2, EIF2AK4, EIF2B5, EIF2C2, EIF2S1, EIF3G, EIF4EBP1, EIF4G3, ELMO3, ELP2, ELP3, EMD, EMG1, EML3, ENDOV, ENO3, ENTPD8, EOMES, EPHB4, EPN1, ERBB2, ERN1, ESPN, ESR1, ESRRAP2, ETNK2, ETV6, EVI5, EVL, EVPL, EXD3, EXOC3, EXOC3L4, EXOSC4, EXOSC6, EZR, FAAH, FAH, FAM100A, FAM102A, FAM104B, FAM107B, FAM108C1, FAM113B, FAM116B, FAM125A, FAM134C, FAM153A, FAM175A, FAM178A, FAM183A, FAM186B, FAM203B, FAM211B, FAM213B, FAM40B, FAM43A, FAM46B, FAM46C, FAM50A, FAM63A, FAM65A, FAM69B, FAM71F1, FAM73A, FAM83A, FAM83G, FAM83H, FAM98A, FANCE, FAR1, FBLN5, FBRSL1, FBXL17, FBXL6, FBXO27, FBXW4, FBXW9, FCAR, FCHO1, FDPS, FERMT2, FGB, FGD1, FGD3, FGFR4, FHL2, FHOD1, FIBCD1, FICD, FKBP11, FKBP4, FKTN, FLOT2, FOSB, FOXJ2, FOXM1, FOXO4, FOXP1-IT1, FOXRED1, FRG1, FSHB, FUK, FURIN, FUT6, FZD2, G6PC3, GAA, GADD45G, GADD45GIP1, GALK1, GALNT3, GALNT6, GATS, GBP2, GCAT, GCN1L1, GDF11, GDI1, GFOD1, GINS2, GIT1, GLT25D1, GLTPD1, GMPPA, GNA11, GNB2, GNL3L, GPATCH3, GPC2, GPER, GPKOW, GPR1, GPR108, GPR137, GPR37L1, GPSM1, GPX2, GRIPAP1, GRWD1, GSDMB, GSDMD, GSTM2, GSTM3, GSTO2, GTF2F1, GTF3C1, GUCY1B2, H1FX, HABP4, HADHA, HARS, HAUS2, HCFC1R1, HCG9, HCN2, HCN3, HDAC6, HDGF, HDHD2, HEATR6, HES1, HEXDC, HEY2, HGS, HIATL2, HINT2, HIP1R, HIST1H1D, HIST1H4C, HIVEP3, HJURP, HKR1, HLA-DMA, HMG20A, HMG20B, HMGCR, HMGCS1, HN1L, HNRNPD, HNRNPUL2, HOOK1, HOOK2, HOXC10, HOXC13, HOXC8, HOXC9, HPX, HSCB, HSD17B7, HSD3B7, HTT, ICA1, IDUA, IER2, IFI27L2, IFT122, IFT74, IGFBP4, IGFBP5, IGSF9, IKBKE, IL10, IL18, IL27RA, IL34, ILKAP, IMP4, INO80E, INPP4B, INPP5J, INPPL1, INTS1, IPO11, IPO13, IPP, IQCC, IRF3, IRF7, IRX3, ISOC2, ISYNA1, ITFG3, ITGA10, ITIH4, ITPA, ITPK1, ITPK1-AS1, ITPKB, ITPRIP, ITPRIPL2, JMJD8, JOSD2, KAT2A, KCNAB1, KCND1, KCNK12, KCNK6, KCNMB4, KCNQ1OT1, KDELR1, KHSRP, KIAA0195, KIAA0284, KIAA0664, KIAA0664L3, KIAA1324, KIAA1683, KIAA1731, KIF12, KIF22, KIFC2, KLF2, KLF6, KLHDC4, KLHL22, KLHL28, KREMEN2, KRT18P13, KRT18P17, KRT18P19, KRT18P28, KRT7, KRT8, KRTCAP2, LACC1, LAG3, LAMA5, LAMB2, LCN2, LCP1, LDHD, LDLR, LEP, LEPREL4, LETM1, LHPP, LILRB1, LIN52, LINC00173, LINC00174, LINC00265, LINC00323, LINC00341, LINC00476, LMF2,

		LMNA, LMOD3, LONP2, LPAR2, LPP, LRCH4, LRFN3, LRFN4, LRP3, LRRC23, LRRC45, LRRFIP1, LTB, LTB4R, LTBR, LY6E, LYPD6B, LYPLA2, LYRM1, MACF1, MACROD1, MAF1, MAGT1, MAML3, MAN1B1, MAN2B1, MAN2B2, MAN2C1, MAOA, MAP1S, MAP3K11, MAP3K12, MAP3K6, MAP4K2, MAPK8IP3, MAPKAPK3, MAPRE3, MAST3, MAT2A, MBD3, MBD4, MBD6, MBOAT2, MBTD1, MCART1, MCF2L,
		MUC20, MUM1, MVD, MVK, MVP, MX1, MX2, MXD3, MYB, MYH14, MYH3, MYL5, MYO1C, MYO3B, MYO9B, MYOM1, N4BP2, NAA10, NACC1, NAGLU, NAGPA, NAPRT1, NARFL, NAT14, NBEAL2, NBL1, NBPF20, NBPF8, NCKAP5L, NCLN, NDE1, NDST1, NDUFB10, NDUFV1, NEAT1, NEIL2, NEK8, NELF, NFIB, NFIX, NFKB2, NFKBIA, NFKBIE, NFYB, NINJ1, NINL, NKX2-2, NLRP8, NME3, NMRAL1, NOL6, NOP14, NOTCH1, NOXA1, NPW, NR1H3, NR2C2AP, NR2E3, NR2F6, NRCAM, NRSN2, NSDHL, NSMCE1, NT5DC2, NTHL1, NUAK1, NUBPL, NUCB1, NUCKS1, NUDC, NUDT3, NUPR1, NYNRIN, OBSCN, ODZ3, OGFR, OPLAH, OPRL1, ORAI1, OSBPL5, OSBPL7, OTUB1, OVGP1, P2RX2, P2RY6, PABPN1, PACS1, PACSIN1, PACSIN3, PAF1, PAFAH1B3, PALM, PALM3, PAQR4, PARP10, PARP12, PATE2, PBX1, PBX2P1, PCDHA3, PCDHB9, PCGF2, PCIF1, PCNT, PCNX, PCNXL3, PCSK1N, PCYT2, PDDC1, PDE1A, PDE4C, PDE9A, PDIA4, PDP2, PDZD4, PEF1, PELI3, PELP1, PEX11G, PEX16, PGAP2, PGR, PHF15, PHF21B, PHKA2, PHKG2, PHLDA2, PI4KB, PIAS4, PICK1, PIEZO1, PIGQ, PIGU, PIGX, PIP5K1C, PITPNM1, PKMYT1, PKN1, PKP1, PLA2G10, PLA2G2D, PLAC8L1, PLBD2, PLCD3, PLD6, PLEKHA4, PLEKHA6, PLEKHH3, PLEKHM2, PLEKHO2, PLIN5, PLK2, PLXNA1, PLXNA3, PLXNA4, PLXNB1, PMPCA, PNCK, PNKP, PNPLA6, PNPLA7, PNPT1, POC1A, PODXL2, POLA2, POLD1, POLD2P1, POLQ, POLR1B, POLR3F, POLRMT, POMGNT1, POMT2, PPDPF, PPFIBP2, PPM1F, PPM1K, PPM1M, PPP1R10, PPP1R13B, PPP1R26, PPP1R9A, PPP2R1A, PPP2R4, PPP6R1, PPRC1, PRDM11, PREB, PRKCZ, PRKD2, PRODH, PROM2, PRPF19, PRPF31, PRPH, PRR14, PRR22, PRR24, PRRC2A, PRRG2, PRRG4, PRRT2, PRRT3, PRSS22, PRSS23, PRSS8, PSD4, PSMB10, PSMD8, PSME4, PTBP1, PTDSS2, PTGER4, PTGR2, PTK6, PTP4A2, PTP4A3, PTPLAD2, PTPN23, PTPN6, PUSL1, PYCARD, PYCRL, PYGO2, QARS, QRFPR, QTRT1, R3HDM4, RAB11FIP3, RAB11FIP4, RAB13, RAB17, RAB26, RAB33B, RAB3IL1, RAB9B, RABAC1, RAC1P2, RAD23A, RAD54L2, RAD9A, RANGAP1, RAP1GAP, RAPGEFL1, RARA, RARRES3, RASD1, RASIP1, RASSF6, RAVER1, RAX2, RBFA, RBKS, RBM42, RBM6, RDBP, RDH13, RDH16, RDH5, REC8, RECQL4, RERE, RET, REXO1, RFTN1, RFX1, RGS11, RGS17, RHBDD2, RHBDL1, RHBDL2, RHOBTB3, RHOG, RHPN1, RIMS2, RIMS3, RIPK1, RN5S9, RNASEH2A, RND1, RNF10, RNF213, RNF25, RNF31, RNMTL1, RNU1-3, RNU1-5, RNU6-1, RNU6-15, RNY3, ROGDI, RPL14, RPL28, RPL7L1, RPP40, RPUSD1, RPUSD2, RRAGC, RRP1, RRP12, RRP7A, RRS1, RTN4RL1, RUSC1, RUVBL2, RXRA, S100A16, S100A7, S100A8, S1PR3, SAA2-SAA4, SAC3D1, SAFB, SALL4, SAMD1, SAMM50, SAP30BP, SBF1, SBNO2, SCARNA9, SCIN, SCNN1A, SCNN1B, SCNN1D, SDC1, SDC4, SDF2L1, SDSL, SELENBP1, SELRC1, SEMA3B, SEMA3E, SEMA3F, SEMA4A, SEMA4C, SEPN1, SERINC2, SERPINA3, SERPINB6, SERPINE2, SERTAD4, SESN2, SF3A2, SF3A3, SF3B3, SFMBT2, SFN, SFXN5, SGSH, SGSM2, SGSM3, SH3BGRL3, SH3GLB2, SHANK2, SHARPIN, SHB, SHBG, SIGIRR, SIL1, SIN3B, SIPA1L2, SIX5, SKA3, SKIV2L, SLC11A2, SLC12A9, SLC15A3, SLC16A3, SLC16A5, SLC19A1, SLC24A6, SLC25A1, SLC25A10, SLC25A11, SLC25A23, SLC25A28, SLC25A29, SLC26A2, SLC29A2, SLC2A6, SLC2A8, SLC30A3, SLC30A7, SLC35C2, SLC38A7, SLC43A2, SLC44A2, SLC4A11, SLC4A2, SLC4A8, SLC52A2, SLC52A3, SLC5A8, SLC6A16, SLC7A8, SLC9A3R1, SLC9A3R2, SLC9A8, SMARCA4, SMCR5, SMUG1, SNAPC1, SNAPC2, SNAPC4, SNF8, SNHG11, SNORA29, SNORD104, SNORD13, SNORD57, SNORD99, SNRNP70, SNRPA, SNX29P2, SOCS2, SOGA3, SORBS3, SP1, SP100, SPC24, SPDEF, SPDYE1, SPHK1, SPIRE2, SPTBN2, SRF, SRGAP1, SRGAP3, SRM, SRRM2, SRSF6, SSH3, SSPO, SSRP1, SSTR2, ST3GAL4, ST3GAL5, ST6GALNAC2, STAP2, STAR, STARD10, STARD5, STAT6, STK11, STK11IP, STK19P, STK25, STK36, STOML2, STX16-NPEPL1, STX1A, STXBP2, SULT1A1, SUN2, SUPT5H, SURF2, SUSD2, SUV39H1, SYAP1, SYMPK, SYNJ2BP, SYS1-DBNDD2, SYT12, SYT13, SYT17, SYT7, SYTL4, TACC3, TACO1, TAF13, TAF4B, TAF6L, TATDN2, TBC1D10B, TBC1D13, TBC1D15, TBC1D16, TBC1D17, TBCD, TBL1X, TBL3, TCEA3, TCF25, TDRD1, TEAD2, TECPR1, TEF, TFPT, TGFB1, THADA, THBS3, THNSL2, THOC2, THOC5, THOP1, TIAF1, TIMM17B, TIMP1, TIMP3, TJP3, TKT, TLCD1, TLE2, TLN1, TM4SF1, TMC4, TMC6, TMEM105, TMEM106A, TMEM120A, TMEM125, TMEM127, TMEM132A, TMEM141, TMEM156, TMEM175, TMEM205, TMEM214, TMEM219, TMEM222, TMEM229B, TMEM238, TMEM241, TMEM44, TMEM63B, TMEM79, TMEM86B, TMEM91, TMEM97, TMPRSS13, TNFAIP2, TNFAIP8L1, TNFSF14, TNFSF15, TNK2, TNNT1, TNPO2, TNPO3, TOMM40L, TPM2, TRABD, TRAF2, TRAPPC2L, TRAPPC6A, TRAPPC9, TRERF1, TREX2, TRIB3, TRIM11, TRIM46, TRIM66, TRIP6, TRMT1, TRMT12, TRMT61A, TROAP, TRPM4, TSC2, TSC22D3, TSEN34, TSEN54, TSPAN15, TSPAN17, TSPAN31, TSPAN33, TSPAN9, TSSC4, TSTA3, TTC21A, TTC38, TTC7A, TTLL12, TTLL5, TYK2, TYRO3, TYW3, UBA1, UBA7, UBE2J1, UBE2M, UBL4A, UBQLN4, UCP2, UPF3A, UPK2, URGCP, UROS, USP49, USP5, VAPB, VARS, VARS2, VAT1, VCX, VIPR1, VPS11, VPS13C, VPS18, VPS28, VPS37B, WARS, WAS, WASH6P, WASH7P, WBSCR27, WDR13, WDR18, WDR24, WDR25, WDR34, WDR46, WDR6, WDR73, WDR74, WDR81, WDR83, WFS1, WHAMM, WIBG, WNK4, WNT10B, WSB2, WWC1, XAB2, XAF1, XRCC1, YBX2, YIPF3, YPEL3, YWHAE, ZADH2, ZBTB17, ZBTB3, ZBTB42, ZBTB43, ZBTB48, ZC3H12A, ZC3H3, ZCWPW1, ZDHHC24, ZER1, ZFP42, ZFPM1, ZFYVE19, ZHX2, ZKSCAN1, ZMAT4, ZMYM1, ZNF133, ZNF140, ZNF142, ZNF148, ZNF165, ZNF219, ZNF223, ZNF276, ZNF296, ZNF320, ZNF324, ZNF346, ZNF358, ZNF385A, ZNF408, ZNF419, ZNF444, ZNF462, ZNF467, ZNF468, ZNF486, ZNF524, ZNF526, ZNF557, ZNF562, ZNF577, ZNF579, ZNF581, ZNF593, ZNF600, ZNF618, ZNF629, ZNF641, ZNF652, ZNF669, ZNF687, ZNF689, ZNF691, ZNF707, ZNF716, ZNF738, ZNF750, ZNF76, ZNF763, ZNF767, ZNF773, ZNF783, ZNF785, ZNF786, ZNF816, ZNF827, ZNF860, ZNF880, ZNHIT2, ZRSR2, ZSCAN5A, ZSWIM1, ZYX, 79 other genes with no HGNC symbol
Low	Up	AACSP1, ACOX1, ACP1, ARPC3, ATP5C1P1, B2M, BOLA3, C9orf167, CAP2, CD9, CHCHD2P9, CNIH, COPS4, CXCR7, CXorf64, CYB5A, DDX21, DDX3X, DLD, DLEC1, EEF1A1P12, EIF4A1P2, ELF1, ELOVL5, ERH, FAM195A, FEN1P1, FTH1P7, GJB4, HINT1, HIST1H4H, HNRNPA1P12, ID3, IFI44L, LXN, MAL2, ME1, MGST3, MICA, MIR557, MORF4L2, MRPS35, MYC, NDUFA12, NGRN, NMI, NPM1P5, OSGIN2, OSTC, PCNP, PDGFC, PFN2, PIGY, PIPSL, POLR2B, PPA1, PRDX3, PSMC1P9, PSMD6, RAB9A, RBM23, RFXAP, RPL10A, RPL10P3, RPL17, RPL18AP16, RPL21, RPL26, RPL9, RPLP0, SEC23B, SEMA3C, SLC2A1, SLC39A6, SMG1, SPATS2L, SQLE, STX4, SUMO2, TMED2, TMEM126A, TMEM14A, TMEM14B, TOR1AIP1, TRIM37, TSFM, TUBA1A, UBB, VPS4B, WDR45L, XBP1, XPO1, ZNF217, 19 other genes with no HGNC symbol
	Down	ADAM12, AOAH, APOE, ARHGAP4, BSG, CASKIN2, CD63, CEACAM19, CHPF, COX19, DDX6, DGAT2, DUSP27, DZANK1, ECSCR, FAM100A, FGB, FGF23, FOSB, GPR176, HCN2, HMGCR, IFT74, IL34, KCNK17, KRTAP3-3, LCN2, LINC00323, MEPCE, MIR1282, NAPRT1, NOTCH1, PLXNB3, PRODH, PRSS8, QARS, REXO1, REXO4, SF3B3, SNAPC4, SNF8, SNORD13, SNORD57, SSTR2, TMEM106C, TMEM79, TRIM46, TYW3, USP4, VAPB, ZDHHC24, ZNF148, ZNF526, ZNF600, 3 other genes with no HGNC symbol

Supplementary Table 6 ***Differentially expressed genes in PEA1 cells after treatment with Oncamex.***

		PEA1 (differentially expressed genes after high or low treatment with Oncamex)
High	Up	38777, ABCB6, ADAMTS1, ADM, ADORA2B, ADPRHL2, ADRBK1, AEN, AFAP1L1, AGPAT5, AGRN, AK4, ALDH18A1, ALDOA, ALKBH5, ANG, ANGPTL4, ANKRD37, ANKZF1, APLN, APOL2, ARC, ARHGEF2, ARHGEF37, ARHGEF7, ARID3A, ARL5B, ASF1B, ASNS, ATF3, ATG9A, AVPI1, B3GNT4, B4GALT7, BAG3, BBX, BCL11A, BCL3, BCL6, BHLHE40, BHLHE41, BIRC3, BNIP3, BNIP3L, BTAF1, BTG2, BTN2A1, C10orf10, C10orf28, C11orf84, C12orf29, C14orf43, C15orf42, C15orf48, C17orf58, C17orf96, C1orf35, C1QL1, C2orf49, C3orf39, C3orf58, C4orf47, C7orf49, C8orf58, CA12, CARD10, CBX4, CCL20, CCND1, CCNE1, CCNE2, CCNJL, CCRN4L, CD83, CDC42EP2, CDK18, CDKN1A, CEBPB, CERS6, CHD7, CHIC2, CHPF, CHST14, CHST15, CHST3, CHSY1, CHSY3, CITED2, CKB, CLDND1, CLK3, CNOT8, COL7A1, CREG1, CRISPLD2, CRKL, CSF2, CSRNP1, CSRP2, CXCL1, CXCL2, CYB5D1, CYGB, DAZ1, DDIT4, DDX41, DENND2A, DENND3, DGCR8, DGKD, DHX32, DLX1, DMWD, DNAJB2, DNAJB9, DOK3, DPYSL4, DTL, DUSP1, DUSP14, DUSP5, E2F7, EDEM1, EDN2, EFNB2, EGLN1, EIF4A3, ELL2P1, ENO2, EPAS1, EPHA2, ERF, ERO1L, ERRFI1, ETS1, ETV5, FAM107B, FAM117B, FAM162A, FAM210A, FAM214B, FAM216A, FAM43A, FAM46A, FAM46C, FAM57A, FBXO32, FEM1C, FER1L4, FGFRL1, FHDC1, FOSL1, FOSL2, FOXC1, FOXO3, FRMD8, FSTL3, FUT11, G0S2, GADD45A, GADD45B, GALNTL4, GANAB, GBE1, GFPT2, GJA3, GLRX, GPT2, GRPEL1, HAGH, HBA2, HBEGF, HELZ, HES4, HES6, HILPDA, HK2, HLA-A, HNF1B, HOXA5, IER2, IER3, IER5, IER5L, IFFO2, IFNGR2, IGFBP3, IGKV1-33, IL4R, IL6, IMP3, ING2, INSIG2, IRAK2, IRF1, IRF2BPL, IRS2, IRX3, ISM2, ITPRIP, JARID2, JUN, JUNB, KCTD11, KDM3A, KDM5B, KIAA0355, KIAA0513, KIAA1715, KIRREL, KLF2, KLF6, KLHDC5, KLHL21, KLHL3, KRBA1, LDHA, LGALS8, LIF, LONRF1, LOX, LPCAT1, LRRC41, LUZP1, MAFF, MALL, MAP1LC3B, MAP2K1, MAP3K14, MAP3K8, MAP3K9, MAP6D1, MAPK7, MAPK8IP3, METTL21B, MFNG, MGAT1, MICB, MIDN, MIR155HG, MKNK2, MNT, MOAP1, MOB2, MSX1, MT1X, MTHFD2, MYBL1, MYEF2, MYLIP, NAB2, NADSYN1, NARF, NCKAP5L, NCKIPSD, NCOA7, NDRG1, NFE2L1, NFIL3, NFIX, NFKB1, NFKB2, NFKBIA, NFKBID, NFKBIE, NGLY1, NINJ1, NIPA1, NKX3-1, NLRP3, NOG, NOL3, NOTCH1, NPHP3, NPIPP1, NRIP1, NUAK2, NUDT18, NXF1, NXT1, OBFC2A, OXR1, OXSR1, P4HA1, P4HA2, PABPC1L, PAPD7, PAPSS2, PAQR4, PFKFB3, PFKFB4, PGK1, PHLDA1, PIEZO1, PIGA, PIK3C2B, PIK3IP1, PIM2, PIM3, PLAU, PLAUR, PLCXD1, PLEKHA2, PLEKHA8P1, PLEKHG3, PLEKHH1, PLEKHH3, PLEKHO2, PLIN2, PLOD2, PLXNA3, PMAIP1, PMP22, PNP, POLR2H, POM121B, POM121C, POU5F1, POU5F1B, POU5F1P5, PPAN-P2RY11, PPAT, PPFIA4, PPP1R14C, PPP1R15A, PPP1R16A, PPP1R3C, PPP1R3E, PPP2R5B, PPP3CC, PPP3R1, PPTC7, PREP, PRR5L, PRR7, PRSS53, PSORS1C3, RAB11FIP3, RAB11FIP5, RAB20, RAB2B, RAB38, RAB40C, RAB9A, RAD54L, RAI1, RALGDS, RAP2A, RASD1, RASL11B, RASSF1, RASSF7, RAVER1, RBM14, RBM4B, RELB, RHOB, RIMKLA, RIOK3, RIPK4, RIT1, RLF, RNASET2, RND3, RNF144B, RNF165, RNF24, RNMT, RPL14P1, RRAGA, RRAGD, RTN4R, RTTN, RUNDC1, RUNX1, RUSC1, S100A1, SAP30, SDC4, SEC61G, SEC63P1, SEMA4B, SERPINE1, SERTAD1, SERTAD2, SESN1, SGK1, SGSM2, SH2B3, SH2D4A, SH3BP1, SH3BP2, SH3PXD2A, SHB, SHPK, SIAH2, SIK1, SLC1A4, SLC25A36, SLC2A1, SLC35E1, SLC38A2, SLC39A14, SLC41A1, SLC6A10P, SLC6A8, SLC7A1, SLC7A5, SLC9A1, SLCO4A1, SLCO5A1, SLFN11, SMAD3, SMAP2, SNHG12, SNORA61, SNORA79, SNTA1, SNX33, SOCS3, SOX9, SPAG4, SPRED1, SPRY1, SRSF7, ST3GAL1, STAMBPL1, STARD5, STC1, STC2, SYDE1, TACC1, TACSTD2, TAF15, TBC1D2B, TBK1, TBX2, TERF2IP, TFB1M, TGFA, TGIF2, TINAGL1, TINF2, TIPARP, TK1, TMEM189, TMEM41A, TMEM47, TMEM74B, TNF, TNFAIP2, TNFAIP3, TNFRSF10B, TNFRSF12A, TNFSF9, TNIP1, TOB1, TOB2, TPI1, TPI1P1, TPI1P2, TRIB2, TRIB3, TRIM32, TRIM47, TSPAN5, TUBB2A, TUBB2B, TULP3, TWIST1, TXNRD1, UBE2O, UPRT, USP37, VASN, VEGFA, VKORC1, VLDLR, VTRNA1-3, WDR45L, WDR90, WSB1, XPNPEP1, YEATS2, ZDHHC7, ZFP82, ZIC2, ZMYND19, ZNF114, ZNF250, ZNF275, ZNF295, ZNF296, ZNF324, ZNF343, ZNF395, ZNF470, ZNF672, ZNF696, ZNF770, ZP1, 21 other genes with no HGNC symbol
	Down	ABCB7, ABCC4, ACACA, AGPS, AKR1C3, ALDH1B1, ALPK2, AMOT, ANAPC13, ANLN, ANXA1, ANXA3, ARHGAP4, ASF1A, ASPM, ATF6, AURKA, AURKB, AVEN, BCMO1, BEX1, BICC1, BIVM, C12orf32, C17orf97, C21orf7, C4orf33, CABYR, CAMKMT, CCDC106, CCNA2, CCNB1, CCNB2, CCT6B, CD9, CDC20, CDCA3, CDH6, CDKN3, CENPA, CENPB, CENPE, CENPF, CGNL1, CKS2, CLDN11, CLDN16, COBLL1, CPE, CYP1B1, DBN1, DCDC2, DDAH2, DEFB1, DEPDC1, DHCR7, DICER1-AS1, DLGAP5, DNALI1, DOCK11, DUS2L, E2F5, EARS2, ECT2, EFHB, EHHADH, FAM171A1, FAM198B, FAM64A, FAM83D, FAM84B, FDFT1, FGF2, FOPNL, FZD2, GCNT3, GPKOW, GPR56, GRB14, GYG2, H1F0, HABP4, HEATR1, HENMT1, HES1, HIST2H2AC, HLF, HMGCR, HMGCS1, HMMR, HN1, HNRNPD, HOGA1, HOXB5, HTATIP2, HYLS1, ID1, ID2, ID3, IDI1, IFI44L, IFIH1, IGF2BP3, IL20RB, IMPA2, INPP4B, INSIG1, KIF12, KIF14, KIF20A, KIF23, KLF11, KLHDC8B, KLHL14, KPNA2, KRT80, LCN2, LDLR, LPIN1, LRRC61, LTBR, MAPKAPK3, ME1, METTL5, MIS18BP1, MRPL1, MTA2, MVK, MX1, NCAPD2, NDC80, NEXN, NR2F6, NTHL1, NUCKS1, NUSAP1, OIP5, PACSIN3, PALLD, PAQR8, PDGFC, PDIA3P, PDZK1, PDZK1P1, PHF11, PIF1, PIGM, PKHD1L1, PLLP, PMVK, PPIL1, PPP1R10, PPP1R35, PRC1, PRR11, PSMC1P9, PSME4, PSRC1, PTPN13, PXDNL, RAB3IL1, RAB7L1, RALBP1, RANGAP1, RBM47, RBMX, REPIN1, RNF26, RPP40, RTN4IP1, SCG5, SDPR, SHROOM3, SLC12A8, SLC35F5, SMARCAL1, SNORD13, SNX2, SORBS2, SOX4, SQLE, SRGAP1, STEAP4, STK32B, STX3, SUMO3, SYNE2, SYS1-DBNDD2, SYT13, TACC3, TACO1, TAF7, TAF9B, TBL1X, THBS1, THOC6, TM4SF18, TMED10, TMEM60, TMEM97, TNFSF10, TNS3, TOP2A, TP53INP1, TPX2, TRIM2, TRIM6, TRIP6, TROAP, TSPAN31, TTK, UCHL5, UPF3A, VCAN, WBP11P1, WDR34, WDR73, WEE1, WNT2B, WWC1, XRCC5, ZBED2, ZC3H4, ZC3HAV1, ZFP3, ZMYM4, ZNF212, ZNF358, ZNF425, ZNF426, ZNF518B, ZNF594, ZNF783, ZNF83, 11 other genes with no HGNC symbol
Low	Up	38777, ABHD14B, ALPP, ATN1, BLVRB, CD63, CINP, CKB, CTDNEP1, CXCL14, DLX2, DMWD, DPP9, EPHX1, FAM215B, FLNA, GANAB, GMPPA, GUCA1A, HAUS2, HIATL2, KDELR1, KIRREL, LYPD3, MAPK8IP3, MAST2, MBTD1, MIR129-2, MIR296, MXD3, NAT14, NELF, NFIX, NPNT, NRAP, PCNT, PFDN6, PIP5K1A, PLIN5, PLP1, POGK, RARRES2, RHBDL1, RHEBL1, S100A1, SLC6A17, SLC9A2, SMCR5, SNORD104, SSTR2, TAF15, TELO2, TFF1, TFPT, USP49, VAMP8, WDR62, XAB2, ZNF692, ZNF786, ZNF833P, 2 other genes with no HGNC symbol
	Down	AASDHPPT, ABCB7, ACTG1, ACTL6A, AFF4, ATAD2, C1orf55, C5orf24, CA2, CCNE2, CDK1, CLPX, CNIH, COPB1, CPE, CUTC, DEPDC1, DHTKD1, DUSP1, DYNC1I2, EHHADH, EIF3J, ENOPH1, FAM18B1, FAM3C2, FAM83D, FOPNL, FOS, FOSB, GINS4, GNG10, GNG12, GOLPH3L, GRAMD3, HLTF, HNRNPA1P12, HNRNPKP4, HSPD1P1, IFIH1, IGF2BP3, ITFG1, ITGAV, JAK1, KCTD9, KPNA3, LAP3, LIPA, LYAR, MAD2L1, ME1, METTL5, MFSD1, MORF4L2, MYCBP2, NCKAP1, NDFIP2, NFE2L2, NPM1P5, NUP153, OAT, OSGIN2, OSTCP2, OTUD4, PALLD, PCNP, PDGFC, PFN2, PGAM1, PIP5KL1, PNMA2, POLR2B, PRAMEF4, PRDX3, PRNP, PTPN13, QPCT, RAB5A, RAD51AP1, RCN2, RRAS2, RRM2, RTCD1, SDCBP, SDHD, SENP6, SFXN1, SGOL2, SIPA1L3, SLC35B4, SLC35F5, SNORD13, SPP1, SQLE, SRP9P1, SRPK1, STRN3, STXBP3, SUCLA2, TAF2, TCF12, TFDP1, THBS1, TJP1, TMED10, TMED7, TMEM123, TMX3, TSPAN13, UCHL5, USP40, VBP1, VN1R2, WDR47, WEE1, YME1L1, ZC3H15, ZNF425, ZNF426, ZNF791, ZNF83, 7 other genes with no HGNC symbol

Supplementary Table 7 ***Differentially expressed genes in PEA2 cells after treatment with Oncamex.***

		PEA2 (differentially expressed genes after high or low treatment with Oncamex)
High	Up	38777, ABCB6, ABHD5, ACIN1, ACVR1, ADM, AK4, AKAP8L, ALPP, ANG, ANGPTL4, ANKRD37, ANKRD54, ANKZF1, AP3M2, APOL2, APPL1, ARFGAP1, ARID3A, ASNS, ATG12, ATG14, BCL3, BCL6, BCYRN1, BHLHE40, BLCAP, BNIP3, BNIP3L, BRD9, C10orf10, C10orf137, C11orf83, C12orf23, C17orf96, C19orf33, C19orf77, C1GALT1, C1orf116, C1orf51, C1orf63, C3orf39, C5orf54, C7orf49, C8orf58, C9orf171, CARS2, CBLB, CCDC127, CCDC77, CCDC88A, CCNE2, CDS1, CEP350, CHI3L1, CHMP4C, CHSY1, CHURC1-FNTB, CNIH4, CNOT8, CNPPD1, COMMD2, COPZ2, COX7B, CPOX, CRIP1, CTSK, CXorf40A, CYP4F11, DCAF8, DDIT4, DEDD2, DENND2A, DGKQ, DHDH, DMWD, DNAJB1, DNAJB2, DNTTIP1, DOK4, DPCD, DTNA, DUSP18, DUSP3, DUSP5, DYNLL1, EFNA1, EGLN1, EGLN3, EIF1AD, ELOVL4, ENO2, EXOSC8, F3, FAM108C1, FAM110C, FAM123C, FAM133B, FAM162A, FAM214B, FAM217B, FAM46A, FAM57A, FGF11, FKBP15, FOXP1-IT1, FRG1, FUT11, FUT6, GABARAPL1, GABRG2, GAD1, GADD45B, GADD45GIP1, GCC1, GCK, GDI1, GLRX, GOLGB1, GOLPH3L, GORASP2, GPI, GPKOW, GPRC5C, GPT2, GRB7, GUK1, HDAC3, HECA, HIATL2, HILPDA, HK1, HK2, HOOK1, HOXA5, HSPA1A, HSPA1B, IER5L, IFFO2, IFI27L2, IFT20, IGFBP3, IGIP, IMP3, IMPA1, INHBB, INSIG2, INTS8, IRS2, ISCA1P6, ITFG2, ITGA5, ITGAE, ITPRIPL2, JHDM1D, JUNB, KCTD11, KDM3A, KDM5A, KDM5B, KDM6B, KHDRBS3, KIAA0513, KIRREL, LDHA, LGALS8, LIMS3, LPCAT1, LRRC14, LRRC9, LRRFIP1, LUZP1, MAGEB6P1, MAP3K14, MAP3K2, MAP3K9, MAP6D1, MAST3, MBD4, MCTS1, MED20, MED21, MIP, MIR4720, MIR658, MIR877, MKNK2, MKRN1, MOB2, MOB3A, MRGPRE, MRPL54, MT1X, MTF2, MUC1, MXD4, MYEOV, MYL3, NADSYN1, NARF, NDRG1, NDUFA2, NDUFB9, NETO1, NEURL1B, NIPA1, NIPBL, NISCH, NLRP8, NOL3, NOTCH1, NUCB2, OPN5, P4HA1, PAG1, PAPD5, PARP16, PCMTD1, PDK3, PEX11A, PFDN5, PFKFB3, PFKFB4, PGAM4, PGK1, PHF13, PIK3C3, PLCXD1, PLEKHA8P1, PLEKHH1, PLIN2, PLIN5, PLK1S1, PLOD2, PLXNA3, POLR2H, POU5F1B, POU5F1P5, PPFIA4, PPME1, PPP1R16A, PPP1R3C, PRKAB2, PRSS53, PSMD11, PSORS1C3, RAB40C, RAB8B, RALGAPA1, RARA, RASD2, RASSF7, RBM4B, RLF, RNASET2, RNF183, RNF24, RNGTT, RNU1-3, RNU1-5, RNY1, RNY4, RPL23, RPL9P9, RPN2, RPS3AP26, RRAGA, RSBN1, RUNDC1, RUSC2, SACM1L, SAP30BP, SAP30L, SAR1A, SCARNA9, SDC4, SDF2, SECISBP2L, SFXN5, SH2B1, SH3BP5L, SH3GL1, SLC25A47, SLC26A6, SLC29A3, SLC2A1, SLC2A3, SLC38A2, SLC6A10P, SLC9A1, SLC9A3R1, SMG5, SMYD4, SNORA12, SNORD13, SNORD3D, SNX11, SNX33, SOGA3, SPAG4, SPTAN1, SRPRB, SSTR2, STC1, STK35, SYAP1, TBC1D7, TFAP2C, TICAM2, TMEM127, TMEM139, TMEM208, TMEM74B, TMEM75, TOB2, TPBG, TPI1, TPI1P1, TPI1P2, TRIB2, TRIM11, TRMT12, TTC14, TUBA4A, TUBB2A, TUBB6, TXNDC17, UBE2O, UBR3, UPF3B, UQCRC2, UROC1, USH1G, USP37, USP49, VKORC1, VLDLR, VN1R2, VPS37D, VTRNA1-3, WDR26, WDR70, WSB1, XCR1, YEATS2, YIPF1, ZCCHC17, ZFYVE27, ZNF207, ZNF282, ZNF318, ZNF322P1, ZNF337, ZNF395, ZNF511, ZNF609, ZNF738, ZNF763, ZNF770, ZNF91, ZYG11B, 28 other genes with no HGNC symbol
	Down	ADAMTS1, ADAMTS9, ADAP2, ADAT1, ADORA2B, ADSS, AEN, AFAP1L1, AIMP2, AKNA, ALDH1A3, ALDH1B1, ANAPC13, AOX1, APEX1, APP, ARAP3, ARHGEF4, ARL6IP6, ARMC4, ATP2A2, AURKA, B3GNT3, BASP1, BEX1, BICC1, BRI3, BRIX1, C10orf81, C12orf32, C14orf159, C1orf186, C4orf19, C4orf26, C8orf4, C8orf55, C9orf46, CA2, CAB39, CABLES1, CASK, CBX1, CBX5, CCDC129, CCDC86, CCNA2, CD2AP, CD44, CD81, CDCA8, CDH18, CDH6, CDKAL1, CENPA, CENPB, CEP41, CIRBP, CKAP2L, CLDN1, CLIP4, CMTM7, COBL, CPSF2, CREB3L2, CSDAP1, CTGF, CUTC, CX3CL1, CXCL1, CXCL10, CXCL2, CXCL5, CXCR3, CYFIP1, CYR61, DAB1, DCDC2, DCK, DCTPP1, DDX10, DDX21, DDX28, DEPTOR, DHCR7, DICER1-AS1, DLGAP5, DNAAF2, DOCK1, DOCK9, DUS2L, DYNC2LI1, DYSF, E2F5, EEF1E1, EHF, EHHADH, EPS15L1, EREG, ERVMER34-1, ESRRA, ETV6, EXOSC2, EXPH5, FADS1, FADS2, FAM113B, FAM171A1, FAM208A, FAM3C2, FAM83D, FAM84B, FASN, FDFT1, FGF2, FHOD3, FJX1, FNDC3B, FRMD4A, FRMD6, FTSJD1, FZD2, GAB2, GADD45A, GART, GBP1, GCNT3, GCSH, GDF15, GJB2, GNE, GNG10, GNG11, GTF2E1, GULP1, H2AFY2, H3F3B, HEATR1, HENMT1, HERC5, HERPUD1, HES1, HMBS, HMGCR, HMGCS1, HMGN1P38, HNRNPA1P28, HNRNPA3, HNRNPD, HNRNPKP4, HOOK2, HOXB2, HOXB8, HPS3, HS3ST1, HS3ST3A1, HSPBAP1, HUWE1, IARS, IBSP, IFI16, IFI44, IFI44L, IFIT3, IGFBP4, IL1A, IL1B, IL1RAPL1, IL1RN, IL23A, IL6, IL8, INO80C, INSIG1, IPO5, IQCD, IRAK2, IRAK3, ITCH, ITGAV, KIAA0247, KIF14, KIF22, KIF23, KIFC1, KLF4, KRTAP2-3, KYNU, LACTB2, LDLR, LIMA1, LIPG, LPIN1, LPXN, LRIG1, LTB, LTBP2, LTV1, LY6E, LYAR, LYRM2, MAGOH, MANSC1, MAP3K5, MAP7, MAPK6, MCCC2, MEOX1, METTL5, MGLL, MGST1, MIR23B, MKI67IP, MKX, MLPH, MMP25, MOK, MPP6, MRPL33, MRPS30, MTA3, MTM1, MTMR12, MX1, MYC, MYOF, NCKAP1, NCOA7, NDUFAF4, NEDD4L, NEURL3, NOP2, NPAS2, NPC1, NPM1P5, NR3C2, NRP1, NSMCE4A, NUP35, NUP62, OAT, OSBPL3, OSGIN2, PACSIN3, PAFAH1B1, PALB2, PALLD, PCNP, PFN2, PHLDB1, PISD, PLAT, PLAU, PLEKHF1, PLLP, PLSCR1, PPAP2B, PPFIBP2, PPP1R10, PPP1R11, PPP1R3F, PPRC1, PRDX3, PRIM1, PRKCH, PRMT3, PRMT6, PRRG1, PRRX2, PSD, PTGER4, PTGES2, PTGS2, PTPRM, QPCT, RAB17, RAD50, RAP1GAP2, RASL11B, RBL2, RBM47, RBMS2, RBMX, RC3H1, REPIN1, RGCC, RGL1, RGS20, RHOBTB3, RIPK2, RMI2, RNF144B, RPL14P1, RPL22, RPL6, RPRD1A, RPUSD2, RRM2, RRP9, RRS1, RTN4IP1, S100A2, SDCBP, SEMA3A, SESTD1, SETP18, SFR1, SGK1, SH2B3, SHISA2, SHROOM3, SLC19A1, SLC20A1, SLC2A12, SLC35F5, SLC39A6, SLC6A12, SNORA24, SNX5, SPATS2L, SPRY2, SPTBN1, SQLE, SRGAP3, SRGN, SRPX, SSFA2, STAU2, STEAP1, SYNCRIP, TAGLN2P1, TANC1, TANC2, TAP2, TBX15, TCF4, TEX10, TGFBR2, THBS1, THOC6, THSD4, TIGD2, TINAGL1, TJP3, TMED10, TMEM171, TMEM187, TMEM241, TMEM55B, TMEM60, TMEM69, TMEM97, TMOD1, TMPRSS2, TNC, TNFAIP2, TNFRSF11B, TNFRSF21, TNFSF10, TNS3, TOP2A, TPD52L1, TPX2, TRIP6, TRMT11, TSEN2, TSPAN4, TTF2, UBE2T, UCP2, USP13, VANGL2, VNN1, WBP2, WDR12, WDR92, WDSUB1, WEE1, WNT7A, XBP1, XPOT, ZBED4, ZC3H12C, ZDHHC14, ZNF165, ZNF239, ZNF518B, ZNHIT2, ZNHIT6, ZNRF3, 23 other genes with no HGNC symbol
Low	Up	38777, AQP12B, ARPC3, ATP5E, BST2, C11orf83, CACNB3, CCL15, CD55, CDK5, CENPH, CFLAR, CHCHD2P9, CLDN8, CLEC2L, CNTNAP3, COTL1, COX6A1P2, CRIP1, CRIP2, CTSZ, DDX23, DDX27, DNAH10, DNPEP, DUSP8, EEF1B2, EHD3, EML2, ETV7, EXOC3, FAM133A, FAM43B, FAM65B, FBXO25, GEMIN7, GPKOW, GPR108, GPR143, GSPT2, GUK1, HIST3H2A, HLA-A, HNRNPA1P7, HSPE1, IFI27, IFI27L2, IFI6, IGFLR1, KCNMB2-IT1, KIF9, LMNB1, LMTK2, MAP3K10, MIR1234, MIR1267, MRPL34, MRPL54, MRPS7, NEDD8-MDP1, NEURL1B, NPM1P5, NRK, OR5G5P, PIPSL, PKN2, PSAPL1, PTRHD1, RAB13, RFPL3, RNF166, RNF216P1, RNY3, RNY4, RPL10A, RPL21, RTP4, SALL4, SCNN1D, SERPINA5, SERPINH1, SH2B1, SLC25A47, SNORA29, SNORD12, SNORD17, SNORD3C, SNORD3D, SNX11, SPDYE6, SPTB, STARD3, SUFU, TAF15, TCF7, TCIRG1, TFAP4, TFEC, TMEM160, TMEM208, TRAPPC6A, TSPAN15, TSPAN32, TTC17, UNC45B, USP41, VTI1A, WDR70, XCR1, ZNF264, ZNF775, ZNF91, ZNHIT1, 15 other genes with no HGNC symbol

	Down	AAK1, ADO, ARID4B, ASH2L, ATP13A3, BAG3, BICC1, C1orf55, C6orf72, CBX5, CCDC8, CEBPZ, CPSF6, CREB3L2, CWC25, DCP2, DNAJB14, DYNLT3, EFCAB6, EID3, ELK3, EPRS, FAM133B, FAM168A, FNDC3B, FTSJD1, GJB2, GK5, HIST1H4C, HIST2H2AC, HOOK1, HOXB8, HS3ST1, IGF2BP2, IGF2R, IL8, IRF2BPL, ITPRIPL2, LY86, MAPK6, MEGF11, MEX3C, MPDZ, MTF2, NFAT5, NFE2L2, NIPAL1, NPC1, ODZ4, OXR1, PABPC1, PAK2, PAPD5, PAPD7, PDE12, PPFIBP1, PRDM13, PRR11, PTGER4, PTGS2, PTPN1, RAB11FIP2, RB1CC1, RBM12B, RBM26, RFX1, SCYL2, SEMA3D, SERINC1, SET, SFXN1, SHISA2, SLC25A36, SLC35F5, SLC52A3, SNX16, SOWAHA, SPIN1, SPON1, SPTY2D1, SRFBP1, SSH1, TAF4, TAOK1, TAP2, TMED10, TMED5, TMEM106B, TMEM179, TMPRSS15, TNS3, TRMT11, TSPAN18, UGGT1, USP10, WBP2, ZCCHC6, ZNF385C, 7 other genes with no HGNC symbol

Supplementary Table 8 ***Overlapping differentially expressed genes between MCF-7 and MDA-MB-231 cells treated with Oncamex.***

		MCF-7 & MDA-MB-231 (Venn diagrams: overlap in changes genes after treatment with high/low Oncamex)	
High	Up	MCF-7 only	ADPGK, AKNAD1, ALDOC, AP4B1, AQP3, ARL6IP6, ASF1B, BAMBI, BCL6, BTBD11, BTG2, C11orf68, C11orf75, C17orf58, C1orf51, C2orf49, CCDC28A, CCNA2, CCNE2, CCNG2, CDK7, CDKN1B, CEBPD, CELF1, CENPW, CEP152, CGA, CHMP1B, CHRM3, CLDN12, CLDND1, CLK3, CMC1, CMTM6, CNIH, CPOX, CRIPT, CRKL, CXADR, DCUN1D3, DEDD2, DENND5A, DHX32, DLX2, DNAJB6, DNAJC24, E2F7, EFNA1, ELP4, EXO1, FAM111A, FARP2, FBXO8, FHL3, FKBP15, FOS, FOXP1-IT1, GADD45B, GLCE, GON4L, GPR37, HES1, HMG20A, HOXA5, HSD17B1, HSPA1A, HSPA1B, HSPH1, ID1, IGHV5-78, IRF2BPL, JUNB, KBTBD2, KCTD6, KDM2A, KIAA0355, KIAA0907, KIDINS220, KIFAP3, KIRREL3-AS2, KLHL12, KLHL9, LEMD3, LPIN1, MAP3K13, MED30, MFAP1, MFAP3, MIR21, MLL5, MMD, MTHFSD, MTRNR2L1, MXD4, NEK7, NFE2L1, NFYA, NMI, NPC1, NR4A2, NSMCE2, NUDT18, NXN, OXSR1, PDRG1, PGAM1, PGAM4, PGK1, PGM1, PGPEP1L, PIAS1, PIAS4, PIR, PLEKHA8P1, PNRC1, POLR2H, POLR3GL, POU2F1, PPIP5K1, PRDX3, PRKRIP1, PRPF3, PTPN21, RAB23, RAB2B, RAB9A, RAD54B, RBM14, RBM4B, RFFL, RHBDL1, RIC8B, RIMKLA, RN7SL1, RNASEL, RNF122, RNF144A, RNFT1, RNGTT, SEC22A, SLC25A4, SPRED1, SPRY1, SSH2, STARD3NL, STC2, STK3, SYT5, TBKBP1, TDO2, TERF2IP, TFAP2C, TOB1, TRIB1, TSPYL1, TTC1, TTI1, VPS4B, WDR26, WDR27, WDR54, WSB1, YPEL2, ZBTB41, ZC2HC1A, ZFP36, ZFYVE20, ZIC2, ZNF217, ZNF248, ZNF295, ZNF337, ZNF395, ZNF654, ZSWIM5, 13 other genes with no HGNC symbol
		MDA only	38777, ABCB6, ABCD1, ABHD5, ADAM8, ADRB2, AHSA1, AK4, ANG, ANKRD54, ANKZF1, ARC, ARHGEF16, ARHGEF40, ARID5B, ARMC7, ASUN, ATAD2B, ATG12, ATG9A, AVL9, B3GALNT2, B3GNT5, BBC3, BCYRN1, BLCAP, BLID, BLZF1, BMS1P5, BTAF1, C10orf10, C10orf118, C11orf96, C12orf23, C2orf69, C3orf52, C3orf58, C5orf30, C7orf71, C8orf58, C8orf80, C9orf84, CAPN5, CAPRIN2, CARS, CBLB, CCND2, CCNE1, CCRN4L, CDC42EP2, CDK12, CDKN1C, CHMP7, CHPF, CHST11, CHSY1, CHSY3, CIR1, CKB, CLCF1, CNOT8, CPO, CSF2, CTSZ, CXCL1, DACT3, DCP2, DDA1, DDAH1, DENND2C, DGKQ, DLC1, DNAJB2, DNAJB9, DOK1, DUSP18, DUSP5, DUSP5P, EIF2C2, ELP2, ENTPD7, ERRFI1, EYA3, F3, FAM107B, FAM117B, FAM13A, FAM162A, FAM179B, FAM195B, FAM46A, FAM63A, FAT4, FER1L4, FGFR3, FICD, FLNC, FUT6, G0S2, GALNT3, GALNTL4, GFPT2, GJA3, GLRX, GLS, GM2A, GNPNAT1, GOLGB1, GPR137B, GPT2, GSK3B, HAND1, HBEGF, HES4, HIATL2, HMHA1, HOXD1, HSD17B7, HSPA4L, IFFO1, IFT20, IGFBP3, IL11, IL1RAPL1, IL27RA, IL8, IMPA1, ISCA1P1, ITFG2, ITGA5, ITPK1-AS1, ITPKA, KCTD11, KDM5A, KIAA1715, KIAA1958, KIF1B, KIRREL, KLF6, KLHDC1, KRTAP2-3, LGALS8, LIF, LIN37, LINC00342, LOX, LRRC14, LUZP1, MAFF, MAGT1, MAK16, MAN2A1, MAP1LC3B, MAP2K1, MAP6D1, MBD4, MCTS1, METRNL, MFHAS1, MGAT1, MGEA5, MIR1275, MIR17HG, MIR507, MIR759, MKNK2, MOB3A, MOSPD1, MT1X, MTF2, MYO3B, NANS, NARF, NCBP1, NFKBID, NIPA1, NIPAL1, NOC3L, NOG, NR2F2, OBFC2A, ODZ1, OFD1, OR1S2, OR5C1, OSBPL8, P4HB, PABPC1L, PAG1, PAM, PANX1, PAPD7, PCNX, PCSK5, PDK1, PHF23, PIK3C3, PIM1, PKIA, PLA2G15, PLAT, PLAUR, PLCXD1, PLEKHG3, PLOD2, PNP, PNPLA2, PNPLA8, POM121B, PPAN-P2RY11, PPP1R16A, PPP2R2A, PPP3R1, PPTC7, PRSS8, PUS3, RAB11FIP3, RAB20, RAB38, RAD54L2, RALGAPA1, RASSF7, RBM15, RECQL4, RGS4, RNF113A, RORA, RPS4XP16, RRAD, RRAGD, RUNDC1, SAMD4A, SDC4, SEC11C, SEC63P1, SERPINB8, SERPINE1, SERPINE2, SGMS2, SH3BP5L, SIPA1L2, SLC22A25, SLC25A36, SLC2A1, SLC2A14, SLC2A3, SLC41A1, SLC5A8, SLC6A10P, SLC6A8, SLC7A2, SLIT2, SMAP2, SNORA5C, SNX33, SOGA3, SPAG4, SPHK1, SPIRE1, SRGAP1, SSTR2, ST8SIA2, STK35, TAF15, TCF19, TCF24, TEAD3, TIGD5, TLR4, TMEM115, TMEM156, TMEM51, TMEM57, TNIP1, TNIP2, TPBG, TPI1P1, TRIM27, TRIM58, TRIP12, TTC14, TUBB2A, UAP1, UBE4A, UGCG, UGDH, UPRT, USP38, USP49, VEGFC, VGF, VMP1, VPS18, VPS37A, WFIKKN1, ZBTB40, ZCCHC12, ZCCHC6, ZDHHC18, ZFAND2A, ZFP36L1, ZNF140, ZNF148, ZNF17, ZNF175, ZNF193, ZNF207, ZNF215, ZNF224, ZNF322P1, ZNF335, ZNF35, ZNF470, ZNF653, ZNF668, ZNF672, ZNF695, ZNF772, ZNF786, ZNF800, ZNF841, ZNFX1, 12 other genes with no HGNC symbol
		Both	ADM, ANGPTL4, ANKRD37, ARID3A, ASNS, BHLHE40, BNIP3, BNIP3L, C10orf28, C17orf96, CHIC2, CITED2, CSRNP1, CSRP2, DDIT4, DUSP1, EGLN1, ENO2, ERO1L, FAM57A, FUT11, GBE1, HILPDA, HK2, INSIG2, JUN, KDM3A, LDHA, MAPK8, MAPK9, NDRG1, NFIL3, NXF1, P4HA1, P4HA2, PFKFB3, PFKFB4, PHF13, PPFIA4, PPME1, PPP2R5B, RAB30, RIOK3, RLF, RNF24, RNMT, RUNDC3B, SLC38A2, STC1, TICAM2, VLDLR, YEATS2, ZNF770, 6 other genes with no HGNC symbol
	Down	MCF-7 only	40787, ACOT4, ACSS1, AEN, AFF3, AK2P2, ALKBH2, ARHGEF16, ARHGEF19, ARPC3, AVEN, B4GALT1, BCL2, BLMH, BOP1, C10orf81, C14orf126, C14orf39, C15orf59, C16orf74, C17orf70, C19orf10, C19orf46, C4orf19, C6orf211, CAMK2N1, CAPN1, CCDC155, CCDC86, CCDC88C, CCDC94, CCND1, CDH18, CHD4, CHGA, CLN3, COMTD1, COPG2, CRIP2, CUTC, CXCL12, DCAF13, DEGS2, DEPTOR, DHX33, DNPEP, DRAM1, DUS1L, DUS3L, EFCAB4A, EFHD1, EIF3B, ELFN2, ELOVL2, EMG1, EML3, ERMP1, ESR1, EXOSC6, EXOSC8, F12, FADS1, FADS2, FAH, FAM173A, FAM195A, FAM213B, FAM35A, FAM5B, FAM63A, FAM65A, FAM70A, FBXO27, FDPS, FFAR2, FGD3, FHL2, FKBP4, FLNA, FLNB, FOXE3, GALNT6, GGT6, GJA1, GLA, GNB1L, GPR68, GRPR, GSDMD, GSTM3, HCG18, HIST1H1B, HIVEP3, HPDL, HPGD, HSD3B7, HSPA5, HSPB8, ICAM3, IGFBP5, IL17D, IL19, IL27RA, INPP4B, IPCEF1, ISOC2, ITPK1, KAZALD1, KIAA0182, KIAA0664, KIF12, KRT18P13, KRT18P17, KRT18P19, KRT18P28, KRT8P33, KRT8P9, KTN1-AS1, KYNU, LCP1, LEPREL4, LMOD3, LPO, LRP5L, LRRFIP1, LTBR, LYRM1, MAML3, MAP3K14, MAPKAPK3, METTL1, MIR373, MIR635, MLLT6, MOCOS, MPPED2, MRP63, MRPS2, MRTO4, MTA2, MYADM, MYBBP1A, MYO3B, NAA10, NAGLU, NCOR2, NINJ1, NME2P1, NOP14, NOP16, NOP58, NPY1R, NR2E3, NR5A2, NTHL1, NUCB2, PALLD, PBX1, PDCD4, PDIA3P, PINK1-AS, PLIN5, PLXNB1, POLR3K, PPP1R35, PPRC1, PREX1, PRKCD, PRLR, PRSS23, PTGR2, PUS1, RAC3, RAD50, RAI14, RAP1GAP, RASL11A, RASL11B, RBPMS2, RDBP, RELL2, RERG, RHBDL2, RPP40, RPS26P35, RPS26P47, RPUSD1, RRP1, RRS1, SAPCD2, SCARNA9, SCIN, SDC1, SDC4, SELENBP1, SEMA3C, SEMA3F, SERPINH1, SFPQ, SGK3, SHANK2, SHISA5, SIPA1L3, SLC19A1, SLC25A11, SLC25A13, SLC25A22, SLC39A10, SLC4A2, SLC7A2, SLC7A8, SLC9A3, SLC9A3R1, SLITRK4, SMARCD2, SOAT2, SPOCD1, SRM, SRPK1, SSH3, STARD10, STEAP3, SUSD3, SYS1-DBNDD2, SYT12, SYTL1, TBC1D16, TBL1X, TEAD2, TEKT4, TGFB3, TIGD5, TMEM229B, TOMM40, TRIB3, TRIM65, TRMT1, TRMT6, TRPS1, TSPAN4, TUFT1, TYRO3, UBL3, UFSP1, VASP, VPS11, VTRNA1-3, WDR46, WDR90, WSB2, XCR1, YBX2, ZHX2, ZNF239, ZNF346, ZNF358, ZNF467, ZNF593, ZNF75A, ZNF768, ZNF787, ZNHIT2, 14 other genes with no HGNC symbol
		MDA only	ABR, ADAM19, ADORA2B, AIMP2, AMD1, AMDHD2, ANAPC13, ANGPTL2, ANP32AP1, APCDD1L, APEX1, APOBEC3B, ARMCX1, ARMCX2, ASPM, ASXL1, AURKA, AURKB, BAIAP2L1, BAMBI, BMP4, BRI3, BTF3L4, BUB1, C12orf32, C15orf23, C16orf53, C17orf98, C1orf109, C1orf123, C20orf72, C7orf53, C9orf3, C9orf40, CALM3, CAP2, CARD10, CAV1, CAV2, CBR1, CBX1, CCDC102A, CCDC106, CCDC99, CCNA2, CCNB2, CCNF, CD207, CD58, CDCA2, CDCA3, CDCA8, CDH11, CDK1, CDKN2D, CDKN3, CENPA, CENPE, CENPF, CEP41, CEP55, CKAP2, CKAP2L, CKS2, CLIC6, COL4A2, COQ2,

			CRADD, CST1, CST4, CTDSPL, CTIF, CTNNBIP1, CUEDC2, CUL9, CYB5A, CYP1B1, CYR61, DENND5B, DLGAP5, DNAAF2, DNAH2, DSN1, EHBP1, ESPL1, ETS2, F2RL1, FAM171A1, FAM46B, FAM75A1, FAM83D, FHOD3, FKBP1C, FUT8, FZD2, GBAP1, GBP1, GCA, GEMIN2, GJB2, GLT25D2, GNG10, GNG12, GPR56, GTF2H4, H1F0, H2AFX, HAUS8, HCAR1, HDDC3, HES1, HIF1A, HIST1H2AC, HIST1H4C, HIVEP1, HLA-DPA1, HMBS, HMGB3, HMGCR, HMGCS1, HMGN1P38, HMMR, HNRNPA0, HNRNPA3, HSPE1, HTRA2, HYLS1, ID3, IGF2BP3, IMPA2, INSIG1, KCNN4, KIAA1671, KIF11, KIF14, KIF18A, KIF20A, KIF22, KIF23, KIF2C, KIF4A, KIFC1, KLF15, KRT80, LAMA5, LAMTOR1, LAYN, LIMA1, LMNB2, LMTK3, LPAL2, LPP, LPXN, LRP5, LTV1, LYRM2, MAD2L1, MAMDC2, MAMLD1, MCM5, MED26, MELK, METTL5, MGAT2, MIR586, MKI67, MLPH, MMACHC, MRPL34, MRPS18C, MTA3, MXD3, MYLIP, MYO5C, MYOF, NASP, NCAPD2, NDC80, NDP, NDUFA12, NEDD8-MDP1, NEXN, NFE2L3, NGF, NIF3L1, NNMT, NOXA1, NPAS2, NR1H3, NR3C2, NREP, NRP1, NRXN1, NSMCE4A, NUP35, NUP37, NUSAP1, OBFC1, OGFR, OIP5, OLFML2A, OPRK1, OSBPL10, PAAF1, PAFAH1B1, PAPPA, PARP4, PCCA, PDCD11, PDE7B, PFN2, PHF19, PIF1, PIGT, PIGV, PIGY, PITX1, PKP2, PLAU, PLEK2, PLEKHA6, PLK1, PLK4, PLLP, PLXNA1, PMEPA1, POC1A, POC5, POLE2, PPAP2B, PPAPDC1A, PPARG, PPIL1, PPP1R10, PPP5C, PRC1, PRDM8, PRDX3, PRICKLE2, PRIM1, PRNP, PSPC1P1, PSRC1, PXDN, RAB7L1, RACGAP1, RAD23B, RAD51AP1, RAN, RARRES3, RGS20, RHOJ, RPL39L, SAMD9L, SCRN1, SDPR, SEMA3A, SH3PXD2A, SH3RF3, SHISA2, SLC35B3, SLC37A1, SLC37A2, SLC46A3, SLCO4A1, SNORA73B, SNORD117, SNRPD1, SORBS2, SOX4, SPATS2L, SPCS1, SRBD1, SRRM1, SUN2, SUSD5, SUV39H1, SVIL, SYNCRIP, TACC2, TACC3, TANC1, TANC2, THBS1, THOC6, TIMELESS, TIMM10, TIMP3, TIPARP, TMCO3, TMEM116, TMEM14A, TMEM163, TMEM237, TMEM60, TMEM71, TMEM75, TNFRSF11B, TNFRSF14, TNFRSF21, TNS3, TOP2A, TOX2, TPX2, TRERF1, TRIM6, TRIM8, TRIP13, TROAP, TTF2, TTK, TUBB, TYMS, UBE2C, UBE2L6, UBE2T, UPF3AP1, UTP18, VIPR1, WDR67, WDR92, WEE1, ZFAND5, ZMIZ1, ZNF627, 21 other genes with no HGNC symbol
		Both	ASAP3, CA12, CABLES1, CCNB1, CDC20, CENPB, CMBL, CREB3L4, DBN1, DNAJC9, HNRNPD, IGFBP4, LDLR, PACSIN3, PER3, PHF15, POLA2, RAB3IL1, REPIN1, SCNN1A, SLC29A2, SNORD13, SPDEF, SRF, SRSF6, TCEA3, TRIP6 other genes with no HGNC symbol
Low	Up	MCF-7 only	C16orf11, C1orf105, C5orf55, FAM110B, FAM210B, FAM83F, FGFBP3, GAS2L2, HERC2P2, KCND3, MFAP4, MIR26B, NFIX, OR2T11, PCDH9, PRSS30P, PTPRU, RNU6-15, SNORA2B, SNORD113-3, SUDS3, ZC3H6, 2 other genes with no HGNC symbol
		MDA only	ADCY10, ARPC3, ATF5, CTSZ, DDI1, HMOX2, KIRREL, PLXDC1, PRR21, SCARNA14, TAF15, TRIB3, TXN2, VASP, ZNF365, 3 other genes with no HGNC symbol
	Down	MCF-7 only	ALX3, ATP2C2, C16orf74, CLDN4, CNGA3, COPG2, F12, FGF6, HIST3H2A, KRT18P19, MRPS34, MTMR8, NBPF20, PDIA3P, PINK1-AS, PLIN5, PPARGC1A, SERPINH1, SLC25A22, SNHG10, TEKT4, TMEM174, YIPF3, ZDHHC18, 13 other genes with no HGNC symbol
		MDA only	ARL4D, BLOC1S1, C17orf65, CPXM2, CRISP1, CSF2, CST1, EDN1, FAM65B, HOGA1, KLF7, MIR23B, MVP, OPRK1, PAX9, PCP2, RAB13, SERPINA5, TFF1, TMEM65, TMEM75, ZNF785, 2 other genes with no HGNC symbol
		Both	C19orf10

Supplementary Table 9 ***Overlapping differentially expressed genes between MCF-7, LCC1, LCC2 and LCC9 cells treated with Oncamex.***

		MCF-7, LCC1, LCC2 & LCC9 (Venn diagrams: overlap in changes genes after treatment with high/low Oncamex)	
High	Up	MCF-7 only	AKNAD1, AP4B1, AQP3, ARL6IP6, ASF1B, ASNS, BAMBI, BCL6, BTBD11, C10orf28, C11orf68, C11orf75, CCDC28A, CCNA2, CDKN1B, CENPW, CEP152, CGA, CLK3, CMC1, CSRNP1, DCUN1D3, DEDD2, DLX2, EFNA1, ELP4, EXO1, FAM111A, FARP2, FHL3, FKBP15, FOXP1-IT1, GON4L, GPR37, HES1, HMG20A, IGHV5-78, IRF2BPL, JUN, JUNB, KCTD6, KIFAP3, KIRREL3-AS2, LEMD3, LPIN1, MTHFSD, MXD4, NR4A2, NXF1, PDRG1, PGPEP1L, PHF13, PIAS1, PIAS4, PLEKHA8P1, PNRC1, POLR3GL, POU2F1, PPIP5K1, PRKRIP1, PRPF3, RAB23, RAB30, RAD54B, RBM14, RFFL, RHBDL1, RN7SL1, RNGTT, RUNDC3B, SEC22A, SLC38A2, SSH2, SYT5, TBKBP1, TDO2, TFAP2C, TICAM2, TOB1, TRIB1, TTC1, TTI1, WDR27, ZBTB41, ZC2HC1A, ZFP36, ZFYVE20, ZNF248, 8 other genes with no HGNC symbol
		LCC1 only	AGK, APLF, ARHGEF7, ARL8B, ARNTL, ATP6V0E1, BRD1, C4orf29, C4orf3, CACNB4, CDH10, CEBPG, CFI, CHFR, CLDN1, CPE, CXorf23, EDA, FAF2, FAM129A, FCHO2, FOXO3, HDAC3, HMOX1, HNRNPA2B1, HSDL1, IFIT3, KCTD9, LONRF2, LRRC37BP1, MALSU1, MAP3K2, MBD3L3, METTL18, MSANTD3, MYO9A, NETO2, NOP58, NRIP1, ORC4, PARP16, PFDN2, PIM2, PLCG2, PPP2R2A, PUM1, PVRL4, RAB3GAP2, RAI1, RAI2, RNF113A, RSL24D1, SART3, SESN1, SLC22A25, SLC41A2, SRSF4, SSH1, STK39, SULT1C4, TNKS2, UAP1L1, VGF, VWA7, WIPI1, ZNF160, ZNF429, ZNF673, ZNF813, ZUFSP, 2 other genes with no HGNC symbol
		LCC2 only	ADPRHL2, AGPAT9, APRT, ARHGAP28, ASCL2, ATG9A, B4GALT5, BEX2, BEX5, BSPRY, C14orf133, C19orf10, C1orf122, CAGE1, CBX8, CCNA1, CCRN4L, CDKN2D, CEBPB, CLDN7, CNTNAP4, CTSL3, CXorf64, DALRD3, DCTN5, DEFB107B, DNAJC5, DNMT3A, DOK3, DPP4, DUSP18, EIF4E2, ELK1, ENO1P1, EPDR1, ETFDH, FAM127B, FAM131A, FAM219A, GDAP1, GLS, HBEGF, HES3, HLA-A, HLA-DRB1, HLA-DRB6, HLA-H, IFI27, IL17C, KLHL35, LARP6, LPIN3, MAP1LC3B, MAP2, MAPK7, MESDC1, MLEC, MTHFD1L, MTO1, NAF1, NARF, NAT10, NDUFB2, NEUROG3, ODC1, ORAI2, ORC1, OSGIN1, OVOL1, PELI1, PEX11B, PIM1, PITHD1, PKM2, PPIL1, PPP1R16A, PRAMEF4, PRSS45, PUS7, PYGL, QSOX1, REV1, RGS6, RNF41, RPRD1B, RRP15, SAMD4A, SERPINB8, SH3BP4, SLC35B2, SLC7A1, SNORA67, SPAG4, SPRED2, STIP1, TCF24, TINF2, TMEM174, TMEM45A, TNFRSF21, TNKS1BP1, TP53, TPI1P1, TTC26, TUBB2A, TUBB2B, TUBB4B, ULBP1, UPK1A, WBP11P1, WRAP73, ZW10, 7 other genes with no HGNC symbol
		LCC9 only	39326, AASDHPPT, ABCB10, ABCE1, ABHD3, ABHD5, ABRACL, ACAP2, ACOX1, ACTR10, ACTR2, ACTR3, ACVR1, ADAT1, ADNP, AFF4, AGGF1, ALDH18A1, ALDH9A1, ALG10B, ALG13, ALS2, ALYREF, AMZ2, ANAPC13, ANAPC7, ANKIB1, ANKRA2, ANKRD46, ANKRD49, ANLN, ANO6, ANXA7, AP1G1, AP1S1, AP1S2, AP3S1, AP5M1, APAF1, API5, APIP, ARCN1, ARIH1, ARL6, ARL6IP1, ARMC10, ARMCX5, ARPC1A, ARPC3, ARRDC4, ARV1, ASB8, ASCL1, ASF1A, ASH2L, ASNSD1, ASXL2, ATAD1, ATAD2, ATG16L1, ATG3, ATG4C, ATP2A2, ATP2C1, ATP5F1, ATP5J, ATP6AP2, ATP6V1A, AUH, AZIN1, BBS10, BCAR3, BCAS2, BECN1, BFAR, BMI1, BMPR1A, BMPR2, BRK1, BRMS1L, BRP44, BRP44L, BSDC1, BTAF1, BTBD1, BTBD10, BTBD6, BTF3, BTF3L4, BTG3, BTN2A1, C10orf32, C11orf1, C11orf67, C11orf73, C11orf82, C12orf23, C12orf26, C12orf75, C14orf149, C14orf166, C14orf167, C14orf2, C14orf43, C15orf24, C16orf80, C1orf131, C1orf43, C1orf52, C1orf53, C1orf55, C1orf63, C1QBP, C2orf28, C2orf47, C3orf14, C3orf38, C4orf27, C6orf72, C8orf59, C9orf46, C9orf78, C9orf89, CALM2, CAND1, CAPN7, CASC4, CASP7, CAT, CBFB, CBL, CBLL1, CBWD5, CBX1, CCDC112, CCDC117, CCDC47, CCDC53, CCDC72, CCDC99, CCNC, CCNDBP1, CCNG1, CCNYL1, CCT2, CCZ1B, CD2, CD2AP, CD46, CD58, CD9, CDC42SE1, CDC5L, CDH1, CDK1, CDK2, CDK8, CENPK, CENPQ, CEP120, CEP44, CERS2, CHCHD2P6, CHCHD2P8, CHCHD3, CHMP5, CHPT1, CLASP2, CLDN23, CLNS1A, CMAS, CMPK1, CNEP1R1, CNOT7, COG6, COMMD10, COMMD6, COPB1, COPB2, COPS4, COPS5, COX5B, COX6B1, COX6C, COX7C, CPNE3, CRADD, CREBZF, CRK, CRY1, CSNK1G3, CSNK2A1, CST9, CTCF, CTNNAL1, CTSL2, CUL5, CYB5A, CYB5R4, CYBASC3, CYC1, CYCSP55, CYFIP1, DDX60, DET1, DHRS7, DHX15, DHX36, DIP2B, DLD, DLEU1, DNAAF2, DNAJA4, DNAL4, DPF2, DPM1, DPY19L1, DPY19L4, DPY30, DR1, DTWD1, DUSP11, DUSP16, DYNLT3, DYRK1A, E2F5, EAF1, EDEM3, EEF1A1P27, EEF1B2, EEF1E1, EFR3A, EHHADH, EI24, EID2, EIF2AK3, EIF4A3, EIF4B, EIF4E3, ELOVL5, EML4, ENOPH1, ENPP4, ENSA, EPCAM, EPHB1, EPRS, ERLIN1, ESD, EXOC1, EXOC5, EXOSC3, F2RL1, F9, FAM122B, FAM126B, FAM149B1, FAM174A, FAM18B1, FAM18B2-CDRT4, FAM190B, FAM199X, FAM206A, FAM214A, FAM216A, FAM217B, FAM3C2, FAM45A, FAM82B, FAM83D, FAM96A, FAT1, FBXL3, FBXO28, FBXO33, FBXO45, FBXW11, FNDC3B, FNTA, FOXA1, FOXN2, FRMD6, FTH1, FTH1P7, FTLP3, FTSJD1, FUNDC1, FZD1, G3BP2, GABARAPL2, GALNT12, GCH1, GCSH, GEMIN2, GFPT1, GGH, GJB2, GLRX2, GLRX3, GNA13, GNAQ, GNG10, GNPTAB, GPAM, GRAMD3, GRB2, GTF2B, GTF2E1, GTF2H5, GTF3C3, HAT1, HBP1, HCAR1, HEATR5B, HELZ, HIGD1A, HIST1H2AE, HIST1H2AG, HIST1H2BJ, HIST1H2BK, HIST1H3H, HIST1H4A, HIST2H2BB, HIST2H2BE, HIST2H3C, HLTF, HMGB2, HMGN1, HMGN2P17, HNRNPA0, HNRNPA1P12, HNRNPH1, HNRNPH2, HNRNPK, HNRNPKP4, HPS3, HRSP12, HSD17B4, HSP90B1, HSPA14, HSPA4L, HTATIP2, ID2, ID3, IFI44L, IFIH1, IFNK, IL6ST, IL8, ILF2, IMPA1, IMPAD1, INTS2, IPO7P2, ISOC1, ITFG1, ITGA2, ITGAE, ITGAV, ITGB1, ITGB1BP1, ITGB3BP, ITM2B, ITPR1, JAK1, KAL1, KAT2B, KBTBD4, KCNK1, KCTD18, KCTD3, KIAA0101, KIAA0196, KIAA0247, KIAA0391, KIAA1033, KIAA1279, KIAA1324L, KIAA1468, KIAA1715, KIF21A, KIF3B, KLHDC2, KLHDC5, KLHL20, KRT10, LACTB, LAMP2, LANCL1, LAP3, LCLAT1, LCMT2, LGMN, LHX2, LIMA1, LINC00116, LINC00493, LMBR1, LMBRD1, LNX2, LRP8, LRRC57, LSM3, LTV1, LXN, LYRM2, LYRM5, LYSMD2, MAD2L1, MAP3K8, MAPK1IP1L, MARCKS, MARS2, MBLAC2, MBTPS1, MCEE, MCFD2, MCU, ME1, ME2, MED27, MED7, MELK, METTL21D, METTL23, METTL5, MEX3C, MEX3D, MFF, MFSD8, MGAT2, MICA, MLH1, MMGT1, MNAT1, MOAP1, MOB1A, MOB4, MPHOSPH6, MPP5, MRFAP1, MRPL13, MRPL18, MRPL22, MRPL32, MRPL33, MRPL39, MRPL45, MRPL50, MRPS18C, MRPS21, MRPS30, MRPS31, MRPS35, MRS2, MTDH, MTM1, MTMR6, MTPN, MYC, MYO5C, MYOF, NAA20, NBN, NCAPG2, NCK1, NCOR1, NCSTN, NDFIP2, NDUFA4, NDUFA7, NDUFB3, NDUFB5, NDUFS4, NECAP1, NFXL1, NGDN, NGRN, NOA1, NOL7, NPM1P5, NPTN, NRBF2, NREP, NSA2, NTAN1, NUDCD2, NUDT21, NUP153, NUP160, NUP54, NUPL2, OAT, OBFC2A, OCRL, OR2D3, OSGIN2, OST4, OSTCP2, OTUD4, OXR1, PABPC3, PAIP2, PAN3, PAPD4, PAPSS1, PAQR3, PARP4, PATE3, PPCS, PPIAP29, PPIC, PPM1D, PPP1CC, PPP1R12A, PPP1R2P3, PPP1R3D, PPP2CB, PPP3CC, PPP3R1, PPTC7, PRAMEF6, PRDM6, PREP, PREPL, PRKAG1, PRKAR1A, PTPLB, PTPN12, PTS, PUM2, PUS7L, PWWP2A, RAB11FIP2, RAB22A, RAB5A, RABGGTB, RAD51C, RALGAPA1, RAPGEF2, RARS2, RASA1, RB1CC1, RBM23, RBM43, RBX1, RC3H2, RCN2, RDH10, RGL3, RINT1, RIOK2, RIPK2, RMI1, RND3, RNF103, RNF13, RNF4, RNF5P1, RPAP3, RPL10P3, RPL12, RPL15,

			SLIRP, SLK, SLMO2, SMARCAD1, SNRPB2, SNX19, SNX2, SNX27, SNX3, SNX30, SNX4, SNX5, SOX4, SPAG9, SPATS2, SPCS1, SPG11, SPPL2A, SPTSSB, SQLE, SRP14, SRP54, SRP9, SRP9P1, SRRM1, SRSF7, SSFA2, SSR1, STARD7, STRADBP1, STRBP, STRN3, STXBP3, SUCLA2, SUMO2, SUMO2P3, SYBU, SYNCRIP, SYPL1, SYS1, SYVN1, TADA1, TAF12, TAF2, TAF4, TAF7, TANC1, TBCAP1, TBCK, TBL2, TEFM, TFB2M, TFDP1, TFF1, THAP11, THOC3, THUMPD1, TIA1, TIAL1, TM2D1, TM2D3, TM9SF4, TMBIM4, TMED10, TMED7, TMEM126B, TMEM14A, TMEM14D, TMEM165, TMEM167A, TMEM192, TMEM2, TMEM230, TMEM245, TMEM33, TMEM39A, TMEM59, TMEM64, TMEM85, TMTC2, TMTC3, TMX1, TOMM20, TOP2A, TOP2B, TPGS2, TPK1, TRAPPC11, TRAPPC4, TRAPPC8, TRIM32, TRIM33, TRIP4, TSC22D2, TSEN15, TSG101, TSHZ1, TSNAX, TSPAN13, TSPAN3, TTC19, TTC5, TTF2, TUSC3, TWSG1, TXNDC16, TXNDC17, UBA5, UBB, UBE2A, UBE3C, UBE4A, UBL3, UBQLN1, UBXN2B, UCHL5, UNC50, UPF3AP1, UQCRFS1, UQCRQ, USMG5, USP3, USP34, USP8P1, VAMP4, VBP1, VIM, VKORC1L1, VPS29, WASF3, WDR12, WDR36, WDR37, WDR47, WDSUB1, WRB, WRNIP1, XBP1, XPC, XRCC5, XRN2, YEATS4, YIPF6, YME1L1, YTHDF3, ZBTB34, ZC3H15, ZCCHC8, ZDHHC13, ZFAND1, ZFAND6, ZFP106, ZFX, ZNF189, ZNF277, ZNF330, ZNF397, ZNF614, ZNF680, ZNF791, ZNHIT3, ZZZ3, 64 other genes with no HGNC symbol
		MCF-7 & LCC1	HSD17B1, MAPK8, NFYA, NMI, NUDT18, RNF144A, TERF2IP, ZNF337
		MCF-7 & LCC2	CPOX, GADD45B, MLL5, NXN, PTPN21, 1 other genes with no HGNC symbol
		MCF-7 & LCC9	CCNG2, CMTM6, CRIPT, GLCE, MED30, MMD, MTRNR2L1, NEK7, NPC1, PIR, PRDX3, RLF, RNASEL, STARD3NL, STK3, VPS4B, YPEL2, ZNF217, 1 other genes with no HGNC symbol
		LCC1 & LCC2	ATP6V1E2, C15orf42, CASC3, CCDC58, CFDP1, CHD7, CNNM1, DDX41, DDX50, DTNA, FAM110C, FJX1, FZD9, GPI, GPT2, H3F3B, HIRA, JAG2, LGALS8, MED20, NCKIPSD, PALLD, PDK1, PKD1, POLG, POLR2D, PRSS53, RAB11FIP5, RAB32, RCOR2, RIPK4, SEL1L3, SH2B2, SLC7A11, SLCO2A1, TMEM18, TMEM74B, 1 other gene with no HGNC symbol
		LCC1 & LCC9	39142, ACTG1, ACTL6A, ANAPC10, ANKRD12, ANKS1A, AP3M1, ARF4, ARGLU1, ATP5C1P1, B2M, BCL11B, BCL2L13, BCL2L2, C12orf5, C14orf109, C14orf129, C14orf135, C18orf25, C3orf70, C7orf23, CAP2, CCDC59, CDKN3, CEP350, CGRRF1, CHMP2B, CHURC1, CISD2, CLIC4, CLPX, CNOT8, COMMD3, CTDSPL2, CUL2, CYP1B1, CYP20A1, DDX3X, DDX5, DERA, DHX29, DMTF1, DNAJA1, DOCK7, DVL3, DYNC1I2, EEF1A1P19, EEF1A1P6, EIF1, EIF4A1P2, EIF4G2, EIF4H, ELL2P1, ENY2, ERLEC1, ETFA, EXD2, EXOC2, FAM210A, FAM220CP, FAM82A2, FAM84B, FBXO21, FEZ2, FZD6, GCA, GHITM, GLB1, GOLGA5, GOLPH3, GOLT1B, H2AFZ, HECTD1, HIST1H2AC, HIST1H2BD, HIST1H4E, HIST2H4A, HIST3H2A, HMGN2P7, HMGN4, ING2, JKAMP, KHDRBS1, KHDRBS3, KIAA1191, KLF9, KPNA3, KPNA4, LAPTM4B, LIPA, LPIN2, MANBA, MBIP, METAP1, MINPP1, MMADHC, MON2, MTERFD1, MTX2, MTX3, NFE2L2, NIPA1, NMD3, OSTC, PELO, PEX2, PFN2, PGM3, PGRMC1, PHLPP2, PIGY, PLS3, POLG2, PPA1, PPPDE1, PPWD1, PQLC3, PRKRIR, PROSER1, PRRC2C, PTGES3, RAB20, RAB21, RALGAPA1P, RDX, REXO2, RPL21, RRAGA, RSBN1, SCAF8, SCO1, SCOC, SCYL2, SDF2, SFXN1, SH3GL3, SH3GLB1, SLC33A1, SLC35F5, SMEK2, SMG8, SMNDC1, SNRNP27, SPATA5L1, SRSF8, STAM, TBC1D14, THAP6, THOC7, TIMM21, TMEM126A, TMEM209, TMEM237, TMEM41A, TMEM87A, TOR1AIP1, TPD52L1, TRAM1, TRIM37, TRMT112, USO1, USP10, VAMP7, WASL, XPO1, YAP1, YWHAG, ZBED4, ZC3H12C, ZCCHC14, ZFAND5, ZFR, ZNF83, 11 other genes with no HGNC symbol
		LCC2 & LCC9	ADIPOR1, AHSA1, AP2M1, BET1, BOLA3, C15orf61, C4orf47, CALU, CANT1, CHCHD2P9, CNO, COX17, CYB5D1, DAD1, DCUN1D5, DDT, DPH3, DYNLT1, ELF1, EPT1, FAM168B, FAM195A, FTL, GIGYF2, HBXIPP1, HERC1, HIBADH, HINT1, HLA-B, HOMER1, HSPA8, IARS2, KCTD5, LAMTOR1, LHX6, LRRC58, LYPLAL1, MAD2L1BP, MAPRE1, MORF4L1P1, MORN2, MRPS23, NDUFA12, NDUFB6, NOP10, OXSM, PDCD2L, PNPO, POLR2B, PPPDE2, RAN, RBBP5, RPL13AP7, RPL15P3, RPL30, RPLP0, RPS4X, RQCD1, SEC23IP, SH3BP1, SIAH2, SKIV2L2, SLC25A5, SLC39A14, SPATS2L, STRAP, TAX1BP3, TBP, THUMPD3, TMCO3, TNFAIP1, TNFRSF12A, TOR1B, TUBB, TXN, UBFD1, UFM1, UHRF2, USP37, VDAC1, WBP4, XPNPEP1, ZNFX1, 9 other genes with no HGNC symbol
		MCF-7, LCC1 & LCC2	ADPGK, CEBPD, HOXA5, NFE2L1, RNF24, SPRED1, WDR54
		MCF-7, LCC2 & LCC9	BTG2, C2orf49, CDK7, E2F7, HSPA1A, ID1, KDM2A, KIAA0355, NSMCE2, POLR2H, RAB9A, RNF122, RNFT1
		MCF-7, LCC1 & LCC9	CCNE2, CHMP1B, CHRM3, CLDN12, CNIH, DNAJC24, FBXO8, KIAA0907, MAP3K13, MAPK9, MFAP1, MFAP3, PGAM1, RIC8B, TSPYL1, WDR26, WSB1, ZNF654

		LCC1, LCC2 & LCC9	ABCB6, ACP1, ADORA2B, AGPAT5, AHCY, AK4, ALDOA, ALKBH5, ANKZF1, ANXA3, ANXA5, AP4E1, ATG9B, B3GNT4, BNIP2, BRI3, C3orf58, C7orf42, CA5B, CAB39, CECR5, CHST14, CHST7, CHSY1, CHURC1-FNTB, CLINT1, COMMD2, COPS8, COX20, COX7A2L, CREG1, CRLS1, CSRNP2, CSTB, DDX18, DDX21, DERL1, DPYSL4, DSCR3, DUSP14, DYNLL1, EDEM1, EEF1A1P12, EEF1G, EIF1B, EIF3J, EIF4EBP2, ENDOG, ENOSF1, FAM162A, FAM60A, FBXO34, FNBP1L, FSCN1, FZD3, GALNTL4, GAPDH, GDF15, GLO1, GRPEL1, GTF2A2, GYS1, HAGH, HBXIP, HIST1H2BG, HIST1H4H, HLA-A, HPRT1, IARS, IDH1, IFIT2, IMP3, ISCA1, ISCA1P6, KCTD11, KDELR2, LAMC1, LRP11, MAL2, MAP2K1, MAP6D1, MAPK6, MDH1, MGST3, MKI67IP, MKRN2, MORF4L2, MTHFD2, NEDD8-MDP1, NOL3, NPHP3, NPIPP1, NUP37, OSBPL10, OTUD6B, PAICS, PAM, PAPD7, PCBP1, PDK3, PEX11A, PEX13, PFKP, PIGA, PIPSL, PLEKHH1, PLOD2, PNMA1, PPP1R3C, PPP1R3E, PRDX2, PRDX4, PRPSAP2, PSAT1, PTRF, PTTG1IP, RAP2A, RIT1, RNF145, RPL10A, RPL17, RPL18AP16, RPL18P13, RPL26, RUNDC1, SAP30, SAV1, SC5DL, SEC23B, SEC61G, SERTAD2, SLC2A1, SLC35E3, SMAD4, SMG1, SMS, SRSF9, SRXN1, STX3, SYDE1, TBK1, TFRC, TJP1, TMED2, TMED5, TMEM123, TMEM14B, TMEM185B, TMEM43, TPI1, TRIT1, TSPYL5, TUBA1A, TUBA1B, TUBB6, TXNIP, TXNRD1, TYMS, VKORC1, WDR45L, WDR61, XPOT, YARS2, ZCCHC9, ZNF511, ZNHIT3, 9 other genes with no HGNC symbol
		MCF-7, LCC1, LCC2 & LCC9	ADM, ALDOC, ANGPTL4, ANKRD37, ARID3A, BHLHE40, BNIP3, BNIP3L, C17orf58, C17orf96, C1orf51, CELF1, CHIC2, CITED2, CLDND1, CRKL, CSRP2, CXADR, DDIT4, DENND5A, DHX32, DNAJB6, DUSP1, EGLN1, ENO2, ERO1L, FAM57A, FOS, FUT11, GBE1, HILPDA, HK2, HSPA1B, HSPH1, INSIG2, KBTBD2, KDM3A, KIDINS220, KLHL12, KLHL9, LDHA, MIR21, NDRG1, NFIL3, OXSR1, P4HA1, P4HA2, PFKFB3, PFKFB4, PGAM4, PGK1, PGM1, PPFIA4, PPME1, PPP2R5B, RAB2B, RBM4B, RIMKLA, RIOK3, RNMT, SLC25A4, SPRY1, STC1, STC2, VLDLR, YEATS2, ZIC2, ZNF295, ZNF395, ZNF770, ZSWIM5, 9 other genes with no HGNC symbol
	Down	MCF-7 only	40787, ACOT4, AEN, ARPC3, AVEN, BCL2, C14orf126, C14orf39, C15orf59, C16orf74, C19orf10, C4orf19, C6orf211, CA12, CCDC155, CCDC86, CCDC88C, CCNB1, CDH18, CHGA, CMBL, COPG2, CUTC, CXCL12, DCAF13, DEPTOR, DHX33, DNPEP, DRAM1, DUS1L, EFHD1, EIF3B, ELOVL2, ERMP1, EXOSC8, F12, FADS1, FADS2, FAM173A, FAM195A, FAM35A, FAM5B, FAM70A, FFAR2, FLNA, FLNB, FOXE3, GGT6, GJA1, GLA, GNB1L, GPR68, GRPR, HCG18, HIST1H1B, HPDL, HPGD, HSPA5, HSPB8, ICAM3, IL17D, IL19, IPCEF1, KIAA0182, KRT8P33, KRT8P9, KTN1-AS1, LPO, LRP5L, MAP3K14, MIR373, MOCOS, MPPED2, MYADM, MYBBP1A, NCOR2, NME2P1, NOP16, NOP58, NPY1R, NR5A2, PALLD, PDCD4, PER3, PINK1-AS, POLR3K, PPP1R35, PREX1, PRKCD, PUS1, RAC3, RAD50, RAI14, RASL11A, RASL11B, RELL2, REPIN1, RERG, RPS26P35, RPS26P47, SEMA3C, SERPINH1, SFPQ, SGK3, SHISA5, SLC25A13, SLC25A22, SLC39A10, SLC7A2, SLC9A3, SLITRK4, SMARCD2, SOAT2, SPOCD1, SRPK1, SYTL1, TEKT4, TIGD5, TOMM40, TRIM65, TRMT6, TRPS1, UBL3, UFSP1, VASP, VTRNA1-3, WDR90, XCR1, ZNF239, 7 other genes with no HGNC symbol
		LCC1 only	ACOX3, ADCY10, AKR1B1, ARMCX1, ATF5, ATP2A3, BEGAIN, BLOC1S1, C12orf66, C16orf42, C17orf82, C19orf53, C19orf54, C1orf138, C6orf100, CAB39L, CAMK1G, CCDC137, CROT, CRX, CUL7, DEGS1, DENND1B, EEF1A2, EFEMP2, ENC1, FAT2, FNIP2, FOLR2, GALNT14, GCGR, GRAMD1A, GSC, GTF2A1, HAND2, HDAC11, HLA-DMB, HNRNPKP4, HOXC6, IFI35, IL16, IL4R, KIF18B, KLHDC8B, LGALS12, LINGO1, LMAN2, LRG1, MAP2K2, MAPK3, MGAT3, MIR2278, MIR7-3HG, MOB3C, MT1G, NCF1C, NDUFC2, NDUFS7, NEU4, NMNAT1, NPAS4, NXNL1, OR11H12, OR5M4P, OR8B12, PAGE2B, PITX1, PLEKHG2, PLK1, PNPLA2, POF1B, POTEI, PPOX, PRAF2, PRAMEF6, PRDM6, PSCA, PSMC3, PSORS1C2, RAP2C, RAPGEF3, RASSF5, RBM47, RCHY1, RNASEH2B, RUNX3, SAMD11, SCAMP5, SH3BGRL2, SLC10A4, SPINK4, SWSAP1, SYT2, TCHH, TMEM121, TOR2A, TP53INP2, TRIM3, UXS1, ZDHHC1, ZNF329, ZNF428, ZSWIM7, 11 other genes with no HGNC symbol
		LCC2 only	ACAA2, ACTG2, ADCY4, ALCAM, ALKBH8, ANKRD1, APOA1, APOC1, AQP11, AR, ATP6V1C1, AURKA, BARD1, BCAS1, BCL3, BMF, C10orf68, C19orf71, C1orf162, CCDC149, CCDC25, CDC25B, CDC42EP4, CFI, CLLU1, CMTM8, COL9A2, CRISP2, CRYGB, CSN1S1, CTDSPL, DLC1, DLGAP5, DNAH2, E2F1, ECT2, EID3, ELF5, EPN3, ERGIC1, FAM200A, FAM27L, FBXO18, FEZF2, FLT3LG, FOXC1, FZD4, GALM, GAS2L3, GRM4, GYG2, HGD, HMGB1P1, IL20, IRF2BPL, IRS2, IRX5, ISG20L2, JPX, KCNJ13, KCNK5, LEPROT, LMTK3, LRP1, LRRCC1, MAGEB5, MARVELD1, MARVELD3, MDK, MIR1914, MIS18BP1, MTF2, NAT9, NBPF14, NBR2, NCAPG, NEMF, NIPAL1, NIPAL3, NR4A3, OAF, PAPD5, PCYOX1, PDZRN3, PEX6, PHLDB1, PI3, PKIB, PKN2, PLEKHF1, PLEKHN1, PPIG, PRR11, PSPC1P1, RBM12B, REEP5, RPS6KA5, RYBP, SENP3, SLC25A25, SLCO4C1, SNORD46, STAC, TACC2, TAGLN, TAOK1, TAS2R39, TBX2, TCEA1P2, TERF1P4, TFEB, TMEM135, TMEM183A, TMEM45B, TNRC6B, TOB1, TP53INP1, TRIM38, TTC12, TTC32, TTK, TUBD1, UGDH, USP36, VN1R2, VTCN1, ZBTB2, ZCCHC6, ZFHX3, ZFP2, ZG16, ZMYND10, ZNF281, ZNF354A, ZNF418, ZNF644, ZNF91, 12 other genes with no HGNC symbol
		LCC9 only	36951, 40057, AAGAB, AARSD1, AATF, ABCA3, ABCA7, ABCC12, ABHD14B, ACAD9, ACP6, ACTN1, ACTR1A, ACTR5, ADAP1, ADCK1, ADCK4, ADCY3, ADM2, ADRBK1, AES, AGRN, AHR, AKR1D1, ALDH8A1, AMDHD2, AMH, AMT, ANKMY1, ANKRD13B, ANKRD30A, ANKRD30B, ANKRD52, ANKRD54, ANKS3, ANO9, ANXA11, ANXA2R, AP5Z1, APOA5, APOE, APOL2, ARAP1, ARFGAP1, ARFGAP2, ARHGDIB, ARHGEF2, ARL6IP4, ARPC4-TTLL3, ARRB1, ASIC3, ASL, ASMTL, ATAD3A, ATF7IP2, ATG12, ATG16L2, ATG7, ATOX1, ATP5D, ATP6AP1, ATP6V1B1, ATXN2, ATXN7L2, AURKAIP1, AZI1, B3GALT6, B3GAT3, BAG6, BCAS4, BCKDK, BGN, BIN3, BRAT1, BRD9, BRF1, BRSK1, BSG, BTBD2, C10orf114, C11orf83, C12orf10, C12orf44, C14orf102, C14orf159, C14orf79, C16orf48, C16orf57, C16orf59, C16orf7, C16orf79, C16orf93, C17orf61, C19orf21, C19orf24, C19orf33, C1orf135, C20orf96, C21orf58, C22orf25, C2orf55, C4orf48, C5, C6orf170, C6orf47, C6orf52, C7orf41, C7orf50, C8orf73, C8orf82, C9orf114, C9orf142, C9orf37, C9orf86, CACFD1, CACNA1H, CAD, CAMK1, CAMK2B, CAMK2N2, CAPZB, CARD9, CARM1, CATSPER2, CCDC101, CCDC102A, CCDC12, CCDC124, CCDC125, CCDC154, CCDC92, CD320, CD96, CD99L2, CDC34, CDC42EP2, CDK10, CEL, CENPT, CEP164, CES2, CFB, CFLAR, CHAC1, CHD5, CHMP1A, CHPF, CHTF18, CIC, CIRH1A, CIZ1, CLASRP, CLIP2, CLN6, CLPTM1, CNNM3, CNTROB, COG2, COL1A1, COL5A1, COL6A1, COL7A1, CORO7, CPT1B, CRIPAK, CROCC, CRYBA2, CSF2RA, CSK, CSNK1G2, CST1, CTC1, CUEDC2, CUL9, CUX2, CYB5R1, CYBA, CYP4F12, D2HGDH, DAGLB, DAXX, DBNDD1, DBNL, DCXR, DDX27, DDX28, DDX39A, DDX51, DDX56, DEF6, DENND4B, DGAT1, DGAT2, DGCR5, DGCR6L, DGKD, DHCR7, DHRS2, DHX37, DIP2C, DIS3L, DMAP1, DMWD, DNM1, DOK7, DOLK, DPEP2, DPP9, DTNB, E2F2, EBF4, ECHDC2, ECSIT, EFHD2, EHMT2, EIF3G, EIF4EBP1, ELMO3, ELP2, ELP3, ENO3, ENTPD8, EPHB4, EPN1, ERN1, ESPN, ETNK2, EVL, EVPL, EXOC3, EXOSC4, EZR, FAAH, FAM102A, FAM104B, FAM108C1, FAM116B, FAM125A, FAM134C, FAM153A, FAM178A, FAM186B, FAM203B, FAM40B, FAM69B, FAM73A, FAM83G, FAM98A, FANCE, FBLN5, FBRSL1, FBXL17, FBXL6, FBXW4, FBXW9,

			FCAR, FCHO1, FERMT2, FGB, FKBP11, FKTN, FLOT2, FOXJ2, FOXM1, FOXO4, FOXRED1, FRG1, FSHB, FUK, FURIN, G6PC3, GAA, GADD45GIP1, GALK1, GDF11, GDI1, GFOD1, GINS2, GIT1, GLT25D1, GLTPD1, GMPPA, GNA11, GNL3L, GPATCH3, GPC2, GPR108, GPR137, GPSM1, GPX2, GRIPAP1, GRWD1, GSDMB, GSTM2, GSTO2, GTF3C1, H1FX, HABP4, HADHA, HCN2, HCN3, HDGF, HEATR6, HEXDC, HEY2, HGS, HINT2, HIP1R, HJURP, HLA-DMA, HMG20A, HMG20B, HMGCR, HNRNPUL2, HOOK2, HPX, HSCB, HTT, ICA1, IDUA, IFI27L2, IFT122, IL10, IL18, IL34, IMP4, INO80E, INTS1, IPO11, IPO13, IRF7, ITFG3, ITGA10, ITIH4, ITPA, ITPKB, JMJD8, JOSD2, KAT2A, KCNAB1, KCND1, KCNK6, KCNMB4, KDELR1, KHSRP, KIAA0284, KIAA0664L3, KIAA1324, KIFC2, KLHDC4, KLHL22, KREMEN2, KRT8, KRTCAP2, LACC1, LAG3, LDHD, LEP, LINC00173, LINC00265, LINC00323, LINC00341, LMF2, LPAR2, LPP, LRFN3, LRFN4, LRRC23, LY6E, LYPD6B, LYPLA2, MACF1, MACROD1, MAF1, MAN1B1, MAN2B1, MAN2C1, MAOA, MAP1S, MAP3K6, MAP4K2, MAPK8IP3, MAPRE3, MAT2A, MBD6, MBOAT2, MCART1, MCM5, MDC1, MED16, MED24, MED25, MEG3, METTL16, MFSD3, MGMT, MIIP, MIR1282, MIR2116, MKI67, MLF2, MLLT4, MLPH, MLST8, MLXIPL, MMP15, MNF1, MNT, MOK, MRPL37, MRPL38, MSL3, MST1P2, MSTO1, MSX1, MT1F, MTA1, MTF1, MUC1, MUM1, MXD3, MYH3, MYL5, MYO1C, MYO9B, MYOM1, NACC1, NAGPA, NARFL, NBL1, NBPF8, NDST1, NDUFV1, NEIL2, NFKB2, NINL, NMRAL1, NOL6, NOTCH1, NOXA1, NR2C2AP, NSMCE1, NT5DC2, NUCB1, NUDC, NUDT3, NUPR1, OGFR, OPLAH, OPRL1, ORAI1, OSBPL7, P2RX2, P2RY6, PABPN1, PACSIN1, PAFAH1B3, PALM, PALM3, PAQR4, PARP10, PARP12, PBX2P1, PCIF1, PCNT, PCNX, PCSK1N, PDDC1, PDE1A, PDIA4, PDP2, PDZD4, PEF1, PELI3, PEX11G, PEX16, PHF21B, PHKG2, PI4KB, PIAS4, PICK1, PIEZO1, PIP5K1C, PKMYT1, PKN1, PLA2G10, PLA2G2D, PLAC8L1, PLCD3, PLD6, PLEKHH3, PLEKHM2, PLEKHO2, PLXNA1, PLXNA3, PNCK, PNPT1, POLD1, POLD2P1, POLQ, POLRMT, POMGNT1, PPM1K, PPM1M, PPP1R26, PPP2R1A, PPP2R4, PPP6R1, PRDM11, PRKCZ, PRKD2, PRPF19, PRPF31, PRPH, PRR14, PRR22, PRR24, PRRG4, PRRT2, PRSS22, PSMD8, PSME4, PTBP1, PTK6, PTP4A2, PTP4A3, PTPN23, PTPN6, PUSL1, PYCARD, PYCRL, PYGO2, QARS, QTRT1, R3HDM4, RAB11FIP3, RAB11FIP4, RAB17, RAB33B, RAB9B, RABAC1, RAC1P2, RAD23A, RANGAP1, RAPGEFL1, RARRES3, RASIP1, RASSF6, RAVER1, RBFA, RBKS, RBM6, RDH13, RDH5, RECQL4, RERE, RET, REXO1, RFTN1, RGS11, RHBDD2, RHBDL1, RHOG, RIPK1, RNASEH2A, RNF10, RNF213, RNF25, RNMTL1, RNU6-1, RNU6-15, RNY3, ROGDI, RPL14, RPL28, RPUSD2, RRAGC, RRP12, RRP7A, RUSC1, RUVBL2, RXRA, S100A16, S100A7, S100A8, SAA2-SAA4, SAC3D1, SAFB, SAMD1, SAMM50, SAP30BP, SBF1, SBNO2, SCNN1B, SCNN1D, SELRC1, SEMA3B, SEMA3E, SEMA4A, SEMA4C, SEPN1, SERINC2, SERPINB6, SERPINE2, SESN2, SF3A2, SF3A3, SFXN5, SGSH, SGSM3, SH3BGRL3, SH3GLB2, SHARPIN, SHB, SHBG, SIGIRR, SIN3B, SIPA1L2, SKA3, SLC24A6, SLC25A1, SLC25A28, SLC2A8, SLC35C2, SLC44A2, SLC52A2, SLC6A16, SLC9A8, SMUG1, SNAPC1, SNAPC2, SNF8, SNHG11, SNORA29, SNORD104, SNORD57, SNORD99, SNRNP70, SORBS3, SP1, SP100, SPDYE1, SPHK1, SPIRE2, SRGAP3, SRRM2, SSRP1, STARD5, STAT6, STK11, STK11IP, STK25, STOML2, STX1A, SULT1A1, SUN2, SUPT5H, SURF2, SYAP1, SYT13, SYT7, SYTL4, TACO1, TAF4B, TATDN2, TBC1D13, TBC1D15, TBC1D17, TBCD, TECPR1, TFPT, THADA, THBS3, THNSL2, THOC5, TIAF1, TIMM17B, TIMP3, TKT, TLE2, TLN1, TMC4, TMEM105, TMEM106A, TMEM125, TMEM127, TMEM132A, TMEM141, TMEM156, TMEM175, TMEM214, TMEM219, TMEM222, TMEM238, TMEM63B, TMEM86B, TMPRSS13, TNFAIP8L1, TNFSF14, TNFSF15, TNK2, TNNT1, TNPO2, TOMM40L, TPM2, TRABD, TRAF2, TRAPPC2L, TRAPPC6A, TRERF1, TREX2, TRIM11, TRIM46, TRMT12, TRMT61A, TRPM4, TSC2, TSC22D3, TSEN34, TSPAN17, TSPAN9, TSSC4, TSTA3, TTC21A, TTC38, TTC7A, TTLL12, TTLL5, TYK2, UBA1, UBE2J1, UBE2M, UBL4A, UBQLN4, UCP2, UPK2, URGCP, USP5, VARS, VARS2, VAT1, VPS13C, VPS18, VPS28, VPS37B, WARS, WAS, WASH6P, WASH7P, WBSCR27, WDR13, WDR25, WDR6, WDR81, WFS1, WHAMM, WWC1, XAB2, XRCC1, ZBTB17, ZBTB3, ZBTB42, ZBTB48, ZC3H3, ZFP42, ZFPM1, ZMAT4, ZMYM1, ZNF133, ZNF142, ZNF165, ZNF276, ZNF296, ZNF320, ZNF324, ZNF408, ZNF419, ZNF524, ZNF526, ZNF557, ZNF577, ZNF581, ZNF629, ZNF652, ZNF669, ZNF687, ZNF689, ZNF691, ZNF707, ZNF716, ZNF76, ZNF767, ZNF783, ZNF880, ZRSR2, ZSWIM1, ZYX, 43 other genes with no HGNC symbol
		MCF-7 & LCC1	CAPN1, MIR635, PDIA3P, PRLR, SUSD3, TSPAN4, ZNF768, ZNF787
		MCF-7 & LCC2	KAZALD1, NUCB2, SAPCD2, SIPA1L3, 1 other gene with no HGNC symbol
		MCF-7 & LCC9	AFF3, ALKBH2, BLMH, CCDC94, CCND1, COMTD1, CRIP2, DEGS2, DUS3L, EMG1, EXOSC6, FAH, FAM213B, FHL2, FKBP4, HNRNPD, IGFBP4, LCP1, LTBR, LYRM1, MAML3, MAPKAPK3, METTL1, MRP63, MRPS2, MRTO4, NAA10, NOP14, NR2E3, PPRC1, PRSS23, PTGR2, RAB3IL1, RPP40, RPUSD1, RRP1, RRS1, SCIN, SHANK2, SLC19A1, SLC4A2, STARD10, SYS1-DBNDD2, TBC1D16, TBL1X, TRIB3, TRIP6, YBX2, ZNHIT2, 2 other genes with no HGNC symbol
		LCC1 & LCC2	ABCA12, ABCB4, ARID5B, ASGR1, ASNA1, BASP1, CPEB3, CYR61, DOK4, ELOVL6, ERCC2, FIZ1, GABARAP, GNL1, MAP3K5, MAP9, PKP4P1, PLA2G3, PLA2G4F, PXMP4, RENBP, SBK1, SREBF1, TIPARP, TMSB4XP8, TNFRSF14, VASN, 1 other gene with no HGNC symbol
		LCC1 & LCC9	38777, ABCD1, ACSS2, ACTN4, ADAT3, AEBP1, AGAP11, AIP, AIRE, ALDH16A1, ALKBH6, ANKRD33, ARAF, ARHGAP10, ARHGDIA, ARL2, ARMC5, ARMC7, ATG2A, ATP13A1, BATF, BLVRB, BMP7, BNIPL, BST2, C11orf2, C14orf80, C17orf28, C19orf66, C1orf86, C20orf27, C2CD4B, C6orf141, C9orf106, C9orf64, CALML5, CBFA2T3, CDC42EP5, CDT1, CEACAM6, CERCAM, CHST1, CITED4, CPSF1, CRIP1, CRY2, CXXC1, DAPK3, DCAKD, DDAH2, DNAJC3-AS1, DOCK6, DTX3, DUS2L, EIF2B5, EIF2S1, EIF4G3, EMD, EOMES, ESRRAP2, EXD3, FAM43A, FAM50A, FAM71F1, FAM83A, FGD1, FZD2, GBP2, GNB2, GPKOW, GTF2F1, HARS, HCFC1R1, HCG9, HDAC6, HDHD2, HKR1, HOXC10, HOXC13, IGSF9, IKBKE, ILKAP, INPPL1, IQCC, IRF3, ISYNA1, KCNK12, KLF2, LAMB2, LCN2, LETM1, LILRB1, LMNA, LONP2, LRP3, MBD3, MICAL1, MMAB, MOV10, MRPL2, MTX1P1, MUC20, MVP, MX2, MYH14, NAPRT1, NCLN, NDUFB10, NELF, NPW, NRSN2, NSDHL, OTUB1, PAF1, PATE2, PCNXL3, PDE9A, PGR, PHLDA2, PIGQ, PIGU, PITPNM1, PLBD2, PLEKHA4, PMPCA, POC1A, POMT2, PPDPF, PREB, PRRC2A, PRSS8, PSMB10, PTDSS2, RAD54L2, RGS17, RNU1-3, RPL7L1, RTN4RL1, SDF2L1, SIL1, SLC11A2, SLC15A3, SLC25A10, SLC25A23, SLC25A29, SLC30A3, SLC38A7, SLC4A8, SLC52A3, SLC9A3R2, SNX29P2, SPC24, SPTBN2, STAP2, STK19P, TAF13, TAF6L, TBL3, TEF, TGFB1, THOP1, TIMP1, TJP3, TLCD1, TMC6, TMEM120A, TMEM205, TMEM79, TMEM97, TNFAIP2, TSEN54, TSPAN15, TSPAN31, TSPAN33, UBA7, UROS, VCX, VIPR1, WDR18, WDR24, WDR74, WDR83, WNK4, WNT10B, YIPF3, YWHAE, ZC3H12A, ZDHHC24, ZER1, ZFYVE19, ZNF444, ZNF468, ZNF618, 11 other genes with no HGNC symbol

		LCC2 & LCC9	ABCB7, ACACA, ACACB, ACSF2, AFAP1L2, AKAP8L, ARID4B, ARL6IP5, ARMC1, BLZF1, BMS1P5, BRD3, C1orf54, C21orf56, C6orf225, C8orf37, CAPN9, CC2D1A, CCNF, CD63, CDKN2AIPNL, CENPF, CERS4, CGN, CNST, DEM1, DHCR24, DLX3, DNAJC22, DUSP19, E4F1, EDC4, EFNB3, EGR1, EHD1, EIF2C2, ENDOV, ETV6, FAM175A, FAM183A, FAR1, FGFR4, FOXP1-IT1, FUT6, GCN1L1, GPR1, GPR37L1, HN1L, IER2, IFT74, ITPK1-AS1, ITPRIPL2, KCNQ1OT1, KIAA0195, KIAA1731, KLHL28, KRT7, LAMA5, LIN52, LINC00174, LRCH4, MAGT1, MAN2B2, MAST3, MIDN, MRPL28, N4BP2, NEAT1, NFIB, NFIX, NFKBIA, NFKBIE, NUAK1, NUCKS1, PCGF2, PDE4C, PGAP2, PLEKHA6, PLXNA4, PNPLA7, PODXL2, POLR3F, PPP1R9A, PROM2, QRFPR, RBM42, REC8, RFX1, RHOBTB3, RHPN1, RIMS3, RNF31, SERTAD4, SF3B3, SKIV2L, SLC26A2, SLC30A7, SLC4A11, SMARCA4, SOCS2, STAR, STX16-NPEPL1, SUSD2, SUV39H1, TACC3, TBC1D10B, TCF25, TDRD1, TMEM91, TNPO3, TRIM66, TROAP, TYW3, UPF3A, WDR34, ZADH2, ZBTB43, ZKSCAN1, ZNF140, ZNF562, ZNF579, ZNF785, ZNF816, ZNF860, 7 other genes with no HGNC symbol
		MCF-7, LCC1 & LCC2	ELFN2, KYNU, RBPMS2, STEAP3, TGFB3, TUFT1, ZNF75A
		MCF-7, LCC2 & LCC9	CABLES1, CREB3L4, FAM63A, FGD3, GSTM3, IGFBP5, LEPREL4, LMOD3, LRRFIP1, MYO3B, RHBDL2, SDC4, SELENBP1, SRSF6, ZNF346
		MCF-7, LCC1 & LCC9	ARHGEF16, ARHGEF19, B4GALT1, BOP1, C17orf70, DNAJC9, FAM65A, FDPS, GSDMD, HSD3B7, IL27RA, KRT18P19, POLA2, SCARNA9, SDC1, SLC25A11, SLC7A8, SLC9A3R1, SRM, SYT12, TRMT1, ZNF593
		LCC1, LCC2 & LCC9	ACP2, ALG1L, ALPP, ANKRD34A, ANKRD44, APOF, ARHGAP4, ATHL1, ATIC, ATN1, B4GALNT1, BCYRN1, BLVRA, BMP8B, C10orf27, C14orf28, C14orf93, C15orf52, C17orf53, C17orf67, C20orf94, C9orf169, CACYBP, CBX5, CECR7, CGNL1, CHD8, CHST12, CISH, CLIC3, COASY, COL16A1, COX19, CSRNP1, CTGF, CUEDC1, DCLRE1C, DDX6, DIAPH2, DICER1-AS1, DLG4, DNAAF3, DUSP2, DUSP5, EDN1, EDN2, EGR2, EHBP1L1, EIF2AK4, ERBB2, EVI5, EXOC3L4, FAM100A, FAM107B, FAM113B, FAM211B, FAM46B, FAM46C, FAM83H, FHOD1, FIBCD1, FICD, FOSB, GADD45G, GALNT3, GATS, GCAT, GPER, GUCY1B2, HAUS2, HES1, HIATL2, HIST1H1D, HIST1H4C, HMGCS1, HOOK1, HOXC8, HOXC9, HSD17B7, INPP5J, IPP, IRX3, ITPRIP, KIAA1683, KIF22, KLF6, LHPP, LINC00476, LRRC45, LTB, LTB4R, MAP3K11, MAP3K12, MBD4, MBTD1, MCF2L, MEPCE, MFSD11, MMP25, MSRB2, MVD, MVK, MX1, MYB, NAT14, NBEAL2, NBPF20, NCKAP5L, NDE1, NEK8, NFYB, NKX2-2, NLRP8, NME3, NR1H3, NR2F6, NRCAM, NUBPL, NYNRIN, OBSCN, ODZ3, OSBPL5, OVGP1, PACS1, PCDHA3, PCDHB9, PCYT2, PELP1, PHKA2, PIGX, PKP1, PLK2, PNKP, PNPLA6, POLR1B, PPFIBP2, PPM1F, PPP1R10, PPP1R13B, PRODH, PRRG2, PRRT3, PSD4, PTGER4, PTPLAD2, RAB13, RAB26, RAD9A, RARA, RASD1, RAX2, RDH16, RIMS2, RN5S9, RND1, RNU1-5, S1PR3, SALL4, SDSL, SERPINA3, SFMBT2, SFN, SGSM2, SIX5, SLC12A9, SLC16A3, SLC16A5, SLC2A6, SLC43A2, SLC5A8, SMCR5, SNAPC4, SNRPA, SOGA3, SRGAP1, SSPO, SSTR2, ST3GAL4, ST3GAL5, ST6GALNAC2, STK36, STXBP2, SYMPK, SYNJ2BP, SYT17, THOC2, TM4SF1, TMEM241, TMEM44, TRAPPC9, USP49, VAPB, WDR73, WIBG, XAF1, YPEL3, ZCWPW1, ZNF148, ZNF219, ZNF223, ZNF385A, ZNF462, ZNF486, ZNF600, ZNF641, ZNF738, ZNF750, ZNF763, ZNF773, ZNF786, ZNF827, ZSCAN5A, 13 other genes with no HGNC symbol
		MCF-7, LCC1, LCC2 & LCC9	ACSS1, AK2P2, ASAP3, C10orf81, C19orf46, CAMK2N1, CDC20, CENPB, CHD4, CLN3, DBN1, EFCAB4A, EML3, ESR1, FBXO27, GALNT6, HIVEP3, INPP4B, ISOC2, ITPK1, KIAA0664, KIF12, KRT18P13, KRT18P17, KRT18P28, LDLR, MLLT6, MTA2, NAGLU, NINJ1, NTHL1, PACSIN3, PBX1, PHF15, PLIN5, PLXNB1, RAP1GAP, RDBP, SCNN1A, SEMA3F, SLC29A2, SNORD13, SPDEF, SRF, SSH3, TCEA3, TEAD2, TMEM229B, TYRO3, VPS11, WDR46, WSB2, ZHX2, ZNF358, ZNF467, 4 other genes with no HGNC symbol
Low	Up	MCF-7 only	C16orf11, C1orf105, C5orf55, FAM110B, FAM210B, FAM83F, FGFBP3, GAS2L2, HERC2P2, KCND3, MFAP4, MIR26B, NFIX, OR2T11, PCDH9, PRSS30P, PTPRU, RNU6-15, SNORA2B, SNORD113-3, SUDS3, ZC3H6, 2 other genes with no HGNC symbol
		LCC1 only	ANO3, C19orf26, CADPS, CCDC19, CHODL, CTGF, EHD3, FADS6, FAM197Y8, FZD10, HNRNPA3, HNRNPA3P3, IER3, KCNJ8, MAML3, MIR708, MTX3, NFAM1, NRAP, NRIP1, OIT3, PRSS45, RAI2, RRH, SCGB3A2, SIAH2, SLC35F1, SLC41A2, SMCP, SULT1C4, TAS2R4, TIPARP, TM4SF20, 6 other genes with no HGNC symbol
		LCC2 only	ASNA1, BAI2, C16orf74, C1orf109, CBX5, CLLU1, CRYGB, DYDC2, EID3, FAM132B, FAM27L, HOXD10, KLRG1, MIR1914, NEMF, NIPAL1, OBP2B, PKN2, PLIN5, RIBC1, SENP3, SNORD46, SNRPD3, SPTY2D1, STARD8, TELO2, TK2, TMEM81, ZMYND10, 6 other genes with no HGNC symbol
		LCC9 only	AACSP1, ACOX1, ACP1, ARPC3, ATP5C1P1, B2M, BOLA3, C9orf167, CAP2, CD9, CHCHD2P9, CNIH, COPS4, CXCR7, CXorf64, CYB5A, DDX21, DDX3X, DLD, DLEC1, EEF1A1P12, EIF4A1P2, ELF1, ELOVL5, ERH, FAM195A, FEN1P1, FTH1P7, GJB4, HINT1, HIST1H4H, HNRNPA1P12, ID3, IFI44L, LXN, MAL2, ME1, MGST3, MICA, MIR557, MORF4L2, MRPS35, MYC, NDUFA12, NGRN, NMI, NPM1P5, OSGIN2, OSTC, PCNP, PDGFC, PFN2, PIGY, PIPSL, POLR2B, PPA1, PRDX3, PSMC1P9, PSMD6, RAB9A, RBM23, RFXAP, RPL10A, RPL10P3, RPL17, RPL18AP16, RPL21, RPL26, RPL9, RPLP0, SEC23B, SEMA3C, SLC2A1, SLC39A6, SMG1, SPATS2L, SQLE, STX4, SUMO2, TMED2, TMEM126A, TMEM14A, TMEM14B, TOR1AIP1, TRIM37, TSFM, TUBA1A, UBB, VPS4B, WDR45L, XBP1, XPO1, ZNF217, 18 other genes with no HGNC symbol

		LCC2 & LCC9	1 gene with no HGNC symbol
	Down	MCF-7 only	ALX3, ATP2C2, C16orf74, C19orf10, CLDN4, CNGA3, COPG2, F12, FGF6, HIST3H2A, KRT18P19, MRPS34, MTMR8, NBPF20, PDIA3P, PINK1-AS, PPARGC1A, SERPINH1, SLC25A22, SNHG10, TEKT4, TMEM174, YIPF3, ZDHHC18, 13 other genes with no HGNC symbol
		LCC1 only	ADCY10, ALPP, BLVRB, C1orf138, C8orf85, CIT, CRX, EFEMP2, ETAA1, FAT2, FNIP2, GALNT3, GPR112, HAND2, HIST1H1D, KCTD8, LRFN2, MBTD1, MGAT3, MIR1267, MIR2278, MIR635, NDUFC2, NXT2, OTOF, PGLYRP4, PHC1, PLAA, POLR1A, PSAPL1, PSCA, PSORS1C2, RAD54L2, RPS26P35, RPS28, SCARNA9, SEC31B, SLC10A4, SLC38A11, SMCR5, SNX32, SPRR1B, SSU72P1, TOP1P1, TOR2A, WSB2, ZNF223, 18 other genes with no HGNC symbol
		LCC2 only	BATF2, C1orf216, C9orf57, CD1C, CDY2B, CUL3, EXOSC8, FGFBP3, HIST1H2BO, HMCN2, HSPB8, IFI44L, IGFBP4, IL5RA, KRTAP5-10, MEGF10, MIR639, OR2AG2, OSMR, OTC, PLG, TBC1D3B, TKTL1, TNIP3, TSKU, TSSK6, UBQLN4P1, 1 other gene with no HGNC symbol
		LCC9 only	ADAM12, AOAH, APOE, ARHGAP4, BSG, CASKIN2, CD63, CEACAM19, CHPF, COX19, DGAT2, DUSP27, DZANK1, ECSCR, FAM100A, FGB, FGF23, GPR176, HCN2, HMGCR, IFT74, IL34, KCNK17, KRTAP3-3, LCN2, LINC00323, MEPCE, MIR1282, NAPRT1, NOTCH1, PLXNB3, PRODH, PRSS8, QARS, REXO1, REXO4, SF3B3, SNAPC4, SNF8, SNORD13, SNORD57, TMEM106C, TMEM79, TRIM46, TYW3, USP4, VAPB, ZDHHC24, ZNF148, ZNF526, ZNF600, 3 other genes with no HGNC symbol
		MCF-7 & LCC1	PLIN5
		LCC1 & LCC9	DDX6,SSTR2
		LCC2 & LCC9	FOSB

Supplementary Table 10 ***Overlapping differentially expressed genes between PEA1 and PEA2 cells treated with Oncamex.***

		PEA1 & PEA2 (Venn diagrams: overlap in changes genes after treatment with high/low Oncamex)	
High	Up	PEA1 only	ADAMTS1, ADORA2B, ADPRHL2, ADRBK1, AEN, AFAP1L1, AGPAT5, AGRN, ALDH18A1, ALDOA, ALKBH5, APLN, ARC, ARHGEF2, ARHGEF37, ARHGEF7, ARL5B, ASF1B, ATF3, ATG9A, AVPI1, B3GNT4, B4GALT7, BAG3, BBX, BCL11A, BHLHE41, BIRC3, BTAF1, BTG2, BTN2A1, C10orf28, C11orf84, C12orf29, C14orf43, C15orf42, C15orf48, C17orf58, C1orf35, C1QL1, C2orf49, C3orf58, C4orf47, CA12, CARD10, CBX4, CCL20, CCND1, CCNE1, CCNJL, CCRN4L, CD83, CDC42EP2, CDK18, CDKN1A, CEBPB, CERS6, CHD7, CHIC2, CHPF, CHST14, CHST15, CHST3, CHSY3, CITED2, CKB, CLDND1, CLK3, COL7A1, CREG1, CRISPLD2, CRKL, CSF2, CSRNP1, CSRP2, CXCL1, CXCL2, CYB5D1, CYGB, DAZ1, DDX41, DENND3, DGCR8, DGKD, DHX32, DLX1, DNAJB9, DOK3, DPYSL4, DTL, DUSP1, DUSP14, E2F7, EDEM1, EDN2, EFNB2, EIF4A3, ELL2P1, EPAS1, EPHA2, ERF, ERO1L, ERRFI1, ETS1, ETV5, FAM107B, FAM117B, FAM210A, FAM216A, FAM43A, FAM46C, FBXO32, FEM1C, FER1L4, FGFRL1, FHDC1, FOSL1, FOSL2, FOXC1, FOXO3, FRMD8, FSTL3, G0S2, GADD45A, GALNTL4, GANAB, GBE1, GFPT2, GJA3, GRPEL1, HAGH, HBA2, HBEGF, HELZ, HES4, HES6, HLA-A, HNF1B, IER2, IER3, IER5, IFNGR2, IGKV1-33, IL4R, IL6, ING2, IRAK2, IRF1, IRF2BPL, IRX3, ISM2, ITPRIP, JARID2, JUN, KIAA0355, KIAA1715, KLF2, KLF6, KLHDC5, KLHL21, KLHL3, KRBA1, LIF, LONRF1, LOX, LRRC41, MAFF, MALL, MAP1LC3B, MAP2K1, MAP3K8, MAPK7, MAPK8IP3, METTL21B, MFNG, MGAT1, MICB, MIDN, MIR155HG, MNT, MOAP1, MSX1, MTHFD2, MYBL1, MYEF2, MYLIP, NAB2, NCKAP5L, NCKIPSD, NCOA7, NFE2L1, NFIL3, NFIX, NFKB1, NFKB2, NFKBIA, NFKBID, NFKBIE, NGLY1, NINJ1, NKX3-1, NLRP3, NOG, NPHP3, NPIPP1, NRIP1, NUAK2, NUDT18, NXF1, NXT1, OBFC2A, OXR1, OXSR1, P4HA2, PABPC1L, PAPD7, PAPSS2, PAQR4, PHLDA1, PIEZO1, PIGA, PIK3C2B, PIK3IP1, PIM2, PIM3, PLAU, PLAUR, PLEKHA2, PLEKHG3, PLEKHH3, PLEKHO2, PMAIP1, PMP22, PNP, POM121B, POM121C, POU5F1, PPAN-P2RY11, PPAT, PPP1R14C, PPP1R15A, PPP1R3E, PPP2R5B, PPP3CC, PPP3R1, PPTC7, PREP, PRR5L, PRR7, RAB11FIP3, RAB11FIP5, RAB20, RAB2B, RAB38, RAB9A, RAD54L, RAI1, RALGDS, RAP2A, RASD1, RASL11B, RASSF1, RAVER1, RBM14, RELB, RHOB, RIMKLA, RIOK3, RIPK4, RIT1, RND3, RNF144B, RNF165, RNMT, RPL14P1, RRAGD, RTN4R, RTTN, RUNX1, RUSC1, S100A1, SAP30, SEC61G, SEC63P1, SEMA4B, SERPINE1, SERTAD1, SERTAD2, SESN1, SGK1, SGSM2, SH2B3, SH2D4A, SH3BP1, SH3BP2, SH3PXD2A, SHB, SHPK, SIAH2, SIK1, SLC1A4, SLC25A36, SLC35E1, SLC39A14, SLC41A1, SLC6A8, SLC7A1, SLC7A5, SLCO4A1, SLCO5A1, SLFN11, SMAD3, SMAP2, SNHG12, SNORA61, SNORA79, SNTA1, SOCS3, SOX9, SPRED1, SPRY1, SRSF7, ST3GAL1, STAMBPL1, STARD5, STC2, SYDE1, TACC1, TACSTD2, TAF15, TBC1D2B, TBK1, TBX2, TERF2IP, TFB1M, TGFA, TGIF2, TINAGL1, TINF2, TIPARP, TK1, TMEM189, TMEM41A, TMEM47, TNF, TNFAIP2, TNFAIP3, TNFRSF10B, TNFRSF12A, TNFSF9, TNIP1, TOB1, TRIB3, TRIM32, TRIM47, TSPAN5, TUBB2B, TULP3, TWIST1, TXNRD1, UPRT, VASN, VEGFA, WDR45L, WDR90, XPNPEP1, ZDHHC7, ZFP82, ZIC2, ZMYND19, ZNF114, ZNF250, ZNF275, ZNF295, ZNF296, ZNF324, ZNF343, ZNF470, ZNF672, ZNF696, ZP1, 12 other genes with no HGNC symbol
		PEA2 only	ABHD5, ACIN1, ACVR1, AKAP8L, ALPP, ANKRD54, AP3M2, APPL1, ARFGAP1, ATG12, ATG14, BCYRN1, BLCAP, BRD9, C10orf137, C11orf83, C12orf23, C19orf33, C19orf77, C1GALT1, C1orf116, C1orf51, C1orf63, C5orf54, C9orf171, CARS2, CBLB, CCDC127, CCDC77, CCDC88A, CDS1, CEP350, CHI3L1, CHMP4C, CHURC1-FNTB, CNIH4, CNPPD1, COMMD2, COPZ2, COX7B, CPOX, CRIP1, CTSK, CXorf40A, CYP4F11, DCAF8, DEDD2, DGKQ, DHDH, DNAJB1, DNTTIP1, DOK4, DPCD, DTNA, DUSP18, DUSP3, DYNLL1, EFNA1, EGLN3, EIF1AD, ELOVL4, EXOSC8, F3, FAM108C1, FAM110C, FAM123C, FAM133B, FAM217B, FGF11, FKBP15, FOXP1-IT1, FRG1, FUT6, GABARAPL1, GABRG2, GAD1, GADD45GIP1, GCC1, GCK, GDI1, GOLGB1, GOLPH3L, GORASP2, GPI, GPKOW, GPRC5C, GRB7, GUK1, HDAC3, HECA, HIATL2, HK1, HOOK1, HSPA1A, HSPA1B, IFI27L2, IFT20, IGIP, IMPA1, INHBB, INTS8, ISCA1P6, ITFG2, ITGA5, ITGAE, ITPRIPL2, JHDM1D, KDM5A, KDM6B, KHDRBS3, LIMS3, LRRC14, LRRC9, LRRFIP1, MAGEB6P1, MAP3K2, MAST3, MBD4, MCTS1, MED20, MED21, MIP, MIR4720, MIR658, MIR877, MKRN1, MOB3A, MRGPRE, MRPL54, MTF2, MUC1, MXD4, MYEOV, MYL3, NDUFA2, NDUFB9, NETO1, NEURL1B, NIPBL, NISCH, NLRP8, NUCB2, OPN5, PAG1, PAPD5, PARP16, PCMTD1, PDK3, PEX11A, PFDN5, PGAM4, PHF13, PIK3C3, PLIN5, PLK1S1, PPME1, PRKAB2, PSMD11, RAB8B, RALGAPA1, RARA, RASD2, RNF183, RNGTT, RNU1-3, RNU1-5, RNY1, RNY4, RPL23, RPL9P9, RPN2, RPS3AP26, RSBN1, RUSC2, SACM1L, SAP30BP, SAP30L, SAR1A, SCARNA9, SDF2, SECISBP2L, SFXN5, SH2B1, SH3BP5L, SH3GL1, SLC25A47, SLC26A6, SLC29A3, SLC2A3, SLC9A3R1, SMG5, SMYD4, SNORA12, SNORD13, SNORD3D, SNX11, SOGA3, SPTAN1, SRPRB, SSTR2, STK35, SYAP1, TBC1D7, TFAP2C, TICAM2, TMEM127, TMEM139, TMEM208, TMEM75, TPBG, TRIM11, TRMT12, TTC14, TUBA4A, TUBB6, TXNDC17, UBR3, UPF3B, UQCRC2, UROC1, USH1G, USP49, VN1R2, VPS37D, WDR26, WDR70, XCR1, YIPF1, ZCCHC17, ZFYVE27, ZNF207, ZNF282, ZNF318, ZNF322P1, ZNF337, ZNF511, ZNF609, ZNF738, ZNF763, ZNF91, ZYG11B, 19 other genes with no HGNC symbol
		Both	38777, ABCB6, ADM, AK4, ANG, ANGPTL4, ANKRD37, ANKZF1, APOL2, ARID3A, ASNS, BCL3, BCL6, BHLHE40, BNIP3, BNIP3L, C10orf10, C17orf96, C3orf39, C7orf49, C8orf58, CCNE2, CHSY1, CNOT8, DDIT4, DENND2A, DMWD, DNAJB2, DUSP5, EGLN1, ENO2, FAM162A, FAM214B, FAM46A, FAM57A, FUT11, GADD45B, GLRX, GPT2, HILPDA, HK2, HOXA5, IER5L, IFFO2, IGFBP3, IMP3, INSIG2, IRS2, JUNB, KCTD11, KDM3A, KDM5B, KIAA0513, KIRREL, LDHA, LGALS8, LPCAT1, LUZP1, MAP3K14, MAP3K9, MAP6D1, MKNK2, MOB2, MT1X, NADSYN1, NARF, NDRG1, NIPA1, NOL3, NOTCH1, P4HA1, PFKFB3, PFKFB4, PGK1, PLCXD1, PLEKHA8P1, PLEKHH1, PLIN2, PLOD2, PLXNA3, POLR2H, POU5F1B, POU5F1P5, PPFIA4, PPP1R16A, PPP1R3C, PRSS53, PSORS1C3, RAB40C, RASSF7, RBM4B, RLF, RNASET2, RNF24, RRAGA, RUNDC1, SDC4, SLC2A1, SLC38A2, SLC6A10P, SLC9A1, SNX33, SPAG4, STC1, TMEM74B, TOB2, TPI1, TPI1P1, TPI1P2, TRIB2, TUBB2A, UBE2O, USP37, VKORC1, VLDLR, VTRNA1-3, WSB1, YEATS2, ZNF395, ZNF770, 9 other genes with no HGNC symbol
	Down	PEA1 only	ABCB7, ABCC4, ACACA, AGPS, AKR1C3, ALPK2, AMOT, ANLN, ANXA1, ANXA3, ARHGAP4, ASF1A, ASPM, ATF6, AURKB, AVEN, BCMO1, BIVM, C17orf97, C21orf7, C4orf33, CABYR, CAMKMT, CCDC106, CCNB1, CCNB2, CCT6B, CD9, CDC20, CDCA3, CDKN3, CENPE, CENPF, CGNL1, CKS2, CLDN11, CLDN16, COBLL1, CPE, CYP1B1, DBN1, DDAH2, DEFB1, DEPDC1, DNALI1, DOCK11, EARS2, ECT2, EFHB, FAM198B, FAM64A, FOPNL, GPKOW, GPR56, GRB14, GYG2, H1F0, HABP4, HIST2H2AC, HLF, HMMR, HN1, HOGA1, HOXB5, HTATIP2, HYLS1, ID1, ID2, ID3, IDI1, IFIH1, IGF2BP3, IL20RB, IMPA2, INPP4B, KIF12, KIF20A, KLF11, KLHDC8B, KLHL14, KPNA2, KRT80, LCN2, LRRC61, LTBR, MAPKAPK3, ME1, MIS18BP1, MRPL1, MTA2, MVK, NCAPD2, NDC80, NEXN, NR2F6, NTHL1, NUCKS1, NUSAP1, OIP5, PAQR8, PDGFC, PDIA3P, PDZK1, PDZK1P1, PHF11, PIF1, PIGM, PKHD1L1, PMVK, PPIL1, PPP1R35, PRC1, PRR11, PSMC1P9, PSME4, PSRC1, PTPN13, PXDNL, RAB3IL1, RAB7L1, RALBP1, RANGAP1, RNF26, RPP40, SCG5, SDPR, SLC12A8, SMARCAL1, SNORD13, SNX2, SORBS2, SOX4, SRGAP1, STEAP4, STK32B, STX3, SUMO3, SYNE2, SYS1-DBNDD2, SYT13, TACC3, TACO1,

			TAF7, TAF9B, TBL1X, TM4SF18, TP53INP1, TRIM2, TRIM6, TROAP, TSPAN31, TTK, UCHL5, UPF3A, VCAN, WBP11P1, WDR34, WDR73, WNT2B, WWC1, XRCC5, ZBED2, ZC3H4, ZC3HAV1, ZFP3, ZMYM4, ZNF212, ZNF358, ZNF425, ZNF426, ZNF594, ZNF783, ZNF83, 25 other genes with no HGNC symbol
		PEA2 only	ADAMTS1, ADAMTS9, ADAP2, ADAT1, ADORA2B, ADSS, AEN, AFAP1L1, AIMP2, AKNA, ALDH1A3, AOX1, APEX1, APP, ARAP3, ARHGEF4, ARL6IP6, ARMC4, ATP2A2, B3GNT3, BASP1, BRI3, BRIX1, C10orf81, C14orf159, C1orf186, C4orf19, C4orf26, C8orf4, C8orf55, C9orf46, CA2, CAB39, CABLES1, CASK, CBX1, CBX5, CCDC129, CCDC86, CD2AP, CD44, CD81, CDCA8, CDH18, CDKAL1, CEP41, CIRBP, CKAP2L, CLDN1, CLIP4, CMTM7, COBL, CPSF2, CREB3L2, CSDAP1, CTGF, CUTC, CX3CL1, CXCL1, CXCL10, CXCL2, CXCL5, CXCR3, CYFIP1, CYR61, DAB1, DCK, DCTPP1, DDX10, DDX21, DDX28, DEPTOR, DNAAF2, DOCK1, DOCK9, DYNC2LI1, DYSF, EEF1E1, EHF, EPS15L1, EREG, ERVMER34-1, ESRRA, ETV6, EXOSC2, EXPH5, FADS1, FADS2, FAM113B, FAM208A, FAM3C2, FASN, FHOD3, FJX1, FNDC3B, FRMD4A, FRMD6, FTSJD1, GAB2, GADD45A, GART, GBP1, GCSH, GDF15, GJB2, GNE, GNG10, GNG11, GTF2E1, GULP1, H2AFY2, H3F3B, HERC5, HERPUD1, HMBS, HMGN1P38, HNRNPA1P28, HNRNPA3, HNRNPKP4, HOOK2, HOXB2, HOXB8, HPS3, HS3ST1, HS3ST3A1, HSPBAP1, HUWE1, IARS, IBSP, IFI16, IFI44, IFIT3, IGFBP4, IL1A, IL1B, IL1RAPL1, IL1RN, IL23A, IL6, IL8, INO80C, IPO5, IQCD, IRAK2, IRAK3, ITCH, ITGAV, KIAA0247, KIF22, KIFC1, KLF4, KRTAP2-3, KYNU, LACTB2, LIMA1, LIPG, LPXN, LRIG1, LTB, LTBP2, LTV1, LY6E, LYAR, LYRM2, MAGOH, MANSC1, MAP3K5, MAP7, MAPK6, MCCC2, MEOX1, MGLL, MGST1, MIR23B, MKI67IP, MKX, MLPH, MMP25, MOK, MPP6, MRPL33, MRPS30, MTA3, MTM1, MTMR12, MYC, MYOF, NCKAP1, NCOA7, NDUFAF4, NEDD4L, NEURL3, NOP2, NPAS2, NPC1, NPM1P5, NR3C2, NRP1, NSMCE4A, NUP35, NUP62, OAT, OSBPL3, OSGIN2, PAFAH1B1, PALB2, PCNP, PFN2, PHLDB1, PISD, PLAT, PLAU, PLEKHF1, PLSCR1, PPAP2B, PPFIBP2, PPP1R11, PPP1R3F, PPRC1, PRDX3, PRIM1, PRKCH, PRMT3, PRMT6, PRRG1, PRRX2, PSD, PTGER4, PTGES2, PTGS2, PTPRM, QPCT, RAB17, RAD50, RAP1GAP2, RASL11B, RBL2, RBMS2, RC3H1, RGCC, RGL1, RGS20, RHOBTB3, RIPK2, RMI2, RNF144B, RPL14P1, RPL22, RPL6, RPRD1A, RPUSD2, RRM2, RRP9, RRS1, S100A2, SDCBP, SEMA3A, SESTD1, SETP18, SFR1, SGK1, SH2B3, SHISA2, SLC19A1, SLC20A1, SLC2A12, SLC39A6, SLC6A12, SNORA24, SNX5, SPATS2L, SPRY2, SPTBN1, SRGAP3, SRGN, SRPX, SSFA2, STAU2, STEAP1, SYNCRIP, TAGLN2P1, TANC1, TANC2, TAP2, TBX15, TCF4, TEX10, TGFBR2, THSD4, TIGD2, TINAGL1, TJP3, TMEM171, TMEM187, TMEM241, TMEM55B, TMEM69, TMOD1, TMPRSS2, TNC, TNFAIP2, TNFRSF11B, TNFRSF21, TPD52L1, TRMT11, TSEN2, TSPAN4, TTF2, UBE2T, UCP2, USP13, VANGL2, VNN1, WBP2, WDR12, WDR92, WDSUB1, WNT7A, XBP1, XPOT, ZBED4, ZC3H12C, ZDHHC14, ZNF165, ZNF239, ZNHIT2, ZNHIT6, ZNRF3, 17 other genes with no HGNC symbol
		Both	ALDH1B1, ANAPC13, AURKA, BEX1, BICC1, C12orf32, CCNA2, CDH6, CENPA, CENPB, DCDC2, DHCR7, DICER1-AS1, DLGAP5, DUS2L, E2F5, EHHADH, FAM171A1, FAM83D, FAM84B, FDFT1, FGF2, FZD2, GCNT3, HEATR1, HENMT1, HES1, HMGCR, HMGCS1, HNRNPD, IFI44L, INSIG1, KIF14, KIF23, LDLR, LPIN1, METTL5, MX1, PACSIN3, PALLD, PLLP, PPP1R10, RBM47, RBMX, REPIN1, RTN4IP1, SHROOM3, SLC35F5, SQLE, THBS1, THOC6, TMED10, TMEM60, TMEM97, TNFSF10, TNS3, TOP2A, TPX2, TRIP6, WEE1, ZNF518B, 6 other genes with no HGNC symbol
Low	Up	PEA1 only	ABHD14B, ALPP, ATN1, BLVRB, CD63, CINP, CKB, CTDNEP1, CXCL14, DLX2, DMWD, DPP9, EPHX1, FAM215B, FLNA, GANAB, GMPPA, GUCA1A, HAUS2, HIATL2, KDELR1, KIRREL, LYPD3, MAPK8IP3, MAST2, MBTD1, MIR129-2, MIR296, MXD3, NAT14, NELF, NFIX, NPNT, NRAP, PCNT, PFDN6, PIP5K1A, PLIN5, PLP1, POGK, RARRES2, RHBDL1, RHEBL1, S100A1, SLC6A17, SLC9A2, SMCR5, SNORD104, SSTR2, TELO2, TFF1, TFPT, USP49, VAMP8, WDR62, XAB2, ZNF692, ZNF786, ZNF833P, 2 other genes with no HGNC symbol
		PEA2 only	AQP12B, ARPC3, ATP5E, BST2, C11orf83, CACNB3, CCL15, CD55, CDK5, CENPH, CFLAR, CHCHD2P9, CLDN8, CLEC2L, CNTNAP3, COTL1, COX6A1P2, CRIP1, CRIP2, CTSZ, DDX23, DDX27, DNAH10, DNPEP, DUSP8, EEF1B2, EHD3, EML2, ETV7, EXOC3, FAM133A, FAM43B, FAM65B, FBXO25, GEMIN7, GPKOW, GPR108, GPR143, GSPT2, GUK1, HIST3H2A, HLA-A, HNRNPA1P7, HSPE1, IFI27, IFI27L2, IFI6, IGFLR1, KCNMB2-IT1, KIF9, LMNB1, LMTK2, MAP3K10, MIR1234, MIR1267, MRPL34, MRPL54, MRPS7, NEDD8-MDP1, NEURL1B, NPM1P5, NRK, OR5G5P, PIPSL, PKN2, PSAPL1, PTRHD1, RAB13, RFPL3, RNF166, RNF216P1, RNY3, RNY4, RPL10A, RPL21, RTP4, SALL4, SCNN1D, SERPINA5, SERPINH1, SH2B1, SLC25A47, SNORA29, SNORD12, SNORD17, SNORD3C, SNORD3D, SNX11, SPDYE6, SPTB, STARD3, SUFU, TCF7, TCIRG1, TFAP4, TFEC, TMEM160, TMEM208, TRAPPC6A, TSPAN15, TSPAN32, TTC17, UNC45B, USP41, VTI1A, WDR70, XCR1, ZNF264, ZNF775, ZNF91, ZNHIT1, 15 other genes with no HGNC symbol
		Both	38777, TAF15
	Down	PEA1 only	AASDHPPT, ABCB7, ACTG1, ACTL6A, AFF4, ATAD2, C5orf24, CA2, CCNE2, CDK1, CLPX, CNIH, COPB1, CPE, CUTC, DEPDC1, DHTKD1, DUSP1, DYNC1I2, EHHADH, EIF3J, ENOPH1, FAM18B1, FAM3C2, FAM83D, FOPNL, FOS, FOSB, GINS4, GNG10, GNG12, GOLPH3L, GRAMD3, HLTF, HNRNPA1P12, HNRNPKP4, HSPD1P1, IFIH1, IGF2BP3, ITFG1, ITGAV, JAK1, KCTD9, KPNA3, LAP3, LIPA, LYAR, MAD2L1, ME1, METTL5, MFSD1, MORF4L2, MYCBP2, NCKAP1, NDFIP2, NPM1P5, NUP153, OAT, OSGIN2, OSTCP2, OTUD4, PALLD, PCNP, PDGFC, PFN2, PGAM1, PIP5KL1, PNMA2, POLR2B, PRAMEF4, PRDX3, PRNP, PTPN13, QPCT, RAB5A, RAD51AP1, RCN2, RRAS2, RRM2, RTCD1, SDCBP, SDHD, SENP6, SGOL2, SIPA1L3, SLC35B4, SNORD13, SPP1, SQLE, SRP9P1, SRPK1, STRN3, STXBP3, SUCLA2, TAF2, TCF12, TFDP1, THBS1, TJP1, TMED7, TMEM123, TMX3, TSPAN13, UCHL5, USP40, VBP1, VN1R2, WDR47, WEE1, YME1L1, ZC3H15, ZNF425, ZNF426, ZNF791, ZNF83, 6 other genes with no HGNC symbol
		PEA2 only	AAK1, ADO, ARID4B, ASH2L, ATP13A3, BAG3, BICC1, C6orf72, CBX5, CCDC8, CEBPZ, CPSF6, CREB3L2, CWC25, DCP2, DNAJB14, DYNLT3, EFCAB6, EID3, ELK3, EPRS, FAM133B, FAM168A, FNDC3B, FTSJD1, GJB2, GK5, HIST1H4C, HIST2H2AC, HOOK1, HOXB8, HS3ST1, IGF2BP2, IGF2R, IL8, IRF2BPL, ITPRIPL2, LY86, MAPK6, MEGF11, MEX3C, MPDZ, MTF2, NFAT5, NIPAL1, NPC1, ODZ4, OXR1, PABPC1, PAK2, PAPD5, PAPD7, PDE12, PPFIBP1, PRDM13, PRR11, PTGER4, PTGS2, PTPN1, RAB11FIP2, RB1CC1, RBM12B, RBM26, RFX1, SCYL2, SEMA3D, SERINC1, SET, SHISA2, SLC25A36, SLC52A3, SNX16, SOWAHA, SPIN1, SPON1, SPTY2D1, SRFBP1, SSH1, TAF4, TAOK1, TAP2, TMED5, TMEM106B, TMEM179, TMPRSS15, TNS3, TRMT11, TSPAN18, UGGT1, USP10, WBP2, ZCCHC6, ZNF385C, 6 other genes with no HGNC symbol
		Both	C1orf55, NFE2L2, SFXN1, SLC35F5, TMED10, 1 other genes with no HGNC symbol

Supplementary Table 11 ***Overlapping differentially expressed genes between MCF-7, MDA-MB-231 and PEA1 cells treated with Oncamex.***

		MCF-7, MDA-MB-231 & PEA1 (Venn diagrams: overlap in changes genes after treatment with high/low Oncamex)	
High	Up	MCF-7 only	ADPGK, AKNAD1, ALDOC, AP4B1, AQP3, ARL6IP6, BAMBI, BTBD11, C11orf68, C11orf75, C1orf51, CCDC28A, CCNA2, CCNG2, CDK7, CDKN1B, CEBPD, CELF1, CENPW, CEP152, CGA, CHMP1B, CHRM3, CLDN12, CMC1, CMTM6, CNIH, CPOX, CRIPT, CXADR, DCUN1D3, DEDD2, DENND5A, DLX2, DNAJB6, DNAJC24, EFNA1, ELP4, EXO1, FAM111A, FARP2, FBXO8, FHL3, FKBP15, FOS, FOXP1-IT1, GLCE, GON4L, GPR37, HES1, HMG20A, HSD17B1, HSPA1A, HSPA1B, HSPH1, ID1, IGHV5-78, KBTBD2, KCTD6, KDM2A, KIAA0907, KIDINS220, KIFAP3, KIRREL3-AS2, KLHL12, KLHL9, LEMD3, LPIN1, MAP3K13, MED30, MFAP1, MFAP3, MIR21, MLL5, MMD, MTHFSD, MTRNR2L1, MXD4, NEK7, NFYA, NMI, NPC1, NR4A2, NSMCE2, NXN, PDRG1, PGAM1, PGAM4, PGM1, PGPEP1L, PIAS1, PIAS4, PIR, PNRC1, POLR3GL, POU2F1, PPIP5K1, PRDX3, PRKRIP1, PRPF3, PTPN21, RAB23, RAD54B, RFFL, RHBDL1, RIC8B, RN7SL1, RNASEL, RNF122, RNF144A, RNFT1, RNGTT, SEC22A, SLC25A4, SSH2, STARD3NL, STK3, SYT5, TBKBP1, TDO2, TFAP2C, TRIB1, TSPYL1, TTC1, TTI1, VPS4B, WDR26, WDR27, WDR54, YPEL2, ZBTB41, ZC2HC1A, ZFP36, ZFYVE20, ZNF217, ZNF248, ZNF337, ZNF654, ZSWIM5, 7 other genes with no HGNC symbol
		MDA only	ABCD1, ABHD5, ADAM8, ADRB2, AHSA1, ANKRD54, ARHGEF16, ARHGEF40, ARID5B, ARMC7, ASUN, ATAD2B, ATG12, AVL9, B3GALNT2, B3GNT5, BBC3, BCYRN1, BLCAP, BLID, BLZF1, BMS1P5, C10orf118, C11orf96, C12orf23, C2orf69, C3orf52, C5orf30, C7orf71, C8orf80, C9orf84, CAPN5, CAPRIN2, CARS, CBLB, CCND2, CDK12, CDKN1C, CHMP7, CHST11, CIR1, CLCF1, CPO, CTSZ, DACT3, DCP2, DDA1, DDAH1, DENND2C, DGKQ, DLC1, DOK1, DUSP18, DUSP5P, EIF2C2, ELP2, ENTPD7, EYA3, F3, FAM13A, FAM179B, FAM195B, FAM63A, FAT4, FGFR3, FICD, FLNC, FUT6, GALNT3, GLS, GM2A, GNPNAT1, GOLGB1, GPR137B, GSK3B, HAND1, HIATL2, HMHA1, HOXD1, HSD17B7, HSPA4L, IFFO1, IFT20, IL11, IL1RAPL1, IL27RA, IL8, IMPA1, ISCA1P1, ITFG2, ITGA5, ITPK1-AS1, ITPKA, KDM5A, KIAA1958, KIF1B, KLHDC1, KRTAP2-3, LIN37, LINC00342, LRRC14, MAGT1, MAK16, MAN2A1, MBD4, MCTS1, METRNL, MFHAS1, MGEA5, MIR1275, MIR17HG, MIR507, MIR759, MOB3A, MOSPD1, MTF2, MYO3B, NANS, NCBP1, NIPAL1, NOC3L, NR2F2, ODZ1, OFD1, OR1S2, OR5C1, OSBPL8, P4HB, PAG1, PAM, PANX1, PCNX, PCSK5, PDK1, PHF23, PIK3C3, PIM1, PKIA, PLA2G15, PLAT, PNPLA2, PNPLA8, PPP2R2A, PRSS8, PUS3, RAD54L2, RALGAPA1, RBM15, RECQL4, RGS4, RNF113A, RORA, RPS4XP16, RRAD, SAMD4A, SEC11C, SERPINB8, SERPINE2, SGMS2, SH3BP5L, SIPA1L2, SLC22A25, SLC2A14, SLC2A3, SLC5A8, SLC7A2, SLIT2, SNORA5C, SOGA3, SPHK1, SPIRE1, SRGAP1, SSTR2, ST8SIA2, STK35, TCF19, TCF24, TEAD3, TIGD5, TLR4, TMEM115, TMEM156, TMEM51, TMEM57, TNIP2, TPBG, TRIM27, TRIM58, TRIP12, TTC14, UAP1, UBE4A, UGCG, UGDH, USP38, USP49, VEGFC, VGF, VMP1, VPS18, VPS37A, WFIKKN1, ZBTB40, ZCCHC12, ZCCHC6, ZDHHC18, ZFAND2A, ZFP36L1, ZNF140, ZNF148, ZNF17, ZNF175, ZNF193, ZNF207, ZNF215, ZNF224, ZNF322P1, ZNF335, ZNF35, ZNF653, ZNF668, ZNF695, ZNF772, ZNF786, ZNF800, ZNF841, ZNFX1, 10 other genes with no HGNC symbol
		PEA1 only	ADAMTS1, ADORA2B, ADPRHL2, ADRBK1, AEN, AFAP1L1, AGPAT5, AGRN, ALDH18A1, ALDOA, ALKBH5, APLN, APOL2, ARHGEF2, ARHGEF37, ARHGEF7, ARL5B, ATF3, AVPI1, B3GNT4, B4GALT7, BAG3, BBX, BCL11A, BCL3, BHLHE41, BIRC3, BTN2A1, C11orf84, C12orf29, C14orf43, C15orf42, C15orf48, C1orf35, C1QL1, C3orf39, C4orf47, C7orf49, CA12, CARD10, CBX4, CCL20, CCND1, CCNJL, CD83, CDK18, CDKN1A, CEBPB, CERS6, CHD7, CHST14, CHST15, CHST3, COL7A1, CREG1, CRISPLD2, CXCL2, CYB5D1, CYGB, DAZ1, DDX41, DENND2A, DENND3, DGCR8, DGKD, DLX1, DMWD, DOK3, DPYSL4, DTL, DUSP14, EDEM1, EDN2, EFNB2, EIF4A3, ELL2P1, EPAS1, EPHA2, ERF, ETS1, ETV5, FAM210A, FAM214B, FAM216A, FAM43A, FAM46C, FBXO32, FEM1C, FGFRL1, FHDC1, FOSL1, FOSL2, FOXC1, FOXO3, FRMD8, FSTL3, GADD45A, GANAB, GRPEL1, HAGH, HBA2, HELZ, HES6, HLA-A, HNF1B, IER2, IER3, IER5, IER5L, IFFO2, IFNGR2, IGKV1-33, IL4R, IL6, IMP3, ING2, IRAK2, IRF1, IRS2, IRX3, ISM2, ITPRIP, JARID2, KDM5B, KIAA0513, KLF2, KLHDC5, KLHL21, KLHL3, KRBA1, LONRF1, LPCAT1, LRRC41, MALL, MAP3K14, MAP3K8, MAP3K9, MAPK7, MAPK8IP3, METTL21B, MFNG, MICB, MIDN, MIR155HG, MNT, MOAP1, MOB2, MSX1, MTHFD2, MYBL1, MYEF2, MYLIP, NAB2, NADSYN1, NCKAP5L, NCKIPSD, NCOA7, NFIX, NFKB1, NFKB2, NFKBIA, NFKBIE, NGLY1, NINJ1, NKX3-1, NLRP3, NOL3, NOTCH1, NPHP3, NPIPP1, NRIP1, NUAK2, NXT1, OXR1, PAPSS2, PAQR4, PHLDA1, PIEZO1, PIGA, PIK3C2B, PIK3IP1, PIM2, PIM3, PLAU, PLEKHA2, PLEKHH1, PLEKHH3, PLEKHO2, PLIN2, PLXNA3, PMAIP1, PMP22, POM121C, POU5F1, POU5F1B, POU5F1P5, PPAT, PPP1R14C, PPP1R15A, PPP1R3C, PPP1R3E, PPP3CC, PREP, PRR5L, PRR7, PRSS53, PSORS1C3, RAB11FIP5, RAB40C, RAD54L, RAI1, RALGDS, RAP2A, RASD1, RASL11B, RASSF1, RAVER1, RELB, RHOB, RIPK4, RIT1, RNASET2, RND3, RNF144B, RNF165, RPL14P1, RRAGA, RTN4R, RTTN, RUNX1, RUSC1, S100A1, SAP30, SEC61G, SEMA4B, SERTAD1, SERTAD2, SESN1, SGK1, SGSM2, SH2B3, SH2D4A, SH3BP1, SH3BP2, SH3PXD2A, SHB, SHPK, SIAH2, SIK1, SLC1A4, SLC35E1, SLC39A14, SLC7A1, SLC7A5, SLC9A1, SLCO4A1, SLCO5A1, SLFN11, SMAD3, SNHG12, SNORA61, SNORA79, SNTA1, SOCS3, SOX9, SRSF7, ST3GAL1, STAMBPL1, STARD5, SYDE1, TACC1, TACSTD2, TBC1D2B, TBK1, TBX2, TFB1M, TGFA, TGIF2, TINAGL1, TINF2, TIPARP, TK1, TMEM189, TMEM41A, TMEM47, TMEM74B, TNF, TNFAIP2, TNFAIP3, TNFRSF10B, TNFRSF12A, TNFSF9, TOB2, TPI1, TPI1P2, TRIB2, TRIB3, TRIM32, TRIM47, TSPAN5, TUBB2B, TULP3, TWIST1, TXNRD1, UBE2O, USP37, VASN, VEGFA, VKORC1, VTRNA1-3, WDR45L, WDR90, XPNPEP1, ZDHHC7, ZFP82, ZMYND19, ZNF114, ZNF250, ZNF275, ZNF296, ZNF324, ZNF343, ZNF696, ZP1, 10 other genes with no HGNC symbol
		MCF-7 & MDA	MAPK8, MAPK9, PHF13, PPME1, RAB30, RUNDC3B, TICAM2, 3 other genes with no HGNC symbol
		MDA & PEA1	38777, ABCB6, AK4, ANG, ANKZF1, ARC, ATG9A, BTAF1, C10orf10, C3orf58, C8orf58, CCNE1, CCRN4L, CDC42EP2, CHPF, CHSY1, CHSY3, CKB, CNOT8, CSF2, CXCL1, DNAJB2, DNAJB9, DUSP5, ERRFI1, FAM107B, FAM117B, FAM162A, FAM46A, FER1L4, G0S2, GALNTL4, GFPT2, GJA3, GLRX, GPT2, HBEGF, HES4, IGFBP3, KCTD11, KIAA1715, KIRREL, KLF6, LGALS8, LIF, LOX, LUZP1, MAFF, MAP1LC3B, MAP2K1, MAP6D1, MGAT1, MKNK2, MT1X, NARF, NFKBID, NIPA1, NOG, OBFC2A, PABPC1L, PAPD7, PLAUR, PLCXD1, PLEKHG3, PLOD2, PNP, POM121B, PPAN-P2RY11, PPP1R16A, PPP3R1, PPTC7, RAB11FIP3, RAB20, RAB38, RASSF7, RRAGD, RUNDC1, SDC4, SEC63P1, SERPINE1, SLC25A36, SLC2A1, SLC41A1, SLC6A10P, SLC6A8, SMAP2, SNX33, SPAG4, TAF15, TNIP1, TPI1P1, TUBB2A, UPRT, ZNF470, ZNF672, 2 other genes with no HGNC symbol

		MCF-7 & PEA1	ASF1B, BCL6, BTG2, C17orf58, C2orf49, CCNE2, CLDND1, CLK3, CRKL, DHX32, E2F7, GADD45B, HOXA5, IRF2BPL, JUNB, KIAA0355, NFE2L1, NUDT18, OXSR1, PGK1, PLEKHA8P1, POLR2H, RAB2B, RAB9A, RBM14, RBM4B, RIMKLA, SPRED1, SPRY1, STC2, TERF2IP, TOB1, WSB1, ZIC2, ZNF295, ZNF395, 6 other genes with no HGNC symbol
		MCF-7, MDA & PEA1	ADM, ANGPTL4, ANKRD37, ARID3A, ASNS, BHLHE40, BNIP3, BNIP3L, C10orf28, C17orf96, CHIC2, CITED2, CSRNP1, CSRP2, DDIT4, DUSP1, EGLN1, ENO2, ERO1L, FAM57A, FUT11, GBE1, HILPDA, HK2, INSIG2, JUN, KDM3A, LDHA, NDRG1, NFIL3, NXF1, P4HA1, P4HA2, PFKFB3, PFKFB4, PPFIA4, PPP2R5B, RIOK3, RLF, RNF24, RNMT, SLC38A2, STC1, VLDLR, YEATS2, ZNF770, 3 other genes with no HGNC symbol
	Down	MCF-7 only	40787, ACOT4, ACSS1, AEN, AFF3, AK2P2, ALKBH2, ARHGEF16, ARHGEF19, ARPC3, B4GALT1, BCL2, BLMH, BOP1, C10orf81, C14orf126, C14orf39, C15orf59, C16orf74, C17orf70, C19orf10, C19orf46, C4orf19, C6orf211, CAMK2N1, CAPN1, CCDC155, CCDC86, CCDC88C, CCDC94, CCND1, CDH18, CHD4, CHGA, CLN3, COMTD1, COPG2, CRIP2, CUTC, CXCL12, DCAF13, DEGS2, DEPTOR, DHX33, DNPEP, DRAM1, DUS1L, DUS3L, EFCAB4A, EFHD1, EIF3B, ELFN2, ELOVL2, EMG1, EML3, ERMP1, ESR1, EXOSC6, EXOSC8, F12, FADS1, FADS2, FAH, FAM173A, FAM195A, FAM213B, FAM35A, FAM5B, FAM63A, FAM65A, FAM70A, FBXO27, FDPS, FFAR2, FGD3, FHL2, FKBP4, FLNA, FLNB, FOXE3, GALNT6, GGT6, GJA1, GLA, GNB1L, GPR68, GRPR, GSDMD, GSTM3, HCG18, HIST1H1B, HIVEP3, HPDL, HPGD, HSD3B7, HSPA5, HSPB8, ICAM3, IGFBP5, IL17D, IL19, IL27RA, IPCEF1, ISOC2, ITPK1, KAZALD1, KIAA0182, KIAA0664, KRT18P13, KRT18P17, KRT18P19, KRT18P28, KRT8P33, KRT8P9, KTN1-AS1, KYNU, LCP1, LEPREL4, LMOD3, LPO, LRP5L, LRRFIP1, LYRM1, MAML3, MAP3K14, METTL1, MIR373, MIR635, MLLT6, MOCOS, MPPED2, MRP63, MRPS2, MRTO4, MYADM, MYBBP1A, MYO3B, NAA10, NAGLU, NCOR2, NINJ1, NME2P1, NOP14, NOP16, NOP58, NPY1R, NR2E3, NR5A2, NUCB2, PBX1, PDCD4, PINK1-AS, PLIN5, PLXNB1, POLR3K, PPRC1, PREX1, PRKCD, PRLR, PRSS23, PTGR2, PUS1, RAC3, RAD50, RAI14, RAP1GAP, RASL11A, RASL11B, RBPMS2, RDBP, RELL2, RERG, RHBDL2, RPS26P35, RPS26P47, RPUSD1, RRP1, RRS1, SAPCD2, SCARNA9, SCIN, SDC1, SDC4, SELENBP1, SEMA3C, SEMA3F, SERPINH1, SFPQ, SGK3, SHANK2, SHISA5, SIPA1L3, SLC19A1, SLC25A11, SLC25A13, SLC25A22, SLC39A10, SLC4A2, SLC7A2, SLC7A8, SLC9A3, SLC9A3R1, SLITRK4, SMARCD2, SOAT2, SPOCD1, SRM, SRPK1, SSH3, STARD10, STEAP3, SUSD3, SYT12, SYTL1, TBC1D16, TEAD2, TEKT4, TGFB3, TIGD5, TMEM229B, TOMM40, TRIB3, TRIM65, TRMT1, TRMT6, TRPS1, TSPAN4, TUFT1, TYRO3, UBL3, UFSP1, VASP, VPS11, VTRNA1-3, WDR46, WDR90, WSB2, XCR1, YBX2, ZHX2, ZNF239, ZNF346, ZNF467, ZNF593, ZNF75A, ZNF768, ZNF787, ZNHIT2, 13 other genes with no HGNC symbol
		MDA only	ABR, ADAM19, ADORA2B, AIMP2, AMD1, AMDHD2, ANGPTL2, ANP32AP1, APCDD1L, APEX1, APOBEC3B, ARMCX1, ARMCX2, ASXL1, BAIAP2L1, BAMBI, BMP4, BRI3, BTF3L4, BUB1, C15orf23, C16orf53, C17orf98, C1orf109, C1orf123, C20orf72, C7orf53, C9orf3, C9orf40, CALM3, CAP2, CARD10, CAV1, CAV2, CBR1, CBX1, CCDC102A, CCDC99, CCNF, CD207, CD58, CDCA2, CDCA8, CDH11, CDK1, CDKN2D, CEP41, CEP55, CKAP2, CKAP2L, CLIC6, COL4A2, COQ2, CRADD, CST1, CST4, CTDSPL, CTIF, CTNNBIP1, CUEDC2, CUL9, CYB5A, CYR61, DENND5B, DNAAF2, DNAH2, DSN1, EHBP1, ESPL1, ETS2, F2RL1, FAM46B, FAM75A1, FHOD3, FKBP1C, FUT8, GBAP1, GBP1, GCA, GEMIN2, GJB2, GLT25D2, GNG10, GNG12, GTF2H4, H2AFX, HAUS8, HCAR1, HDDC3, HIF1A, HIST1H2AC, HIST1H4C, HIVEP1, HLA-DPA1, HMBS, HMGB3, HMGN1P38, HNRNPA0, HNRNPA3, HSPE1, HTRA2, KCNN4, KIAA1671, KIF11, KIF18A, KIF22, KIF2C, KIF4A, KIFC1, KLF15, LAMA5, LAMTOR1, LAYN, LIMA1, LMNB2, LMTK3, LPAL2, LPP, LPXN, LRP5, LTV1, LYRM2, MAD2L1, MAMDC2, MAMLD1, MCM5, MED26, MELK, MGAT2, MIR586, MKI67, MLPH, MMACHC, MRPL34, MRPS18C, MTA3, MXD3, MYLIP, MYO5C, MYOF, NASP, NDP, NDUFA12, NEDD8-MDP1, NFE2L3, NGF, NIF3L1, NNMT, NOXA1, NPAS2, NR1H3, NR3C2, NREP, NRP1, NRXN1, NSMCE4A, NUP35, NUP37, OBFC1, OGFR, OLFML2A, OPRK1, OSBPL10, PAAF1, PAFAH1B1, PAPPA, PARP4, PCCA, PDCD11, PDE7B, PFN2, PHF19, PIGT, PIGV, PIGY, PITX1, PKP2, PLAU, PLEK2, PLEKHA6, PLK1, PLK4, PLXNA1, PMEPA1, POC1A, POC5, POLE2, PPAP2B, PPAPDC1A, PPARG, PPP5C, PRDM8, PRDX3, PRICKLE2, PRIM1, PRNP, PSPC1P1, PXDN, RACGAP1, RAD23B, RAD51AP1, RAN, RARRES3, RGS20, RHOJ, RPL39L, SAMD9L, SCRN1, SEMA3A, SH3PXD2A, SH3RF3, SHISA2, SLC35B3, SLC37A1, SLC37A2, SLC46A3, SLCO4A1, SNORA73B, SNORD117, SNRPD1, SPATS2L, SPCS1, SRBD1, SRRM1, SUN2, SUSD5, SUV39H1, SVIL, SYNCRIP, TACC2, TANC1, TANC2, TIMELESS, TIMM10, TIMP3, TIPARP, TMCO3, TMEM116, TMEM14A, TMEM163, TMEM237, TMEM71, TMEM75, TNFRSF11B, TNFRSF14, TNFRSF21, TOX2, TRERF1, TRIM8, TRIP13, TTF2, TUBB, TYMS, UBE2C, UBE2L6, UBE2T, UPF3AP1, UTP18, VIPR1, WDR67, WDR92, ZFAND5, ZMIZ1, ZNF627, 15 other genes with no HGNC symbol
		PEA1 only	ABCB7, ABCC4, ACACA, AGPS, AKR1C3, ALDH1B1, ALPK2, AMOT, ANLN, ANXA1, ANXA3, ARHGAP4, ASF1A, ATF6, BCMO1, BEX1, BICC1, BIVM, C17orf97, C21orf7, C4orf33, CABYR, CAMKMT, CCT6B, CD9, CDH6, CGNL1, CLDN11, CLDN16, COBLL1, CPE, DCDC2, DDAH2, DEFB1, DEPDC1, DHCR7, DICER1-AS1, DNALI1, DOCK11, DUS2L, E2F5, EARS2, ECT2, EFHB, EHHADH, FAM198B, FAM64A, FAM84B, FDFT1, FGF2, FOPNL, GCNT3, GPKOW, GRB14, GYG2, HABP4, HEATR1, HENMT1, HIST2H2AC, HLF, HN1, HOGA1, HOXB5, HTATIP2, ID1, ID2, IDI1, IFI44L, IFIH1, IL20RB, KLF11, KLHDC8B, KLHL14, KPNA2, LCN2, LPIN1, LRRC61, ME1, MIS18BP1, MRPL1, MVK, MX1, NR2F6, NUCKS1, PAQR8, PDGFC, PDZK1, PDZK1P1, PHF11, PIGM, PKHD1L1, PMVK, PRR11, PSMC1P9, PSME4, PTPN13, PXDNL, RALBP1, RANGAP1, RBM47, RBMX, RNF26, RTN4IP1, SCG5, SHROOM3, SLC12A8, SLC35F5, SMARCAL1, SNX2, SQLE, SRGAP1, STEAP4, STK32B, STX3, SUMO3, SYNE2, SYT13, TACO1, TAF7, TAF9B, TM4SF18, TMED10, TMEM97, TNFSF10, TP53INP1, TRIM2, TSPAN31, UCHL5, UPF3A, VCAN, WBP11P1, WDR34, WDR73, WNT2B, WWC1, XRCC5, ZBED2, ZC3H4, ZC3HAV1, ZFP3, ZMYM4, ZNF212, ZNF425, ZNF426, ZNF518B, ZNF594, ZNF783, ZNF83, 4 other genes with no HGNC symbol
		MCF-7 & MDA	ASAP3, CA12, CABLES1, CMBL, CREB3L4, DNAJC9, IGFBP4, PER3, PHF15, POLA2, SCNN1A, SLC29A2, SPDEF, SRF, SRSF6, TCEA3
		MDA & PEA1	ANAPC13, ASPM, AURKA, AURKB, C12orf32, CCDC106, CCNA2, CCNB2, CDCA3, CDKN3, CENPA, CENPE, CENPF, CKS2, CYP1B1, DLGAP5, FAM171A1, FAM83D, FZD2, GPR56, H1F0, HES1, HMGCR, HMGCS1, HMMR, HYLS1, ID3, IGF2BP3, IMPA2, INSIG1, KIF14, KIF20A, KIF23, KRT80, METTL5, NCAPD2, NDC80, NEXN, NUSAP1, OIP5, PIF1, PLLP, PPIL1, PPP1R10, PRC1, PSRC1, RAB7L1, SDPR, SORBS2, SOX4, TACC3, THBS1, THOC6, TMEM60, TNS3, TOP2A, TPX2, TRIM6, TROAP, TTK, WEE1, 6 other genes with no HGNC symbol

		MCF-7 & PEA1	AVEN, INPP4B, KIF12, LTBR, MAPKAPK3, MTA2, NTHL1, PALLD, PDIA3P, PPP1R35, RPP40, SYS1-DBNDD2, TBL1X, ZNF358, 1 other genes with no HGNC symbol
		MCF-7, MDA & PEA1	CCNB1, CDC20, CENPB, DBN1, HNRNPD, LDLR, PACSIN3, RAB3IL1, REPIN1, SNORD13, TRIP6
Low	Up	MCF-7 only	C16orf11, C1orf105, C5orf55, FAM110B, FAM210B, FAM83F, FGFBP3, GAS2L2, HERC2P2, KCND3, MFAP4, MIR26B, OR2T11, PCDH9, PRSS30P, PTPRU, RNU6-15, SNORA2B, SNORD113-3, SUDS3, ZC3H6, 2 other genes with no HGNC symbol
		MDA only	ADCY10, ARPC3, ATF5, CTSZ, DDI1, HMOX2, PLXDC1, PRR21, SCARNA14, TRIB3, TXN2, VASP, ZNF365, 3 other genes with no HGNC symbol
		PEA1 only	38777, ABHD14B, ALPP, ATN1, BLVRB, CD63, CINP, CKB, CTDNEP1, CXCL14, DLX2, DMWD, DPP9, EPHX1, FAM215B, FLNA, GANAB, GMPPA, GUCA1A, HAUS2, HIATL2, KDELR1, LYPD3, MAPK8IP3, MAST2, MBTD1, MIR129-2, MIR296, MXD3, NAT14, NELF, NPNT, NRAP, PCNT, PFDN6, PIP5K1A, PLIN5, PLP1, POGK, RARRES2, RHBDL1, RHEBL1, S100A1, SLC6A17, SLC9A2, SMCR5, SNORD104, SSTR2, TELO2, TFF1, TFPT, USP49, VAMP8, WDR62, XAB2, ZNF692, ZNF786, ZNF833P, 2 other genes with no HGNC symbol
		MDA & PEA1	KIRREL, TAF15
		MCF-7 & PEA1	NFIX
	Down	MCF-7 only	ALX3, ATP2C2, C16orf74, CLDN4, CNGA3, COPG2, F12, FGF6, HIST3H2A, KRT18P19, MRPS34, MTMR8, NBPF20, PDIA3P, PINK1-AS, PLIN5, PPARGC1A, SERPINH1, SLC25A22, SNHG10, TEKT4, TMEM174, YIPF3, ZDHHC18, 13 other genes with no HGNC symbol
		MDA only	ARL4D, BLOC1S1, C17orf65, CPXM2, CRISP1, CSF2, CST1, EDN1, FAM65B, HOGA1, KLF7, MIR23B, MVP, OPRK1, PAX9, PCP2, RAB13, SERPINA5, TFF1, TMEM65, TMEM75, ZNF785, 2 other genes with no HGNC symbol
		PEA1 only	AASDHPPT, ABCB7, ACTG1, ACTL6A, AFF4, ATAD2, C1orf55, C5orf24, CA2, CCNE2, CDK1, CLPX, CNIH, COPB1, CPE, CUTC, DEPDC1, DHTKD1, DUSP1, DYNC1I2, EHHADH, EIF3J, ENOPH1, FAM18B1, FAM3C2, FAM83D, FOPNL, FOS, FOSB, GINS4, GNG10, GNG12, GOLPH3L, GRAMD3, HLTF, HNRNPA1P12, HNRNPKP4, HSPD1P1, IFIH1, IGF2BP3, ITFG1, ITGAV, JAK1, KCTD9, KPNA3, LAP3, LIPA, LYAR, MAD2L1, ME1, METTL5, MFSD1, MORF4L2, MYCBP2, NCKAP1, NDFIP2, NFE2L2, NPM1P5, NUP153, OAT, OSGIN2, OSTCP2, OTUD4, PALLD, PCNP, PDGFC, PFN2, PGAM1, PIP5KL1, PNMA2, POLR2B, PRAMEF4, PRDX3, PRNP, PTPN13, QPCT, RAB5A, RAD51AP1, RCN2, RRAS2, RRM2, RTCD1, SDCBP, SDHD, SENP6, SFXN1, SGOL2, SIPA1L3, SLC35B4, SLC35F5, SNORD13, SPP1, SQLE, SRP9P1, SRPK1, STRN3, STXBP3, SUCLA2, TAF2, TCF12, TFDP1, THBS1, TJP1, TMED10, TMED7, TMEM123, TMX3, TSPAN13, UCHL5, USP40, VBP1, VN1R2, WDR47, WEE1, YME1L1, ZC3H15, ZNF425, ZNF426, ZNF791, ZNF83, 7 other genes with no HGNC symbol
		MCF-7 & MDA	C19orf10

Supplementary Table 12 ***Overlapping differentially expressed between MCF-7 cells treated with Oncamex or exposed to hypoxic conditions.***

	MCF-7: Oncamex, Chronic Hypoxia, Acute Hypoxia (Venn diagrams: overlap with genes changed by high/low Oncamex)	
Up	Oncamex only	ADPGK, AKNAD1, ANGPTL4, AP4B1, AQP3, ARL6IP6, ASF1B, BNIP3L, BTBD11, BTG2, C10orf28, C11orf75, C17orf58, C17orf96, CCDC28A, CCNA2, CCNE2, CCNG2, CDK7, CDKN1B, CEBPD, CENPW, CEP152, CGA, CHIC2, CHMP1B, CHRM3, CLDN12, CLDND1, CMC1, CMTM6, CNIH, CPOX, CRIPT, CRKL, CSRP2, CXADR, DCUN1D3, DENND5A, DHX32, DLX2, DNAJB6, DNAJC24, DUSP1, E2F7, EGLN1, ELP4, ERO1L, EXO1, FAM111A, FAM57A, FARP2, FBXO8, FHL3, FOS, GBE1, GLCE, GON4L, GPR37, HMG20A, HOXA5, HSD17B1, HSPH1, ID1, IGHV5-78, INSIG2, JUNB, KBTBD2, KCTD6, KDM2A, KIAA0355, KIAA0907, KIDINS220, KIFAP3, KIRREL3-AS2, KLHL12, KLHL9, LDHA, LEMD3, LPIN1, MAP3K13, MAPK8, MAPK9, MED30, MFAP1, MFAP3, MIR21, MLL5, MMD, MTHFSD, MTRNR2L1, MXD4, NEK7, NFIL3, NFYA, NMI, NPC1, NR4A2, NSMCE2, NXF1, OXSR1, P4HA1, P4HA2, PDRG1, PGAM1, PGAM4, PGPEP1L, PHF13, PIAS1, PIR, PLEKHA8P1, PNRC1, POLR2H, POLR3GL, PPIP5K1, PRDX3, PRKRIP1, RAB23, RAB2B, RAB9A, RAD54B, RBM14, RBM4B, RFFL, RHBDL1, RIC8B, RIMKLA, RN7SL1, RNASEL, RNF144A, RNF24, RNFT1, RNGTT, RNMT, RUNDC3B, SEC22A, SLC25A4, SLC38A2, SPRED1, SPRY1, SSH2, STARD3NL, STK3, SYT5, TBKBP1, TDO2, TERF2IP, TFAP2C, TICAM2, TSPYL1, TTC1, TTI1, VPS4B, WDR26, WDR27, YPEL2, ZBTB41, ZC2HC1A, ZFP36, ZFYVE20, ZIC2, ZNF217, ZNF248, ZNF295, ZNF654, ZNF770, ZSWIM5, 15 other genes with no HGNC symbol
	Chronic only	ABCA12, ABCC3, AGRN, AKR1C2, AKR1C3, ARC, ARID5B, ATN1, ATP1B1, BCAR3, BCAS1, BCL3, BCL9L, C14orf132, C14orf159, C15orf52, CCND1, CDKN1A, CLIC3, COL5A1, CX3CL1, CXCR7, CYP1A2, CYP1B1, DEGS1, DGKD, DLC1, DNAJC30, DSP, EFS, EGR2, EGR3, EGR4, ERRFI1, EVL, EXOC3, FAM46C, FICD, FRG1B, GAPDH, GATA3, GPER, GUSBP4, HLA-B, HMOX1, HOXC8, HOXC9, ID3, IER3, IER5, INHA, INHBB, IRF2BP2, IRS1, IRS2, IRX5, ITPRIPL2, KCNK12, LCN2, LDLR, LINC00243, LMCD1, LZTS2, MAP3K5, MAT1A, MED13P1, MUC1, MYLIP, NBPF20, NFKBIA, NVL, NYNRIN, PCDHA3, PCOLCE, PGM5, PKP4P1, PPP1R3E, PPTC7, PRRC2B, RGS16, RHOBTB3, RHOV, RND1, RNF43, RNU4-2, RNU4ATAC, RXRA, S100A16, S100A4, S100A8, S100A9, SALL4, SAMD1, SCARB1, SCARNA9, SETP18, SIK1, SLC38A1, SNORA67, SNORD13, SNORD57, SRRM4, ST3GAL5, TAF13, TM4SF1, TNS3, TPM4, TTC17, UGCG, VTCN1, YWHAE, ZDHHC8P1, ZMYND8, 4 other genes with no HGNC symbol
	Acute only	AARS, AARSD1, AATF, ABCB7, ACBD6, ACOT9, ACTG2, ACTN1, ACTN4, ADAM9, AGAP11, AHNAK2, AIP, AKAP8L, ALG9, ALKBH2, AMY1A, ANKRD1, ANXA1, ANXA2R, ANXA3, AP4M1, AP5S1, APOOL, ARFGAP1, ARFGEF2, ARHGAP10, ARHGEF3, ARHGEF35, ARIH1, ASS1, ASXL1, ATHL1, ATL3, ATOH8, ATXN2, AVL9, AVPI1, B4GALT3, BAG6, BATF, BCKDK, BMP7, BOP1, BRAF, BRI3P1, BYSL, C10orf12, C11orf83, C12orf10, C17orf48, C17orf49, C17orf53, C19orf47, C1orf50, C20orf20, C20orf94, C21orf56, C2orf82, C8orf58, CACYBP, CARS, CBLB, CBX8, CCDC101, CCDC107, CCDC12, CCDC124, CCDC130, CCDC154, CCDC9, CCDC94, CCNB1IP1, CD36, CD55, CDC20, CDK19, CDKL2, CDKN2D, CEBPB, CEBPZ, CENPF, CEP89, CGN, CHD3, CHD7, CHST12, CHST3, CHTF18, CHTOP, CIC, CIR1, CLASRP, CLDN1, CLDN3, COBLL1, COG4, COMMD1, CREBRF, CSNK1D, CSNK2A1P, CSRP1, CTC1, CTGF, CYP4F22, CYR61, DAPK3, DAXX, DBN1, DCP2, DDAH2, DDIT3, DDX10, DDX39A, DLG4, DMAP1, DNAJA2, DNAJB11, DNAJC3, DTNA, DUS3L, DUSP16, DYNC1H1, EEA1, EGLN2, EHMT2, EIF2A, EIF2B5, EIF3D, EMD, ENO3, ERBB2, ERF, ERN1, EYA3, EZR, FAM108C1, FAM158A, FAM160A2, FAM162A, FAM210A, FAM219B, FAM46B, FAM50A, FAM83G, FAM91A1, FEM1A, FERMT2, FHL2, FIP1L1, FJX1, FLCN, FLNA, FOXJ2, FOXO3, FOXP1, FSTL3, GABPB1, GADD45G, GANAB, GARS, GBF1, GDI1, GIGYF1, GMEB1, GMPPA, GNL1, GNL2, GPATCH3, GPC5, GPCPD1, GPSM1, GPT2, GRWD1, GSG2, GSK3B, GTF2F2, H3F3C, HADHA, HARS2, HBEGF, HCFC1R1, HDAC6, HEY2, HIST1H1A, HIST1H1C, HIST1H1D, HIST1H3D, HIST1H3F, HIST1H3H, HIST2H2AA3, HIST2H2BB, HIST2H2BD, HIST2H3C, HIST3H2BB, HOOK1, HOXC10, HOXC11, HRK, HSP90B1, IDH2, IFFO2, INPP4B, INPP5J, INPPL1, IRF6, ITFG2, ITPK1, JAG2, JUND, KCNF1, KCTD15, KDM5A, KIAA0195, KIAA0922, KIF5B, KIFC2, KLC1, KLF6, KPNA4, KRT18P28, KRTCAP2, LAMB2, LARP6, LARS, LCP1, LGALS1, LONP1, LPP, LRIG2, LRRC28, MAGT1, MANF, MAP1S, MAPK8IP3, MB21D2, MBD6, METTL16, MICALL1, MIDN, MIIP, MLLT4, MMS19, MNT, MOB3A, MRPL2, MRPL37, MRPL44, MRPS5, MYO1B, NAMPT, NBAS, NMD3, NOB1, NOC3L, NOP2, NSMCE1, OSGIN1, PACSIN2, PAM16, PAPD5, PAWR, PCNX, PDE4A, PDLIM1, PDLIM7, PHAX, PHF17, PHF21A, PHF23, PHIP, PLEKHF2, PLEKHG2, PLOD1, PLXNA3, PNKP, POLL, POLRMT, PPAN-P2RY11, PPIG, PPP2R2A, PRICKLE3, PSAT1, PTGER4, PTRF, PUSL1, PYGB, RAB13, RAB33B, RAB3GAP1, RAB3IL1, RAB40C, RALGAPB, RASSF3, RBM28, RBM42, RBM6, RBMS2, RDBP, RDH13, REXO1, REXO4, RFX1, RGS17, RGS2, RHBDD1, RHBDF1, RHOG, RIPK4, RIT1, RN5S9, RNF169, RNF20, RNF31, RNU1-3, RNU1-5, RNU11, RP9, RPF2, RPL28, RRAGC, RRAGD, RRAS, RRP12, RRP8, RSPRY1, RTN4RL1, SAMD4A, SARS, SAT2, SELRC1, SEMA3B, SERGEF, SF3A2, SF3B2, SFMBT2, SHMT2, SIN3B, SIPA1L2, SKIV2L, SLC16A9, SLC25A38, SLC2A1, SLC38A7, SLC3A2, SLC9A1, SMTN, SNORD35B, SNORD3C, SNORD3D, SNRPA, SOST, SOX4, SPAG7, SPANXA1, SPANXB2, SPIN1, SPTAN1, SRRM2, SSRP1, STX1A, STXBP2, SUGT1, SUPT5H, SUPV3L1, SURF6, SUV420H1, TBC1D15, TBL3, TEF, TERF1P4, TFAP4, TFPI, TGM1, THADA, THAP8, THBS3, THOC2, THOC5, TIAM2, TMC6, TMEM136, TMEM170A, TNFRSF12A, TNIP1, TNPO2, TNPO3, TPCN1, TPM2, TPR, TRIP6, TRMT61A, TSPAN15, TSSC4, TTC39C, U2AF1L4, UBE2HP1, UBR4, UBXN1, UIMC1, ULBP1, USP30, VARS, VARS2, VPS18, VPS26B, VPS37D, VPS4A, WARS, WASF2, WDR25, WDR33, WDR74, WEE1, WHSC2, WWP2, XAB2, XPO6, YARS, ZBTB10, ZBTB17, ZBTB2, ZBTB3, ZBTB46, ZCCHC7, ZDHHC20-IT1, ZFAND2A, ZNF133, ZNF16, ZNF205, ZNF212, ZNF25, ZNF263, ZNF282, ZNF296, ZNF317, ZNF322P1, ZNF408, ZNF433, ZNF444, ZNF451, ZNF524, ZNF579, ZNF593, ZNF600, ZNF628, ZNF641, ZNF653, ZNF692, ZNF707, ZNF775, ZNF783, ZNF841, ZRSR2, ZSCAN29, 20 other genes with no HGNC symbol
	Oncamex & Chronic	BHLHE40, CITED2, HES1, HK2, PGK1, PGM1, TOB1, TRIB1, VLDLR
	Oncamex & Acute	AGPAT9, ARHGEF2, ARTN, ATF3, BRSK1, C19orf33, C20orf111, CBX4, CCRN4L, CDH3, CSDE1, CYP1A1, DBP, DDX27, DDX41, DDX6, DENND4B, DKK1, DLX3, DUSP3, DUSP5, DUSP8, EDN1, EDN2, EIF2C2, EIF4A2, EPB41L4A-AS1, EPPK1, FAM100A, FAM107B, FAM129A, FGD3, FLOT1, FSCN1, GADD45A, GBP2, GDF15, GPI, IER5L, IRX3, ITPRIP, KDM5B, KRT17, KRT80, MUS81, MYH9, NEU1, NOTCH1, NUPR1, PAN2, PHLDA3, PIM3, PKD1, PLD6, PLK2, PPFIBP2, PPP1R15A, RAB26, RASD1, RASEF, RN7SK, RND3, RNF165, RYBP, S100A14, S100P, SLC2A3, SNORA28, SYDE1, TBX2, TEX19, TLE1, TRIB3, TSC22D3, TUBB2B, TUFT1, UBE2O, ZBTB43, ZC3H12A, ZNF148, ZNF467, ZNF581, ZRANB1, ZYX

	Chronic & Acute	ASNS, C11orf68, C2orf49, CELF1, CLK3, DEDD2, FKBP15, FUT11, GADD45B, HILPDA, HSPA1A, HSPA1B, IRF2BPL, JUN, NUDT18, NXN, PIAS4, POU2F1, PPP2R5B, PRPF3, PTPN21, RAB30, RIOK3, RLF, RNF122, WSB1, YEATS2, ZNF337, 1 other gene with no HGNC symbol
	Oncamex, Chronic & Acute	ADM, ALDOC, ANKRD37, ARID3A, BAMBI, BCL6, BNIP3, C1orf51, CSRNP1, DDIT4, EFNA1, ENO2, FOXP1-IT1, KDM3A, NDRG1, NFE2L1, PFKFB3, PFKFB4, PPFIA4, PPME1, STC1, STC2, WDR54, ZNF395
Down	Oncamex only	40787, ACOT4, ACSS1, AEN, AFF3, AK2P2, ALKBH2, ARHGEF16, ARHGEF19, ASAP3, AVEN, B4GALT1, BCL2, BLMH, BOP1, C10orf81, C14orf126, C14orf39, C17orf70, C19orf10, C19orf46, C4orf19, CA12, CABLES1, CAMK2N1, CAPN1, CCDC155, CCDC86, CCDC88C, CCDC94, CCND1, CDC20, CDH18, CENPB, CHD4, CHGA, CLN3, CMBL, COMTD1, COPG2, CREB3L4, CRIP2, CUTC, DBN1, DCAF13, DEGS2, DEPTOR, DHX33, DNPEP, DRAM1, DUS1L, DUS3L, EFCAB4A, EFHD1, EIF3B, ELFN2, EMG1, EML3, ERMP1, EXOSC6, F12, FADS1, FADS2, FAH, FAM173A, FAM213B, FAM35A, FAM5B, FAM63A, FAM65A, FAM70A, FBXO27, FDPS, FFAR2, FGD3, FHL2, FKBP4, FLNA, FLNB, FOXE3, GALNT6, GGT6, GLA, GNB1L, GPR68, GRPR, GSDMD, HCG18, HIST1H1B, HIVEP3, HNRNPD, HPDL, HSD3B7, HSPA5, HSPB8, ICAM3, IGFBP4, IL19, INPP4B, IPCEF1, ISOC2, ITPK1, KAZALD1, KIAA0182, KIAA0664, KIF12, KRT18P13, KRT18P17, KRT18P19, KRT18P28, KRT8P33, KRT8P9, KTN1-AS1, LCP1, LDLR, LEPREL4, LMOD3, LPO, LRP5L, LRRFIP1, LTBR, LYRM1, MAML3, MAP3K14, MAPKAPK3, METTL1, MIR373, MIR635, MLLT6, MOCOS, MPPED2, MRP63, MRPS2, MRTO4, MTA2, MYADM, MYBBP1A, MYO3B, NAA10, NAGLU, NCOR2, NINJ1, NME2P1, NOP14, NOP16, NOP58, NPY1R, NTHL1, NUCB2, PACSIN3, PALLD, PBX1, PDCD4, PDIA3P, PER3, PHF15, PINK1-AS, PLIN5, PLXNB1, POLR3K, PPP1R35, PPRC1, PREX1, PRKCD, PRLR, PRSS23, PTGR2, PUS1, RAB3IL1, RAC3, RAD50, RAI14, RAP1GAP, RASL11A, RASL11B, RBPMS2, RDBP, RELL2, REPIN1, RHBDL2, RPP40, RPS26P35, RPS26P47, RPUSD1, RRP1, RRS1, SAPCD2, SCARNA9, SCIN, SCNN1A, SDC1, SDC4, SELENBP1, SEMA3F, SERPINH1, SFPQ, SHANK2, SHISA5, SIPA1L3, SLC19A1, SLC25A11, SLC25A22, SLC29A2, SLC39A10, SLC4A2, SLC7A2, SLC7A8, SLC9A3, SLC9A3R1, SMARCD2, SNORD13, SOAT2, SPDEF, SPOCD1, SRF, SRM, SRPK1, SSH3, STARD10, STEAP3, SYS1-DBNDD2, SYT12, SYTL1, TBC1D16, TBL1X, TCEA3, TEAD2, TEKT4, TIGD5, TMEM229B, TOMM40, TRIB3, TRIM65, TRIP6, TRMT1, TRMT6, TRPS1, TUFT1, TYRO3, UFSP1, VASP, VPS11, VTRNA1-3, WDR46, WDR90, WSB2, XCR1, YBX2, ZHX2, ZNF239, ZNF346, ZNF358, ZNF467, ZNF593, ZNF75A, ZNF768, ZNF787, ZNHIT2, 12 other genes with no HGNC symbol
	Chronic only	ARPC5, ASPM, BUB1, C2orf47, CCDC109B, CCND3, CDKN3, CLEC3A, COQ3, CPE, E2F3, EFHA1, ELOVL6, FABP5P1, FAM102B, FKBP5, GLRX2, HIGD1A, HSPH1, IBTK, ITGAE, MTX1, NAA50, NDUFAF2, PARPBP, PRRT3, PSMD14, PTGES3, RPF1, SDF4, SDHD, SNRPA1, SPIN4, TOP2A, TRGC2, UCHL5, VRK1, WRB, 1 other gene with no HGNC symbol
	Acute only	ABCE1, ABHD3, ACLY, ACP1, ACTL6A, ACY1, ADAT1, ADCY3, AFF4, AGGF1, AHCY, AKR7A3, ALDH5A1, ALG10B, AMD1, ANAPC13, ANAPC7, ANKRD20A5P, ANKRD46, ANKRD49, ANXA7, AP1G1, AP2M1, AP3M1, AP3S1, AP4E1, AP5M1, APIP, APPBP2, APPL2, ARF4, ARL1, ARL6IP6, ARPP19, ARV1, ASF1A, ASF1B, ASTE1, ATP1B1, ATP2A2, ATP5C1P1, ATP5F1, ATP5J, ATP6V1A, ATP6V1E2, B2M, B4GALT5, BCDIN3D, BCL11B, BET1, BEX5, BMPR2, BOLA3, BRK1, BRP44, BTF3, BTF3L4, C10orf32, C10orf57, C12orf26, C14orf109, C14orf129, C14orf167, C16orf53, C16orf59, C17orf58, C1orf122, C1orf53, C1QBP, C20orf11, C20orf160, C20orf72, C3orf14, C4orf27, C7orf23, C8orf55, C9orf46, C9orf78, CALM1, CALM2, CALM3, CANT1, CAT, CBFB, CBR4, CCDC14, CCDC47, CCDC97, CCNDBP1, CCT2, CCZ1B, CD58, CD9, CDC42EP5, CDC42SE1, CDK4, CELSR2, CEP85, CHAMP1, CHCHD2P9, CHURC1, CKLF, CKS2, CLDN7, CLINT1, CMAS, CMC1, CMTM6, CNOT6, COA5, COMMD3, COMMD6, COX20, CPNE3, CREG1, CRNDE, CSRNP2, CSTF2T, CSTF3, CTDSP2, CUL5, CYB561D1, CYB5A, CYC1, CYCS, CYFIP1, CYP2R1, DAZAP2, DCAF12, DCAF16, DCLRE1B, DCUN1D5, DDX21, DDX3X, DDX46, DDX5, DERA, DERL1, DEXI, DHX15, DHX36, DNAAF2, DNAJB6, DNAJC19, DNMT1, DOLK, DPM1, DPY19L1, DTL, DUSP28, DVL3, DYNLL1, DYNLT1, E2F2, E2F7, EBP, EEF1A1P12, EEF1A1P19, EEF1E1, EGR1, EGR2, EHF, EI24, EID2, EIF3J, EIF4A1P2, EIF4EBP2, ELF1, ELOVL5, ENSA, EPCAM, ETFA, FADD, FAM108A2, FAM111A, FAM120AOS, FAM122B, FAM214A, FAM217B, FAM84B, FAM96A, FCRLB, FOS, FOSB, FTH1, FTSJD1, G3BP2, GCA, GCSH, GGCT, GLB1, GLCE, GLRX3, GOLPH3, GOLT1B, GPAA1, GTF2A2, GXYLT1, H2AFX, H2AFZ, H3F3AP4, H3F3AP6, HBXIPP1, HES6, HIBADH, HINT1, HLTF, HMGN1, HMGN2P17, HN1, HNRNPA0, HNRNPA3, HNRNPAB, HNRNPH2, HNRNPH3, HNRNPK, HPRT1, HPS3, HPS6, HSPE1, HTATIP2, IDI1, IGFBP2, IMP3, IMPA2, INSIG1, INTS2, ISCA1, ITGAV, ITGB1BP1, ITM2B, ITPR1, JKAMP, JTB, JUNB, KIAA0146, KIAA0196, KIAA0494, KIAA0907, KIAA1324, KRT18, LACTB2, LAMP2, LANCL1, LANCL2, LAPTM4B, LARGE, LARP4B, LCMT2, LINC00116, LIPA, LITAF, LRIG1, LRP10, LRP11, LRR1, LRRC8B, LYPLAL1, LYRM2, MAD2L1, MAL2, MAPK9, MAPRE1, MARCKSL1, MARS2, MASTL, MBIP, MBTPS1, MCEE, MCM10, MCM3, MCM4, MDH1, ME1, MELK, METTL3, MFF, MFSD1, MGP, MGST1, MGST3, MICA, MITD1, MLEC, MLH1, MMADHC, MOAP1, MOB4, MORF4L1P1, MORF4L2, MPV17, MRI1, MRPL33, MRPL45, MRPL49, MRPL50, MRPS21, MRPS35, MUCL1, MXD4, MYC, MYD88, MYO5C, NAB1, NAE1, NDFIP2, NDUFA1, NDUFA12, NDUFB3, NDUFB6, NEDD8-MDP1, NETO2, NPDC1, NPM1P5, NPTN, NSMCE4A, NUP153, NUP160, NUP35, NUP37, NUPL2, OAT, OSTC, OSTCP2, PAFAH1B1, PAICS, PAPOLA, PAQR4, PCDH19, PCMTD2, PCNP, PDCD2, PDIK1L, PDLIM3, PDSS1, PEX11B, PEX2, PFN2, PGRMC1, PHLPP2, PHOSPHO2, PHTF1, PIGB, PIGM, PIGT, PIGY, PIK3R2, PIP, PIPSL, PLAGL2, PLEKHH1, PMS2P5, PNMA1, PNPO, POLR2B, POLR2J2, PON2, PPIAP29, PPIC, PPP1CA, PPP1R10, PPP1R3D, PPP2R2C, PPP2R3C, PPPDE1, PPPDE2, PQLC3, PRADC1, PRDX2, PREPL, PRIM1, PRMT6, PROSC, PROSER1, PRPF38B, PRRC1, PSMA3, PSMC1P9, PSMC4, PSMD10, PSME3, PTPLA, PUM2, RAB11A, RAB11FIP2, RAB22A, RAB5A, RAD51C, RAD54B, RAP2A, RAP2C, RBBP5, RBM23, RCN2, RET, RFC4, RFC5, RFWD3, RFX5, RIMS2, RMI2, RNF103, RNF5P1, RPA1, RPA3, RPL15, RPL15P3, RPL17, RPL18AP16, RPL22, RPL23AP4, RPL34, RPL39L, RPL6, RPL8, RPLP0,

		RPRD1B, RPS27L, RPS3AP5, RPS6KA5, RRP1B, S1PR3, SAR1A, SEC23B, SEL1L3, SEPHS2, SET, SFT2D1, SIDT1, SIVA1, SKP1, SLC22A5, SLC25A4, SLC25A44, SLC27A2, SLC2A10, SLC35B2, SLC35B3, SLC35E2B, SLC39A6, SLC46A3, SNHG9, SNORA12, SNORA61, SNRPD1, SNRPD3, SNX4, SOX3, SPCS1, SPG11, SPTSSA, SQLE, SRP14, SRSF1, SRSF2, SRSF5, SRSF7, SRSF9, STAG3, STARD7, STRAP, STXBP3, SUB1, SYBU, TACC1, TAF2, TBC1D14, TBK1, TCFL5, TCTEX1D2, TFB2M, TFF1, TFF3, THAP11, THOC3, THOC7, TIMM21, TM9SF2, TM9SF4, TMBIM4, TMED10, TMED2, TMED7, TMEM109, TMEM123, TMEM14B, TMEM14D, TMEM160, TMEM194A, TMEM209, TMEM216, TMEM230, TMEM245, TMEM41A, TMEM5, TMEM60, TMEM85, TMX1, TOM1L1, TOP2B, TOR1A, TOR1AIP1, TPD52L1, TPGS2, TRA2B, TRAM1, TRAM2, TRIM37, TRIM44, TSEN2, TSPAN3, TSPO, TSPYL1, TSPYL5, TST, TSTD1, TTC19, TTC31, TTF2, TUBA1A, TUBA1C, TUBB4B, TUSC1, TWSG1, TXN, TYMS, UBB, UBE2N, UBE3C, UBE4B, UBR7, UFM1, UNC50, UPF3AP1, USMG5, USP38, VAMP7, VDAC1, VGF, VMA21, VPS29, VPS4B, WBP4, WDR36, WDR61, XBP1, XRCC5, XRCC6BP1, YWHAB, ZCCHC14, ZCCHC9, ZDHHC6, ZFP3, ZNF594, ZNF680, ZNF789, ZNF791, 41 other genes with no HGNC symbol
	Oncamex & Chronic	CCNB1, DNAJC9, EXOSC8, POLA2, TGFB3, 1 other gene with no HGNC symbol
	Oncamex & Acute	AP1S1, ARPC1A, ARRDC4, ATAD2, C11orf82, C12orf75, C14orf142, CCNE2, CDC45, CDC7, CENPK, CHMP2B, CHPT1, CNIH, CNTNAP2, DLD, EPDR1, FZD6, GAGE12H, GAGE12I, GAGE12J, GAGE2B, GAGE2C, GINS2, GMNN, GNG10, H3F3B, HAT1, HENMT1, HMBS, HMGN2P7, IL17RB, ISOC1, KIF11, LAP3, LYSMD2, MCM6, MLF1IP, MRPS28, MRPS34, NDUFA4, OIP5, PARP1, PCNA, PDZK1, PDZK1P1, POLE2, PPM1E, PRDX3, PRMT3, PRPS2, PSMG1, RAD51AP1, RBBP7, RMI1, RNFT1, RRM2, SLBP, SLC39A8, SNX10, SRP9P1, TAMM41, TEX30, TFDP1, TMEM14A, TSPAN13, TUBA1B, TXNIP, UBE2T, YEATS4, 6 other genes with no HGNC symbol
	Chronic & Acute	ARPC3, C15orf59, C16orf74, C6orf211, ESR1, GSTM3, IGFBP5, IL17D, IL27RA, KYNU, NR2E3, NR5A2, RERG, SEMA3C, SGK3, SLITRK4, SRSF6, TSPAN4, UBL3
	Oncamex, Chronic & Acute	CXCL12, ELOVL2, FAM195A, GJA1, HPGD, SLC25A13, SUSD3, 1 other gene with no HGNC symbol

Supplementary Table 13 ***Overlapping differentially expressed between MDA-MB-231 cells treated with Oncamex or exposed to hypoxic conditions.***

	MDA-MB-231: Oncamex, Chronic Hypoxia, Acute Hypoxia (Venn diagrams: overlap in genes changed by high/low Oncamex)	
Up	Oncamex only	ABCB6, ABCD1, ABHD5, ADAM8, ADM, AHSA1, AK4, ANGPTL4, ANKRD54, ANKZF1, ARC, ARHGEF16, ARHGEF40, ARID5B, ARMC7, ASNS, ASUN, ATAD2B, ATG12, AVL9, B3GALNT2, B3GNT5, BBC3, BCYRN1, BHLHE40, BLCAP, BLZF1, BMS1P5, BNIP3L, BTAF1, C10orf118, C10orf28, C11orf96, C12orf23, C17orf96, C2orf69, C3orf52, C3orf58, C5orf30, C7orf71, C8orf80, C9orf84, CAPN5, CAPRIN2, CARS, CCNE1, CCRN4L, CDC42EP2, CDK12, CDKN1C, CHIC2, CHMP7, CHPF, CHST11, CHSY1, CHSY3, CIR1, CITED2, CKB, CLCF1, CNOT8, CPO, CSRNP1, CSRP2, CTSZ, CXCL1, DACT3, DCP2, DDA1, DDAH1, DDIT4, DENND2C, DGKQ, DNAJB2, DNAJB9, DOK1, DUSP1, DUSP18, DUSP5P, EGLN1, ELP2, ENTPD7, ERRFI1, EYA3, F3, FAM117B, FAM162A, FAM179B, FAM195B, FAM46A, FAM57A, FAM63A, FER1L4, FGFR3, FICD, FLNC, FUT11, FUT6, G0S2, GALNT3, GALNTL4, GBE1, GFPT2, GJA3, GLRX, GLS, GM2A, GNPNAT1, GOLGB1, GPR137B, GPT2, HAND1, HBEGF, HES4, HIATL2, HILPDA, HK2, HMHA1, HOXD1, HSD17B7, HSPA4L, IFFO1, IFT20, IL11, IL27RA, IMPA1, INSIG2, ISCA1P1, ITFG2, ITPK1-AS1, ITPKA, JUN, KCTD11, KDM3A, KDM5A, KIAA1715, KIAA1958, KIF1B, KIRREL, KLHDC1, KRTAP2-3, LDHA, LGALS8, LIF, LIN37, LINC00342, LRRC14, LUZP1, MAFF, MAGT1, MAK16, MAN2A1, MAP1LC3B, MAP2K1, MAP6D1, MAPK8, MAPK9, MBD4, MCTS1, METRNL, MFHAS1, MGAT1, MGEA5, MIR1275, MIR17HG, MIR507, MIR759, MKNK2, MOSPD1, MTF2, MYO3B, NANS, NCBP1, NFIL3, NFKBID, NIPA1, NIPAL1, NOC3L, NR2F2, NXF1, OBFC2A, ODZ1, OFD1, OR1S2, OR5C1, OSBPL8, P4HA2, P4HB, PABPC1L, PAG1, PAM, PANX1, PAPD7, PCSK5, PDK1, PFKFB3, PHF13, PIK3C3, PKIA, PLA2G15, PLAT, PLAUR, PLCXD1, PLOD2, PNP, PNPLA2, PNPLA8, POM121B, PPME1, PPP2R2A, PPP2R5B, PPP3R1, PPTC7, PRSS8, RAB11FIP3, RAB20, RAB30, RAB38, RAD54L2, RALGAPA1, RBM15, RGS4, RIOK3, RLF, RNF113A, RNF24, RNMT, RORA, RPS4XP16, RRAD, RUNDC3B, SAMD4A, SDC4, SEC11C, SEC63P1, SERPINB8, SERPINE1, SGMS2, SH3BP5L, SLC22A25, SLC25A36, SLC2A1, SLC2A14, SLC41A1, SLC5A8, SLC6A10P, SLC6A8, SLC7A2, SLIT2, SMAP2, SNORA5C, SNX33, SOGA3, SRGAP1, SSTR2, ST8SIA2, STC1, STK35, TAF15, TCF19, TCF24, TEAD3, TICAM2, TMEM115, TMEM156, TMEM51, TMEM57, TNIP2, TPI1P1, TRIM27, TRIM58, TRIP12, TUBB2A, UAP1, UBE4A, UGCG, UGDH, UPRT, USP38, VGF, VLDLR, VMP1, VPS18, VPS37A, WFIKKN1, YEATS2, ZBTB40, ZCCHC12, ZDHHC18, ZFP36L1, ZNF140, ZNF17, ZNF175, ZNF193, ZNF207, ZNF215, ZNF322P1, ZNF335, ZNF35, ZNF470, ZNF668, ZNF672, ZNF695, ZNF770, ZNF772, ZNF800, ZNFX1, 11 other genes with no HGNC symbol
	Chronic only	AARS, ABI3BP, AHNAK2, AIP, ALDOC, AMT, ANKDD1A, AP1G2, AP3M2, ASS1, ATF3, B3GALTL, BCL11A, BEX2, BFSP1, BMP8B, C11orf35, C11orf68, C12orf47, C19orf66, C21orf7, C2orf42, C7orf61, CADM1, CAMK2N1, CAMLG, CBX7, CCDC130, CCDC85B, CDA, CDCP1, CDK5RAP3, CFB, CFLAR, CHAC1, CLDND2, CNST, CPA4, CREBRF, CTC1, CUBN, CYB5R2, CYP1B1, DDIT3, DDIT4L, DDX10, DDX41, DEFB103A, DENND4B, DFNB31, DHDH, DLG4, DNAAF3, DNASE2, DOCK6, DPCD, EEF2, EIF3G, EIF3H, ENDOV, ENO3, EPB41L4A-AS1, EPOR, ERCC2, EXOC3, F2RL2, FAM108C1, FAM113B, FAM167A, FAM214B, FAM219B, FAM83G, FAM91A1, FLT4, FOXA2, FOXC1, FZD2, FZD4, FZD8, GAB2, GABARAPL1, GBA2, GDI1, GJC2, GLTSCR2, GMPPA, GNPTG, GPSM3, HCFC1R1, HDAC6, HEATR6, HEXIM2, HGS, HIST1H1C, HIST1H2BD, HIST2H2AA3, HIST2H2BE, HLX, HMG20A, IGDCC4, IL24, INPP4B, INTS5, IRF2BP1, IRF3, KIAA2013, KIFC2, KLF9, LAMB2, LAMC2, LARP6, LEMD2, LINC00243, LOXL4, LY96, LZTS2, MAN2C1, MAP3K12, MIF4GD, MIR185, MIR21, MIR29C, MMP3, MORC2, MRPS6, MST1P2, MUC1, MUTED, MYOM1, MZF1, NEK6, NFKBIA, NPC1L1, NUAK1, OGT, OXTR, PAN2, PAQR7, PGF, PHF1, PHF21A, PHKA2, PLD1, PLD3, PLEKHF1, PLEKHM2, PLXNA3, PNPLA6, POLRMT, PPFIBP2, PPP1R3E, PRG2, PROS1, PSG4, PTGS2, PTPRH, PVRL3, RAB33B, RAB3IL1, RAB40C, REM2, RERE, RGCC, RIMBP3, RIN1, RN5S9, RN7SK, RNU1-3, RNU1-5, RNU11, RNU4-2, RPL13AP20, RPL13AP6, RPL17, RPL28, RRAS, RRNAD1, RSAD1, RSPRY1, RUSC2, S100P, SAT2, SCG5, SFTA1P, SGK1, SKIV2L, SLAMF7, SLC23A3, SLC25A38, SLC25A6, SLC5A3, SNAPC4, SNORA12, SNORD13, SNORD3A, SNORD3C, SNORD3D, SPINK1, SPNS2, SPSB3, SSR4, ST3GAL6, STK19P, STK36, SUN3, SUPT5H, SYT11, TBC1D16, TBL1X, TCAP, TEF, TFAP2C, TGFBR3, TINF2, TMEM136, TMEM171, TMEM205, TMEM45A, TMEM91, TPM2, TRABD, TRIB3, TRIM27, TRNP1, TSC22D3, TSPAN31, UBL4A, UBXN1, UCN, USP36, VEGFA, WASH7P, WDR13, WDR19, WDR66, WFDC10B, WFDC3, YPEL3, ZBTB4, ZC3H10, ZER1, ZMIZ2, ZNF133, ZNF248, ZNF296, ZNF337, ZNF358, ZNF524, ZNF526, ZNF579, ZNF581, ZNF783, ZNF827, ZSWIM1, 22 other genes with no HGNC symbol
	Acute only	ANKRD33, C11orf83, C14orf80, C17orf53, C17orf70, C19orf33, CD63, COL5A1, DPP9, FOS, GPI, GRWD1, HAUS2, JAG1, KRT7, LCP1, MAP3K6, MYO9B, NCLN, PHLDB1, PIEZO1, PIGQ, PIGU, POC1A, POLQ, RRP1, SF3B3, SH3RF2, SLC16A3, STARD8, SYNJ2BP, TAF13, TMEM106C, TPI1P2, TTLL12, TUBA4A, ZNF600, ZNF692, ZNF738, ZNF767, 3 other genes with no HGNC symbol
	Oncamex & Chronic	ANG, ANKRD37, ARID3A, BLID, BNIP3, C10orf10, C8orf58, CBLB, CCND2, DUSP5, EIF2C2, ERO1L, FAM107B, FAM13A, GSK3B, IL1RAPL1, IL8, LOX, MT1X, NARF, NOG, P4HA1, PCNX, PIM1, PPFIA4, PUS3, RUNDC1, SERPINE2, SIPA1L2, SLC2A3, SLC38A2, SPHK1, SPIRE1, TLR4, TNIP1, TPBG, TTC14, VEGFC, ZCCHC6, ZFAND2A, ZNF224, ZNF786, ZNF841, 5 other genes with no HGNC symbol
	Oncamex & Acute	ABCA7, C15orf52, C1orf110, C20orf20, C5orf46, CA9, COL7A1, CST1, DUSP3, EDN1, FOSB, HIST2H2AC, LIMCH1, LINC00476, LRFN3, MMP1, NR4A2, PAGE5, PCDHB9, PLOD1, PPP1R13L, RNF31, SCARNA9, TRIML2, ZBTB3, ZNF223
	Chronic & Acute	ADRB2, ATG9A, CSF2, PFKFB4, PLEKHG3, PPAN-P2RY11, PPP1R16A, RASSF7, RECQL4, USP49, 1 other gene with no HGNC symbol
	Oncamex, Chronic & Acute	38777, DLC1, ENO2, FAT4, IGFBP3, ITGA5, KLF6, MOB3A, NDRG1, PHF23, RRAGD, SPAG4, TIGD5, ZNF148, ZNF653, 1 other gene with no HGNC symbol

Down	Oncamex only	ABR, ADORA2B, AIMP2, AMD1, AMDHD2, ANAPC13, ANGPTL2, ANP32AP1, APCDD1L, APEX1, ARMCX1, ARMCX2, ASAP3, ASXL1, BAIAP2L1, BMP4, BRI3, C16orf53, C17orf98, C1orf109, C1orf123, C7orf53, C9orf3, C9orf40, CA12, CABLES1, CARD10, CAV2, CBR1, CBX1, CCDC102A, CCDC106, CD207, CD58, CDH11, CENPB, CEP41, CLIC6, CMBL, COL4A2, CRADD, CREB3L4, CST1, CST4, CTDSPL, CTIF, CTNNBIP1, CUEDC2, CUL9, CYB5A, CYP1B1, CYR61, DBN1, DENND5B, DNAAF2, DNAH2, DNAJC9, DSN1, EHBP1, ETS2, F2RL1, FAM171A1, FAM75A1, FKBP1C, FUT8, FZD2, GBAP1, GCA, GEMIN2, GJB2, GLT25D2, GNG12, GPR56, GTF2H4, H1F0, HCAR1, HDDC3, HES1, HIF1A, HIST1H2AC, HIVEP1, HMBS, HNRNPA0, HNRNPA3, HTRA2, ID3, IGF2BP3, IMPA2, KCNN4, KIAA1671, KIF22, KLF15, KRT80, LAMA5, LAMTOR1, LAYN, LIMA1, LMTK3, LPAL2, LPP, LPXN, LRP5, LTV1, LYRM2, MAMLD1, MED26, METTL5, MGAT2, MIR586, MLPH, MMACHC, MRPL34, MRPS18C, MTA3, MYO5C, MYOF, NASP, NDP, NEDD8-MDP1, NEXN, NFE2L3, NGF, NIF3L1, NNMT, NOXA1, NPAS2, NR1H3, NR3C2, NREP, NRP1, NRXN1, NSMCE4A, NUP35, OBFC1, OGFR, OPRK1, OSBPL10, PAAF1, PACSIN3, PAFAH1B1, PAPPA, PARP4, PCCA, PDCD11, PDE7B, PER3, PFN2, PHF15, PIF1, PIGT, PIGV, PITX1, PKP2, PLEK2, PLEKHA6, PLK1, PLLP, PMEPA1, POC5, POLA2, PPAP2B, PPAPDC1A, PPARG, PPIL1, PPP1R10, PPP5C, PRDM8, PRICKLE2, PSPC1P1, PXDN, RAB3IL1, RAB7L1, RAD23B, REPIN1, RGS20, RHOJ, RPL39L, SAMD9L, SCRN1, SDPR, SEMA3A, SH3PXD2A, SH3RF3, SHISA2, SLC29A2, SLC35B3, SLC37A1, SLC37A2, SLC46A3, SLCO4A1, SNORA73B, SNORD117, SNORD13, SORBS2, SOX4, SPCS1, SPDEF, SRBD1, SRF, SRRM1, SRSF6, SUN2, SUSD5, SVIL, TACC2, TANC1, TANC2, TCEA3, THOC6, TIMELESS, TIPARP, TMEM116, TMEM60, TMEM75, TNFRSF11B, TNFRSF14, TNFRSF21, TNS3, TOX2, TRERF1, TRIM6, TRIM8, TRIP6, TUBB, UBE2L6, UTP18, VIPR1, WDR92, WEE1, ZFAND5, ZMIZ1, ZNF627, 14 other genes with no HGNC symbol
	Chronic only	ABCB10, ABCC4, ACACA, ACAT2, ACLY, ACOX2, ACTL6A, ALDH7A1, ALYREF, ANLN, ANXA2P1, AP1M2, AP3B1, APOO, ARL6IP1, ASF1B, ATAD2, ATP5A1, BAG3, BASP1, BIRC5, BOLA3, BORA, BRP44, BUB3, C11orf82, C1orf112, C1orf53, C1QBP, C4BPB, C4orf46, CALM2, CBFB, CBR3, CCDC34, CCNE2, CD97, CDC25A, CDC25C, CDC45, CDCA5, CDCA7, CDT1, CENPI, CENPK, CENPL, CENPM, CENPN, CENPW, CEP85, CHAF1B, CHEK1, CKAP5, CKB, CMC2, CMTM6, CNN3, COL4A1, COTL1, CSRP2, CTPS, CTSD, CYCSP55, DBI, DCUN1D5, DDX5, DEK, DEPDC1, DHCR24, DHRS11, DHX15, DIAPH3, DNMT1, DTL, DUSP12, DYNLT1, E2F2, EBP, ECT2, EFEMP1, ELOVL5, ELOVL6, EML4, ENC1, ENY2, EPHX1, ERCC6L, ERH, ETFA, EXO1, EXOSC8, EXOSC9, EZH2, FADS2, FAM102B, FAM111A, FAM64A, FAM96A, FANCI, FBP1, FDPS, FH, FKBP5, FOXM1, FSTL1, G0S2, GAS2L3, GGCX, GINS2, GLRX2, GMNN, GTF2A2, H2AFZ, HADH, HAUS1, HIGD1A, HIGD1AP1, HJURP, HLA-DRA, HLTF, HMGB1P1, HMGB2, HMGN1, HMGN2, HMGN2P17, HMGN2P7, HN1, HNRNPA1P12, HNRNPAB, HNRNPH1, HPRT1, HSDL2, HSPA14, HSPB11, ISOC1, ITGAE, KDELC2, KIAA0101, KIAA0922, KIF15, KIF20B, KNTC1, KPNA2, KPNB1, KRT8, LAP3, LAPTM4B, LMNB1, LPCAT3, LRRC8B, LSM3, LXN, MAPKAPK3, MAPRE1, MCM10, MCM4, MCM6, MGST1, MLF1IP, MLH1, MMD, MND1, MORC4, MRPL13, MRPL39, MVK, MYH10, NCAPD3, NCAPG, NCAPG2, NDUFB6, NEK2, NMU, NOP58, NQO1, NRGN, PAICS, PAPSS2, PARP1, PARPBP, PBK, PCNA, PDSS1, PGD, PHTF1, PPIAP29, PRPS1, PRR11, PRTFDC1, PSMA3, PSMA5, PSMC1P9, PSMC2, PSMD1, PSMD14, PSMG1, PTPLA, PTPLB, PTPN1, PTTG1, PTTG3P, QDPR, RANBP1, RBBP7, RFC4, RFC5, RMI1, RPA3, RPL6, RQCD1, RRM1, RRM2, RSRC1, SAP30, SAPCD2, SGOL2, SIVA1, SKA1, SKA2, SKA3, SLIRP, SMC4, SNORA61, SNRNP40, SNRPF, SNRPGP5, SPA17, SPAG5, SPC24, SPIN4, SRP9P1, SRSF2, SSBP1, STIL, STMN1, TAX1BP3, TEX30, TFDP1, TFF2, TFF3, TGM2, THOC7, TIMM23, TINAGL1, TK1, TMEM97, TMSB15B, TPGS2, TRA2B, TSPAN9, TUBA1A, TUBA1B, TUBA1C, TUBB4B, TXN, TXNIP, UCP2, USP1, USP13, USP32P2, VPS29, VRK1, WDR61, WDR62, XPO1, YBX1P1, YEATS4, ZCCHC24, 22 other genes with no HGNC symbol
	Acute only	AFF4, ASNS, ATF4, C20orf111, C9orf89, CBX4, CCNDBP1, CD9, CRISPLD2, CSRNP2, DNAJB9, EIF1B, ENPP1, EPAS1, FBXO32, FRAT2, GDF15, GFPT2, GLRX, GTF2B, HERPUD1, HIBADH, HIST1H2BD, HSPA1A, HSPA1B, HSPA5, IRAK2, JUNB, MANF, MSMO1, MXD1, MYC, NIPSNAP1, NXF1, PELI1, RAB2B, RASD1, RGCC, RNF103, SC5DL, SERPINB1, SERTAD1, SFT2D1, SIRT1, SNORA12, SQSTM1, SRXN1, TACSTD2, TM7SF2, TM9SF4, TMED10, TNFSF9, TUFT1, XBP1, ZNHIT3, 3 other genes with no HGNC symbol
	Oncamex & Chronic	ADAM19, APOBEC3B, ASPM, AURKA, AURKB, BTF3L4, BUB1, C12orf32, C15orf23, C20orf72, CALM3, CAP2, CAV1, CCDC99, CCNA2, CCNB1, CCNB2, CCNF, CDC20, CDCA2, CDCA3, CDCA8, CDK1, CDKN2D, CDKN3, CENPA, CENPE, CENPF, CEP55, CKAP2, CKAP2L, CKS2, COQ2, DLGAP5, ESPL1, FHOD3, GBP1, H2AFX, HAUS8, HIST1H4C, HLA-DPA1, HMGB3, HMGN1P38, HMMR, HNRNPD, HSPE1, HYLS1, IGFBP4, KIF11, KIF14, KIF18A, KIF20A, KIF23, KIF2C, KIF4A, KIFC1, LMNB2, MAD2L1, MAMDC2, MCM5, MELK, MKI67, MXD3, NCAPD2, NDC80, NDUFA12, NUP37, NUSAP1, OIP5, OLFML2A, PHF19, PIGY, PLAU, PLK4, PLXNA1, POC1A, POLE2, PRC1, PRDX3, PRIM1, PRNP, PSRC1, RACGAP1, RAD51AP1, RAN, RARRES3, SCNN1A, SNRPD1, SPATS2L, SUV39H1, SYNCRIP, TACC3, THBS1, TIMM10, TMEM14A, TMEM163, TMEM237, TMEM71, TOP2A, TPX2, TRIP13, TROAP, TTF2, TTK, TYMS, UBE2C, UBE2T, WDR67, 5 other genes with no HGNC symbol
	Oncamex & Acute	AHCY, CLINT1, DHCR7, DNAJB1, EFNB2, EPDR1, FAM53C, FASN, FDFT1, IDH1, IDI1, KCTD5, LIPA, LPIN1, MARCKSL1, OAT, PCSK9, SPINK4, SRGN, VASN, 3 other genes with no HGNC symbol
	Chronic & Acute	BAMBI, FAM46B, MYLIP, TMCO3
	Oncamex, Chronic & Acute	FAM83D, GNG10, HMGCR, HMGCS1, INSIG1, LDLR, TIMP3, UPF3AP1, 2 other genes with no HGNC symbol

Appendix 3: Publications

Section 1.1.5. in Chapter 1 was the basis for a published literature review:

Novel flavonoids as anti-cancer agents: mechanisms of action and promise for their potential application in breast cancer

Martínez-Pérez C, Ward C, Cook G, Mullen P, McPhail D, Harrison, DJ and Langdon SP.

Biochemical Society Transactions **42**, 1017-1023 (2014)

Chapters 3 and 4 were the basis for a published research article:

Antitumour activity of the novel flavonoid Oncamex in preclinical breast cancer models

Martínez-Pérez C, Ward C, Turnbull AK, Mullen P, Cook G, Meehan J, Jarman EJ, Thomson PIT, Campbell CJ, McPhail D, Harrison, DJ and Langdon SP.

British Journal of Cancer 114, 905-906 (2016)

Biochemical Society TRANSACTIONS

Novel flavonoids as anti-cancer agents: mechanisms of action and promise for their potential application in breast cancer

Carlos Martinez-Perez*[1], Carol Ward*, Graeme Cook†, Peter Mullen‡, Donald McPhail†, David J. Harrison‡ and Simon P. Langdon*

*University of Edinburgh Division of Pathology Laboratories, Institute of Genetics and Molecular Medicine, Western General Hospital, Crewe Road South, Edinburgh EH4 2XU, U.K.

†Antoxis Limited, IMS Building, Foresterhill, Aberdeen AB25 2ZD, U.K.

‡Systems Pathology, Medical and Biological Sciences Building, University of St. Andrews, North Haugh, St. Andrews, Fife KY16 9TF, U.K.

Abstract

Flavonoids are a large group of ubiquitous polyphenolic secondary metabolites in plants with a wide range of properties, including a widely reported anti-cancer effect. The present review focuses on the different known mechanisms partaking in said anti-tumour effects, with particular emphasis on breast cancer. Their structure and reactivity allows flavonoids to work as antioxidant agents and phyto-oestrogens, modulating oestrogen signalling and metabolism to induce an overall anti-proliferative response. Other effects include the ability of flavonoids to modulate the CYP1 (cytochrome P450 1) and ABC (ATP-binding cassette) protein families, involved in carcinogenesis and drug delivery respectively. They can also induce apoptosis and cell cycle arrest and regulate other signalling pathways involved in the development and progression of cancer. In conclusion, there is accumulating evidence on the versatility of flavonoids and the numerous activities contributing to their anti-tumour effect. The complex, yet effective, mechanism of action of flavonoids, together with their interesting pharmacological properties, is the basis for their potential application in breast and other cancers. This rationale has led to the current interest in the application of flavonoids, including clinical trials currently underway and the development of novel flavonoids with improved properties, which hold great promise for tackling breast cancer.

Introduction

Flavonoids account for the largest group of secondary metabolites in the plant kingdom. They comprise over 5000 ubiquitous compounds with a common polyphenolic backbone (Table 1) and have essential roles in plants [1].

Among other health-promoting properties, numerous studies have reported interesting pre-clinical activity of flavonoids in cancer models for a wide range of cancers, suggesting their potential use in treatment and prevention of cancer. This has been the basis for numerous studies and trials in different models and cancer types, including extensive research on breast tumours [2–4].

Research has reported the involvement of numerous mechanisms in the effect of flavonoids against cancer. These are not mutually exclusive, but evidence supports the potential of these compounds to target different pathways and mechanisms underlying the complexity of cancer as a disease. Owing to limitations of space, the present review does not cover the numerous clinical trials and studies demonstrating the effect of flavonoids on cancer. Instead, it focuses on the most relevant of their different properties and summarizes their complex potential mechanism of action in breast cancer in particular.

Key words: antioxidant, breast cancer, flavonoid, oestrogen, phyto-oestrogen.

Abbreviations: ABC, ATP-binding cassette; AhR, aryl hydrocarbon receptor; AI, aromatase inhibitor; BCRP, breast cancer-resistance protein; CYP, cytochrome P450; E_2, 17β-oestradiol; ER, oestrogen receptor; MDR, multidrug resistance; PAH, polycyclic aromatic hydrocarbon; P-gp, P-glycoprotein; ROS, reactive oxygen species.

[1]To whom correspondence should be addressed (email c.martinez@sms.ed.ac.uk).

Flavonoids as antioxidants

The role of flavonoids as antioxidants has been the subject of research for decades [5,6]. The numerous hydroxy groups in the flavonoid structure, in combination with a highly conjugated π-electron system, allow them to act as free radical scavengers via hydrogen atom or electron donating activities. Furthermore, they can block the formation of ROS (reactive oxygen species), such as the hydroxyl radical, through chelation of redox-active transition metal ions [6]. This can have a positive effect on cancer prevention by the minimization of phenomena such as oxidative damage to DNA.

Research on breast cancer cell lines has shown that polyphenols exert strong inhibitory effects due to their antioxidant properties of antagonizing the oxidizing activity of H_2O_2 by scavenging ROS or inhibiting ROS production [7]. Interestingly, there is also evidence that they can act as pro-oxidative compounds. For instance, myricetin can undergo auto-oxidation and reduce molecular oxygen to the

Table 1 | Flavonoids are polyphenolic derivates consisting of a 3-ring basic backbone: two fused rings (aromatic A ring and heterocyclic C ring), connected to another aromatic B ring through a carbon–carbon bridge

According to changes in this molecular backbone and the presence of hydroxy groups and other moieties, flavonoids can then be categorized into a further seven subclasses [1], most of which are found in numerous dietary sources. The Table includes examples for each flavonoid subclass, dietary sources and E.D.I. (estimated daily intakes) [19]. Flavanonols have not been reported at significant levels in dietary sources N/A, not applicable.

Subclass	Structure	Examples	Dietary sources	E.D.I. (mg)
Flavonols	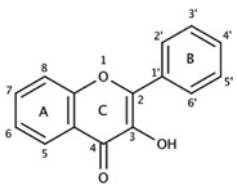	Quercetin, kaempferol, myricetin and their glycosides	Onions, red wine, tea, fruits, berries and herbs	12.9
Flavones	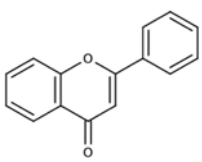	Luteolin, apigenin and tangeretin	Herbs, celery and chamomile tea	1.6
Flavanones	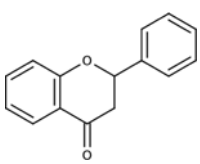	Naringenin, hesperetin (found in diet mainly as glycosides)	Citrus fruits	14.4
Flavanols	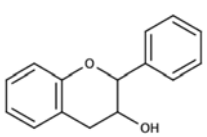	Catechin, epicatechin, epigallocatechin	Cocoa or dark chocolate, apples, grape, red wine and green tea	156.9
Anthocyanidins	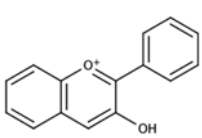	Cyanidin, delphinidin, pelargonidin, malvidin	Berries and other fruits	3.1
Isoflavones	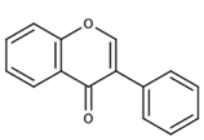	Genistein, daidzein, glycitein and their glycosides	Soya products	1.2
Flavanonol	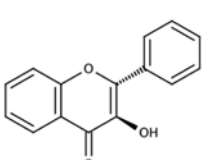	Taxifolin, aromadedrin	N/A	N/A

superoxide free radical [8]. This dual effect suggests that a balance of both anti- and pro-oxidative properties might be essential to the role of flavonoids in the prevention or treatment of disease.

Flavonoids as phyto-oestrogens

Some subtypes of flavonoids have often been referred to as phyto-oestrogens due to their ability to mimic oestrogen-like responses. They resemble the most important type of oestrogen in humans, E_2 (17β-oestradiol), due to the existence of hydroxy groups and phenolic rings [required for binding ER (oestrogen receptors) α and β] [9].

Flavonoids can bind both isoforms of ER, mainly as agonists competing with E_2 [7], inducing biological responses traditionally associated with the binding of the natural hormone in a dose-dependent manner [10,11]. Studies have reported that some of the ER-mediated responses induced by flavonoids are nonetheless comparable with, or even higher than, those induced by physiological levels of E_2, one reason

some flavonoids are still described as full oestrogen agonists [12].

Unlike E_2, several studies have reported a stronger affinity of flavonoids for the ERβ isoform [13] and also that flavonoids binding ERβ induce the transcription of oestrogen target genes to much greater levels than when binding ERα [14]. Critically, ERβ is known to exert a response opposing the proliferative effects of ERα activation [15]. Indeed, interaction between both types of receptors and their substrates provides a regulation for the overall effect of oestrogens and the ratio of ERα/ERβ is used as a prognostic marker in breast tumours [16]. This means that physiological levels of phyto-oestrogens are likely to activate ERβ but not the ERα-mediated pro-cancer signalling (or activate this to a much lower extent), therefore facilitating a beneficial anti-proliferative effect.

Phyto-oestrogens can also alter the level of oestrogen biosynthesis, acting as AIs (aromatase inhibitors) on CYP19 (cytochrome P450 19) aromatase, 17β-HSD (hydroxysteroid dehydrogenases) and oestrone sulfatase and sulfotransferase [17], all involved in the generation of oestradiol in breast tissue and associated with breast cancer when overexpressed. Some flavonoids have been shown to induce a significant decrease in circulating oestrogen concentration. Although their efficacy is lower than that of clinically used steroidal AIs, they could be very beneficial to treat tumours which exhibit a lack of response to common therapies. Additionally, flavonoids can also alter oestrogen-metabolizing enzymes, thus reducing the production of genotoxic metabolites. Some *in vivo* studies have been carried out on animal models, although the complexity of these modulations needs to be further elucidated [18].

Flavonoids as CYP1A1 inhibitors/substrates

The impact of diet and environment on the development and progression of cancer is partially due to the exposure to PAHs (polycyclic aromatic hydrocarbons) and other xenobiotic carcinogenic compounds. PAHs such as BaP [benzo(α)pyrene], found in tobacco smoke or charred foods, can give rise to cancer after being subject to oxidation by CYP1, a family of extrahepatic enzymes with mono-oxygenase activity.

The CYP1 family has been implicated in carcinogenesis and cancer progression through three main mechanisms: first, the CYP1 family modifies and activates PAHs and other pro-carcinogens, allowing them to bind DNA and give rise to cellular and genetic damage, essential in the cancer initiation stage [20]; secondly, the CYP1B1 isoform is involved in the modification of steroidal hormones such as oestradiol, contributing to the initiation of mammary carcinogenesis [21]; finally, the same isoform has also been shown to hinder cancer treatment by inactivation of a range of clinically used anti-cancer drugs [22].

Following the role of CYP1 in the development of cancer, extensive research has been carried out to tackle its effects. Flavonoids such as resveratrol have been identified as potent inhibitors of CYP1 induction both *ex vivo* and *in vivo* by acting as competitive antagonists for the AhR (aryl hydrocarbon receptor), involved in the activation of CYP1 expression [23]. This is possibly due to structural similarities with typical AhR ligands [24], which means that compounds with different structural features can have more potent inhibitory effects in different isoforms of the enzyme. For example, myricetin and quercetin are potent CYP1B1 inhibitors but appeared to be less effective on the CYP1A1 and CYP1A2 isoforms [25].

Furthermore, other authors have reported the role of some flavonoids as AhR agonists and CYP1 substrates [24]. In this case, the expression of CYP1 isoforms is facilitated via AhR-mediated induction of the *Cyp1* gene, but structural similarities of flavonoids to steroid hormones make flavonoids likely substrates [25], diminishing the harmful activity of CYP1 enzymes when they are targeted in lieu of PAHs and other pro-carcinogens. Additionally, enzymatic modification of flavonoids often gives rise to structures with improved anti-carcinogenic properties upon delivery at CYP1-expressing tumour sites [25].

Overall, flavonoids can exert different effects on the CYP1 family, acting either as AhR-antagonists/inhibitors, as AhR-agonists/substrates or having a combined inhibitor/substrate effect. The latter is the case with resveratrol, which can also be transformed into molecules with improved anti-carcinogenesis properties [24].

Flavonoids as ABC (ATP-binding cassette) transporter regulators

The ABC superfamily is an evolutionarily conserved family of transporters that comprises P-gp (P-glycoprotein), BCRP (breast cancer resistance protein, also known as ABCG2) and MRPs (multidrug resistance proteins) 1 and 2. These membrane proteins are involved in the absorption, disposition and secretion of xenobiotic compounds. They are the main family of drug efflux transporters and are involved in the disposition of clinically used drugs [26]. Particularly, BCRP has been detected in a number of human tumours, including breast cancer, and represents a prominent mechanism for the development of MDR (multidrug resistance). Its overexpression in tumour sites leads to active exclusion of cytotoxic agents, limiting their absorption and intracellular accumulation and therefore hindering the effect of some cancer treatments [27].

There is accumulating evidence for the existence of flavonoid-drug interaction with BCRP. In the last decade extensive screenings have proved the effect of flavonoids as inhibitors of BCRP [26,28], showing that their intake during cancer treatment can cause an increase in the bioavailability and accumulation of anti-neoplastic agents [29], thus reversing MDR.

Flavonoids induce these effects by acting as inhibitors of the transporters, limiting the ATP-hydrolysing action that leads to exclusion of anti-cancer drugs from tumour

tissues [30]. This probably takes place by binding to NBD (nucleotide binding domain), which is targeted by flavonoids both in BCRP and P-gp [31]. Despite the positive alteration of drug pharmacokinetics induced by flavonoids, their interaction with BCRP is yet to be completely understood. For instance, some flavonoids can act as BCRP substrates (competing for the transporter with other substrates [26]), whereas other compounds can even induce expression of ABC transporters, stimulating BCRP-mediated MDR [32].

Effect of flavonoids on apoptosis, cell cycle arrest and other signalling pathways

Numerous flavonoids have been shown to induce apoptosis in a wide range of cancers (including breast [33]) through both main apoptotic pathways: intrinsic, caspase-9 and mitochondrial-driven apoptosis; and extrinsic, caspase-8 and death receptor-driven apoptosis [34].

They can also modulate other important regulators of apoptosis, including PARP (poly ADP-ribose polymerase) [35], anti-apoptotic protein families FLIP {FLICE [FADD (Fas-associated death domain)-like interleukin 1β-converting enzyme] inhibitory protein} and Bcl-2 (B-cell lymphoma 2) [33,36] or regulatory genes such as *p53* [37]. Flavonoids such as quercetin can also inhibit proteins involved in the evasion of apoptosis, such as sphingosine kinase [37] and PKB [protein kinase B (also known as Akt)] [38].

Ultimately, these discoveries highlight the broad and complex effect of flavonoids as pro-apoptotic drugs. In fact, some flavonoids have also been observed to play a counterintuitive role as competitive inhibitors for some caspases, suggesting that alternative, non-caspase dependent apoptosis pathways may be involved in their actions [39].

Cell-cycle arrest has also been identified as one of the main mechanisms behind the anti-tumour effect of flavonoids. Both naturally occurring and novel flavonoids have been shown to arrest proliferation at the G2/M checkpoint in several different cancer types [7,37], mainly through modulation of the expression level of different cyclins [35].

Through different mechanisms, linked to their properties as antioxidants, oestrogen-agonists or CYP1-inhibitors, flavonoids can also modulate proliferation, invasion or inflammatory signals. For instance, resveratrol inhibits COXs (cyclooxygenases) 1 and 2 [40], involved in the production of prostaglandins that subsequently leads to cell proliferation, angiogenesis and immunosuppression [2]. Different flavonoids have also been reported to modulate inflammatory signalling by mechanisms such as down-regulation or inhibition of NF-κB (nuclear factor κB) [41], therefore inhibiting proliferation and survival.

A recent meta-analysis has shown the relationship between flavonoid consumption and the reduction of chronic systemic inflammation mediators [42], while other reviews have shown evidence supporting the ability of flavonoids to inhibit metastasis, invasion and progression of cancer [43].

Promise of flavonoids as pharmacological agents against breast cancer

A major factor in the potential of flavonoids as anti-cancer agents lies in the complex manner in which they exert different effects. First, research has described the anti-tumour effects of flavonoids as being not only dose-dependent, but also biphasic [36]: whereas lower concentrations that could easily derive from a regular dietary intake have anti-apoptotic or cytoprotective effects, higher concentrations (by a factor between 5 and 10) can cause a pro-apoptotic response involving phenomena such as DNA damage [44]. Indeed, low concentrations of flavonoids such as genistein, resveratrol or myricetin may act as oestrogen agonists and cause proliferation of breast tumour tissues in an ER-dependent manner, whereas higher concentrations in the micromolar range exert AI and cytotoxic effects [10,12]. Nevertheless, the concentrations required to exert the desirable effects of flavonoids are still feasible from a pharmacological point of view, as opposed to other models in which anti-mutagens and anti-carcinogens are administered at unrealistically high doses, which would probably hinder the translation of these therapeutic strategies to the clinical setting [45]. Additionally, a major setting for the application of flavonoids is as sensitizers or co-treatments to achieve synergistic effects in combination with other therapies, which means the concentrations required in treatment would potentially be lower and their administration and delivery easily achievable.

Furthermore, the anti-cancer effect of flavonoids has been proved to be broad (affecting most types of cancers) but cancer-specific, since normal cells remain unaffected by concentrations that induce pro-apoptotic effects on cancer cells [36]. This is probably due to the fact that flavonoids target pathways typically characteristic of cancer cells. For instance, the CYP1 family of enzymes has been shown to be selectively expressed in tumour cells and pre-malignant tissue, not being significantly present in normal surrounding tissues [25]. This shows a great potential for the development of therapies targeted specifically to the abnormal tissue, and this specificity could also be enhanced because the compounds used are often only bioactivated when exposed to the effect of these enzymes.

Flavonoids also work in an additive manner. Hence the combination of different polyphenols administered concomitantly with anti-cancer treatments has been suggested as one of the promising strategies for the application of flavonoids to cancer treatment [46]. Interestingly, research has also shown that flavonoids do not hinder other natural anti-cancer processes (such as the effect of phase II detoxifying enzymes [47]).

Conclusions

Research in the last few decades has provided extensive evidence of the great versatility of flavonoids and the numerous targets that make them a family of compounds with great potential as anti-cancer agents. These properties seem

Figure 1 | **Anti-tumour properties of flavonoids**

A broad range of beneficial anti-tumour properties have been reported for flavonoids. Their effect on oestrogen production and signalling pathways has been linked to their role as AIs and their interaction with ER and oestrogen-metabolizing enzymes. They act as BCRP inhibitors and interact with CYP1 both as inhibitors and substrates. Research has also shown their ability to induce apoptosis and cell-cycle arrest and to alter numerous signalling pathways involved in cancer-related phenomena such as inflammation and proliferation.

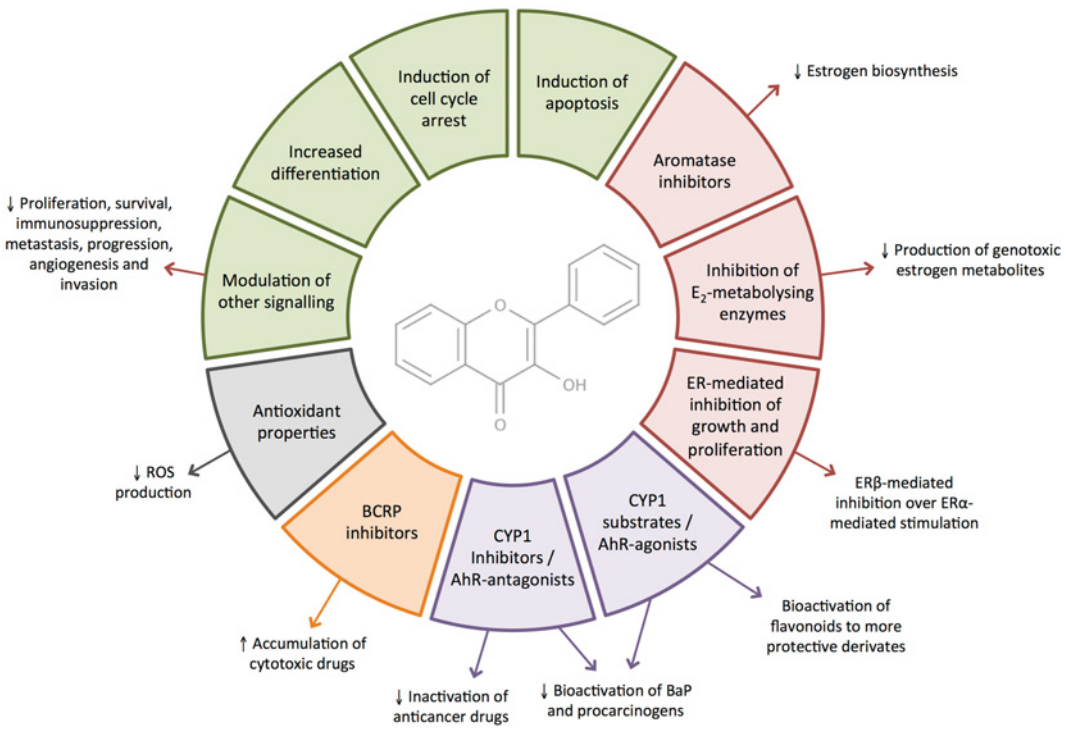

to be largely linked to their relatively simple structure: the presence of conjugated electron systems and aromatic rings make them stable and reactive, whereas their overall structure allows them to act as substrates, inhibitors or agonists for numerous enzymes or molecules involved in the development and progression of cancer.

To summarize, the combination of said multiple targets of flavonoids and the positive pharmacological characteristics of the effects they exert add up to the potential of these compounds in cancer treatment. Such versatile biological activity implies a great underlying complexity in the true mechanisms of action of different flavonoids, often dependent on a fine balance between pro- and anti-oxidant properties or between other beneficial and detrimental effects (Figure 1). Further study is needed for a better understanding of this, also taking into consideration the consequences of long-term exposure to compounds as ubiquitous as these or the variable effects due to specific structure–activity relationships [29–31].

In relation to this, the *in vivo* availability of dietary flavonoids, which can be poorly absorbed and rapidly conjugated, has been questioned. This could be a limitation to some of the *in vivo* actions of flavonoids. However, novel flavonoids currently under study [48] incorporate side chains or specific moieties such as methoxylations that address these obstacles by allowing improved bioavailability and delivery of the compound to the cancerous tissues targeted.

Despite this complexity, meta-analyses of controlled intervention trials and studies *in vivo* have shown that the application of flavonoids in the right setting and conditions can ultimately lead to a very positive outcome: decreasing indicators of inflammation, limiting proliferation, increasing latency and reducing both tumour size and metastasis [42]. The accumulating knowledge on the mechanism of action of flavonoids, as briefly summarized in the present review, together with information on different structure–activity relationships has led to promising new research rationales. In fact, there are several examples of promising novel flavonoids with improved properties that are currently at different stages of development towards their potential application in the treatment of ovarian and breast cancer [48–50].

Acknowledgements

We thank all of our colleagues and collaborators for helping in the preparation of this article, particularly Dr Arran Turnbull for his support and a critical reading of the review before submission.

Funding

Our work is supported by SULSA (Scottish Universities of Life Sciences Alliance), funded by the Biotechnology and Biological Sciences Research Council and Scottish Funding Council, as part of a BioSKAPE Industry Ph.D. studentship in collaboration with Antoxis Ltd (Aberdeen).

References

1 Ververidis, F., Trantas, E., Douglas, C., Vollmer, G., Kretzschmar, G. and Panopoulos, N. (2007) Biotechnology of flavonoids and other phenylpropanoid-derived natural products. Part I: Chemical diversity, impacts on plant biology and human health. Biotechnol. J. **2**, 1214–1234 CrossRef PubMed
2 Romagnolo, D.F. and Selmin, O.I. (2012) Flavonoids and cancer prevention: a review of the evidence. J. Nutr. Gerontol. Geriatr. **31**, 206–238 CrossRef PubMed
3 Tomé-Carneiro, J., Larrosa, M., González-Sarrías, A., Tomás-Barberán, F., García-Conesa, M. and Espín, J. (2013) Resveratrol and clinical trials: the crossroad from *in vitro* studies to human evidence. Curr. Pharm. Des. **19**, 6064–6093 CrossRef PubMed
4 Pan, H., Zhou, W., He, W., Liu, X., Ding, Q., Ling, L., Zha, X. and Wang, S. (2012) Genistein inhibits MDA-MB-231 triple-negative breast cancer cell growth by inhibiting NF-κB activity via the Notch-1 pathway. Int. J. Mol. Med. **30**, 337–343 PubMed
5 Bors, W. and Saran, M. (1987) Radical scavenging by flavonoid antioxidants. Free Radic. Res. Commun. **2**, 289–294 CrossRef PubMed
6 McPhail, D.B., Hartley, R.C., Gardner, P.T. and Duthie, G.G. (2003) Kinetic and stoichiometric assessment of the antioxidant activity of flavonoids by electron spin resonance spectroscopy. J. Agric. Food Chem. **51**, 1684–1690 CrossRef PubMed
7 Damianaki, A., Bakogeorgou, E., Kampa, M., Notas, G., Hatzoglou, A., Panagiotou, S., Gemetzi, C., Kouroumalis, E., Martin, P.M. and Castanas, E. (2000) Potent inhibitory action of red wine polyphenols on human breast cancer cells. J. Cell. Biochem. **78**, 429–441 CrossRef PubMed
8 Chobot, V. and Hadacek, F. (2011) Exploration of pro-oxidant and antioxidant activities of the flavonoid myricetin. Redox Rep. **16**, 242–246 CrossRef PubMed
9 Sirtori, C.R., Arnoldi, A. and Johnson, S.K. (2005) Phytoestrogens: end of a tale? Ann. Med. **37**, 423–438 CrossRef PubMed
10 Maggiolini, M., Bonofiglio, D., Marsico, S., Panno, M.L., Cenni, B., Picard, D. and Andò, S. (2001) Estrogen receptor α mediates the proliferative but not the cytotoxic dose-dependent effects of two major phytoestrogens on human breast cancer cells. Mol. Pharmacol. **60**, 595–602 PubMed
11 Bowers, J.L., Tyulmenkov, V.V., Jernigan, S.C. and Klinge, C.M. (2000) Resveratrol acts as a mixed agonist/antagonist for estrogen receptors α and β. Endocrinology **141**, 3657–3667 PubMed
12 Matsumura, A., Ghosh, A., Pope, G.S. and Darbre, P.D. (2005) Comparative study of oestrogenic properties of eight phytoestrogens in MCF7 human breast cancer cells. J. Steroid Biochem. Mol. Biol. **94**, 431–443 CrossRef PubMed
13 Kuiper, G.G.J.M., Lemmen, J.G., Carlsson, B., Corton, J.C., Safe, S.H., van der Saag, P.T., van der Burg, B. and Gustafsson, J.-Å. (1998) Interaction of estrogenic chemicals and phytoestrogens with estrogen receptor β. Endocrinology **139**, 4252–4263 PubMed
14 Harris, D.M., Besselink, E., Henning, S.M., Go, V.L.W. and Heber, D. (2005) Phytoestrogens induce differential estrogen receptor α- or β-mediated responses in transfected breast cancer cells. Exp. Biol. Med. **230**, 558–568
15 Koehler, K.F., Helguero, L.A., Haldosén, L.-A., Warner, M. and Gustafsson, J.-Å. (2005) Reflections on the discovery and significance of estrogen receptor β. Endocr. Rev. **26**, 465–478 CrossRef PubMed
16 Balfe, P., McCann, A., McGoldrick, A., McAllister, K., Kennedy, M., Dervan, P. and Kerin, M.J. (2004) Estrogen receptor α and β profiling in human breast cancer. Eur. J. Surg. Oncol. **30**, 469–474 CrossRef PubMed
17 Rice, S. and Whitehead, S.A. (2006) Phytoestrogens and breast cancer: promoters or protectors? Endocr. Relat. Cancer **13**, 995–1015 CrossRef
18 Mense, S.M., Hei, T.K., Ganju, R.K. and Bhat, H.K. (2008) Phytoestrogens and breast cancer prevention: possible mechanisms of action. Environ. Health Perspect. **116**, 426–433 CrossRef PubMed
19 Chun, O.K., Chung, S.J. and Song, W.O. (2007) Estimated dietary flavonoid intake and major food sources of U.S. adults. J. Nutr. **137**, 1244–1252 PubMed
20 Wen, X. and Walle, T. (2006) Methylated flavonoids have greatly improved intestinal absorption and metabolic stability. Drug Metab. Dispos. **34**, 1786–1792 CrossRef PubMed
21 Bugano, D.D.G., Conforti-Froes, N., Yamaguchi, N.H. and Baracat, E.C. (2008) Genetic polymorphisms, the metabolism of estrogens and breast cancer: a review. Eur. J. Gynaecol. Oncol. **29**, 313–320 PubMed
22 Rochat, B., Morsman, J.M., Murray, G.I., Figg, W.D. and Mcleod, H.L. (2001) Human CYP1B1 and anticancer agent metabolism: mechanism for tumor-specific drug inactivation? J. Pharmacol. Exp. Ther. **296**, 537–541
23 Ciolino, H.P., Daschner, P.J. and Yeh, G.C. (1999) Dietary flavonols quercetin and kaempferol are ligands of the aryl hydrocarbon receptor that affect CYP1A1 transcription differentially. Biochem. J. **340**, 715–722 CrossRef PubMed
24 Arroo, R.R.J., Androutsopoulos, V., Beresford, K., Ruparelia, K., Surichan, S., Wilsher, N. and Potter, G.A. (2009) Phytoestrogens as natural prodrugs in cancer prevention: dietary flavonoids. Phytochem. Rev. **8**, 375–386 CrossRef
25 Arroo, R.R.J., Androutsopoulos, V., Patel, A., Surichan, S., Wilsher, N. and Potter, G.A. (2008) Phytoestrogens as natural prodrugs in cancer prevention: a novel concept. Phytochem. Rev. **7**, 431–443 CrossRef
26 Tan, K.W., Li, Y., Paxton, J.W., Birch, N.P. and Scheepens, A. (2013) Identification of novel dietary phytochemicals inhibiting the efflux transporter breast cancer resistance protein (BCRP/ABCG2). Food Chem. **138**, 2267–2274 CrossRef PubMed
27 Natarajan, K., Xie, Y., Baer, M.R. and Ross, D.D. (2012) Role of breast cancer resistance protein (BCRP/ABCG2) in cancer drug resistance. Biochem. Pharmacol. **83**, 1084–1103 CrossRef PubMed
28 Katayama, K., Masuyama, K., Yoshioka, S., Hasegawa, H., Mitsuhashi, J. and Sugimoto, Y. (2007) Flavonoids inhibit breast cancer resistance protein-mediated drug resistance: transporter specificity and structure–activity relationship. Cancer Chemother. Pharmacol. **60**, 789–797 CrossRef PubMed
29 Zhang, S., Yang, X., Coburn, R.A. and Morris, M.E. (2005) Structure activity relationships and quantitative structure activity relationships for the flavonoid-mediated inhibition of breast cancer resistance protein. Biochem. Pharmacol. **70**, 627–639 CrossRef PubMed
30 Zhang, S., Yang, X. and Morris, M.E. (2004) Flavonoids are inhibitors of breast cancer resistance protein (ABCG2)-mediated transport. Mol. Pharmacol. **65**, 1208–1216 CrossRef PubMed
31 Morris, M.E. and Zhang, S. (2006) Flavonoid-drug interactions: effects of flavonoids on ABC transporters. Life Sci. **78**, 2116–2130 CrossRef PubMed
32 Tirona, R.G. and Bailey, D.G. (2006) Herbal product-drug interactions mediated by induction. Br. J. Clin. Pharmacol. **61**, 677–681 CrossRef PubMed
33 Huang, C., Chen, X., Guo, B., Huang, W., Shen, T., Sun, X., Xiao, P. and Zhou, Q. (2012) Induction of apoptosis by icariside II through extrinsic and intrinsic signaling pathways in human breast cancer MCF7 Cells. Biosci. Biotechnol. Biochem. **76**, 1322–1328 CrossRef PubMed
34 Kamsteeg, M., Rutherford, T., Sapi, E., Hanczaruk, B., Shahabi, S., Flick, M., Brown, D. and Mor, G. (2003) Phenoxodiol – an isoflavone analog – induces apoptosis in chemoresistant ovarian cancer cells. Oncogene **22**, 2611–2620 CrossRef PubMed
35 Park, K.I., Park, H.S., Nagappan, A., Hong, G.E., Lee, D.H., Kang, S.R., Kim, J.A., Zhang, J., Kim, E.H., Lee, W.S. et al. (2012) Induction of the cell cycle arrest and apoptosis by flavonoids isolated from Korean *Citrus aurantium* L. in non-small-cell lung cancer cells. Food Chem. **135**, 2728–2735 CrossRef PubMed
36 Ramos, S. (2007) Effects of dietary flavonoids on apoptotic pathways related to cancer chemoprevention. J. Nutr. Biochem. **18**, 427–442 CrossRef PubMed
37 Brown, D.M., Kelly, G.E. and Husband, A. (2005) Flavonoid compounds in maintenance of prostate health and prevention and treatment of cancer. Mol. Biotechnol. **30**, 253–270 CrossRef PubMed
38 Siegelin, M.D., Reuss, D.E., Habel, A., Herold-Mende, C. and von Deimling, A. (2008) The flavonoid kaempferol sensitizes human glioma cells to TRAIL-mediated apoptosis by proteasomal degradation of survivin. Mol. Cancer Ther. **7**, 3566–3574 CrossRef PubMed
39 White, J.B., Beckford, J., Yadegarynia, S., Ngo, N., Lialiutska, T. and D'Alarcao, M. (2012) Some natural flavonoids are competitive inhibitors of caspase-1, -3 and -7 despite their cellular toxicity. Food Chem. **131**, 1453–1459 CrossRef PubMed

40 Subbaramaiah, K., Chung, W.J., Michaluart, P., Telang, N., Tanabe, T., Inoue, H., Jang, M., Pezzuto, J.M. and Dannenberg, A.J. (1998) Resveratrol inhibits cyclooxygenase-2 transcription and activity in phorbol ester-treated human mammary epithelial cells. J. Biol. Chem. **273**, 21875–21882 CrossRef PubMed
41 Pozo-Guisado, E., Merino, J.M., Mulero-Navarro, S., Lorenzo-Benayas, M.J., Centeno, F., Alvarez-Barrientos, A. and Fernandez-Salguero, P.M. (2005) Resveratrol-induced apoptosis in MCF-7 human breast cancer cells involves a caspase-independent mechanism with downregulation of Bcl-2 and NF-κB. Int. J. Cancer **115**, 74–84 CrossRef PubMed
42 Peluso, I., Raguzzini, A. and Serafini, M. (2013) Effect of flavonoids on circulating levels of TNF-α and IL-6 in humans: a systematic review and meta-analysis. Mol. Nutr. Food Res. **57**, 784–801 CrossRef PubMed
43 Yang, J. and Weinberg, R.A. (2008) Epithelial–mesenchymal transition: at the crossroads of development and tumor metastasis. Dev. Cell **14**, 818–829 CrossRef PubMed
44 Wätjen, W., Michels, G., Steffan, B., Niering, P., Chovolou, Y., Kampkötter, A., Tran-Thi, Q.J., Proksch, P. and Kahl, R. (2005) Low concentrations of flavonoids are protective in rat H4IIE cells whereas high concentrations cause DNA damage and apoptosis. J. Nutr. **135**, 525–531 PubMed
45 Knasmüller, S., Steinkellner, H., Majer, B.J., Nobis, E.C., Scharf, G. and Kassie, F. (2002) Search for dietary antimutagens and anticarcinogens: methodological aspects and extrapolation problems. Food Chem. Toxicol. **40**, 1051–1062 CrossRef PubMed
46 Zhang, S., Yang, X. and Morris, M.E. (2004) Combined effects of multiple flavonoids on breast cancer resistance protein (ABCG2)-mediated transport. Pharm. Res. **21**, 1263–1273 CrossRef PubMed
47 Kensler, T.W. (1997) Chemoprevention by inducers of carcinogen detoxication enzymes. Environ. Health Perspect. **105**, 965–970 CrossRef PubMed
48 Martinez-Perez, C., Mullen, P., Ward, C., Cook, G., McPhail, D., Harrison, D.J. and Langdon, S.P. (2014), Investigation of the role of ROS modulation in the antitumour effect of a novel breast cancer drug candidate, http://www.biochemistry.org/Portals/0/Conferences/abstracts/SA155/SA155P032.pdf (Abstract)
49 Pant, S., Burris, 3rd, H.A., Moore, K., Bendell, J.C., Kurkjian, C., Jones, S.F., Moreno, O., Kuhn, J.G., McMeekin, S. and Infante, J.R. (2014) A first-in-human dose-escalation study of ME-143, a second generation NADH oxidase inhibitor, in patients with advanced solid tumors. Invest. New Drugs **32**, 87–93 CrossRef PubMed
50 Kurkjian, C., Pant, S., Burris, III, H.A., Bendell, J.C., Jones, S.F., Moore, K.N., Moreno, O., Mass, R.D. and Infante, J.R. (2012) ME-143, a novel inhibitor of tumor-specific NADH oxidase (tNOX): results from a first-in-human phase I study. J. Clin. Oncol. **30** (Suppl.), 3067, (Abstract)

Received 8 April 2014
doi:10.1042/BST20140073

FULL PAPER

BJC

British Journal of Cancer (2016), 1–12 | doi: 10.1038/bjc.2016.6

Keywords: breast cancer; preclinical models of cancer; ROS modulation; novel flavonoids; animal models of cancer; natural products; SAR studies; xenograft models; novel antitumour agents

Antitumour activity of the novel flavonoid Oncamex in preclinical breast cancer models

Carlos Martínez-Pérez*[,1], Carol Ward[1], Arran K Turnbull[1], Peter Mullen[2], Graeme Cook[3], James Meehan[1], Edward J Jarman[1], Patrick IT Thomson[4], Colin J Campbell[4], Donald McPhail[3], David J Harrison[2] and Simon P Langdon[1]

[1]Division of Pathology Laboratories, Institute of Genetics and Molecular Medicine, University of Edinburgh, Western General Hospital, Edinburgh EH4 2XU, UK; [2]School of Medicine, University of St Andrews, St Andrews KY16 9TF, UK; [3]Antoxis Limited, IMS Building, Foresterhill Health and Research Complex, Aberdeen AB25 2ZD, UK and [4]EaSTCHEM, School of Chemistry, University of Edinburgh, Joseph Black Building, Edinburgh EH9 3FJ, UK

Background: The natural polyphenol myricetin induces cell cycle arrest and apoptosis in preclinical cancer models. We hypothesised that myricetin-derived flavonoids with enhanced redox properties, improved cell uptake and mitochondrial targeting might have increased potential as antitumour agents.

Methods: We studied the effect of a second-generation flavonoid analogue Oncamex in a panel of seven breast cancer cell lines, applying western blotting, gene expression analysis, fluorescence microscopy and immunohistochemistry of xenograft tissue to investigate its mechanism of action.

Results: Proliferation assays showed that Oncamex treatment for 8 h reduced cell viability and induced cytotoxicity and apoptosis, concomitant with increased caspase activation. Microarray analysis showed that Oncamex was associated with changes in the expression of genes controlling cell cycle and apoptosis. Fluorescence microscopy showed the compound's mitochondrial targeting and reactive oxygen species-modulating properties, inducing superoxide production at concentrations associated with antiproliferative effects. A preliminary *in vivo* study in mice implanted with the MDA-MB-231 breast cancer xenograft showed that Oncamex inhibited tumour growth, reducing tissue viability and Ki-67 proliferation, with no signs of untoward effects on the animals.

Conclusions: Oncamex is a novel flavonoid capable of specific mitochondrial delivery and redox modulation. It has shown antitumour activity in preclinical models of breast cancer, supporting the potential of this prototypic candidate for its continued development as an anticancer agent.

Flavonoids account for the largest and most ubiquitous group of plant secondary metabolites. They comprise seven different subclasses of polyphenols with a common backbone consisting of two fused rings linked to another aromatic ring (Weng and Yen, 2012). Beyond their numerous roles in plant biology, flavonoids have long been identified as possessing a wide range of bioactivities, including protective and therapeutic effects against cancer, cardiovascular and neurodegenerative diseases, and thus have great potential for clinical application (Romano *et al*, 2013).

In particular, extensive preclinical evidence has accumulated for their antiproliferative effects against several types of cancer, including breast (Pan *et al*, 2012), prostate (Brown et al, 2005), lung (Park *et al*, 2012) and colorectal cancers (Ko *et al*, 2005a). However, their use in a therapeutic context is presently hampered by poor drug-like attributes resulting in low bioavailability and metabolic stability, limited cell uptake and ineffective delivery to important cellular compartments such as the mitochondria.

*Correspondence: C Martínez-Pérez; E-mail: c.martinez@sms.ed.ac.uk

Revised 17 November 2015; accepted 16 December 2015

Previous research has reported the anticancer effect of flavonoids on breast tumours through multiple mechanisms (Martinez-Perez *et al*, 2014). Structural similarities to the hormone 17β-oestradiol allow for interaction with the oestrogen receptors (ERs) (Limer and Speirs, 2004), although the effect is predominantly beneficial due to a stronger affinity for the proliferation-inhibiting isoform ERβ (Ström *et al*, 2004; Harris *et al*, 2005; McCarty, 2006). In addition, flavonoids can block the bioactivation of procarcinogens (Ciolino and Yeh, 1999; Moon *et al*, 2006) and act as inhibitors for oestrogen-producing and metabolising enzymes (Sanderson *et al*, 2004; Rice and Whitehead, 2006) and for the breast cancer resistance protein (BCRP), involved in the development of multidrug resistance (Katayama *et al*, 2007; Tan *et al*, 2013).

Flavonoids exert these antitumour activities in a concentration- and time-dependent manner, and have been shown to be effective in the treatment of numerous cancer types specifically targeting malignant cells (Ramos, 2007). Such properties support flavonoids as strong candidates for the development of novel anticancer treatments. Indeed, research has shown that administration of flavonoids can lead to a decrease in inflammation, proliferation, tumour size and metastasis (Limer and Speirs, 2004; Peluso *et al*, 2013). Further potential lies in their application as re-sensitisers in tumours clinically resistant to TRAIL (tumour necrosis factor-related apoptosis-inducing ligand) (Siegelin *et al*, 2009), radiotherapy (Yi *et al*, 2008), endocrine therapy (Mai *et al*, 2007; Tu *et al*, 2013) or chemotherapeutic agents like Centchroman (Singh *et al*, 2012).

The flavonol myricetin is a natural flavonoid with powerful antioxidant activity that has been shown to have a therapeutic effect in different cancers both *in vitro* and *in vivo*. It exerts apoptotic effects in combination with TRAIL (Siegelin *et al*, 2009) or by other mitochondrial-dependent pathways (Ko *et al*, 2005b), as well as inducing G_2/M cell cycle arrest (Zhang *et al*, 2008). We hypothesised that myricetin-derived, synthetic flavonoids with improved antioxidant properties, specific mitochondrial targeting and optimised physicochemical properties and drug-like attributes (McPhail *et al*, 2009) may have enhanced potential as antitumour agents.

In this study, we characterise a small library of these myricetin-derived new chemical entities. We assessed their antitumour properties in a panel of breast cancer cell lines, describing structure–activity relationships (SARs) and investigating the mechanism of action of these compounds, including the role of reactive oxygen species (ROS) modulation in their antitumour effects. The potential application of such synthetic derivatives in an *in vivo* setting was also assessed in a human breast cancer xenograft model.

MATERIALS AND METHODS

Cell culture. Breast cancer cell lines MCF-7, MDA-MB-231, BT-549 and HBL-100 (all obtained from ATCC) were cultured in Dulbecco's Modified Eagle Medium (DMEM) supplemented with 10% heat-inactivated foetal calf serum (FCS) and 100 IU ml^{-1} penicillin/streptomycin. These cell lines correspond to different molecular subtypes of breast cancer, with hormone-dependent MCF-7 expressing ERs (ER+) and MDA-MB-231, BT-549 and HBL-100 being characterised as triple-negative cell lines, lacking in receptors for oestrogen, progesterone and human epidermal growth factor (ER− PR− HER2−) and, hence, hormone-independent. The LCC1, LCC2 and LCC9 (hormone-independent cells established by derivation of selected subpopulations of MCF-7 cells (Brünner *et al*, 1993b, 1997; Thompson *et al*, 1993)) were cultured in phenol red-free DMEM supplemented with 5% heat-inactivated FCS charcoal-stripped of steroids. Cells were incubated at 37 °C in a humidified atmosphere containing 5% CO_2. Cells were grown to confluence with periodic medium changes and collected by brief incubation with trypsin/ethylenediaminetetraacetic acid solution. All cell lines were authenticated by short tandem repeat profiling undertaken by the Public Health England (Salisbury, UK) in December 2014.

Sulforhodamine B assay. Cells (500–2000 cells per well, depending on doubling time) were typically plated in 96-well microplates, and medium changed to 2.5% FCS DMEM after 24 h, following preliminary experiments that showed an improved effect of drugs for lower serum concentrations (Supplementary Figure 1). Cells were treated after a further 24 h with a library of eight compounds, including myricetin and lead compounds AO-1530 and Oncamex (Table 1). Treatments included a range of micromolar concentrations between 0.01 and 100 μM for all compounds. Each experiment was repeated at least once.

After treatment cells were fixed with 50 μl per well of cold 25% trichloroacetic acid for 1 h at 4 °C and washed 10 times with H_2O. After drying, plates were stained for 30 min with 50 μl per well of 0.4% (w/v) sulforhodamine B (SRB) (in 1% acetic acid) and washed four times with 1% acetic acid. Protein-bound SRB was solubilised in 150 μl per well of 10 mM Tris solution (pH 10.5), followed by measurement of optical density (OD) at 540 nm in a BP800 Microplate Reader (Biohit, Helsinki, Finland). Results were processed, subtracting average values of blanks and day 0 controls and normalising to untreated controls.

Fluorescence microscopy. Cells were grown on coverslips and treated with Oncamex for 15 min, 1 or 6 h at 37 °C, adding 25 nM Mitotracker Deep Red (Life, Eugene, OR, USA) for the last 30 min (or 15 min for the shortest incubation). Cells were fixed in 4% parafarmoldehyde for 45 min, washed three times in phosphate-buffered saline (PBS) and allowed to air-dry before mounting on Superfrost Plus microscope slides (Thermo Scientific, Braunschweig, Germany) using ProLong Gold antifade mountant with DAPI (4′,6-diamidino-2-phenylindole, Life, Bleiswijk, Netherlands). Oncamex possesses fluorescent properties, with a stable signal measurable at 550 nm_{EXC}/570 nm_{EM}. Cells were visualised, captures obtained and analysed using a PM-2000 AQUA (Automated Quantitative Analysis) system (HistoRX, New Haven, CT, USA) and an Axioplan 2 fluorescence microscope (Zeiss, Cambridge, UK).

The production of ROS was detected by fluorescence microscopy. The method above was followed with additional staining of cells with mitochondrial probes following the manufacturers' guidelines, incubating with 10 μM MitoPY1 (Tocris, Bristol, UK) or 2.5 μM MitoSOX (Life) to detect mitochondrial production of hydrogen peroxide and superoxide, respectively.

Cell spotting. A total of 10^5 MCF-7 cells per well were plated in triplicate in six-well plates. After treatment and incubation, cells were trypsinised and centrifuged for 5 min at 2000 r.p.m. Resulting pellets were resuspended in 100 μl of FCS and transferred to Cytofunnels EZ Single (Fisher, Braunschweig, Germany) mounted on Superfrost Plus slides (VWR International, Leuven, Belgium) to be spun for 3 min at 500 r.p.m. in a Cytospin 4 Cytocentrifuge (Thermo Fisher, Chesire, UK). Slides were allowed to air-dry and stained using the Reastain Quick Diff kit (Reagena, Toivala, Finland), to fix and dye both protein and DNA. After rinsing and air-drying, cells were observed on an Olympus BX51 microscope (Olympus, Hamburg, Germany) and images were captured using the software package Q-Capture Pro (Q Imaging, Surrey, BC, Canada).

Plate-based assays. The CellTox Green Cytotoxicity and ApoTox-Glo Triplex assay kits (Promega, Madison, WI, USA) were used to measure cytotoxicity at different timepoints and to assess the

Table 1. Library of novel flavonoids screened for their antitumour properties

Compound	Structure	Characteristics/properties
Myricetin	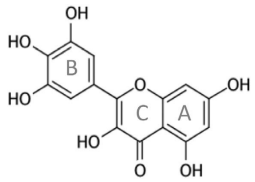	Naturally occurring flavonoid identified as particularly powerful antioxidant
AO-1530	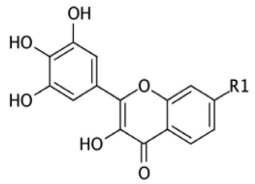	Myricetin-based novel flavonoid, mitochondria-targeted and with active redox properties. Non-redox-active OH groups removed and a decyl chain similar to the one found in vitamin E has been added to improve permeability and targeting
Oncamex (R1)	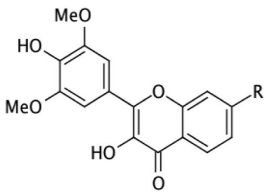	Bi-methoxylated second-generation analogue of AO-1530
AO-1486 (R2)		Same backbone as AO-1530, but nonspecific targeting
AO-1487 (R3)		Same backbone as AO-1530, but nonspecific targeting
AO-594 (R4)		Same backbone as AO-1530, but weaker specificity for the mitochondrial compartment
AO-155-179	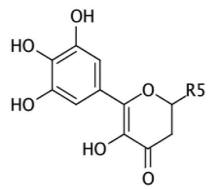	Similar backbone to that of AO-1530 but one of the fused rings has been removed, leaving a less flavonoid-like structure
AO-714A	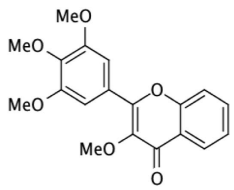	Fully blocked redox activity
AO-594	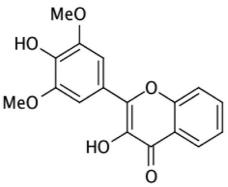	Same backbone as AO-1530, but nonspecific targeting

Abbreviations: R1 = $(CH_2)_9$-CH_3; R2 = $(CH_2)_3$-NH-$(CH_2)_4$-NH_2; R3 = CH_2-(C_6H_8)-NH_2.HCl; R4 = no radical; R5 = $(CH_2)_{10}$-CH_3. The addition of different moieties and radicals granted distinctive redox potential and intracellular targeting to analogues in a library of seven novel, myricetin-derived flavonoids.

mechanism of action of the drugs studied, respectively. In all, 10^4 cells per well were plated in 96-well microplates (black walls for CellTox assay and white for ApoTox), changing the medium to phenol red-free DMEM after 24 h. The protocols were carried out following the manufacturer's instructions, and fluorescence and luminescence were measured in a Labsystems Fluoroskan Ascent FL (Thermo, Vantaa, Finland) plate reader.

Cell lysates. In all, 3×10^6 MCF-7 cells per dish were plated in 140-cm^2 Petri dishes. After treatment, cells were washed in PBS and incubated for 10 min on ice in 400 μl of lysis buffer (50 mM Tris, 5 mM EGTA and 150 mM NaCl) containing Complete Protease Inhibitor Tablet (Roche, Mannheim, Germany; 1 tablet per 10 ml), 1 : 100 of phosphatase inhibitor cocktails 2 and 3 (Sigma, St Louis, MO, USA), 1 : 200 aprotinin (Sigma) and 1 : 100

Triton X (Sigma). Lysates were centrifuged at 13 000 r.p.m. at 4 °C for 6 min. Supernatants were recovered and stored at −70 °C.

Bicinchoninic acid assay. Protein concentration in cell lysates was determined by bicinchoninic acid (BCA) assay. Bovine serum albumin (BSA, G Biosciences, St Louis, MO, USA) was used as protein standard, preparing serial dilutions (0–1000 $\mu g\,ml^{-1}$) in distilled water (dH_2O), while aliquots of cell lysates were also diluted 1 : 10 in dH_2O. A volume of 1 ml of a 1 : 50 copper sulphate : BCA solution was added to 50 μl of each protein solution in borosilicate glass tubes. Tubes were incubated at 60 °C for 15 min before cooling briefly and dispensing replicates of each solution to a 96-well microplate. The OD at 540 nm was measured in a BP800 Microplate Reader (Biohit) and protein concentration in each lysate was extrapolated from BSA dilutions standard curves.

Electrophoresis and western blot. Cell lysates (40 μg of protein in 1 : 4 volume of 5 × loading buffer (5% SDS, 25% 2-mercaptoethanol, 50% glycerol, 0.02% bromophenol blue and 0.04 M Tris)) were denatured at 60 °C for 1 h and electrophoretically separated by polyacrylamide gel electrophoresis on Mini-gel equipment (BioRad, Hemel Hempstead, UK). Prestained protein marker, Broad Range (7–175 kDa, New England BioLabs, Ipswich, MA, USA), diluted 1 : 3 in 1 × loading buffer, was used as marker.

Proteins were transferred to a polyvinylidene fluoride membrane for 90 min at a constant voltage of 100 V and in cold, stirred transfer buffer (25 mM Tris and 19.2 mM glycine). After blocking for 1 h at 4 °C in BB : PBS (1 : 1 dilution of Odyssey Blocking buffer (Li-Cor, Lincoln, NE, USA) in PBS), membranes were incubated with mouse anti-cleaved PARP (poly(ADP-ribose) polymerase; 1 : 8000 dilution, Cell Signaling, Hitching, UK) and rabbit anti-human β-tubulin (1 : 6000 dilution, Abcam, Cambridge, UK) antibodies overnight at 4 °C. Staining with secondary goat anti-mouse IRDye 800CW and goat anti-rabbit IRDye 680CW antibodies (both 1 : 10 000 dilution, Li-Cor) was followed by scanning on Li-Cor Odyssey Scanner (Li-Cor).

Analytical electrochemistry. To prepare solutions of analytes, 0.5 mg of solid sample was suspended in 1 ml of 100 mM tetrabutylammonium hexafluorophosphate dissolved in acetonitrile (MeCN), and the suspension was treated with ultrasound in a water bath (40 °C) for 30 min. Cyclic voltammograms were acquired using a Autolab PGStat (Eco-Chemie, Utrecht, Netherlands) at a scan rate of 100 $mV\,s^{-1}$, using only the tenth and final scan unless otherwise stated, to estimate the reduction potential of the analytes. A saturated calomel (Hg_2Cl_2) electrode was used as a reference and a fine platinum gauze (0.1 mm wire, 1 cm^2) as a counter electrode. A straight platinum wire (1 mm diameter) was used as a working electrode, and the experiments were carried out under a blanket of argon.

RNA processing, microarray hybridisation and data analysis. Raw and normalised gene expression files are available from the National Center for Biotechnology Information Gene Expression Omnibus (Barrett *et al*, 2005) under the accession number GSE70949.

Ten samples were collected comprising five breast cancer cell lines (MCF-7, MDA-MB-231, LCC1, LCC2 and LCC9) in two different conditions: untreated vehicle control (DMSO) and treated cells (6 h in 10 μM Oncamex). For this, 3×10^6 cells per cell line were treated, trypsinised and stored at −70 °C. The RNA was extracted using the Qiagen RNeasy Mini kit (Qiagen, Hilden, Germany), amplified and labelled using the Ambion Illumina TotalPrep RNA Amplification kit (Life, Carslbad, CA, USA) (in both steps as per the manufacturers' instructions) and hybridised to HumanHT-12 v4 Illumina BeadChips (Illumina, Cambridge, UK). Arrays were scanned using an Illumina iScan (Illumina).

Raw gene expression files were log2-transformed and quantile-normalised using the *lumi* Bioconductor package (Du *et al*, 2008), mapped to Ensembl gene identifiers and detection-filtered using re-annotation and pre-processing approaches previously described (Turnbull *et al*, 2012). Differential gene expression analysis was performed using pair-wise rank products (Breitling *et al*, 2004) between control and treated groups. Functional enrichment analysis of differentially expressed genes was performed using DAVID (Database for Annotation, Visualization and Integrated Discovery) Bioinformatics Resources 6.7 (Huang *et al*, 2009a, b). Heatmaps of differentially expressed genes belonging to clusters enriched for cell cycle and apoptosis were generated using log2 fold change expression values calculated between treated and control conditions for each cell line. Heatmaps were generated using TM4 microarray software suite's MultiExperiment Viewer (Saeed *et al*, 2003, 2006) and genes were ordered by Euclidean distance. Genes belonging to the apoptosis cluster were differentiated into pro- and anti-apoptosis clusters using Qiagen's custom referenced apoptosis PCR array literature (references therein).

Xenograft experiments. The xenograft studies were undertaken under a UK Home Office Project Licence in accordance with the Animals (Scientific Procedures) Act 1986, and studies were approved by the University of Edinburgh Animal Ethics Committee. The MDA-MB-231 xenografts were implanted subcutaneously into the flanks of adult (>8 weeks) female CD-1 immunodeficient mice (Charles River Laboratories, Tranent, UK), using 10 xenografts per experimental group of 6 mice, implanted in one or both flanks. Treatment was started when the mean tumour volume reached 0.25 cm^3 (day 0) and mice were treated daily intraperitoneally with Oncamex (25 $mg\,kg^{-1}$ per day) or with solvent control (10% DMSO in saline) on days 0–4 and 7–11. Changes in tumour size over 14 days were measured using Vernier callipers and volumes calculated ($V = l \times w^2/2$). Changes in mean body weight were recorded every 2 days over 14 days. The initial dose selection of 25 $mg\,kg^{-1}$ per day was based on the similarity of this structure to another compound for which 25 $mk\,kg^{-1}$ per day had been a safe dose. This dose was confirmed to be safe in an initial dose-testing experiment and no untoward effects were noted.

Immunohistochemistry. Xenograft tissue was collected, fixed in formalin and embedded in paraffin. Sections were dewaxed in xylene for 5 min and washed in alcohol and water before incubating in heated antigen retrieval solution (0.1 M sodium citrate and 0.1 M citric acid, pH 6). Slides were washed in PBS, incubated in 3% dH_2O_2 for 10 min and washed again in PBST (0.1% Tween-20 PBS) before incubating for 10 min in Total Protein Block (Dako, Ely, UK). Sections were incubated for 1 h in mouse monoclonal anti-Ki-67 antibody (1 : 300 dilution, Dako), followed by 30 min in Envision labelled polymer (Dako) and 10 min in DAB (1 : 50 dilution in buffer, Dako), with washes in PBST between each step. Finally, slides were counterstained in haematoxylin for 1 min and taken through graded alcohols to xylene before mounting in DPX mountant medium (Sigma-Aldrich, Dorset, UK).

Immunohistochemistry (IHC) scores were calculated by counting average positively stained cells across sections for each of the 10 xenografts for treated and control groups, using the average of calculations by three users to ensure unbiased estimations. Percentage of viability was assessed using the image-processing package Image J (NIH, Bethesda, MD, USA) to measure the viable areas in each section.

Other materials. Novel flavonoids tested (Table 1) were supplied by Antoxis Limited (Aberdeen, UK) from their library of proprietary compounds (Caldwell *et al*, 2007). They were custom synthesised and their purity was ascertained to be >95% by liquid

chromatography mass spectrometry and nuclear magnetic resonance. Unless otherwise stated, any other reagents and solvents were of analytical grade from Sigma-Aldrich and were used without further purification.

Statistical analysis. For analysis of SRB and other plate-based assays, all experiments were repeated at least once, and six technical replicates were used to calculate means and s.d. Results were processed, subtracting average values of blanks and day 0 controls and normalising to untreated controls. Cell proliferation curves were fitted to a model for sigmoidal regression using the Excel package Fit Designer 2D (IDBS, Guildford, UK), excluding outliers outside of a 95% confidence interval, for the calculation of half maximal inhibitory concentration (IC_{50}) values.

For statistical analysis of xenograft and IHC results, Prism 6 (GraphPad Software, La Jolla, CA, USA) was used to compare control and treated groups using unpaired *t*-test.

RESULTS

Novel flavonoid Oncamex exerts a potent antitumour effect in breast cancer cell lines. Among the eight compounds tested (Table 1) in a panel of SRB assays, AO-1530 and its second-generation methoxylated analogue Oncamex showed the strongest antiproliferative effects (Figure 1A and B). Oncamex was the most potent myricetin derivative of the series tested and exerted similar antiproliferative responses in MCF-7, BT-549, MDA-MB-231 and HBL-100 cells. For hormone-independent cell lines LCC1, LCC2 and LCC9, the two lead compounds were still more effective than myricetin although the overall effect was weaker.

Oncamex's IC_{50} values were between 4- and 140-fold lower than those of myricetin in all cell lines, while the potency and IC_{50} values of the other analogues were more variable (Figure 1C and D). Analogues AO-714A and AO-155-179 typically exerted antiproliferative effects closer to those of the lead compounds, whereas other analogues exerted weaker effects, with IC_{50} values closer to, or even higher, than those of myricetin.

Oncamex specifically targets the mitochondrial compartment, with rapid delivery and stable accumulation. Drug uptake and intracellular location was assessed by microscopic visualisation. Images obtained demonstrated a specific targeting of the mitochondrial compartment by Oncamex in the model breast cancer cell line MDA-MB-231 (selected for its better adherence when grown on coverslips; Figure 2). The compound was co-localised with Mitotracker (and absent from nuclei and cytoplasm) as early as 15 min after treatment and was still retained in the mitochondrial compartment after 6 h. Previous work in another cancer cell line has shown the ability of AO-1530 to target the mitochondria, whilst other analogues with weaker antiproliferative effects have less specific intracellular localisation (Supplementary Figure 2).

Oncamex exerts its antitumour effect through induction of cytotoxicity and apoptosis. Microscopic observation of MCF-7 cells showed that treatment with Oncamex induced substantial changes after 24 h, including a reduction of cell density and division, alterations in nuclear morphology and appearance of apoptotic cells (Figure 3A–D). By 72 h after treatment these changes were generalised, with abundant apoptotic, phagocytised and dead cells. These results suggested the involvement of apoptosis in Oncamex's mechanism of action.

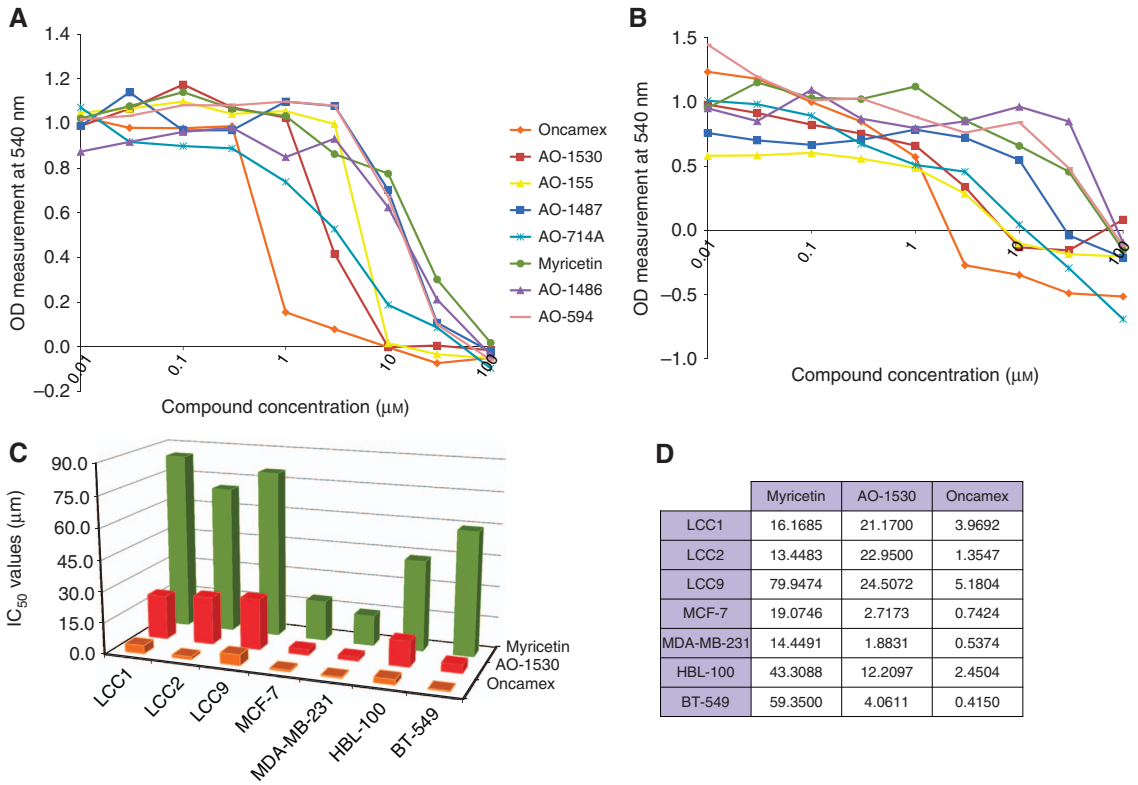

	Myricetin	AO-1530	Oncamex
LCC1	16.1685	21.1700	3.9692
LCC2	13.4483	22.9500	1.3547
LCC9	79.9474	24.5072	5.1804
MCF-7	19.0746	2.7173	0.7424
MDA-MB-231	14.4491	1.8831	0.5374
HBL-100	43.3088	12.2097	2.4504
BT-549	59.3500	4.0611	0.4150

Figure 1. Antitumour effect of Oncamex on breast cancer cell lines. The antiproliferative effect of a library of novel flavonoids was first assessed through SRB assays on a panel of seven breast cancer cell lines. Cells were treated for 4 days with drug concentrations in the 0.01–100 μM range concentration in all treatments. Results were comparable in all models, including MCF-7 (**A**) and MDA-MB-231 cells (**B**), with second-generation analogue Oncamex showing the strongest anticancer properties, markedly greater than those of myricetin. Analysis of concentration–response curves obtained from SRB assays allowed for the calculation of IC_{50} values for myricetin and the lead compounds (**C**, **D**), which reflected the stronger potency of Oncamex.

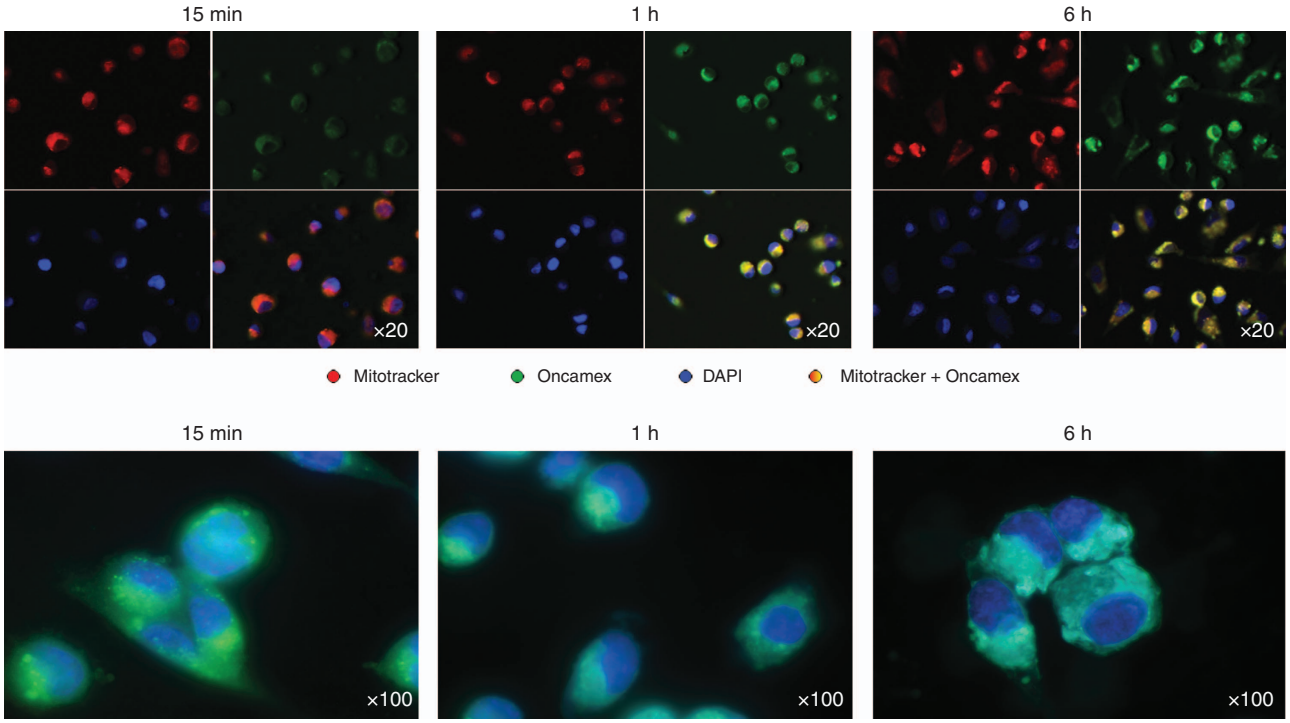

Figure 2. Intracellular localisation of Oncamex. Fluorescence microscopy on MDA-MB-231 cells treated with Oncamex demonstrated the rapid delivery of the drug and its localisation within the mitochondrial compartment, as shown by the overlap of the drug's fluorescent signal with that of Mitrotracker Deep Red (visualised as an orange–yellow signal resulting from the overlap of red and green fluorescences). The compound is delivered to the mitochondria as early as 15 min after the treatment and accumulates over time, retaining its organelle-specific targeting after 6 h. Visualisation of the cells at higher magnifications showed the change in cell morphology after 6 h, indicative of the induction of apoptosis.

SRB assays on cells exposed to different lengths of treatment (8, 16, 24, 48, 72 and 96 h) provided an insight into the timing of the anticancer effects observed (Supplementary Figure 3). Results showed that besides the more potent effect of Oncamex over AO-1530, the former also exerts a more rapid effect, inducing a significant reduction in cell density after 8 h comparable to the levels observed after 96 h, whereas AO-1530's effect was weaker and more delayed, not affecting cells until 24 h into treatment. CellTox plate assays showed that Oncamex produced an increase in cytotoxicity by 8 h after treatment in all cell lines (or earlier in some of them), reaching levels between 2- and 10-fold greater than the baseline signal by 24 h (Figure 3E).

Further investigation of Oncamex's mechanism of action using ApoTox multiplex assays showed that treatment of MCF-7, MDA-MB-231, HBL-100 and BT-549 cells with micromolar Oncamex concentrations for 8 h induced concentration-dependent, inversely correlated changes in cytotoxicity and cell viability, together with caspase-3/-7 activation, consistent with apoptosis (Figure 3G).

Induction of apoptosis was also measured by western blotting detection of PARP cleavage. Treatment with micromolar concentrations of AO-1530 or Oncamex led to cleavage of PARP. Oncamex exerted a more rapid effect, with cleaved PARP being detectable after 8 h, whereas 24-h incubation with AO-1530 was required for PARP cleavage to occur (Figure 3F).

ROS modulation is linked to Oncamex's properties. Oncamex displays an active redox profile. Analysis of electrochemical activity by cyclic voltammetry showed that Oncamex undergoes a reversible reduction, with a midpoint potential of $+145$ mV *vs* normal hydrogen electrode (Supplementary Figure 4).

To assess the role of ROS modulation in Oncamex's antitumour effect, ApoTox assays were repeated with the addition of a 30-min pre-incubation stage using an antioxidant agent (5 or 10 mM *N*-acetyl cysteine, NAC). Results with both model cell lines used (MCF-7 and MDA-MB-231, selected to include both an ER-positive and a triple-negative cell line, respectively) showed pre-treatment with 10 mM NAC caused a partial, but not complete, blockage of the cytotoxic and apoptotic signals induced by treatment with Oncamex (Figure 3H).

To investigate the effect of Oncamex on ROS production, MDA-MB-231 cells (selected for their better adherence when grown on coverslips) were stained with the novel fluorescent probes MitoPY1 or MitoSOX for the specific detection of mitochondrial hydrogen peroxide (mH_2O_2) and superoxide (mSO), respectively. The signal generated by MitoPY1 was not intense enough to allow for sensitive quantification, but provided qualitative results in the form of bright specks localised in the mitochondrial department. The induction of mH_2O_2 was observed 1 h after treatment with 0.3 μM Oncamex but no significant signals arose after longer incubations (Figure 4A). MitoSOX results showed a quantifiable, significant increase in mSO production in cells treated with higher concentrations of Oncamex for longer treatment times (Figure 4B and C).

Oncamex induces gene expression changes related to cell cycle and apoptosis regulation. Results from microarray experiments showed that 6-h treatment with Oncamex altered the expression profile of genes related to cell cycle and apoptosis (Figure 5). Genes involved in cell cycle regulation were downregulated by treatment in all cell lines studied. These include genes encoding proteins with well-known biological functions such as cyclins (encoded by *CCND1*, *CCNF* or *CCNB1*), regulators of proliferation (*AURKA* and *MKI67*) and other cell division-promoting proteins (*CDC20*, *MCM5* or *MCM3*).

Functional enrichment analysis showed that Oncamex induces different effects in two clusters of apoptosis-related genes. Pro-apoptotic genes were upregulated by treatment, including genes encoding apoptosis-inducing proteins (such as *BNIP3*,

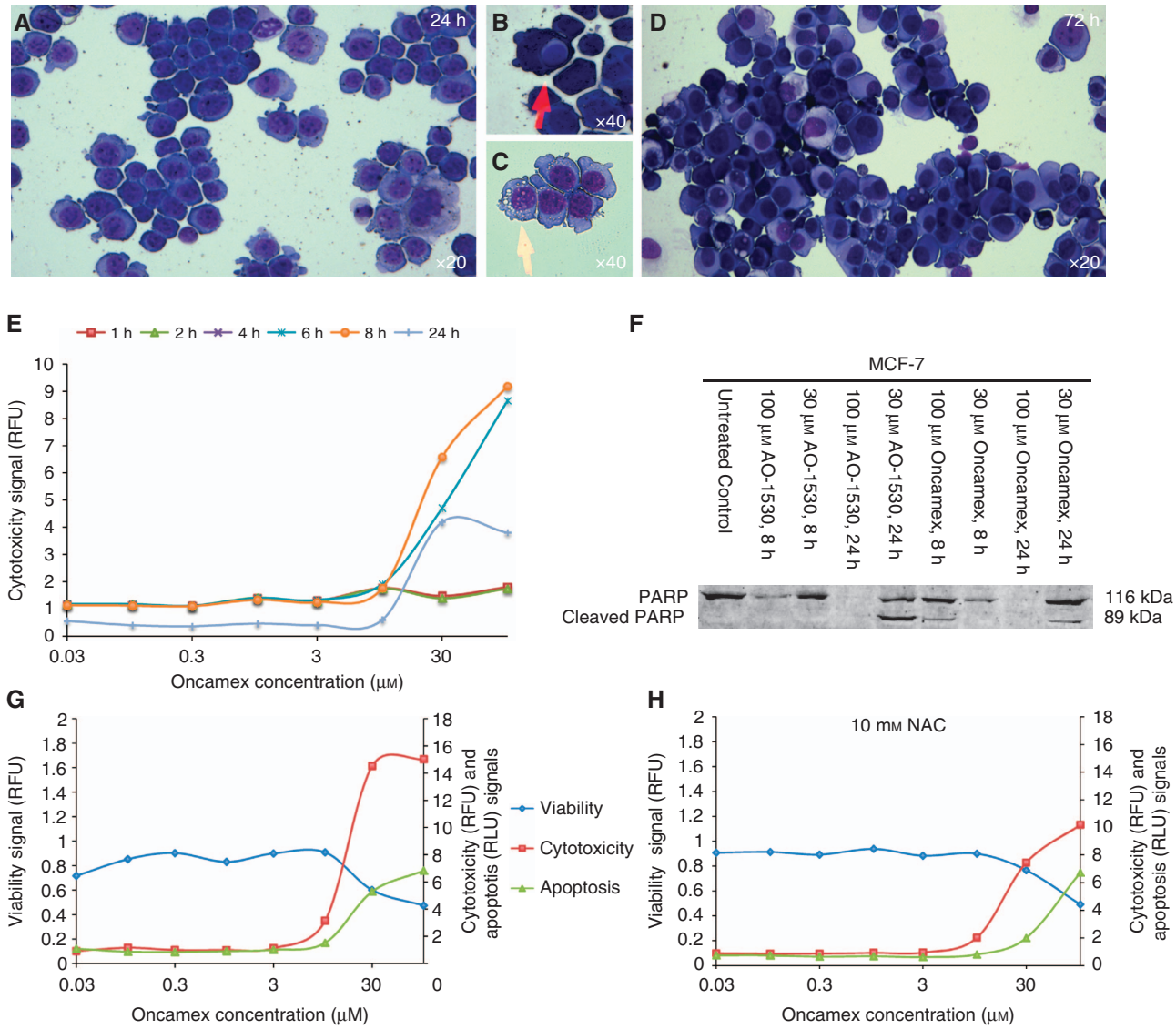

Figure 3. Cytotoxic and apoptotic effects of Oncamex. Initial evidence on the mechanism of action of Oncamex was obtained from study of breast cancer cell line models MCF-7 and MDA-MB-231. Microscopic visualisation of MCF-7 cells treated with 30 μM Oncamex showed a reduction in cell density, changes in cell morphology and the appearance of apoptotic and dead cells after 24 h (**A–C**), which was generalised by 72 h after treatment (**D**). CellTox Green plate assays supported preliminary results by direct measurement of the induction of cytotoxicity in treated MDA-MB-231 cells, peaking 8 h after treatment (**E**). Western blotting was used to measure PARP cleavage in treated MCF-7 cells (**F**): Oncamex seemed to induce apoptosis faster, with PARP cleavage occurring after 8 h treatment with the highest concentrations, whereas 24-h incubation was required with AO-1530. The 24-h incubation with the highest concentrations seemed to induce further cell degradation, preventing protein detection. Apoptosis was confirmed by an additional method using ApoTox plate assays, which reported an dose-dependent increase in cytotoxicity and apoptosis, inversely proportional to cell viability (**G**). These antitumour effects were partially blocked by 30 pre-treatment with 10 mM of the antioxidant NAC (**H**).

BNIP3L or *CRADD*) and caspases (*CASP7*). Anti-apoptotic genes were downregulated, including decreased expression of genes involved in apoptosis inhibition (*DFFA*, *BCL2*, *BIRC6* or *BIRC5*) or survival and proliferation (*IL10*).

Oncamex inhibits tumour proliferation and viability in a mouse *in vivo* model. Results from a first *in vivo* model in mice implanted with MDA-MB-231 xenografts (selected for the better ability of these cells to grow as xenografts) showed that treatment with Oncamex (25 mg kg^{-1} per day) had a significant effect ($P<0.05$), inhibiting tumour growth as indicated by changes in xenograft volume compared with untreated mice (Figure 6A). Treatment did not entail significant changes in mean body weight (<4% loss over 20 days) (Figure 6B).

IHC processing of collected xenograft tissue identified a significant decrease in Ki-67 expression, from 60% in controls to 36% in mice treated with Oncamex (Figure 6C–F), suggesting that this compound inhibits cell proliferation *in vivo*. Similarly, the percentage of viable areas was significantly reduced from 56 to 37% (Figure 6C–E and G).

DISCUSSION

In this study, we have identified several novel flavonoids with greater potency than myricetin when assessed in a panel of seven breast cancer cell lines. AO-1530, a synthetic analogue of myricetin

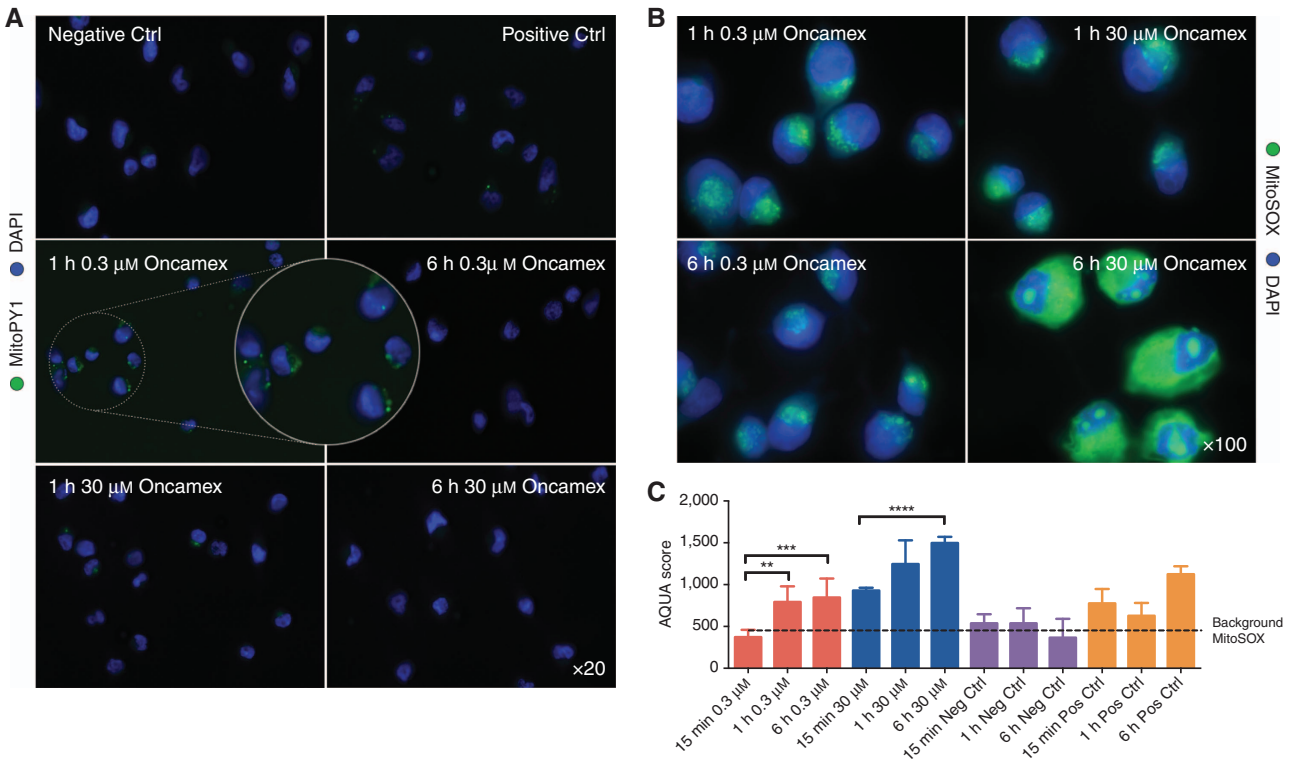

Figure 4. Effect of Oncamex on production of mitochondrial ROS. The production of ROS in MDA-MB-231 cells exposed to Oncamex in different treatment conditions was assessed using mitochondrial, species-specific fluorescent probes for microscopic visualisation of production of different species *in situ*. MitoPY1 produced a signal too weak for reliable quantification, but provided qualitative results showing an increase in mH_2O_2 after short incubations with 0.3 μM Oncamex (**A**), visible as bright specks in the mitochondrial compartment similar to the ones observed in the positive control treated with 100 μM H_2O_2. Measurement of MitoSOX reported a quantifiable, significant increase in mSO 6 h after treatment with 30 μM Oncamex (**B**), as supported by statistical analysis of measurements (**C**). *P*-values from unpaired *t*-test: $^{**}P<0.01$; $^{***}P<0.001$; $^{****}P<0.0001$. Where not shown $P>0.05$ (nonsignificant).

in which the non-redox-active OH groups on the A-ring of the flavonoid have been removed and a decyl chain has been added to improve cell membrane permeability (analogous to the function of the chain in vitamin E), had previously been identified as a more potent antioxidant than myricetin (McPhail *et al*, 2009). Results from SRB assays have indicated that AO-1530's strong antiproliferative properties are surpassed by Oncamex, a second-generation bi-methoxylated analogue.

We aimed to identify the SAR properties contributing to the stronger potency of these novel analogues. The library of compounds studied included molecules specifically designed to achieve distinct intracellular targeting and effective redox properties. One of the defining characteristics of Oncamex is the inclusion of two methoxy moieties in its structure. Previous research has suggested contrasting effects of methoxy substitutions in chemical entities: it has been reported that they may have unfavourable steric effects, compromising redox-modulating and cytochrome P450 (CYP1)-inhibitory capabilities (Heim *et al*, 2002; Arroo *et al*, 2009), while the extent of the BCRP-inhibitory properties of flavonoids also depends on the number and location of these modifications (Katayama *et al*, 2007; Pick *et al*, 2011; Tan *et al*, 2013). Nevertheless, the enhanced potency of Oncamex is most likely the result of methoxylation leading to improved pharmacokinetic properties and increased stability: methoxylated compounds are less prone to modifications such as glucuronidation and sulphation, and are thus more chemically and metabolically stable (Androutsopoulos *et al*, 2010). Added to improved uptake and membrane transport, such alterations may provide these compounds with increased bioavailability (Walle, 2007; Arroo *et al*, 2009). Moreover, it has been reported that upon delivery, methoxylated compounds are targeted by tumour-specific *O*-demethylases that provide free hydroxyl groups and hence an increase in redox properties (Androutsopoulos *et al*, 2008; Arroo *et al*, 2009). Therefore, it seems reasonable that chain-bearing, methoxylated novel flavonoids could make promising candidates as potential chemotherapeutic agents, providing improved pharmacological attributes, including cancer-specific activation.

Although Oncamex was the most potent compound in this series, the effect of the other analogues was more variable. Interestingly, the fully methoxylated molecule AO-714A showed a potent effect with variable but generally low IC_{50} values. This also supports the notion that flavonoids may not require free hydroxyl groups to be active anticancer agents due to their propensity to undergo demethylation *in vivo* by *O*-demethylases (Arroo *et al*, 2009). Similar to Oncamex, AO-714A presents multiple methoxylations that would improve its bioavailability and these are located in the 3′, 4′ and 5′ positions, reported as structural features that significantly increase the BCRP-inhibitory activity of flavonoids (Katayama *et al*, 2007; Tan *et al*, 2013). These observations suggest that different mechanisms such as induction of oxidative phosphorylation-independent cell death (as previously reported with myricetin (Ko *et al*, 2005b)) could also be relevant to their anticancer effect. Finally, other analogues expected to have a redox potential comparable to that of AO-1530 but with no specific targeting for mitochondria showed lower potency, highlighting the importance of targeted drug delivery.

Overall, these results indicate that particular SARs are relevant for the application of flavonoids to cancer treatment. The antitumour effect of these novel molecules is most likely the result of a combination of different structural traits and properties,

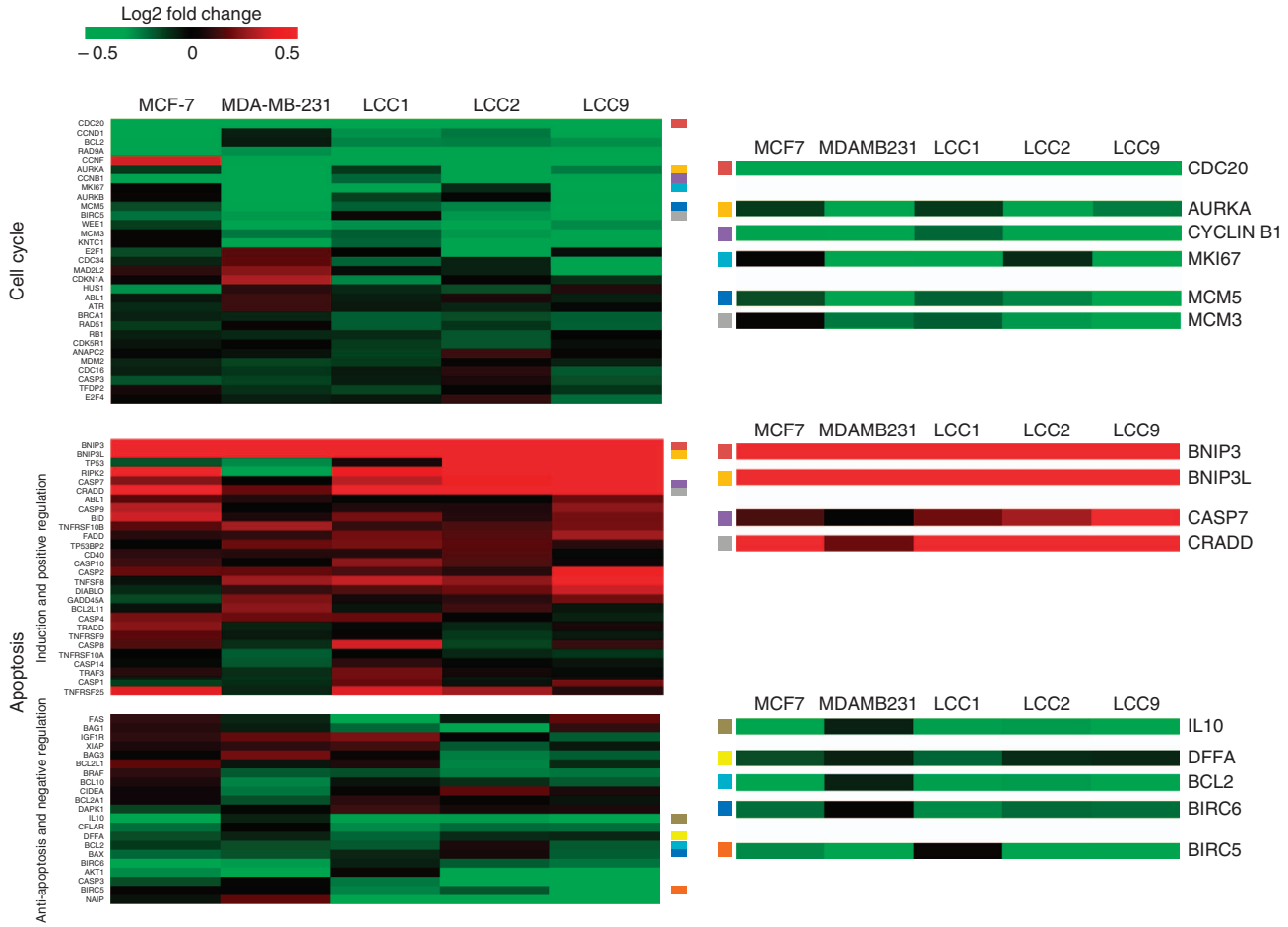

Figure 5. Modulation of gene expression by treatment with Oncamex. Heatmaps based on log2 fold changes between control and treated (6 h 10 μM Oncamex) summarising changes in gene expression in cell cycle and apoptosis function groups. Red and green represent high and low log2 gene expression fold changes, respectively. Genes are ordered by Euclidean distance. Representative examples of well-characterised genes in each pathway, which are up- or downregulated the most on treatment, are enlarged in panels to the right and their position in the overall heatmap is indicated by colour-coded markers.

including optimum redox potential and structural resemblance to the flavonoid backbone, which has been shown to allow for a wide range of molecular interactions for different polyphenols (Martinez-Perez *et al*, 2014). In addition, the substitution with electron-donating moieties, methoxylated residues and mitochondrial targeting provide significantly stronger antitumour properties.

Oncamex exerts an antiproliferative effect on cancer cells and has been found to induce apoptosis, as suggested by the development of responses as soon as 8 h after treatment by detection of caspase activation and PARP cleavage. Results from the panel of breast cancer cell lines studied suggest that the antitumour effect of Oncamex is independent of ER status, as triple-negative cell lines MDA-MB-231, BT-549 and HBL-100 cells showed susceptibility similar to that of ER-positive cells. This suggests that Oncamex's effect does not rely on modulation of hormonal signals and thus may be applicable to cancers of a more varied nature. We observed that LCC cell lines, which are ER-positive but hormone-independent MCF-7 variants, are less sensitive to Oncamex, but this is most likely due to the lower baseline proliferation rate of LCC cells (Brünner *et al*, 1993a, b, 1997).

The cytotoxic and apoptotic signals induced by Oncamex were partially blocked by pre-incubation with an antioxidant, suggesting that the compound's redox activity, studied by electrochemical analysis, is at least partially involved in the induction of these responses through ROS modulation. The production of ROS was detected by fluorescence microscopy using species-specific probes to obtain *in situ* visualisation. Results reported the induction of different mitochondrial ROS production in a concentration- and time-dependent manner. Whereas mH_2O_2 was produced shortly after treatment with nanomolar concentrations of Oncamex, mSO was produced after 6 h treatment with higher concentrations, in the same timeframe and concentration range linked to Oncamex's antitumour properties. The redox profile for Oncamex showed that it undergoes a reversible reduction with a midpoint potential of $+145$ mV, a value substantially more positive than the physiological resting redox potential in either cytoplasm or mitochondria (Auchinvole *et al*, 2012; Mallikarjun *et al*, 2012). This supports the notion that although aspects such as kinetics and biostability may affect its reactivity, Oncamex would most likely be found in its reduced form in the mitochondrial compartment and thus be able to donate an electron to oxygen to form the superoxide radical anion. Hence, results obtained from the study of mitochondrial ROS suggest that production of superoxide in the mitochondrial compartment might be associated with the antitumour effects exerted but also support the existence of a biphasic effect, previously reported for polyphenols such as flavonoids (Ramos, 2007), by which different, possibly opposing effects might be exerted by a compound depending on a fine concentration balance.

Gene expression analysis was carried out to study the effect of Oncamex on breast cancer cell line models at gene expression level.

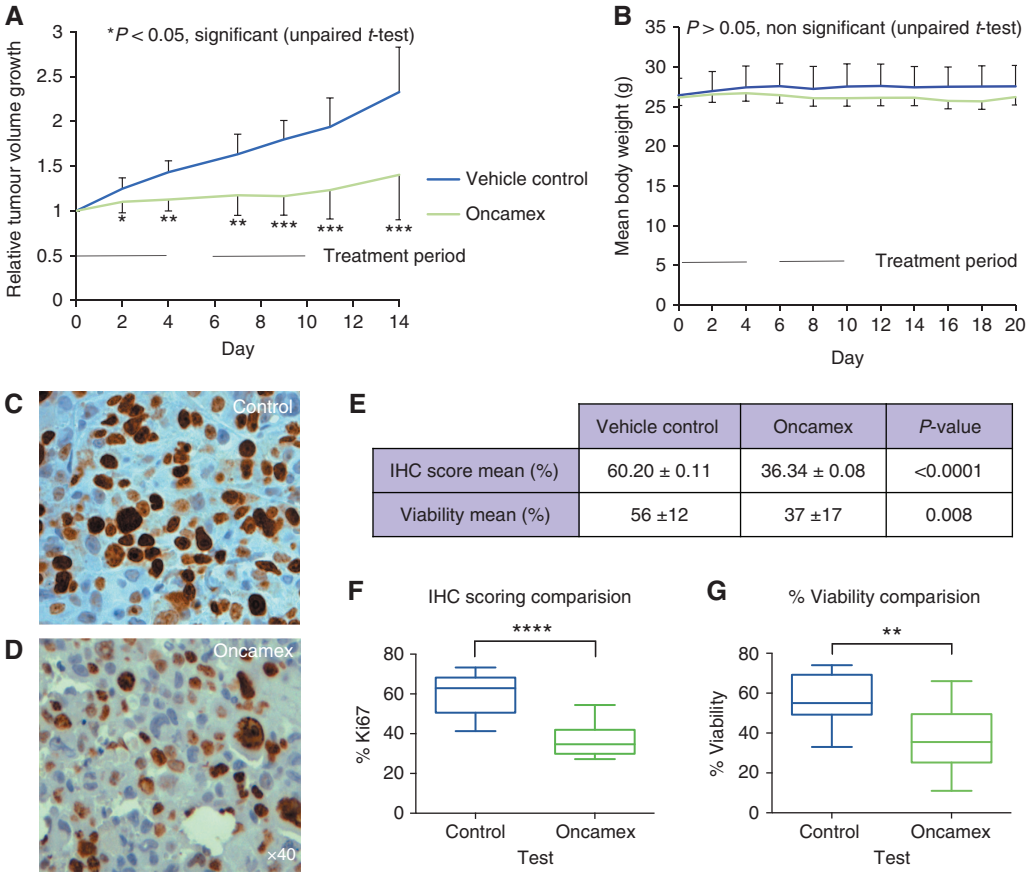

	Vehicle control	Oncamex	*P*-value
IHC score mean (%)	60.20 ± 0.11	36.34 ± 0.08	<0.0001
Viability mean (%)	56 ±12	37 ±17	0.008

Figure 6. Effect of Oncamex on xenografts in an *in vivo* mice model. Treatment of mice implanted with MDA-MB-231 xenografts with Oncamex (25 mg kg^{-1} per day, treating for 4 consecutive days with a 2-day rest in between) showed to exert a significant growth-inhibitory effect in comparison to untreated animals (**A**). Mean body weight was registered every second day for 20 days (**B**). Ki-67 activation was measured by immunohistochemistry in controls (**C**) and xenografts treated with Oncamex (**D**). Statistical study reported a statistically significant decrease in expression of the proliferation-linked protein as reported unpaired *t*-test analysis (**E**, **F**). Image analysis with the open-access processing programme ImageJ also showed a statistically significant reduction in the percentage of viable areas in the tissue (**E**, **G**). *P*-values from unpaired *t*-test: *$P<0.05$; **$P<0.01$; ***$P<0.001$; ****$P<0.0001$. Where not shown $P>0.05$ (nonsignificant).

Cells were exposed to treatment levels that had been shown to exert changes in proliferation and cell death, as well as to induce changes in ROS signalling. Results supported the antiproliferative and pro-apoptotic effects previously measured using cytotoxicity assays, western blotting and different plate assays. This suggests that the rapid delivery of Oncamex to the mitochondria is also translated either directly or indirectly into regulation of these pathways at gene expression level. Importantly, Oncamex induced largely the same effect across different cell lines despite their inherent biological differences.

The ROS status has been established as a major regulator in the development and advancement of cancer and, as the site of cell respiration, the mitochondrial compartment is the main source of ROS-linked signalling. Hence, a number of different mechanisms could be altered by the effect of these ROS-modulating drugs in the mitochondria. Given the versatility of flavonoids as anticancer agents, these results show that while Oncamex's promise as an antitumour agent has been demonstrated, its mechanism of action is probably complex and further study will be required for a better understanding.

Oncamex demonstrated significant growth-inhibitory activity in the MDA-MB-231 breast cancer xenograft model at a dose level that was not associated with any indications of toxicity. The proliferative marker Ki-67 was reduced by treatment with the drug consistent with an antiproliferative effect. Further studies are now required to observe whether other breast cancer xenografts are sensitive to this drug and to further study the pharmacokinetic and pharmacodynamic properties of this agent.

In conclusion, we have shown the potential of the prototypic novel compound Oncamex as an antitumour agent. This suggests that myricetin's natural scaffold can be modified to enhance its activity and shows the potential for mitochondrial targeted, redox-active molecules in cancer therapy. The results reported in this study have provided evidence of the anticancer effect of Oncamex in *in vitro* cell culture models, as well as preliminary antitumour activity in an *in vivo* xenograft model in mice.

ACKNOWLEDGEMENTS

We are grateful to Professor Robert Clarke for the use of the LCC1, LCC2 and LCC9 cell lines; to Sonya Uddin and Chrysi Xintaropoulou for their help with the gene extraction procedures; to Paul Perry for his assistance with microscopy; and to Helen Caldwell and Elaine McLay for sectioning of formalin-fixed and paraffin-embedded tissues. We thank SULSA (Scottish Universities Life Science Alliance) for supporting this project through a SULSA BioSkape Industry PhD Studentship and Antoxis Limited for providing additional funding. We also thank the Seventh Framework Programme of the European Union (METOXIA project; HEALTH-F2-2009-222741) for support.

CONFLICT OF INTEREST

DM and GC are employees of Antoxis Limited. The remaining authors declare no conflict of interest.

AUTHOR CONTRIBUTIONS

CM-P, CW, DJH, DM and SPL conceived of the study and participated in its design and coordination, and helped to draft the manuscript; CM-P, AKT, JM and EJJ participated in the gene extraction and IHC procedures; PM and CW assisted with cell culture; GC assisted with microscopy; PITT and CJC assisted with analytical electrochemistry and participated in cyclic voltammetry experiments; DM, PITT and CJC provided guidance on chemistry and ROS biology; CM-P and AKT carried out the gene expression analysis; SPL carried out the *in vivo* experiments; all authors contributed to and approved the final manuscript.

REFERENCES

Androutsopoulos V, Arroo RRJ, Hall JF, Surichan S, Potter GA (2008) Antiproliferative and cytostatic effects of the natural product eupatorin on MDA-MB-468 human breast cancer cells due to CYP1-mediated metabolism. *Breast Cancer Res* **10**: R39.

Androutsopoulos VP, Papakyriakou A, Vourloumis D, Tsatsakis AM, Spandidos DA (2010) Dietary flavonoids in cancer therapy and prevention: substrates and inhibitors of cytochrome P450 CYP1 enzymes. *Pharmacol Ther* **126**: 9–20.

Arroo RRJ, Androutsopoulos V, Beresford K, Ruparelia K, Surichan S, Wilsher N, Potter GA (2009) Phytoestrogens as natural prodrugs in cancer prevention: dietary flavonoids. *Phytochem Rev* **8**: 375–386.

Auchinvole CAR, Richardson P, McGuinnes C, Mallikarjun V, Donaldson K, McNab H, Campbell CJ (2012) Monitoring intracellular redox potential changes using SERS nanosensors. *ACS Nano* **6**: 888–896.

Barrett T, Suzek TO, Troup DB, Wilhite SE, Ngau W-C, Ledoux P, Rudnev D, Lash AE, Fujibuchi W, Edgar R (2005) NCBI GEO: mining millions of expression profiles—database and tools. *Nucleic Acids Res* **33**: D562–D566.

Breitling R, Armengaud P, Amtmann A, Herzyk P (2004) Rank products: a simple, yet powerful, new method to detect differentially regulated genes in replicated microarray experiments. *FEBS Lett* **573**: 83–92.

Brown DM, Kelly GE, Husband A (2005) Flavonoid compounds in maintenance of prostate health and prevention and treatment of cancer. *Mol Biotechnol* **30**: 253–270.

Brünner N, Boulay V, Fojo A (1993a) Acquisition of hormone-independent growth in MCF-7 cells is accompanied by increased expression of estrogen-regulated genes but without detectable DNA amplifications. *Cancer Res* **53**: 283–290.

Brünner N, Boysen B, Jirus S, Brunner N, Frandsen T, Spang-thomsen M, Skaar TC, Hoist-hansen C, Fuqua SAW (1997) MCF7/LCC9: an antiestrogen-resistant MCF-7 variant in which acquired resistance to the steroidal antiestrogen ICI 182, 780 confers an early cross-resistance to the nonsteroidal antiestrogen tamoxifen. *Cancer Res* **57**: 3486–3493.

Brünner N, Frandsen TL, Holst-hansen C, Brãnner N, Lippman ME, Clarke R, Bei M, Thompson EW, Wakeling AE (1993b) MCF7/LCC2: a 4-hydroxytamoxifen resistant human breast cancer variant that retains sensitivity to the steroidal antiestrogen ICI 182, 780. *Cancer Res* **53**: 3229–3232.

Caldwell ST, Bennett CJ, Hartley RC, McPhail DB, Duthie GG (2007) Flavonoid compounds as therapeutic antioxidants. Patent no. WO 2004/007475 A1.

Ciolino HP, Yeh GC (1999) Inhibition of aryl hydrocarbon-induced cytochrome P-450 1A1 enzyme activity and CYP1A1 expression by resveratrol. *Mol Pharmacol* **56**: 760–767.

Du P, Kibbe WA, Lin SM (2008) lumi: a pipeline for processing Illumina microarray. *Bioinformatics* **24**: 1547–1548.

Harris DM, Besselink E, Henning SM, Go VLW, Heber D (2005) Phytoestrogens induce differential estrogen receptor alpha- or beta-mediated responses in transfected breast cancer cells. *Exp Biol Med* **230**: 558–568.

Heim KE, Tagliaferro AR, Bobilya DJ (2002) Flavonoid antioxidants: chemistry, metabolism and structure-activity relationships. *J Nutr Biochem* **13**: 572–584.

Huang DW, Sherman BT, Lempicki RA (2009a) Bioinformatics enrichment tools: paths toward the comprehensive functional analysis of large gene lists. *Nucleic Acids Res* **37**: 1–13.

Huang DW, Sherman BT, Lempicki RA (2009b) Systematic and integrative analysis of large gene lists using DAVID bioinformatics resources. *Nat Protoc* **4**: 44–57.

Katayama K, Masuyama K, Yoshioka S, Hasegawa H, Mitsuhashi J, Sugimoto Y (2007) Flavonoids inhibit breast cancer resistance protein-mediated drug resistance: transporter specificity and structure-activity relationship. *Cancer Chemother Pharmacol* **60**: 789–797.

Ko C-H, Shen S-C, Lee TJF, Chen Y-C (2005a) Myricetin inhibits matrix metalloproteinase 2 protein expression and enzyme activity in colorectal carcinoma cells. *Mol Cancer Ther* **4**: 281–290.

Ko CH, Shen S-C, Hsu C-S, Chen Y-C (2005b) Mitochondrial-dependent, reactive oxygen species-independent apoptosis by myricetin: roles of protein kinase C, cytochrome c, and caspase cascade. *Biochem Pharmacol* **69**: 913–927.

Limer JL, Speirs V (2004) Phyto-oestrogens and breast cancer chemo-prevention. *Breast Cancer Res* **6**: 119–127.

Mai Z, Blackburn GL, Zhou J (2007) Genistein sensitizes inhibitory effect of tamoxifen on the growth of estrogen receptor-positive and HER2-overexpressing human breast cancer cells. *Mol Carcinog* **46**: 534–542.

Mallikarjun V, Clarke DJ, Campbell CJ (2012) Cellular redox potential and the biomolecular electrochemical series: a systems hypothesis. *Free Radic Biol Med* **53**: 280–288.

Martinez-Perez C, Ward C, Cook G, Mullen P, McPhail D, Harrison DJ, Langdon SP (2014) Novel flavonoids as anti-cancer agents: mechanisms of action and promise for their potential application in breast cancer. *Biochem Soc Trans* **42**: 1017–1023.

McCarty MF (2006) Isoflavones made simple - Genistein's agonist activity for the beta-type estrogen receptor mediates their health benefits. *Med Hypotheses* **66**: 1093–1114.

McPhail DB, Cook GJ, Johnstone AS, Docherty K (2009) Protection of mESCs from oxidative stress-induced cell death by a novel class of mitochondrial-targeted, high-potency antioxidant. *British Pharmacological Society Summer Meeting 2009 Abstract*.

Moon YJ, Wang X, Morris ME (2006) Dietary flavonoids: effects on xenobiotic and carcinogen metabolism. *Toxicol In Vitro* **20**: 187–210.

Pan H, Zhou W, He W, Liu X, Ding Q, Ling L, Zha X, Wang S (2012) Genistein inhibits MDA-MB-231 triple-negative breast cancer cell growth by inhibiting NF-κB activity via the Notch-1 pathway. *Int J Mol Med* **30**: 337–343.

Park KI, Park HS, Nagappan A, Hong GE, Lee DH, Kang SR, Kim JA, Zhang J, Kim EH, Lee WS, Shin SC, Hah YS, Kim GS (2012) Induction of the cell cycle arrest and apoptosis by flavonoids isolated from Korean Citrus aurantium L. in non-small-cell lung cancer cells. *Food Chem* **135**: 2728–2735.

Peluso I, Raguzzini A, Serafini M (2013) Effect of flavonoids on circulating levels of TNF-α and IL-6 in humans: a systematic review and meta-analysis. *Mol Nutr Food Res* **57**: 784–801.

Pick A, Müller H, Mayer R, Haenisch B, Pajeva IK, Weigt M, Bönisch H, Müller CE, Wiese M (2011) Structure-activity relationships of flavonoids as inhibitors of breast cancer resistance protein (BCRP). *Bioorg Med Chem* **19**: 2090–2102.

Ramos S (2007) Effects of dietary flavonoids on apoptotic pathways related to cancer chemoprevention. *J Nutr Biochem* **18**: 427–442.

Rice S, Whitehead SA (2006) Phytoestrogens and breast cancer – promoters or protectors? *Endocr Relat Cancer* **13**: 995–1015.

Romano B, Pagano E, Montanaro V, Fortunato AL, Milic N, Borrelli F (2013) Novel insights into the pharmacology of flavonoids. *Phytother Res* **27**: 1588–1596.

Saeed AI, Bhagabati NK, Braisted JC, Liang W, Sharov V, Howe EA, Li J, Thiagarajan M, White JA, Quackenbush J (2006) TM4 microarray software suite. *Methods Enzymol* **411**: 134–193.

Saeed AI, Sharov V, White J, Li J, Liang W, Bhagabati N, Braisted J, Klapa M, Currier T, Thiagarajan M, Sturn A, Snuffin M, Rezantsev A, Popov D, Ryltsov A, Kostukovich E, Borisovsky I, Liu Z, Vinsavich A, Trush V, Quackenbush J (2003) TM4: a free, open-source system for microarray data management and analysis. *Biotechniques* **34**: 374–378.

Sanderson JT, Hordijk J, Denison MS, Springsteel MF, Nantz MH, van den Berg M (2004) Induction and inhibition of aromatase (CYP19) activity by natural and synthetic flavonoid compounds in H295R human adrenocortical carcinoma cells. *Toxicol Sci* **82**: 70–79.

Siegelin MD, Gaiser T, Habel A, Siegelin Y (2009) Myricetin sensitizes malignant glioma cells to TRAIL-mediated apoptosis by down-regulation of the short isoform of FLIP and bcl-2. *Cancer Lett* **283**: 230–238.

Singh N, Zaidi D, Shyam H, Sharma R, Balapure AK (2012) Polyphenols sensitization potentiates susceptibility of MCF-7 and MDA MB-231 cells to Centchroman. *PLoS One* **7**: e37736.

Ström A, Hartman J, Foster JS, Kietz S, Wimalasena J, Gustafsson J-Å (2004) Estrogen receptor β inhibits 17β-estradiol-stimulated proliferation of the breast cancer cell line T47D. *Proc Natl Acad Sci USA* **101**: 1566–1571.

Tan KW, Li Y, Paxton JW, Birch NP, Scheepens A (2013) Identification of novel dietary phytochemicals inhibiting the efflux transporter breast cancer resistance protein (BCRP/ABCG2). *Food Chem* **138**: 2267–2274.

Thompson EW, Brünner N, Torri J, Johnson MD, Boulay V, Wright A, Lippman ME, Steeg PS, Clarke R (1993) The invasive and metastatic properties of hormone-independent but hormone-responsive variants of MCF-7 human breast cancer cells. *Clin Exp Metastasis* **11**: 15–26.

Tu S-H, Ho C-T, Liu M-F, Huang C-S, Chang H-W, Chang C-H, Wu C-H, Ho Y-S (2013) Luteolin sensitises drug-resistant human breast cancer cells to tamoxifen via the inhibition of cyclin E2 expression. *Food Chem* **141**: 1553–1561.

Turnbull AK, Kitchen RR, Larionov AA, Renshaw L, Dixon JM, Sims AH (2012) Direct integration of intensity-level data from Affymetrix and Illumina microarrays improves statistical power for robust reanalysis. *BMC Med Genomics* **5**: 35.

Walle T (2007) Methylation of dietary flavones greatly improves their hepatic metabolic stability and intestinal absorption. *Mol Pharm* **4**: 166–170.

Weng C-J, Yen G-C (2012) Flavonoids, a ubiquitous dietary phenolic subclass, exert extensive in vitro anti-invasive and in vivo anti-metastatic activities. *Cancer Metastasis Rev* **31**: 323–351.

Yi T, Li H, Wang X, Wu Z (2008) Enhancement radiosensitization of breast cancer cells by deguelin. *Cancer Biother Radiopharm* **23**: 355–362.

Zhang Q, Zhao X-H, Wang Z-J (2008) Flavones and flavonols exert cytotoxic effects on a human oesophageal adenocarcinoma cell line (OE33) by causing G2/M arrest and inducing apoptosis. *Food Chem Toxicol* **46**: 2042–2053.

Supplementary Information accompanies this paper on British Journal of Cancer website (http://www.nature.com/bjc)